TRANSPORTATION RESEARCH
RECORD

No. 1500

Highway and Facility Design; Highway Operations, Capacity, and Traffic Control

Geometric Design, Roadside Safety Features, Roadside Hardware Monitoring, and Scenic Loop Tours

A peer-reviewed publication of the Transportation Research Board

TRANSPORTATION RESEARCH BOARD
NATIONAL RESEARCH COUNCIL

NATIONAL ACADEMY PRESS
WASHINGTON, D.C. 1995

Transportation Research Record 1500
ISSN 0361-1981
ISBN 0-309-06157-1
Price: $45.00

Subscriber Category
IIA highway and facility design
IVA highway operations, capacity, and traffic control

Printed in the United States of America

Sponsorship of Transportation Research Record 1500

GROUP 2—DESIGN AND CONSTRUCTION OF TRANSPORTATION FACILITIES
Chairman: Michael G. Katona, U.S. Air Force Armstrong Laboratory

General Design Section
Chairman: Hayes E. Ross, Jr., Texas A&M University System

Committee on Photogrammetry, Remote Sensing, Surveying, and Related Automated Systems
Chairman: John E. Haverberg, Wisconsin Department of Transportation
Darrel L. Baker, William C. Beanland, John D. Bossler, Christopher C. Brooks, Roger R. Chamard, Larry L. Christenson, Frank F. Cooper, Paul J. Demers, Carl I. Fonnesbeck, David M. Gorg, Jack H. Hansen, Brian D. Hart, Thomas E. Henderson, Louis Keller, Donald W. Little, T. Dwane Moore, Richard A. Pearsall, Donald R. Rich, Frank L. Scarpace, A. Keith Turner, Donald E. Wilbur

Committee on Geometric Design
Chairman: John M. Mason, Jr., Pennsylvania State University
Secretary: Daniel B. Fambro, Texas A&M University System
Robert J. Behar, James K. Cable, Milton S. E. Carrasco, Michael M. Christensen, Donald E. Cleveland, William M. Dubose III, Said M. Easa, Dennis A. Grylicki, Elizabeth Hilton, David S. Johnson, Rudiger Lamm, Joel P. Leisch, Angel (Andy) Martinez, John R. McLean, Samuel P. Owusu-Ofori, Abishai Polus, Deborah V. Richmond, John L. Sanford, Seppo I. Sillan, Bob L. Smith, Nikiforos Stamatiadis, Larry Francis Sutherland, Matthew B. Tondl, Ross J. Walker, Keith M. Wolhuter

Committee on Roadside Safety Features
Chairman: John F. Carney III, Vanderbilt University
Robert F. Baker, Maurice E. Bronstad, James E. Bryden, Julie Anna Cirillo, Owen S. Denman, Arthur M. Dinitz, John C. Durkos, Vittorio Giavotto, Don Jay Gripne, Malcolm D. MacDonald, Mark A. Marek, Charles F. McDevitt, J. T. Peacock, David H. Pope, Richard D. Powers, Robert Quincy, Hayes E. Ross, Jr., Larry A. Scofield, Robert K. Seyfried, Rudolph Kenneth Shearin, Jr., Dean L. Sicking, Roger L. Stoughton, E. Debra Swanson, Harry W. Taylor, Thomas Turbell, Ta-Lun Yang

Committee on Landscape and Environmental Design
Chairman: E. LeRoy Brady, Arizona Department of Transportation
Secretary: Barbara M. Schaedler
Nicholas R. Close, Jerrold S. Corush, David H. Fasser, Lawrence E. Foote, Wilfrid L. Gates, Jr., Eugene Johnson, Edward N. Kress, Harlow C. Landphair, Charles R. Lee, Derek Lovejoy, Mark D. Masteller, Teresa Mitchell, Charles P. Monahan, Bob Moore, Carroll L. Morgenson, Barbara A. Petrarca, Charles R. Reed, James F. Ritzer, Elga Ronis, Jacquelyn A. Ross, Armen S. Sardarov, Michael C. Saunders, Richard C. Smardon, Grady Stem, Howard R. Wagner

GROUP 3—OPERATION, SAFETY, AND MAINTENANCE OF TRANSPORTATION FACILITIES
Chairman: Jerome W. Hall, University of New Mexico

Facilities and Operation Section
Chairman: Jack L. Kay, JHK & Associates

Committee on Operational Effects of Geometrics
Chairman: Daniel S. Turner, University of Alabama
Secretary: Douglas W. Harwood, Midwest Research Institute
Rahim F. Benekohal, Myung-Soon Chang, John E. Fisher, Kay Fitzpatrick, J. L. Gattis, Don Jay Gripne, Michael F. Hankey, Jeffrey P. Hartman, Warren E. Hughes, Raymond A. Krammes, Ken Lazar, Mark A. Marek, Patrick T. McCoy, John J. Nitzel, K. F. Phillips, Abishai Polus, Justin True, Walter E. Witt, Paul H. Wright

Transportation Research Board Staff
Robert E. Spicher, Director, Technical Activities
D.W. Dearasaugh, Engineer of Design
Richard A. Cunard, Engineer of Traffic and Operations
Nancy A. Ackerman, Director, Reports and Editorial Services

Sponsorship is indicated by a footnote at the end of each paper. The organizational units, officers, and members are as of December 31, 1994.

Transportation Research Record 1500

Contents

Foreword

The 24 papers in this volume were peer reviewed by the TRB Committee on Geometric Design, Committee on Roadside Safety Features, Committee on Photogrammetry, Remote Sensing, Surveying, and Related Automated Systems, Committee on Landscape and Environmental Design, and Committee on Operational Effects of Geometrics.

Carrasco describes a computer-aided design and drafting application that provides an interactive means of simulating turning vehicles. Medina and Kahl use a geographic information system for determining the feasibility of alternative corridors for an Illinois highway. Krammes et al. describe the development of a module for evaluating horizontal alignment consistency to be incorporated in an interactive highway safety design model. Kahl and Fambro propose a change in object height for stopping sight distance calculations. Hassan et al. discuss horizontal sight distances with continuous lateral obstructions around a curve or complicated horizontal alignments.

Mak et al. describe the development and testing of a slotted rail terminal for W-beam guardrails. Seo et al. discuss efforts in Japan to develop guardrails for high speed impacts. Gauthier et al. developed and tested a side impact system that will project a crash test vehicle in a side skid at a specified yaw angle. Menges et al. describe the development and crash testing of the Truck Thrie beam Transition, called the Triple T. Alberson et al. discuss the design and performance of two bridge railings tested at AASHTO performance Level 1 specified for low-volume rural roads. At the other end of the spectrum, Menges et al. describe two bridge railings designed to restrain and redirect commercial trucks and buses and tested at AASHTO performance Level 3. Rosson et al. discuss the development and testing of two bridge railings for longitudinal timber bridges, tested at AASHTO performance Level 2 and at NCHRP report 350 test Level 4. Viner uses accident data to evaluate rollovers in ran-off-road crashes. Mak et al. present results of a study to determine appropriate and cost-beneficial clear zones along suburban high-speed arterial highways.

Mastandrea et al. describe a comprehensive automated infrastructure inventory and management system. Ksaibati et al. summarize the findings of a study of national trends in the effectiveness of scenic loop tours.

The final eight papers in this volume are related by their examination of the role that roadway geometry plays in traffic operations and accidents.

Turning Vehicle Simulation: Interactive Computer-Aided Design and Drafting Application

MILTON S. E. CARRASCO

The use of computer-aided design and drafting (CADD) systems in transportation engineering is having a profound effect on the design process being undertaken by the designers of transportation facilities. The spatial requirements and turning capabilities of vehicles are important factors in the design of such facilities. Until now, designers have depended for the most part on the use of plastic turning vehicle templates to guide them in the design process. This paper describes a CADD application that provides an interactive means of simulating turning vehicles and determining their tire and swept paths in a flexible, efficient, and accurate way. As a result vehicle simulation and design development are maintained in the same graphics environment. The paper describes the use of the program and demonstrates its accuracy for design purposes. Several advantages of the program are noted, including the increased efficiency that can result from working in a single CADD environment, the ability to review alternative paths and vehicle types quickly, the ability to work in either metric or English units of measurement, and the ability to analyze the turning maneuvers of vehicles still in the development stage.

The design of a transportation facility such as a roadway intersection or truck terminal is influenced by the turning capability of one or more design vehicles and their swept paths.

Until the late 1970s, most highway design projects were completed "on the drawing board," that is, the designs were generated either manually or through a combination of stand-alone computer programs and manual drafting. The typical design process included the use of plastic turning vehicle templates to determine manually the swept paths of design vehicles. Designers manually placed the plastic templates or other generated plots onto the design to determine the location of appropriate design features such as curbs and gutters, traffic islands, lane widths and lane markings, pavement edges, retaining walls, and other physical features. Several design iterations were typically required before the design could be finalized.

The advent of the personal computer (PC) and computer-aided design and drafting (CADD) software has had a significant impact on the design and drafting procedures in all areas of engineering. These systems allow for an integrated design and drafting process. An interactive program that can simulate vehicle turning maneuvers and operates seamlessly in a CADD environment can enhance the efficiency of the design of transportation facilities and the preparation of design drawings.

In this paper the algorithm that is the basis of the CADD model presented is described. The extension of the basic algorithm for determining tracking and swept paths is also described.

PBK Engineering Ltd., 2150 West Broadway, Vancouver, British Columbia, V6Y 1J5 Canada.

Finally, a model known as AutoTURN, which is based on the principles and algorithms described above, is described. An overview of the model's operation is described demonstrating its flexibility and ease of use. Output from the CADD program is compared with other methods including turning templates, analytical methods, and field measurements.

EXISTING SIMULATION PROGRAMS

Despite the various mathematical and graphical methods that have been developed over the years, only a few computer programs have been developed in North America to simulate vehicle offtracking and swept paths. The programs are all based on the "constant pursuit method" (also known as the "incremental method of analysis" or "bicycle" model) and, as such, are kinematic models.

A program developed by Sayers (*1*) of the University of Michigan Transportation Research Institute (UMTRI) is one of the first computer simulations of turning vehicles to be documented. The program uses Cartesian coordinate geometry to calculate a vehicle's position as it traverses a given geometric path and was originally written for the Apple II computer. It provides a relatively quick way to produce swept paths for most vehicle combinations. The developers of the program note, however, that a major disadvantage of the program is the long execution time (from several minutes to about 20 mins) to produce plots of the desired path.

Fong and Chenu (*2*) have adapted the simulation portion of the UMTRI program and have developed a mainframe version of the program (known as "TOM"), which is being used at the California Department of Transportation (Caltrans) to improve the processing speed and plot quality. A major advantage of TOM (and by association, the UMTRI program) over other methods described previously is its flexibility in path and vehicle inputs. Virtually any simple and compound circular curves can be used as the vehicle path, and virtually any vehicle type and tractor-trailer combination can be modeled.

The Ministry of Transportation and Highways of British Columbia (*3*) has developed a PC DOS-based program known as "TRACKER," which is similar to TOM but has an added advantage in that the program output can be exported in DXF format to CADD software such as AutoCAD or MicroStation.

A major disadvantage of these computer programs is that they do not work in an interactive manner. As a result the designer must complete a simulation by inputting detailed vehicle path geometry on a separate computer or outside the CADD platform, then import the output into CADD or manually check the design.

To overcome this disadvantage an interactive turning vehicle simulation program that works directly within the CADD environment is required. Such a program must allow the designer to work directly within the design base (i.e., the drawing file), input a steering path, select or define the design vehicle's dimensions, and determine its swept path. The resulting output will allow the designer to evaluate or set design details, such as edge of pavement and traffic islands, and prepare detailed drawings all within the same working environment—the CADD environment.

In the following section the principles on which the CADD model presented in this paper is based are discussed. The term swept path refers to the aerial space between the outer and inner extremities of a vehicle, which may consist of vehicle units that are significantly wider than the axle widths. The term tracking path represents the path resulting from the tracing of the outer tire walls of outermost tires of a vehicle's steering and rear axles (or the geometric center of the rear axle group in the case of a multiaxle rear bogey).

CADD-BASED MODEL

The CADD model in this paper utilizes an algorithm based on the graphical method developed by Vaughan and Sims (*4*) and on Sayers' (*1*) model, that is, the incremental method of analysis or the constant pursuit method. The algorithm consists essentially of an analytical means of duplicating the operation of the tractrix integrator, and uses CADD routines to simplify input for analysis and to facilitate plotting of the desired vehicle paths. A geometry-based approach was selected because tire mechanics, in most practical situations, do not significantly affect offtracking.

Figure 1 (*a*) and (*b*) illustrate the basis of the algorithm as it applies to a single-unit vehicle and a multiple-unit vehicle, respectively. These vehicle units are represented by a "bicycle" model, with multiple axles represented by the geometric center of the axle group.

In coordinate geometry terms, the analysis for a single-unit vehicle reduces to the solution of the following equations to obtain the coordinates of the center of the rear axle:

$$x_{i2} = (x_{i1} - x_{(i-1)2})/[(1_{i(i-1)} - 1_{wb})/(1_{i(i-1)})] + x_{(i-1)2} \quad (1)$$

$$y_{i2} = (y_{i1} - y_{(i-1)2})/[(1_{i(i-1)} - 1_{wb})/(1_{i(i-1)})] + y_{(i-1)2} \quad (2)$$

where

i = the incremental location for which
1 = the geometric center of the front axle or towing point,

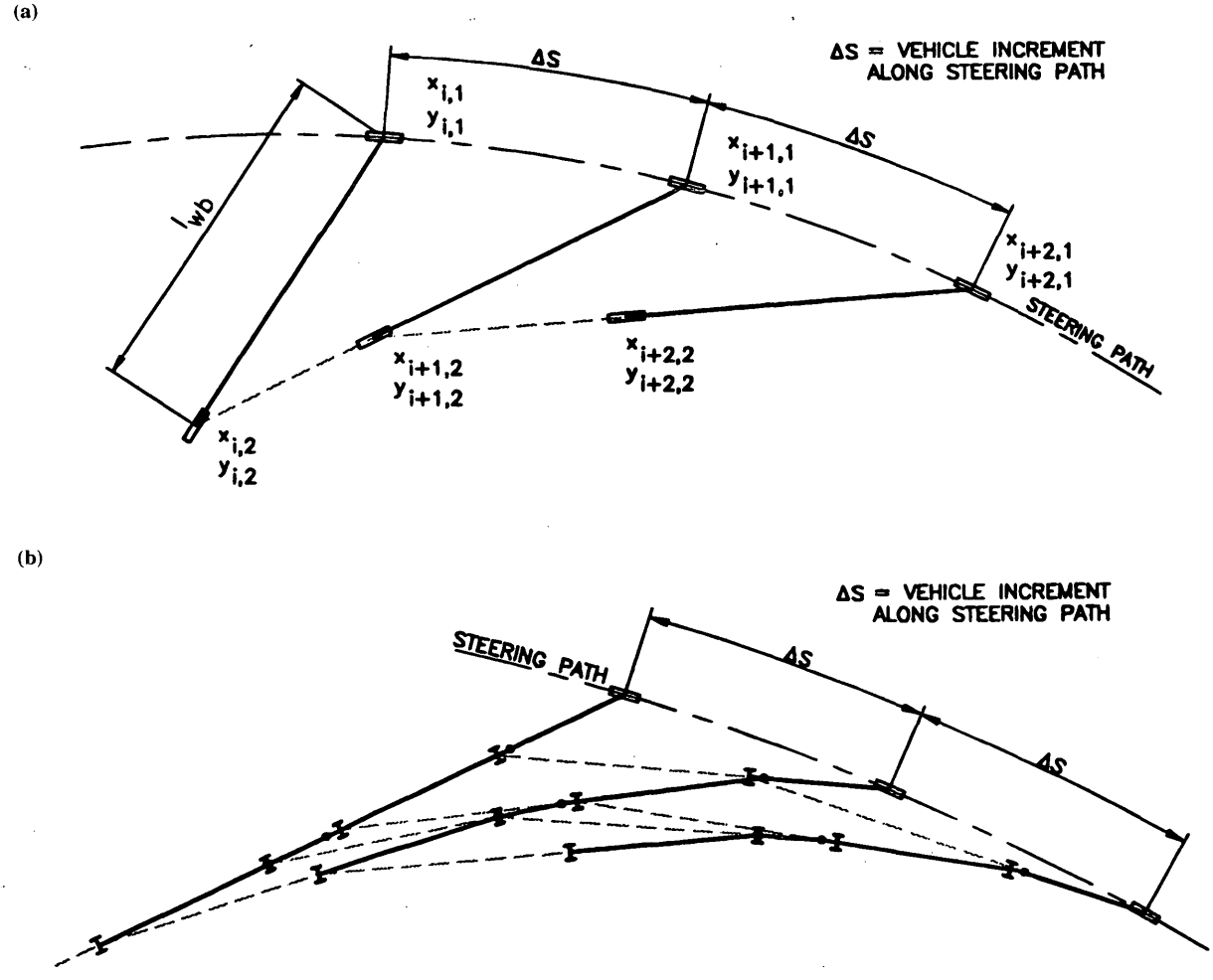

FIGURE 1 Application of algorithm to (*a*) single-unit vehicles and (*b*) multiple-unit vehicles (tractor semitrailer plus fulltrailer).

2 = the geometric center of the rear axle,

$l_{i(i-1)} = [(x_{i1} - x_{(i-1)2})^2 + (y_{i1} - y_{(i-1)2})^2]^{1/2}$
and is the distance from the steering or towing point at the ith location to the rear axle at the $(i - 1)$th location, and

l_{wb} = simple wheelbase of vehicle unit.

Derivation of this and other key equations pertaining to the CADD model is presented elsewhere (*5*).

The incremental position of the steering or towing point is set at a fixed distance equal to some small number relative to real-world vehicle and turning dimensions. In this model the incremental distance is set at 1/100th of a vehicle width, equaling about 25 mm. This incremental distance is selected because it represents the point at which smaller increments provide no appreciable change in offtracking values. Through coordinate geometry calculations, the coordinates of the incremental points and the rear axle point are obtained by solving Equations 1 and 2.

The same principle can be used for a vehicle consisting of several units, because there will always be two similar equations to solve to obtain the rear axle coordinates. Towing points such as a fifth wheel or a hinge point can be obtained once the position of the towing vehicle has been determined.

Application of Algorithm to Tracking and Swept Paths

The algorithm applies to the bicycle model concept and, in this configuration, is only good for obtaining offtracking values for a particular vehicle. For the model to be useful in determining tracking and swept paths, it must be enhanced. The bicycle model is used because it has been found to be reasonably accurate for design purposes, and it simplifies the analysis of the tracking and swept paths. Consequently it provides a shorter execution time. The following sections describe the process used to determine vehicle tracking paths and vehicle swept paths.

Determination of Vehicle Tracking Path

Figure 2 illustrates the concept used to develop the vehicle tracking path from the base bicycle model. The following briefly describes the step-by-step process that is built into the model.

1. For each incremental step, after the new bicycle position has been determined, the axle configurations of the vehicle in its new position are located using the vehicle body and axle dimensions.
2. The coordinates of the outer extremities of the axles are then calculated based on the axle width and are stored in a data base.
3. These calculations are repeated for each incremental step producing coordinates for the outer edges of the tires of the first and the last axles (or geometric center of the axle groups) of the vehicle. The data are stored in the data base until the analysis of the entire path is complete.
4. The coordinates of the stored tracking path points are then plotted and lines are drawn connecting the points. In this manner complex curves representing the path of the steering and the rearmost axles are plotted. These curves represent the tracking path of the vehicle.

Determination of Vehicle Swept Path

Using the basic bicycle model to determine the swept path of a vehicle requires a slightly different approach. Figure 3 illustrates the method used in this model and the following describes the procedure that is incorporated in the model for developing the swept path:

1. As in the development of tracking paths, coordinates for the body of the vehicle are calculated for each incremental step. The term "body" includes any oversize loads that may be carried on the vehicle.
2. Screen lines are established along the travel path at close intervals (the model uses an interval of 1/10 of the vehicle width—

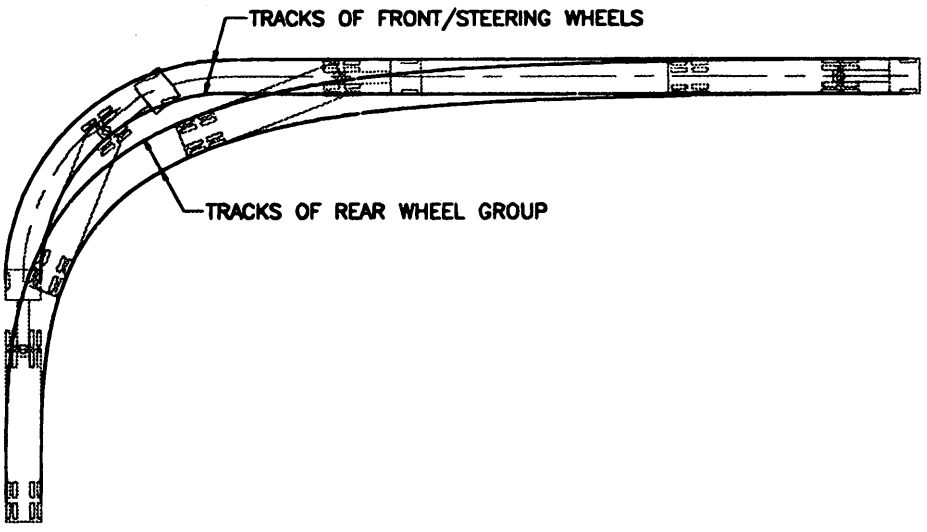

FIGURE 2 Vehicle tracking path.

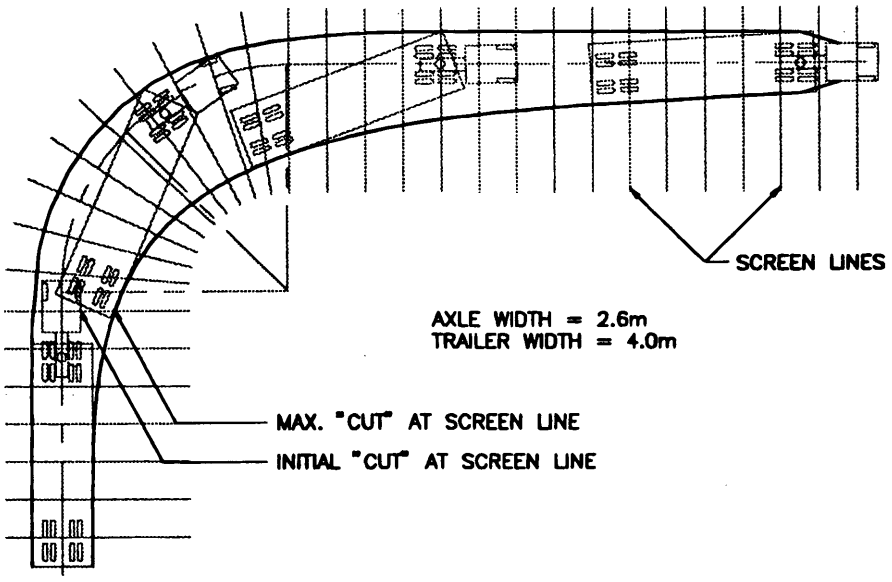

FIGURE 3 Vehicle swept path model.

approximately 250-mm intervals). The screen lines are typically set normal to the travel path.

3. As the vehicle crosses the screen lines with each incremental calculation, the coordinates at the intersection of the vehicle body with the screen line are calculated and stored. As the vehicle progresses along the travel path with each successive increment, the position of the extremities of the vehicle at each of the screen lines is compared with the previous vehicle position. In the process the maximum cut is determined and stored into a data base.

4. The coordinates of the maximum cut at each screen line are then plotted and a curve is drawn between the points to obtain the swept path of the vehicle.

Incorporating Vehicle Turning Limitations

This model and the tracking and swept path enhancements by themselves are insufficient to simulate fully "real world" turning conditions. Because the CADD model is essentially a kinematic model, the only way to incorporate the effects of turn limitation is through empirical means. Field tests were conducted using a tractor with a semitrailer to verify model results and to obtain an understanding of turn limitations.

Field tests showed that in a tight cornering situation, with steering wheels at their maximum turn position, a tractor with a semitrailer reaches a position where side frictional forces acting on the rear tandem axles become so large that the vehicle cannot proceed any further. Field measurements for the test vehicle showed the maximum steering angle to be approximately 27 degrees and the angle between the tractor and the semitrailer, under tight turn conditions, to be approximately 76 degrees.

A review of vehicle specifications of newer tractors shows that the maximum steering angle has steadily increased from previous values of 27 degrees to 30 degrees to values of as much as 40 degrees, making it possible for the new vehicles to negotiate sharper radii turns than older tractors.

With each incremental step in the CADD model, the steering angle and tractor-to-trailer or trailer-to-trailer angle (for multitrailer-unit vehicles) is calculated using the vehicle and path dimensions provided. The calculated values can then be compared with the limitations of the specified vehicle. If the calculated values exceed the specified turn limitations, it is possible to flag such an occurrence, warning the user of a problem with the simulation.

AUTOTURN—A CADD APPLICATION FOR SIMULATING TURNING VEHICLES

This section describes a working CADD model, known as AutoTURN, that is based on the model algorithm described previously. Enhancements pertaining to the determination of tracking and swept paths have also been included in this CADD model. The AutoTURN program is a CADD-based program and is written in the C programming language. It is a menu-driven graphics program that operates on a Cartesian coordinate system. This capability makes it ideal for undertaking the design and drafting of transportation facilities, because the determination of tracking and swept paths is an important element in setting or evaluating the design of such facilities. In turn, relating these parameters to the real world involves establishing coordinates of the design geometry utilizing either a local or universal system of coordinates and elevation data. CADD is an ideal environment for completing coordinate geometry calculations and for preparing design drawings to exact coordinates. As a result it permits total automation of the design and drafting process.

AutoTURN allows the user to establish a vehicle's turn requirements or check a vehicle's turning maneuver, and to finalize design and produce final drawings in a single working environment. This advantage is further enhanced by its interactive capability, whereby the user can quickly refine or review other alignments and compare the paths of other vehicles. The program will trace the path of specific points on the vehicle as it traverses a defined path and can even be used to determine turning needs of vehicles in the development stage.

Program Logic

The logic of the program as it applies within an AutoCAD environment is illustrated in Figure 4. Data entry, execution, and output are achieved through three distinct processes.

Data is entered via the CADD environment. Vehicle dimensions and the steering path are input by simply editing predefined vehicle dimensions and selecting predefined path entities. After being entered, data files are prepared for use in the execution phase.

Execution of the program is undertaken using C language to perform the coordinate geometry calculations; coordinates are calculated for the incremental points on the steering path and for the vehicle's axle and tire points. The resulting coordinates are then written to a Path.dxb file. The Path.dxb file is the data base file that is imported into CADD for drawing preparation.

CADD software provides a suitable environment in which not only is the data entry considerably simplified, but also the user is allowed to receive directly plots of the resulting paths. Program execution typically takes between 15 and 30 sec (using a 486 PC) from the time selection of vehicle and path configuration is completed to the time an "on-screen" plot of the desired path is produced.

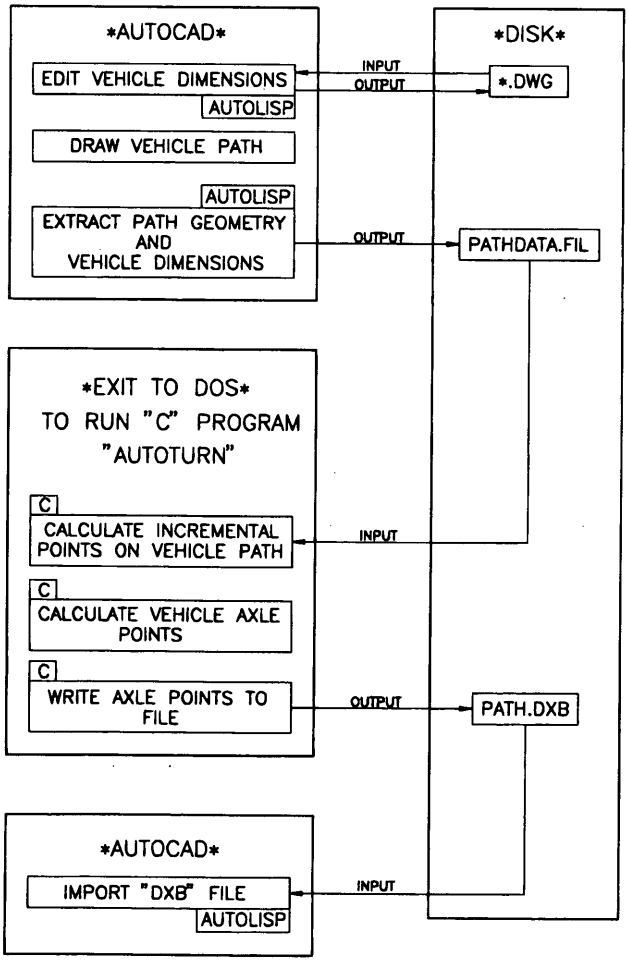

FIGURE 4 Program logic.

Ease of Use

The purpose of this section is to illustrate the ease of using the program. Figure 5 provides an overview of the steps involved, and a service road access design, shown in Figure 6(*a*), is used to demonstrate a practical application of the program. AutoTURN will be used to evaluate the design for accommodation of a WB-12 standard Road and Transportation Association of Canada (*6*) design vehicle, which is equivalent to a WB-40 AASHTO (*7*) design vehicle.

Step 1—Select Design Base

The designer selects the design base in AutoCAD. This may involve a drawing showing the layout of a proposed or existing facility such as a roadway intersection, parking lot, or a transit terminal. In the case of frontage road, the design base consists of the road layout prepared using AutoCAD.

Step 2—Draw Vehicle Path

The program requires as input the vehicle's steering path, which is the path to be followed by the center of the front axle of the vehicle. In the case of a roadway this path will typically be the centerline of the lane (Figure 6) and consists of a contiguous series of line and arc entities. Setting the steering path generally requires a knowledge of the start and end positions of the vehicle. Two vehicle paths, the major and minor left turns, will be tested in the example.

Step 3—Load AutoTURN

After the drawing containing the steering path is loaded into AutoCAD, the AutoTURN program is loaded by selecting the Load AutoTURN command from the AutoTURN pull-down menu.

Step 4—Set Configuration Menu

The next step is to set simulation parameters using the configuration menu of the program. This menu contains parameters relating to the type of vehicle being studied, the vehicle's start position, the type of simulation (i.e., tracking or swept path), the type of output files desired, drawing layering, and dimension units desired. The first three parameters affect the simulation output, and hence the design. The remaining parameters aid the drawing preparation process.

Step 5—Run Simulation

After the configuration menu parameters have been selected, the program is executed by selecting the Run Simulation option from the pull-down menu. The user is then prompted to select the steering path entities in the order and direction of travel.

Step 6—Evaluate Vehicle Path

Once the drawing of the required vehicle path is produced, the proposed steering path can be evaluated against available maneuvering

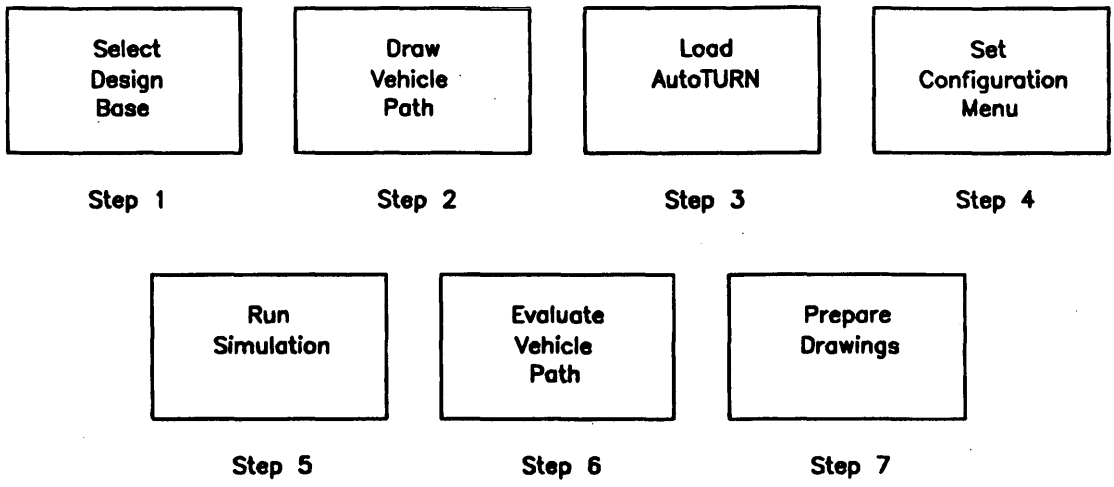

FIGURE 5 Program use.

space, taking into account conflicts with curbs, utility poles, buildings, or structural elements. If conflicts occur, the user can modify the path, if feasible, or consider the possibility of relocating the conflicting elements so that they lie outside the vehicle's swept path. Figure 6*b* shows the resulting swept paths for the vehicle paths selected. The design appears to accommodate the WB-12 design vehicle adequately except for the service road curb return radius. The adjusted radius is set using AutoCAD and is shown by a broken line.

Step 7—Prepare Drawings

Design details and drawings can be completed without leaving the AutoCAD graphics environment once an acceptable swept path and alignment has been obtained.

Program Validation

Validation of the AutoTURN outputs was undertaken through comparison with several offtracking methods and turning templates, as well as with field measurements. The following comparisons were made:

1. AASHTO templates;
2. Caltran's offtracking software (TOM);
3. Jindra's (*8*) and Woodroofe's (*9*) equations;
4. Jensen's (*10*) tire mechanics model; and
5. Field measurements.

AASHTO's turning templates and Caltran's TOM program are both used for design purposes. AutoTURN outputs matched AASHTO templates well with no noticeable differences in the swept paths. TOM and AutoTURN produced identical tire tracking outputs. Fong and Chenu (*2*) note that the results from TOM were found to be accurate to within 2 percent when compared with field measurements.

Jindra's (*8*) and Woodroofe's (*9*) equations are numerical approximations for estimating transient and steady-state values of offtracking. In addition the equations use an equivalent wheelbase to represent articulated vehicles. A comparison of the results of the equations with the outputs from AutoTURN is illustrated in Figure 7. The comparison shows that Jindra's (*8*) equations and AutoTURN produce results similar to within 14 percent when actual vehicle dimensions are used in the AutoTURN program. Results from Woodroofe's (*9*) equations match AutoTURN output (based on actual vehicle dimensions) to within 8 percent. Neither of these comparisons can be considered conclusive evidence of the absolute accuracy of the AutoTURN program, because the author is not aware of the level of validation of these equations with field measurement or the extent of any such testing.

Comparison with Jensen's (*10*) tire mechanics model (Figure 8) shows that offtracking values generated by AutoTURN agree to within 6 percent; the AutoTURN results tending to be larger in value and therefore more conservative.

Of these methods, only conducting field measurements provides a measure of the absolute accuracy of the AutoTURN program. All of the other methods provide a measure of the relative accuracy of the program. Unfortunately, not only are extensive field measurements impractical but conducting field measurements requires considerable planning and careful execution to obtain valid measurements, as Morrison (*11*) noted. In a field test conducted by the author, AutoTURN produced results accurate to within 3.5 percent of the maximum offtracking width, with a maximum difference of 165 mm (Figure 9).

Discussion

A factor that must be considered in determining an acceptable degree of accuracy for the program is the design consideration in accommodating vehicle turning maneuvers. The designer of transportation facilities, in particular, highways, must be considerate of the skills and abilities of the drivers and vehicle types and configurations that will use those facilities. To account for these conditions, good design practice suggests allowing for a forgiving clearance on either side of the swept path. The author suggests that a forgiving clearance of a minimum of 0.6 m on each side of a vehicle's actual swept path (for a total widening of 1.2 m) be provided to establish the minimum travel path for the design turn. In absolute terms, the

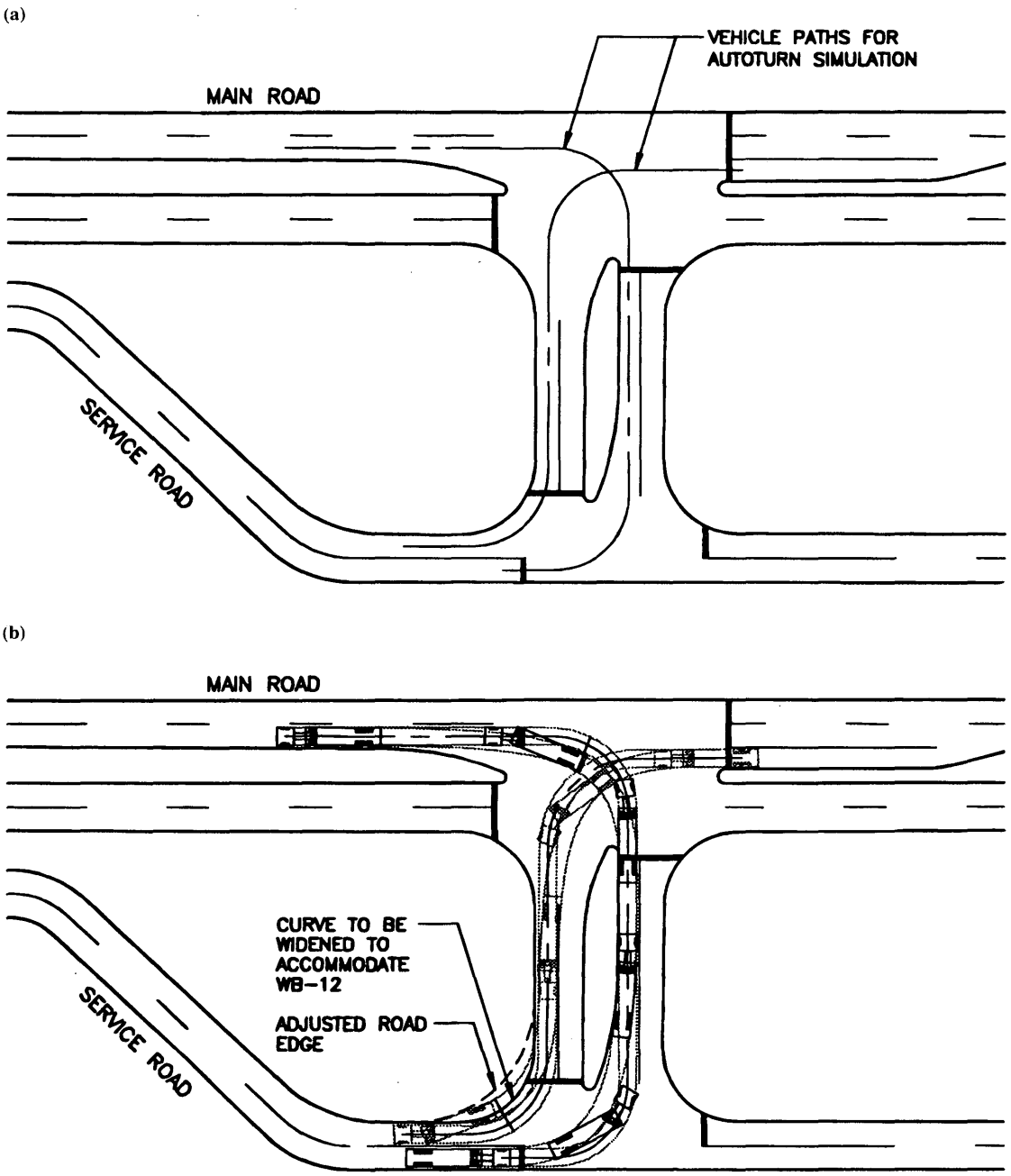

FIGURE 6 Service road access (*a*) base design and (*b*) base design with AutoTURN run.

author suggests that the calculated path widths should not encroach into this forgiving space by more than 25 percent. The CADD model described here appears to provide an accuracy that is well within this suggested limit.

Jensen's research (*10*), however, shows that there are potential limitations in using a kinematic model such as AutoTURN to simulate nonstandard vehicles, for example, those having multiple, widely spaced fixed-axle bogeys with short wheelbases, steerable or freely castering rear bogeys, or other vehicle or axle configuration in which frictional effects on the wheels can have a significant effect on offtracking dimensions. The program is also unable to model slippery or icy pavement surfaces, which can affect offtracking. A further limitation of the program is the effect of vehicle speed and the resulting centrifugal forces that act on a high-speed turning vehicle. This effect tends to produce lower offtracking values than lower speed maneuvers.

CONCLUSIONS

The AutoTURN program, which is based on the CADD model discussed in this paper, is an interactive CADD application that provides the designer with an alternative means of simulating turning vehicles. The advantages of this program include the following:

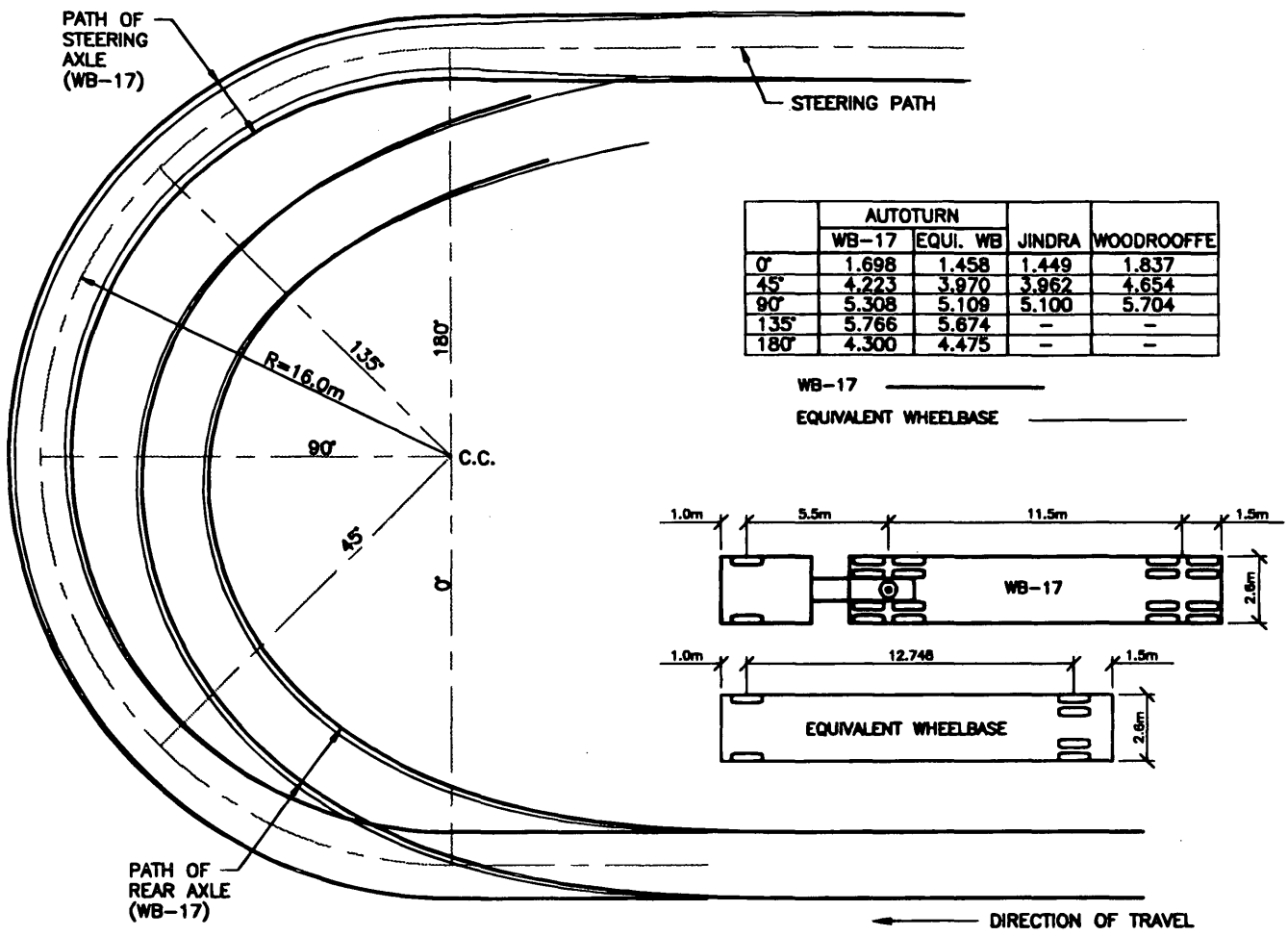

	AUTOTURN		JINDRA	WOODROOFFE
	WB-17	EQUI. WB		
0°	1.698	1.458	1.449	1.837
45°	4.223	3.970	3.962	4.654
90°	5.308	5.109	5.100	5.704
135°	5.766	5.674	–	–
180°	4.300	4.475	–	–

FIGURE 7 AutoTURN versus Jindra's (*8*) and Woodroofe's (*9*) calculations.

1. By operating directly within a CADD environment, it eliminates the need for importing simulation plots generated externally as most other programs do, and it eliminates the need for manual verification of vehicle swept paths.
2. The program enhances the automation capability of CADD in that it works directly within the design base (i.e., design drawings), produces vehicle paths that can be evaluated, and allows changes to be made to the design as required.
3. It can be used to simulate virtually any vehicle type with nonstandard dimensions.
4. It can be used to evaluate the turning maneuvers of vehicles still in the development phase.
5. Unlike turning templates, which are generally provided for a single radius of turn, AutoTURN can simulate any steering path geometry consisting of circular curves and tangent sections.
6. It is easy to operate and produces outputs relatively quickly.
7. It can determine both tracking and swept paths.
8. The program can identify maneuvers in which turn limitations are likely to be exceeded.
9. It can operate with any unit of measurement, that is, English or metric.

The AutoTURN program has been validated through comparisons with other methods of analysis, computer programs, and field measurements. The comparisons show that offtracking values generated by AutoTURN agree to within 6 percent with similar values generated by Jensen's (*10*) tire mechanics model, with the AutoTURN results tending to be larger in value. In absolute terms the maximum difference is approximately 200 mm. AutoTURN results also compare well against field measurements, producing a maximum error of 165 mm or 3.5 percent of offtracking values.

These comparisons and comparisons with other commonly used design methods confirm the acceptability of AutoTURN as a design tool for establishing vehicle tracking and swept paths for the design of roadways and other transportation facilities.

Although the program appears to produce acceptable results for most standard vehicle types, further research is required to establish its suitability or limitations when simulating certain nonstandard vehicles.

RECOMMENDATIONS

As noted above, a CADD model such as the AutoTURN program clearly has several advantages when compared with other non-CADD programs or any other methods that currently exist. The program can be improved further if the following features can be included:

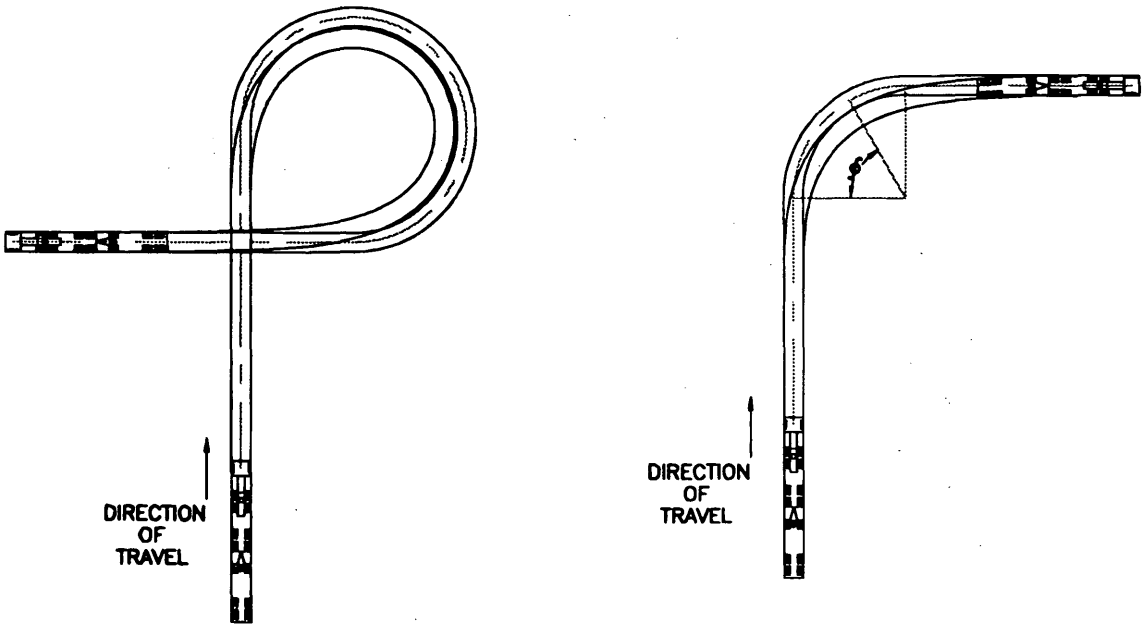

BASED ON A–TRAIN WITH 3.0m TRACKWIDTH

	STEADY–STATE TURN				90° DEGREE TURN		
	SAE MODEL	SIMPLE MODEL	JENSEN'S MODEL	AUTOTURN	JENSEN'S MODEL	AUTOTURN	∮
A–TRAIN	–	–	3.063	2.919	2.651	2.566	60°
C–TRAIN (FIXED AXLE)	2.295	3.120	3.161	3.300	2.795	2.820	60°
C–TRAIN (FREE AXLE)	1.637	2.234	3.336	3.437	2.207	2.340	65°

NOTES:

1. OFFTRACKING VALUES SHOWN IN METRES. ∮ REPRESENTS APPROXIMATE LOCATION OF MAX. OFFTRACKING.
2. SAE AND SIMPLE MODEL OFFTRACKING VALUES OBTAINED FROM JENSEN'S THESIS
3. JENSEN'S VALUES BASED ON DRY ROAD CONDITIONS
4. JENSEN REFERS TO C–TRAIN CONFIGURATION AS B–DOLLY

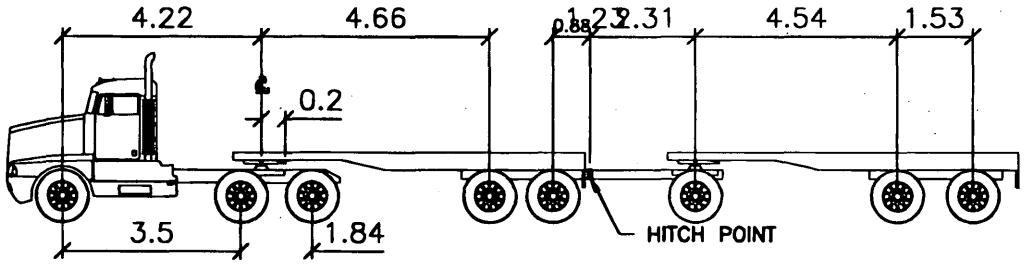

FIGURE 8 AutoTURN versus Jensen's model (*10*).

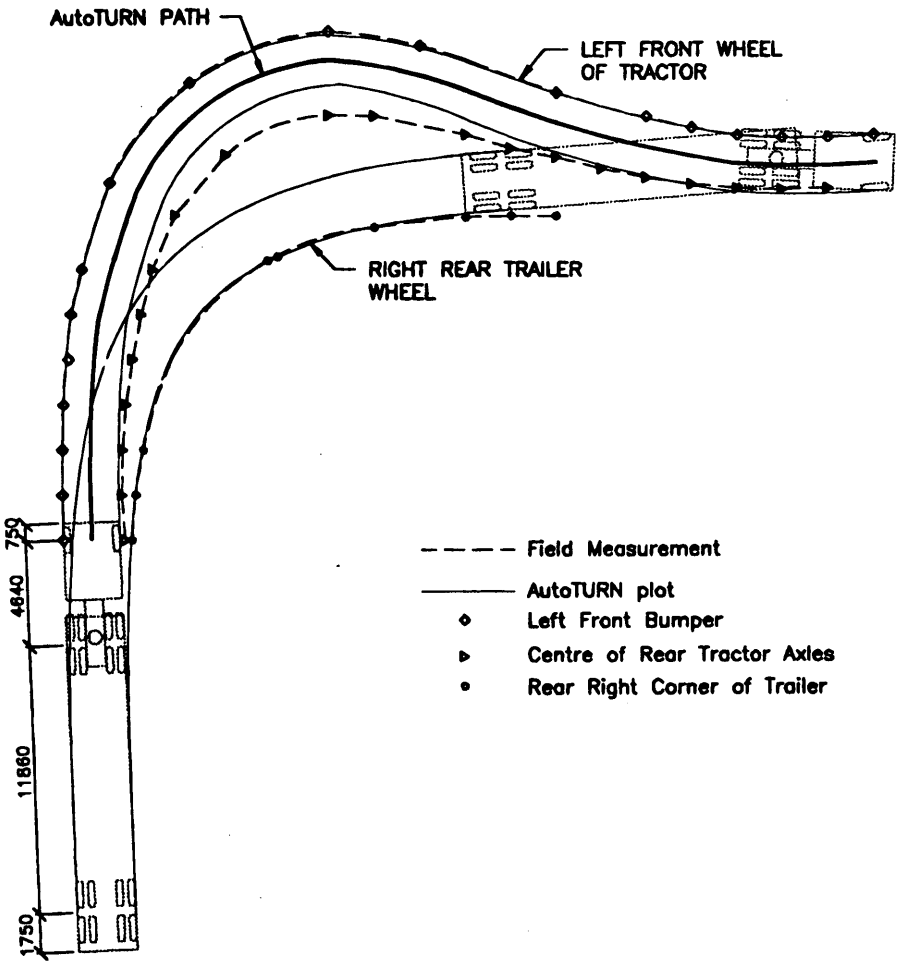

FIGURE 9 AutoTurn versus field measurements.

1. The effects of tire mechanics;
2. Reverse maneuvers of articulated vehicles;
3. Simulation of other types of vehicles such as aircrafts, trains, street cars and light rail transit, and trolley buses;
4. Steerable or freely castering rear bogeys; and
5. Interactive user-controlled steering simulations.

It is recommended that further research and development be undertaken to develop a program that includes these enhancements to make a more complete and versatile turning vehicle simulation program.

ACKNOWLEDGEMENTS

The author wishes to acknowledge Dr. John Morrall of the University of Calgary for his encouragement and support in undertaking this project. A very special note of appreciation is extended to Tim Evans, whose programming skills resulted in the development of the AutoTURN program. The assistance of Canadian Freightways Ltd., which provided the vehicle, driver, and facilities for conducting field tests, is also acknowledged.

REFERENCES

1. Sayers, M. W. The University of Michigan Transportation Research Institute. Vehicle Offtracking Models. In *Transportation Research Record 1054,* TRB, National Research Council, Washington, D.C., 1985.
2. Fong, K. T., and D. C. Chenu. *Simulation of Truck Turns with a Computer Model.* Report 86-1. Division of Transportation Planning, California Department of Transportation, Jan. 1986.
3. Garlick, G., D. N. Kanga, and G. G. Miller. TRACKER: A Program to Generate Vehicle Offtracking Templates. *Compendium of Technical Papers,* ITE District 7—1991 Annual Conference, Victoria, British Columbia, Canada, Vol. II, pp. 283–302.
4. Vaughan, R. G., and A. G. Sims. *Determination of Swept Paths of Vehicles.* Traffic Accident Research Unit, Department of Motor Transport, New South Wales, Australia, July 1970.
5. Carrasco, M. S. E. *Computerized Vehicle-Turning Simulation—An Interactive Application.* M. E. Thesis. University of Calgary, Alberta, 1992.

6. *Manual of Geometric Design Standards for Canadian Roads, 1986 Metric Edition.* Road and Transportation Association of Canada, Ottawa, Canada, 1986.
7. *A Policy on Geometric Design of Highways and Streets.* AASHTO, Washington, D.C., 1990.
8. Jindra, F. Offtracking of Tractor-Trailer Combinations. *Automotive Engineer,* Vol. 53, March 1966, pp. 96–101.
9. Woodroofe, J. H. F., C. A. M. Smith, and L. E. Morisset. A Generalized Solution of Non-Steady State Vehicle Offtracking in Constant Radius Curves. *SAE Technical Paper Series,* Truck and Bus Meeting and Exposition, Chicago, Illinois, Dec. 1985.
10. Jensen, L. G. A Mathematical Model for the Low-Speed Offtracking of Articulated Vehicles That Includes Tire Mechanics. M. S. Thesis, University of Calgary, Oct. 1987.
11. Morrison, W. R. B. A Swept Path Model Which Includes Tyre Mechanics. *Australian Road Research Board Proceedings,* Vol. 6, Part 1, 1972.

Publication of this paper sponsored by Committee on Geometric Design.

Geographic Information System Applications in the Heart of Illinois Highway Feasibility Study

ISABEL CAÑETE MEDINA AND KAREN B. KAHL

Local governments and businesses in central Illinois believe that a new highway connection between the metropolitan areas of Peoria and Chicago will shorten travel times and foster economic development. A geographic information system (GIS) that was used to determine the feasibility of alternative corridors being considered for an improved highway within the 10-county, 7,700-km^2 (3,000 mi^2) study area is discussed. The development of the GIS required the compilation and integration of large amounts of geographic and environmental data. The data base was developed using a personal computer based GIS. Overlay analysis was used to map environmentally sensitive areas and possible engineering constraints. Previously developed corridor alternatives were entered into the GIS, and their locations and alignment designs were adjusted to avoid major engineering obstacles and environmental impacts. After the corridor locations were finalized, the GIS was used in the alternatives evaluation to assess the effects of the proposed corridors.

Geographic information systems (GIS) in transportation have been widely used in such applications as travel demand modeling, traffic forecasting, intelligent vehicle highway systems and traffic management systems, and road management systems, including highway facilities inventory and pavement data management. However, only recently have the capabilities of GIS been explored for highway planning and route location studies.

A GIS was developed for the Heart of Illinois Highway Feasibility Study to serve as a decision support tool in determining suitable corridor locations and in evaluating their potential impacts. The GIS was used to (*a*) inventory the location and feature descriptions of known environmental resources, (*b*) revise and adjust corridor alignment, and (*c*) evaluate corridor impacts. In addition, the GIS was used for address-matching of origin-and-destination (O-D) data and for map and report production.

PROJECT BACKGROUND

Support for a direct highway connection between Peoria and Chicago has continued to grow among business and government leaders in north central Illinois. The Heart of Illinois Highway Feasibility Study was conducted to examine potential corridor locations for a new freeway or expressway between the two metropolitan areas. The feasibility of corridor alternatives was based on engineering, environmental, and economic considerations.

I. C. Medina, CM Technologies, 1034 Asbury Avenue, Evanston, Ill. 60202. K. B. Kahl, CH2M Hill, 411 E. Wisconsin, Suite 1600, Milwaukee, Wis. 53202.

The Heart of Illinois Highway Feasibility Study began in May 1993 and is scheduled for completion in the spring of 1995. The project is funded by the Illinois Department of Transportation (IDOT) and the FHWA. The study area covers more than 7,700 km^2 (3,000 mi^2) encompassing rural and metropolitan areas within 10 counties, as well as scenic and environmentally sensitive regions along the Illinois River. More than 1,000 km (620 mi) of corridor alternatives (80 segments) were developed from previous studies and reports, field reconnaissance, and extensive input by members of the Study Advisory Group and the community (Figure 1). Because of the large project area, the corridor alternatives were divided into three bands representing directions of travel: north, northeast, and east.

After the identification of alternatives, the corridors within each study band were evaluated using a three-step screening process in which each level of screening increased in detail. The initial screening eliminated alternatives that clearly did not merit further analysis. The criteria used in the elimination process included: redundancy because of an existing freeway, adverse travel conditions discontinuity or overlap, and diagonal severance of agricultural land. The second step was a preliminary screening of several groups of corridor alternatives, which would provide essentially the same traffic service over slightly different routes. The corridors were evaluated and one alternative in each group was selected for inclusion in the more detailed screening. The third step involved the evaluation of the remaining corridors based on transportation cost, planning and accessibility, and environmental factors to select one or more corridors for each study band. After the three-step screening process, the "finalist" corridors were then the subject of more detailed engineering, environmental, and economic analyses. The GIS was used in the assessment of corridor alternatives in the preliminary and detailed screening steps.

DATA BASE DEVELOPMENT

Hardware and Software

The GIS was implemented using a personal computer (PC)-based system. The computer hardware included a 486 DX/66 MHz work station with 8 megabytes of extended memory and 350 megabytes of disk storage. A Summagraphics 30.48 × 45.72cm (12-in. × 18-in.) digitizing tablet was used for data input. The software chosen for implementation was Atlas GIS, version 2.1, by Strategic Mapping, Inc. (Palo Alto, Calif.). An import and export utility from the same company was used in translating existing GIS data bases such as TIGER/Line and Arc/Info files into Atlas GIS format. The

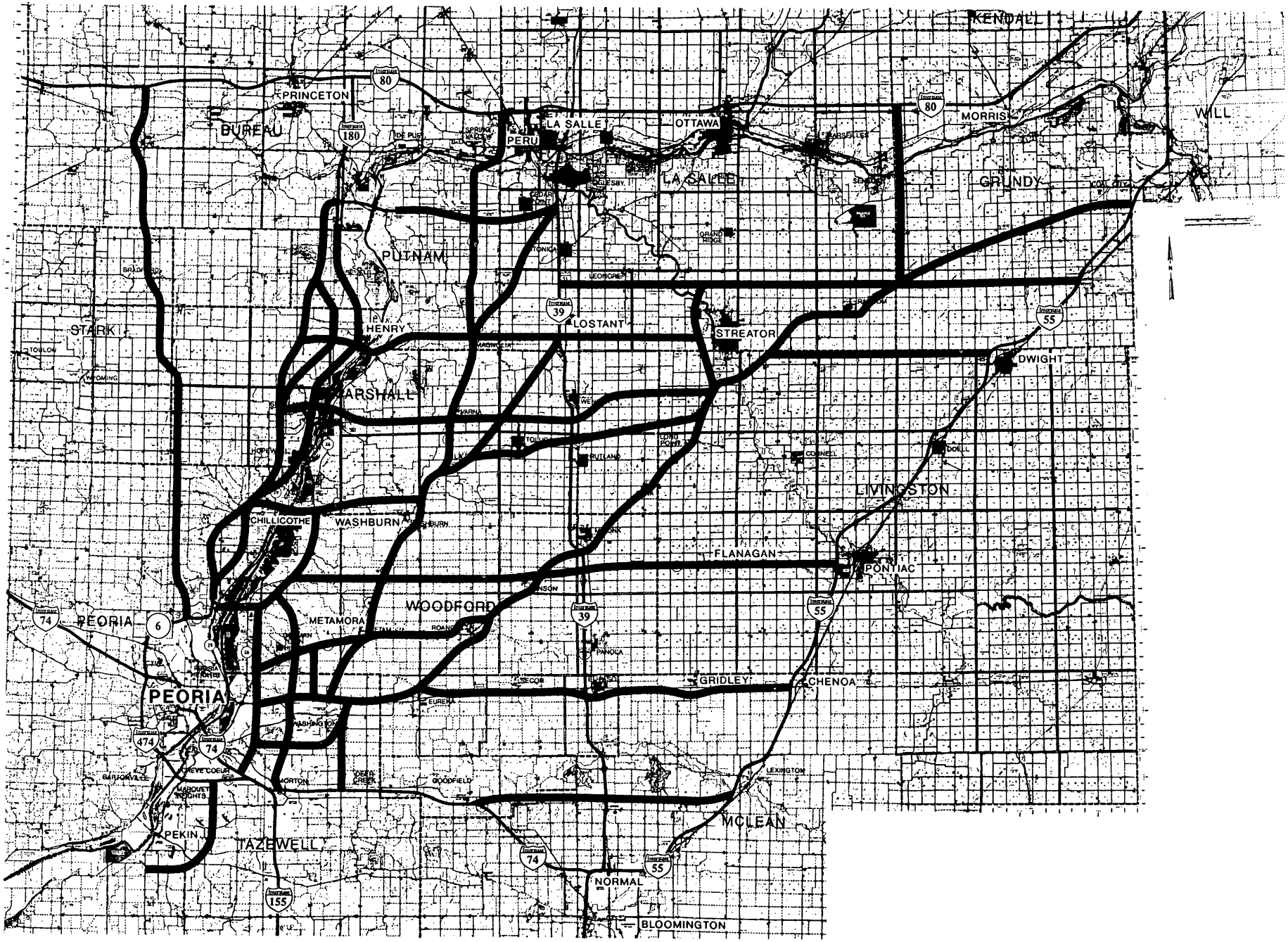

FIGURE 1 Preliminary corridor alternatives.

Excel spreadsheet program was also used for entering data base information such as street addresses, which were later imported into Atlas GIS.

Data Sources

The sources of information for the GIS data base are shown in Table 1. The data were available in both digital (computer file) and analog (printed map) formats and were provided in various scales and map projections. The geographic and environmental features were originally compiled using latitude-longitude coordinates. The geographic data were later projected to Universal Transverse Mercator, Zone 16 (UTM-16) coordinates.

Data Integration

The compilation and integration of data for such a large study area involved considerable work, with an enormous amount of data entered into the GIS. The base map for the data base was developed from TIGER/Line files translated to Atlas GIS format. GIS data bases from state agencies also were imported into Atlas GIS. Problems occasionally occurred in file translation, requiring manual edits of imported data. After the base map was completed, other types of geographic data were entered into the system. The most common problem encountered during data input was discrepancies with map information provided by different sources (e.g., United States Geological Survey maps versus county plat books). Researchers had to decide which sources provided the most accurate information for various types of geographic data. Information also was updated based on the most recent aerial photographs and field reconnaissance. Wetlands and flood plain information were not included in the GIS because the data were too detailed and extensive.

GEOGRAPHIC INFORMATION SYSTEM APPLICATIONS

The implementation of a GIS for the Heart of Illinois Highway Feasibility Study provided opportunities for developing new techniques in highway planning and route location studies. GIS applications are compared with current practices and methods in the following sections.

Origin-and-Destination Study

An (O-D) study was performed as part of the Heart of Illinois Highway Feasibility Study. The results of the O-D study were used to project travel demand between Peoria and Chicago for the purpose of identifying alternative highway corridors. The data collection for the O-D study used a combination of roadside personal interviews and mail-back questionnaires at 14 sites. The primary data collected from approximately 11,000 motorists included the trip origin and destination by address or nearest cross streets.

The survey processing required developing traffic analysis zone (TAZ) codes for each origin and destination address. The TAZ were based primarily on 1990 census tract boundaries and were delineated in the GIS using tract boundaries from TIGER/Line files. With information from the TIGER/Line data base such as street names and street numbers, the GIS was able to match 75 percent (572 of 747) of the addresses collected on the O-D survey forms to their corresponding TAZ codes. Approximately 6 person hours were required to process the address matches, which were primarily performed on origins and destinations in the Peoria metropolitan area. For the remaining data, the TAZ codes were determined by locating addresses using detailed street maps. The results of the O-D study were used to develop traffic forecasts to compare the costs and benefits of various corridor alternatives.

Environmental Resources Inventory

The base map for the environmental resources inventory consisted of county and municipal boundaries, roadways, railroads, and hydrographic features. Other geographic features were added to the base map using various data sources (see Table 1). The boundaries of some environmental features were digitized using printed maps. Others were available in digital format from state agencies. The location of hazardous waste sites and historic resources was entered into the system by matching their addresses to corresponding map coordinates.

The geographic features considered in the inventory include:

- Archaeological sites
- Cemeteries
- Community facilities
- Other developed areas
- Gas storage areas
- Hazardous waste sites (CERCLIS)
- Historic resources
- Surface and underground mines
- Natural areas and wildlife refuges
- Nature preserves
- Pipelines (gas)
- Power lines (transmission lines)
- Power plants and substations
- Prime farmland
- Protected agricultural lands
- Pumping stations
- Quarries, pits
- Radio towers
- Sewage disposal areas
- Steep slopes
- State parks, conservation areas and recreation areas
- Other public lands and parks
- Park trails
- Threatened and endangered species
- Unique and highly valued aquatic resources
- Woodlands

Each feature was represented as a single layer on the GIS. The layers were combined and overlaid to produce an environmental resources inventory map. The most sensitive land uses are located along the Illinois River and included archaeological sites, developed areas, hazardous waste sites, historic resources, natural areas and nature preserves, public lands and parks, habitats of threatened and endangered species, wooded areas, and steep slopes. The remaining sections of the study area are primarily composed of prime farmland.

The conventional procedure for developing an environmental resources inventory map is to compile the necessary information and manually draw or delineate the features on an aerial photo mosaic or USGS map. Maps of environmental features are usually provided in various scales (Table 1) and have to be manually transformed or translated into the appropriate scale and coordinate system used for the base map. Because of the time and work effort

TABLE 1 Sources of Information

Data/Map Name	Source	Date Compiled	Data Format(1)	Map Scale(2)	Map Projection(3)
TIGER/Line Census Files	Bureau of Census	1990	F	1:100,000	Latitude-Longitude
USGS Topographic Maps	US Geological Survey	1985-1991	M	1:100,000	
				1:24,000	UTM-16
				1,250,000	
County Plat Books	Rockford Map Publishers	1988-1993	M	ns	ns
General Soil Maps	Soil Conservation Service	1972-1993	M	various	ns
Illinois Coal Mines	Illinois State Geological Survey	Jan. 1989	M	1:62,500	UTM
Coal Industry in Illinois	Illinois State Geological Survey	July 1984	M	1:500,000	Lambert Conformal Conic
Biologically Sensitive Areas	Illinois Natural History Survey	1993	F (Arc/Info)	1:52,000	Latitude-Longitude
Illinois Official Highway Map	IL Department of Tansportation	1993	M	1"=12 miles	ns
Official Highway Map	Peoria County	1993	M	1"=1 mile	ns
General Highway Maps	IL Department of Tansportation	1987-1990	M	1"=2 miles	State Plane Coordinate
Archaeological Sites	Illinois State Museum	1993	F	ns	Lambert Conformal Conic
The National Register of Historic Places	Illinois Historic Preservation Agency	1993	D	na	na
Historic Illinois Places	Illinois Historic Preservation Agency		M	ns	ns
A Directory of Illinois Nature Preserves	Illinois Department of Conservation	1991	D;M	ns	ns
Inventory of Public Recreation Lands	Illinois Department of Transportation	1977	D;M	ns	ns
Forest Park Foundation	Forest Park Foundation		M		
Illinois Land Atlas & Gazetteer	Delorme		M		
CERCLIS List	US EPA Superfund Program	1993	D	na	na
Gas Storage Areas	Ancona Gas Company	1993	M	ns	ns
Protected Agricultural Lands	US Dept. of Agriculture	1993	M	ns	ns

(1) F = Computer Files; M = Printed Maps; D = Documents
(2) na = not applicable; ns = not specified
(3)na = not applicable; ns = not specified

involved, not all features are added to the base map. Instead, several maps are compiled and used as references for the engineering and environmental analysis.

With GIS, geographic features can be digitized using their specific map scale and coordinate system and translated into the scale used for the base map. Moreover, a variety of environmental data from state agencies are already available in GIS format, allowing the integration of data in an inventory map. Using GIS, it took two people approximately 4 months to develop the data base. With manual techniques, it may take less time to prepare an inventory because not all environmental features are added to the base map. A GIS map containing a variety of features, however, provides a more comprehensive description or visual representation of the study area.

Location Engineering

The preliminary alternatives for the study represented the broadest range of possible corridor locations and were the starting point for alternatives evaluation. Before screening the alternatives, the GIS was used to revise and adjust corridor locations and alignments.

Preliminary alignments of the corridor alternatives were entered into the GIS and represented more than 1,000 km (620 mi) of potential highway. These initial locations disregarded any impacts to the surrounding areas and were based mostly on the alignment of existing roads and highways. The corridors were plotted as a 1-km (0.62-mi) band on an overlay to the environmental resources inventory map. The corridors were narrowed to a width of 0.5 km (0.31 mi) within the 1-km band, avoiding as much of the major engineering obstacles and environmentally sensitive areas as possible. If a large impact area could not be avoided within the 1-km band, the preliminary alignments were adjusted to reduce or eliminate the impacts. For example, a bypass around a town was relocated from the south side to the north side to avoid a forested area and a new residential development. The corridor alternatives were never narrowed to the width of a highway right-of-way, because the objective of the study was to determine the feasibility of corridors and not to determine the best alignment.

Current methods for adjusting corridor locations involve a process of mapping corridors, assessing impacts, and revising corridors. Often, adjustments made to avoid impacts on one resource result in additional impacts to other resources. Several corridor revisions are usually required to minimize overall impacts.

With a GIS base map, route locations are adjusted and revised not only to avoid impacts on certain resources, but also to reduce overall impacts on the environment and avoid major engineering obstacles. The cumulative effects of corridor impacts can be visually represented when the alternatives are overlaid on an environmental resources map. GIS allows the designer to adjust route locations and at the same time visually assess environmental effects. This process can be performed without the use of GIS as long as a base map is developed containing most, if not all, of the environmental data. The use of a GIS, however, facilitates the integration of information from various sources.

Environmental Impact Assessment

After the corridor locations were finalized, the GIS was used to calculate the impacts of the proposed corridors. Two methods were employed in assessing environmental impacts. The first method used the printed environmental resources inventory map with corridor overlays. The second method utilized GIS analytical operations such as buffering and intersection techniques. Impacts were calculated by counting the number or extent of resources within the 0.5-km (0.31-mi)-wide corridors. Aerial photographs and other more detailed maps (e.g., flood plain and wetlands maps) also were used as references in assessing the effects of the corridor alternatives. Table 2 provides examples of impact calculations.

Existing methods for evaluating impacts involve overlaying corridor alternatives on maps compiled for the environmental analysis. Areas, lengths, and number of sites affected are calculated using a planimeter and a scale. If the environmental data are not contained in one base map, corridor overlays must be prepared for each environmental map to be analyzed, especially if the maps are of different scales. With GIS, the base map contains most of the environmental features to be analyzed, hence requiring only one corridor overlay. Areas, lengths, and number of sites affected can be calculated by the system in one-fourth the time it would take using manual methods.

Maps and Presentation Graphics

For this project, maps were easily generated by the GIS for report production and graphic display purposes. An environmental resources inventory map was produced using a Novajet Inkjet Plotter and printed on photographic bond at a scale of 1:50,000. Maps of corridor alternatives (approximate scale 1:150,000) were also generated using a Versatec Color Plotter and printed on bond paper. The GIS maps were mounted on boards and used as exhibits in public meetings and informational drop-in centers. For report production, 30.48 × 45.72 cm (8-in. × 11-in.) maps were produced using a Hewlett Packard Laserjet printer and a Versatec Color Plotter. Color transparencies of corridor alternatives also were generated for presentations to IDOT officials and the study advisory group.

The GIS was able to produce maps in one-eighth the time it would normally take using manual or other computer graphics methods. This capability is extremely valuable for future studies and evaluations and for presentations of study results to a concerned and perhaps more demanding public when it comes to environmental assessments.

Costs and Benefits of Using Geographic Information System

The development of the data base was the most time-consuming and costly aspect of the GIS implementation. Nevertheless, the use of GIS for analysis and map production provided many benefits. GIS reduced the work effort involved in matching addresses to TAZ codes, in assessing environmental impacts, and in generating graphics for presentation purposes. The data base that was developed will also be used for future planning studies in the project area, providing deferred cost savings. Most importantly, it was the ability of GIS to integrate and visually represent data that was beneficial to the designers, planners, and decision makers.

The application of GIS did not significantly affect the overall cost of the project because of the extensive data input process. The techniques that were developed for the study, however, made significant contributions in improving the planning and design process.

TABLE 2 Environmental Impact Assessment

	Alt. N3	Alt. N4	Alt. N5	Alt. N6
Farmland Impacts				
Illinois Agricultural Areas				
Affected - Number	4	2	3	1
- Area	570 ha (1,410 ac)	220 ha (540 ac)	510 ha (1,260 ac)	160 ha (400 ac)
Prime Farmland Affected				
Area > 75% prime	2,690 ha (6,640 ac)	1970 ha (4,870 ac)	3,100 ha (7,660 ac)	2,330 ha (5,760 ac)
25-75% prime	840 ha (2,070 ac)	870 ha (2,150 ac)	700 ha (1,730 ac)	460 ha (1,140 ac)
< 25% prime	350 ha (860 ac)	350 ha (860 ac)	220 ha (540 ac)	220 ha (540 ac)
Conservation/Natural Areas Affected,Area	o Root Cemetery Nature Preserve, Status Pending, 1 ha (2 ac) o Magnolia Hill Prairies Natural Area, 10 ha (25 ac)	o Root Cemetery Nature Preserve, Status Pending, 1 ha (2 ac) o Magnolia Hill Prairies Natural Area, 10 ha (25 ac)	o Root Cemetery Nature Preserve, Status Pending, 1 ha (2 ac) o Sparland State Conservation Area, 10 ha (25 ac)	o Root Cemetery Nature Preserve, Status Pending, 1 ha (2 ac) o Sparland State Conservation Area, 10 ha (25 ac)
Threatened and Endangered Specie Sites Encountered	0	0	Invertebrate found along IL River adjacent to corridor	Invertebrate found along IL River adjacent to corridor
Parkland Affected	Adjacent to Forest Park Foundation Land	Adjacent to Forest Park Foundation Land	Adjacent to Forest Park Foundation Land	Adjacent to Forest Park Foundation Land
Area of Woodland Affected	480 ha (1,190 ac)	480 ha (190 ac)	410 ha (1,010 ac)	330 ha (820 ac)
Cultural Resources Encountered				
Archaeological sites	11 small sites 1 medium site	8 small sites 1 medium site	10 small sites	7 small sites
Cemeteries	0	0	0	1
Hazardous Waste Sites (CERCLIS) Encountered	Adjacent to site	0	Adjacent to site	0
Steep Slopes Encountered	330 ha (820 ac)	330 ha (820 ac)		
Mining Areas Encountered	1 gravel pit; 1 mining area 10 ha (20 ac)	1 mine	1 gravel pit; 1 mining area 10 ha (20 ac)	0

CONCLUSION

For the Heart of Illinois Highway Feasibility Study, the GIS was used to process O-D survey forms, compile and integrate data to create an environmental resources inventory map, revise and adjust corridor locations and alignments, quantify the effects of proposed alternatives on environmentally sensitive areas, and produce maps and exhibits for presentation and report production. These functions were performed using a PC-based system,which did not require software customization. The development of the GIS data base for an area covering 7,700 km^2 (3,000 mi^2) was the most expensive and time-consuming aspect of GIS implementation. When the data base was completed, however, the GIS was able to produce maps quickly and easily, and reduce the work effort involved in assessing and quantifying corridor impacts.

The experience gained from the Heart of Illinois study indicates how GIS can influence decision making and improve the process of identifying and evaluating corridor alternatives. If state agencies continue to inventory their resources using GIS, then data base development may become less costly and state departments of transportation may use geographic information systems more frequently for roadway location studies. Furthermore, as planners and engineers are required to consider environmental issues along with engineering and cost issues, GIS can be used to synthesize and analyze data for highway planning. GIS has the potential to affect roadway planning as significantly as computer-aided design has changed the process of roadway design.

GLOSSARY

TIGER/Line files: GIS data base developed by the Bureau of Census containing a variety of information, including roadways, municipal boundaries, hydrographic features, railroads, etc.

Arc/Info files: GIS data bases developed and stored using Arc/Info software by Environmental Research Systems, Inc.

Buffering techniques: A type of GIS operation in which an area is generated or delineated around a point or a line. For example, a 5-mi radius buffer around a point results in the generation of a circle 10 mi in diameter around the point.

Intersection techniques: A type of GIS operation in which two areas are overlaid and a new area is generated or delineated based on their intersection.

ACKNOWLEDGMENTS

The authors acknowledge the contributions of Kate Hunter of the Illinois Natural History Survey, Michael Wiant of the Illinois State Museum, Dan Plomb of CH2M Hill, and Omar Santos formerly of LS Gallegos & Associates for their help in data collection. Thanks also to Jim Saag, Larry Martin, and Tracy Frommelt of CH2M Hill for their support in implementing the GIS for the study.

The work reported in this paper was conducted as part of The Heart of Illinois Highway Feasibility Study. The study was funded by the Illinois Department of Transportation and the FHWA. The project team included CH2M Hill, LS Gallegos & Associates, and Wilbur Smith Associates.

Publication of this paper sponsored by Committee on Geometric Design.

Highway Geometric Design Consistency Evaluation Software

RAYMOND A. KRAMMES, KETHIREDDIPALLI S. RAO, AND HOON OH

Previous research has concluded that horizontal curves on which design speeds are less than drivers' desired speeds exhibit operating speed inconsistencies that increase accident potential, and that current AASHTO design policy is unable to identify and address these inconsistencies. One step to address these concerns is the development by the FHWA of an Interactive Highway Safety Design Model that incorporates a consistency module. A Highway Geometric Design Consistency Program has been developed to serve as a basis for this consistency module. The program is a menu-driven microcomputer procedure for evaluating horizontal alignment consistency on rural two-lane highways using two preliminary models: an operating speed profile model and a driver workload profile model. This paper reviews these preliminary models, describes the menu-driven procedure for using them, and recommends future development of the models and procedure.

Previous research on rural two-lane highway operations and safety has concluded that horizontal curves on which design speeds are less than drivers' desired speeds exhibit operating speed inconsistencies that increase accident potential (*1–3*). Current AASHTO design policy is unable to identify and address operating speed inconsistencies (*4*). Therefore, it has been recommended that the design process for horizontal alignments on rural two-lane highways on which design speeds are less than 100 km/hr (62.1 mi/hr) be modified to incorporate a consistency evaluation that identifies and addresses operating speed inconsistencies (*1*). FHWA is taking steps toward implementing this recommendation by incorporating a consistency module in its Interactive Highway Safety Design Model (*5*).

This paper describes a program that has been developed to serve as the basis for the consistency module (*6*). The program is a menu-driven microcomputer procedure for evaluating horizontal alignment consistency on rural two-lane highways using two preliminary models: an operating speed profile model and a driver workload profile model. Both models have the same modest data requirements: the stationing of the point of curvature (PC) and the point of tangency (PT) of each horizontal curve along an alignment and each curve's radius or degree of curvature. Currently, the procedure requires the user to extract these data from roadway plans and enter it into an input data screen. In the ultimate implementation in the Interactive Highway Safety Design Model, the data required for the consistency module would be extracted automatically from the data base of the commercial computer-aided design (CAD) package that will be the hub of the model.

This paper is organized into three main sections. First, preliminary speed profile and workload profile models, which have been reported elsewhere, are reviewed. Next, the microcomputer procedure for using these models is described. Last, recommendations are made for further development of both the preliminary models and the procedures for using them.

Texas Transportation Institute, Texas A&M University, College Station, Tex. 77843-3135.

PRELIMINARY MODELS FOR EVALUATING CONSISTENCY

Conceptual Framework

The causes and consequences of geometric inconsistencies are best explained within the context of driver-vehicle-roadway interactions. The driving task is principally an information-processing and decision making task. Driver workload is a principal measure of driver information processing and is defined as "the time rate at which drivers must perform a given amount of work of driving task" (*7*). The roadway geometry and other factors (including the roadside environment, weather, traffic control devices, traffic conditions, etc.) are the primary inputs to the driving task. The outputs are control actions that translate into vehicle operations that, in turn, can be observed and characterized by traffic measurements (e.g., operating speed).

Drivers generally devote sufficient attention to accommodation of the workload demands they expect of the roadway. Most rural highways have relatively low workload demands; therefore, drivers often have relatively low attention levels on them. Geometric inconsistencies, however, impose higher workloads and demand more attention than are typically required and, therefore, more than drivers expect. Drivers who recognize the disparity between their expectation and the actual workload requirements of a feature increase their attention level and appropriately adjust their speed or path. Drivers who fail to recognize or are slow to recognize the disparity may make speed or path errors that increase the likelihood of accidents. Therefore, abrupt speed or path changes are common manifestations of the unexpectedly high workload demands associated with geometric inconsistencies. In theory, geometric inconsistencies could be measured by either increases in driver workload requirements or decreases in operating speeds between successive features (*8*).

Operating Speed–Based Consistency Evaluation

Concerns about and procedures for evaluating consistency on rural two-lane highways have focused on horizontal curves. Curves have higher average accident rates than tangent sections (*9*), and average accident rates on curves increase as the required speed reduction from an approach tangent to a curve increases (*3*).

Most of the procedures for evaluating horizontal alignment consistency are based on operating speed reductions. Switzerland was probably the first country to incorporate into their design procedures

a speed-profile model for evaluating speed reductions (*10*). Leisch and Leisch (*11*) were the first in the United States to publish an operating speed–based procedure for evaluating horizontal and vertical alignment consistency. Lamm et al. (*12*), Lamm and Choueiri (*13*), and Lamm et al. (*14*) played a significant role in renewing U.S. concerns about consistency considerations.

The speed profile model in the microcomputer program described in this paper has the same form as the Swiss model (*10*), uses the basic equations and assumptions reported by Lamm et al. (*14*), and was calibrated by Ottesen and Krammes (*2*). The speed profile model estimates the 85th percentile speed at each point along a horizontal alignment. This profile is used to calculate the decrease in 85th percentile operating speed from an approach tangent to a curve, which is the measure of consistency associated with a curve.

Calibrating the speed-profile model required three types of information:

- A regression equation for the 85th percentile speed on a horizontal curve as a function of curve geometry;
- The 85th percentile desired speed on long tangents, which is defined as the speed maintained by the 85th percentile driver on the portion of long tangents outside the influence of adjoining horizontal curves; and
- Deceleration and acceleration rates entering and departing curves.

The regression equation for 85th percentile speed on a horizontal curve was developed based on free-flow passenger vehicle speed data from 138 curves in five states (New York, Oregon, Pennsylvania, Texas, and Washington). The roadways on which data were collected were low- to moderate-volume rural collectors or minor arterials in level to rolling terrain (i.e., grades $\leq$ 5 percent). Other characteristics of the roadways included: design speed $\leq$ 100 km/hr (62.1 mi/hr), lane widths between 3.05 and 3.66 m (10 and 12 ft), and shoulder widths between 0 and 2.44 m (0 and 8 ft).

Twelve curve geometry, cross-section, and approach-condition variables were considered as predictors of 85th percentile speed on curves, and several equation forms were tested. The following multiple-linear regression model, with an R^2 value of 0.82, a root mean square error of 5.1 km/hr (3.1 mi/hr), and a P value of 0.0001; was recommended (*2*):

$$V85 = 102.45 - 1.54D + 0.0037L - 0.10I \quad (1)$$

where

$V85$ = 85th percentile speed on the curve (km/hr),
D = degree of curvature (degrees),
L = length of curve (m), and
I = deflection angle (degrees).

The desired speed on long tangents was based on speed data from 78 approach tangents that were long enough for drivers to reach and maintain a maximum desired speed. Attempts to model the desired speed on long tangents using predictor variables, including tangent length, parameters of the adjoining curves, cross-section width, terrain type, and geographical region of the United States, were unsuccessful. Therefore, the model uses 97.9 km/hr (60.8 mi/hr), the mean of the 85th percentile speed on the 78 long tangents, as the desired speed on long tangents.

The speed profile model assumes that speeds are constant through horizontal curves and that deceleration and acceleration occur only on the tangents approaching and departing the curve. These assumptions are simplifications of reality; the research literature reports some results supporting these assumptions and other results suggesting that acceleration and deceleration occur within curves. The error in estimated speed reductions resulting from these simplifications, however, is likely to be small. Acceleration and deceleration rates are assumed to be equal. The 0.85-m/sec^2 (2.8 ft/sec^2) rate reported by Lamm et al. (*14*) was used in the model without validation. This rate is similar to the 0.8-m/sec^2 (2.6 ft/sec^2) rate assumed in the Swiss procedure (*10*).

The speed profile model uses basic equations of motion in combination with the calibration data (speeds on curves, speeds on long tangents, and deceleration and acceleration rates) to estimate the 85th percentile speed at each point along a horizontal alignment. The equations of motion are used to determine what speed could be attained on the tangent and over how much of the tangent deceleration and acceleration would occur so that the appropriate speed (estimated by Equation 1) would be reached on the horizontal curves and the desired speed on long tangents would not be exceeded.

Driver Workload-Based Consistency Evaluation

The use of driver workload as a measure of consistency has been much more limited than operating speed. Messer et al. (*7*) developed a model for estimating driver workload based on roadway geometry and incorporated it into a procedure for evaluating rural highway design consistency. Preliminary evaluations suggest that these workload estimates are good indicators of high accident locations on rural two-lane highways (*15,16*). The procedure is manual, however, and has had only very limited application.

One strength of driver workload as a measure of consistency is that, in theory, it can be applied to any geometric feature, unlike operating speed reduction, which is limited in application to horizontal, and possibly vertical, alignment. The principal weakness of driver workload is that it is difficult to measure. The Messer et al. model (*7*) is based on subjective appraisals rather than objective measurements, which makes it difficult to validate and, therefore, limits its credibility.

The workload profile model used in the microcomputer procedure described herein was developed by Shafer et al. (*17*). To address the criticism about the subjective basis of driver workload estimates, they used the vision occlusion method, which is an objective method for measuring driver workload.

In the vision occlusion method, drivers voluntarily occlude their vision, opening their eyes only when they think it necessary to extract information for the guidance task. If vehicle speed is constant and lane integrity is not violated, then the amount of time that drivers are unwilling to have their vision occluded over a fixed length of roadway represents the mental workload required for the guidance task. Workload is defined as the proportion of total driving time that drivers need to look at the roadway. The lower the information-processing demands for guiding the vehicle along the roadway, the longer the drivers will voluntarily keep their vision occluded. Conversely, the greater the information-processing demands, the more a driver will need to look at the roadway and thus the higher the mental workload.

Calibrating the workload profile model requires two types of information: a regression equation for driver workload on a horizontal curve as a function of curve geometry and driver workload on tangents.

The vision occlusion method was used to measure driver workload on curves (without superelevation) and tangents on test courses laid out on former airport runways at the Texas A & M Proving Ground Research Facility. Selected degrees of curvature (3 degrees, 6 degrees, 9 degrees, and 12 degrees) and deflection angles (20 degrees, 45 degrees, and 90 degrees) were studied. Shafer et al. (*17*) describe the test method in detail. For each curve and tangent, the workload measurements of all subjects were averaged. A total of 55 subjects participated in the tests.

A regression equation was developed for the average workload on curves. Degree of curvature and deflection angle were tested as predictor variables. The following simple-linear regression equation for average workload as a function of degree of curvature was recommended:

$$WL = 0.193 + 0.016D \quad (2)$$

where WL is the average workload of curve and D is the degree of curvature (degrees).

This equation had an R^2 value of 0.90, a root mean square error of 0.020, and P value of 0.0001. Driver workload on curves increases approximately linearly with increasing degree of curvature.

The mean of the workload observations on tangent sections of the test courses, 0.176, was used as the driver workload on tangents in the workload profile model. This value indicates that subjects required vision only 17.6 percent of the time on the tangent sections of the test courses.

The workloads measured are likely to be lower than would be experienced by drivers on an actual highway. The test courses were flat, and nothing in the environment beyond the courses required the subjects' attention. The workload estimates are considered a relatively pure measure of the workload demands of the guidance task of path-following on curves and tangents.

The current form of the workload profile model is very preliminary. The model consists only of the mean workload value on tangents and the workload estimates from Equation 2 for curves. Workload changes abruptly at the beginning and end of a curve. The gradual transitions in workload that were observed during data collection have not been represented in the model.

MICROCOMPUTER PROCEDURE FOR USING PRELIMINARY MODELS

The Highway Geometric Design Consistency Program facilitates the use of these preliminary models for consistency evaluations of rural two-lane highway horizontal alignments. This menu-driven microcomputer program provides tabular screens for entering and editing input data and creates output files of model results that can be presented in tabular or graphical form. The program is available in both metric- and English-units versions (*6,18*). The hardware requirement is an IBM-compatible, DOS-based microcomputer with a minimum of 270K RAM.

The data for which the models were calibrated limit the scope of the consistency evaluations that can be performed using the program to horizontal alignments consisting of horizontal curves and tangents on rural two-lane highways with design speeds $\leq$ 100 km/hr (62.1 mi/hr) in level to rolling terrain. There is no provision for evaluating transition curves. The speed profile model applies to horizontal radii $\geq$58 m (190 ft) and vertical grades $\leq$5 percent. The workload profile model applies to horizontal radii $\geq$145 m (476 ft) and deflection angles $\leq$90 degrees.

Input Data

The data requirements to perform consistency evaluations using the metric units version of the program are modest: stationing of the PC and PT of each horizontal curve, radius of each curve, and station equations. These data can be obtained from standard roadway plans.

Figure 1 is the tabular input data screen. By way of example, data for an 8-km section of rural two-lane highway in Texas have been entered and are shown on the screen.

The screen includes columns for:

- Curve number (in consecutive order);
- PC station (in metric stationing notation);
- PT station (that should be used in calculating the curve's length);
- Station equation (i.e., the PT station that should be used in calculating the subsequent tangent's length);
- Radius in meters;
- 85th percentile speed in km/hr (calculated automatically by the program using the regression equation for 85th percentile speeds on curves in the speed profile model based on the radius that has been entered); and
- Drive workload (calculated automatically by the program based on the regression equation for driver workload on curves in the driver workload profile model based on the radius that has been entered).

Output

The procedure provides both tabular and graphical output of the measures of consistency and profiles of 85th percentile speed and workload. Figure 2 shows the form of the procedure's tabular output from the speed and workload profile models. The output corresponds to the input data in Figure 1. For each curve, the tabular output indicates the estimated reduction in 85th percentile speed and the increase in driver workload from the approach tangent to the curve. These measures of consistency are computed from the speed profile and workload profile that are illustrated graphically in Figures 3 and 4, respectively.

Both Figures 3 and 4 have two parts. The top part is a bar chart depicting the sharpness of each horizontal curve along the alignment. The height of a bar represents the radius of the curve in meters; the higher the bar, the smaller the radius and, therefore, the sharper the curve. The width of a bar represents the length of curve in kilometers. The bottom part of the graphical output is either the speed profile or the workload profile. On the speed profile in Figure 3, the horizontal elements represent speed on a curve or on the portion of a long tangent on which the 85th percentile desired speed is attained; the diagonal lines represent deceleration and acceleration on the tangent approaching and departing a curve. The workload profile in Figure 4 illustrates the increase in workload on a curve relative to the base workload value of 0.176 for tangents.

Designers can use the 85th percentile speed profile to check the appropriateness of their design speed selections and to identify probable locations of operating speed inconsistencies that may

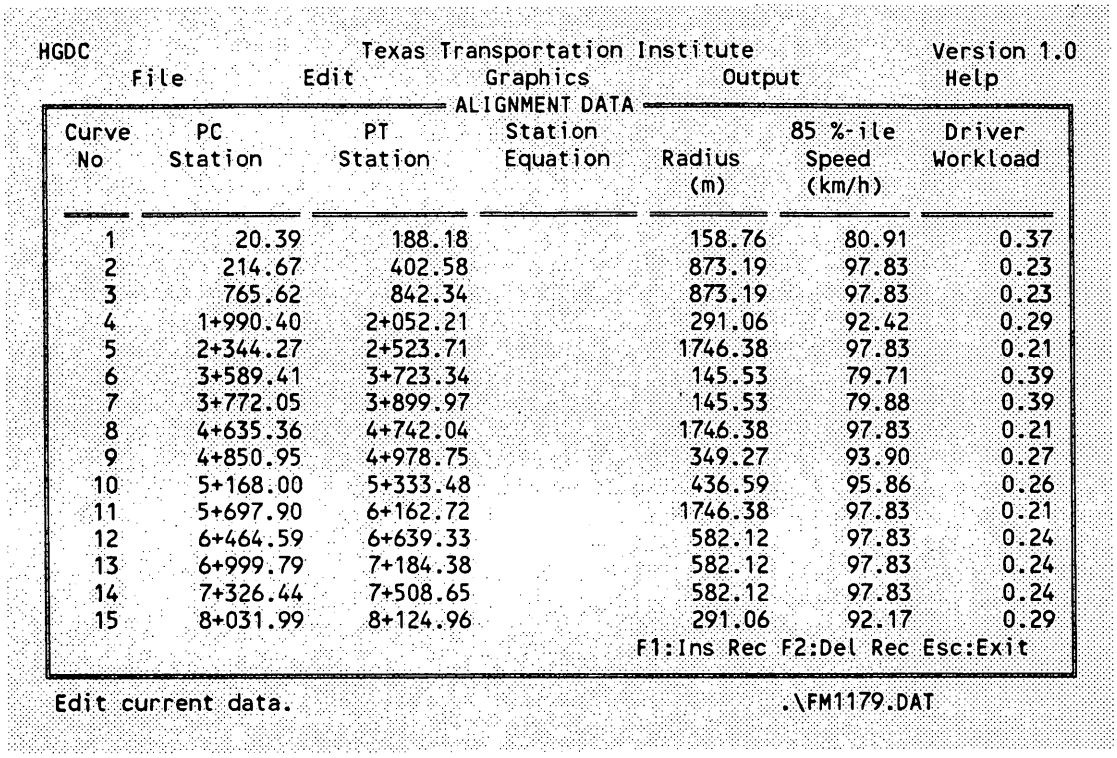

FIGURE 1 **Input data screen.**

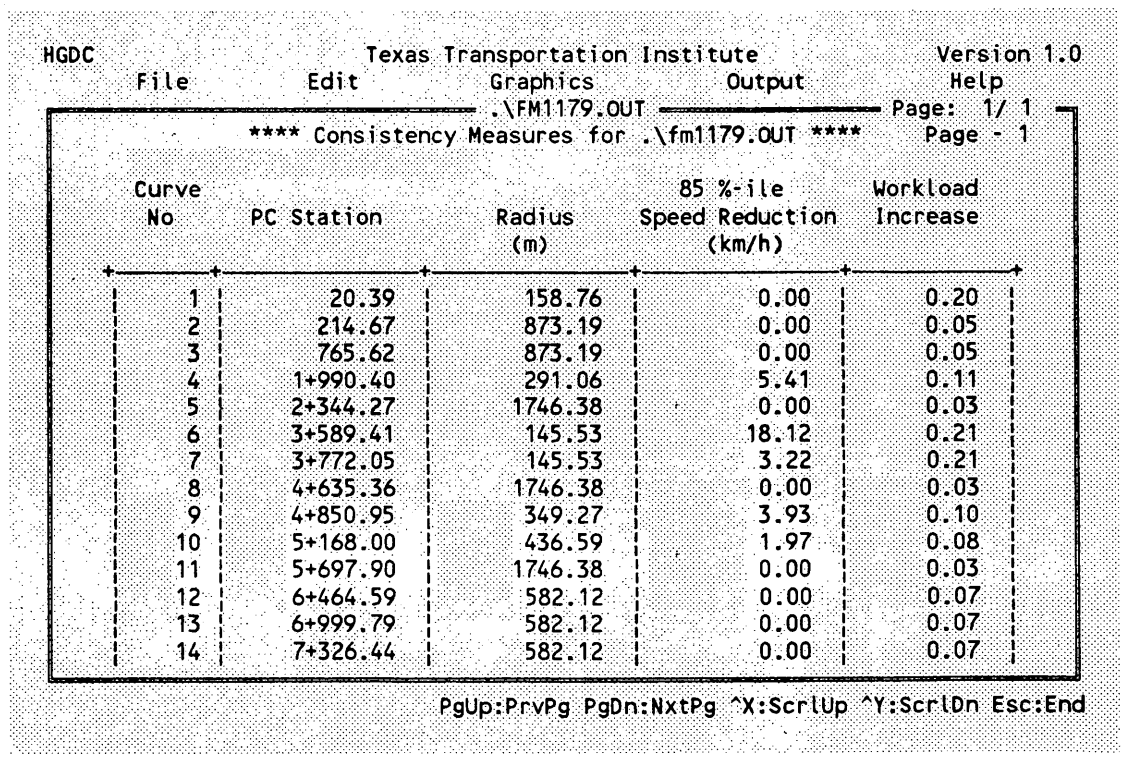

FIGURE 2 **Tabular output screen.**

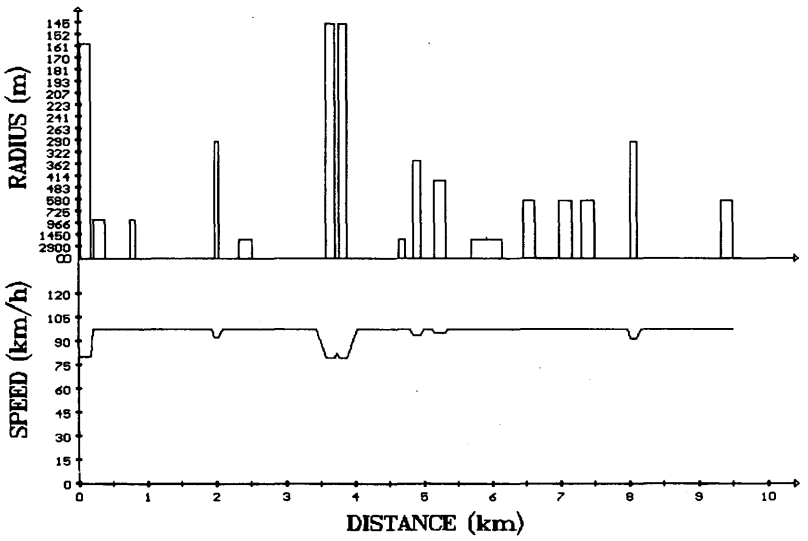

FIGURE 3 Graphical speed profile output screen.

require special attention in the design process. Statistical analyses indicate that the speed reduction estimates from the model are good indicators of accident potential on horizontal curves, with expected accident rates increasing approximately linearly as the estimated speed reduction increases (*3*). Leisch and Leisch (*11*) and Lamm et al. (*14*) have suggested that required speed reductions between successive alignment elements should not exceed 16 to 20 km/hr (10 to 12 mi/hr). If greater speed reductions are estimated, then accident experience should be checked to determine what safety improvements, if any, are warranted.

In summary, the microcomputer program provides an easy-to-use, menu-driven procedure for performing consistency evaluations of rural two-lane highway horizontal alignments using preliminary speed and workload profile models. Both tabular output of measures of consistency for each horizontal curve along an alignment (including the reduction in 85th percentile speed and increase in workload from the approach tangent to each curve) and graphical output (including speed and workload profiles) are provided.

RECOMMENDED FUTURE DEVELOPMENTS

Although the speed profile model is at a more refined stage than the driver workload model, both are considered preliminary models that require further development. Furthermore, the menu-driven microcomputer procedure is intended for interim use until the consistency module is implemented in the Interactive Highway Safety Design Model.

Speed profile models similar to the one described herein have been used for many years in other countries; therefore, the basic approach and assumptions are probably reasonable. Furthermore, the speeds on curves and on long tangents have been calibrated

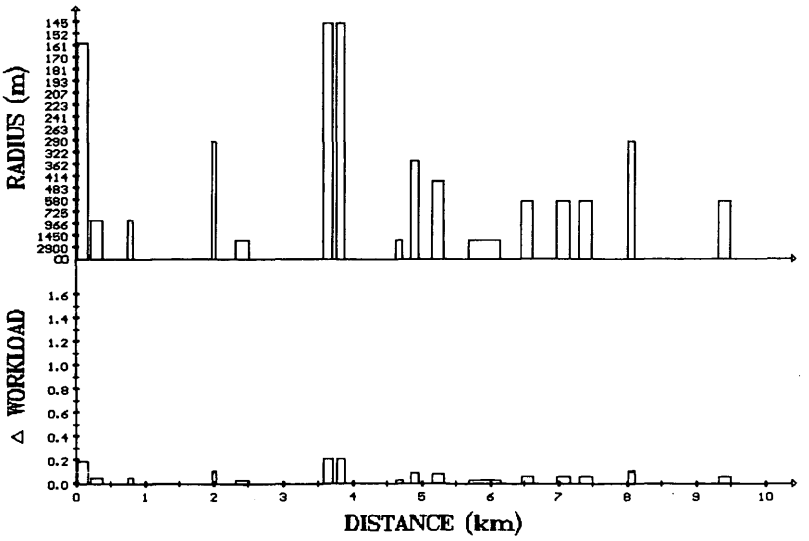

FIGURE 4 Graphical workload profile output screen.

using a moderately large data base of 138 curves and 78 of their approach tangents in five states representing three regions of the United States. The data are believed to be representative of relatively isolated horizontal curves (i.e., with relatively long approach tangents and sight distance) on typical state-maintained rural, two-lane collectors and minor arterials with design speeds ≤100 km/hr (62.1 mi/hr) in level to rolling terrain (i.e., with grades ≤5 percent). However, additional validation of the model is recommended to determine its accuracy for alignment conditions and geographical regions different from those for which the model was calibrated. Validation is also recommended on the assumptions about deceleration and acceleration rates: that is, that the rates are equal to 0.85 m/sec^2 (2.8 ft/sec^2), and the deceleration and acceleration occur only on the tangents approaching and departing the curve. Furthermore, consideration should be given to enhancing the model to account for other factors that may influence operating speeds, including vertical alignment, at-grade intersections, and changes in cross-section, and to estimate speed profiles for heavy vehicles as well as passenger cars. Additional analysis is also required to establish guidelines on desirable or absolute maximum speed reductions between successive geometric features and between vehicle types.

The workload profile model is very preliminary. It was calibrated based on data for 55 subjects on curves without superelevation on test courses that simulate actual roadways but lack such roadways' richness of visual inputs to drivers. It is recommended that the model be validated using data obtained with the vision occlusion method on actual roadways. It is also recommended that the model be refined to reflect more accurately the gradual transitions that occur in workload (much as they occur in speeds) approaching and departing curves. Finally, consideration should be given to applying the vision occlusion method for measuring driver workload to other geometric features (e.g., at-grade intersections and narrow bridges) that exhibit higher-than-average accident experience.

The menu-driven microcomputer procedure is an easy-to-use interim tool that can be used until the Interactive Highway Safety Design Model is completed. The consistency module in this model should, as planned, extract the required input data automatically from the data base of the commercial CAD package integrated with the model.

Previous research and experience in other countries suggest that consistency evaluations of rural two-lane highways with design speeds less than 100 km/hr (62.1 mi/hr) can promote the design of safer alignments. Implementation of consistency evaluations in U.S. design practice may have been slowed, in part, by the lack of easy-to-use procedures. It is hoped that the microcomputer procedure reported herein will encourage experimentation with the preliminary models for consistency evaluation so that the state of the art in the United States can be improved and, in time, enhanced models can be incorporated as a consistency module in FHWA's Interactive Highway Safety Design Model.

REFERENCES

1. Krammes, R. A. Design Speed and Operating Speed in Rural Highway Alignment Design. Paper No. 940996. Presented at 73rd Annual Meeting of the Transportation Research Board, Washington, D.C., Jan. 1994.
2. Ottesen, J. L., and R. A. Krammes. Speed Profile Model for a U.S. Operating-Speed-Based Design Consistency Evaluation Procedure. Paper No. 940995. Presented at 73rd Annual meeting of the Transportation Research Board, Washington, D.C., Jan. 1994.
3. Anderson, I. B., and R. A. Krammes. Speed Reduction as a Surrogate for Accident Experience at Horizontal Curves on Rural Two-Lane Highways. Paper No. 940994. Presented at 73rd Annual Meeting of the Transportation Research Board, Washington, D.C., Jan. 1994.
4. *A Policy on Geometric Design of Highways and Streets.* AASHTO, Washington, D.C., 1990.
5. Reagan, J. A. The Interactive Highway Safety Design Model: Designing for Safety by Analyzing Road Geometrics. *Public Roads,* Vol. 58, No. 1, 1994, pp. 37–43.
6. Rao, K. S., H. Oh, and R. A. Krammes. *Users Manual for the Highway Geometric Design Consistency Program (Metric Units).* Report No. FHWA-RD-94-039. FHWA, U.S. Department of Transportation, 1994.
7. Messer, C. J., J. M. Mounce, and R. Q. Brackett. *Highway Geometric Design Consistency Related to Driver Expectancy,* Vol. III. *Methodology for Evaluating Geometric Design Consistency.* Report No. FHWA/RD-81-038. FHWA, U.S. Department of Transportation, 1981.
8. Krammes, R. A., R. Q. Brackett, M. A. Shafer, J. L. Ottesen, I. B. Anderson, K. L. Fink, K. M. Collins, O. J. Pendleton, and C. J. Messer. *Horizontal Alignment Design Consistency for Rural Two-Lane Highways.* Report No. FHWA/RD-81-038. FHWA, U.S. Department of Transportation, 1994.
9. Zegeer, C. V., J. M. Twomey, M. L. Heckman, and J. C. Hayward. *Safety Effectiveness of Highway Design Features,* Vol. II. *Alignment.* Report No. FHWA-RD-91-045. FHWA, U.S. Department of Transportation, 1992.
10. *Geschwindigkeit als Projektierungselement.* Swiss Norm 640 080b. Vereingung Schweizerischer Strassenfachleute, Zurich, Switzerland, 1992.
11. Leisch, J. E., and J. P. Leisch. New Concepts in Design-Speed Application. In *Transportation Research Record 702,* TRB, National Research Council, Washington, D.C., 1979, pp. 53–63.
12. Lamm, R., J. C. Hayward, and J. C. Cargin. Comparison of Different Procedures for Evaluating Speed Consistency. In *Transportation Research Record 1100,* TRB, National Research Council, Washington, D.C., 1986, pp. 10–20.
13. Lamm, R., and E. M. Choueiri. Recommendations for Evaluating Horizontal Design Consistency Based on Investigations in the State of New York. In *Transportation Research Record 1122,* TRB, National Research Council, Washington, D.C., 1987, pp. 68–78.
14. Lamm, R., E. M. Choueiri, J. C. Hayward, and A. Paluri. Possible Design Procedure to Promote Design Consistency in Highway Geometric Design on Two-Lane Rural Roads. In *Transportation Research Record 1195,* TRB, National Research Council, Washington, D.C., 1992, pp. 1–10.
15. Krammes, R. A., and S. W. Glascock. Geometric Inconsistencies and Accident Experience on Two-Lane Rural Highways. In *Transportation Research Record 1356,* TRB, Washington, D.C., 1992, pp. 1–10.
16. Wooldridge, M. D. Design Consistency and Driver Error. Paper No. 930722. Presented at 72nd Annual Meeting of TRB, National Research Council, Washington, D.C., 1993.
17. Shafer, M. A., R. Q. Brackett, and R. A. Krammes. Driver Mental Workload as a Measure of Geometric Design Consistency for Horizontal Curves. Paper No. 950706. Submitted for Presentation at 74th Annual Meeting of TRB, National Research Council, Washington, D.C., 1994.
18. Rao, K. S., H. Oh, and R. A. Krammes. *Users Manual for the Highway Geometric Design Consistency Program (English Units).* Report No. FHWA-RD-94-038. FHWA, U.S. Department of Transportation, 1994.

Publication of this paper sponsored by Committee on Geometric Design.

Investigation of Object-Related Accidents Affecting Stopping Sight Distances

KAREN B. KAHL AND DANIEL B. FAMBRO

Stopping sight distance (SSD) is an integral part of the highway design process because it is the minimum sight distance required at all points along the roadway. The current SSD model uses a critical sight distance situation in which the driver detects a small object in the roadway, recognizes it as a hazard, and stops before striking it. Some researchers have questioned the assumptions and variables used in the SSD model because they do not appear to represent a realistic, real-world situation when combined in the existing model. The 150-mm (6-in.) object is one of these questionable variables because this height was not based on the probability of encountering such an object in the roadway environment. The objective of this research was to investigate the characteristics of objects encountered in the roadway that represent a realistic hazard for the driver. A detailed examination of accident data was performed to evaluate the characteristics. Three types of accidents in two states were studied: other-object, animal, and evasive-action. The study results showed that only 0.07 percent of the reportable accidents involved small objects in the roadway. More than 90 percent of these objects accidents occurred at night on straight, flat roadways (conditions in which sight distance is not limited by the roadway's geometry), and they did not result in serious injuries. These findings suggest that accidents with small objects are neither frequent enough nor severe enough to justify their use as the critical situation in the SSD model. The authors recommend that the object height used in the design should represent the smallest object that poses a hazard to the driver: the minimum legal taillight height of a vehicle.

Stopping sight distance (SSD) is an integral part of the highway design process because it is the minimum sight distance required at all points along the roadway. The current SSD model uses a critical sight distance situation in which the passenger car driver, traveling at or near the design speed on a wet pavement, detects a small object in the roadway, recognizes it as a hazard, performs a locked-wheel brake, and stops before striking the object. The same parameter values are used for all types of roadways and conditions. Over time, several of these model parameters (including the object height) have changed, resulting in longer vertical curve length requirements; however, it has not been proven that longer curve lengths improve safety or that shorter curve lengths increase the potential for accidents (*1*).

The current SSD model is based on detection and recognition of a 150-mm (6-in.) object; however, several researchers have questioned this value and the assumptions in the SSD model because they do not appear to represent a realistic, real-world situation (*2*). The selection of the object height was not based on the frequency or severity of encountering such objects, and the selection appears to have been unrelated to the operational requirements for safe stopping sight distances (*3*). The initial rationale for the object height was a tradeoff between the cost of excavation and the ability of the driver to see the roadway, however in recent years it has been related to the height of the vehicle's undercarriage. Regardless of the rationale, objects of this size do not represent a hazardous situation for motorists if they do not cause accidents. Woods (*4*) found that a driver is 125 times more likely to be in an accident involving another vehicle than in an accident involving a small unknown "object."

In addition to the probability of striking a 150-mm (6-in.) object, research has not considered whether the chosen object height is actually visible to the average, or 85th percentile, driver. At night, the driver's visibility is limited to the headlight illumination distance, which is generally less than the required SSD. If the driver cannot recognize the object as a hazard or even see it at the required SSD, then the design criteria are not compatible with a driver's visual abilities.

The objective of this study was to investigate the characteristics of objects encountered in the roadway environment that could affect safe SSD. A secondary objective of the study was to determine whether any of these characteristics were different for different types of roadways.

HISTORY OF THE OBJECT HEIGHT

The need for sight distance on roadways was recognized in textbooks on highway engineering as early as 1914 (*5*). In 1921, Harger (*6*) was one of the first to attach lengths and heights to sight distance requirements by creating a line of sight between two points 1.7 m (5.5 ft) above the ground. In 1936, Gutmann (*7*) introduced the German standard for sight distance, which used two objects to determine the sight distance over a crest vertical curve: a standard passenger car 1.5 m (4.9 ft) high and an object 200 mm (8 in.) above the roadway surface.

Since the development of the first SSD models, object height has been a controversial topic. Throughout the 1930s, many highway agencies in the United States considered an approaching vehicle to be the critical encounter for evaluating sight distance; in 1940, the AASHO's SSD publication provided a standard by defining the critical object as a 100-mm (4-in.) object (*8*), the so-called "dead cat" rule (*9*). The 1954 AASHO policy (*10*) further supported the choice of the 100-mm (4-in.) object height by concluding that it offered a compromise between the cost of excavation and the ability of the driver to see the road ahead. "A 4-in. control was considered the approximate point of diminishing returns."

In the 1965 AASHO policy (*11*), the object height was increased from 100 to 150 mm (4 to 6 in.); however, the rationale used to

K. B. Kahl, CH2M HILL, 411 East Wisconsin Avenue, Suite 1600, Milwaukee, Wis. 53202. D. B. Fambro, Department of Civil Engineering, Texas A&M University System, Suite 303, CE/TTI Building, College Station, Tex. 77843.

justify the 150-mm 6-in.) object was the same rationale used for the 100-mm (4-in.) object in 1954. It represented the approximate point of diminishing returns between excavation and visibility. The literature at that time did not contain data to support the increase, but it has been suggested that the object height was increased to offset a decrease in driver's eye height and thus keep the required lengths of crest vertical curves relatively constant.

In 1984, the rationale for using the 150-mm (6-in.) object changed. The 1984 and the 1990 Green Books (*12,13*) emphasize that a 150-mm (6-in.) object represents the lowest object that can create a hazardous situation. They state that an object height of 150 mm (6 in.) is "largely an arbitrary rationalization of possible hazardous objects and a driver's ability to perceive and react to a hazardous situation." In summary, neither the original object height of 100 mm (4 in.) nor the current object height of 150 mm (6 in.) has supporting research to show that either represents an object or situation that is hazardous to a driver.

DATA COLLECTION

Accident records and narratives provide the best information for researchers studying what types of objects are encountered on the roadway as well as what circumstances are associated with object-related accidents. This study reviewed the records and narratives of object-related accidents from two large states to determine what types of objects are being struck on the roadways and the characteristics of the resultant accidents. Three types of single-vehicle accidents were examined in this study: other-object, animal, and evasive-action. These accident types were selected because they had the closest representation to the SSD situation: an unsuspecting driver encountering an unexpected object in the roadway. After these three accident data subsets were compiled, the characteristics of the object-related accidents were compared with characteristics of all accidents to investigate whether there were differences associated with object-related accidents.

The object-related accident characteristics were obtained from computerized data bases compiled from state accident reports; therefore, the type and amount of accessible data were limited to the information found in the state accident reports. The accident variables extracted from the data base included the object type, the accident severity, and the roadway type. The narrative accident reports were reviewed to determine the actual objects or animals struck and their approximate heights.

The accident data were separated according to the type of roadway to investigate whether the types of object struck differed by roadway classification. The roadway classification categories were limited by the variables available in the data bases; therefore, the variables were used to create a set of roadway classifications that could be applied to the data in both states. The classification categories were organized according to features that affected the geometric design of the road, such as the type of area (rural or urban), access control, number of lanes, median treatment, and shoulder treatment. Five road classifications were developed in a hierarchical order: freeways, multilane divided, multilane undivided, two-lane with shoulder, and two-lane without shoulder. These classifications were further divided into rural and urban areas, with four annual average daily traffic groups within each category.

Characteristics of unreported object-related accidents could not be investigated and therefore were a concern to the authors. For example, Griffin (*14*) reported that because fewer noninjury accidents are being reported, a larger percentage of the total number of accidents reported is composed of injury accidents. Griffin stated that accident data bases created through local, state, or federal governments tend to only include accidents that resulted in physical injury or property damage. This limitation could also apply to object-related accidents. For instance, if the object in the roadway did not cause physical injury or property damage, then it may not have been reported; however, these unreported accidents did not create a critical situation for the driver. Discounting these accidents would skew the data toward accidents with higher objects and more severe injuries. Thus, although unreported object-related accidents may be missing from the data base, the results will overestimate the percentage of critical situations caused by objects in the road.

State 1 Data Base

The first accident data set was obtained directly from the accident data base in State 1. The data base only included roadway information for the state-maintained highway system (on-system accidents); therefore, only those accidents occurring on state roads could be evaluated. There were 381,446 reported accidents in the state in 1991, but only 187,024 (49 percent) of the accidents were on the state-maintained system and could be included in the data base for this study.

The accidents used in the study were limited to single-vehicle accidents that occurred on the roadway. (If several vehicles were involved, then the accident description focused on the collision and not necessarily on the object that caused it.) The accident also had to occur on the roadway to directly pertain to the SSD critical situation. Single-vehicle, on-roadway accidents represented 9 percent (34,414) of all accidents in 1990. Within the single-vehicle, on-roadway accident subset, there were 523 object-related accidents and 2,619 animal-related accidents. Evasive-action accidents were also investigated; however, the accidents reviewed were not limited to single-vehicle accidents because the analysis focused on the cause of the evasive maneuver. There were 377 evasive-action accidents in which drivers swerved or slowed to avoid objects and 1,042 evasive-action accidents in which they swerved or slowed to avoid animals.

State 2 Data Base

The second set of accident data was taken from a highway safety data base developed by the FHWA Highway Safety Information System (HSIS). HSIS is a location-based accident system that combines accident, roadway, and traffic data in a computer-linkable format (*15*). The five states involved in HSIS have provided different information about their respective accidents; therefore, each data base had to be reviewed to determine which had variables that most closely matched those in the State 1 data base. As with State 1, the selected state data base contained only those accidents that could be linked to a specific location reference; these were usually accidents on higher order roadways that belonged to the state-maintained system.

Approximately 400,000 accidents were reported in State 2 in 1990; however, only 153,796 accidents were entered in the data base because of the location reference requirement. Twenty-one percent (32,233 accidents) of the accidents in the data base were single-vehicle accidents. Within the single-vehicle accident subset, 619 were object-related accidents and 6,237 were animal-related accidents. In summarizing the evasive-action accidents in State 2,

there were 164 accidents in which drivers swerved or slowed to avoid objects and 731 accidents where in which drivers slowed or swerved to avoid animals.

DATA ANALYSIS

The three subsets of accidents that involved objects on the roadway were other-object, animal, and evasive-action. All other-object accident reports and a random sample of animal accident reports (14 percent) and evasive-action accident reports (38 percent) were reviewed to determine what objects were struck. The objects that caused these accidents were recorded, and their heights were established. Six height categories were created to help organize the data. If the object height was unknown, then the location of the damage and the vehicle damage severity were used to estimate an object height.

Other-Object Accidents

Other-object accidents occur when the driver strikes something that would not normally be encountered in the roadway environment and the encounter results in an accident. As mentioned previously, only those accidents that occurred on the roadway were examined because they represented situations that could result from limited SSD. Other-object accidents had the closest representation to the critical situation in the SSD model: a driver encountering an unexpected object on the roadway.

All of the single-vehicle, other-object accident reports were reviewed to determine what objects caused the accidents and if the objects or their characteristics differed according to roadway classification. In State 1 there were 238 other-object accidents on rural roads (45 percent) and 285 other-object accidents on urban roads (55 percent). The largest percentage of other-object accidents in State 1 occurred on freeways: 37 percent occurred in rural areas and 79 percent in urban areas. In State 2, 186 of the other-object accidents occurred on rural roads (30 percent) and 433 on urban roads (70 percent). As with State 1, the largest percentage of other-object accidents occurred on freeways: 48 percent in rural areas and 46 percent in urban areas.

Some of the more common objects struck on all types of roads included tires, hay bales, car parts, poles (lights or signs that had fallen across the road), trees or branches, construction barrels, railroad ties, and metal debris. On rural two-lane roads without shoulders, 53 percent of the accidents involved striking trees that had fallen across the road. Some of the more common objects struck on urban freeways appeared to be items that had fallen from moving vans or trucks, as well as poles that had fallen across the roadway.

Animal Accidents

An animal accident occurs when an animal is struck on the roadway. The accident data bases had limited reporting capabilities, which prompted questions about the nature of the animal accidents; the animal could have darted in front of the vehicle just before impact or it could have been standing in the roadway and the driver was unable to stop before striking it. In the first case, SSD was not a problem; however, in the latter case, it might have been a contributing factor to the accident. Because the purpose of this study was to determine the probability of encountering an object or animal in the roadway, all types of animal accidents were considered.

In State 1, 2,619 single-vehicle, animal accidents were reported in 1990. A random sample of 270 (10 percent) of these accident reports were reviewed. Ninety percent of the animal accidents occurred on rural roads and 10 percent occurred on urban roads. In State 2 there were more than 6,616 single-vehicle, animal accidents; 96 percent of them involved deer, and 4 percent involved other animals. Seventy-three percent of the animal accidents occurred on rural roads, 21 percent on urban roads, and 6 percent were not classified. One noticeable difference between the two states was the significantly higher number of deer accidents in State 2 than in State 1.

The animals were identified from the accident reports and separated according to size. Large animals were taller than 600 mm (24 in.) and included cows, horses, deer, or goats. Ninety-four percent of the animals struck in State 1 and more than 96 percent of the animals struck in State 2 were large animals. A medium-sized animal had an average height of between 450 and 600 mm (18 and 24 in.). They included dogs, pigs, and sheep and represented 5 percent of the animal-related accidents in State 1. Small animals had average heights of between 50 and 150 mm (2 to 6 in.) and included rabbits, raccoons, squirrels, skunks, armadillos, or other small animals. Small animals represented 1 percent of the animal accidents in State 1. The height of the animals from the random sample of 270 accidents was considered representative of all animal accidents. In State 2, however, the animal heights were heavily weighted toward large animals because of the large number of accidents with deer.

Evasive-Action Accidents

Evasive-action accidents occur when a driver attempts to avoid a hazard on the roadway. The drivers are usually successful in their attempt to avoid the hazard but subsequently strike another roadway element. In a study by Ketvirtis (*16*), subjects were given the choice to stop completely, go around, or pass over an object in the roadway; most chose to pass over almost all objects up to 100 mm (4 in.) in height. When the object was 150 mm (6 in.) high, approximately half chose to pass over and half chose to go around the hazard. Most subjects elected to perform an evasive maneuver and go around an object higher than 200 mm (8 in.).

The accidents that occurred because the driver attempted to avoid an object in the roadway were reviewed because they could be related to SSD. These accidents are relevant because they describe drivers' actions when faced with a situation similar to the one described by the SSD model: a driver encountering an unexpected object in the roadway. In State 1, pertinent evasive-action accident categories included: swerved to avoid object, swerved to avoid animal, slowed to avoid object, and slowed to avoid animal. These accidents represented 0.8 percent (1,419 accidents) of the total number of on-system accidents in State 1. Objects were avoided more often on urban roads and animals were avoided more often on rural roads. In State 2, evasive-action accidents were labeled "avoided foreign object" and "avoided animal." These accidents represented approximately 0.06 percent (895 accidents) of all accidents in the data base.

Accident Severity

The severity of the object accidents was determined using severity ratings based on human injury. These severity ratings did not nec-

essarily have a direct correlation to the cause of the accident because the severity could have been influenced by other factors, including the use of seat belts or the size and type of the vehicle. In addition, the accident severity depended on the size of the object struck and the impact location on the vehicle. If the vehicle struck a piece of tire, lost control, and rolled over, then it probably sustained more damage than if it had simply struck the tire and pulled onto the shoulder. The five levels of severity included: no injury, possible injury, nonincapacitating injury, incapacitating injury, and fatality. Low-severity accidents included those in which there was no injury, possible injury, and nonincapacitating injury. Severe-injury accidents included those that resulted in fatalities and incapacitating injuries.

When considering the percentage of accidents resulting in severe injuries for the different types of accidents in State 1, other-object and animal accidents had two of the three lowest percentages of severe injury accidents. In State 2, other-object and animal accidents also had some of the lowest percentages of severe injury accidents. Animal-related accidents had the lowest percentage of injury accidents on rural roads.

To further investigate differences in accident severity, the occupant severity for object-related accidents in State 1 was compared with the occupant severity for all accidents. Table 1 shows that object and animal accidents on rural roads resulted in more low-severity accidents than all other types of accidents in 1990. On urban roads, the percentage of moderate-severity accidents was similar for all types of accidents. These results suggest that accidents with objects or animals on rural roads do not represent the most severe or the most hazardous situations for drivers.

Accident Characteristics

The accident characteristics may have contributed to the cause of the accident; therefore, they offer a comparison of the object-related accidents in this study with all types of accidents. The object-related accidents were an average of the other-object, animal, and evasive-action accidents reviewed from State 1. The characteristics that were reviewed included light, surface, and road conditions; weather; and alignment. Table 1 presents the percentage of accidents that occurred under the given conditions for all accidents and for object-related accidents. The percentages in the tables were an average of all 1990 accidents in State 1. The following situations were chosen for comparison from each accident condition: dry surfaces; clear weather; straight, level alignment; no roadway defects; and dark lighted and unlighted roadways.

A large percentage of object-related accidents occurred in clear weather on dry pavements; therefore, the roadway surface condition was the same for object-related accidents as it was for all accidents. The roadway alignment was also not a significant factor for most object-related accidents; thus, there was not a large difference between all accidents and object-related accidents. In addition, there were slightly fewer roadway defects in object-related accidents than in all accidents.

The light condition was an important contributory factor for the object-related accidents reviewed in this study. On rural and urban roads, approximately 30 to 40 percent more object-related accidents occurred under dark, unlighted conditions. Under dark, lighted conditions on urban roads, there also were more object-related accidents than other types of accidents. Although light conditions may have been important for all types of accidents, it was a more critical feature for accidents involving objects in the road.

RESULTS

The critical situation assumed by AASHTO is that the driver encounters a small unexpected object, recognizes it as a hazard, and then stops within the available SSD. The results of this study discuss the frequency at which these small obstacles result in a reported accident. This section also analyzes the accident conditions as they relate to the SSD critical encounter.

TABLE 1 Comparison of Critical Accident Characteristics in State 1 (by Percentage)

Accident Characteristics	Rural		Urban	
	All Accidents	Object Accidents[a]	All Accidents	Object Accidents[a]
Occupant Severity				
Low Severity	89.2	94.6	95.6	96.2
Light Condition				
Dark Unlit	27.2	70.0	7.4	33.7
Dark Lit	7.7	4.7	20.2	25.1
Surface Condition				
Dry	81.1	85.3	80.5	88.2
Weather				
Clear/Cloudy	86.4	87.7	86.0	90.4
Alignment				
Straight, Level	85.4	89.3	96.6	97.5
Road Condition				
No Defects	89.2	95.5	80.5	92.7

[a] Object-related accidents are an average of other-object, animal, and evasive-action accidents.

TABLE 2 Number of Rural Accidents in State 1 According to Height

Roadway Classification	Object Heights, mm[b]					
	0-50	50-150	150-300	300-450	450-600	> 600
Freeway	4	26	27	19	65	204
Multilane Divided	1	4	3	6	54	185
Multilane Undivided	0	4	4	5	42	176
Two-Lane High	0	8	16	9	129	754
Two-Lane Low	1	9	4	7	304	1091
Summary	6	51	54	46	594	2410
	0.2%	1.6%	1.7%	1.5%	18.8%	76.2%

[a] There were 82,705 rural accidents in the State 1 data base in 1990. This table summarizes other-object, animal, and evasive-action accidents.
[b] 1 inch = 25.4 mm.

Critical Object Heights

The object accident study has considered three types of accidents in which the driver could encounter a situation similar to that assumed by the SSD model: object, animal, and evasive-action. A breakdown of the results of the object heights in State 1 is presented in Tables 2 and 3. When considering all reported accidents in State 1, only 2 percent involved objects or animals; of those 2 percent, less than 4 percent involved an object smaller than 150 mm (6 ins.). More than 96 percent involved objects taller than 150 mm (6 ins.). Therefore, approximately 0.07 percent of the accidents in the State 1 data base involved objects less than 150 mm (6 ins.) high. Similar tables are not presented for State 2 because the accident reports for evasive-action accidents were not available. Thus, the distribution of actual object heights could not be determined.

The study also showed that many of the object-related accidents occurred at night when better roadway geometry would not have improved the drivers' sight distance because their visibility was limited by the headlight illumination distance and not the roadway geometry. Therefore, the only accidents that might be eliminated by increasing SSD would be those that took place during the day. In State 1, the percentage of total accidents involving small objects during the day was only 0.026 percent. Furthermore, it was assumed that a severe injury accident would represent the most critical occurrence to be avoided. The data showed that accidents involving small objects resulted in severe injuries only 0.004 percent of the time.

Considering these percentages, an accident with a small object that occurs in the daylight and results in a severe injury represents less than 0.001 percent of all accidents. In addition, the accident must also occur on or near a curve to apply to the SSD critical situation. Thus, the encounter becomes even less probable because only 0.7 percent of the small-object accidents occurred on vertical or horizontal alignment.

The results of this study were extrapolated to the 11.5 million accidents that occurred in the United States in 1990 (*17*) to determine the number of accidents that might be eliminated by increasing the curve length (i.e., decreasing the object height). Using the preceding percentages there would be approximately 3,000 accidents in the United States in 1 year in which an object 150 mm (6 ins.) or smaller would have been struck during daylight (11.5 million $\times$ 0.00026 = 3,000). Only 460 small object accidents would result in severe occupant injuries (11.5 million $\times$ 0.00004 = 460).

TABLE 3 Number of Urban Accidents in State 1 According to Height

Roadway Classification	Object Heights, mm[b]					
	0-50	50-150	150-300	300-450	450-600	> 600
Freeway	10	59	90	27	107	118
Multilane Divided	0	3	5	1	45	63
Multilane Undivided	1	4	2	2	32	62
Two-Lane High	0	3	1	3	24	50
Two-Lane Low	0	1	1	1	24	35
Summary	11	70	99	34	232	328
	1.4%	9.0%	12.8%	4.4%	30.0%	42.4%

[a] There were 298,741 urban accidents in the State 1 data base in 1990. This table summarizes other-object, animal, and evasive-action accidents.
[b] 1 inch = 25.4 mm.

Thus, the probability of an accident resulting from an encounter with a small object during the day on vertical alignment that caused a severe injury would be quite small.

Roadway Functional Classification

When the accidents were grouped into different roadway classification categories, no significant differences were observed among the types of objects struck in each category. However, some roadway classifications did not have enough data to make general conclusions about all roadways of that type; a future study using larger samples might yield different results.

The roadway classifications did show a difference among the heights of objects struck on rural and urban roads. On urban roads, 10.4 percent of the objects struck were below 150 mm (6 ins.) in height, but on rural roads only 1.8 percent were below 150 mm (6 ins.) in height. The visibility conditions would not explain this difference because urban roadways tend to be better lighted than rural roadways; however, drivers in urban areas may not be able to swerve to avoid an object in their lane because of high traffic volumes or the conditions of the roadway environment outside their lane. Drivers in rural areas with less traffic may have more opportunity to avoid an object. Given that urban and rural areas represent unique environments, perhaps SSD should be related to the area type.

CONCLUSIONS

The objective of this study was to analyze a representative sample of accidents to evaluate the characteristics of objects encountered on the roadway that would affect SSD. Currently, the SSD model uses a 150-mm (6-in.) object as the critical object height. The critical situation is the moment at which the driver detects an object on the roadway as a hazard just in time to stop before striking it. The conclusions, as stated below, do not support the current object height of 150 mm (6-in.) nor the critical situation used in the SSD model.

1. Two percent of all reported accidents involved objects or animals on the roadway, and only 0.07 percent of all reported accidents involved objects or animals less than 150 mm (6 in.) high. Therefore, small objects and animals were not struck often enough to justify their use as the critical encounter in the SSD model.
2. More than 90 percent of the object-related accidents occurred on straight, level roads where the driver's visibility was not limited by the geometry of the roadway. Therefore, available SSD was not a major contributory factor in the object-related accidents.
3. Most of the object-related accidents occurred at night when longer SSD and curve lengths would not necessarily increase the driver's visibility in these situations.
4. More than 95 percent of the accidents studied resulted in low-severity injuries; therefore, a small object is not the most critical, hazardous encounter in the SSD situation.
5. The study results did not substantiate the use of roadway classifications for identifying different critical object heights for different roadway classes; however, the study did suggest a difference in objects struck between roads in rural and urban areas.

The results of this study do not support the continued use of the existing 150-mm (6-in.) object height; therefore, the following recommendations are made.

1. The object height should represent the smallest realistic hazard encountered in the roadway; therefore, it appears that the height should be greater than 150 mm.
2. The taillight height of a vehicle is an object height that is frequently encountered and can be seen during both daytime and nighttime. Future research on the object height should focus on a 380-mm (15-in.) vehicle taillight because it represents a realistic hazard to the driver.
3. Research also should consider the drivers' visual abilities and limitations because the object height should represent an object that the driver can see.

ACKNOWLEDGMENTS

This research was performed at the Texas Transportation Institute, Texas A&M University.

REFERENCES

1. Neuman, T. R., J. C. Glennon and J. E. Leisch. Functional Analysis of Stopping Sight Distance Requirements. In *Transportation Research Record 923,* TRB, National Research Council, Washington, D.C., 1983, pp. 57–64.
2. Hall, J. W., and D. S. Turner. Stopping Sight Distance: Can We See Where We Now Stand? In *Transportation Research Record 1208.* TRB, National Research Council, Washington, D.C., 1988 pp. 4–13.
3. *State of the Art Report 6: Relationship Between Safety and Key Highway Features.* TRB, National Research Council, Washington, D.C., 1987.
4. Woods, D. L. Sensitivity Analysis of the Factors Affecting Highway Vertical Curve Design. Presented at 68th Annual Meeting of the Transportation Research Board, Washington, D.C., Jan. 1989.
5. Blanchard, A. H., and H. B. Drowne. *Text-Book on Highway Engineering,* 1st ed. John Wiley and Sons, New York, 1914.
6. Harger, W. G. *The Location, Grading and Drainage of Highways,* 1st ed. McGraw-Hill, New York, 1921.
7. Gutmann, I. Engineering Sets High Mark on German Superhighways. *Engineering News-Record.* New York, Aug. 1936, pp. 296–297.
8. *A Policy on Sight Distance for Highways.* AASHO, Washington, D.C., 1940.
9. Cron, F. W. Highway Design for Motor Vehicles: A Historical Review, Part 7: The Evolution of Highway Grade Design. *Public Roads,* Vol. 40, No. 2. Sept. 1976, pp. 78–86.
10. *A Policy on Geometric Design of Rural Highways.* AASHO, Washington, D.C., 1954.
11. *A Policy on Geometric Design of Rural Highways.* AASHO, Washington, D.C., 1965.
12. *A Policy on Geometric Design of Highways and Streets.* AASHTO, Washington, D.C., 1984.
13. *A Policy on Geometric Design of Highways and Streets.* AASHTO, Washington, D.C., 1990.
14. Griffin, L. I. III. Estimating the Effectiveness of Occupant Protection Safety Devices From State Accident Data. Prepared for the Conference on the Collection and Analysis of State Highway Safety Data, San Diego, Calif., 1990.
15. Council, F. M., and C. D. Williams. *Guidebook for the HSIS State Data Files.* Highway Safety Information System, FHWA, Washington, D.C., 1991.
16. Ketvirtis, A., and P. J. Cooper. Detection of Critical Size Object as a Criterion for Determining Drivers Visual Needs. Presented at 76th Annual Meeting of the Transportation Research Board, Washington, D.C., Jan. 1977.
17. *Accident Facts, 1991 Edition.* National Safety Council, Chicago, 1991.

Publication of this paper sponsored by Committee on Geometric Design.

Sight Distance on Horizontal Alignments with Continuous Lateral Obstructions

YASSER HASSAN, SAID M. EASA, AND A. O. ABD EL HALIM

For safe and efficient highway operation, sight distance has been of great interest to researchers in the field of highway geometric design. Several formulas have been developed to relate the available sight distance to the horizontal and vertical alignment of the highway and the existing obstructions. Among these formulas is the one presented by (AASHTO) to determine the available sight distance on a simple horizontal curve with a length greater than the sight distance. For shorter curves in which the sight distance is greater than the curve length, other methods have been developed. However, none of these methods considered the case of continuous lateral obstructions or complicated horizontal alignments. Consequently, it has been recommended that the available sight distance be checked graphically or in the field. For this study, general analytical procedures were developed to check the available sight distance on horizontal alignments with single and continuous obstructions. A horizontal alignment may consist of any combination of horizontal components, such as straight segments, circular curves, and spiral curves. Based on the analytical procedure, a computer software program was developed to establish the no-passing zones on two-lane highways, according to the specifications used by the Ministry of Transportation of Ontario, Canada. The developed procedures and computer software proved to be very accurate. Using them would save time and effort and would avoid possible human errors when the sight distance is checked using current graphical or field techniques. The computer software can also be used to develop design tables and charts for the available sight distance on different horizontal alignments.

Sight distance is vital for safe and efficient highway operation. The driver must be able to see ahead a distance sufficient for stopping to avoid hitting an unexpected object on the roadway. Moreover, it is recommended that the design of two-lane rural highways should provide drivers with a sight distance sufficient to pass slower vehicles. In many cases, however, the sight distance is restricted to a certain length. On horizontal curves, the driver's sight line may be limited by lateral objects such as trees, buildings, and cut slopes. On crest vertical curves, the sight line may be limited by the vertical curve itself. Also, sight distance on sag vertical curves may be limited to the farthest point covered by the vehicle's headlight beam. Therefore, the designer must check the available sight distance against the required stopping site distance (SSD) or decision site distance (DSD) on any highway, and the passing site distance (PSD) on two-lane rural highways.

For horizontal curves, many models have been developed to relate the available sight distance to the lateral clearance. Among these models is the one presented by the AASHTO for the case of $S \leq L$, where S is the sight distance on the curve and L is the curve length (*1*). Although this formula is easy and direct, it is "of limited practical value except on long curves" (*1*). Therefore, AASHTO recommends that "the designer must use graphical methods to check sight distance on horizontal curves" (*1*).

Y. Hassan and A. O. Abd El Halim, Department of Civil Engineering, Carleton University, Ottawa, Ontario K1S 5B6, Canada. S. M. Easa, Department of Civil Engineering, Lakehead University, Thunder Bay, Ontario PTB SE1, Canada.

The other case in which the sight distance is greater than the curve length has been studied by many researchers. Neuman and Glennon (*2*), Waissi and Cleveland (*3*), Berg et al. (*4*), and Easa (*5*) developed different methods to check the required lateral clearance on simple horizontal curves. Easa (*6,7*) also studied the case of a single lateral obstruction on compound and reverse curves and developed other formulas to relate the lateral clearance to the available sight distance. None of these methods has considered the case of continuous obstructions. According to the standards of the Manual of Uniform Traffic Control Devices (MUTCD), which is used by the Ministry of Transportation of Ontario (MTO), Canada, for establishing the no-passing zones (*8*), the available sight distance for drivers in the inside lane is limited by a continuous obstruction represented by a theoretical 3 m wide shoulder. Continuous obstructions also may be encountered because of cut slopes.

For this study, general analytical methods were developed to evaluate sight distance on horizontal alignments for both cases of continuous and single obstructions. The terms "horizontal alignment" and "horizontal curve" refer to any combination of horizontal highway components, such as straight segments, circular curves, or clothoid spiral curves. A computer software program was developed to determine the available sight distance and, in turn, the no-passing zones on two-lane rural highways according to the standards of MUTCD used by MTO.

THEORETICAL DEVELOPMENT

This study examines available sight distance (which may be SSD, DSD, or PSD) on general horizontal curves consisting of any combination of straight segments, circular curves, and spiral curves. Figure 1 shows some of the cases of horizontal alignments that are covered in this report. More complicated alignments that can be encountered on actual highways are also covered in this paper.

Continuous Obstruction: General Procedures

Assuming a constant lane width and lateral clearance, the continuous obstruction will be parallel to and have the same geometry of the highway centerline; the sight distance will be restricted by having the sight line tangent to the obstruction. The point of tangency may be located on a circular curve, spiral curve, or the point of intersection of two successive straight segments without curves. The following sections present general procedures that can be used to determine the available sight distance, regardless of the components of the horizontal curve. Relationships are then presented for the special alignments of intersecting long tangents without a curve and for the simple circular curve.

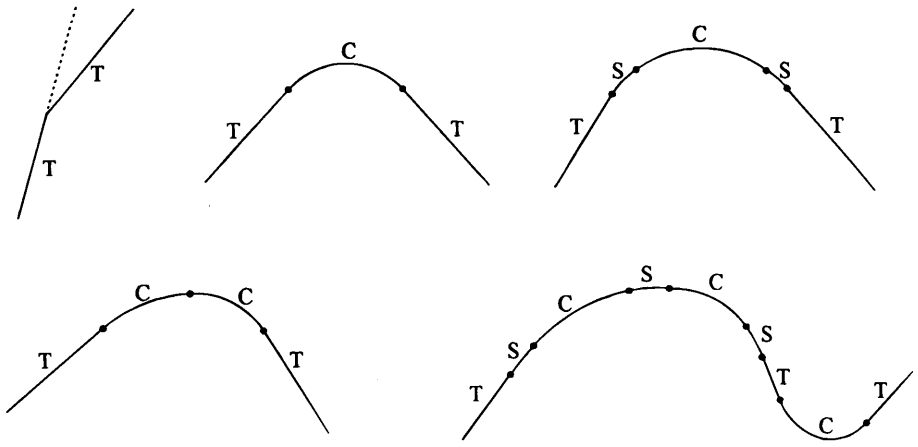

FIGURE 1 Examples of possible horizontal alignments.

In the following sections, the azimuth of the lines, defined as the angle from the north direction to the line, measured clockwise, is referred to as Φ. Also, the east and north coordinates of the points are referred to as (x, y), respectively. However, because it is the relative positioning of the points to each other (not the absolute positions) that determines the available sight distance, the coordinates and azimuths can be taken relative to any reference point and direction. In all of the following derivations, the lateral clearance between the obstruction and the center of the lane is assumed to be constant and is referred to as m.

Sight Line Tangent to a Circular Curve

In this case, the obstruction restricting the sight line is a circular curve, as shown in Figure 2. In general, the beginning and the end of the sight line may be positioned on any horizontal highway segment (a straight or circular segment or a spiral curve). The general procedure developed for this study is iterative, the sight distance is initially assumed as S. Then S is checked and decreased or increased until the sight line becomes tangent to the obstruction. The procedure involves the following steps:

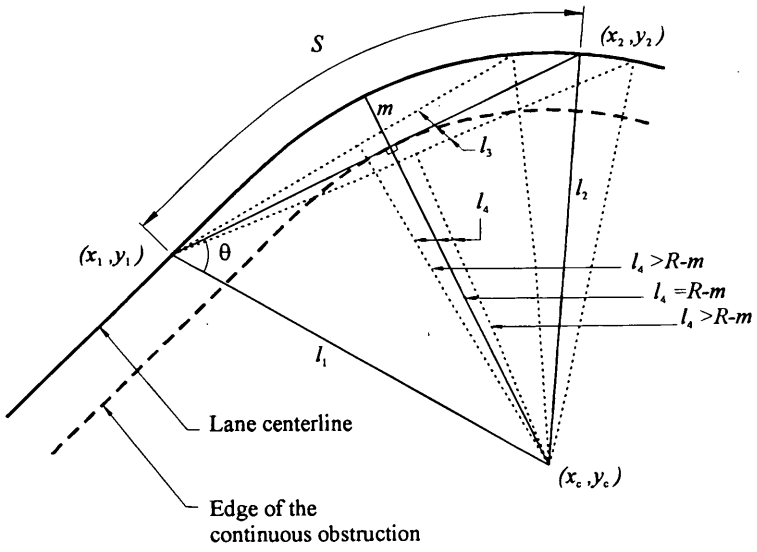

FIGURE 2 General procedure: Sight line tangent to circular curve (continuous obstruction).

1. Determine the coordinates of the beginning of the sight line and the center of the curve (x_1, y_1) and (x_c, y_c), respectively.
2. Calculate the length l_1 as

$$l_1 = [(x_1 - x_c)^2 + (y_1 - y_c)^2]^{1/2} \quad (1)$$

3. Determine the coordinates of the end of the sight line (x_2, y_2).
4. Calculate l_2 and l_3 similar to l_1.
5. From the basics of trigonometry, l_1, l_2, l_3, and θ can be related by the following equation:

$$l_2^2 = l_1^2 + l_3^2 - 2\, l_1\, l_3 \cos\theta \quad (2)$$

or

$$\theta = \cos^{-1}\left(\frac{l_1^2 + l_3^2 - l_2^2}{2\, l_1\, l_3}\right) \quad (3)$$

6. Calculate the length l_4 as

$$l_4 = l_1 \sin\theta \quad (4)$$

7. If $l_4 < R\text{-}m$, S is greater than the actual sight distance. Decrease S and repeat Steps 3 to 6.
8. If $l_4 > R\text{-}m$, S is less than the actual sight distance. Increase S and repeat Steps 3 to 6.
9. If $l_4 = R\text{-}m$, S is equal to the actual sight distance. End iterations.

Although the lengths l_1, l_2, and l_3 can be calculated without using the coordinates, a unique sequence of calculations is required for each possible combination of horizontal segments.

On the other hand, using the coordinates of the points makes the procedure applicable regardless of the positions of the beginning and end of the sight line and also makes it very easy for computer programming.

Sight Line Tangent to Spiral Curve

Generally, a spiral curve is a curve with varying radius, beginning with a straight segment ($R \rightarrow \infty$); as the curve's length increases, the corresponding radius decreases. Many mathematical formulas can be used to represent spiral curves and may be found in mathematics textbooks, such as in *Survey of Applicable Mathematics* (*9*). Among these formulas, Euler's spiral, known as the clothoid spiral, is the most commonly used in road design (*1,10*). Defining l as segment length of a spiral curve beginning with a straight segment R as the corresponding radius and δ as the deflection angle of this segment in radian, Euler's spiral is formulated as follows:

$$A^2 = l * R = \frac{l^2}{2\,\delta} = R^2 * 2\delta \quad (5)$$

where A is the spiral parameter.

As illustrated in Figures 3 and 4, this case is similar to the previous case, but the obstruction restricting the sight line is a spiral curve. The beginning and the end of the sight line may be positioned on any horizontal highway segment (straight or circular segment or spiral curve). In this case, three iterative procedures were developed, any of which can be used to determine the available sight distance (*11*). Only the first procedure is presented because, as will be shown later, the same technique can be used for the case of a single obstruction. The procedure involves the following steps:

1. Determine the coordinates of the beginning of the sight line (x_1, y_1).

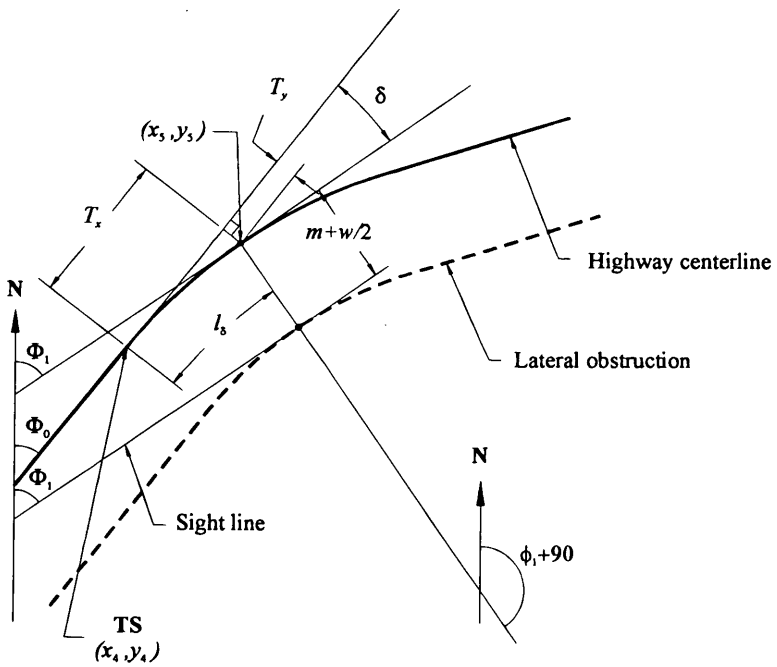

FIGURE 3 Coordinate determination involving spiral curves.

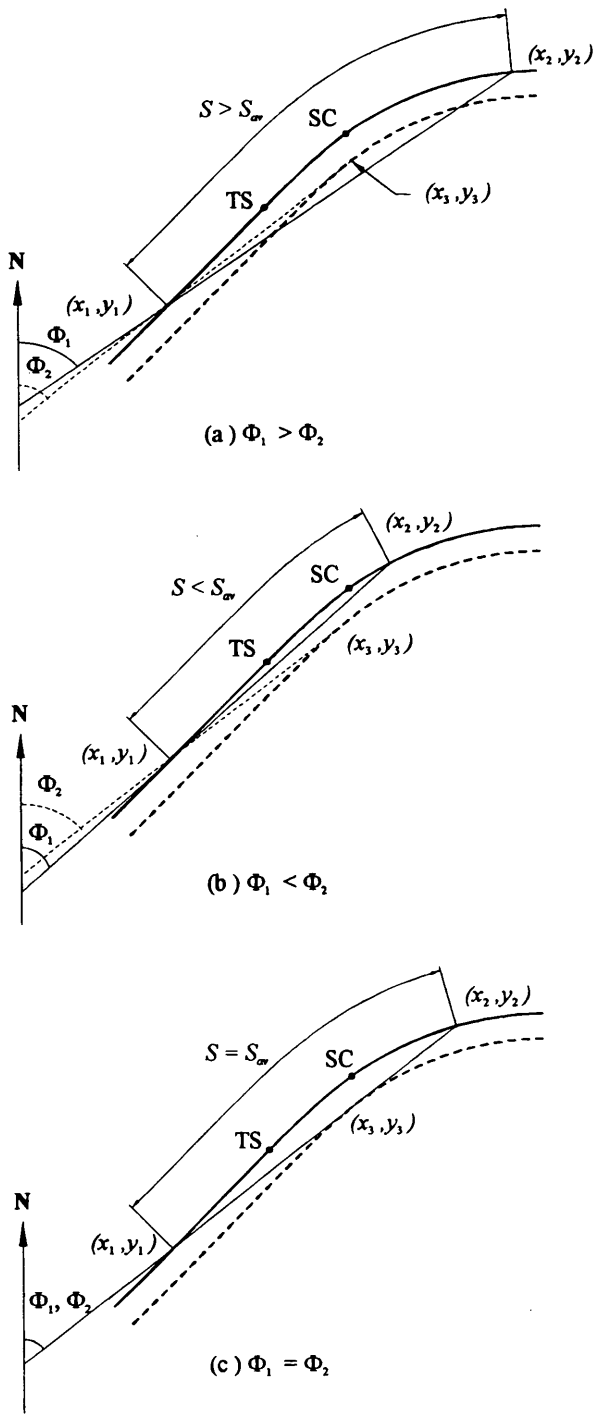

FIGURE 4 General procedure: Sight line tangent to spiral curve (continuous obstruction).

2. Determine the coordinates of the end of the sight line (x_2, y_2).
3. Calculate the azimuth of the sight line, Φ_1, as

$$\Phi_1 = \tan^{-1}\left(\frac{x_2 - x_1}{y_2 - y_1}\right) \tag{6}$$

4. Knowing the azimuth of the tangent to the spiral, Φ_0, determine the coordinates of the point of tangency of a line having an azimuth Φ_1 and the given obstruction, (x_3, y_3). For right-turn spirals beginning with a straight segment, (x_3, y_3) can be determined by considering another point, (x_5, y_5), defined as the point of tangency of a line having an azimuth Φ_1 and the highway's centerline. As shown in Figure 3, the coordinates (x_5, y_5) can be determined as follows

$$\delta = (\Phi_1 - \Phi_0) \times \frac{\pi}{180°} \tag{7}$$

Using the spiral formula presented in Equation 5,

$$l_\delta = A \times \sqrt{2\delta} \tag{8}$$

From the general characteristics of Euler's spiral (*9*),

$$T_x = A\sqrt{2\delta}\left(1 - \frac{\delta^2}{5 * 2!} + \frac{\delta^4}{9 * 4!} - \frac{\delta^6}{13 * 6!} + \ldots\right)$$

$$\approx l_\delta - \frac{l_\delta\,\delta^2}{10} \tag{9}$$

$$T_y = A\sqrt{2\delta}\left(\frac{\delta}{3} - \frac{\delta^3}{7 * 3!} + \frac{\delta^5}{11 * 5!} - \ldots\right) \approx \frac{l_\delta\,\delta}{3} \tag{10}$$

Defining (x_4, y_4) as the coordinates of the tangent-spiral (TS) point on the centerline of the highway, then

$$x_5 = x_4 + T_x \sin\Phi_0 + T_y \cos\Phi_0 \tag{11}$$

$$y_5 = y_4 + T_x \cos\Phi_0 - T_y \sin\Phi_0 \tag{12}$$

Defining w as the lane width, the line from (x_5, y_5) to (x_3, y_3) will have an azimuth of $\Phi_1 + 90°$ and a length of $m + w/2$. Therefore, (x_3, y_3) can be calculated as follows:

$$x_3 = x_5 + (m + w/2)\sin(\Phi_1 + 90°) \tag{13}$$

$$y_3 = y_5 + (m + w/2)\cos(\Phi_1 + 90°) \tag{14}$$

5. Calculate the azimuth of the line between Points 1 and 3, Φ_2.
6. For right-turn curves, if $\Phi_1 > \Phi_2$ (if $\Phi_1 < \Phi_2$, for left-turn curves), S is greater than the actual sight distance (see Figure 4 for illustration). Decrease S and repeat Steps 2 to 5.
7. For right-turn curves, if $\Phi_1 < \Phi_2$ (if $\Phi_1 > \Phi_2$, for left-turn curves), S is less than the actual sight distance (see Figure 4 for illustration). Increase S and repeat Steps 2 to 5.
8. If $\Phi_1 = \Phi_2$, S is equal to the actual sight distance (see Figure 4 for illustration). End iterations.

Because the azimuth is always less than 360 degrees, some caution is required in the last check if for right-turn curves, Φ_1 is slightly greater than zero and Φ_2 is slightly less than 360 degrees (or if Φ_2 is slightly greater than zero and Φ_1 is slightly less than 360 degrees for left-turn curves). For example, for right-turn curves, if Φ_2 is slightly less than 360 degrees, and S is greater than the available sight distance, Φ_1 may be slightly greater than zero. In this case, S should be decreased and another iteration is required.

Continuous Obstruction: Special Cases

The following procedures present closed-form solutions derived for the special alignments of intersecting two long straight segments without a curve and for the simple circular curve.

Intersecting Straight Segments Without a Curve

In this case, only two long straight segments are intersecting with a small deflection angle, as shown in Figure 1. Although no circular or spiral curves are involved in this case, it represents a possible horizontal alignment and therefore was considered in this paper. In general, the beginning and the end of the sight line may be located on any horizontal highway segment. However, the straight segments in this case are usually long enough for the beginning and the end of the sight line to be located on the two intersecting straight segments. Therefore, only this case is presented; other cases can be found elsewhere *(11)*.

Figure 5 presents two straight segments with a deflection angle Δ. The driver is at a distance l_1 from the point of intersection (PI). As shown the sight line will touch the continuous obstruction at its PI. From Figure 5,

$$l_3 = m/\tan\frac{180° - \Delta}{2} \tag{15}$$

$$\alpha = \tan^{-1}[m/(l_1 - l_3)] \tag{16}$$

$$\beta = \Delta - \alpha \tag{17}$$

$$l_2 = l_1 \sin\alpha/\sin\beta \tag{18}$$

Then, the available sight distance is

$$S = l_1 + l_2 \tag{19}$$

Simple Circular Curve

In this case, the horizontal curve consists of a simple circular curve, having a radius, R, with two straight segments (tangents) at the two ends. Obviously, the sight line can only be restricted by touching a circular curved obstruction. Therefore, the general procedure presented previously can be applied. However, other closed-form relationships were developed for this special case to determine the available sight distance more easily and accurately. These formulas can be considered extensions to the work of Easa (*5*), which considered only a single (or multiple) lateral obstruction.

For the case of a simple curve, there are four possibilities for the beginning and the end of the sight line touching the obstruction:

1. Sight line begins on first tangent and ends on curve.
2. Sight line begins on first tangent and ends on second tangent.
3. Sight line begins and ends on curve.
4. Sight line begins on curve and ends on second tangent.

Case 1: Sight Line Begins on First Tangent and Ends on Curve As presented in Figure 6

$$l_2 = (R^2 + l_1^2)^{1/2} \tag{20}$$

where l_1 is the distance between the river and the point of curve (PC).

$$\delta_1 = \tan^{-1}(l_1/R) \tag{21}$$

$$\delta_2 = \cos^{-1}\left(\frac{R - m}{l_2}\right) \tag{22}$$

$$\delta_3 = \cos^{-1}\left(1 - \frac{m}{R}\right) \tag{23}$$

$$\Delta_1 = \delta_2 + \delta_3 - \delta_1 \tag{24}$$

Then, the available sight distance is

$$S = l_1 + R\,\Delta_1 \times \frac{\pi}{180°} \tag{25}$$

Case (2): Sight Line Begins on First Tangent and Ends on Second Tangent As shown in Figure 6, δ_1 and δ_2 can be determined as in Case (1). Defining Δ as the total deflection angle of the curve, then

$$\delta_3 = \Delta + \delta_1 - \delta_2 \tag{26}$$

$$m_2 = [R^2 + (R-m)^2 - 2R\,(R - m)\cos\delta_3]^{1/2} \tag{27}$$

$$\theta_1 = \sin^{-1}(R\sin\delta_3/m_2) \tag{28}$$

$$\theta_2 = \sin^{-1}[(R - m)\sin\delta_3/m_2] \tag{29}$$

As shown in Figure 6, the angle α is in a triangle whose other two angles are $(\theta_1 - 90°)$ and $(\theta_2 + 90°)$. Therefore,

$$\alpha = 180° - \theta_1 - \theta_2 \tag{30}$$

$$l_4 = m_2 \sin(\theta_1 - 90°)/\sin\alpha \tag{31}$$

Then, the available sight distance is

$$S = l_1 + R\,\Delta \times \frac{\pi}{180°} + l_4 \tag{32}$$

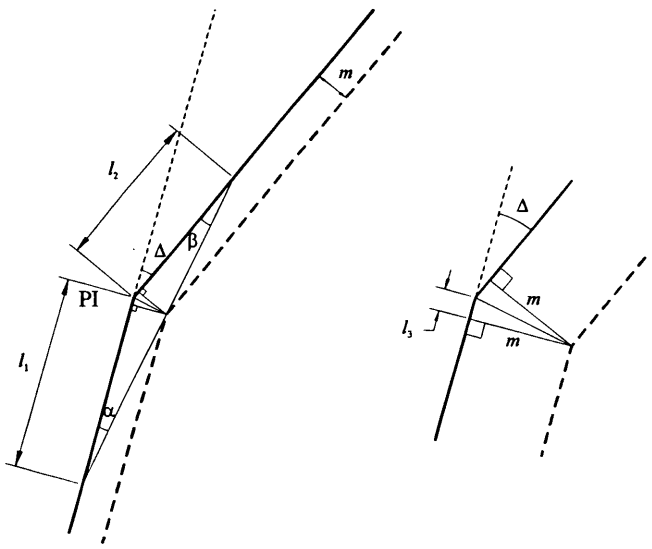

FIGURE 5 Special case: Intersecting straight segments without curves (continuous obstruction).

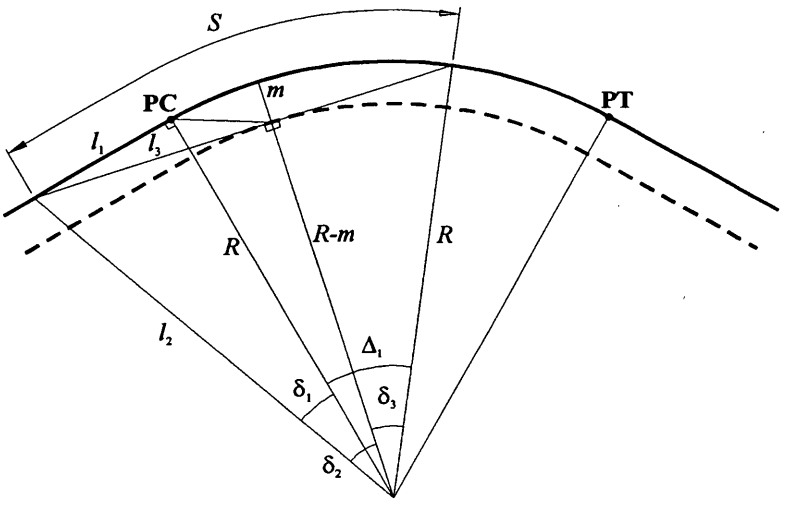

Sight Line Begins on Tangent and Ends on Curve.

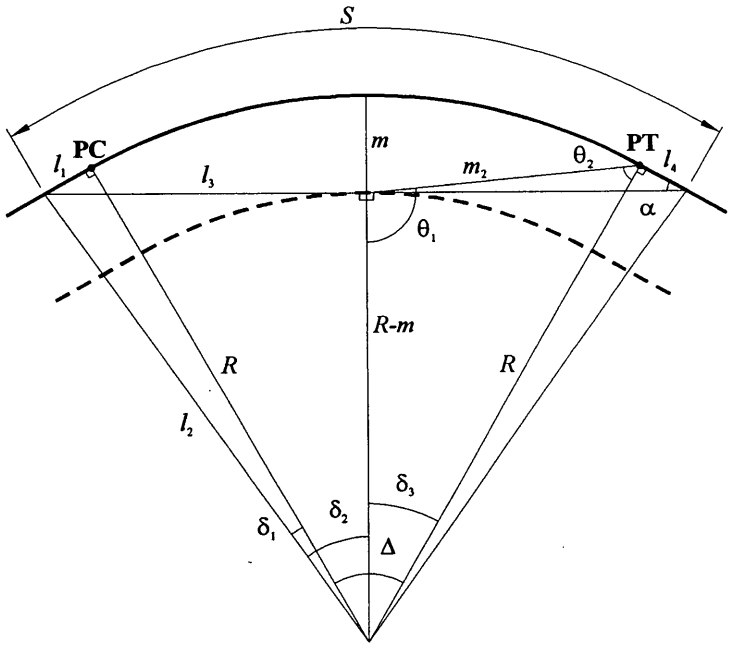

Sight Line Begins and Ends on Tangents.

FIGURE 6 Special case: Simple circular curve (continuous obstruction).

Case (3): Sight Line Begins and Ends on Curve In this case, the formula presented by AASHTO (*1*) can be applied as follows:

$$S = 2R \times \cos^{-1}(1 - m/R) \times \frac{\pi}{180^\circ} \quad (33)$$

Case 4: Sight Line Begins on Curve and Ends on Second Tangent The relationships involved in this case (*11*) are backward derivations for Case (1) and, therefore will not be presented.

Single Obstruction

As previously mentioned, the case of a single obstruction has been extensively studied. Formulas relating the available sight distance to the lateral clearance on simple horizontal curves already exist. For this study a general iterative procedure was developed to check the available sight distance regardless of the components of the horizontal curve or the positions of the beginning and end of the sight line. The procedure uses the azimuths of the lines in a way similar to the procedure of the continuous obstruction, with the sight line tangent to a spiral curve. However, in this case, the coordinates of the obstruction are directly used instead of using the point of tangency (x_3, y_3).

COMPUTER SOFTWARE PROGRAM FOR NO-PASSING ZONES

The theoretical procedures previously presented were translated to a computer software program written in Microsoft Quick Basic, which

determines the available passing sight distance and no-passing zones on two-lane highways. The software uses the MUTCD standards for no-passing zones, which are used by the MTO (*8*). In these standards, lateral obstructions on the two lanes are considered differently. On the inside lane, defined as the lane nearer to the center(s) of the curve(s), the driver's sight line is always limited by the edge of a theoretical shoulder 3 m wide. On the other hand, the sight line of drivers on the outside lane can cross the right-of-way and is limited only by any existing lateral obstruction. For both lanes, the sight distance is measured along the centerline of the lane. The sight line of a driver on the outside lane obviously does not cross the lane on which the driver travels, and the driver sees the entire opposing lane. For this reason, the sight line would be limited by existing obstructions. For a driver on the inside lane, however, the sight line crosses the lane on which the driver travels, and part of the opposing lane may be hidden from the driver's view. In this case, the edge of a 3-meter theoretical shoulder is considered an obstruction to confine the sight line near the traveled way and to improve the visual conditions for the passing driver.

For the inside lane, the program uses the previous special relationships for continuous obstructions, if applicable, to calculate the available sight distance. If, because of the geometry of the curves, these relationships are not applicable, the program uses the general procedures for continuous obstructions to determine the available sight distance. However, the program was designed to interpret the alignment data specified by the user in the form of the station and the radius at each point between two horizontal segments ($R = 0$ is used to specify straight segments). The program determines whether the special or the general procedures will be used, generates the parameters required in either case, and determines the available sight distance. The width of the theoretical shoulder is a variable specified by the user.

For the outside lane, lateral obstructions are defined by the user as an input to the program; they may be continuous or single obstructions. Continuous obstructions are treated exactly as in the case of the inside lane, for single obstructions, the program uses only the general procedures to determine the available sight distance. In the case of more than one obstruction, the program will check the available sight distance against each obstruction and determine the minimum available sight distance.

For both lanes, the user specifies the minimum sight distance, S_m, required to be checked. If the available sight distance is less than S_m, the program determines the available sight distance, S_{av}, every user-specified incremental step, STEP, and for a user-specified accuracy, ACC. The values of S_m, STEP, and ACC are defined by the user in the input file, which also contains the alignment and obstructions data. If S_{av} is greater than or equal to S_m, the current station will be skipped, and the available sight distance at the next station will be checked. It should be noted that S_m need not be taken at exactly the minimum required PSD for the highway of interest. It is better to specify a greater value for S_m so the user has a better idea about the change of S_{av} on the highway. The user can then establish the marking of the no-passing zones manually according to the actual value of the minimum required PSD.

Program Verification

The developed methods and program were verified by comparing the results obtained by the software with those obtained graphically for numerical examples having alignments similar to those shown in Figure 1. The parameters specified for the program were as follows: S_m = 250 m, STEP = 20 m, and ACC = 0.1 m. The actual available sight distances were determined by drawing the same curves using Auto-Computer Assisted Design (AutoCAD). Then, the available sight distances on the inside lane were determined by drawing sight lines tangent to the theoretical shoulder. On the outside lane, the sight lines were drawn passing through certain obstructions input in to the program. The results obtained by the program for all cases were in very good agreement with those obtained graphically (*11*).

APPLICATION EXAMPLE

The developed computer program was applied to a two-lane stretch on Highway 17 in Ontario to check the available sight distance and to establish no-passing zones. The lane width was 3.75 m and the speed limit was 90 kph. As shown in Figure 7 and Table 1, the stretch contained two curves; each was a circular curve with two spirals. The alignments before the first curve and after the second curve were assumed to be straight segments.

According to the MUTCD specifications used by MTO, the minimum required PSD is 300 m for a 90-kph speed (*8*). This required sight distance is much less than the corresponding distances required by AASHTO (*1*) and the Roads and Transportation Association of Canada (RTAC) (*10*). However, based on a model of the kinematic relationships among the passing, passed, and opposing vehicles, Harwood and Glennon (*12*) agreed with the MUTCD criteria for PSD for a passenger car passing a passenger car. In passing maneuvers involving trucks, the required PSD was greater than that recommended by MUTCD but less than that recommended by AASHTO. Based on this discussion and because the highway is supervised by the MTO, the 300-m minimum PSD was adopted for establishing the no-passing zones. Also, because of the lack of information about single obstructions for the outside lane, the no-passing zones were established for the continuous obstruction represented by the 3-m theoretical shoulder only.

The parameters for the program were: S_m = 300 m, STEP = 5 m, and ACC = 0.1 m. Table 2 shows a sample of the program output, which gives the sight distance less than S_m. Because of the large number of stations having S_{av} less than S_m, the results presented in Table 2 are given for both lanes every 50 m. In Figure 8, the available PSD on both lanes was also plotted against the highway stations to show the variation of the available PSD caused by the existing horizontal alignment. The appropriate marking for passing is also given in Figure 8.

DESIGN VALUES FOR SPECIAL ALIGNMENTS

For design purposes, the computer program was used to determine the available PSD on the inside lane of two-lane highways because of the horizontal alignment, according to MTO specifications. Three types of horizontal alignments were considered: simple curves, simple curves with spirals, and compound curves. Assuming a lane width of 3.5 m and therefore a lateral clearance (m) of 4.75 m, the available sight distance for the three alignments was determined every 5 m and to an accuracy of 0.1 m. Then, the minimum S_{av} on each alignment was given and was rounded to the nearest lower integer (see Tables 3–5 for different values of the curve radius R and the deflection angle Δ).

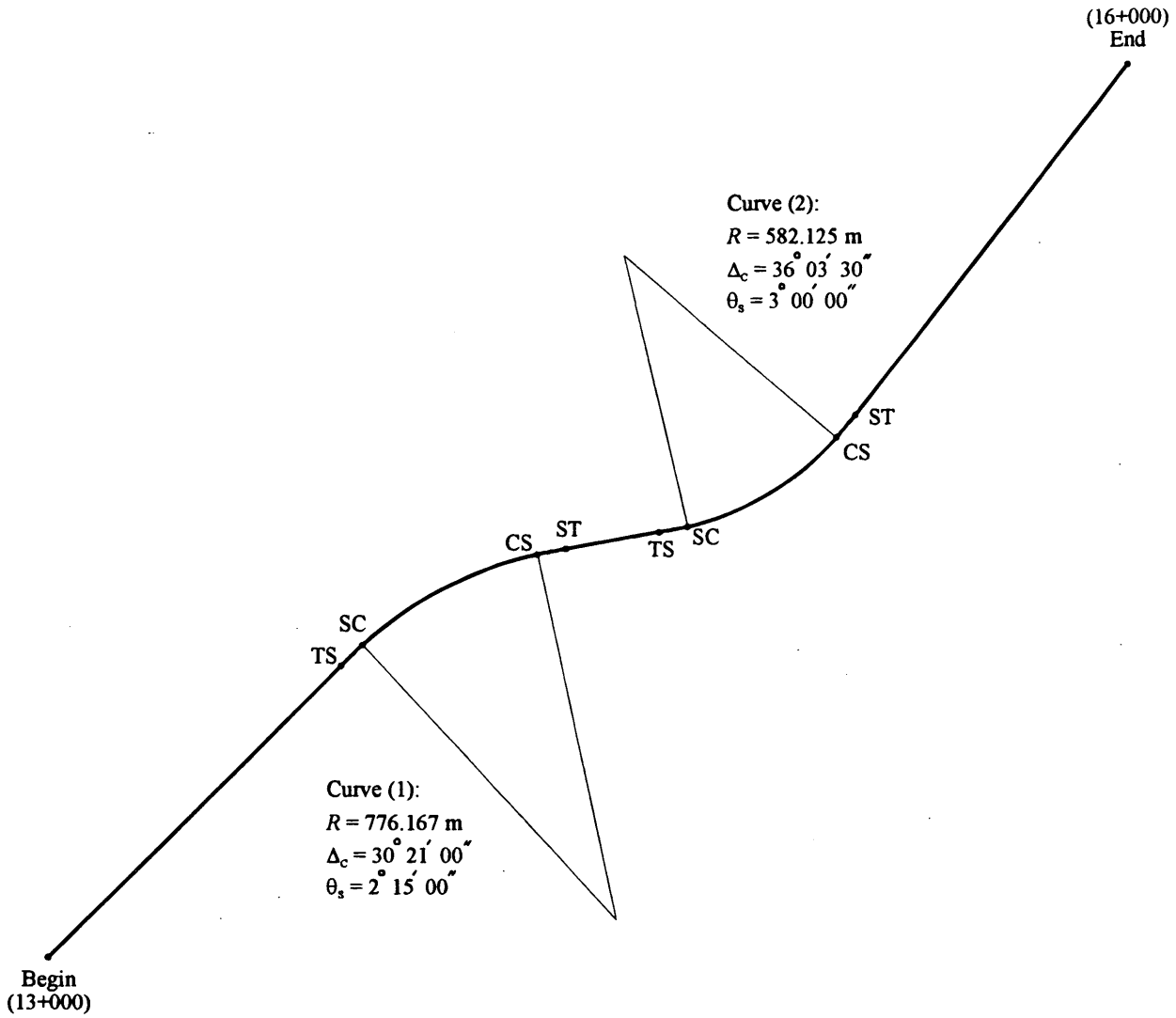

FIGURE 7 Horizontal alignment of the stretch example (Highway 17).

In the first alignment, a simple circular curve, the only variables are R and Δ. Table 3 shows the range used for each variable. In the second alignment, a circular curve with spirals, the spiral parameter, A, is used. The value of A usually depends on the value of R, the design speed, and the maximum superelevation rate. An example of the design values of A is the specifications given by RTAC (*10*). However, because of the differences in the specifications used by different jurisdictions, ideally, values of S_{av} for various R should be given for different values of A. However, when comparing the results in Tables 4 and 5, the change of A from zero (which corresponds to the simple curve) to 200 m resulted in a change in S_{av} ranging from less than 0.1 to about 5 percent. This would suggest that the spiral parameter has a minor effect on the available sight distance. In this study, however, the value of A was set at 200 m to present a sample of the possible design tables that can be produced using the developed computer program. Finally, the parameters associated with the third alignment, a compound curve, are the radii of the two circular curves, R_1 and R_2, and the deflection angle of each curve, Δ_1 and Δ_2. The ratio of R_2/R_1 was set as 1.5, which is the value suggested by AASHTO (*1*) for open highways, and the values of Δ_1 and Δ_2 have the range given in Table 5.

Tables 3 to 5 represent a sample of the design tables that can be developed to determine the PSD on horizontal alignments. For example, if the alignment is a curve with spirals having R = 1000 m, A = 200 m, and Δ = 6°, the available PSD on the inside lane is 236 m, compared with 195 m given by the AASHTO formula.

Tables 3 to 5 also show that, for the same radius, as the angle of deflection increases the curve length increases and the available sight distance approaches the value given in Equation 33. Each curve has a deflection angle beyond which the curve is long enough for Equation 33 to be applicable, and S_{av} will no longer depend on Δ. Applying the AASHTO formula of Equation 33 will considerably underestimate the available sight distance for short curves.

TABLE 1 Horizontal Alignment of Example Highway Stretch

Station[a]	Coordinates[b]		Point Identification[c]
	North	East	
13 + 000.000	4000.000	4000.000	Begin
13 + 857.769	4606.534	4606.534	TS
13 + 918.729	4649.068	4650.197	SC
14 + 329.870	4837.172	5010.389	CS
14 + 390.830	4848.699	5070.245	ST
14 + 588.673	4883.564	5264.992	TS
14 + 649.633	4895.351	5324.794	SC
15 + 015.986	5081.903	5633.081	CS
15 + 076.946	5129.412	5671.268	ST
16 + 000.000	5858.850	6236.907	End

[a] Station 13 + 000 means a point at a distance of 13,000 m from the point of zero chainage, and so on.
[b] the coordinates of the first point and the azimuth of the first segment were assumed as (4000, 4000) m and 45°, respectively.
[c] TS = point of Tangent to Spiral.
SC = point of Spiral to Curve.
CS = point of Curve to Spiral.
TS = point of Spiral to Tangent.

CONCLUSIONS

General analytical procedures to determine the available sight distance on horizontal alignments with single or continuous obstructions were presented. These procedures, along with the developed computer program, can replace the current graphical technique recommended by AASHTO or the field technique used by the MTO to determine the available sight distance, when sight distance is restricted only by the horizontal alignment.

As an application to the no-passing zones according to the specifications of MUTCD, it was shown that the AASHTO formula extremely underestimates the available sight distance when sight distance is greater than the curve length. Therefore, a sample of design tables was developed using the developed procedures and

TABLE 2 Sample of Computer Software Program Output for Example Highway Stretch

Right Lane[a]		Left Lane[a]	
Station	S_{av}	Station	S_{av}
13 + 700	293.6	14 + 750	154.6
13 + 750	249.7	14 + 800	148.6
13 + 800	210.4	14 + 850	148.6
13 + 850	181.7	14 + 900	148.6
13 + 900	172.2	14 + 950	148.6
13 + 950	171.6	15 + 000	148.6
14 + 000	171.6	15 + 050	150.4
14 + 050	171.6	15 + 100	167.8
14 + 100	171.6	15 + 150	203.2
14 + 150	171.6	15 + 200	246.0
14 + 200	174.8	15 + 250	291.6
14 + 250	255.9		

[a] The right and left lanes are relative to a driver travelling in the direction of increasing stations.

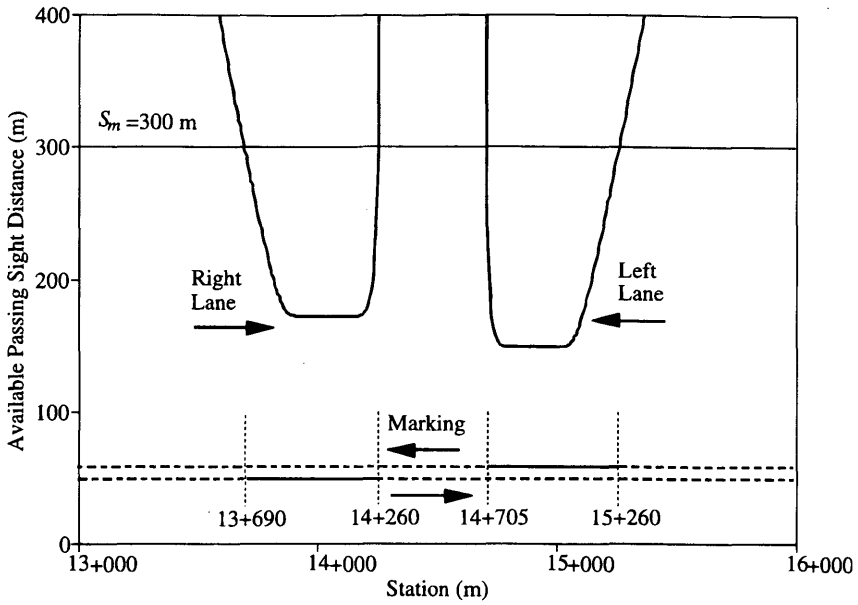

FIGURE 8 Available PSD and corresponding marking for the stretch example.

computer program. The tables can be easily used to check the available PSD on some horizontal alignments, such as simple curves, curves with spirals, and compound curves. For complicated alignments, the program can be used directly to determine the available passing sight distance faster, more conveniently, and more accurately than the techniques now in use.

ACKNOWLEDGMENTS

The authors thank Dennis Siczkar of the MTO, Thunder Bay District, for his support and thoughtful comments during this project. The financial support of the Natural Sciences and Engineering Research Council of Canada is also gratefully acknowledged.

TABLE 3 Available Sight Distance on Simple Horizontal Curves (Continuous Obstruction, m = 4.75 m)

R (m)	S_{av} (m)					
	Δ^a					AASHTO Formula[b]
	2°	4°	6°	8°	10°	
200	547	279	191	150	126	87
400	551	286	202	164	143	123
600	554	293	212	178	161	151
800	558	300	223	191	178	174
1000	561	307	233	205	196	195
1200	565	314	244	219	213	213
1400	568	321	254	233	230	230
1600	572	328	265	247	246	246
1800	575	335	275	261	261	261
2000	579	342	286	275	275	275

[a] Δ = deflection angle of the curve.
[b] See Equation 33.

TABLE 4 Available Sight Distance on Horizontal Curves with Spirals (Continuous Obstruction, A = 200 m, m = 4.75 m)

R (m)	S_{av} (m)					
	Δ^a					AASHTO Formula[b]
	2°	4°	6°	8°	10°	
600	N/A	N/A	N/A	187	168	151
800	N/A	307	228	195	181	174
1000	N/A	310	236	208	197	195
1200	569	316	245	221	214	213
1400	571	322	255	234	230	230
1600	574	329	266	248	246	246
1800	577	335	276	262	261	261
2000	580	342	286	275	275	275

[a] Δ = total deflection angle of the circular curve and the two spirals.
N/A = Not Applicable (the required length of the circular curve ≤ zero).

[b] See Equation 33.

TABLE 5 Available Sight Distance on Compound Horizontal Curves (Continuous Obstruction, R_2/R_1 = 1.5, m = 4.75 m)

Δ_1	Δ_2	S_{av} (m)				
		R_1 (m)				
		400	800	1200	1600	2000
2°	2°	289	307	324	341	359
	4°	210	239	268	297	326
	6°	176	216	256	294	326
	8°	160	211	256	294	326
4°	2°	204	228	251	274	297
	4°	171	205	240	270	297
	6°	155	202	240	270	297
	8°	149	202	240	270	297
6°	2°	165	195	225	254	280
	4°	149	189	224	254	280
	6°	143	189	224	254	280
	8°	142	189	224	254	280
8°	2°	145	181	216	247	275
	4°	137	181	216	247	275
	6°	135	181	216	247	275
	8°	135	181	216	247	275
AASHTO Formula[a]		123	174	213	246	275

[a] See Equation 33.

REFERENCES

1. AASHTO. *A Policy on Geometric Design of Highways and Streets.* AASHTO, Washington, D.C., 1990.
2. Neuman, T. R., and J. C. Glennon. Cost-Effectiveness of Improvements to Stopping Sight Distance. In *Transportation Research Record 923,* TRB, National Research Council, Washington, D.C., 1984.
3. Waissi, G. R., and D. E. Cleveland. Sight Distance Relationships Involving Horizontal Curves. In *Transportation Research Record 1122,* TRB, National Research Council, Washington, D.C., 1987.
4. Berg, W. D., J. Choi, and E. J. Kuipers. Development of Highway Alignment Information from Photolog Data. In *Transportation Research Record 1239,* TRB, National Research Council, Washington, D.C., 1989.
5. Easa, S. M. Lateral Clearance to Vision Obstacles on Horizontal Curves. In *Transportation Research Record 1303,* TRB, National Research Council, Washington, D.C., 1991.
6. Easa, S. M. Lateral Clearance Needs on Compound Horizontal Curves. *ASCE, Journal of Transportation Engineering,* Vol. 119, No. 1, Jan./Feb. 1993, pp. 111–123.
7. Easa, S. M. Design Considerations for Highway Reverse Curves. In *Transportation Research Record,* TRB, National Research Council, Washington, D.C., 1994 (in press).
8. *Manual of Uniform Traffic Control Devices.* Ministry of Transportation of Ontario, Downsview, Ontario, Canada, 1992.
9. Rektorys, K., ed. *Survey of Applicable Mathematics.* M.I.T. Press, Cambridge Mass., 1969.
10. Roads and Transportation Association of Canada. *Manual of Geometric Design Standards for Canadian Roads.* Roads and Transportation Association of Canada, Ottawa, Canada, 1986.
11. Hassan, Y., S. M. Easa, and A. O. Abd El Halim. *User's Guide of MARKH: A Program for Establishing No-Passing Zones on Two-Lane Highways due to Horizontal Alignment,* Research Report LU-TRC-RR-94-1. Transportation Research Center, Lakehead University, Thunder Bay, Ontario, Canada 1994.
12. Harwood, D. W., and J. C. Glennon. Passing Sight Distance Design for Passenger Cars and Trucks. In *Transportation Research Record 1208,* TRB, National Research Council, Washington, D.C., 1989.

Publication of this paper sponsored by Committee on Geometric Design.

Slotted Rail Guardrail Terminal

KING K. MAK, ROGER P. BLIGH, HAYES E. ROSS, JR., AND DEAN L. SICKING

A slotted rail terminal (SRT) for W-beam guardrails was successfully developed and crash-tested in accordance with requirements set forth in NCHRP Report 230. The SRT design is intended as a retrofit or replacement of the standard breakaway cable terminal (BCT) and has better impact performance than the eccentric loader terminal and the modified eccentric loader terminal. The slotted rail concept involves cutting three longitudinal 12.7 mm (½ in.) wide slots into the W-beam rail, one at each peak and valley in the cross section, to reduce the buckling strength while maintaining the tensile capacity. The reduced buckling strength of the slotted rail allows for controlled buckling of the rail, which greatly reduces the yaw rate of the impacting vehicle, thereby minimizing the potential for the buckled rail to directly contact or penetrate the occupant compartment. The SRT terminal is expected to be less sensitive to installation details because the buckling of the rail is controlled by the slots and is at a force level substantially lower than the unmodified W-beam rail. A slot guard is attached to the downstream end of each set of slots to prevent extension of the slots and rupture of the rail. To help reduce inventory and control cost, the SRT terminal uses many of the standard components used with the BCT and other flared terminals. In addition, the layout and configuration of the SRT terminal is similar to that of the standard BCT terminal to facilitate easy retrofit.

The development of crashworthy guardrail end terminals has long been a problem for the roadside safety community. Early guardrails were constructed with untreated stand-up ends, resulting in catastrophic accidents in which rail elements speared and impaled impacting vehicles. Considerable efforts have been undertaken in recent years to develop crashworthy guardrail terminals with good success. Existing safety end treatments for W-beam guardrails include: turndown, breakaway cable terminal (BCT), eccentric loader terminal (ELT), modified eccentric loader terminal (MELT), CAT, SENTRE, BRAKEMASTER, and the ET-2000.

The turndown end terminal is the least expensive of all the end treatments and has been used extensively in several states. However, it has been found that the turndown end terminals could cause impacting vehicles to ramp up and vault over the end treatment, often resulting in rollovers. For this reason, the FHWA has ruled that turndown guardrail end terminals can no longer be installed along high-speed, high-volume federal-aid highways (*1*).

Since its conception and initial testing in 1972, the BCT terminal has become the most widely used W-beam end treatment. The BCT terminal is designed to cause the W-beam rail to "gate," or buckle out of the way of an impacting vehicle, and to allow the vehicle to penetrate behind the guardrail in a controlled manner. However, because the design relies on the dynamic buckling of the W-beam rail, the impact performance of the BCT is very sensitive to installation details, such as barrier flare rate and end offset. Unfortunately, the flare rate and end offset of BCT terminals are not always installed correctly and, consequently, the BCT terminal does not have a favorable service history. Furthermore, even when installed correctly, the BCT terminal has been shown to impart unacceptably high deceleration forces on 817-kg (1,800-lb) minisize vehicles during 96.6-km/hr (60 mph) impacts and has failed to meet the evaluation criteria set forth in NCHRP Report 230 (*2*). The FHWA has recently ruled that BCT terminals will no longer be acceptable for installation along high-speed, high-volume roadways on the national highway system (*3*).

The ELT and MELT terminals are improvements over the standard BCT system. The designs are still based on the "gating" concept and rely on the dynamic buckling of the W-beam rail for energy dissipation and controlled penetration. These end treatments have been successfully crash-tested in accordance with NCHRP Report 230 requirements with a flare offset of 1.22 m (4 ft) (*4*). When tested with a 457-mm (18-in.) offset, the ELT exhibited only marginally acceptable results. Like the standard BCT terminal, the ELT and MELT terminals are sensitive to installation details, and the added complexity of their designs has posed problems in field installations.

Other end treatments, such as the CAT, SENTRE, BRAKEMASTER, and ET-2000, rely on some form of energy attenuation to decelerate impacting vehicles to a safe and controlled stop. These end treatments are considerably more expensive compared with the flared terminals, such as the BCT, ELT, and MELT, and together they comprise only a small percentage of the terminals currently in use.

The slotted rail terminal (SRT) presented in this study is intended as a relatively inexpensive retrofit, or replacement, for the standard BCT terminal. Two designs have been developed based on the slotted rail concept: one intended for use on high-speed (96.6 km/hr or 60 mph) highways (5) and the other for lower-speed roadways with speed limits of 72.4 km/hr (45 mph) or less (*6*). This study presents only the design and evaluation results of the 96.6-km/hr (60-mph) SRT terminal. Development of the SRT designs began in 1992 and was completed in the spring of 1994. The terminal was tested and evaluated in accordance with NCHRP Report 230 criteria. (*2*)

DESIGN CONSIDERATIONS

The SRT terminal is intended as a retrofit and replacement to the BCT terminal, therefore, its design is based on the same gating concept. The BCT, ELT, and MELT terminals all rely on the dynamic buckling of the W-beam rail, which requires a high force level and which is difficult to control in terms of location and manner of buckling. In small car, off-center, head-on impacts with these terminals, the high buckling force caused the vehicle to yaw at a high rate, exposing the occupant compartment of the vehicle to the buckled rail. Thus, the major considerations in the design of the SRT terminal were controlling the dynamic buckling of the W-beam rail and reducing the yaw rate of the impacting vehicle to minimize the potential for the buckled rail to penetrate the occupant compartment.

K. K. Mak, R. P. Bligh, and H. E. Ross, Jr., Texas Transportation Institute, Texas A&M University, College Station, Tex. 77843. D. L. Sicking, Midwest Roadside Safety Facility, University of Nebraska-Lincoln, Lincoln, Nebr. 68588–0531.

Another consideration in the design of the SRT terminal was the ease of retrofit for the standard BCT terminal. The SRT terminal should use as many standard BCT terminal components as possible and have a similar configuration and layout. The impact performance of the BCT, ELT, and MELT terminals are known to be very sensitive to installation details. One of the considerations in the design of the SRT terminal was to reduce the sensitivity of the impact performance to installation details, thus allowing for more latitude and margin of error in case the terminal is not installed exactly according to design.

Costs associated with the terminal were also a major consideration. Most guardrail installations are rarely, if ever, subjected to an impact, and the benefits of even greatly improved impact performance are often not sufficient to justify high terminal costs. Experience has shown that high construction and maintenance costs have prevented the widespread implementation of crashworthy barrier terminals. The SRT terminal is designed to keep the cost of installation and maintenance low and therefore comparable with the costs of the ELT and MELT terminals.

The primary considerations in the development of the slotted rail terminal were to:

- Meet nationally recognized safety standards (*2*),
- Provide controlled dynamic buckling of the W-beam rail,
- Reduce the potential for impact or penetration of the occupant compartment by the buckled rail,
- Be suitable for retrofit of the BCT terminal, and
- Be inexpensive and easy to install and maintain.

SLOTTED RAIL TERMINAL CONCEPT

The slotted rail concept, previously developed at the Texas Transportation Institute as part of another study (*7*), involves cutting longitudinal slots in the W-beam rail to reduce its dynamic buckling strength sufficiently to safely accommodate small car end-on impacts while maintaining adequate capacity to contain and redirect vehicles impacting beyond the length of need. As shown in Figure 1, the W-beam rail cross section can be cut into four relatively flat segments by placing a longitudinal slot at each peak and valley in the cross section. The three 12.7mm (½ in.) wide longitudinal slots reduce the cross-sectional area in the slotted region from 1,284 to 1,181 mm^2 (1.99 to 1.83 in.^{2}), which is still greater than the cross-sectional area of 1,039 mm^2 (1.61 in.^{2}) through the four bolt holes at a splice. Thus, the tensile capacity of the W-beam is not compromised because the tensile capacity of the W-beam rail at the slotted segments is greater than that at a splice.

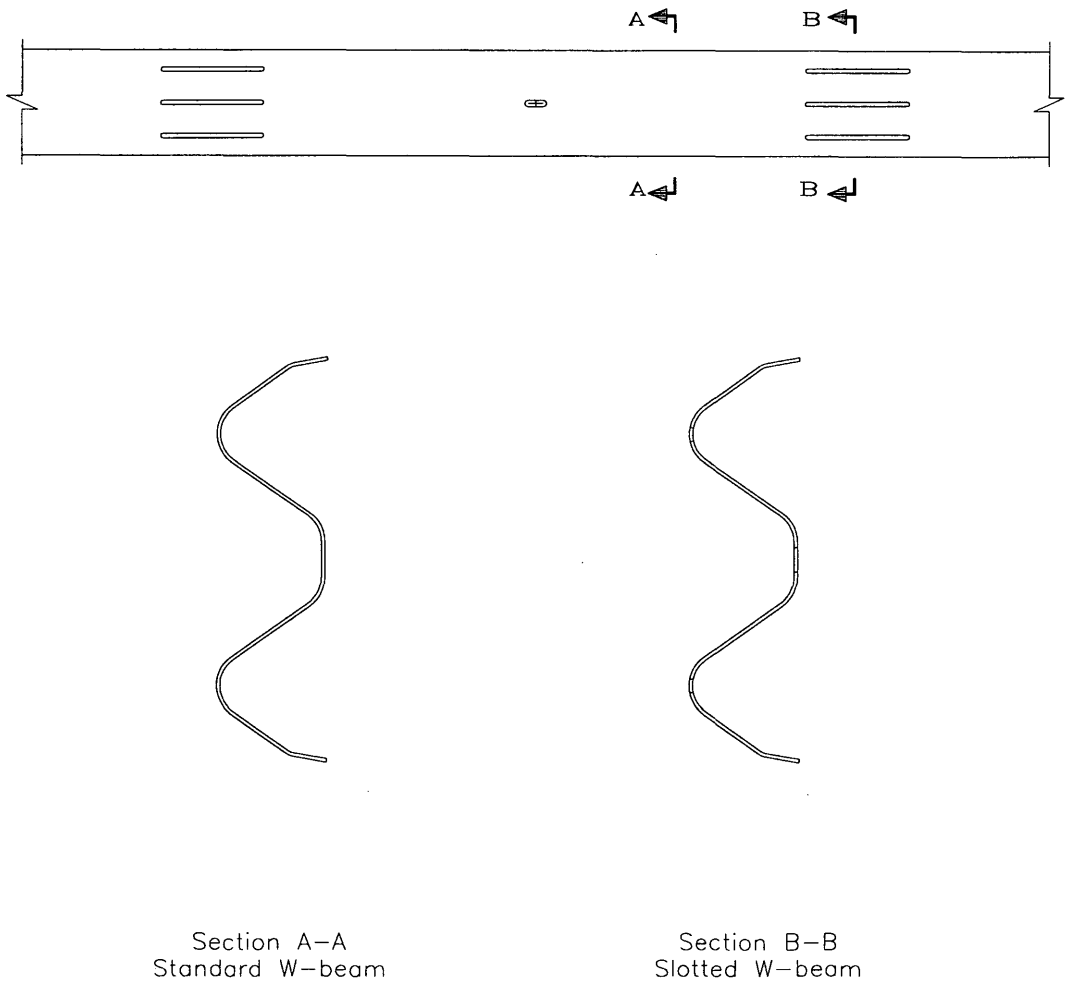

FIGURE 1 Schematic of slot configuration.

On the other hand, the moment of inertia of the W-beam rail is significantly reduced by the presence of the slots. The moment of inertia of an unmodified, 12-gauge W-beam rail is approximately 97×10^4 mm^4 (2.33 in.^{4}). In comparison, the combined moments of inertia of the four relatively flat segments is only 8,325 mm^4 (0.02 in.^{4}). Thus, the buckling strength of a slotted W-beam cross section is only 1 percent of that of an unmodified cross section. The reduced buckling strength of the slotted W-beam allows for controlled, predictable buckling of the rail.

In one of the early developmental crash tests of the slotted rail concept, it was found that intrusion of parts of the impacting vehicle into the slots could lead to tearing, ripping, and extending of one of the slots until it reached a splice, at which point the W-beam rail would rupture and allow the vehicle to penetrate through the guardrail. To alleviate this potential problem, slot guards are attached to the W-beam rail at the downstream ends of each set of slots. The slot guard both reinforces the W-beam rail and provides a 45-degree deflector plate to push the rail away from any vehicle component that may intrude into the slots.

Pendulum tests were conducted to determine the dynamic buckling strength of the slotted W-beam rail, the results of which are summarized in Table 1. Energy dissipation from buckling and collapsing of the slots showed little variation when the slot length was varied from 305 mm to 1.52 m (12 to 60 in.). The same is true for the peak deceleration. Additionally, the slot guard was found to have minimal effect on the buckling and collapsing behavior of the slots or on the peak deceleration or the energy dissipation characteristics of the slotted rail.

In selecting the slot lengths for use with the SRT terminal, consideration was given to the separation of the impulses caused from the buckling of each set in order to minimize the yaw rate of the small car during offset, end-on impacts. This separation of the impulses is provided by the collapsing of the slots after buckling has been initiated. Additionally, it is desirable to select the length and location of the slots such that each set of slots buckles individually and sequentially. Slot lengths that are too short may not provide the desired separation between the buckling impulses. On the other hand, slot lengths that are too long may increase the potential for the bumper or other parts of the impacting vehicle to intrude into the slots. After some consideration, slot lengths of 305 mm (12 in.) and 686 mm (27 in.) were selected for use with the SRT terminal design.

SLOTTED RAIL TERMINAL DESIGN

Figure 2 presents details of the design of the SRT terminal, and Figure 3 includes photographs of the terminal. Brief descriptions of the major components of the SRT terminal design are as follows.

Five sets of slots are used over the first 7.62 m (25 ft) of rail, which may consist of one 7.62-m (25-ft) section or two 3.81-m (12-ft 6-in.) sections of W-beam rail. The slots of the first set are 0.69 m (27 in.) long and are located between Posts 1 and 2. The slots of the second set are 305 mm (12 in.) long and are located at Post 2. The slots of the third set are 0.69 m (27 in.) long and are located between Posts 2 and 3. The slots of the fourth and fifth sets are both 305 mm (12 in.) long and are located between Posts 4 and 5 and between Posts 6 and 7, respectively.

The reason for using longer slots for the first and third sets of slots is to provide longer strokes after initial buckling of these slots,

TABLE 1 Summary of Pendulum Test Results

Slot Length mm (in.)	Slot Guard	Energy Dissipation, KJ (kip-ft)	
		Initial	@ Displacement = 1.22 m (4 ft)
305 (12)	No	12.5 (9.3)	25.4 (18.7)
381 (15)	No	11.8 (8.7)	19.4 (14.3)
457 (18)	No	13.2 (9.7)	25.1 (18.5)
610 (24)	No	11.3 (8.3)	17.1 (12.6)
914 (36)	No	8.9 (6.6)	21.4 (15.8)
1219 (48)	No	11.7 (8.6)	26.3 (19.4)
1524 (60)	No	10.7 (7.9)	18.7 (13.8)
305 (12)	Slot Guard	11.8 (8.7)	31.5 (23.2)
381 (15)	Slot Guard	11.3 (8.3)	N/A
457 (18)	Slot Guard	12.9 (9.5)	28.2 (20.8)

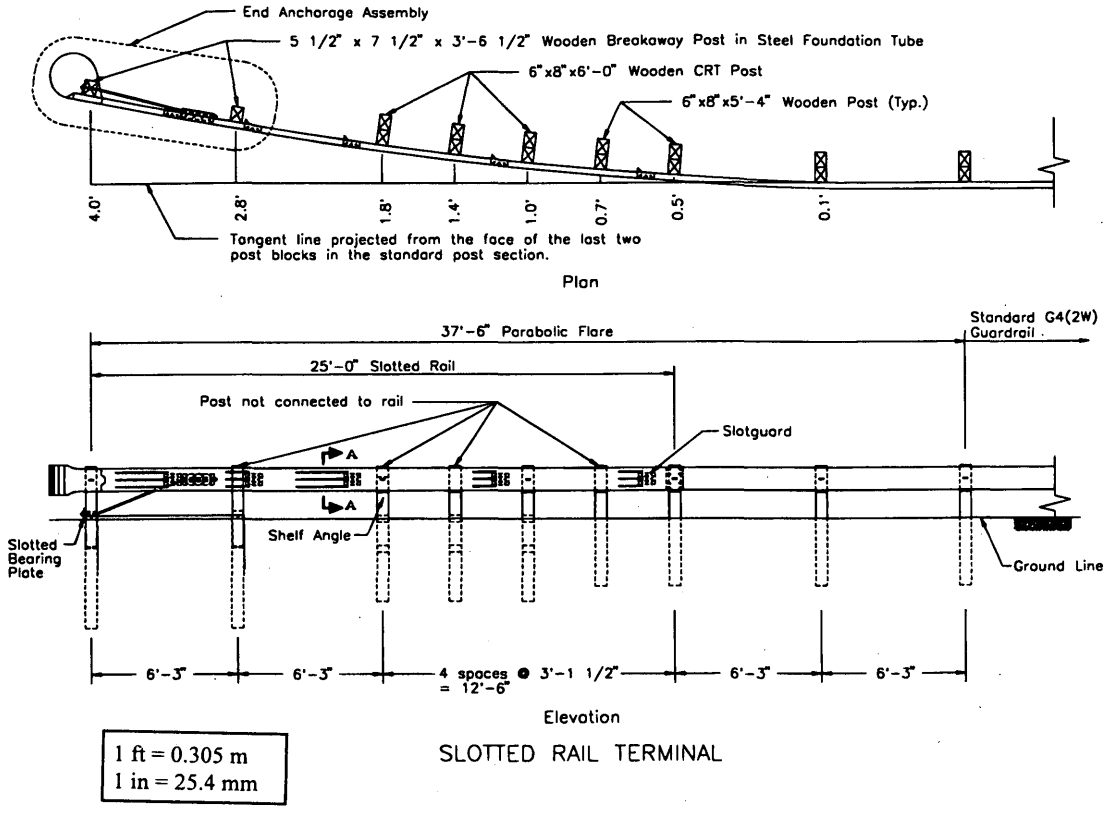

FIGURE 2 Schematic of SRT design.

which helps separate the impulses and reduce the yaw rate of the vehicle in the early stages of impact. The second set of slots at Post 2 is intended to facilitate bending or buckling of the rail at Post 2, thereby reducing the length of the W-beam column created between the first and third set of slots. Shorter slots are used for the fourth and fifth sets of slots (*a*) to reduce the potential for the bumper or other parts of the impacting vehicle to protrude into the slots during redirectional impacts and (*b*) to stiffen the end terminal for large vehicle end-on impacts.

Bolt-on slot guards are attached to the W-beam rail at the downstream end of each set of slots to prevent the bumper or other parts of the impacting vehicle from intruding into and extending the slots. The slot guard reinforces the W-beam rail and provides a 45-degree deflector plate to push the rail away from any vehicle component that may intrude into the slots.

The end anchorage system is similar to that of the ELT and MELT terminals. Two steel foundation tubes connected with a ground channel strut provide the required anchorage capacity. A BCT cable anchorage assembly is attached to the W-beam rail at one end and is anchored through a hole in the base of the wooden end post. A buffered end section, similar to that used with the BCT terminal, is attached to the end of the slotted rail section to distribute the impact load.

A slotted bearing plate is used to distribute the forces in the cable to the wooden end post and foundation tube. The standard bearing plate arrangement used with the BCT cable assembly does not allow the bearing plate to separate from the cable after the wooden end post is broken from impact by the vehicle. Tests have shown that the bearing plate, after releasing from the wooden end post, can potentially be thrown up underneath the vehicle and become caught on the undercarriage. This restrains the forward movement of the vehicle resulting in the vehicle yawing rapidly and coming to an abrupt stop. To eliminate this potential problem, a slotted configuration is incorporated into the bearing plate so the bearing plate can separate from the cable if the wooden end post breaks. To keep the cable anchor bearing plate from being displaced from its proper position should the cable become slack, two lag screws, or bent nails, are used to secure the bearing plate to the wooden end post.

A parabolic flare with an end offset of 1.22 m (4 ft) is used, identical to that used with the BCT terminal. The first five posts (Posts 1–5) are wooden breakaway posts. Posts 1 and 2 are placed in foundation tubes, and Posts 3, 4, and 5 are controlled release terminal (CRT) posts. Standard wooden or steel guardrail posts are then used from Post 6 on. A post spacing of 1.91 m (6 ft 3 in.) is used with the first two spans, followed by four spans of 0.95 m (3 ft 1½ in.) post spacing. The rest of the end terminal section and the standard length-of-need section use the standard 1.91 m (6 ft, 3 in.) post spacing. The W-beam rail is not bolted to Posts 2, 3, 4, or 6. A shelf angle is added at Post 3 to provide intermediate support to the rail between Posts 1 and 5.

COMPLIANCE TESTING

According to guidelines presented in NCHRP Report 230, four compliance crash tests are required to evaluate the performance of

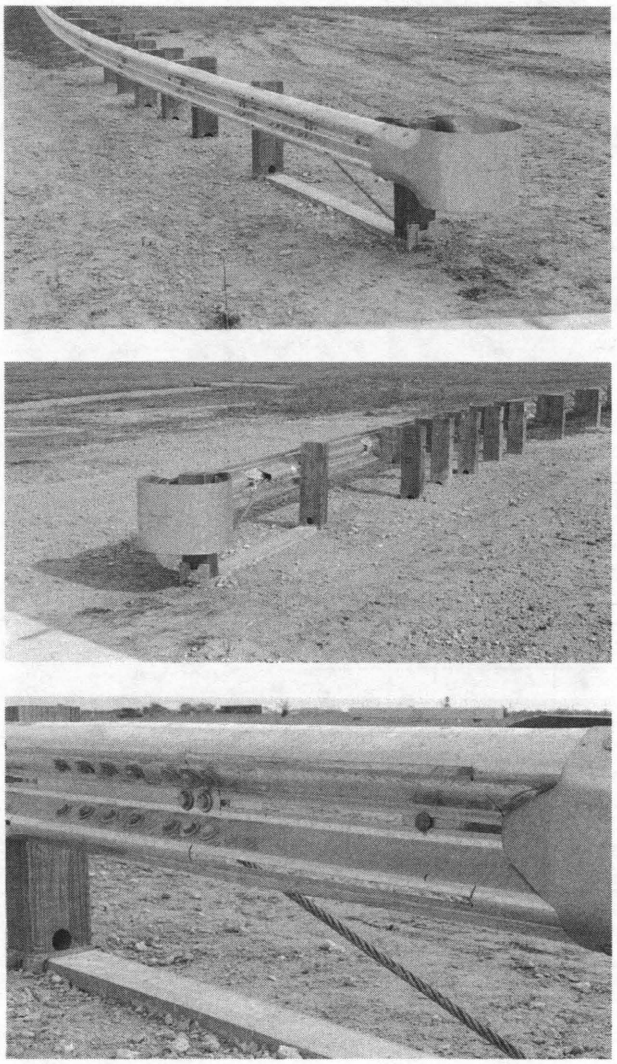

FIGURE 3 Photographs of SRT.

a barrier end terminal design. To evaluate the performance of this SRT terminal design, only three of the four compliance crash tests were deemed necessary. The small car redirective test was considered unnecessary because this crash test was successfully conducted with other BCT-type terminal designs with similar flares and end offsets, and the modifications made to the SRT terminal design should not affect the stability of the vehicle or occupant risk factors for this test. The FHWA agreed with this assessment.

The SRT terminal successfully passed all three recommended crash tests as summarized in Table 2. Sequential photographs for each of the tests are presented in Figure 4.

Large Car Length-of-Need Test

The first compliance crash test involved a 1981 Cadillac Sedan weighing 2,041 kg (4,500 lb) and impacting the test installation at the beginning of length-of-need, which was selected to be at Post 3, or 3.81 m (12.5 ft) downstream from the nose of the terminal. At impact, the test vehicle was traveling at a speed of 91.7 km/hr (57.0 mph) and at an angle of 22.5 degrees relative to the length-of-need section and 30.3 degrees relative to the terminal section. The usual objective of this test is to evaluate the structural adequacy of the guardrail and terminal anchorage. An additional objective of this test was to evaluate the effectiveness of the slot guard in preventing the slots from being extended and thereby resulting in penetration of the vehicle through the W-beam rail.

The impacting vehicle was contained and smoothly redirected by the terminal. All occupant risk factors were well within the recommended limits in NCHRP Report 230. The test vehicle remained upright and stable throughout the test. As shown in Figure 5, damage to the guardrail was moderate considering the severity of the impact. The foundation tube at Post 1 was displaced longitudinally 50.8 mm (2 in.). Posts 3–5 were broken off at ground level, and Posts 6 and 7 were split along their longitudinal axis. The rail element was damaged and partially flattened in the impact area. The maximum dynamic deflection of the rail was 1.0 m (3.3 ft), and the maximum permanent deflection was 0.8 m (2.7 ft), located approximately midspan of Posts 5 and 6. Damage to the vehicle, shown in Figure 5, also was moderate, concentrated at the right front quarter. Maximum crush was 340 mm (13.4 in.) at the right front corner of the vehicle. There was no deformation or intrusion into the occupant compartment.

The vehicle was in contact with the installation for 7.9 m (26.0 ft). The vehicle exited the installation at a speed of 39.2 km/hr (24.4 mph) and at an angle of 15.1 degrees. The vehicle came to rest 26.2 m (86.0 ft) downstream from the initial point of impact and 4.6 m (15 ft) in front of the installation. The change in velocity of the vehicle was 52.5 km/hr (32.6 mph) and the exit angle was 15.1 degrees, these are higher than the recommended limit of 24.1 km/hr (15 mph) and 60 percent of the impact angle (13.5 degrees). However, vehicle trajectory after loss of contact with the guardrail indicated that the vehicle would not have posed a hazard to adjacent traffic.

The major concern with this test was the potential for the vehicle bumper or other parts of the vehicle to intrude into the slots and tear or rip the rail. The slot guard was specifically designed to prevent this. Results of this crash test demonstrated that the slot guards perform as designed in preventing the slots from being torn or ripped apart.

Small Car Head-On Test

The second compliance test involved an end-on impact by a 1988 Chevrolet Sprint, weighing 817 kg (1,800 lb). The test vehicle hit the terminal at a speed of 99.4 km/hr (61.8 mph) and at an angle of 0 degrees relative to the tangent of the length-of-need section. The centerline of the vehicle was offset 381 mm (15.0 in.) toward the traffic face from the centerline of the wooden end post. This orientation will cause the vehicle to rotate clockwise into the rail, maximizing the potential for the buckled rail to hit and penetrate the occupant compartment of the impacting vehicle. In addition to vehicle trajectory, the primary objective of this test was to evaluate occupant risk for small car, end-on impacts.

On impact, the end post (Post 1) was fractured at ground level, releasing the cable anchor mechanism as designed. The vehicle was smoothly decelerated as it proceeded forward, buckling the first, third, and fourth sets of slots and breaking Posts 1–5 at ground level. The vehicle first yawed clockwise and then began to yaw counterclockwise, apparently the result of the left front tire or undercarriage of the vehicle engaging some of the broken posts and debris. The vehicle lost contact with the installation near Post 6,

TABLE 2 Summary of Compliance Crash Test Results

Description		Large Car, Redirection Test	Small Car, Head-On Test	Large Car, Head-On Test
Vehicle Weight		2,043 kg (4,500 lb)	817 kg (1,800 lb)	2,043 kg (4,500 lb)
Impact Conditions	Speed	91.7 km/h (57.0 mph)	99.4 km/h (61.8 mph)	97.6 km/h (60.6 mph)
	Angle	22.5 deg.	0	0
	Offset	N/A	381 mm (15 in.)	0
Exit Conditions	Speed	39.2 km/h (24.4 mph)	37.5 km/h (23.3 mph)	83.1 km/h (51.7 mph)
	Angle	15.1 deg.	15.6 deg.	2.3 deg.
Total Length of Contact		7.9 m (26.0 ft)	9.1 m (30.0 ft)	9.5 m (31.3 ft)
Maximum Dynamic Deflection		1.0 m (3.3 ft)	7.5 m (24.5 ft)	7.6 m (24.9 ft)
Occupant Impact Velocity	Longitudinal	8.1 m/s (26.7 ft/s)	8.4 m/s (27.4 ft/s)	3.8 m/s (12.5 ft/s)
	Lateral	4.6 m/s (15.0 ft/s)	2.6 m/s (8.6 ft/s)	No Contact
Ridedown Acceleration	Longitudinal	-10.3 g	-9.4 g	-6.7 g
	Lateral	-10.8 g	13.5 g	No Contact

traveling at a speed of 37.5 km/hr (23.3 mph) and at an angle of 15.6 degrees relative to the tangent section and was still yawing in a counterclockwise direction. The vehicle came to rest behind the rail facing Post 11, 16 m (52.5 ft) downstream from the point of impact and oriented 120 degrees from the vehicle's initial direction of travel.

The terminal performed as designed, first smoothly decelerating the vehicle and then allowing the vehicle to penetrate behind the guardrail in a controlled manner. As a result of the low buckling strength of the slotted rail, the vehicle exhibited a minimal amount of yaw during the impact sequence. Thus, even though an elbow was formed at the third set of slots of the buckled rail, the orientation of the vehicle was such that it merely sideswiped the slot guard on the back side of the rail, resulting in minor damage to the left rear door. All occupant risk factors were well within the recommended limits in NCHRP Report 230. The occupant impact velocity in the longitudinal direction was 8.4 m/sec (27.4 ft/sec), which is less than the design value of 9.1 m/sec, (30 ft/sec) and below that for most existing end terminals.

The test vehicle remained upright and stable during the impact sequence and after exiting from the installation. The vehicle yawed counterclockwise near the end of impact sequence, apparently as a result of the left front tire or undercarriage of the vehicle becoming engaged with some of the broken posts and debris. However, the vehicle had slowed significantly with most of the impact energy attenuated at that point, and the yaw rate was considered moderate.

Damages sustained by the terminal and vehicle are shown in Figure 6. The first, third, and fourth set of slots were buckled, and the second and fifth set of slots did not activate. Posts 1–5 were broken off at ground level, and Posts 6 and 7 were slightly displaced laterally. The foundation tube was bent at Post 1 and disturbed at Post 2. The vehicle received moderate damage, most of which was concentrated at the front of the vehicle. The maximum crush was 240 mm (9.5 in.) at bumper height near the front center of the vehicle. There was 159 mm (6.3 in.) of deformation into the occupant compartment in the fire wall area near the floor pan on the driver's side. However, the extent of intrusion into the occupant compartment was considered minor and did not pose any significant hazard to the occupant. The vehicle came to rest behind and adjacent to the test installation and did not pose any hazard to adjacent traffic.

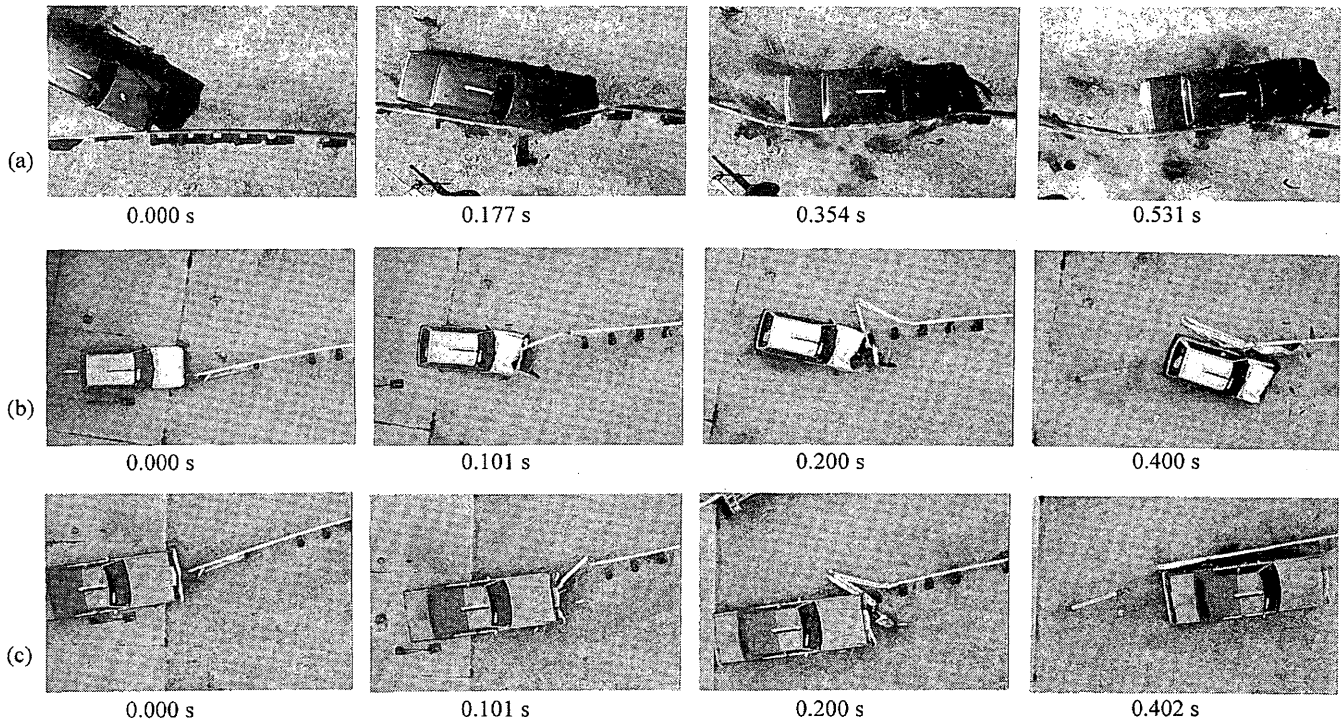

FIGURE 4 Sequential photographs of compliance crash tests: (*a*) large car length-of-need test, (*b*) small car end-on test, and (*c*) large car end-on test.

Large Car Head-On Test

The third compliance crash test involved a 1980 Lincoln Continental, weighing 2,041-kg (4,500 lb). The vehicle hit the end terminal head on at a speed of 97.6 km/hr (60.6 mph) and at an angle of 0 degrees relative to the tangent section of rail. The centerline of the vehicle was aligned with the centerline of the end post. The objective of this test was to evaluate the terminal performance during high-speed, head-on impacts with full-size automobiles.

On impact, the end post was fractured at ground level, releasing the cable anchor mechanism as designed. The vehicle was smoothly decelerated as it proceeded forward, buckling the first four sets of slots and breaking Posts 1–5 at ground level. As the vehicle continued forward, the left front tire made contact with the top of Posts 6, 7, and 8. The vehicle was traveling at 83.1 km/hr (51.7 mph) with an exit trajectory of 2.3 degrees as the vehicle lost contact with Post 8. After the vehicle exited from the guardrail, it landed on the right front tire and began to slide and yaw counterclockwise. The vehicle subsequently turned back toward the barrier and hit the guardrail again near Post 19 and came to rest 51.8 m (170 ft) from the point of initial impact.

The terminal performed as designed, first smoothly decelerating the vehicle and then allowing the vehicle to penetrate behind the guardrail in a controlled manner. Although not required as part of the evaluation criteria, all occupant risk factors were well within the recommended limits set forth in NCHRP Report 230. The test vehicle remained upright and stable during the impact sequence and after exiting the installation. There was some roll and pitch of the vehicle as it traversed over some of the broken posts and debris, but the extent of the roll and pitch was relatively moderate and did not affect the stability of the vehicle.

Damage sustained by the terminal and vehicle is shown in Figure 7. The first through fourth sets of slots were buckled. The fifth set of slots was bent but did not buckle. Posts 1–5 were broken off at ground level, and Posts 6 and 7 were slightly displaced laterally. The foundation tube for the end post was slightly disturbed. The vehicle received moderate damage, most of which was concentrated at the front of the vehicle. Maximum crush was 440 mm (17.3 in.) at bumper height near the front center of the vehicle. There was no deformation into the occupant compartment.

CONCLUSIONS AND RECOMMENDATIONS

An SRT for W-beam guardrails was successfully developed and crash-tested in accordance with requirements in NCHRP Report 230. The slotted rail concept involves cutting three longitudinal 1.3 cm (½ in.) wide slots into the W-beam rail, one at each peak and valley in the cross section. A slot guard is attached to the W-beam rail at the downstream end of each set of slots to prevent extension of the slots and rupture of the rail.

Even though the ELT, MELT, and SRT terminals all meet the recommended design limits for occupant impact velocity and ride-down accelerations set forth in NCHRP Report 230, the SRT terminal is believed to offer a significant improvement over these other systems. The slotted feature of the SRT terminal provides controlled and predictable dynamic buckling of the W-beam rail, whereas the ELT and MELT terminals rely on the buckling behavior of a long, unmodified, eccentrically loaded W-beam rail. The buckling load for the SRT terminal is significantly less than that required by the other two terminals. This reduced buckling load substantially reduces vehicular yaw during the impact sequence,

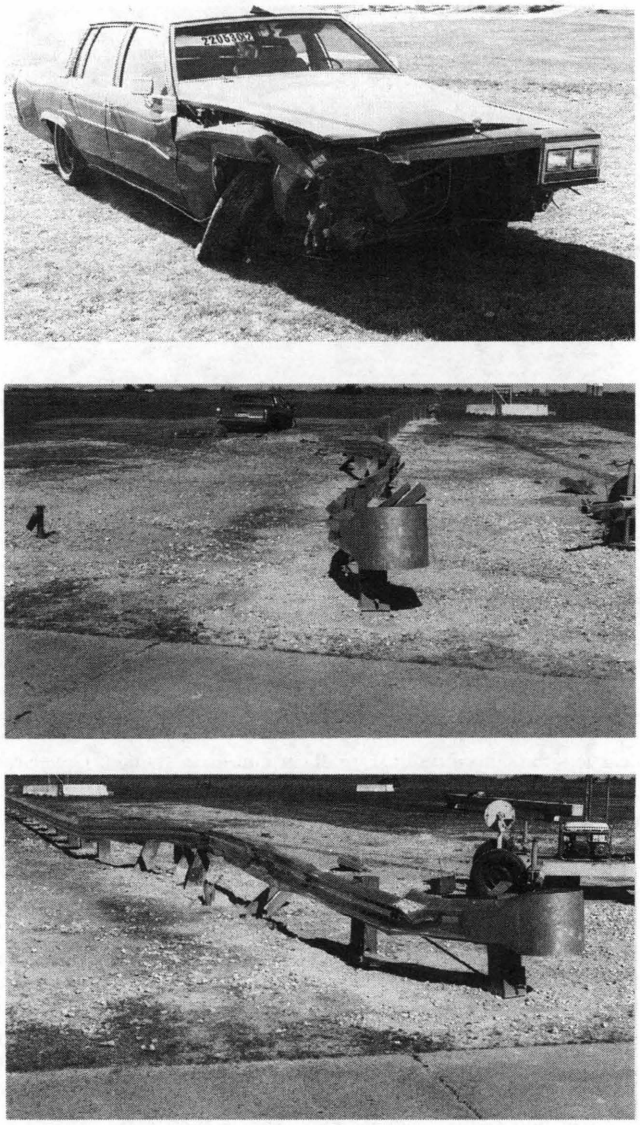

FIGURE 5 Damaged test vehicle and terminal after large car, redirection test.

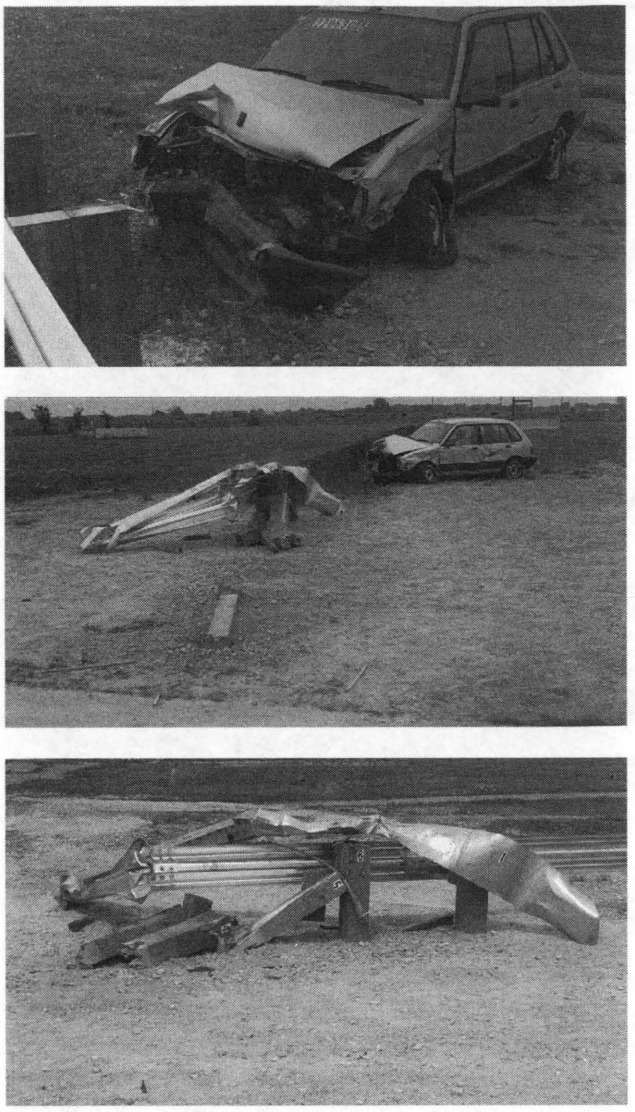

FIGURE 6 Damaged test vehicle and terminal after small car, end-on test.

which in turn minimizes the potential for secondary impact with bent or kinked rail elements that could result in penetration of the occupant compartment. Reduced yaw motion also reduces the potential for vehicle rollover after the terminal impact. The long column length in the ELT and MELT terminal designs results in the buckled W-beam rail initially rebounding away from the impacting vehicle and then forcefully recontacting the side of the vehicle. This type of behavior is much less pronounced with the SRT because of to the relatively short lengths of rail present between the slotted sections. Furthermore, because buckling of the rail for the SRT terminal is controlled by the slots, the impact performance of the SRT terminal is expected to be much less sensitive and more forgiving to installation variations and tolerances.

The SRT design is intended as a retrofit or replacement of the standard BCT terminal. Hence, the SRT design uses many of the standard components common to the BCT terminal. Because the SRT also uses features common to other end treatments, such as a foundation strut and weakened CRT posts, the need for inventory of new components is minimized and the cost of the terminal is kept low. Also of significance in terms of facilitating easy retrofit of existing terminals is that the parabolic flare of the SRT terminal is identical to that of the BCT terminal. The site grading requirement for the SRT terminal should also be similar to that of the BCT terminal (i.e., the SRT terminal should be installed on an essentially level site that has a relatively clear runout area behind and beyond the gating portion of the terminal to ensure proper performance).

Although production and installation costs are extremely difficult to quantify, the material cost for the slotted rail terminal is expected to be comparable with that of the ELT or MELT, with manufacturers' estimates in the range of $900 to $1,100. The installation cost

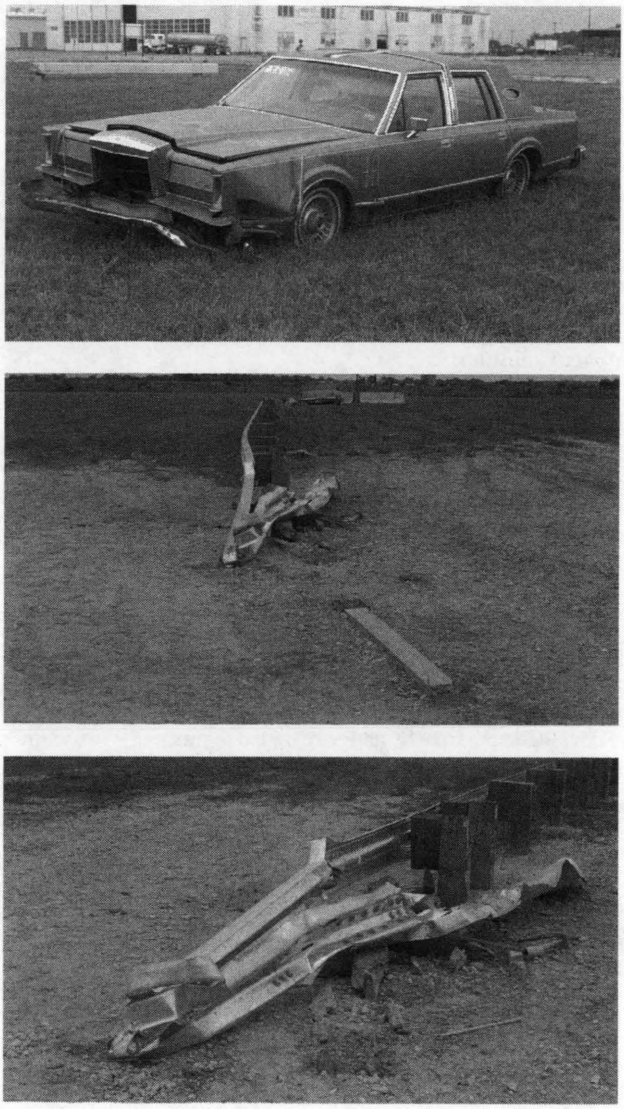

FIGURE 7 Damaged test vehicle and terminal after large car, end-on test.

should be similar to that of the BCT terminal, probably in the range of $200 to $300.

The SRT has been approved by FHWA for use on federal-aid highway projects (*8*). The terminal is offered as a proprietary item and is available for field implementation. As with any new roadside safety device, in-service evaluations to monitor the installation activities and accident experience are recommended to identify and resolve any unforeseen installation, maintenance, or safety problems in a timely manner.

REFERENCES

1. Willett, T. O. Guidelines of Applications of the AASHTO Roadside Design Guide on Federal-Aid Highway Projects. Memorandum, Sept. 7, 1990.
2. Michie, J. D. *NCHRP Report 230: Recommended Procedure for the Safety Performance Evaluation of Highway Appurtenances.* TRB, National Research Council, Washington, D.C., March 1981.
3. Carlson, E. D. Traffic Barrier Safety Policy and Guidance. Memorandum, Sept. 29, 1994.
4. Meczkowski, L. C., *Evaluation of Improvements to Breakaway Cable Terminal.* Report FHWA-RD-91-065. FHWA, U.S. Department of Transportation, Washington, D.C., 1991.
5. Mak, K. K., R. P. Bligh, and W. C. Menges. *W-Beam Slotted End Terminal Design,* Final Report, TTI Project No. 220530. Texas Transportation Institute, Texas A&M University System, College Station, May 1994.
6. Mak, K. K., and R. P. Bligh. *Development of W-Beam Slotted Rail End Terminal Design,* Research Report RF 7199-3F. Texas Transportation Institute, Texas A&M University System, College Station, May 1994.
7. Sicking, D. L., A. B. Qureshy, R. P. Bligh, H. E. Ross, Jr., and C. E. Buth. *Development of New Guardrail End Treatments,* Research Report 404-1F. Texas Transportation Institute, Texas A & M University System, College Station, Oct. 1988.
8. Sillan, S. I. Letter to King K. Mak. Federal-Aid and Design Division, FHWA, U.S. Department of Transportation, Washington, D.C., June 24, 1994.

Publication of this paper sponsored by Committee on Roadside Safety Features.

Development of Guardrails for High-Speed Collisions

TAKUYA SEO, KAZUHIKO ANDO, TOSHINOBU FUKUYA, AND SATORU KAJI

The installation of guardrails in Japan is conducted according to the Guideline of Guard Fences (October 1972) and has served to prevent or alleviate accidents around the country by keeping vehicles from leaving the road. However, since the guideline was first promulgated, traffic characteristics in Japan have changed considerably: the total extension of national expressways is much longer, the performance of vehicles has been improved dramatically, traffic on national expressways is faster, and vehicles are larger. Consequently, the severity of a guardrail collision tends to be much higher than before, and this trend is expected to continue in coming years. For this and similar reasons, a number of investigations and experiments were carried out in 1990 and 1991 to develop new types of guardrails for highways. This paper focuses on a design of guardrails for high-speed impacts that satisfies demands exceeding those specified in the current guideline. A basic design for a guardrail capable of withstanding an impact of 20 degrees by a 20,000-kg truck running at 100 km/hr is described.

The installation of guardrails in Japan is conducted according to the Guideline of Guard Fences (*1*) and has served to prevent or alleviate accidents around the country by keeping vehicles from leaving the road. However, since the guideline was first promulgated, traffic characteristics in Japan have changed considerably. The total extension of national expressways is faster and vehicles are larger. The impact of guardrail collisions has steadily increased and is expected to increase even further.

With the development of highway networks and the construction of bypasses for ordinary roads, traffic moves faster. With the increased importance of road transportation and the enhanced performance of cars and trucks, there is a steady trend toward bigger vehicles. For these reasons, it has become necessary to reexamine the design of guardrails for high-speed impacts to develop new types that are able to withstand impacts larger than those envisioned in the design parameters for the guardrails currently in place.

In addition to revealing guardrail and vehicle impact characteristics under high-speed collisions, we propose a design for a guardrail that is able to provide sufficient strength and occupant safety in the event of an impact in excess of the design parameters for a Type S guardrail (vehicle weight = 14 000 kg; impact velocity = 80 km/hr; impact angle = 15 degrees; impact severity = 232 kJ; see Table 1), which is the strongest type of guardrail currently in use in Japan.

GENERAL DESCRIPTION

The general flow of our research is presented in Figure 1.

T. Seo and K. Ando, Traffic Safety Division, Public Works Research Institute, Ministry of Construction, 1, Asahi, Tsukuba-shi, Ibaraki-ken, 305 Japan. T. Fukuya and S. Kaji, Technical Committee, Steel Barrier Association, 3-2-10, Nihonbashi-kayabacho, Chuo-ku, Tokyo, 103 Japan.

Impact Condition

Impact conditions consist of the vehicle weight, the impact velocity, and the impact angle. The results of our surveys and theoretical studies and our impact conditions are presented in Table 1.

Study of Guardrail Design

As a starting point for modification in the development of a guardrail to accommodate high-speed impact, we chose to begin with a guardrail previously developed for sharp curves (Gr-SS) (*2*). This guardrail has the highest impact resistance of any of the types we developed previously, and we decided to proceed with our modifications after first verifying its high-speed impact characteristics.

Vehicle Impact Tests

To verify the vehicle guidance characteristics, strength, and other barrier performance items, barrier designs that were judged to be promising through design investigations and impact simulations were subjected to impact tests with vehicles.

Outline of Test Facilities

The test facilities used a winch to pull the vehicle into the barrier. The maximum pulling performance of the setup was as follows:

Normal truck: vehicle weight = 20 000 kg; pulling speed = 100 km/hr.

Small passenger car: vehicle weight = 2500 kg; pulling speed = 140 km/hr.

Post Foundation Ground Conditions

The condition of ground into which the barrier posts are sunk has a great effect on pillar deformation and support characteristics. For this reason, it is best that the tests are done under consistent ground conditions. As standard ground conditions for our testing, the typical highway base was adopted.

Measurement Items and Evaluation Items

Measurement items and evaluation items are presented in Table 2.

TABLE 1 Impact Condition

	Class	Vehicle type	Vehicle weight W	Impact velocity V	Impact angle θ	Impact severity IS
Impact conditions for this investigation	SS	Normal truck	20,000 (kg)	100 (km/h)	20 (°)	902 (kJ)
		Small passenger car	1,100 (kg)	140 (km/h)		92 (kJ)
Current Japanese impact standards	S	Normal truck	14,000 (kg)	80 (km/h)	15 (°)	232 (kJ)
		Small passenger car	3,500 (kg)			58 (kJ)
	A	Normal truck	14,000 (kg)	60 (km/h)		130 (kJ)
		Small passenger car	3,500 (kg)			33 (kJ)
	B	Normal truck	14,000 (kg)	40 (km/h)		58 (kJ)
		Small passenger car	3,500 (kg)			14 (kJ)
	C	Normal truck	14,000 (kg)	35 (km/h)		44 (kJ)
		Small passenger car	3,500 (kg)			11 (kJ)

$$\text{Impact severity} = \frac{W}{2g}(V \times \sin\theta)^2 \ldots (1)$$

W: vehicle weight (t)
θ : impact angle (°)
V : impact velocity (m/s)
g : acceleration of gravity (m/s²)

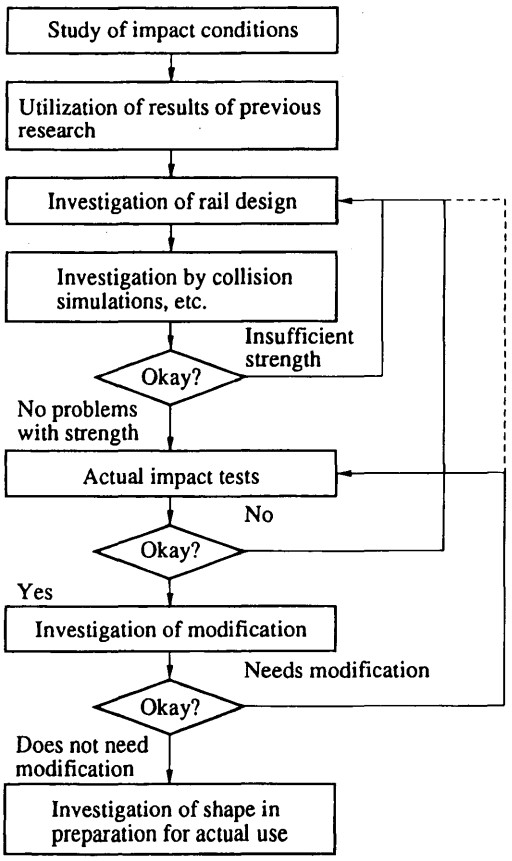

FIGURE 1 General flow of research efforts.

RESULTS

Following the procedures outlined in the previous section, we conducted a total of nine impact tests (normal trucks, six times; small passenger cars, three times) using the procedure presented in Figure 2. In the following sections, we discuss results of basic investigations into the strength and guidance characteristics of the guardrails in collisions with normal trucks. In addition, we discuss results of the investigations of occupant safety in small passenger cars in high-speed collisions. Table 3 presents a compilation of the test results.

Normal Trucks (Tests 1–6)

In the first test we examined the suitability of the guardrail for sharp curves in a high-speed collision (20 000-kg truck, 100 km/hr, 15 degrees, 516 kJ). The truck tipped onto its side on collision. Following up on this result, we modified the basic design of the guardrail and tested the effectiveness of these modifications in Tests 2 through 6. We later described some of the things we were able to confirm through this series of tests. The locations and names of various parts of a guardrail are illustrated in Figure 3.

Beam Height and Beam Strength

Because of the low height of the main beam in Test 1, the inertial force of cargo from the collision was not adequately accommodated. As a result, the truck fell on its side (Figure 4).

We modified the design by adding a cargo acceptance beam about 1300 mm above the center of gravity of the vehicle; guidance

TABLE 2 Measurement and Evaluation Items

Test evaluation	Measurement items	Evaluation items
Barrier strength	Maximum displacement Horizontal post force Beam tension	Barrier contain and redirect the vehicle. Beam-stress is within permission stress. The posts are required to be strong enough to withstand the impact force.
Vehicle behavior	Exit velocity Exit Angle Vehicle trajectory Jump height Slant angle	Vehicle stays on road and does not roll sideway or spin after collision. Exit verocity is no less than impact velocity by more than 20km/h and 25%. Exit angle is within 10degrees and 60% of impact angle.
Occupant Safety	Occupant accelerations Vehicle accelerations Vehicle trajectory	Detached elements from the barrier and the vehicle not penetrated or show potential for penetrating the occupant compartment. HIC<1,000. 50(ms) average accelerations< 25(x), 15(y).

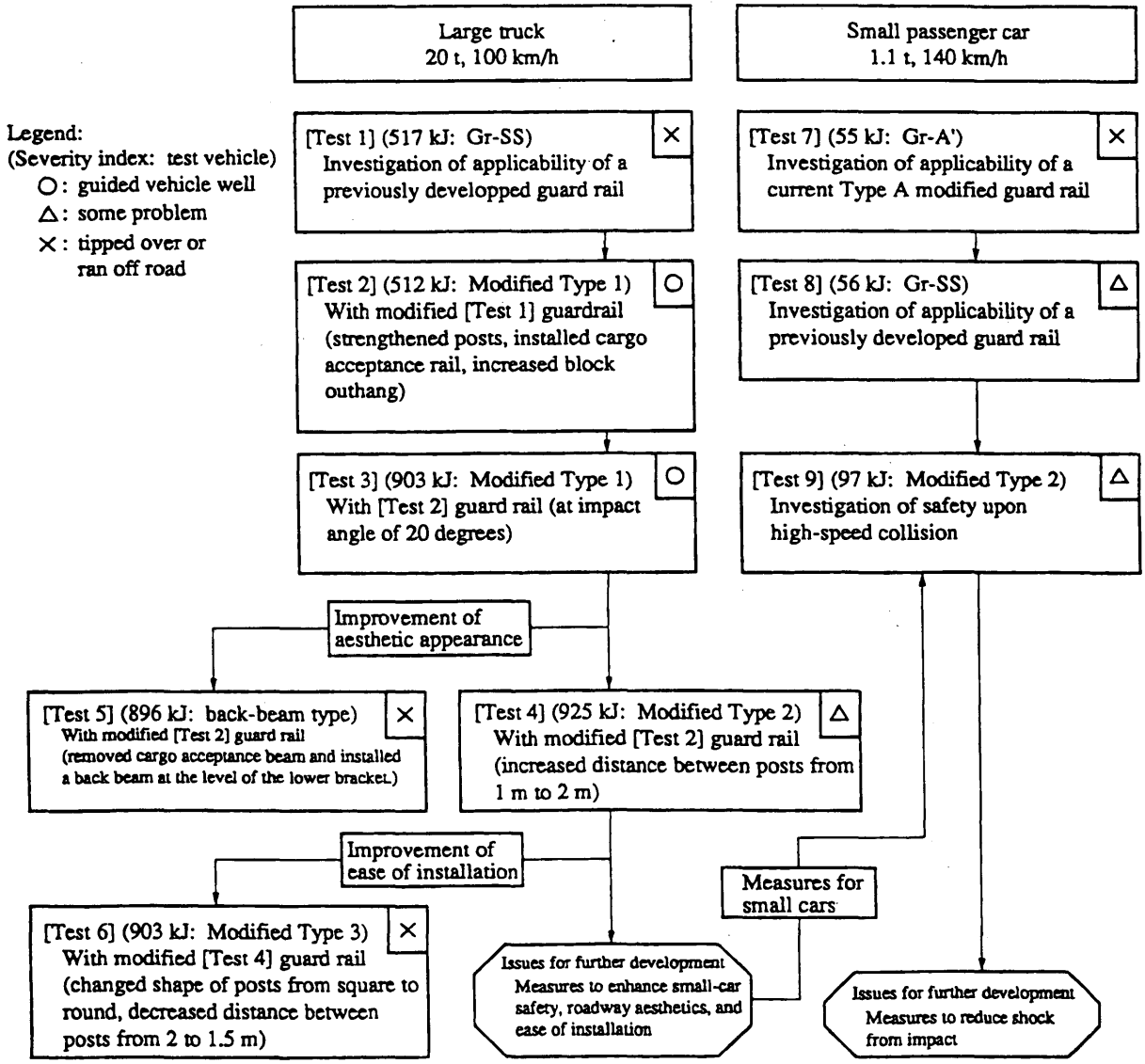

FIGURE 2 Flowchart for impact test results.

TABLE 3 Compilation of Test Results

Test No.		Test 1	Test 2	Test 3	Test 4	Test 5	Test 6	Test 7	Test 8	Test 9
Vehicle type		Large truck						Small passenger car		
Barrier		Gr-SS	Gr-SS Modified Type 1	Gr-SS Modified Type 1	Gr-SS Modified Type 2	Gr-SS back-beam type	Gr-SS Modified Type 3	Gr-A'	Gr-SS	Gr-SS Modified Type 2
Test setup	Sectional plan	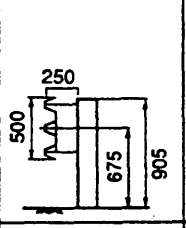	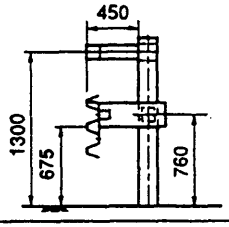		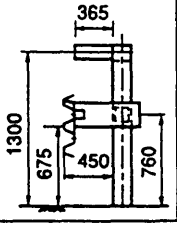	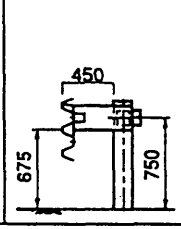	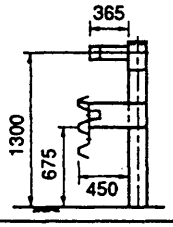	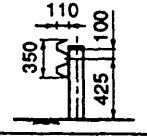	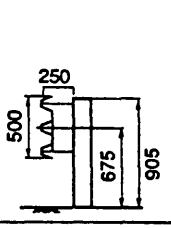	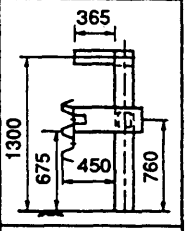
	Post dimensions (mm)	ø139.8x4.5	□100x100x6.0				ø139.8x4.5	ø114.3x4.5	ø139.8x4.5	□100x100x6.0
	Post spacing (m)	1	1		2	1	1.5	4	1	2
	Weight (kg/m)	77.6	144.8		91.8	122.5	94.2	47.3	77.6	91.8
Collision results	Vehicle weight (t)	20.0	20.0	20.0	20.5	20.0	20.0	1.1	1.1	1.1
	Impact velocity (km/h)	100.1	100.0	100.0	100.0	99.6	100.0	138	139.5	139.5
	Impact angle (°)	15	15	20	20	20	20	15	15	20
	Impact severity (t-m) (kJ)	52.7 517	52.7 517	92.1 903	94.4 925	91.4 896	92.1 903	5.6 55	5.7 56	9.9 97
Measurements	Exit velocity (km/h)	Tipped	88.9	76.9	79.5	Tipped	Tipped	Glided	118.5	115
	Exit angle (°)	Tipped	6.2	9.8	7	Tipped	Tipped	Glided	7	5.4
	Contact length (mm) Main beam	17.4	11.5	12.7	19.9	13.5	25.1	11.3	5.23	8.79
	Contact length (mm) Cargo acceptance beam	–	14.5	16.1	21.8	29.0	26.6	–	–	–
	Max. permanent displacement (mm)	1202	678	1086	1602	570	1832	680	90	177
	Ave. horizontal force on pillar (t)	6.0	8.6	8.3	16.4	9.5	9.7	5.4	4.2	6.6
	Max. tension (t) Main beam	26.3	26.6	26.6	25.8	45.9	29.3	4.5	8.0	–
	Max. tension (t) Cargo acceptance beam	–	14.5	12.3	24.4	10.5	37.5	–	–	–
	Acceleration at vehicle COG for first 50 ms (g) Direction of Travel (X)	–4.4	1.8	2.0	1.6	–	–	3.3	3.2	6.7
	Acceleration at vehicle COG for first 50 ms (g) Normal direction to Travel (Y)	3.2	4.2	2.1	1.5	–	–	7.9	–13.9	26.9
	Acceleration at vehicle COG for first 50 ms (g) Resultant	4.9	4.3	2.6	3.5	–	–	8.4	13.9	26.9
	HIC (driver's seat) (front passenger's seat)	14.8 7.3	6.5 146	50.5 22.8	8.3 11.3	– –	– –	424.3 535.7	551.8 1530.9	1311 902
Test evaluation	Barrier strength	Insufficient strength overall	Much structural margin	Little structural margin	Very near performance limit	Insufficient beam height	Insufficient post strength	Insufficient block outhang	Much guard rail rigidity	Much guard rail rigidity
	Vehicle behavior	Broke through and tipped	Normal guidance	Normal guidance	Normal guidance	Tipped on road	Broke through and tipped	Glided and tipped	Normal guidance	Normal guidance
	Occupant safety	×	Good	Good	Good	–	×	×	×	×
	Overall evaluation	×	○	○	○	×	×	×	△	△

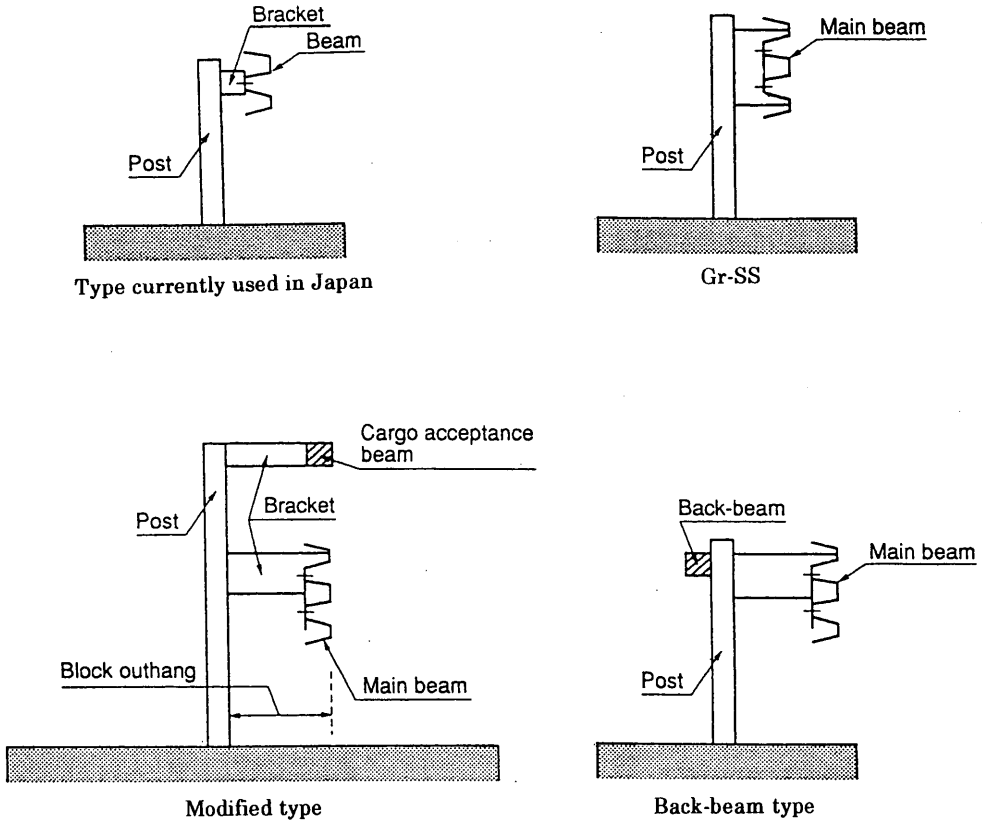

FIGURE 3 Guardrail parts.

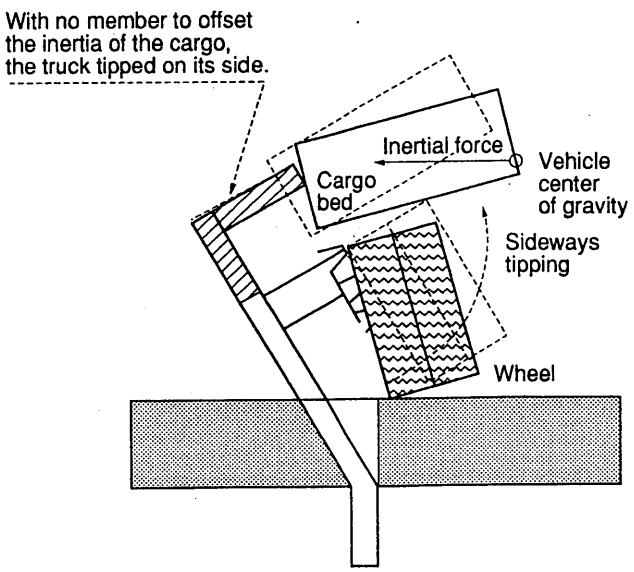

FIGURE 4 Motion of vehicle on collision.

performance was good. To confirm the effectiveness of the cargo acceptance beam, we conducted Test 5 without the cargo acceptance beam (but with a back beam; see Figure 3). In this test, the inertial force of cargo was not fully accommodated, and the vehicle tipped onto its side on the road.

We believe that for the protection of normal trucks it is necessary to install a cargo acceptance beam at a height near that of the vehicle's center of gravity. Furthermore, we confirmed through testing that a suitable location for the main beam is about the height of the vehicle tires, where the load of the collision is concentrated (Figure 5).

The main beam (SS400[3]) receives most of the impact load. It functions as a tension member on impact and must not break. In all of the tests, the resulting stress on the main beam never exceeded

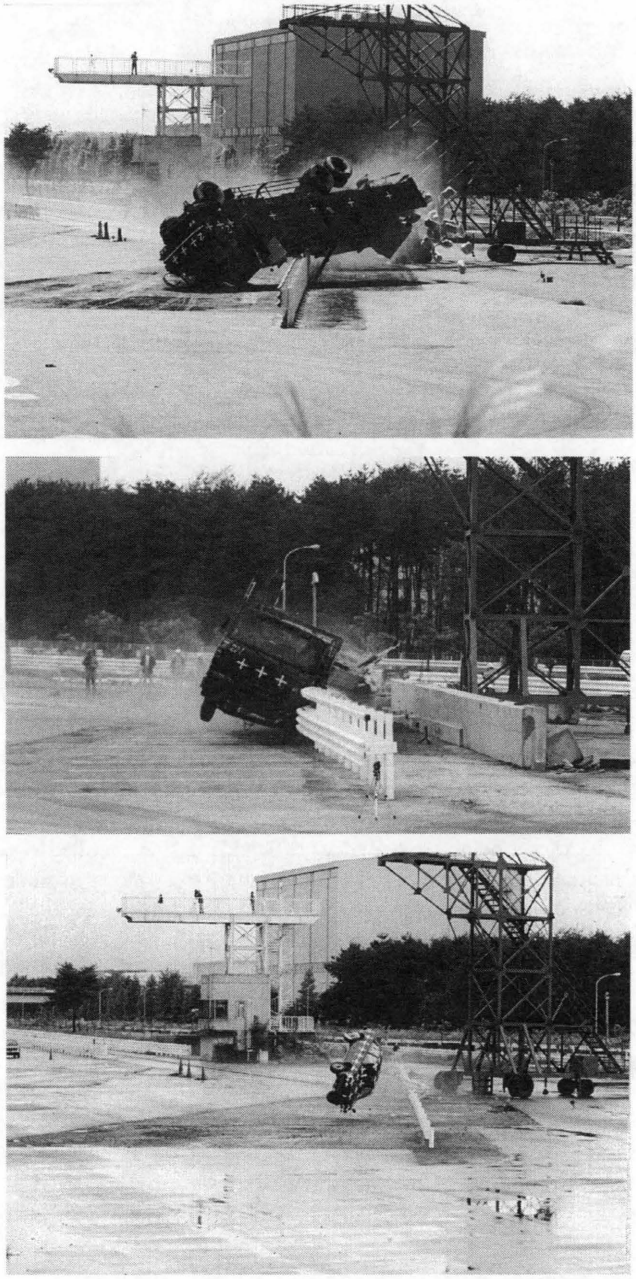

FIGURE 5 Results of impact test: (*top*) Gr-SS, (*middle*) Gr-SS Modified Type 2, (*bottom*) Gr-A′.

tolerance limits and the beam never broke. On the basis of these results, we believe suitable values for the main beam to be as follows: beam cross-sectional surface area = 31.2 cm^2, cross-sectional coefficient = 64 cm^3, and bend rigidity = 57.1 t-m^2. The cargo acceptance beam (STK400[4]) supports the load from the truck cargo and distributes that load among posts over a wide area. In Test 2, 3, and 4, in which vehicle guidance performance was good, the stress acting on the cargo acceptance beam was within limits and the beam did not break. On the basis of these results, we believe suitable values for the cargo acceptance beam to be as follows: beam cross-sectional surface area = 16 cm^2 and bend rigidity = 29 t-m^2. Our recommended shape is square: 100 · 100 · 4.5 (area = 16.7 cm^2; bend rigidity = 52 t-m^2).

Post Strength

The posts (STK400) are required to be strong enough to withstand the impact force and, on deformation, are not to have a sudden drop in supporting force caused by localized buckling or the like at or near ground level.

To make the posts easier to install, we modified them in preparation for Test 6 as presented in Table 4. As a result, however, the guardrail bent back on collision and the vehicle tipped onto its side. Consequently we believe that it is necessary when installing a guardrail intended to withstand severe impacts, to consider the relationships of post spacing, average support force per post, post shape, and other post strength-related factors.

Block Outhang

The block outhang is the distance that the main beam projects from the pole, and it is provided to keep the vehicle from colliding directly into the pole. In Test 1, the block outhang was 250 mm, which was not long enough to prevent the wheels of the truck from running over the poles and bending them down. In effect, this aggravated the problem of low beam height, and as a result, the vehicle tipped over.

From Test 2 onward, the block outhang was set at 450 mm, a distance that, by desktop calculations, we estimated would be effective in keeping the wheels from running over the poles. In the subsequent tests we found that this problem did not occur and that the longer outhang had no adverse effects on the guardrail as a whole. For these reasons, we believe that a block outhang of at least 450 mm is necessary.

The bracket that attaches the beam to the pole must continue to maintain the gap between the two even after the guardrail deforms on collision. For this reason, it must have a high rigidity.

Small Passenger Cars Tests (Tests 7 through 9)

The guardrails used in testing for normal truck collisions must be able to handle high impact energies. For this reason, their structure is such that they do not deform easily on low energy (passenger car) collisions. In Tests 7 through 9, we examined the high-speed passenger car impact behavior of three types of guardrails.

Suitability of Current Guardrails

In Test 7, we examined the ability of a currently used guardrail to handle high-speed collisions with small passenger cars. The test

TABLE 4 Revision from Modified Type 2 to Modified Type 3 Post

Revised item	Modified type 2 post	Modified type 3 post
Post	□-125 × 125 × 6 (STK400)	ø-139.8 × 4.5 (STK400)
Post support force	6 t	4 t
Post spacing	2 m	1.5 m
Support force	3 t/m	2.7 t/m

Notes: • Post support force : determined by post loading tests
• Support force : post support force/post spacing

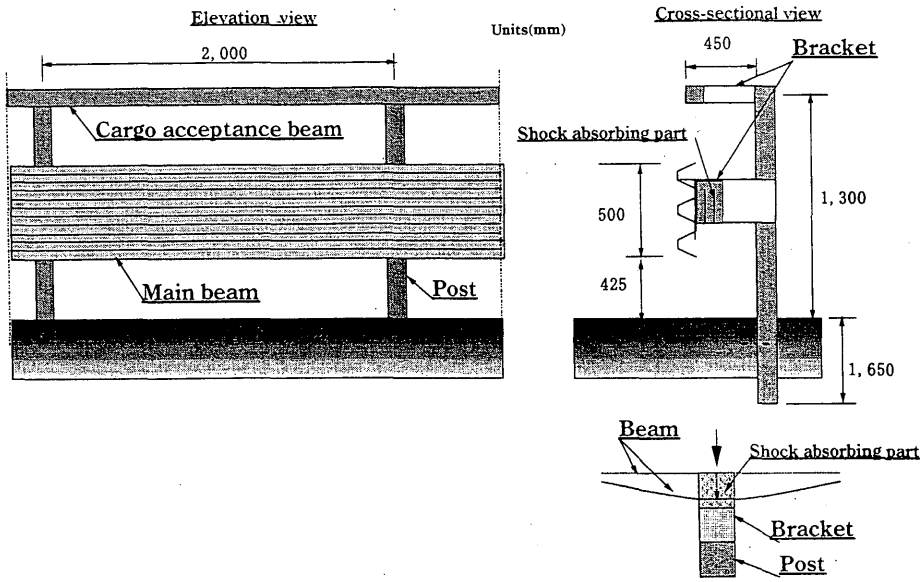

FIGURE 6 Modified Type 2.

revealed that the rail cannot adequately handle a collision at about 140 km/hr; we learned the necessity of providing sufficiently strong posts and a suitable block outhang (Figure 4).

Occupant Safety

In Test 8, we used a guardrail (Gr-SS; see Figure 3) with no cargo acceptance beam. Although it has good guidance characteristics, it imparts to vehicle occupants a head injury criteria (HIC) that exceeds the tolerance limit. The structure of the Gr-SS has a high rigidity in high-speed collisions with small passenger cars.

In Test 9, we examined the small passenger car high-speed collision behavior of the modified Type 2 guardrail, which was shown to be effective for collisions involving large trucks. In this test, tolerance limits for the acceleration at the vehicle center of gravity and for the HIC were exceeded. From this, we can say that a highly rigid rail like the modified Type 2 imparts a high impact load on vehicle occupants and still has much room for improvement in terms of safety.

Based on the results of these three tests, we conducted a separate investigation on the design of a bracket that will protect vehicle occupants. We believe that the development of this type of bracket will make it possible to assure passenger safety, even with a highly rigid guardrail like that of modified Type 2, which was shown to have good guidance characteristics for normal trucks.

Beam Height

In Tests 7 through 9, we confirmed that a beam height of about 425 mm prevents small passenger cars from "burrowing" underneath on collision.

CONCLUSION

In this series of tests with normal trucks, we found that, even with guardrail impact conditions (vehicle weight = 20 000 kg; impact velocity = 100 km/hr; impact angle = 20 degrees; impact severity = 903 kJ) considered severe by world standards, the modified Type 2 guardrail (Figures 4 and 6) has a structure that smoothly guides the vehicle on impact. Also, in three tests with small passenger cars, we examined guardrail behavior characteristics in high speed collisions with such vehicles.

Based on the structure of the modified Type 2 guardrail, which was not able to handle high-speed collisions by normal trucks adequately, we intend to study ways to further improve the performance of the guardrail structure though efforts to lessen the impact shock on passenger cars, to increase the ease of installation, to enhance its economic attractiveness, and to lighten the heavy, oppressive look along our highways.

REFERENCES

1. *Guideline of Guard Fences.* Japan Road Association, October 1972.
2. Yokshitaka, M., K. Ando, Y. Sakai, et al. Study on Development of High Intense Barriers. Joint Research Report No. 41, March 1990.
3. *Rolled Steel for General Structure.* Japan Industrial Standard G3101, 1987.
4. *Carbon Steel Tubes for General Structural Purpose.* Japan Industrial Standard G3444, 1994.

Publication of this paper sponsored by Committee on Roadside Safety Features.

Development of Variable Yaw Angle Side Impact System and Testing on Double Thrie Beam Median Barrier

GARY P. GAUTHIER, JOHN R. JEWELL, AND PAYAM ROWHANI

A side impact system for projecting crash test vehicles in side skids was developed and tested. The system incorporates a side impact carriage (SIC) that can be modified to position the test vehicle at different yaw angles, a guidance rail, an impact attenuator, a skid deck, and tow cable propulsion. The SIC is a modified lightweight test bogie designed to carry test vehicles weighing up to 1170 kg. The SIC is loaded with the vehicle and towed up to the skid deck by a 1-ton pickup truck pulling the cable through a pulley. The SIC hits the skid deck at the wheel supports for the test vehicle, causing them to collapse. The vehicle drops onto the lubricated skid deck, and skids in channels positioned to maintain the correct yaw angle. The SIC travels underneath the deck and slows to a stop after colliding with the impact attenuator. The vehicle skids off the deck and onto the ground surface in front of the test article. After several trial tests, the system was used to project a Honda Civic in a side skid at a counterclockwise yaw angle of 31 degrees, a trajectory angle of 22 degrees, and an impact speed of 66.5 km/hr into a double thrie beam median barrier. The side impact system needs modifications and more testing. The double thrie beam median barrier meets the occupant risk and structural adequacy (but not the vehicle trajectory) evaluation criteria for Test 2-10 of the National Cooperative Highway Research Program Report 350 guidelines. The test indicated the need to conduct more side-skid testing of the double thrie beam median barrier.

To improve the performance of roadside safety features in side-skidding collisions at various yaw angles, a crash-testing system must be developed to replicate this type of vehicle behavior. Although new roadside feature designs are tested adequately for crash worthiness in tracking collisions, side-skidding impacts can result in different occupant injuries, vehicle dynamics, and vehicle damage.

Typically, crash-worthiness tests for longitudinal barriers are performed with tracking vehicles having impact angles of 15, 20, and 25 degrees. In the report *Side Impact Crash Testing of Roadside Structures,* a comprehensive list of side impact tests conducted throughout the world reveals only tests with yaw angles of 90 and 45 degrees into narrow objects (*1*). A literature search revealed that no side skidding or side impact crash tests into longitudinal barriers had been conducted at yaw angles other than 90 degrees. The only operating side impact carriage in the U.S. is at the Federal Outdoor Impact Laboratory of the Federal Highway Administration in Virginia. It has only been used to project vehicles into narrow objects at 90 degree yaw angles.

The California Department of Transportation (Caltrans) Legal Division in Los Angeles requested the researchers to assist in defending a tort liability claim. The claim resulted from a cross-median accident involving a 1989 Honda Civic passing under a cable barrier. The Honda skidded sideways across the soil median center line along a trajectory angle of 22 degrees, at approximately 80.5 km/hr and in a counterclockwise yaw of 32 degrees. Hence, the apparent angle of impact with the barrier was 32 + 22 = 54 degrees. The vehicle was assumed to have translated with no rotation. Crash Test 523 was intended to replicate this accident at the same speed and angles, but with a double thrie beam barrier. The cable barrier at the accident site was subsequently replaced with a double thrie beam barrier.

The objectives of this project were as follows:

1. Develop a side impact system capable of projecting a Honda Civic for Crash Test 523, as described previously. Although this was the only test budgeted for the project, it would be designed for any similarly sized vehicle to be projected into a smooth, translating side skid at any yaw angle and at speeds up to 100 km/hr.
2. Evaluate the performance of a double thrie beam median barrier in a side skid collision based on National Cooperation Highway Research Program (NCHRP) Report 350 guidelines.
3. Conduct a crash test with this system for the Caltrans Legal Division in defense of a legal case scheduled to start trial August 1, 1994. Because of the limited scope of this paper, details of this legal case will not be presented.

TECHNICAL DISCUSSION

Part A: Development of Side Impact System

General

The following design criteria were set for the side impact system:

1. The side impact carriage (SIC) would be the existing Caltrans lightweight crash test bogie, modified to support a vehicle weighing up to 1170 kg in various yaw positions (see Figure 1). It would be able to sustain design uniform accelerations of $-23.5g$.
2. The SIC would be towed by a 1-ton pickup truck with a 2:1 mechanical advantage pulley configuration.
3. An existing portable guidance rail would be used.

The test vehicle is carried on the SIC, supported by collapsible wheel supports. The SIC and vehicle are towed along the guidance rail up to a skid deck that stands at a height just below the wheels of the test vehicle. The skid deck comprises steel channels that receive each wheel as they drop from the collapsing wheel supports.

California Department of Transportation, Engineering Services Center, Office of Materials Engineering and Testing Services, Structural Materials Branch, Roadside Safety Technology Unit, P.O. Box 19128, Sacramento, Calif. 95819

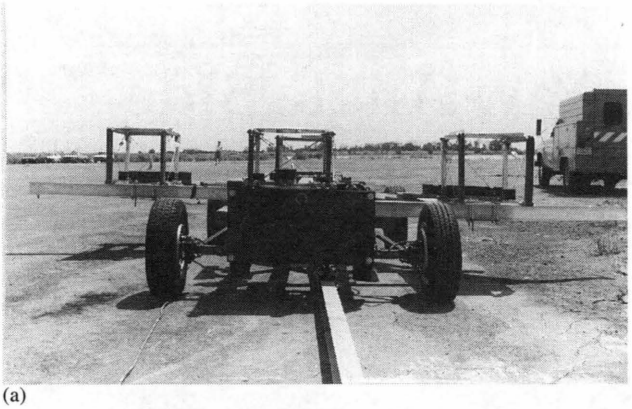

(a)

(b)

(c)

FIGURE 1 SIC: (*a*) front view, (*b*) left side view, and (*c*) loaded with car at impact point with skid deck.

The wheel supports hit the ends of the skid channels and collapse backward against the frame of the SIC. The SIC travels underneath the skid deck and is stopped by an impact attenuator, whereas the test vehicle skids above it on the lubricated deck. The test vehicle skids along the deck until the end, where it slides onto the pavement or soil surface in front of the test article.

Side Impact Carriage Design

To support the test vehicle, the existing lightweight crash test bogie is fitted with 6061-T6 aluminum I-beams cantilevered from the frame. The beams are clamped to the tubular steel frame of the bogie with steel plates and bolts. The locations of the beams can be changed to accommodate vehicles of different sizes and various yaw angles.

For additional strength during the collision with the impact attenuator, wheel struts brace the connection between the axles and the frame and an extra steel plate is bolted to the existing impact plate. In addition, wire rope cables connect the ends of the two longer beams to the bogie frame.

These modifications turned the test bogie into a side impact carriage. A structural dynamic analysis revealed that the SIC can resist horizontal accelerations of $-23.5g$.

Test Vehicle Wheel Supports

The test vehicle wheel supports hold the wheels of the test vehicle above the skid deck, allowing a smooth transition as the vehicle is transferred onto the skid channels (see Figure 2). The wheel supports collapse on impact with the upstream ends of the skid channels. They remain attached to the SIC and can be reused after minor repairs.

The basic design consists of two collapsing four-bar linkages held together in parallel by two plates. The top plate supports the vehicle tire and the bottom plate is bolted onto the aluminum I-beam of the SIC. The two front columns are the only steel members on the supports. All other members are 6061-T6 aluminum. The top and bottom plates are each supported with two solid aluminum bars. The rear columns are two aluminum square tubes welded together. The members are held together by eight bolts that act as hinges. The four-bar linkages are restrained laterally with two diagonal steel cables. Since the supports must collapse during the impact with the skid deck, one cable on each of the sides is spliced with a pin connection that fails when the supports hit the skid channels.

Tow Cable System

The tow cable pulls the SIC along the length of the guidance rail. After the test vehicle is transferred to the skid deck, the tow cable pulls the SIC underneath the skid deck and is released. One end of the cable behind the SIC trails freely, the middle is connected to the SIC, and the other end is attached to a deadman anchor. Between the SIC and dead end of the cable, a 1-ton pickup truck pulls the cable through a pulley attached to the rear bumper.

Guidance System

The guidance rail is composed of sections of aluminum I-beam 127 mm deep. The rails are anchored with brackets and steel spikes set in holes drilled in the asphalt pavement and filled with magnesium-phosphate concrete. The guidance mechanism connecting the SIC to the rail features roller blade wheels, four on each side and four on the top of the rail (see Figure 3).

Impact Attenuator

The impact attenuator brings the SIC to a controlled stop after the test vehicle is released and is skidding above on the skid deck. The attenuator dissipates the energy in the SIC by crushing a fiber-reinforced plastic (FRP) tube (see Figure 4). This design is based on the box-beam guardrail terminal developed for the Wyoming

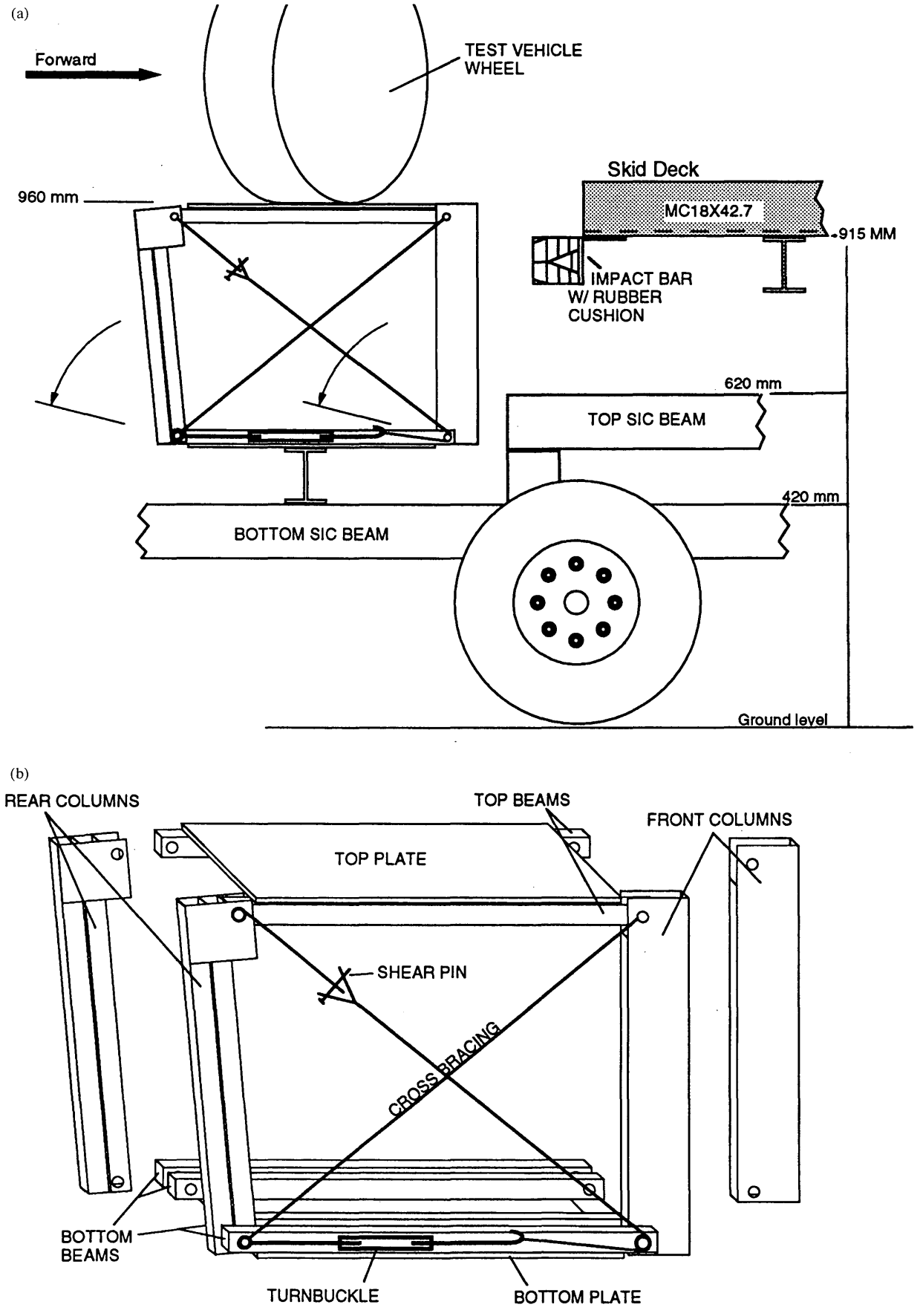

FIGURE 2 SIC wheel support schematic: (*a*) wheel support assembly and (*b*) exploded detail of wheel supports.

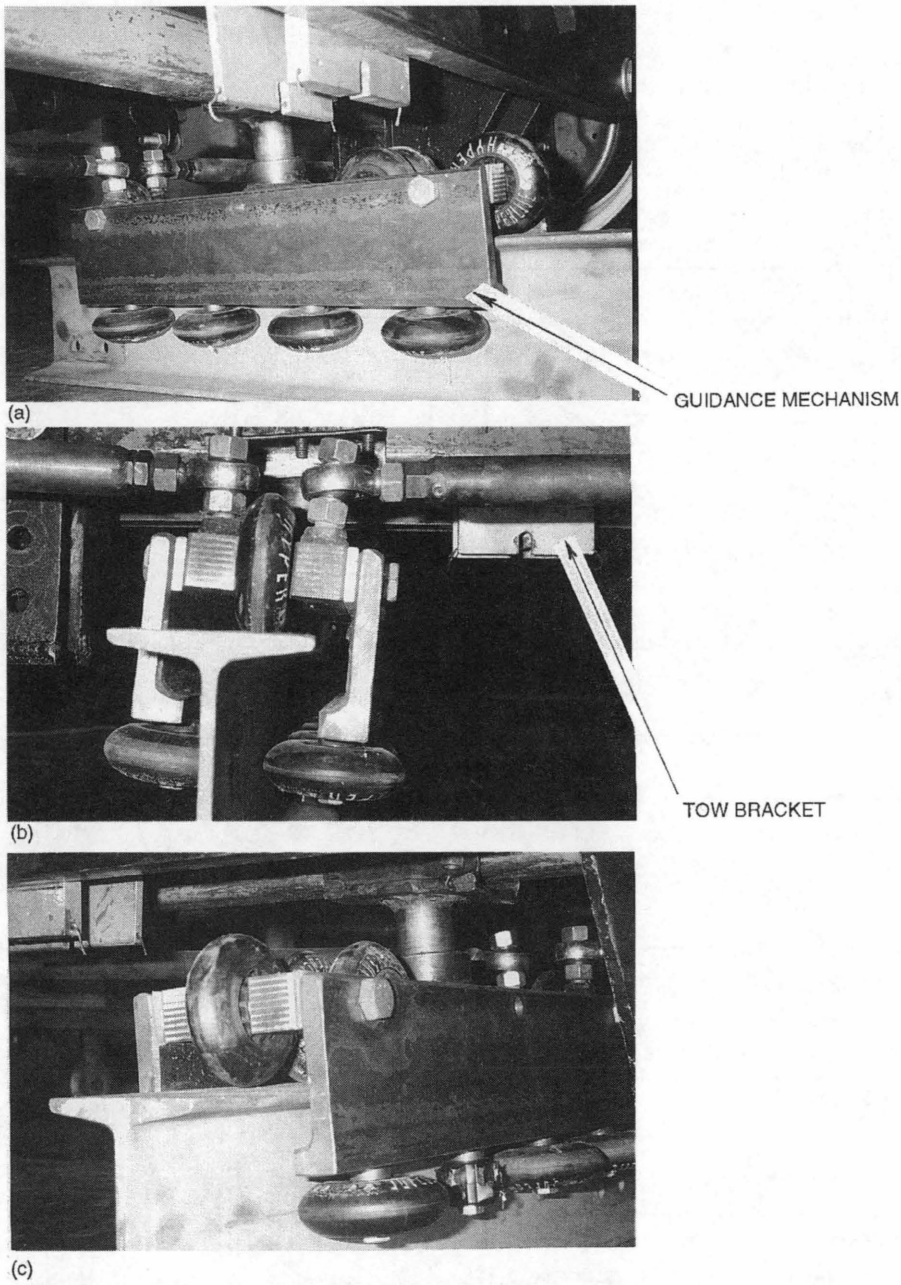

FIGURE 3 Guidance mechanism and tow bracket: (*a*) right side view from front, (*b*) rear view, and (*c*) left side from front (lateral guide wheel is damaged).

Department of Transportation by the Texas Transportation Institute (*2*). The optimum tube size was determined to be a wall tube, 152 mm diameter × 6 mm thick, manufactured with the same specifications as the tube samples in the development of the Wyoming box-beam end terminal.

Skid Deck

The skid deck consists of two, three, or four steel channels supported on four steel wide-flange beams and the median embankment (see Figure 5). For the particular yaw angle of this project, the left channel received the left front wheel of the test vehicle, the middle channel received the right front and left rear wheels, and the right channel received the right rear wheel. They were positioned so that the left front, right rear, and right front wheels dropped onto the skid deck simultaneously, and later hit the dirt median all at the same time. The left rear wheel trailed, skidding in the same channel as the right front wheel.

The webs of the channels are coated with liquid soap, and the inside flange faces are coated with grease. This allows the test vehicle wheels to skid smoothly and with very little friction.

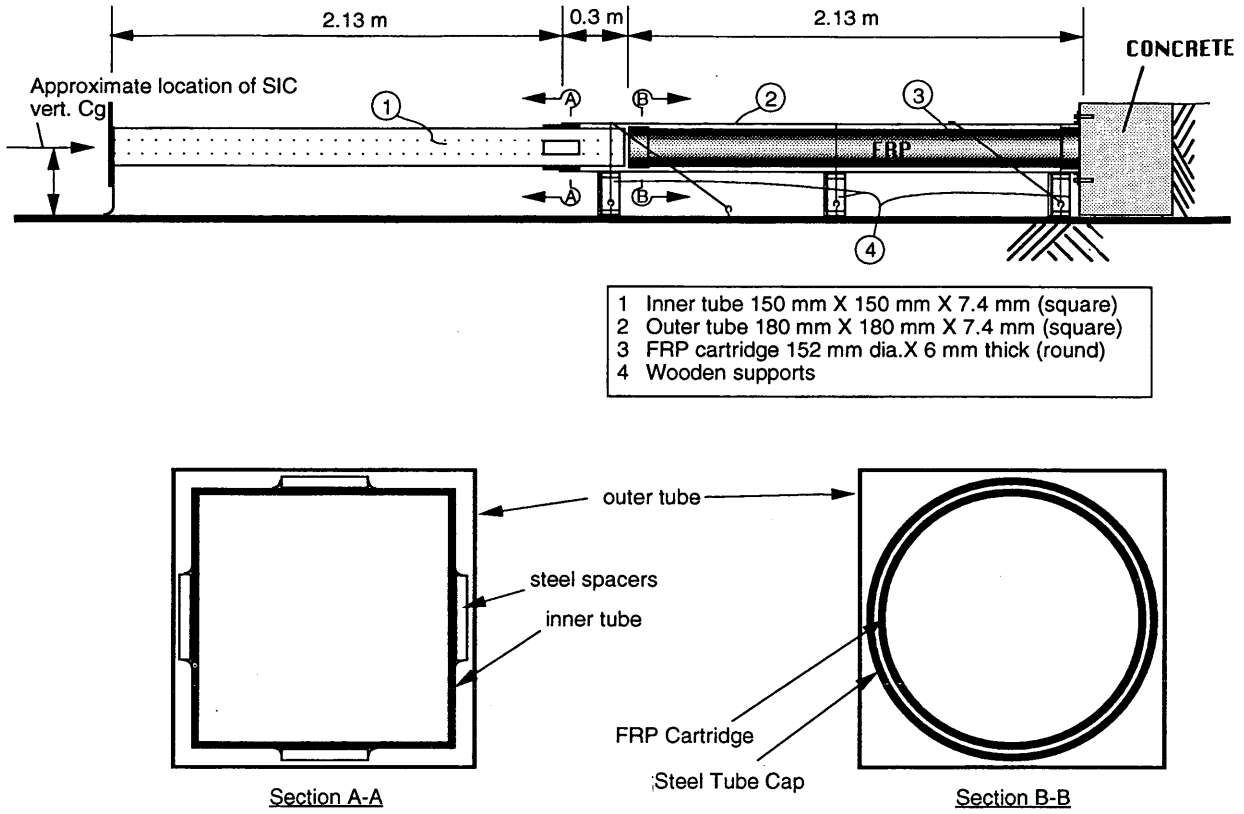

FIGURE 4 Impact attenuator.

Results of Trial Test 1

The purpose of this test was to tow the SIC, without a crash car loaded onto it, into the skid deck and impact attenuator at an estimated final speed of 48 km/hr. Stability of the SIC at this speed, performance of the wheel support collapse mechanism, and performance of the impact attenuator were focal points. In this test, the SIC had an earlier version guidance mechanism and the front wheels were fixed. The guidance rail anchor plates were not attached adequately to the pavement.

Approximately 70 m from the impact attenuator, the guidance rail shifted out of alignment, the guidance mechanism broke off, and the SIC was pulled into the skid deck without guidance. Consequently, the SIC did not reach the skid deck at the correct position and speed.

Results of Trial Test 2

This test had the same purpose as the first, with the addition of testing a modified guidance system. The fixed SIC front wheel connections were rebuilt with hinges to the axle, controlled by two tie rods connected to the guidance mechanism. The guidance mechanism incorporated a larger and stronger frame. The guidance rail anchor plates were fixed securely to the pavement.

The SIC was towed into the skid deck at approximately 48 km/hr with no problems. The wheel supports collapsed properly and the SIC hit the end of the impact attenuator squarely, pushing it in approximately 30–50 cm.

Results of Trial Test 3

A 1975 Toyota Celica hit a temporary cable barrier at an estimated speed of 42 km/hr with a trajectory angle of 25 degrees, and a counterclockwise yaw angle of 35 degrees. The system worked well, except that the test vehicle rotated slightly counterclockwise while translating in a side skid. This resulted in trajectory and yaw angles larger than desired. No signs of vehicle roll were noted; however, the Celica did pitch downward in front on making contact with the dirt. The SIC hit the attenuator squarely, crushing the FRP tube approximately 150 mm.

The Celica's undesired rotation was due to the unrestrained front wheels partially rolling and side skidding, whereas the rear wheels only side skidded since the transmission was in park. With the steering locked in a straight-ahead position, the partial rolling of the front wheels caused the front of the vehicle to track slightly in the direction of the initial yaw angle, whereas the rear translated along the initial trajectory path.

Results of Trial Test 4

The Celica from Trial Test 3 was used again in Trial Test 4. It hit the temporary cable barrier at an estimated speed of 70 km/hr with

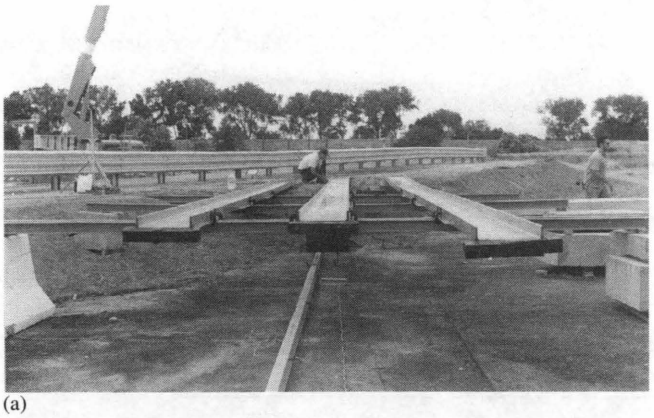

(a)

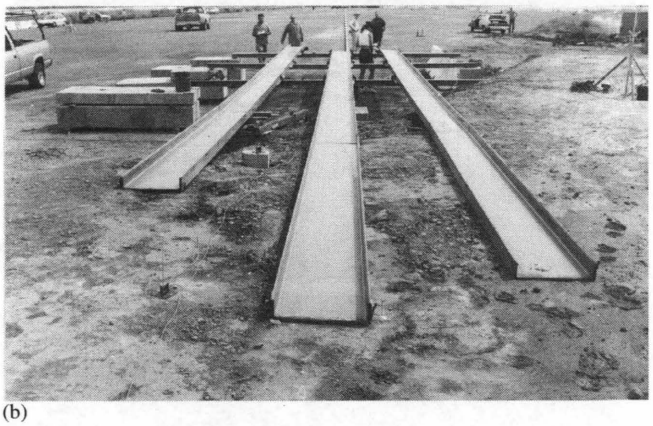

(b)

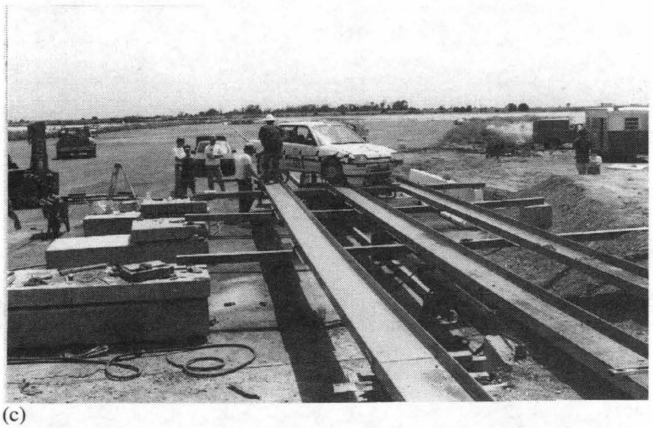

(c)

FIGURE 5 Skid deck: (*a*) looking downstream, (*b*) looking upstream, and (*c*) looking upstream with car at impact point.

a trajectory angle of 22 degrees and a counterclockwise yaw angle of 32 degrees. As the SIC hit the attenuator, the larger rear tube slipped up and off the reaction block, which in turn deflected the center skid channel upward approximately 60 cm. This caused the Celica's front left and right rear wheels to lift off of the skid channels for several feet. The car, however, stayed very close to the intended trajectory and yaw angles as it skidded onto the dirt median. This produced some instability in the car's motion, but it stabilized by the time it hit the temporary barrier.

The results of this test indicated that after modifying the impact attenuator connection to the reaction block the system was ready to be used to conduct Test 523.

Results of Test 523 Pertaining to Side Impact System

This was the final test of the project, using a 1989 Honda Civic hitting a double thrie beam median barrier. The performance of the barrier is covered in Part B.

The SIC loaded with the Honda was towed along the guidance rail without incident, until near the midpoint of the rail, the front wheels of the SIC started to turn to the right. The guidance mechanism was not able to keep the front wheels in proper alignment, probably because it was attached to the SIC frame in only one location (see Figure 3). Lateral forces transmitted from the SIC wheels to the guidance mechanism via the tie rods forced the guidance mechanism connection to the SIC frame to shift 3.18 cm laterally to the left. With the guidance mechanism shifted out of alignment, the SIC wheels were allowed to turn. Hence, the SIC remained on the guidance rail, but slightly out of alignment. The front wheels skidded as the SIC was towed into the skid deck.

The Honda slipped off the wheel supports smoothly and skidded onto the deck. The right front wheel support collapsed properly, but the other three did not, and were damaged beyond repair. The wheel supports hit the skid channels too high at the top plates, snagging and ripping them instead of making contact with the front columns and initiating collapse. The misaligned SIC caused the right front column of the right rear wheel support to miss the skid channel completely, so that the impact force initiating collapse was on only the left column.

The Honda skidded across the skid deck, made contact with the dirt median, and side skidded into the barrier at the desired 22 degrees trajectory angle. The yaw angle was 31 degrees counterclockwise, one degree off the desired 32 degrees. Impact speed was 66.5 km/hr, well below the desired 80.5 km/hr. The lower speed is attributed to the SIC not being towed fast enough because of the added drag on the tow vehicle from the misaligned SIC front wheels.

The SIC hit the attenuator squarely, slowing from 72.4 km/hr to 0 km/hr in 0.457 m, an average acceleration of $-45.2g$. Although this is significantly higher than the design acceleration of $-23.5g$, the SIC frame did not sustain any damage. The FRP tube crush strength was higher than anticipated.

The guidance mechanism problem can be eliminated if it is restrained from lateral movement by connecting it to the SIC frame in an additional location. The problem of the too-high impact with the wheel supports can be corrected by adjusting the skid deck elevations. Crushing tests of the FRP tubes should be conducted to select a smaller size that will allow the SIC to decelerate over a longer distance and decrease the acceleration at a rate closer to the design value.

Part B: Test 523—Performance of Double Thrie Beam Median Barrier in Side Skid Collision

Test Parameters

Test Article Design and Construction The test article was a double thrie beam median barrier built with W 6 × 9 steel posts in accordance with Caltrans Standard Plan A78A (*3*) (see Figure 6 (*a*). This barrier is the same type that was installed at the legal case accident site after the accident. The median was replicated by surveying the accident site area and building the test median to the same dimensions and elevations.

DATA SUMMARY SHEET, TEST 523

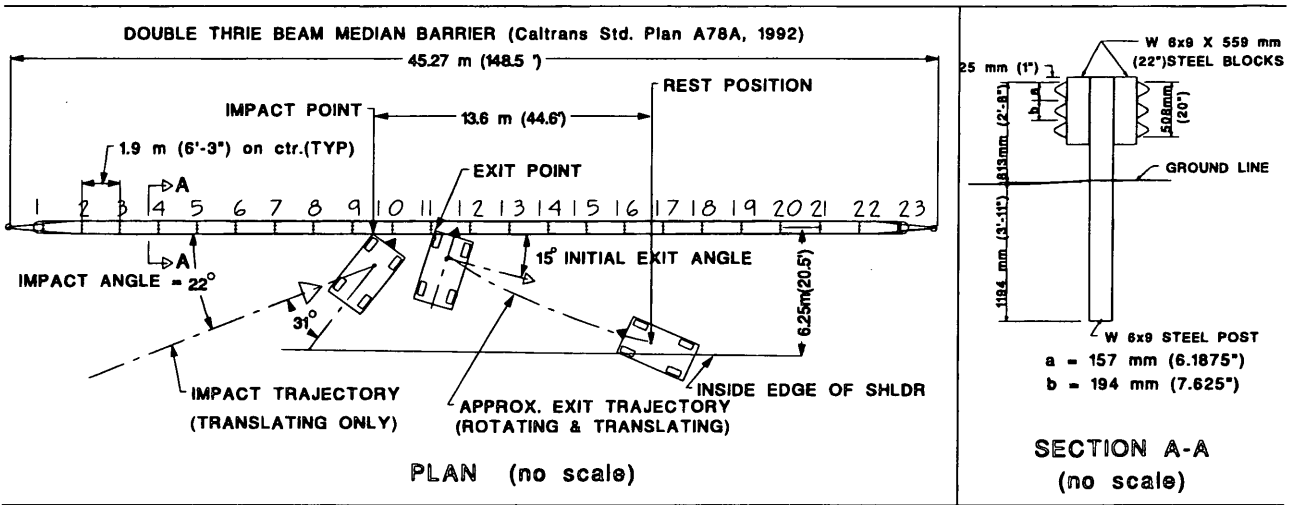

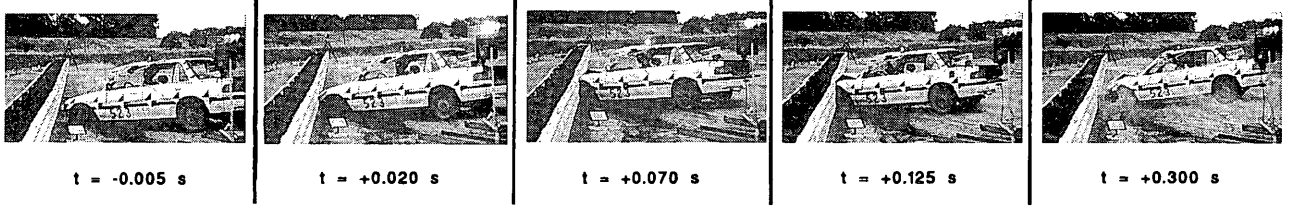

GENERAL INFORMATION		
Test Agency:		California Dept. of Transportation
Test No.		523
Test Date:		July 21, 1994
TEST ARTICLE		
Type:		Double Thrie Beam Median Barrier
Length:		45.27 m
Key elements:		W 6 x 9 steel posts, 12 gage rail
SOIL TYPE		sandy clay (SC) replicated from accident site
TEST VEHICLE		
Type:		Production model
Designation:		Exemplar vehicle for legal case
Model:		'89 Honda Civic
Mass:	Curb:	925 kg
	Test inertial:	1095 kg
	Dummy:	74.8 kg
	Gross Static:	1170 kg
IMPACT CONDITIONS		
Speed:		66.5 km/hr
Trajectory Angle:		22°
Yaw Angle:		31° Counterclockwise
EXIT CONDITIONS		
Speed:		43.4 km/hr
Trajectory Angle:		15° initially (rotating)

OCCUPANT RISK VALUES (calculated from flail space model)	
Theoretical Impact Velocity:	
longitudinal (x):	9.8 m/s
lateral (y):	No theoretical impact
Theoretical Ridedown Acceleration:	
longitudinal (x):	-6.3 g
lateral (y):	No theoretical impact
TEST ARTICLE MAXIMUM DEFLECTIONS	
Lateral:	
dynamic:	0.056 m post #10
permanent:	0.032 m post #10
Longitudinal:	
dynamic:	not measured
permanent:	0.016 m post #10
VEHICLE DAMAGE	
Exterior:	
VDS:	FL4:
CDC:	01FLEW5
Interior:	
OCDI:	LF0010000
POST IMPACT VEHICLE ROTATIONS	
Max Roll Angle:	negligible
Max Pitch Angle:	approximately 5°
Max Yaw Angle:	103°

FIGURE 6 Data summary sheet Test 523.

The barrier dynamic lateral deflections were measured with eight displacement transducers attached to Posts 8 through 15 (see Figure 6(*a*) for post locations). Permanent deflections were measured longitudinally and laterally from benchmarks placed in the ground before impact. Strain gauges were installed on the four anchor rods.

Test Vehicle The test vehicle was a 1989 Honda Civic, similar to the one that was involved in the legal case. With a test inertial mass of 1095 kg, it did not meet the NCHRP 350 requirements for an 820C vehicle (*4*).

The car was instrumented with seven triaxial sets of accelerometers and three rate gyros. High speed cameras were installed outside the driver's door and on the rear window shelf. The transmission of the test vehicle was placed in park, the steering was locked in the straight position, the emergency brake was engaged, and the wheels were restrained from rolling by wire cables. The engine was not running during the test. These actions were taken so that a translating side skid at the designated trajectory and yaw angles could be maintained.

Soil Conditions The test article median was built in an embankment constructed of imported fill that closely replicated the soil conditions at the accident site. Triaxial stress tests on the completed embankment indicated an average shear strength from 96 kPa at a normal stress of 0 kPa to 110 kPa at a normal stress of 24 kPa (depth of 1.2 m).

Test Conditions and Results

Impact Description/Vehicle Behavior The Honda side skidded into the barrier at a 22 degree trajectory angle and 31 degree counterclockwise yaw angle. Impact speed was 66.5 km/hr (see Figure 7).

The vehicle was pitched down slightly as it hit the dirt median, causing the front bumper to drop lower than the bottom of the thrie beam rail. It passed underneath it as the left headlight and hood made first contact with the rail approximately 0.8 m upstream of Post 10. About ¾ of the front-end width crushed and slid against the rail for approximately 3 m before the vehicle left the barrier at an angle of 15 degrees and a speed of 43.4 km/hr. The Honda began to rotate as it exited the barrier, and continued to rotate and translate to a point approximately 14 m downstream, straddling the edge of shoulder 6.25 m from the barrier center line. Total change in yaw from impact was 103 degrees counterclockwise.

Maximum 50-m/sec average accelerations were $-10.7g$ longitudinal, $2.5g$ lateral, and $-2.7g$ vertical. The theoretical occupant impact velocity and ridedown acceleration in the longitudinal direction were 9.8 m/sec and $-6.3g$. There was no theoretical impact in the lateral direction.

Barrier Damage The test article deflected very little (see Figure 6(*b*) for data). Only Post 10 and its front block were damaged significantly. The thrie beam rail on the impact side was bent, but would not require immediate replacement (see Figure 8). The anchor rod on the upstream impact side resisted 28.6 kN of tension, and the anchor rod on the downstream impact side resisted 18.1 kN of tension.

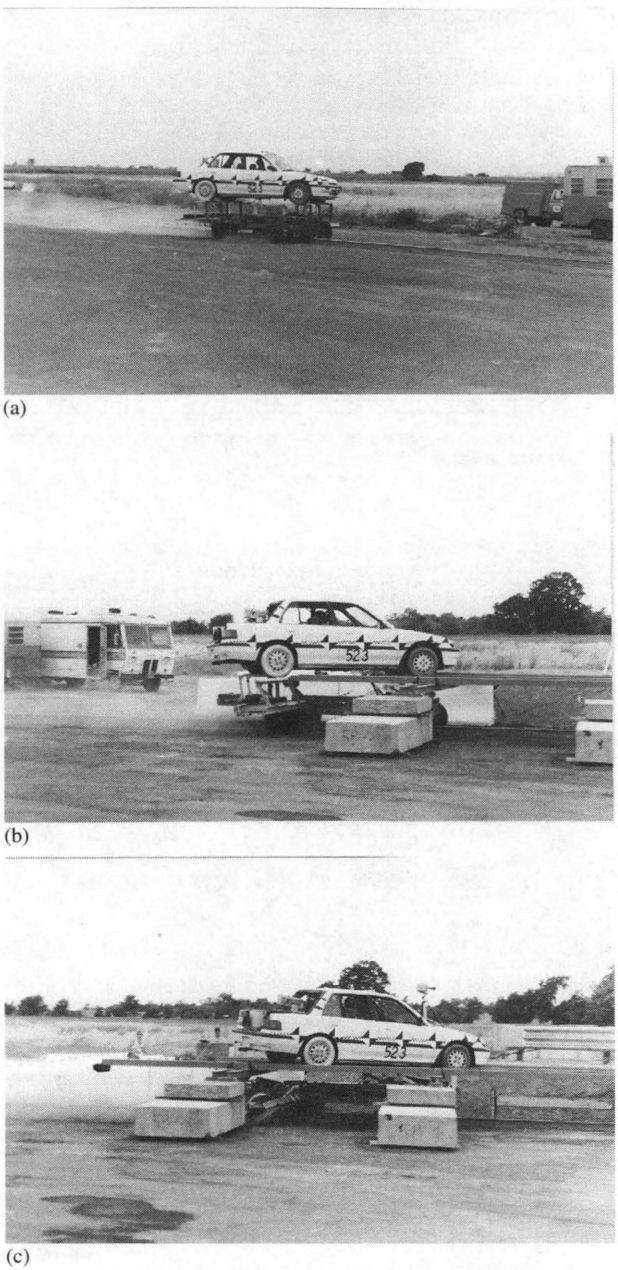

(a)

(b)

(c)

FIGURE 7 Test 523 Sequential Photos: (*a*) 1.940 sec before impact, (*b*) 1.025 sec before impact, (*c*) 0.855 sec before impact, (*d*) 0.500 sec before impact, (*e*) 0.075 sec after impact, (*f*) 0.265 sec after impact, (*g*) 0.465 sec after impact, (*h*) 0.805 sec after impact, and (*i*) 2.260 sec after impact. (*continued on next page*)

Vehicle Damage The vehicle could not be driven after the impact, but most of the damage was confined to the front left corner of the vehicle (see Figure 9). Debris scatter amounted to pieces of plastic from the Honda's lights. A portion of the plastic bumper was ripped off the Honda and got stuck at Post 10. See the Data Summary Sheet, Figure 6(*b*), for damage ratings.

Dummy Behavior A recently calibrated Hybrid III dummy was placed in the driver's seat of the test vehicle. It was restrained with a lap and shoulder belt. The head and chest each had one set of triaxial accelerometers.

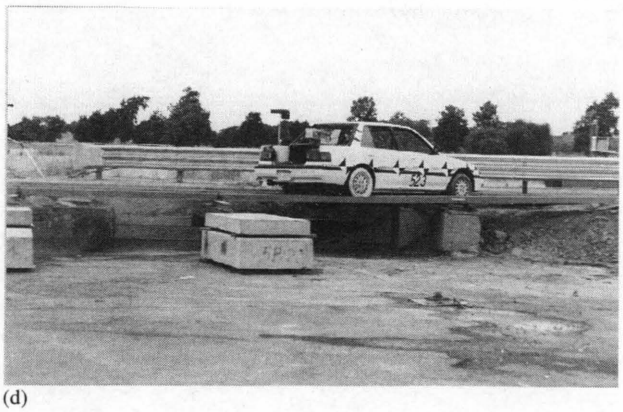
(d)


(e)

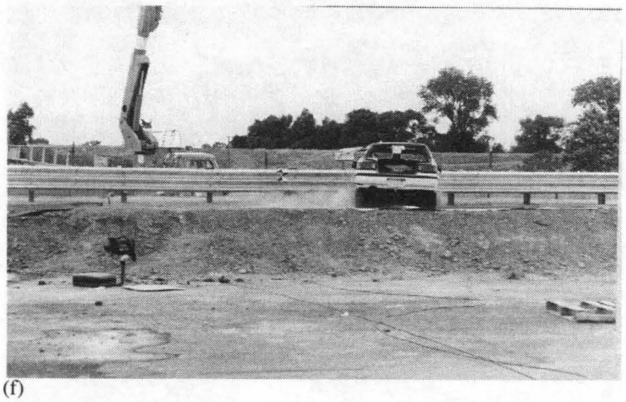
(f)

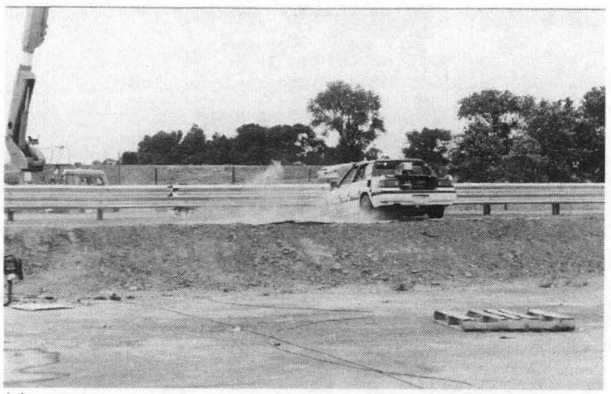
(g)

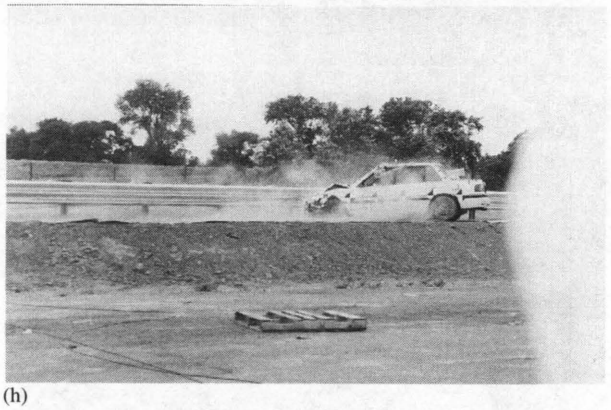
(h)

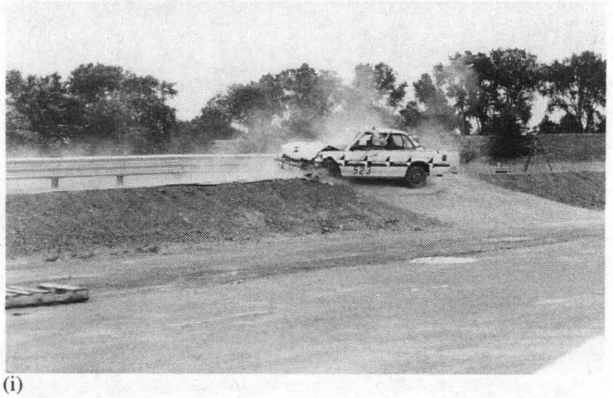
(i)

FIGURE 7 (*continued*)

After impact, the dummy rotated forward about the lap belt, but the head did not hit the steering wheel or the windshield. It rotated backward and swung slightly to the left before coming back to rest against the headrest. The head injury criteria rating was 78.8, and maximum chest accelerations were $-27g$ longitudinal, $6g$ lateral, and $6g$ vertical. The maximum head accelerations were $-15g$ longitudinal, $4g$ lateral, $18g$ vertical, and $20g$ resultant.

Assessment of Test Results

This test was assessed against standard Test 2-10 criteria of NCHRP Report 350 (*4*). Although the conditions for Test 2-10 include a smaller, tracking vehicle, they are the closest to those of Test 523, which were determined by the accident replication.

Occupant Risk The test satisfies all of the occupant risk criteria. The occupant impact velocity was 9.8 m/sec, over the preferred 9 m/sec but less than the maximum of 12 m/sec. No parts or flying debris entered the occupant compartment.

Structural Adequacy The barrier was structurally adequate: it was not penetrated and it redirected the vehicle. It received only minor damage.

Vehicle Trajectory This test did not meet the vehicle trajectory criteria. The vehicle came to rest straddling the median side shoulder line 6.25 m from the barrier center line. With a shoulder width of 0.61 m, the rear of the vehicle projected into the traveled

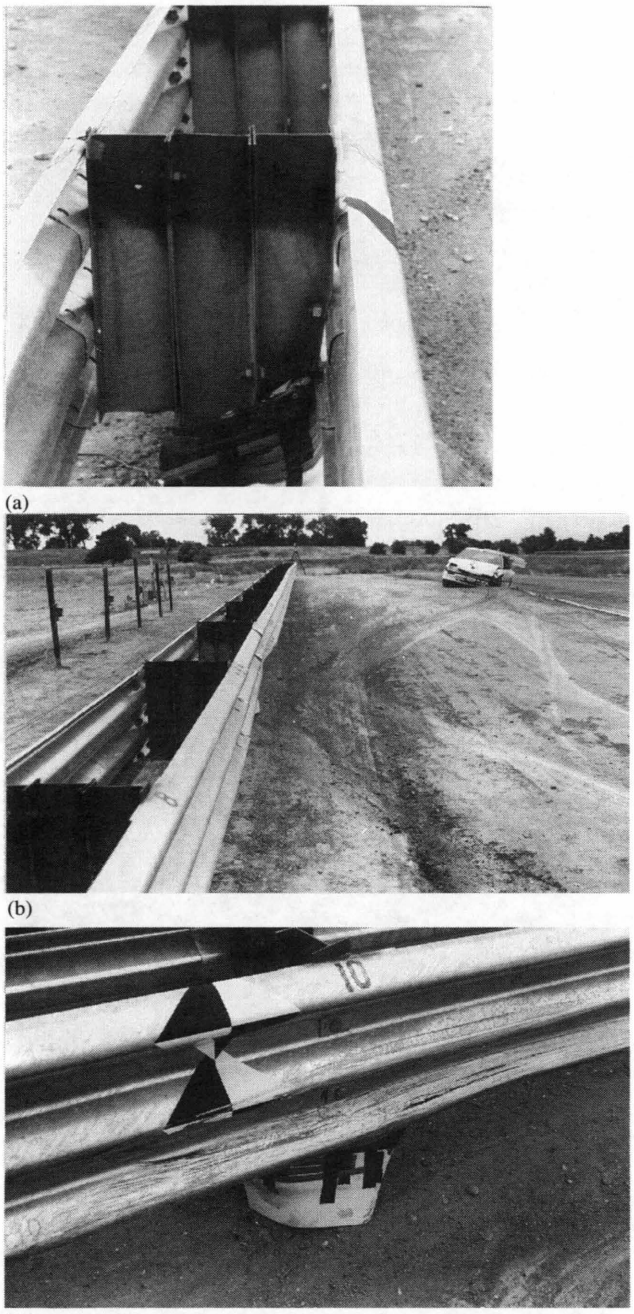

(a)

(b)

(c)

FIGURE 8 Test article damage: (*a*) Post 10 looking downstream, (*b*) looking downstream, and (*c*) impact side of barrier.

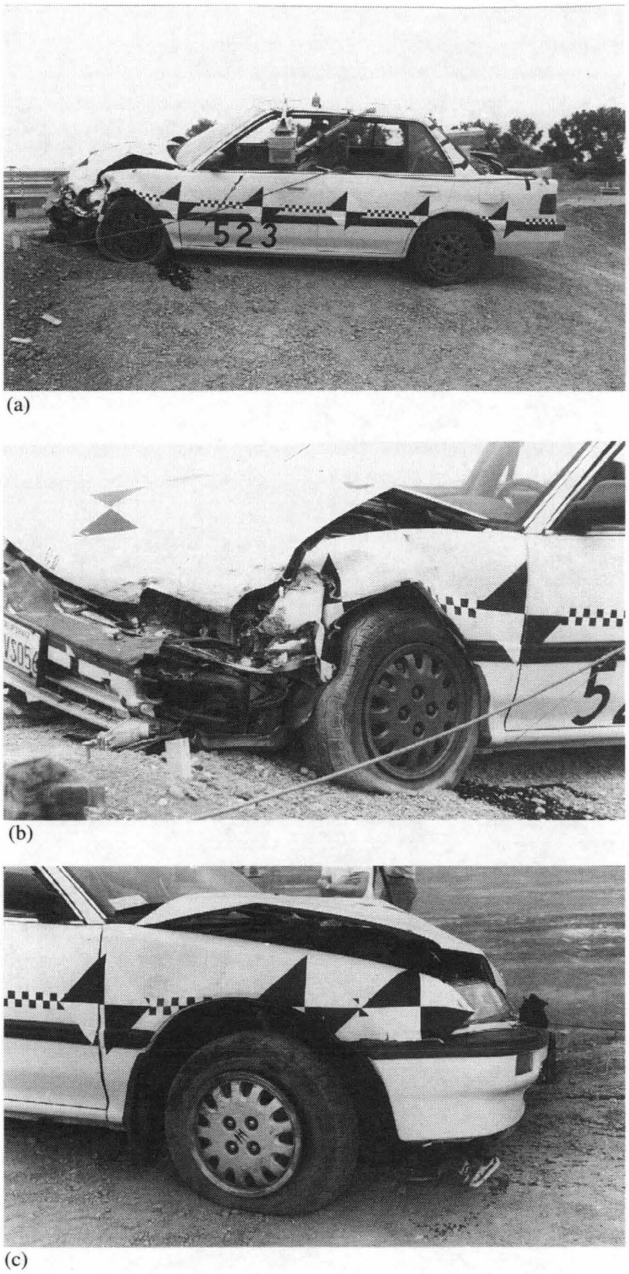

(a)

(b)

(c)

FIGURE 9 Test vehicle damage: (*a*) left side view, (*b*) left front view, and (*c*) right side view.

way. The exit angle of 15 degrees was also not less than 60 percent of the impact angle of 22 degrees.

Overall Assessment On highways with speed limits approximately 70 km/hr, the double thrie beam median barrier may be considered conditionally crashworthy in side skid collisions of the type in this test. In tests with a median width equal to that of Test 523 or smaller, the vehicle could reenter the traveled way. However, this type of barrier is installed typically in freeway medians, where speed limits are approximately 100 km/hr. At this speed, the occupant risks could be unacceptably high. Larger yaw angles could also cause higher decelerations and put the vehicle in more vulnerable positions, in which occupants would be at a higher risk of injury.

CONCLUSIONS AND RECOMMENDATIONS

The side impact system performed well enough to project the Honda properly in Test 523 at a speed of 66.5 km/hr. With an improved guidance mechanism, impact speeds of 100 km/hr should be attainable. Different yaw angles can be achieved by simply relocating the cross beams on the SIC and repositioning the skid deck

channels. With more extensive trial testing this system could be quite useful in a wide variety of side skid crash tests.

This side-skidding test at NCHRP Test Level 2 conditions indicates that the double thrie beam median barrier meets the structural adequacy and occupant risk criteria, but does not meet the vehicle trajectory criterion for medians with widths of approximately 15 m or less. More extensive testing at different yaw angles and in strict adherence to NCHRP Report 350 Test Level 3 conditions would be required to define fully the impact performance limits of the barrier in side skid collisions.

Test 523 was successful in providing information to Caltrans attorneys making decisions pertaining to the defense of the vehicle accident lawsuit.

ACKNOWLEDGMENTS

The authors would like to thank sincerely the following organizations for contributing to this ambitious project: Caltrans Legal Division for initiating the project and providing funds, FHWA for providing research funds, Baldwin Construction Co. for building the test article, and Boster, Kobayashi and Associates for accident reconstruction consultation. Many thanks are also extended to the following Caltrans employees who made it happen: Roger Stoughton, Thang Le, Office of Geology drillers, Gene Weyel, Bill Poroshin, Anne Hernandez, Nasir Khan, Gary Pund, Larry Moore, Del Gans, Bill Ng, Michael White, Michael O'Keefe, Phil Spartz, and many others who may have played smaller roles but no less important ones.

REFERENCES

1. Ray, M. H., and J. F. Carney III. *Side Impact Crash Testing of Roadside Structures.* Report RD-92-079. FHWA, U.S. Department of Transportation, Vanderbilt University, Nashville, Tenn., May 1993.
2. Sicking, D. L., K. K. Mak, and W. B. Wilson. Box-Beam Guardrail Terminal. In *Special Report 940925,* TRB, Texas Transportation Institute, College Station, Jan. 1994.
3. *Standard Plans.* California Department of Transportation, Office of Office Engineer, Sacramento, July 1992.
4. Ross, H. E. Jr., D. L. Sicking, and R. A. Zimmer. *NCHRP Report 350: Recommended Procedures for the Safety Performance Evaluation of Highway Features.* TRB, National Research Council, Washington, D.C., 1993.

Publication of this paper Sponsored by Committee on Roadside Safety Features.

Triple T: Truck Thrie Beam Transition

WANDA L. MENGES, C. EUGENE BUTH, AND CHARLES F. MCDEVITT

The Truck Thrie Beam Transition (Triple T), an 813-mm (32-in.) thrie beam transition, was developed under a recently completed pooled funds study. The study involved 23 states, the District of Columbia, and the Federal Highway Administration. The Triple T was crash-tested according to Performance Level 2 (PL2) requirements of the 1989 AASHTO guide. The transition performed acceptably after modifications were made to the end terminal connection. For testing, the transition was attached to the end of the 813-mm (32-in.) vertical-faced concrete parapet bridge railing. The Triple T is acceptable for use on other PL2 bridge railings if suitable attachment to the bridge railing (such as the modified end terminal connector) is used.

The transportation industry is continually upgrading performance requirements of bridge railing systems. The 1989 AASHTO *Guide Specifications for Bridge Railings* (*1*) defines three levels of performance for bridge railing systems. The demand for Performance Level 2 (PL2) bridge railings, which are used in many states, is expected to increase.

During a recent pooled funds study, a collection of railing designs was developed. The study was sponsored by the FHWA, the District of Columbia, and 23 states. Twelve bridge railing designs were tested at various performance levels to evaluate the different needs of various states (*2*). Four of the bridge railing designs met PL2 requirements of the 1989 AASHTO guide.

Standard W-beam guardrails are used as approach railings to most bridge railings. A transition is used to attach these semirigid railings to the stiffer bridge railings. Transition railings are also semirigid and PL2 bridge railings are usually rigid. Therefore, guardrail-to-bridge rail transitions must be designed to prevent errant vehicles from deflecting the guardrail sufficiently for the vehicle to snag the end of the rigid bridge railing. A transition that prevents this snagging reduces property damage, injuries, and fatalities.

The results of the work performed to develop and test the Truck Thrie Beam Transition (Triple T), an 813-mm (32-in.) thrie beam transition, to meet PL2 requirements, are presented (*2,3*). According to the 1989 AASHTO guide, three tests are required on the transition to meet PL2. The test matrix includes one test with an 817-kg (1,800-lb) passenger car traveling 97 km/hr (60 mph) and at an angle of 20 degrees; one with a 2,452-kg (5,400-lb) pickup truck traveling 97 km/hr (60 mph) and at an angle of 20 degrees; and a third with an 8,172-kg (18,000-lb) single-unit truck traveling 80 km/hr (50 mph) and at an angle of 15 degrees. Four tests were performed on the transition. During the test with a pickup, the end terminal snagged the door, and the door remained lodged on the edge of the terminal. Modifications were made to the end terminal splice bolt connection. Using the modified end terminal design, the pickup truck test was repeated, and the single-unit truck test was conducted.

Details of the design of the transition and modifications made to the end terminal attachment, are discussed in the next section. Crash test procedures and results of the full-scale crash tests are given. After modifications and further testing, the Triple T performed acceptably for PL2 of the 1989 guide specifications.

Texas Transportation Institute, The Texas A&M University System, College Station, Tex. 77843-3135.

DESIGN OF TRUCK THRIE BEAM TRANSITION (TRIPLE T)

The prototype Triple T was attached to an 813-mm (32-in.) vertical-faced concrete parapet bridge railing for testing. Elevation and cross-section views of the transition are shown in Figure 1. The height to the top of the transition thrie beam rail element is 790 mm (31 in.) above the ground. The transition is supported by W6 × 15 posts and 152-mm (6-in.) blocks spaced at 1-m (3-ft 1½-in.) intervals, center-to-center, with a 768-mm (2-ft 6 ¼-in.) space adjacent to the end of the concrete parapet. The transition is composed of two 3.8-m (12 ft-6 in.) sections of 12-gauge thrie beam, one nested inside the other. One 3.8-m (12-ft 6-in.) section of 12-gauge thrie beam is spliced into the nested thrie beams. The single 12-gauge thrie beam transitions to a 3.8 m (12 ft 6 in.) long section of standard W-beam guardrail. The standard W-beam guardrail terminates with a 11.4-m (37-ft 6-in.) breakaway cable terminal. The total installation is 26 m (85 ft) long. Photographs of the completed installation are given in Figure 2.

The nested thrie beams are attached to the 813-mm (32-in.) vertical-faced concrete parapet with a standard American Road and Transportation Builders Association (ARTBA) terminal connector (see Figure 3). The standard ARTBA terminal connector is a section formed in the shape of a thrie beam at one end and tapered to a flat section at the other end. The flat portion of the terminal connector attaches to a bridge abutment or parapet wall, and the rail end is spliced to the guardrail. It is impossible to connect the two layers of nested thrie beam elements to a standard ARTBA terminal connector without damaging the elements. For the first two tests, the terminal connector was lapped onto the traffic face with two layers of thrie beam sandwiched between the terminal connector and the parapet. During the test with the pickup (Test 20), the vehicle's door was peeled off by the exposed edge of the terminal connector. This unacceptable performance showed that a more suitable attachment to the concrete parapet was needed.

Three thicknesses of thrie beam material cannot be bolted together if the conventional hole patterns on the end terminals are used. A proposed remedy for this problem is to punch slotted holes in the terminal connectors, with the holes slanted approximately 45 degrees to the longitudinal axis of the connector. Although such a hole pattern allows the three layers to be bolted together, the strength of such a terminal connection is questionable. Static, axial-load tension tests were performed on several thrie beam and W-beam terminal connectors with different splice bolt patterns to determine their strengths and failure modes (*4*). The different configurations tested are shown in Figure 4, and the results of the

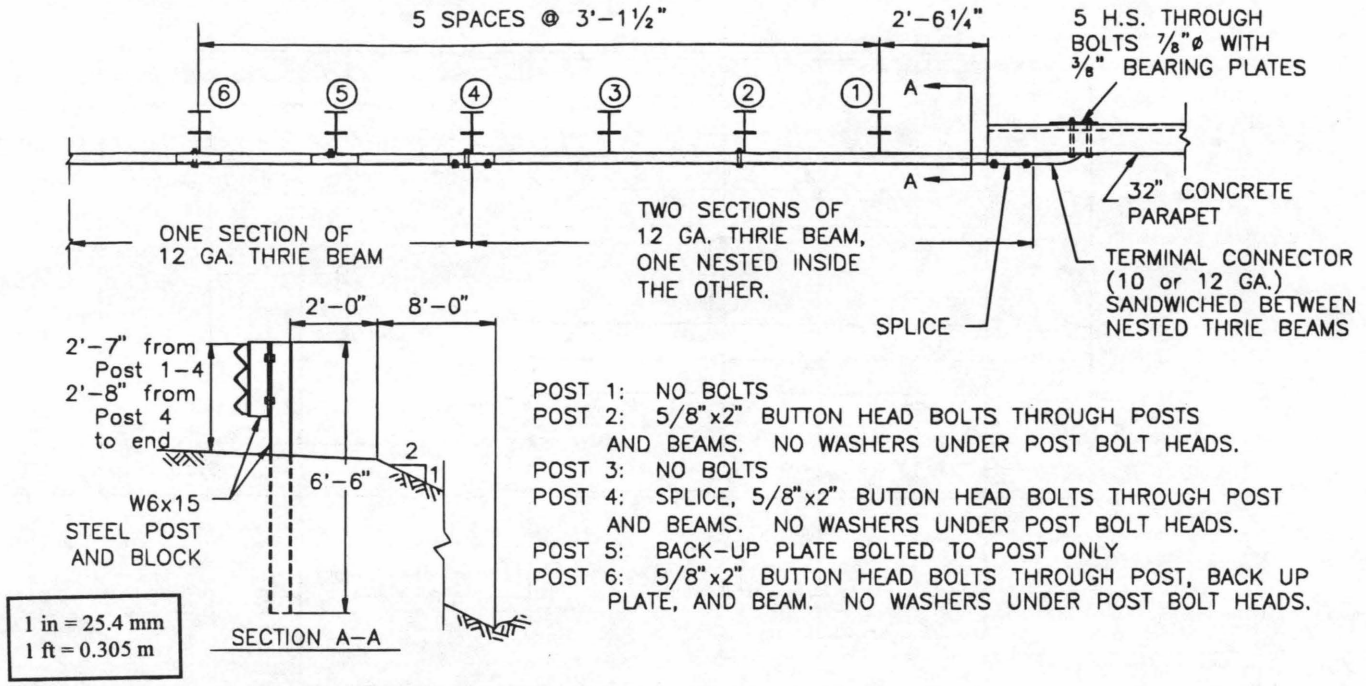

FIGURE 1 Triple T installation.

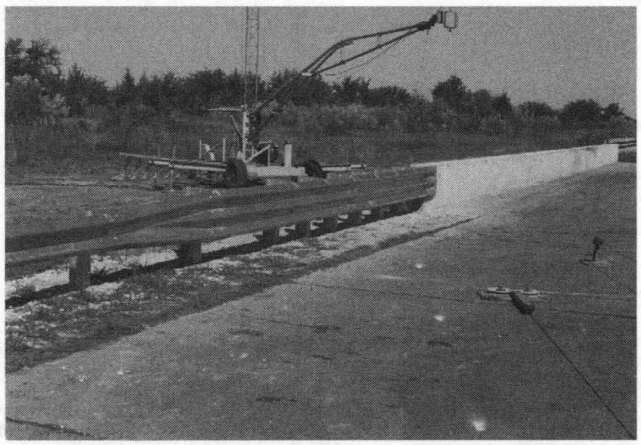

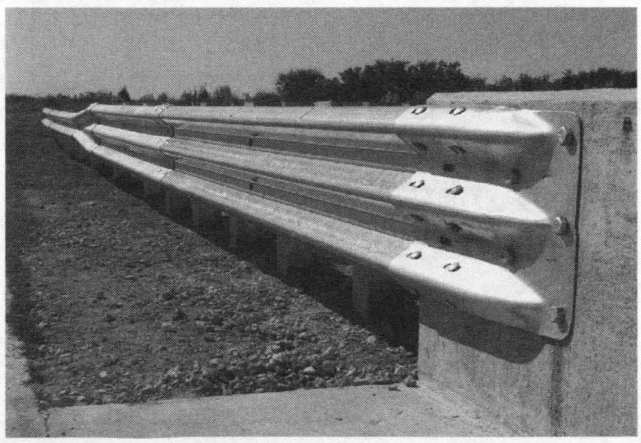

FIGURE 2 Triple T installation for Tests 19 and 20.

strength tests are summarized in Table 1. In all cases, the 25.4-mm (1-in.) holes in the flat section of the terminal exhibited plastic flow and tearing. Use of slotted, angled holes did not reduce the strength of the terminal connector.

Modifications were made only to the terminal connector that connects the transition to the concrete parapet. No modifications were made to the transition area; therefore, the small car test was not repeated. The modified terminal connector shown in Figure 5 was used for retesting the pickup truck (Test 21) and for testing the 8,172-kg (18,000-lb) single-unit truck (Test 29). The modified terminal connector has slanted, slotted holes to ease the assembly of the splice. The connector is sandwiched between the two layers of thrie beam rail element. In Test 21, the connector thickness was 12-gauge; in Test 29, it was 10-gauge.

FULL-SCALE CRASH TESTS

The Triple T was evaluated according to PL2 requirements of the 1989 AASHTO guide. Nominal test conditions for this performance level are as follows:

- 817-kg (1,800-lb) passenger car, 96.6 km/hr (60 mph), 20 degrees;
- 2,452-kg (5,400-lb) pickup, 96.6 km/hr (60 mph), 20 degrees;
- 8,172-kg (18,000-lb) single-unit truck, 80.5 km/hr (50 mph), 15 degrees.

Four tests were performed on the Triple T. The transition performed acceptably with the small car; however, during the pickup test, the exposed end of the terminal connector engaged the door of the test vehicle and separated the door from the vehicle. Modifications and strength tests were made on the end terminal splice con-

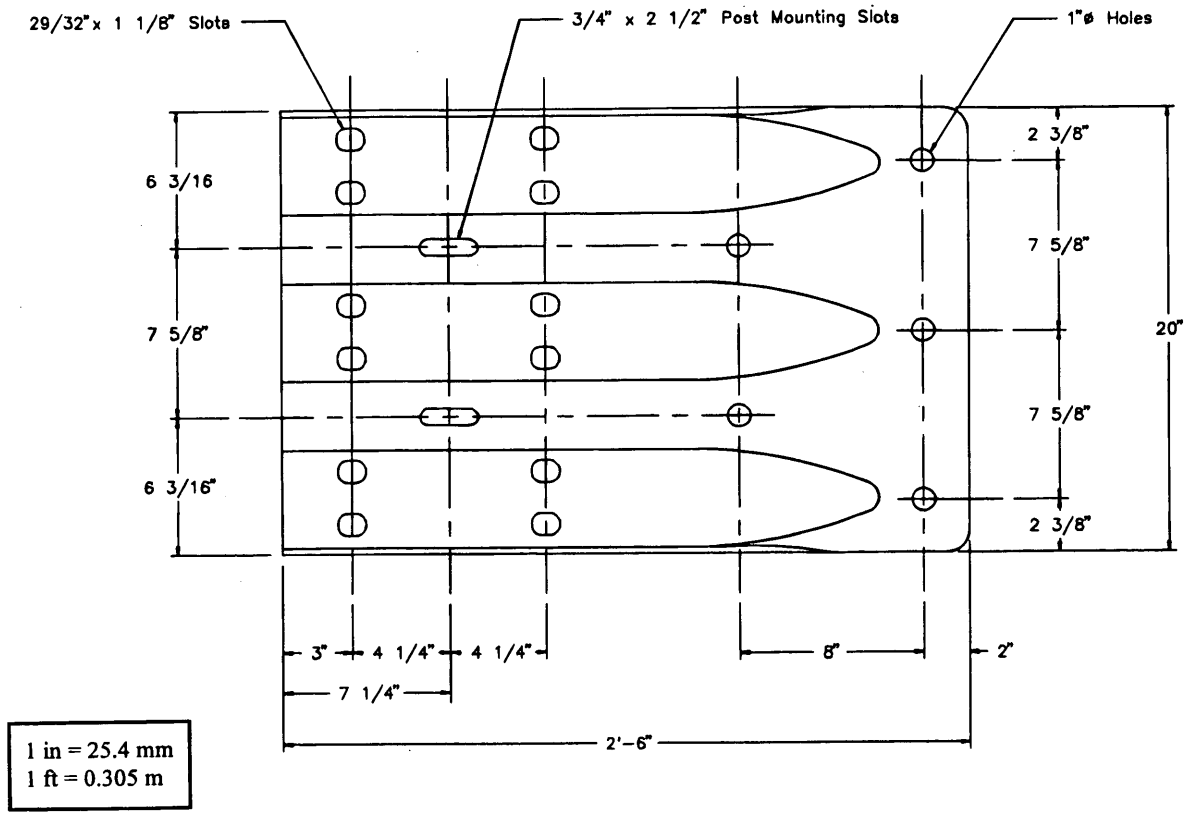

FIGURE 3 Standard ARTBA thrie beam end terminal connector.

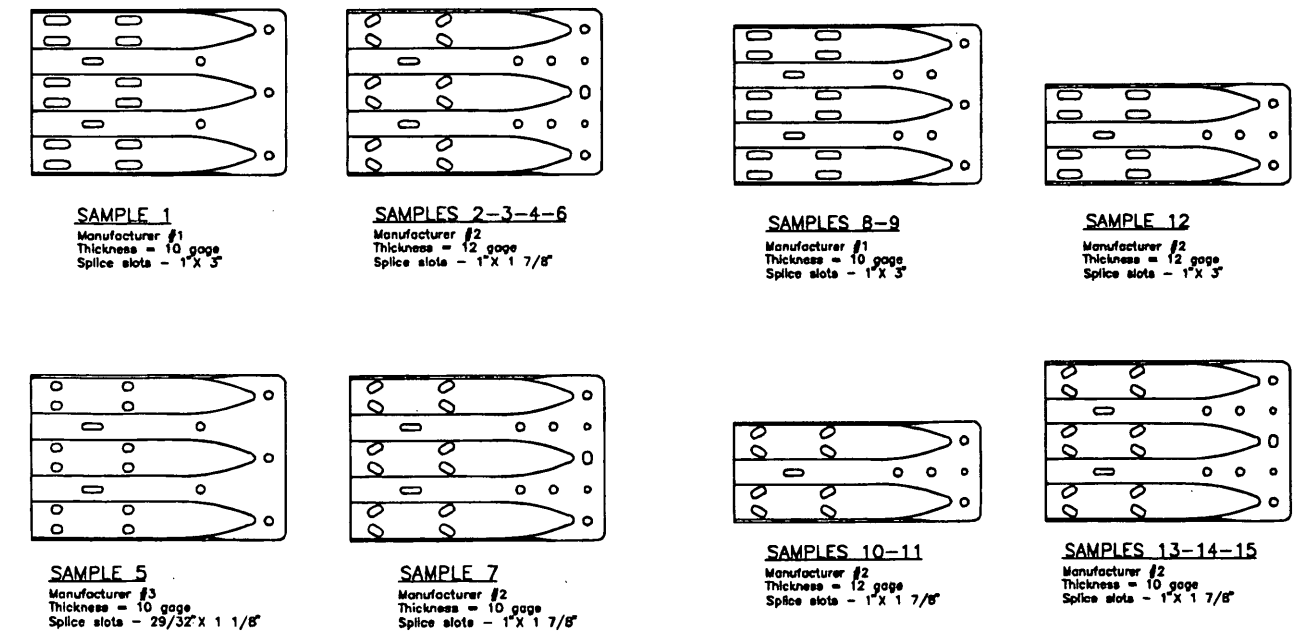

FIGURE 4 End terminal splice bolt configurations tested.

TABLE 1 Ultimate Loads and Properties of W-Beam and Thrie Beam Terminal Connectors

SAMPLE NO	MANUFACTURER	MODEL	HOLE PATTERN	THICKNESS	NO. HOLES	ULTIMATE LOAD
1	NUMBER ONE	THRIE BEAM	ST. LONG SLOTS	10 GAUGE	5[1]	95.9 KIPS (426.6 kN)
2	NUMBER TWO	THRIE BEAM	ANGLED SLOTS	12 GAUGE	9[2]	132.6 KIPS (589.8 kN)
3	NUMBER TWO	THRIE BEAM	ANGLED SLOTS	12 GAUGE	9[2]	126.9 KIPS (564.5 kN)
4	NUMBER TWO	THRIE BEAM	ANGLED SLOTS	12 GAUGE	9[2]	133.7 KIPS (594.7 kN)
5	NUMBER THREE	THRIE BEAM	ST. SHORT SLOTS	10 GAUGE	5[1]	116.7 KIPS (519.1 kN)
6	NUMBER TWO	THRIE BEAM	ANGLED SLOTS	12 GAUGE	9[1]	83.3 KIPS (370.5 kN)
7	NUMBER TWO	THRIE BEAM	ANGLED SLOTS	10 GAUGE	9[1]	---[4]
8	NUMBER ONE	THRIE BEAM	ST. LONG SLOTS	10 GAUGE	7[1]	93.8 KIPS (417.2 kN)
9	NUMBER ONE	THRIE BEAM	ST. LONG SLOTS	10 GAUGE	7[1]	87.7 KIPS (390.1 kN)
10	NUMBER TWO	W-BEAM	ANGLED SLOTS	12 GAUGE	4[3]	65.9 KIPS (293.1 kN)
11	NUMBER TWO	W-BEAM	ANGLED SLOTS	12 GAUGE	4[3]	66.4 KIPS (295.4 kN)
12	NUMBER TWO	W-BEAM	ST. LONG SLOTS	12 GAUGE	4[3]	71.1 KIPS (316.3 kN)
13	NUMBER TWO	THRIE BEAM	ANGLED SLOTS	10 GAUGE	9[1]	102.4 KIPS (455.5 kN)
14	NUMBER TWO	THRIE BEAM	ANGLED SLOTS	10 GAUGE	9[1]	99.3 KIPS (441.7 kN)
15	NUMBER TWO	THRIE BEAM	ANGLED SLOTS	10 GAUGE	9[1]	101.8 KIPS (452.8 kN)

NOTES:
1. Terminal connectors tested with 5-SAE Grade 8, 7/8-in (22-mm) bolts at the flat section.
2. Terminal connectors tested with 7-SAE Grade 8, 7/8-in (22-mm) bolts and 2-SAE Grade 8, 3/4-in (19-mm) bolts at the flat section.
3. Terminal connectors tested with 4-SAE Grade 8, 7/8-in (22-mm) bolts at the flat section.
4. Sample 7 was used in crash test 7069-29.

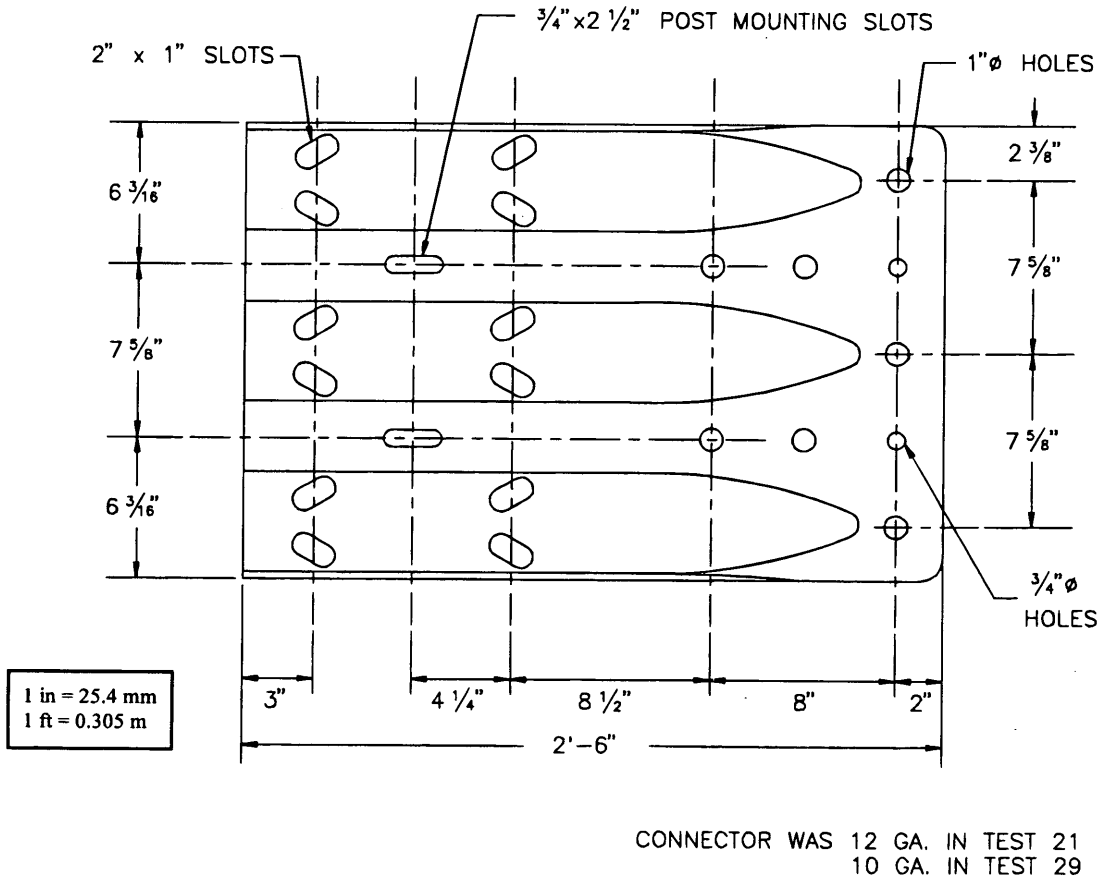

FIGURE 5 Modified end terminal connector used in Tests 21 and 29.

nection, and the pickup test was repeated using a modified end terminal connection on the transition. The modified end terminal connector was also used during the single-unit truck test. The small car test was not repeated because failure during the pickup test occurred at the terminal connector, not on the transition.

All other testing, evaluation, and reporting requirements were in accordance with specifications set forth in NCHRP Report 230 (*5*).

Test 19

For the test with the 817-kg (1,800-lb) passenger car, a 1983 Honda Civic was directed into the Triple T. Test inertia mass of the vehicle was 817 kg (1,800 lb). The gross static mass was 894 kg (1,970 lb). The speed of the vehicle at time of impact was 97.3 km/hr (60.5 mph), and the angle of impact was 19.9 degrees. The vehicle contacted the transition approximately 2.1 m (5.0 ft) from the end of the concrete parapet.

The vehicle began to redirect shortly after impact with the transition. By 0.137 sec, the vehicle was traveling parallel to the transition at a speed of 82.1 km/hr (51.0 mph). At approximately the same time, the rear of the vehicle contacted the transition. The vehicle lost contact with the transition at 0.219 sec, traveling at 76.7 km/hr (47.7 mph) and 6.9 degrees. After the brakes were applied, the vehicle yawed clockwise and subsequently came to rest 73 m (240 ft) down and 30 m (100 ft) forward of the point of impact.

The transition received minor cosmetic damage (see Figure 6). Maximum lateral deformation of the transition was 13 mm (0.5 in.) and occurred at Post 2. Damage to the vehicle included the strut and constant velocity joint on the left side. The left front wheel was canted inward at the bottom and pushed back into the fender well. Maximum crush of the vehicle was 279 mm (11.0 in.) at the left front corner at bumper height.

The transition contained the test vehicle with minimal lateral movement of the transition. Although there was minimal deformation to the occupant compartment, there was no intrusion. The vehicle remained upright and relatively stable during and after the impact sequence. The transition smoothly redirected the vehicle. Effective coefficient of friction (smoothness of the interaction of the vehicle and the transition) was considered fair.

The lateral occupant impact velocity of 7.9 m/sec (25.9 ft/sec) in this test was marginally over the 7.6 m/sec (25 ft/sec) limit specified in the 1989 AASHTO guide. The longitudinal occupant impact velocity and the longitudinal and lateral occupant ridedown accelerations were within the limits. The vehicle trajectory at loss of contact with the transition indicated minimum intrusion into adjacent traffic lanes.

Although the lateral occupant impact velocity was technically over the limit specified in the 1989 guide, performance of the transition in this test was judged acceptable (see Figure 7 and Table 2).

Test 20

The second test used a 1981 Chevrolet C-20 pickup with a test inertia mass of 2,452 kg (5,400 lb). Gross static mass of the pickup was 2,529 kg (5,570 lb). The pickup was traveling 100.9 km/hr (62.7 mph) and contacted the transition at an angle of 19.0 degrees and approximately 2.1 m (7.0 ft) from the end of the concrete parapet.

The vehicle began to redirect shortly after impact with the transition. At approximately 0.103 sec, the driver's-side door began to open and the front edge of the door began to peel away from the hinges. By 0.204 sec, the vehicle was traveling parallel to the transition at a speed of 75.3 km/hr (46.8 mph). At approximately the same time, the rear of the vehicle contacted the transition. Maximum lateral deflection of 274 mm (10.8 in.) occurred at 0.231 sec. The vehicle lost contact with the transition at 0.308 sec, traveling at 67.4 km/hr (41.9 mph). Although the vehicle exited the barrier yawing counterclockwise, the exit angle between the vehicle path and the transition was 9.0 degrees. As the brakes on the vehicle were applied, the vehicle continued to yaw counterclockwise, subsequently coming to rest 41 m (135 ft) down from the point of impact.

The transition received moderate damage, with a maximum lateral deformation of the transition of 165 mm (6.5 in.). The vehicle sustained damage to the left side as shown in Figure 8. Maximum crush at the left front corner at bumper height was 559 mm (22.0 in.). The sway bar and upper and lower control arms on the left side were damaged. The roof was bent and the driver's-side door was detached. The left front wheel was canted inward at the bottom and pushed back into the fender well.

The transition contained the test vehicle with minimal lateral movement of the transition. There was no intrusion of railing components into the occupant compartment; however, the door was

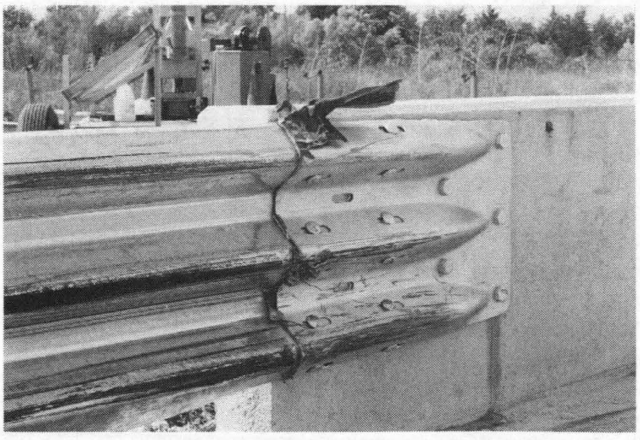

FIGURE 6 Vehicle and end terminal after Test 19.

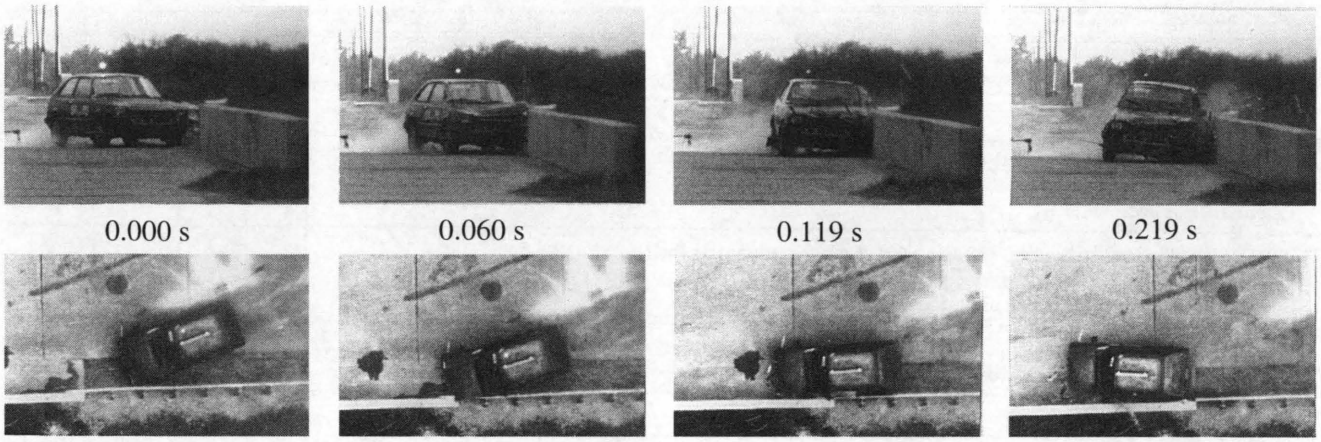

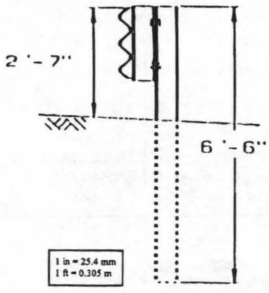

Test No.	7069-19
Date	10/02/90
Test Installation	813 mm (32-in) Thrie Beam Transition
Installation Length	26 m (85 ft)
Test Vehicle	1983 Honda Civic
Vehicle Weight	
Test Inertia	817 kg (1,800 lb)
Gross Static	894 kg (1,970 lb)
Vehicle Damage Classification	
TAD	11FL4 & 11LD6
CDC	11FLEK2 & 11LDEW3
Maximum Vehicle Crush	279 mm (11.0 in)

Impact Speed	97.3 km/h (60.5 mi/h)
Impact Angle	19.9 deg
Speed at Parallel	82.1 km/h (51.0 mi/h)
Exit Speed	76.7 km/h (47.7 mi/h)
Exit Trajectory	6.9 deg
Vehicle Accelerations (Max. 0.050-sec avg)	
Longitudinal	-8.5 g
Lateral	-14.3 g
Occupant Impact Velocity at true c.g.	
Longitudinal	5.9 m/s (19.3 ft/s)
Lateral	7.9 m/s (25.9 ft/s)
Occupant Ridedown Accelerarions	
Longitudinal	-2.3 g
Lateral	-12.5 g

FIGURE 7 Summary of results for Test 19.

detached from the vehicle and remained lodged on the end terminal connector. The vehicle remained upright and relatively stable during and after the collision. The transition redirected the vehicle, but the effective coefficient of friction was quite high. Velocity change of the vehicle during the collision was 33.5 km/hr (20.8 mph). The occupant impact velocities and the occupant ridedown accelerations were within the limits of the 1989 AASHTO guide. The vehicle trajectory at loss of contact indicates minimum intrusion into adjacent traffic lanes.

The transition performed as designed for this test; however, the exposed end of the terminal connector peeled the door from the vehicle. Because of the undesirable performance of the end terminal connector, performance of the transition in this test was judged to be unacceptable (see Figure 9 and Table 2).

After Test 20 it was decided that a more suitable attachment of the transition to the bridge railing was needed before testing could continue. A discussion of these modifications can be found in the Design section.

Test 21

The pickup test was repeated on the Triple T with the modified 12-gauge terminal connector. The modified end terminal has slotted, angled splice bolt holes. A 1984 Chevrolet custom pickup with test inertia mass of 2,452 kg (5,400 lb) and gross static mass of 2,526 kg (5,565 lb) was directed into the transition. The pickup contacted the transition 2.1 m (7.0 ft) from the end of the concrete parapet. The pickup was traveling 98.8 km/hr (61.4 mph) and contacted the transition at an angle of 18.3 degrees.

Shortly after impact, the vehicle began to redirect and then contacted Post 1. Maximum lateral deflection of the transition was 244 mm (9.5 in.) at 0.060 sec after impact. At approximately 0.070 sec, the vehicle contacted the end of the concrete parapet and the left front wheel snagged slightly on the end of the parapet. By 0.178 sec, the vehicle was traveling parallel to the transition at a speed of 80.9 km/hr (50.3 mph). The rear of the vehicle contacted the transition at 0.188 sec. The vehicle lost contact with the transition at 0.314 sec, traveling 80.5 km/hr (50.0 mph) and at an angle of 8.2 degrees. The brakes were applied as the vehicle left the immediate area of the test site, and the vehicle subsequently came to rest 41 m (195 ft) from the point of impact.

The transition received moderate damage with a maximum permanent deformation of 127 mm (5.0 in.). The vehicle sustained damage to the left side with a maximum crush of 381 mm (15.0 in.) at the left front corner at bumper height. The right front corner was deformed outward approximately 121 mm (4.8 in.). The sway bar, A-arms on the left side, and gas tank were damaged. The drive shaft, frame, and roof were bent. The floor pan was pushed into the occupant compartment approximately 127 to 178 mm (5 to 7 in.). The instrument panel moved inward approximately 76 mm (3 in.). The left front wheel was canted inward at the bottom and pushed back into the fender well, reducing the wheelbase on the driver's side by 356 mm (14.0 in.) (see Figure 10).

The transition contained the test vehicle with minimal lateral movement of the transition. Although there was deformation into

TABLE 2 Assessment of Results of Tests on Triple T

AASHTO EVALUATION CRITERIA	ASSESSMENT			
	Test 19	Test 20	Test 21	Test 29
A. The test shall contain the vehicle; neither the vehicle no its cargo shall penetrate or go over the installation. Controlled lateral deflection of the test article is acceptable.	Pass	Pass	Pass	Pass
B. Detached elements, fragments, or other debris from the test article shall not penetrate or show potential for penetrating the passenger compartment or present undue hazard to other traffic.	Pass	Pass	Pass	Pass
C. Integrity of the passenger compartment must be maintained with no intrusion and essentially no deformation.	Pass	Fail	Marginal	Pass
D. The vehicle shall remain upright during and after collision.	Pass	Pass	Pass	Fail*
E. The test article must smoothly redirect the vehicle.	Pass*	Pass*	Pass*	Pass*
F. The smoothness of the vehicle-railing interaction is further assessed by the effective coefficient of friction, μ: μ (0 - .25: Good; .26 - .35: Fair; >.35: Marginal) where $\mu = (\cos\theta - V_p/V)/\sin\theta$	Fair*	Marginal*	Marginal*	Good*
G. The impact velocity shall be less than: Occupant Impact Velocity - m/s (ft/s) Longitudinal 9.2 (30)	Fail	Pass*	Pass*	N/A
Occupant Impact Velocity - m/s (ft/s) Lateral 7.6 (25)	Pass	Pass*	Pass*	N/A
Occupant Ridedown Accelerations - g's Longitudinal 15				
Occupant Ridedown Accelerations - g's Lateral 15				
H. Vehicle exit angle from the barrier shall not be more than 12 degrees.	Pass*	Pass*	Pass*	Pass*

*Desired but not required.

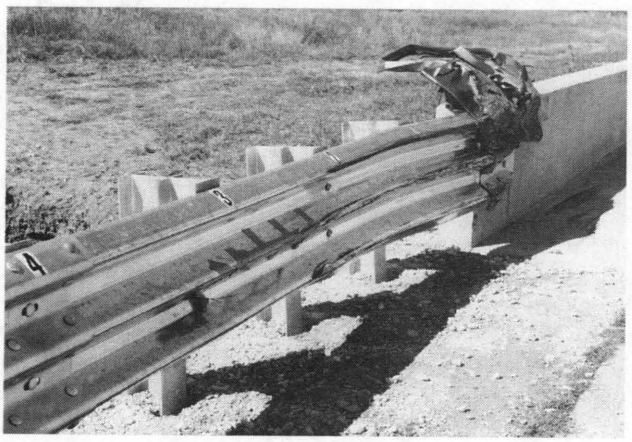

FIGURE 8 Vehicle and transition after Test 20.

the occupant compartment, there was no intrusion of railing components. The vehicle remained upright and relatively stable during and after the collision. The transition redirected the vehicle, but the effective coefficient of friction was quite high. Velocity change of the vehicle during the collision was 17.9 km/hr (11.1 mph). The occupant impact velocities and the occupant ridedown accelerations were within the limits specified in the 1989 AASHTO guide. The vehicle trajectory at loss of contact indicates minimum intrusion into adjacent traffic lanes.

The deformation of the floor pan was of some concern, but was not considered life-threatening. Performance of the transition in this test was judged acceptable (see Figure 11 and Table 2).

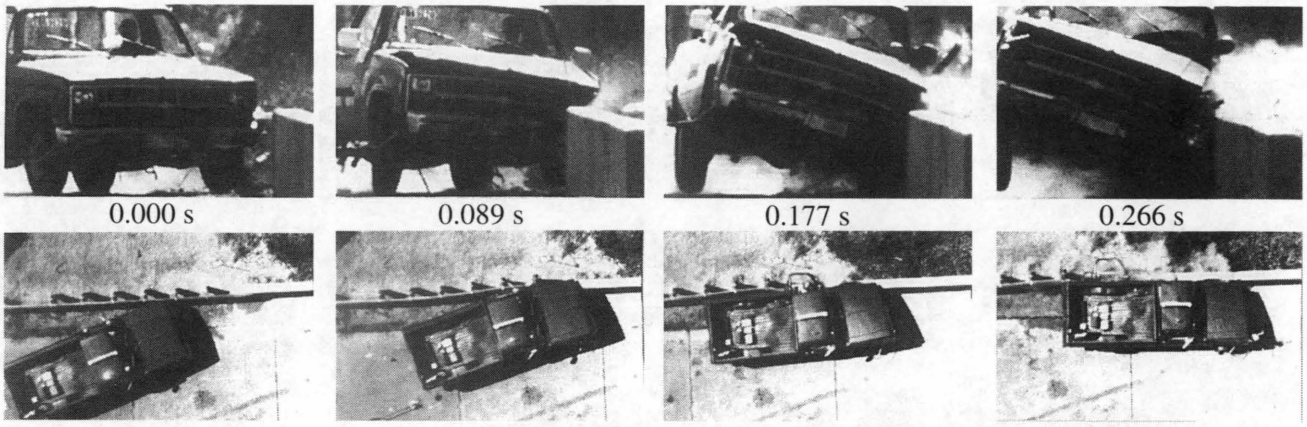

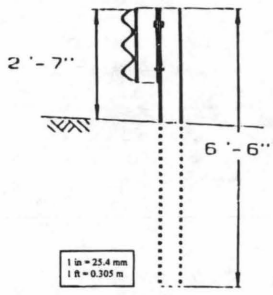

Test No.	7069-20
Date	10/19/90
Test Installation	813 mm (32-in) Thrie Beam Transition
Installation Length	26 m (85 ft)
Test Vehicle	1981 Chevrolet C-20 Pickup
Vehicle Weight	
Test Inertia	2 452 kg (5,400 lb)
Gross Static	2 529 kg (5,570 lb)
Vehicle Damage Classification	
TAD	11FL5 & 11LD7
CDC	11FLEK3 & 11LDEW3
Maximum Vehicle Crush	559 mm (22.0 in)

Impact Speed	100.9 km/h (62.7 mi/h)
Impact Angle	19.0 deg
Speed at Parallel	75.3 km/h (46.8 mi/h)
Exit Speed	67.4 km/h (41.9 mi/h)
Exit Trajectory	9.0 deg
Vehicle Accelerations (Max. 0.050-sec avg)	
Longitudinal	-6.4 g
Lateral	-7.7 g
Occupant Impact Velocity at true c.g.	
Longitudinal	5.9 m/s (19.3 ft/s)
Lateral	5.3 m/s (17.3 ft/s)
Occupant Ridedown Accelerations	
Longitudinal	-5.4 g
Lateral	-13.0 g

FIGURE 9 Summary of results for Test 20.

FIGURE 10 Vehicle and transition after Test 21.

Test 29

In this test, a modified 10-gauge terminal connector was used to attach the Triple T to the concrete parapet. A 1981 Ford single-unit truck was used in the crash test. Test inertia mass of the vehicle was 4,899 kg (10,790 lb), and its gross static mass was 8,172 kg (18,000 lb). The vehicle contacted the transition 3.4 m (11 ft) from the end of the concrete parapet. The speed of the vehicle at impact was 83.0 km/hr (51.6 mph), and the angle of impact was 14.6 degrees.

Shortly after impact the front wheels received a steer input to the left and the vehicle began to redirect. At 0.155 sec, the vehicle contacted the end of the concrete parapet. By 0.262 sec, the vehicle was traveling parallel to the transition at a speed of 78.7 km/hr (48.9 mph). At 0.341 sec, the rear of the vehicle contacted the transition. The vehicle lost contact with the terminal connector at 0.585 sec; however, the van-box remained in contact with the top of the concrete parapet until 1.718 sec after impact. As the vehicle continued forward, it began to yaw clockwise and roll counterclockwise. The brakes were applied at 2.5 sec after impact. The vehicle

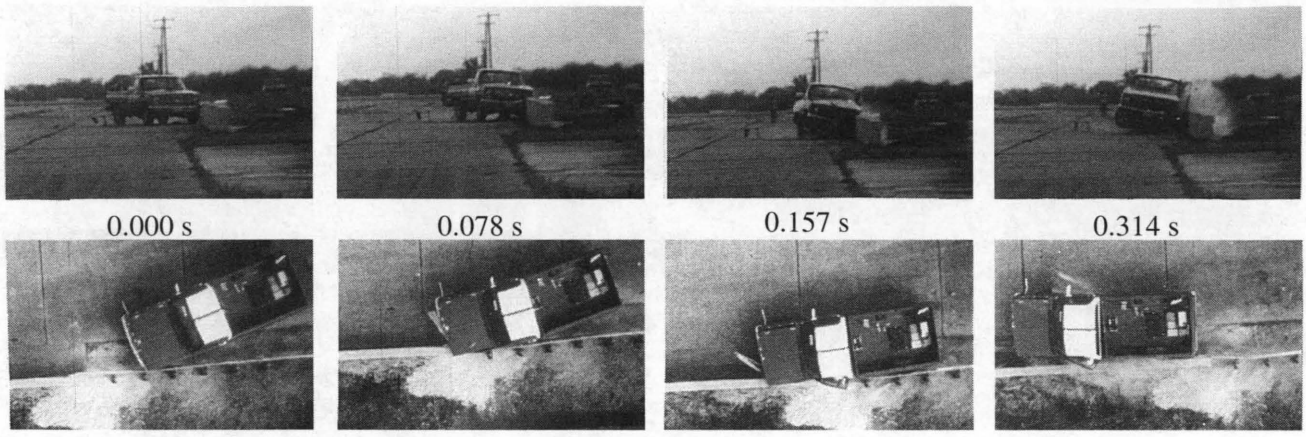

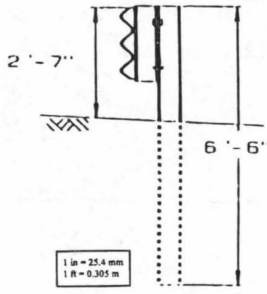

Test No.	7069-21
Date	03/17/92
Test Installation	813 mm (32-in) Thrie Beam Transition
Installation Length	26 m (85 ft)
Test Vehicle	1984 Chevrolet Custom Pickup
Vehicle Weight	
Test Inertia	2 452 kg (5,400 lb)
Gross Static	2 527 kg (5,565 lb)
Vehicle Damage Classification	
TAD	11FL5 & 11LD6
CDC	11FLEK3 & 11LDEW4
Maximum Vehicle Crush	381 mm (15.0 in)

Impact Speed	98.8 km/h (61.4 mi/h)
Impact Angle	18.3 deg
Speed at Parallel	80.9 km/h (50.3 mi/h)
Exit Speed	80.5 km/h (50.0 mi/h)
Exit Trajectory	8.2 deg
Vehicle Accelerations (Max. 0.050-sec avg)	
Longitudinal	-6.9 g
Lateral	-10.3 g
Occupant Impact Velocity at true c.g.	
Longitudinal	5.9 m/s (19.3 ft/s)
Lateral	7.6 m/s (24.8 ft/s)
Occupant Ridedown Accelerarions	
Longitudinal	-3.7 g
Lateral	12.5 g

FIGURE 11 Summary of results for Test 21.

subsequently rolled and came to rest on its left side 50 m (165 ft) down and 14 m (45 ft) forward from the point of impact.

The transition received moderate damage with a maximum permanent deformation of 254 mm (10.0 in.). The end of the concrete parapet where the terminal connector attached was cracked, as shown in Figure 12. The vehicle sustained damage to the left side. Maximum crush at the left front corner at bumper height was 330 mm (13.0 in.). The floor pan was pushed inward, and the cab was bent and twisted. The windshield and rear glass were broken. The frame at the rear axle was bent, and the van box was twisted and torn.

The transition contained the test vehicle with minimal lateral movement of the transition. The floor pan was slightly deformed into the vehicle; however, there was no intrusion of railing components into the occupant compartment. The vehicle remained upright and relatively stable during the test sequence. After exiting the immediate area of the test installation, the vehicle rolled onto its left side. This rollover behavior was attributed to asymmetrical brake application as the vehicle exited the test site. The transition redirected the vehicle with the effective coefficient of friction rated as good. The vehicle trajectory at loss of contact indicates minimal intrusion into adjacent traffic lanes. Performance of the transition in this test was judged acceptable (see Figure 13 and Table 2).

SUMMARY AND CONCLUSIONS

Two tests were performed on the Triple T with a standard ARTBA end terminal connector. Problems were encountered with the end terminal connection attaching the nested thrie beam elements of the transition to the concrete parapet. It was not possible to connect the nested thrie beam elements to the terminal connector with the conventional splice bolt hole pattern without damaging the elements. During the first two tests, the terminal connector was lapped onto the traffic face with two layers of thrie beam sandwiched between the terminal connector and the concrete parapet. The exposed edge of the terminal connector engaged the door of the pickup during the second test, and the door remained lodged on the end terminal connector. To facilitate bolting the three thicknesses of material together, slotted holes were punched in the terminal connector, with the holes slanted 45 degrees to the longitudinal axis of the connector. Because the strength of such a terminal connection was questionable, tests were performed on various splice bolt patterns. During the strength tests, failure first occurred in the flat section of the terminal that attaches to the bridge railing. It was concluded that the splice bolt pattern did not affect the performance or static load capacity of the connection.

A modified terminal connector with slanted, slotted holes was used for retesting the pickup and for testing with the 8,172-kg (18,000-lb) single-unit truck. The Triple T and modified end terminal meet PL-2 criteria of the 1989 AASHTO guide.

The Triple T can be used to transition from the approach guardrail to PL2 bridge railings if an appropriate attachment to the bridge railing is made. Attachment to a bridge railing should provide a smooth tensile capacity of the transition rail element at least as high as values obtained from tests reported in Table 2. An ARTBA end terminal modified by punching angled, slotted holes in the splice bolt connection can be used to attach the Triple T to some PL2 bridge railings.

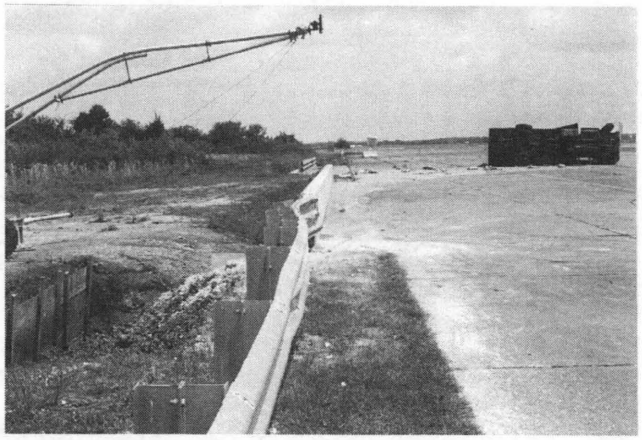

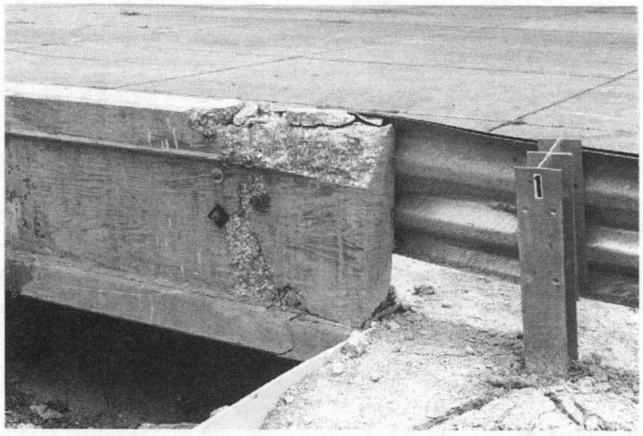

FIGURE 12 Transition after Test 29.

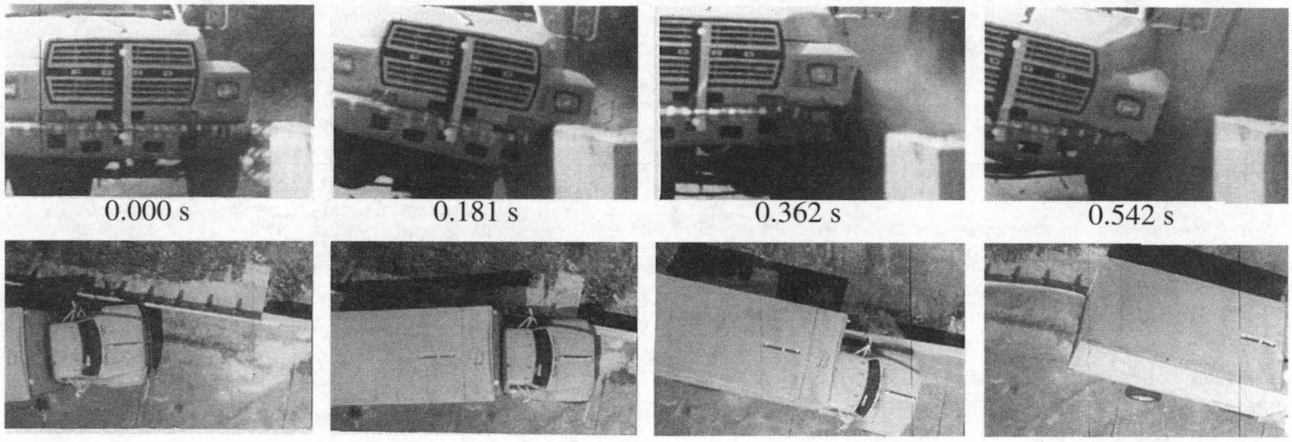

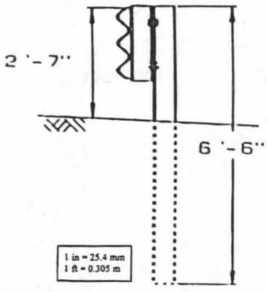

Test No.	7069-29
Date	06/05/92
Test Installation	813 mm (32-in) Thrie Beam Transition
Installation Length	26 m (85 ft)
Test Vehicle	1981 Ford Single-Unit Truck
Vehicle Weight	
Test Inertia	4 899 kg (10,790 lb)
Gross Static	8 172 kg (18,000 lb)
Maximum Vehicle Crush	330 mm (13.0 in)
Max. Perm. Deform.	254 mm (10.0 in)

Impact Speed	83.0 km/h (51.6 mi/h)
Impact Angle	14.6 deg
Speed at Parallel	78.7 km/h (48.9 mi/h)
Exit Speed	N/A
Exit Trajectory	11 deg
Vehicle Accelerations (Max. 0.050-sec avg)	
Longitudinal	-2.3 g
Lateral	6.3 g
Occupant Impact Velocity at true c.g.	
Longitudinal	2.9 m/s (9.4 ft/s)
Lateral	3.6 m/s (11.9 ft/s)
Occupant Ridedown Accelerarions	
Longitudinal	-4.1 g
Lateral	9.0 g

FIGURE 13 Summary of results for Test 29.

REFERENCES

1. *Guide Specifications for Bridge Railings.* American Association of State Highway and Transportation Officials, Washington, D.C., 1989.
2. Buth, C. E., T. J. Hirsch, and W. L. Menges. Technical Report. *Testing of New Bridge Rail and Transition Designs,* Vol. I. Texas Transportation Institute, Texas A & M University, College Station, Sept. 1993.
3. Buth, C. E., T. J. Hirsch, and W. L. Menges. 32-in (813-mm) Thrie Beam Transition. *Testing of New Bridge Rail and Transition Designs,* Vol. XIII, Appendix L, Texas Transportation Institute, Texas A&M University, College Station, Sept. 1993.
4. Buth, C. E., T. J. Hirsch, and M. Henderson. Axial Tensile Strength of Thrie and W-Beam Terminal Connectors. *Testing of New Bridge Rail and Transition Designs,* Vol. XIV, Appendix M, Texas Transportation Institute, Texas A & M University, College Station, Sept. 1993.
5. Michie, J. D. *NCHRP Report 230: Recommended Procedures for the Safety Performance Evaluation of Highway Appurtenances.* TRB, National Research Council, Washington, D.C., March 1981.

Publication of this paper sponsored by Committee on Roadside Safety Features.

Performance Level 1 Bridge Railings

DEAN C. ALBERSON, WANDA L. MENGES, AND C. EUGENE BUTH

Twenty-three states, FHWA, and the District of Columbia sponsored the project Testing of New Bridge Rail and Transition Designs that was completed in September 1993. Bridge railing for Performance Levels 1, 2, and 3, as specified in the 1989 American Association of State Highway and Transportation Officials *Guide Specifications for Bridge Railings*, were tested under the contract. This paper discusses the design and performance of the two bridge railings tested at Performance Level 1. The Oregon side-mounted railing has been used on small bridges on low-volume rural roads and is typically mounted on pre-stressed deck planks. The W6 × 15 posts are mounted on the side face of exterior planks, and a single thickness of 10-gauge thrie beam is mounted to the posts without blockouts. Height to the top of the rail element is 690 mm (27 in.). The BR27D railing design consists of a concrete parapet with a metal beam-and-post railing mounted on top of the parapet. For testing, it was mounted both on top of a sidewalk and flush on the deck.

In August of 1986, a major pooled-funds project was initiated to evaluate numerous bridge railings and transitions (*1*). When the project was completed in 1993, 37 full-scale crash tests were performed. Bridge railings were evaluated at Performance Levels 1, 2, and 3. Objectives of the study were to develop safer bridge rail and transition designs and improve design guidelines. This report focuses on the performance of the PL1 bridge railings tested under the pooled-funds project.

The first railing discussed is the Oregon side-mounted bridge railing. A single thickness 10-guage thrie beam is mounted on W6 × 15 posts spaced 1.9 m (6.25 ft) on center. Maximum deflection from the pickup crash test was 330 mm (13.0 in.) at the top of the thrie beam. This design is somewhat more flexible than the BR27D that was also tested. The BR27D bridge railing consists of two tubular box members atop a 457-mm (18.0-in.) concrete parapet. Tests were performed with and without a sidewalk. Lateral displacement of the top rail element on both tests was 13 mm (0.5 in.). All railings tested at PL1 under this contract were judged to have acceptable performance.

DESIGN CONSIDERATIONS

The 1989 guide specification sets forth three performance levels for bridge railings (*2*). A 2,452-kg (5,400-lb) pickup truck traveling at 72 km/hr (45 mph) with an impact angle of 20 degrees is used to evaluate the strength and height of a PL1 railing. The required minimum height of the resultant of resisting force provided by the railing to prevent the vehicle from rolling over the railing is at or somewhat below the center-of-gravity of the test vehicle. Height to the center-of-gravity of a typical empty 3/4-ton pickup is about 660 mm (26 in.), and the empty weight is about 2,088 kg (4,600 lb). Onboard instrumentation used in tests increases the weight, and ballast (fixed to the vehicle) is typically used to adjust the test inertia weight to 2,452 kg (5,400 lb). The ballast is positioned to provide a center-of-gravity of the total mass at 690 mm (27 in.) above the ground. The recommended design force of 133 kN (30 kips) used for PL1 railings is a uniformly distributed line force 1.07 m (42 in.) long located at least 610 mm (24 in.) above the roadway surface.

Much of the information used to establish recommended values of design force was developed in two earlier FHWA research studies (*3,4*). In those studies, a rigid flat-faced vertical wall was instrumented with load cells and accelerometers to measure transverse forces during crashes under various impact conditions. The force recommended for design of railings is based on highest 0.050-sec averages of measured forces. It is recommended that no factor of safety (i.e., load factor = 1.0) be used with the values of force in ultimate strength analyses of railings for specified test conditions.

Besides providing adequate strength, a railing system must provide suitable geometrics for interaction with the vehicle. Adequate height must be provided to prevent the vehicle from rolling over the railing. Sufficient frontal area must be provided to adequately engage the vehicle and provide a smooth redirection without too much snagging and longitudinal deceleration.

A yieldline analysis procedure was used for the concrete parapet bridge railing (*5*). The expected yieldline failure pattern for a concrete parapet consists of three yield lines extending from a point directly below the center of the load and at the base of the parapet. One line extends vertically and the other two extend diagonally to the top of the parapet.

A plastic hinge failure mechanism analysis technique was used for metal beam and post systems (*5*). Typical failure mechanisms for such railing systems occur in one, two, or three spans with plastic hinges forming at the mid-length of the railing failure mechanism and at the base of posts within the failure mechanism.

FULL-SCALE CRASH TESTS

Two PL1 designs were evaluated. They were:

1. Oregon side-mounted railing.
2. BR27D on sidewalk and on deck.

A summary of the tests performed is presented in Table 1.

Oregon Side-Mounted Railing

The original design for this railing was proposed by the Oregon DOT. It has been used on small bridges on low-volume rural roads and is typically mounted on pre-stressed deck planks. The W6 × 15 posts are mounted on the side face of exterior planks, and a single thickness of 10-gauge thrie beam is mounted to the posts without blockouts. Height to the top of the rail element is 690 mm (27 in.). A drawing for this railing design is shown in Figure 1.

Texas Transportation Institute, The Texas A&M University System, College Station, Tex. 77843.

TABLE 1 Summary of Full-Scale Crash Tests Performed on Performance Level 1 Railings

RAILING DESIGN	TEST NO.	ACTUAL CONDITIONS	OCCUPANT RISK				PERF.
			Vx(m/s)	Vy(m/s)	Ax(g's/10ms)	Ay(g's/10ms)	
OREGON SIDE-MOUNTED	7069-17	894 kg|84.0 km/h|19.7 deg	5.7	5.8	-1.8	4.5	Accept
	7069-18	2605 kg|74.2 km/h|20.9 deg	5.2	3.6	-3.6	8.8	Accept
BR27D ON SIDEWALK	7069-22	893 kg|83.2 km/h|20.8 deg	3.7	1.9	-4.7	-13.3	Accept
	7069-23	2527 kg|72.9 km/h|20.2 deg	4.0	4.3	-2.3	-10.6	Accept
BR27D ON DECK	7069-30	894 kg|82.4 km/h|20.5 deg	4.9	6.6	-3.6	-6.1	Accept
	7069-31	2527 kg|73.4 km/h|18.8 deg	3.6	3.7	2.2	-8.2	Accept

1 kg = 2.2 lb 1 km = 0.6 mi

Test 7069-17: 817-kg (1,800-lb) Honda Civic, 84.0 km/hr (52.2 mph), 19.7 degrees

The vehicle struck the bridge railing approximately 6.3 m (20.6 ft) from the upstream end. The vehicle lost contact with the bridge railing at 0.26 sec traveling at 68.7 km/hr (42.7 mph) and 7.1 degrees. It was in contact with the railing for 2.8 m (9.3 ft).

The railing received moderate damage (Figure 2). Maximum lateral deflection was 13 mm (0.5 in.) at the top of Post 5. At Post 4, the top anchor bolts connecting the post to the bridge deck showed structural distress. One bolt was pulled from the anchor insert in the concrete. Post 5 was bent outward about 13 mm (0.5 in.) at the top, and the top anchor bolts showed structural distress. One of the bolts in this post was also pulled from the anchor insert.

Examination of anchor bolts in all the posts after the tests shows that the bolts had been cut off during construction and, in some, only three or four threads were engaged in the anchor insert. The plans called for a minimum thread engagement of 22 mm (7/8 in). Evidently, concrete had flowed into the anchors during fabrication of the pre-stressed deck slabs and the anchor bolts had been cut off to prevent them from bottoming out. This was not detected during the construction inspection process. Before the next test, concrete was removed from all anchor inserts and new full-length anchor bolts were installed.

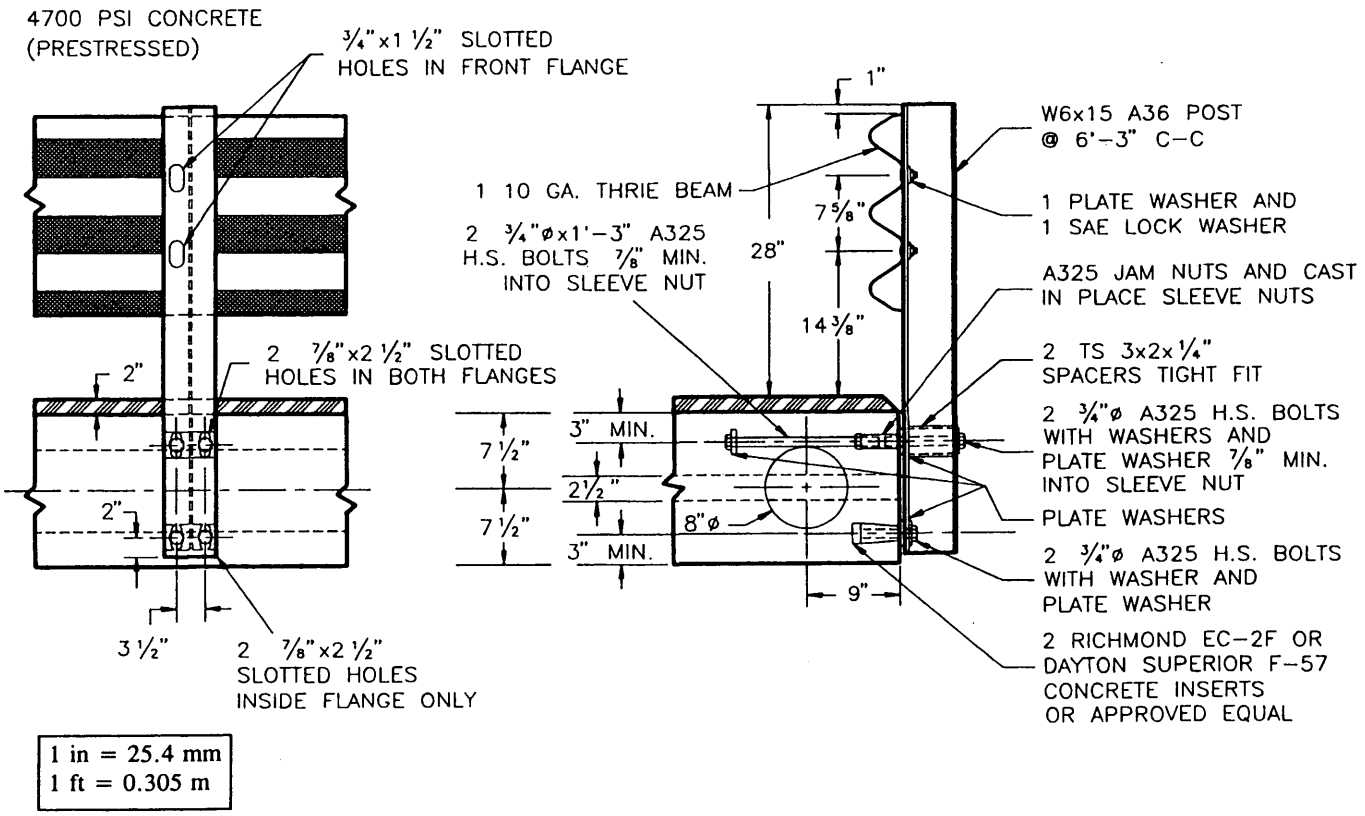

FIGURE 1 Details of Oregon side-mounted bridge railing.

FIGURE 2 Damage to vehicle and railing systems for Test 7069-17.

The vehicle sustained damage to the right side (Figure 2). Maximum crush at the right front corner at bumper height was 229 mm (9.0 in.).

The railing contained the vehicle with minimal lateral movement of the bridge railing. There was no intrusion into the occupant compartment and no deformation of the compartment. The bridge railing smoothly redirected the vehicle, and the effective coefficient of friction was considered fair. The occupant risk factors were within the limits recommended in the 1989 AASHTO guide specifications (*2*). Data and other pertinent information from this test are summarized in Figure 3. The vehicle trajectory at loss of contact indicates minimum intrusion into adjacent traffic lanes.

Performance of the railing in this test is judged to be acceptable.

Test 7069-18: 2,528-kg (5,573-lb) Chevrolet Pickup, 74.2 km/hr (46.1 mph), 20.9 degrees

The vehicle struck the bridge railing approximately 12.6 m (41.3 ft) from the upstream end. The vehicle lost contact with the bridge railing at 0.46 sec traveling at 57.8 km/hr (35.9 mph) and 10.9 degrees. It was in contact with the railing for 5.0 m (16.3 ft).

The railing received moderate damage (Figure 4). At Post 8 the upper deck bolts connecting the post to the bridge deck were bent and the post was bent back 38 mm (1.5 in.) at the bridge deck surface. Post 9 was bent 64 mm (2.5 in.), the upper deck bolt on the right side was bent, and the upper deck bolt on the left side pulled through the outer flange. Post 10 was slightly twisted. Maximum lateral deflection was 330 mm (13.0 in.) at the top of the thrie beam between Posts 8 and 9.

The vehicle sustained damage to the right side as shown in Figure 5. Maximum crush at the right front corner at bumper height was 165 mm (6.5 in.).

The railing contained the vehicle with minimal lateral movement of the bridge railing. There was no intrusion into the occupant compartment and no deformation of the compartment. The railing smoothly redirected the vehicle, and the effective coefficient of friction was considered fair. The occupant risk factors were within the limits recommended in the 1989 AASHTO guide specifications (*2*). Data and other pertinent information from this test are summarized in Figure 6. The vehicle trajectory at loss of contact indicates minimum intrusion into adjacent traffic lanes.

Performance of the railing in this test is judged to be acceptable.

BR27D on Sidewalk

This railing design concept was selected by the project panel to meet a need for a railing for urban areas. Many states are currently using railing designs that are similar to BR27D in that they consist of a concrete parapet with an open metal railing on top. The BR27D

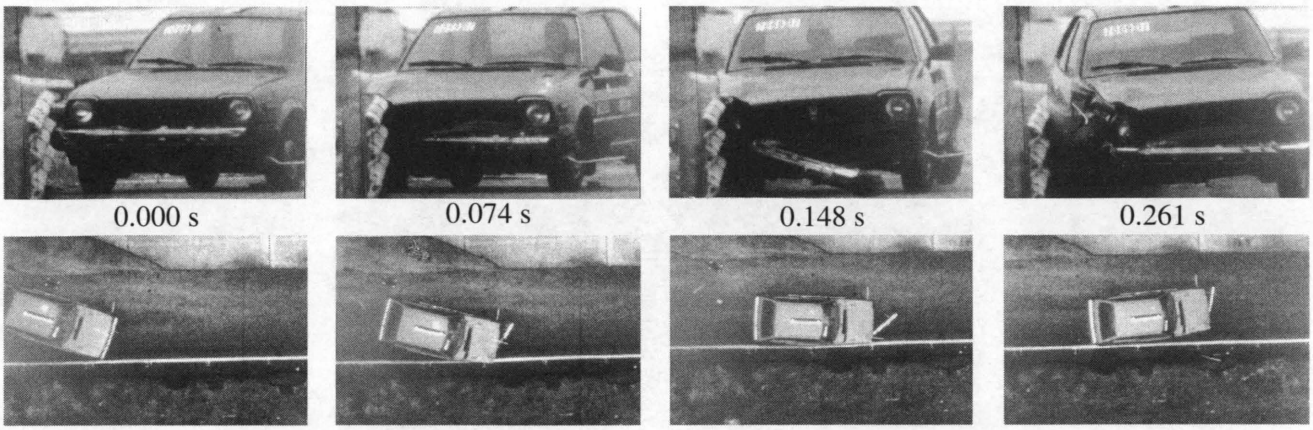

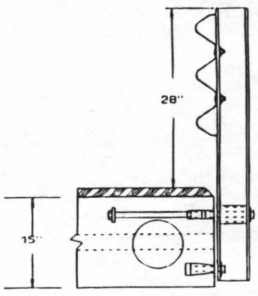

Test No.	7069-17
Date	05/10/89
Test Installation	Oregon Side-Mounted Bridge Railing
Installation Length	26 m (85 ft)
Test Vehicle	1980 Honda Civic
Vehicle Weight	
Test Inertia	817 kg (1,800 lb)
Gross Static	894 kg (1,970 lb)
Vehicle Damage Classification	
TAD	01FR4 & 01RFQ3
CDC	01FREK2 & 01RFEW3
Maximum Vehicle Crush	229 mm (9.0 in)

Impact Speed	84.0 km/h (52.2 mi/h)
Impact Angle	19.7 deg
Speed at Parallel	70.8 km/h (44.0 mi/h)
Exit Speed	68.7 km/h (42.7 mi/h)
Exit Trajectory	7.1 deg
Vehicle Accelerations (Max. 0.050-sec avg)	
Longitudinal	-5.2 g
Lateral	8.47 g
Occupant Impact Velocity at true c.g.	
Longitudinal	5.7 m/s (18.8 ft/s)
Lateral	5.8 m/s (18.9 ft/s)
Occupant Ridedown Accelerations	
Longitudinal	-1.8 g
Lateral	4.5 g

FIGURE 3 Summary of results for Test 7069-17.

consists of two TS 102 × 76 × 6.4-mm (TS 4 × 3 × 1/4-in.) rails attached to TS 102 × 102 × 4.8-mm (TS 4 × 4 × 3/16-in.) posts on 2.0-m (6 ft, 8 in.) centers. The posts are atop a concrete parapet 25 mm (10 in.) wide 457-mm (18.0 in.) tall, that is attached to a 203-mm (8.0-in.) deck.

BR27D was tested to PL1 with and without the curb and sidewalk. A somewhat similar design, BR27C, was tested to PL2 with and without the curb and sidewalk (*1*).

In the analysis and design of BR27D with curb and sidewalk, information on the influence of the curb on vehicle trajectory was needed. Some information on this subject for 1,589-kg (3,500 lb) automobiles was found in the 1977 barrier guide (*6*). No data specifically for vehicles used in tests on BR27D were available. The expected influence of the 200-mm (8.0-in) curb on the trajectory of a Honda Civic, a pickup truck, and an 8,172-kg (18,000-lb) truck was estimated from available data. A design force of 133 kN (30 kips) at 890 mm (35 in) above the top surface of the sidewalk was selected for design of BR27D. A cross section of this railing design is shown in Figure 7.

Test 7069-22: 817-kg (1,800-lb) Honda Civic, 83.2 km/hr (51.7 mph), 20.8 degrees

Upon impact with the curb, the left front tire folded under the vehicle. When the right front wheel reached the top of the curb, the vehicle was totally airborne and remained as such as it struck the concrete parapet at 0.26 sec. The vehicle struck the parapet at Post 5 traveling at a speed of 75.0 km/hr (46.6 mph) and at an angle of 13.4 degrees. The vehicle lost contact with the parapet at 0.61 sec traveling at 65.6 km/hr (40.8 mph) and 6.1 degrees.

The bridge railing system received minimal damage (see Figure 9). There was no measurable permanent deformation to the railing elements and only cosmetic damage to the concrete parapet. There were tire marks on the concrete parapet and on the face of the lower metal railing element in the area of impact, and also on the lower part of Post 6. The vehicle was in contact with the bridge railing for 3.5 m (11.5 ft). Length of contact with the concrete parapet was 2.1 m (7.0 ft).

The vehicle sustained damage to the left side as shown in Figure 8. Maximum crush at the left front corner at bumper height was 152 mm (6.0 in.).

The railing contained the vehicle with no lateral movement of the metal railing element of the bridge railing system. There was no intrusion of railing components into the occupant compartment and no debris to present undue hazard to other traffic. The integrity of the occupant compartment was maintained with no intrusion and no deformation. The bridge railing smoothly redirected the vehicle. The effective coefficient of friction was considered marginal. The occupant impact velocities and the occupant ridedown accelerations were within the limits. Data and other pertinent information from this test are summarized in Figure 9. Vehicle trajectory

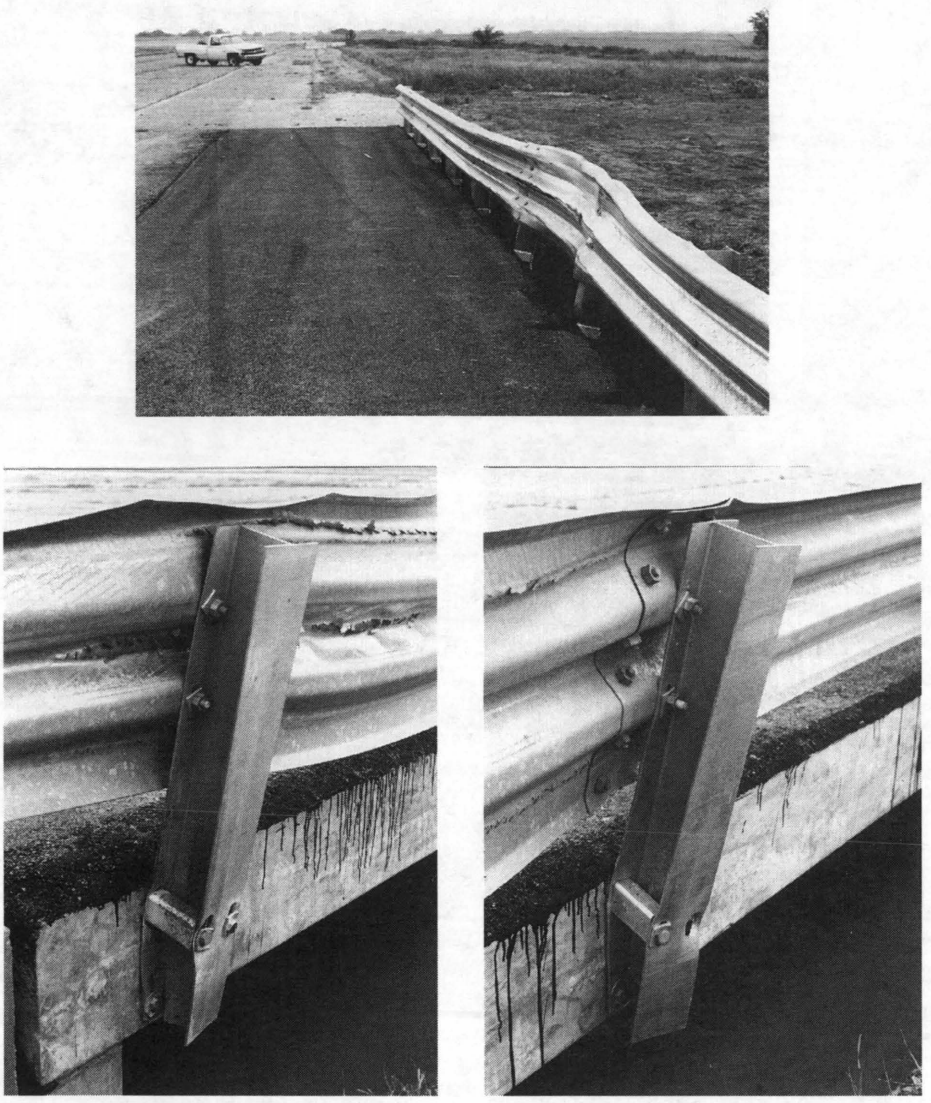

FIGURE 4 Damage to railing in Test 7069-18.

at loss of contact indicated minimum intrusion into adjacent traffic lanes.

Performance of the railing in this test is judged to be acceptable.

Test 7069-23: 2,450-kg (5,400-lb) Chevrolet Pickup, 72.9 km/hr (45.3 mph), 20.2 degrees

The vehicle struck the concrete parapet at 0.22 sec. The vehicle struck the parapet 0.9 m (3 ft) from Post 5 (between Posts 4 and 5) traveling at a speed of 70.5 km/hr (43.8 mph) and at an angle of 19.7 degrees. As the vehicle continued forward, the bumper protruded between the lower metal railing element and the concrete parapet. The vehicle lost contact with the concrete parapet traveling at 59.9 km/hr (37.2 mph) and 5.3 degrees. It was in contact with the railing for 3.9 m (12.8 ft).

The bridge railing received minimal damage (Figure 10). The maximum permanent deformation to the railing element was 13 mm (0.5 in.) between Posts 5 and 6. Posts 5 and 6 were also pushed rearward approximately 5 mm (3/16 in.). There was only cosmetic damage to the concrete parapet. Tire marks were observed on the concrete parapet, on the face of the lower metal railing element in the area of impact, and also on the lower part of Posts 5 and 6.

The vehicle sustained damage to the left side as shown in Figure 10. Maximum crush at the left front corner at bumper height was 318 mm (12.5 in.), and the right side was deformed outward 127 mm (5.0 in.).

The railing contained the vehicle with minimal lateral movement of the metal railing element of the bridge railing system. There was no intrusion of railing components into the occupant compartment and no debris to present undue hazard to other traffic. The integrity of the occupant compartment was maintained with no intrusion and no deformation. The bridge railing smoothly redirected the vehicle. The effective coefficient of friction was considered good. The occupant impact velocities and the occupant ridedown accelerations were within the limits. Data and other pertinent information from

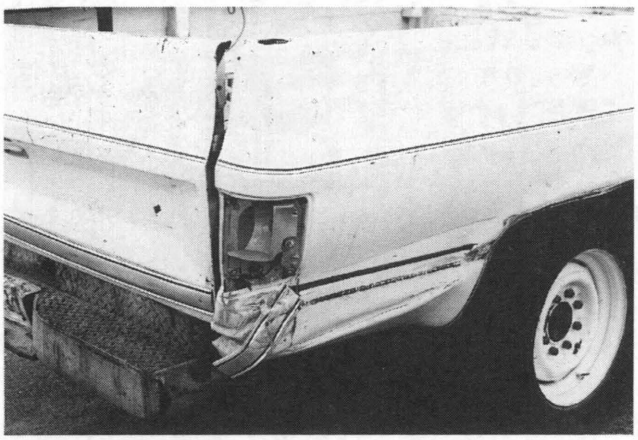

FIGURE 5 Damage to vehicle in Test 7069-18.

this test are summarized in Figure 11. The vehicle trajectory at loss of contact indicated minimum intrusion into adjacent traffic lanes.

Performance of the railing in this test is judged to be acceptable.

BR27D on Deck

Design of this railing was identical to BR27D on sidewalk. It was mounted on the deck without a curb and sidewalk. A cross section of the prototype test railing is similar to the one shown in Figure 8.

Test 7069-30: 817-kg (1,800-lb) Honda Civic, 82.4 km/hr (51.2 mph), 20.5 degrees

Shortly after impact the vehicle began to redirect. At approximately 0.10 sec after impact the dummy struck the driver-side door and shattered the door glass. The vehicle lost contact with the bridge railing at 0.32 sec traveling at 69.2 km/hr (43.0 mph) and 6.8 degrees. It was in contact with the railing for 2.4 m (8.0 ft).

The bridge railing received minimal damage (Figure 12). There was no measurable permanent deformation to the railing elements

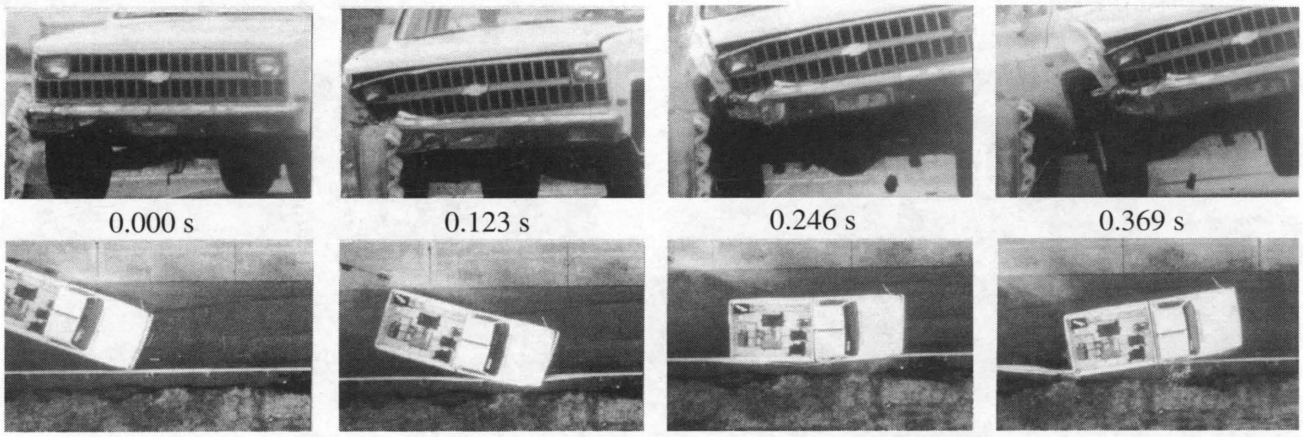

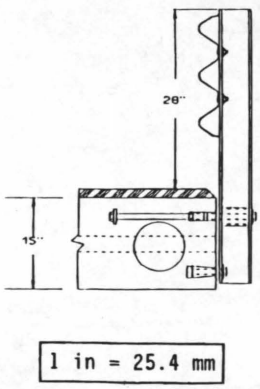

Test No.	7069-18
Date	05/12/89
Test Installation	Oregon Side-Mounted Bridge Railing
Installation Length	26 m (85 ft)
Test Vehicle	1982 Chevrolet Custom Deluxe Pickup
Vehicle Weight	
Test Inertia	2 452 kg (5,400 lb)
Gross Static	2 605 kg (5,737 lb)
Vehicle Damage Classification	
TAD	01RF2 & 01 RFQ3
CDC	01FREK2 & 01RFEW2
Maximum Vehicle Crush	165 mm (6.5 in)

Impact Speed	74.2 km/h (46.1 mi/h)
Impact Angle	20.9 deg
Speed at Parallel	61.5 km/h (38.2 mi/h)
Exit Speed	57.8 km/h (35.9 mi/h)
Exit Trajectory	10.9 deg
Vehicle Accelerations (Max. 0.050-sec avg)	
Longitudinal	-3.8 g
Lateral	6.7 g
Occupant Impact Velocity at true c.g.	
Longitudinal	5.2 m/s (17.1 ft/s)
Lateral	3.6 m/s (11.7 ft/s)
Occupant Ridedown Accelerations	
Longitudinal	-3.6 g
Lateral	8.8 g

FIGURE 6 Summary of results for Test 7069-18.

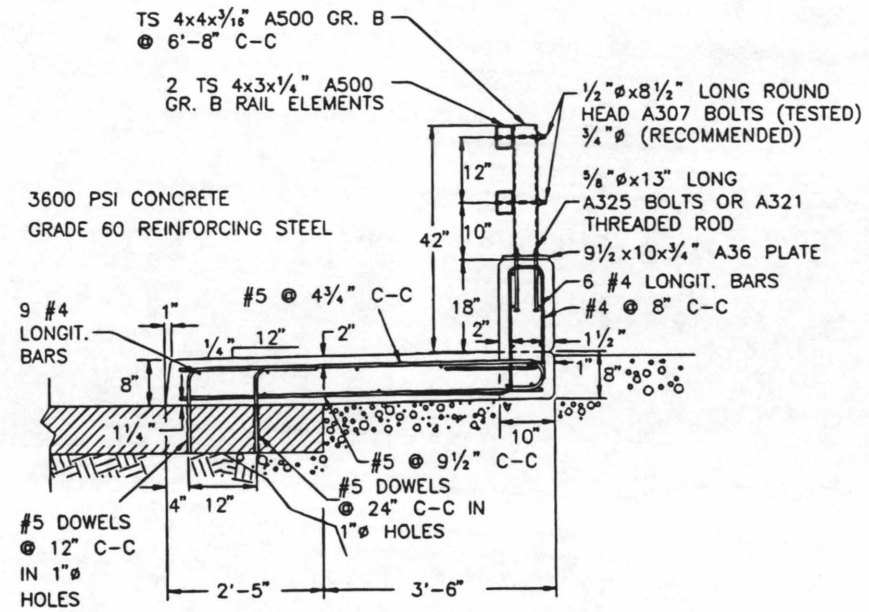

1 in = 25.4 mm
1 ft = 0.305 m

FIGURE 7 Cross section of BR27D bridge railing on sidewalk.

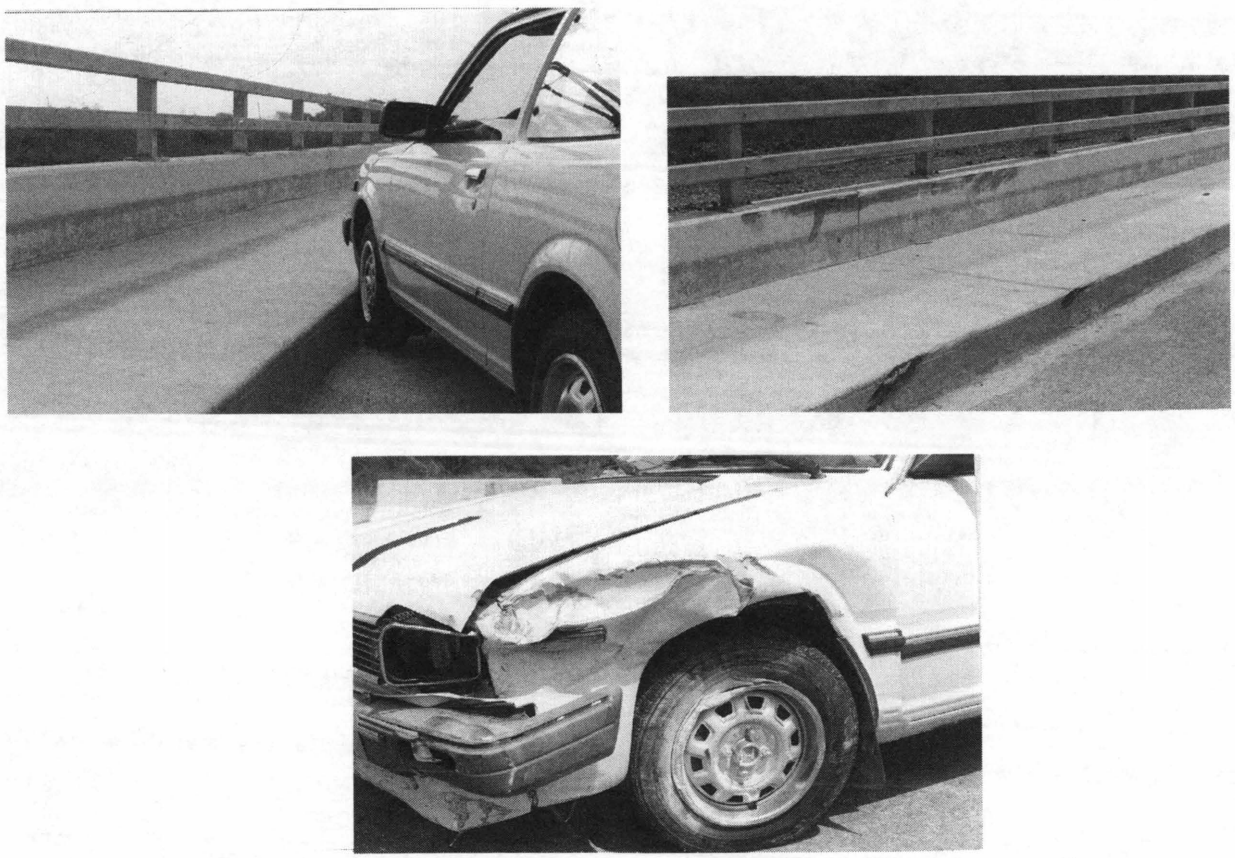

FIGURE 8 Vehicle and railing damage for Test 7069-22.

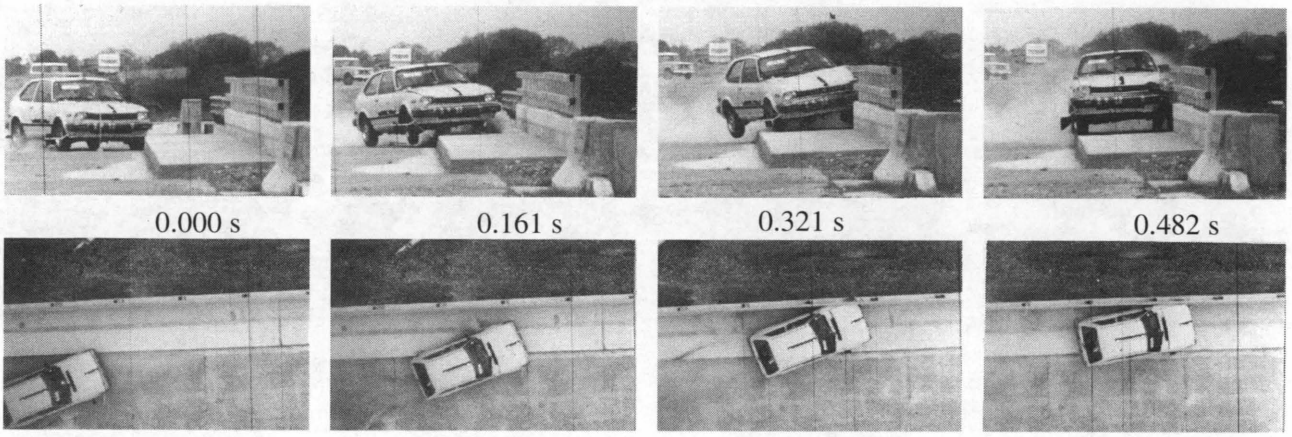

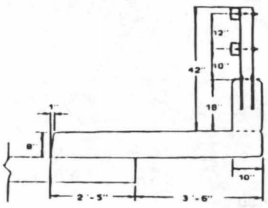

1 in = 25.4 mm

Test No.	7069-22
Date	03/24/92
Test Installation	BR27D Bridge Railing on sidewalk
Installation Length	30 m (100 ft)
Test Vehicle	1983 Honda Civic
Vehicle Weight	
Test Inertia	817 kg (1,800 lb)
Gross Static	893 kg (1,967 lb)
Vehicle Damage Classification	
TAD	11LFQ3
CDC	11LFEK2 & 11LFES2
Maximum Vehicle Crush	152 mm (6.0 in)

Impact Speed	83.2 km/h (51.7 mi/h)
Impact Angle	20.8 deg
Speed at Parallel	66.0 km/h (41.0 mi/h)
Exit Speed	65.6 km/h (40.8 mi/h)
Exit Trajectory	6.1 deg
Vehicle Accelerations (Max. 0.050-sec avg)	
Longitudinal	-4.4 g
Lateral	-6.8 g
Occupant Impact Velocity at true c.g.	
Longitudinal	3.7 m/s (12.2 ft/s)
Lateral	6.3 m/s (1.9 ft/s)
Occupant Ridedown Accelerations	
Longitudinal	-4.7 g
Lateral	-13.3 g

FIGURE 9 Summary of results for Test 7069-22.

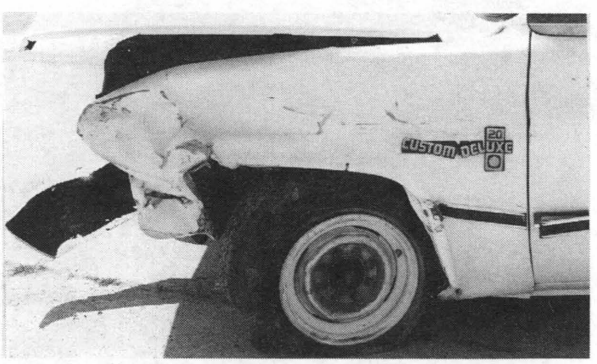

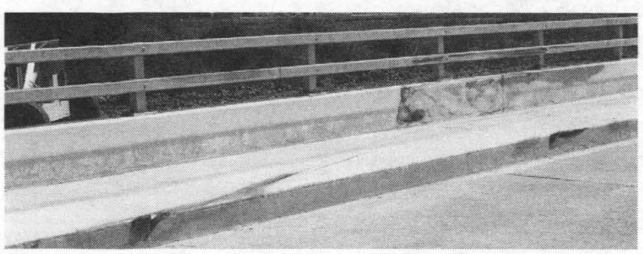

FIGURE 10 Vehicle and railing damage for Test 7069-23.

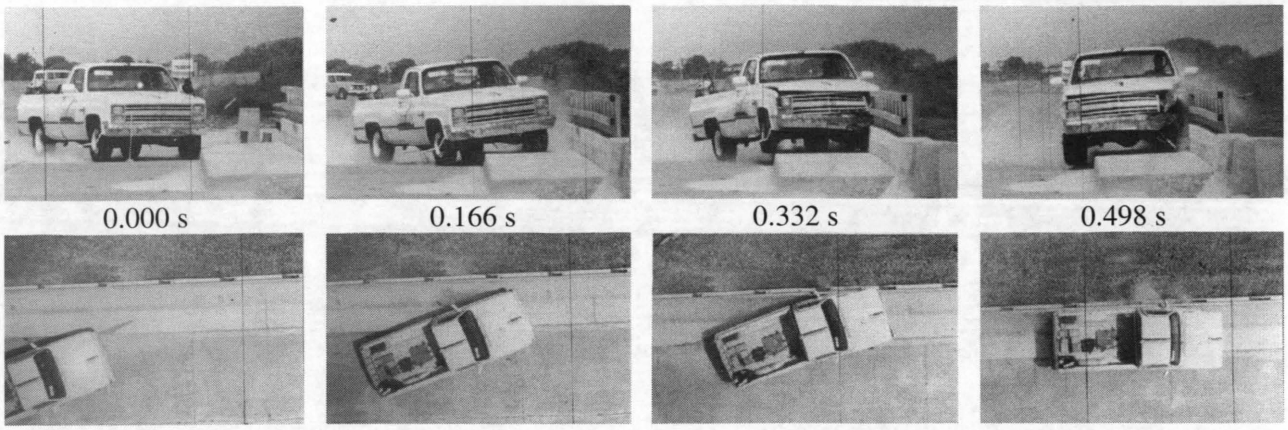

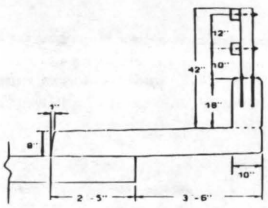

1 in = 25.4 mm

Test No.	7069-23
Date	03/26/92
Test Installation	BR27D Bridge Railing on sidewalk
Installation Length	30 m (100 ft)
Test Vehicle	1984 Chevrolet Custom Pckup
Vehicle Weight	
Test Inertia	2 452 kg (5,400 lb)
Gross Static	2 527 kg (5,565 lb)
Vehicle Damage Classification	
TAD	11FL4 & 11LD4
CDC	11FLEK2 & 11LDEW3
Maximum Vehicle Crush	318 mm (12.5 in)

Impact Speed	72.9 km/h (45.3 mi/h)
Impact Angle	20.2 deg
Speed at Parallel	64.8 km/h (40.3 mi/h)
Exit Speed	59.9 km/h (37.2 mi/h)
Exit Trajectory	5.3 deg
Vehicle Accelerations (Max. 0.050-sec avg)	
Longitudinal	-3.7 g
Lateral	-7.8 g
Occupant Impact Velocity at true c.g.	
Longitudinal	4.0 m/s (13.2 ft/s)
Lateral	4.3 m/s (14.0 ft/s)
Occupant Ridedown Accelerations	
Longitudinal	-2.3g
Lateral	-10.6 g

FIGURE 11 Summary of results for Test 7069-23.

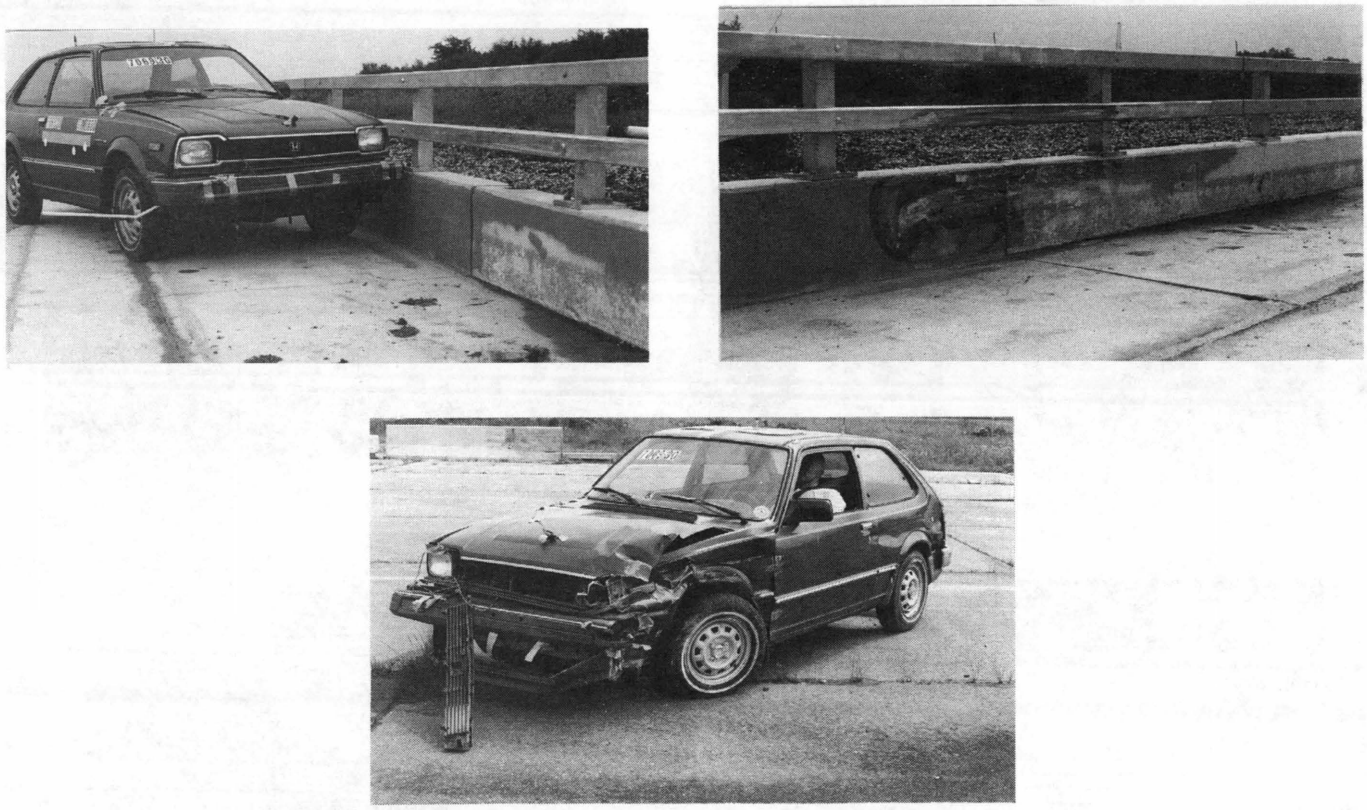

FIGURE 12 Vehicle and railing for Test 7069-30.

and only cosmetic damage to the concrete parapet. Tire marks were observed on the concrete parapet and on the face of the lower metal railing element in the area of impact.

Maximum crush of the vehicle at the left front corner at bumper height was 178 mm (7.0 in.) (Figure 12). The left front strut was damaged and the left front wheel was canted inward at the bottom and pushed back, reducing the wheelbase on the driver side by 57 mm (2.25 in.).

The railing contained the vehicle with no lateral movement of the metal railing element of the bridge railing system. There was no intrusion of railing components into the occupant compartment and no debris to present undue hazard to other traffic. The integrity of the occupant compartment was maintained with no intrusion and no deformation. The bridge railing smoothly redirected the vehicle. The effective coefficient of friction was considered good. The occupant impact velocities and the occupant ridedown accelerations were within the limits. Data and other pertinent information from this test are summarized in Figure 13. The vehicle trajectory at loss of contact indicated minimum intrusion into adjacent traffic lanes.

Performance of the railing in this test is judged to be acceptable.

Test 7069-31: 2,450-kg (5,400-lb) Chevrolet Pickup, 73.4 km/hr (45.6 mph), 18.8 degrees

The vehicle began to redirect at 0.05-sec after impact, and at 0.15 sec the dummy struck the driver-side door and shattered the glass. The vehicle lost contact with the bridge railing at 0.33 sec traveling at 61.1 km/hr (38.0 mph) and 6.2 degrees. It was in contact with the railing for 3.6 m (11.7 ft).

The bridge railing received minimal damage (Figure 14). The maximum permanent deformation to the railing element was 13 mm (0.5 in.) between Posts 5 and 6. There was only cosmetic damage to the concrete parapet. Tire marks were observed on the concrete parapet, on the face of the lower metal railing element in the area of impact, and also on the lower part of Post 6.

Maximum crush of the vehicle at the left front corner at bumper height was 165 mm (6.5 in.), and the right side was deformed outward 102 mm (4.0 in.) (Figure 14).

The railing contained the vehicle with minimal lateral movement of the metal railing element of the bridge railing system. There was no intrusion of railing components into the occupant compartment and no debris to present undue hazard to other traffic. The integrity of the occupant compartment was maintained with no intrusion and no deformation. The bridge railing smoothly redirected the vehicle. The effective coefficient of friction was considered good. The occupant impact velocities and the occupant ridedown accelerations were within the limits. Data and other pertinent information from this test are summarized in Figure 15. The vehicle trajectory at loss of contact indicated minimum intrusion into adjacent traffic lanes.

Performance of the railing in this test is judged to be acceptable.

SUMMARY

The Oregon side-mounted railing is a rather uncomplicated design that uses mostly standard hardware items. It has adequate strength and height for PL1 and, under more severe impact, exhibits plastic deformation that limits accelerations imposed on the vehicle. Plas-

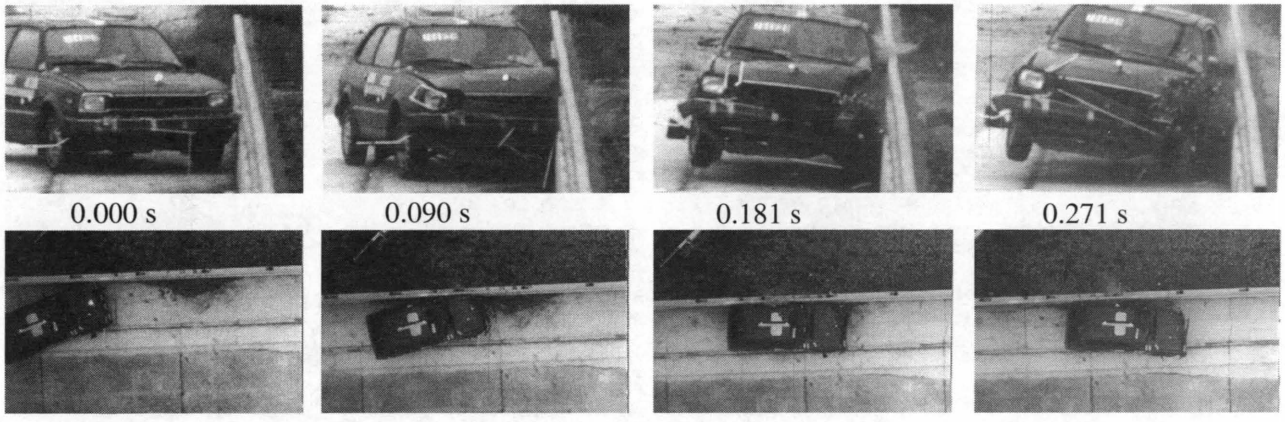

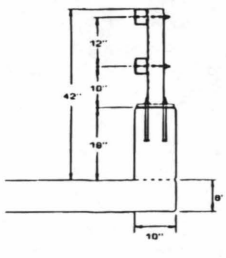

1 in = 25.4 mm

Test No.	7069-30
Date	05/19/92
Test Installation	BR27D Bridge Railing on deck
Installation Length	30 m (100 ft)
Test Vehicle	1983 Honda Civic
Vehicle Weight	
Test Inertia	817 kg (1,800 lb)
Gross Static	894 kg (1,970 lb)
Vehicle Damage Classification	
TAD	11LFQ3
CDC	11FLEK2 & 11LFES2
Maximum Vehicle Crush	178 mm (7.0 in)

Impact Speed	82.4 km/h (51.2 mi/h)
Impact Angle	20.5 deg
Speed at Parallel	70.2 km/h (43.6 mi/h)
Exit Speed	69.2 km/h (43.0 mi/h)
Exit Trajectory	6.8 deg
Vehicle Accelerations (Max. 0.050-sec avg)	
Longitudinal	-7.5 g
Lateral	-12.8 g
Occupant Impact Velocity at true c.g.	
Longitudinal	4.9 m/s (16.0 ft/s)
Lateral	6.6 m/s (21.5 ft/s)
Occupant Ridedown Accelerations	
Longitudinal	-3.6g
Lateral	-6.1 g

FIGURE 13 Summary of results for Test 7069-30.

FIGURE 14 Vehicle and railing for Test 7069-31.

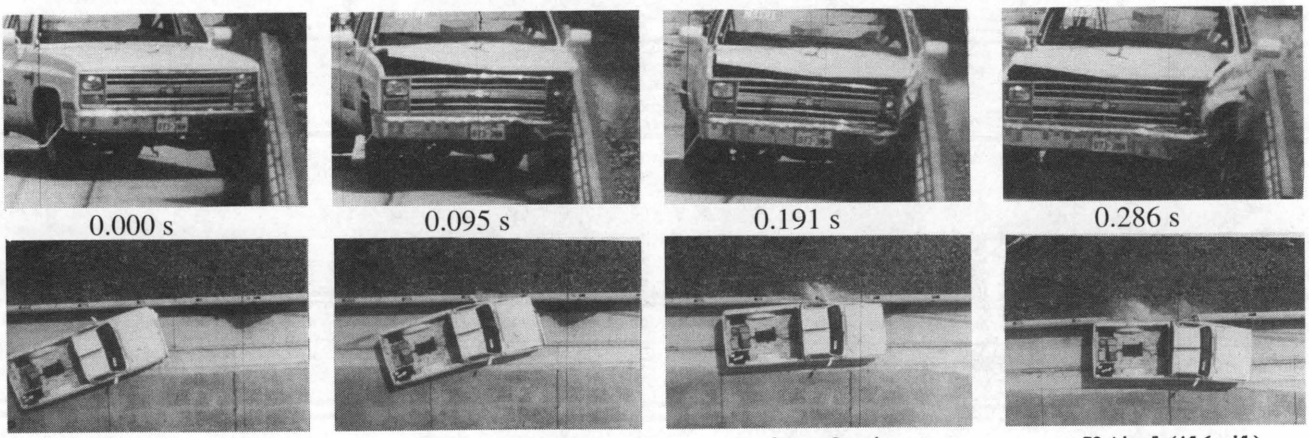

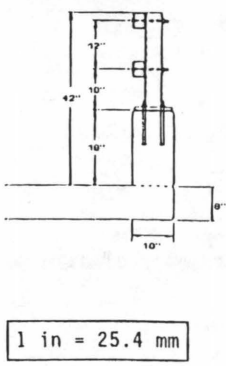

1 in = 25.4 mm

Test No.	7069-31
Date	05/21/92
Test Installation	BR27D Bridge Railing on deck
Installation Length	30 m (100 ft)
Test Vehicle	1985 Chevrolet Custom Pickup
Vehicle Weight	
Test Inertia	2 452 kg (5,400 lb)
Gross Static	2 527 kg (5,566 lb)
Vehicle Damage Classification	
TAD	11LFQ3 & 11LD2
CDC	11FLEK2 & 11LDEW2
Maximum Vehicle Crush	165 mm (6.5 in)

Impact Speed	73.4 km/h (45.6 mi/h)
Impact Angle	18.8 deg
Speed at Parallel	65.6 km/h (40.8 mi/h)
Exit Speed	61.1 km/h (38.0 mi/h)
Exit Trajectory	6.2 deg
Vehicle Accelerations (Max. 0.050-sec avg)	
Longitudinal	-4.1 g
Lateral	-7.5 g
Occupant Impact Velocity at true c.g.	
Longitudinal	3.6 m/s (11.7 ft/s)
Lateral	3.7 m/s (12.3 ft/s)
Occupant Ridedown Accelerations	
Longitudinal	2.2 g
Lateral	-8.2 g

FIGURE 15 Summary of results for Test 7069-31.

tic deformation was confined to metal railing components, and no damage was caused to the deck.

Railing design BR27D was tested to PL1 under two situations. First, it was tested when mounted on a sidewalk 1.5 m (5 ft) wide with a curb 203 mm (8 in.) high at the face of the sidewalk. It also was tested when mounted flush on the deck. Acceptable results were obtained in both series of tests. The small car test yielded lower occupant values when the BR27D was mounted with a curb and sidewalk. Redirection was initiated by the curb impact, thus lowering the occupant risk values when the ultimate redirection occurred with the railing. The curb and sidewalk did not affect the pickup tests in either reducing or increasing the occupant risk values. For the most part, the railing functioned as a "rigid" railing with only a small amount of permanent deformation in the metal railing in the more severe tests.

The results of all tests are summarized in Table 1.

CONCLUSIONS

All PL1 bridge railings tested under this contract performed acceptably. There were deflections in the Oregon side-mounted bridge railing, but the deck remained undamaged. The BR27D performed well with and without curb and sidewalk. There were minor deflections in the top rail of this system and cosmetic damage to the concrete section of the rail. All occupant risk values, as summarized earlier, were within acceptable limits.

PL1 bridge rails provide a cost-effective alternative to state agencies when traffic volume, mix, and speed do not warrant the more expensive PL2 and PL3 bridge rails. The Oregon side-mounted railing and the BR27D railing are full-scale crash-tested systems that are ready for use.

REFERENCES

1. Buth, C. E., T. J. Hirsch, and W. L. Menges. *Testing of New Bridge Rail and Transition Designs.* Technical Report, FHWA Contract DTFH61-86-C-00071, Report FHWA-RD-93-058. Federal Highway Administration, Washington, D.C., Sept. 1993.
2. *Guide Specifications for Bridge Railings.* AASHTO, Washington, D.C., 1989.
3. Buth, C. E. *Safer Bridge Railing Designs.* Final Report, FHWA Contract DOT-FH-11-9181, Report FHWA/RD-82/072. Federal Highway Administration, Washington, D.C., June 1984.
4. Beason, W. L., and T. J. Hirsch. *Measurement of Heavy Vehicle Impact Forces and Inertia Properties.* Texas Transportation Institute, Texas A&M University, College Station, Jan. 1989.
5. Hirsch, T. J. *Analytical Evaluation of Texas Bridge Rails to Contain Buses and Trucks.* Research Report 230-2. Texas Transportation Institute, Texas A&M University, College Station, Aug. 1978.
6. *Guide for Selecting, Locating, and Designing Traffic Barriers.* AASHTO, Washington, D.C., 1977.

Publication of this paper sponsored by Committee on Roadside Safety Features.

Performance Level 3 Bridge Railings

WANDA L. MENGES, C. EUGENE BUTH, D. LANCE BULLARD, JR., AND CHARLES F. MCDEVITT

Many existing bridge railings have been designed to restrain and redirect passenger vehicles. Because of specific site conditions, some locations along the nation's highways require that bridge railings contain and redirect heavier vehicles, such as commercial trucks and buses. These sites include areas where the consequences of failure to contain a vehicle would be severe. Examples include bridges that are grade separation structures crossing heavily congested traffic lanes, areas of reduced radius of curvature, elevated ramps near schools or hospitals, and other areas where additional protection is needed to prevent heavier vehicles from penetrating or rolling over the bridge railing. According to the 1989 American Association of State Highway and Transportation Officials (AASHTO) *Guide Specifications for Bridge Railings,* these sites require Performance Level 3 (PL3) bridge railings. Two PL3 bridge railings were developed under a recently completed pooled funds study sponsored by the Federal Highway Administration, the District of Columbia, and 23 states. The 1.07-m (42-in.) F-shape bridge railing and the 1.07-m (42-in.) concrete parapet were tested and evaluated according to the PL3 requirements of the 1989 AASHTO guide. Both bridge railings performed acceptably.

Many bridge railings throughout the United States have been designed to restrain and redirect passenger cars. Because of specific site conditions, some locations along the nation's highways require bridge railings that are capable of containing and redirecting heavy vehicles, such as commercial buses, truck tractors, and semitrailer combinations. Examples of such locations include bridges that are grade separation structures crossing other densely populated traffic lanes, areas of reduced radius of curvature, elevated ramps near schools or hospitals, and other locations where the consequences of failure to contain a vehicle would be severe.

According to the 1989 American Association of State Highway and Transportation Officials (AASHTO) *Guide Specifications for Bridge Railings (1),* these conditions require Performance Level 3 (PL3) bridge railings. The guide recommends that PL3 bridge railings be used for freeways with variable cross slopes, reduced radius of curvature, higher volumes of mixed heavy vehicles, and maximum tolerable speeds. PL3 bridge railings should also be used where additional protection is needed to prevent heavier vehicles from penetrating or rolling over the bridge railing.

A research study sponsored by the Federal Highway Administration (FHWA), the District of Columbia, and 23 states was recently completed by Texas Transportation Institute. The objective of the study was to develop several bridge railings for each of the three performance levels in the AASHTO guide specifications. Two PL3 bridge railings were developed in this study. The project began in August 1986 while the AASHTO guide specifications were being revised and updated. When the 1.07-m (42-in.) F-shape bridge railing was designed, the proposed 1987 test matrix of the AASHTO guide (Table 1) specified a strength test in which an 18,160-kg (40,000-lb) intercity bus strikes the bridge railing at 96.5 km/hr (60 mph) and at an angle of 15 degrees (*2*). The F-shape bridge railing performed acceptably under those test conditions. However, criteria set forth in the final 1989 AASHTO guide require that a PL3 bridge railing be tested using a 22,700-kg (50,000-lb) van-type tractor-trailer striking the railing at a speed of 80.5 km/hr (50 mph) and at an angle of 15 degrees (Table 2). Therefore, another test was performed under the new conditions, and again the F-shape bridge railing performed acceptably. A 1.07-m (42-in.) vertical-faced concrete parapet, which was designed and tested during the study, also performed acceptably using the 1989 AASHTO guide specifications.

This report documents the design and testing of two PL3 bridge railings: the 1.07-m (42-in.) F-shape bridge railing and the 1.07-m (42-in.) concrete parapet.

Texas Transportation Institute, The Texas A&M University System, College Station, Tex. 77843.

DESIGN CONSIDERATIONS

1.07-m (42-in.) F-Shape

The F-shape bridge railing was initially designed to meet Performance Level 3 of the 1987 *Guide Specifications for Bridge Railings.* The railing was first tested with an 18,160-kg (40,000-lb) intercity bus traveling 96.5 km/hr (60 mph) with an approach angle of 15 degrees (1987 guide specifications). The F-shape was later tested with a 22,700-kg (50,000-lb) tractor-trailer at 80.5 km/hr (50 mph) and 15 degrees. Design impact force for the tractor-trailer test was 552 kN (124 kips) of uniformly distributed line force 2.44 m (96 in.) long and 0.96 m to 1.02 m (38 to 40 in.) above the roadway surface (*3,4*).

A cross section of the 1.07 m (42 in.) high F-shape is shown in Figure 1. The cross-sectional width of the railing is 439 mm (17.3 in.) at its base and tapers inward along the height with an increased cross-sectional width at the top of 230 mm (9 in.) along the top 304.8 mm (12 in.) of the rail. The slope at the bottom of the railing minimizes vehicle damage at low-impact angles by causing the tire to ride up the railing and redirect itself back to the pavement. The increased cross-sectional width at the top of the railing acts as a continuous beam and enhances the longitudinal distribution of forces in the parapet and deck.

Four No. 7 longitudinal bars were used in the increased cross-section at the top of the F-shape and four No. 8 longitudinal bars were placed throughout the tapered portion of the railing. The vertical steel consisted of No. 5 bent stirrups spaced at 203 mm (8 in.) on center. Specified concrete strength was 24,804 kPa (3,600 psi). The cantilevered deck was supported on a foundation so that the deck overhang was 991 mm (39 in.).

Analysis of the strength of the railing is based on the yieldline failure pattern shown in Figure 2 (*5*). The length of the yieldline

TABLE 1 1987 Proposed AASHTO Test Matrix

PERFORMANCE LEVEL	TEST SPEEDS -- mph TEST VEHICLE DESCRIPTIONS AND IMPACT ANGLES			
	Small Automobile Wt = 1.8 kips θ = 20 deg	Pickup Truck Wt = 5.4 kips θ = 20 deg	Intercity Bus (loose ballast) Wt = 40.0 kips θ = 15 deg	Van-Type Tractor-Trailer No. 2 Wt = 80.0 kips θ = 15 deg
PL-1	50	45		
PL-2	60	65		
PL-3	60	65	60	
PL-4	60	65		55

Metric Conversion: 1 kip = 454 kg
1 mph = 1.609 km/h

failure pattern depends on the relative bending moment capacities of the various railing elements. The computed cantilever moment capacity of the parapet, M_c, is 69.9 m-kN/m (15.7 ft-k/ft). The average moment capacity of the parapet about a vertical axis, M_w, is 67.6 m-kN/m (15.2 ft-k/ft). The additional average moment capacity of the stiffening beam along the top of the parapet is 32 m-kN (23.6 ft-kips). The length of the yieldline failure pattern, computed from the equation in Figure 2, is 5.4 m (17.6 ft) and the ultimate strength of the parapet is 565.2 kN (127 kips), which is greater than the design force of 552 kN (124 kips).

1.07-m (42-in.) Concrete Parapet

The concrete parapet, shown in Figure 3, is 254 mm (10 in.) wide at the base and 305 mm (12 in.) wide at the top. The "beam" along the top edge enhances the longitudinal distribution of forces within the parapet and the deck. Two types of vertical reinforcing bars are alternated to provide No. 5 bars spaced at 152 mm (6 in.) in the traffic side face.

The design impact force used was 685 kN (154 kips) uniformly distributed over a longitudinal distance of 2.44 m (96 in.) at 864 mm (34 in.) above the deck surface. The currently recommended design force for PL3 [tractor-trailer; 22,700 kg (50,000 lb); 80.5 km/hr (50 mph); 15 degrees] is a uniformly distributed line force of 552 kN (124 kips) distributed over 2.44 m (96 in.) at 0.96 to 1.02 m (38 to 40 in.) above the deck surface. The concrete parapet meets these design requirements.

Analysis of the strength of the railing is based on the yieldline pattern shown in Figure 2. The force from a colliding vehicle is idealized as being a uniformly distributed line load extending 2.4 m (8.0 ft). The load may be applied at any location along the railing.

The length of the yieldline failure pattern depends on the relative bending moment capacities of the various railing elements. The computed cantilever moment capacity of the parapet, M_c, is 95.2 m-kN/m (21.4 ft-k/ft). The moment capacity of the parapet about a vertical axis, M_w, is 73.4 m-kN/m (16.5 ft-k/ft). The additional moment capacity of the stiffening beam along the top of the parapet is 59.6 m-kN (43.9 ft-kips). The length of the yieldline failure pattern, computed from the equation in Figure 2 is 4.9 m (16.2 ft), and the ultimate strength of the parapet is 881 kN (198 kips).

FULL-SCALE CRASH TESTS

Two bridge railing designs, a 1.07-m (42-in.) F-shape and a 1.07-m (42-in.) vertical-faced concrete parapet, were tested and evaluated according to Performance Level 3 of the AASHTO guide. Both in

TABLE 2 1989 AASHTO Test Matrix

PERFORMANCE LEVEL	TEST SPEEDS -- mph TEST VEHICLE DESCRIPTIONS AND IMPACT ANGLES			
	Small Automobile Wt = 1.8 kips θ = 20 deg	Pickup Truck Wt = 5.4 kips θ = 20 deg	Medium Single-Unit Truck Wt = 18.0 kips θ = 15 deg	Van-Type Tractor-Trailer Wt = 50.0 kips θ = 15 deg
PL-1	50	45		
PL-2	60	60	50	
PL-3	60	60		50

Metric Conversion: 1 kip = 454 kg
1 mph = 1.609 km/h

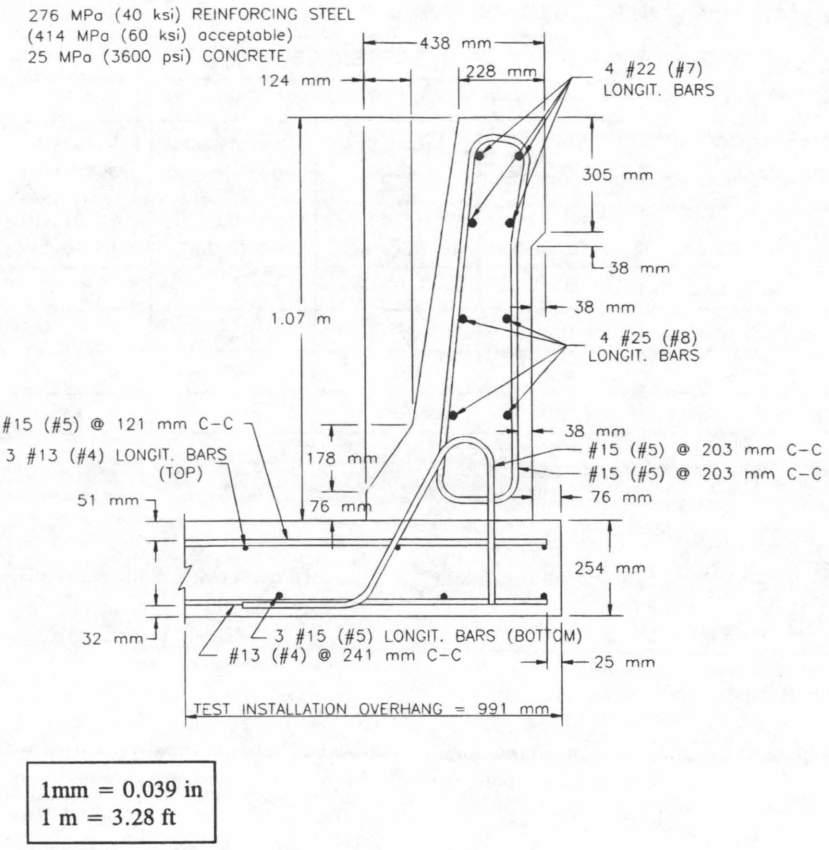

FIGURE 1 Cross section of 1.07-m (42-in.) F-shape bridge railing.

the proposed 1987 and final 1989 AASHTO guide specifications, the PL3 test matrix requires that crash tests be conducted with an 817-kg (1,800-lb) automobile and a 2452 kg (5400-lb) pickup. PL2 crash tests on the 812-mm (32-in.) versions of the F-shape and vertical-faced concrete parapet were conducted earlier in this study (*6*). Because these shorter versions performed acceptably when struck by the small automobile and pickup, it was assumed that these vehicles would perform similarly with the taller versions. Therefore, only the tests with the heavy vehicles were performed on the 1.07-m (42-in.) F-shape and the 1.07-m (42-in.) concrete parapet.

All other testing, evaluation, and reporting requirements were in accordance with specifications established in National Cooperative Highway Research Program Report 230 (*7*). Descriptions of the full-scale crash tests follows.

1.07-m (42-in.) F-shape

Test 7069-7: 18,414 kg (40,560 lb) Intercity Bus, 89.6 km/hr (55.7 mph), 15.7 Degrees

A 1954 GMC Scenic Cruiser bus was directed into the F-shape bridge railing using a remote control guidance system. Curb weight (empty weight) of the vehicle was 13,547 kg (29,840 lb). The gross static mass of the vehicle (including loose ballast) was 18,414 kg (40,560 lb). The vehicle was free-wheeling and unrestrained just before impact.

The vehicle hit the bridge railing 10 m (35 ft) from the upstream end and was smoothly redirected. It was in contact with the bridge railing for 7.6 m (25 ft), briefly lost contact for 7.9 m (26 ft), struck the bridge railing again, and rode off the end of the railing. The vehicle was tracking at loss of contact and was traveling at 68.4 km/hr (42.5 mph).

There was no measurable movement of the bridge railing; however, a longitudinal hairline crack developed in the bridge deck, starting approximately at the point of impact and extending about 11 m (35 ft) parallel to and nominally 610 mm (24 in.) from the base of the railing. Damage to the bridge railing and vehicle is shown in Figure 4. Maximum crush at the right front corner at bumper height was 102 mm (4.0 in.). The front wheel assembly and suspension were damaged.

The F-shape bridge railing contained and smoothly redirected the vehicle with no lateral movement of the bridge railing. There was no debris or detached elements. There was no intrusion into the occupant compartment, although a minimal amount of deformation occurred on the right door. The vehicle trajectory at loss of contact indicated minimum intrusion into adjacent traffic lanes. The vehicle remained upright and stable during and after the crash. Additional information pertinent to this test is presented in Figure 5. Performance of the bridge railing was judged acceptable, as indicated in Table 3.

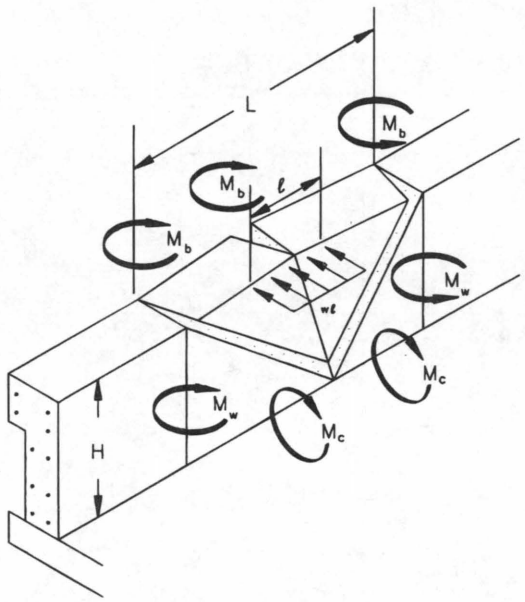

$$L = \frac{l}{2} + \sqrt{\left(\frac{l}{2}\right)^2 + 8H\left(\frac{M_b + M_w H}{M_c}\right)}$$

$$(wl)_{ult} = \frac{8M_b}{L - \frac{l}{2}} + \frac{8M_w H}{L - \frac{l}{2}} + \frac{M_c L^2}{H\left(L - \frac{l}{2}\right)}$$

H	=	height of wall (FT)
L	=	critical length of wall failure (FT)
l	=	length of distributed vehicle impact load on railing (FT)
M_b	=	ultimate moment capacity of beam at top of wall (KFT)
M_c	=	ultimate flexural resistance of wall about horizontal axis
M_w	=	ultimate flexural resistance of wall about vertical axis (KFT/FT)
$(wl)_{ult}$	=	total ultimate load (KIPS)

FIGURE 2 Yieldline failure mechanism for concrete parapet.

Test 7069-10: 22 700 kg (50,000 lb) Tractor-Trailer, 84.0 km/hr (52.2 mph) 14.0 Degrees

A 1979 International Transtar 4200 tractor with a 13.7-m (45-ft) van-trailer was directed into the F-shape bridge railing using a remote controlled guidance system. Test inertia weight (empty weight) of the vehicle was 13,574 kg (29,900 lb). Gross static mass (loaded weight) of the vehicle was 22,700 kg (50,000 lb). The vehicle was free-wheeling and unrestrained just before impact.

Impact occurred 10.1 m (35 ft) from the upstream end of the bridge railing and the vehicle was smoothly redirected. At 0.260 sec, the right-front corner of the vehicle contacted the bridge railing, and at 0.785 sec the rear wheels made contact with the bridge railing. The vehicle rode against the bridge railing for 22 m (72 ft). As the vehicle rode off the end of the bridge railing, the vehicle trajectory path was 0 degrees.

There was no lateral movement of the bridge railing. A small piece of the top of the bridge railing chipped off where the edge of the trailer hit the railing. Both outside right rear wheel rims of the tractor were bent and the tires deflated (see Figure 6). The front wheel assembly and suspension were damaged. The shock mounts were broken, the tie rods and the steering rod were bent, and the springs were loosened. Maximum crush at the right front corner of the vehicle at bumper height was 457 mm (18.0 in.).

The F-shape bridge railing contained and smoothly redirected the vehicle with no lateral movement of the bridge railing. There was no debris or detached elements. There was no intrusion into the occupant compartment, although minimal deformation of the right door occurred. The vehicle trajectory at loss of contact indicated minimal intrusion into adjacent traffic lanes. The vehicle remained upright and stable during and after the crash. Additional information pertinent to this test is presented in Figure 7. Performance of

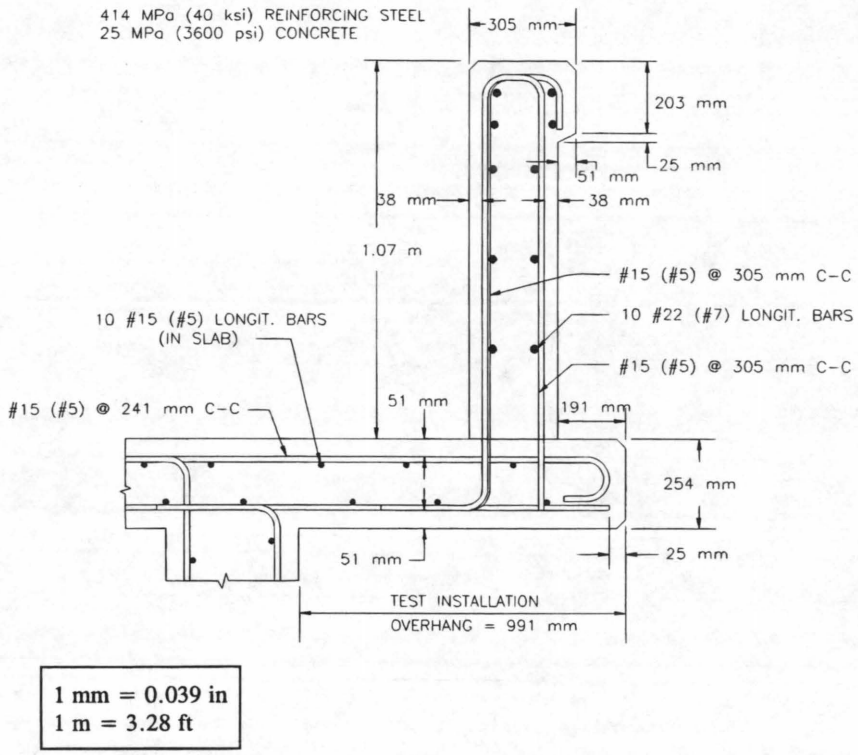

FIGURE 3 Cross section of 1.07-m (42-in.) concrete parapet.

the F-shape bridge railing was judged acceptable, as indicated in Table 4.

1.07-m (42.in.) Concrete Parapet

Only one test was performed on the vertical-faced concrete parapet bridge railing. This test was the 1989 AASHTO PL3 strength test with the 22,700-kg (50,000-lb) tractor-trailer striking the bridge railing at a speed of 80.5 km/hr (50-mph) and at an angle of 15 degrees. The parapet met the requirements for PL3.

Test 7069-13: 22,723 kg (50,050 lb) Tractor-Trailer, 82.7 km/hr (51.4 mph), 16.2 Degrees

A 1979 International Transtar 4200 tractor with a 1977 Pullman van-trailer was directed into the concrete parapet bridge railing using a remote control guidance system. Curb weight (empty weight) of the vehicle was 12,571 kg (27,690 lb). Gross static mass (loaded weight) of the vehicle was 22,723 kg (50,050 lb). The vehicle was free-wheeling and unrestrained just before impact.

The vehicle hit the parapet 7.3 m (24 ft) from the upstream end, and shortly thereafter the vehicle began to redirect. As the vehicle

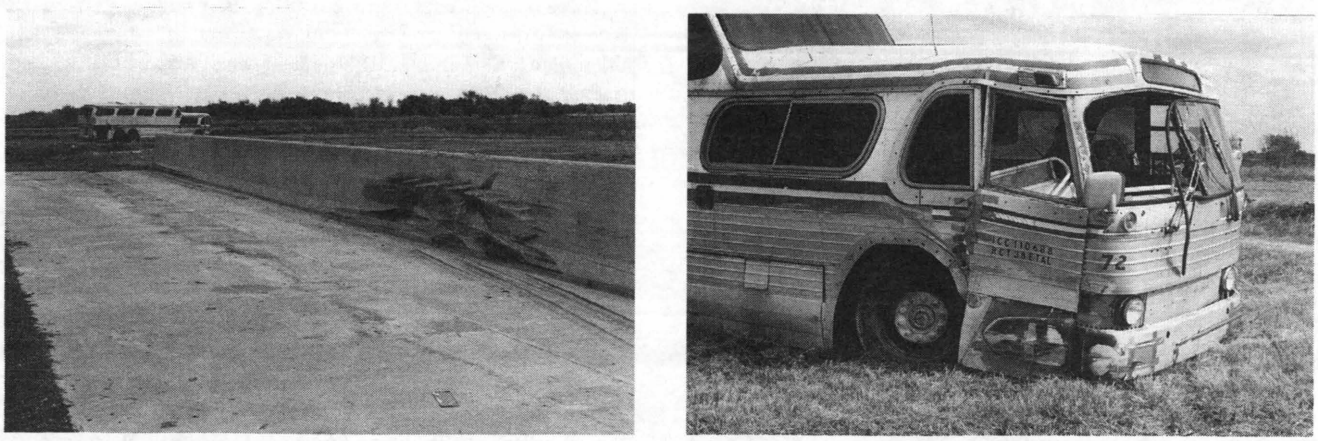

FIGURE 4 Damage to F-shape bridge railing and bus, Test 7069-7.

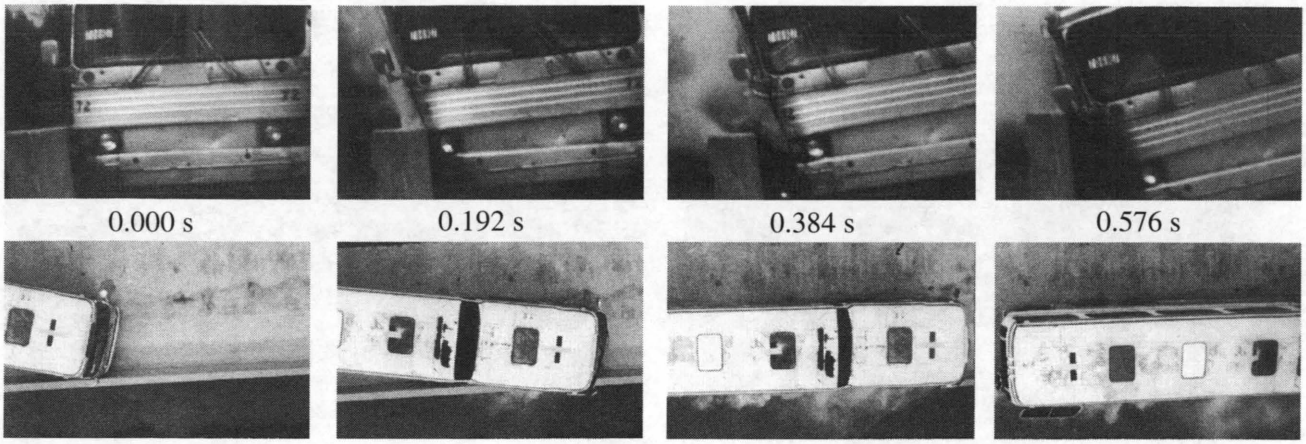

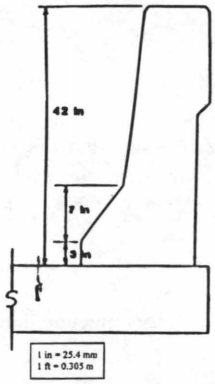

Test No.	7069-7
Date	11/19/87
Test Installation	1.07 m (42-in) F-shape Bridge Railing
Installation Length	30 m (100 ft)
Test Vehicle	1954 GMC Scenicruiser Bus
Vehicle Weight	
Empty Weight	13 547 kg (29,840 lb)
Test Inertia	18 414 kg (40,560 lb)
Vehicle Damage Classification	
TAD	N/A
CDC	N/A
Maximum Vehicle Crush	102 mm (4.0 in)

Impact Speed	89.6 km/h (55.7 mi/h)
Impact Angle	15.7 deg
Exit Speed	68.4 km/h (42.5 mi/h)
Exit Trajectory	0 deg
Vehicle Accelerations (Max. 0.050-sec avg)	
Longitudinal	-1.5 g
Lateral	6.5 g
Occupant Impact Velocity at true c.g.	
Longitudinal	2.4 m/s (7.9 ft/s)
Lateral	1.6 m/s (5.4 ft/s)
Occupant Ridedown Accelerations	
Longitudinal	-2.4 g
Lateral	21.7 g

FIGURE 5 Summary of results for bus test on F-shape bridge railing, Test 7069-7.

TABLE 3 Performance Evaluation for Bus Test on F-Shape, Test 7069-7

	AASHTO EVALUATION CRITERIA*	TEST RESULTS	ASSESSMENT
A.	Must contain vehicle	Vehicle was contained	Pass
B.	Debris shall not penetrate passenger compartment	No debris penetrated passenger compartment	Pass
C.	Passenger compartment must have essentially no deformation	Acceptable deformation	Pass
D.	Vehicle must remain upright during and after collision	Vehicle remained upright	Pass
E.	Must smoothly redirect vehicle	Vehicle was smoothly redirected	Pass
F.	Effective coefficient of friction: μ — Assessment 0 - .25 — Good .26 - .35 — Fair >.35 — Marginal	μ — Assessment .31 — Fair	Pass
G.	Shall be less than: Occupant Impact Velocity - m/s (ft/s) Longitudinal — Lateral 9.2 (30) — 7.6 (25) Occupant Ridedown Accelerations - g's Longitudinal — Lateral 15 — 15	Occupant Impact Velocity - m/s (ft/s) Longitudinal — Lateral 2.4 (7.9) — 1.6 (5.4) Occupant Ridedown Accelerations - g's Longitudinal — Lateral -2.4 — 21.7	N/A
H.	Exit angle shall be less than 12 degrees	Exit angle was 0 degrees	Pass

**A, B, and C are required. D, E, F, and H are desired. G is not applicable for this test.*

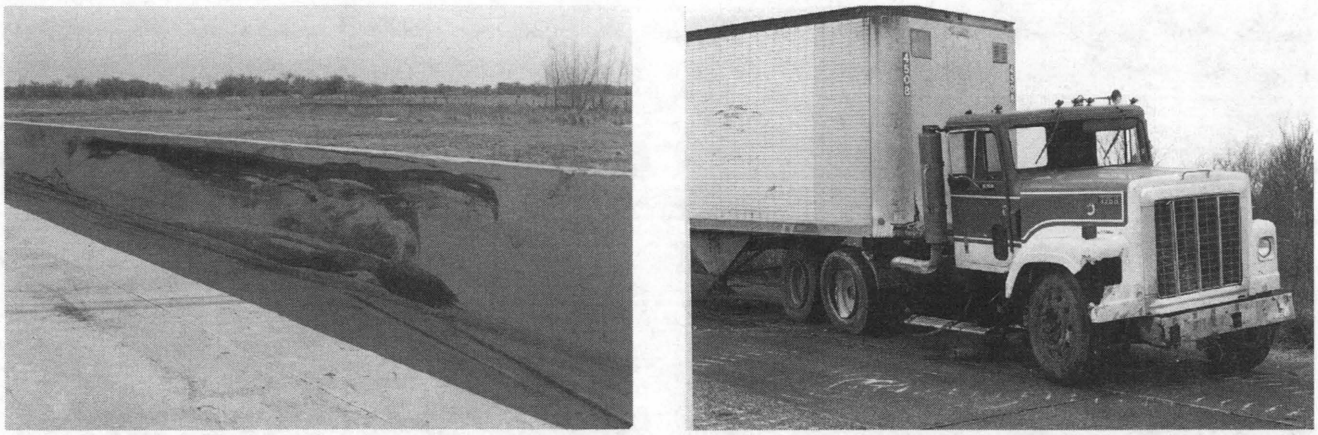

FIGURE 6 Damage to F-shape bridge railing and tractor trailer, Test 7069-10.

continued to ride down the parapet, the trailer began to roll clockwise, attaining a maximum roll of approximately 39 degrees at 1.165 sec The trailer then began to roll counterclockwise, and the vehicle rode off the end of the parapet for a total length of contact of 26 m (85 ft). As the vehicle exited the test area, the brakes on the vehicle were applied and the vehicle subsequently came to rest on its left side.

The parapet received minor damage with a small chip at the top. Damage to the bridge railing and vehicle is shown in Figure 8. The vehicle received damage to the front axle, pitman arm, U bolts, front leaf springs and bolts, front shock mounts, air brake lines, right fuel cell, left rear spring pin and clamp, and exhaust pipe. Maximum crush at the right front corner at bumper height was 457 mm (18.0 in.).

The concrete parapet contained and redirected the vehicle with no lateral movement of the parapet. There was no debris or detached elements. Although minimal deformation occurred on the right door, there was no intrusion into the occupant compartment. The vehicle trajectory at loss of contact indicated minimum intrusion into adjacent traffic lanes. The concrete parapet prevented the vehi-

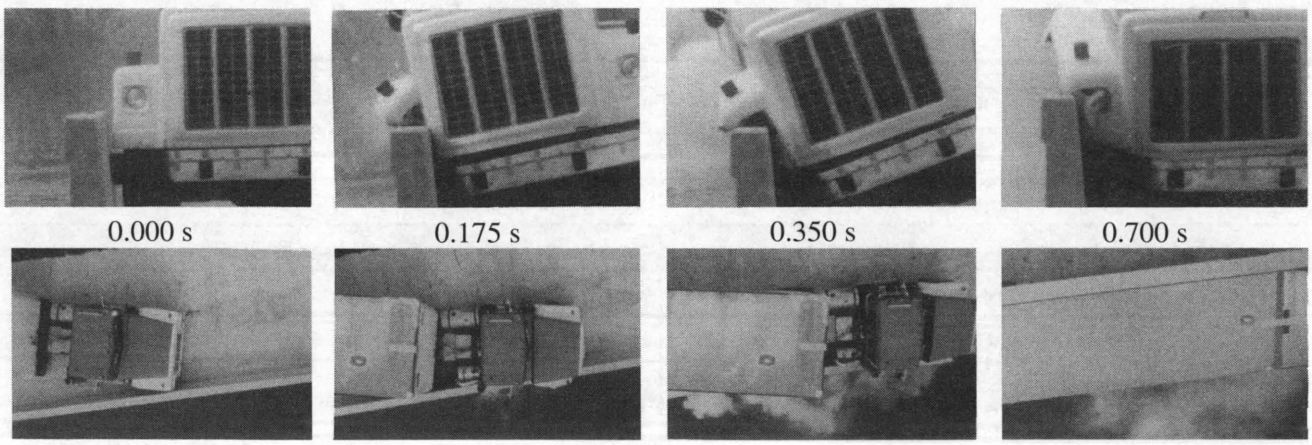

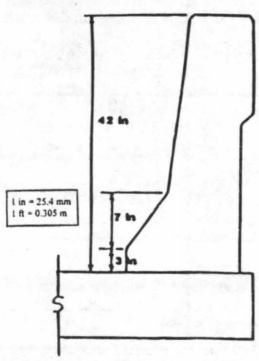

Test No.	7069-10
Date	3/3/88
Test Installation	1.07 m (42-in) F-shape Bridge Railing
Installation Length	30 m (100 ft)
Test Vehicle	1979 International Transtar 4200 Tractor
Vehicle Weight	
Empty Weight	13 574 kg (29,900 lb)
Test Inertia	22 700 kg (50,000 lb)
Maximum Vehicle Crush	457 mm (18.0 in)

Impact Speed	84.0 km/h (52.2 mi/h)
Impact Angle	14.0 deg
Exit Speed	N/A
Exit Trajectory	0 deg
Vehicle Accelerations (Max. 0.050-sec avg)	
Longitudinal	-2.2 g
Lateral	4.7 g
Occupant Impact Velocity at true c.g.	
Longitudinal	2.8 m/s (9.1 ft/s)
Lateral	2.8 m/s (9.3 ft/s)
Occupant Ridedown Accelerations	
Longitudinal	-4.7g
Lateral	3.7 g

FIGURE 7 Summary of results for tractor-trailer test on F-shape, Test 7069-10.

TABLE 4 Performance Evaluation for Tractor-Trailer Test on F-shape, Test 7069-10

	AASHTO EVALUATION CRITERIA*	TEST RESULTS	ASSESSMENT
A.	Must contain vehicle	Vehicle was contained	Pass
B.	Debris shall not penetrate passenger compartment	No debris penetrated passenger compartment	Pass
C.	Passenger compartment must have essentially no deformation	Acceptable deformation	Pass
D.	Vehicle must remain upright during and after collision	Vehicle remained upright	Pass
E.	Must smoothly redirect vehicle	Vehicle was smoothly redirected	Pass
F.	Effective coefficient of friction μ — Assessment 0 - .25 — Good .26 - .35 — Fair >.35 — Marginal	μ — Assessment Not Available — N/A	N/A
G.	Shall be less than: Occupant Impact Velocity - m/s (ft/s) Longitudinal 9.2 (30) — Lateral 7.6 (25) Occupant Ridedown Accelerations - g's Longitudinal 15 — Lateral 15	Occupant Impact Velocity - m/s (ft/s) Longitudinal 2.8 (9.1) — Lateral 2.8 (9.3) Occupant Ridedown Accelerations - g's Longitudinal -4.7 — Lateral 3.7	N/A
H.	Exit angle shall be less than 12 degrees	about 0 degrees	Pass

**A, B, and C, are required. D, E, F, and H are desired. G is not applicable for this test.*

TABLE 5 Performance Evaluation for Tractor-Trailer Test on Vertical Faced Concrete Parapet, Test 7069-13

	AASHTO EVALUATION CRITERIA*	TEST RESULTS	ASSESSMENT
A.	Must contain vehicle	Vehicle was contained	Pass
B.	Debris shall not penetrate passenger compartment	No debris penetrated passenger compartment	Pass
C.	Passenger compartment must have essentially no deformation	Acceptable deformation	Pass
D.	Vehicle must remain upright during and after the collision	Vehicle remained upright during contact with the bridge railing; however, the vehicle rolled after exiting the installation.	Fail
E.	Must smoothly redirect vehicle	Vehicle was smoothly redirected	Pass
F.	Effective coefficient of friction: μ — Assessment 0 - .25 — Good .26 - .35 — Fair >.35 — Marginal	μ — Assessment .55 — Marginal	Pass
G.	Shall be less than: Occupant Impact Velocity - m/s (ft/s) Longitudinal 9.2 (30) — Lateral 7.6 (25) Occupant Ridedown Accelerations - g's Longitudinal 15 — Lateral 15	Occupant Impact Velocity - m/s (ft/s) Longitudinal 3.2 (10.5) — Lateral 3.8 (12.5) Occupant Ridedown Accelerations - g's Longitudinal -2.2 — Lateral 4.6	N/A
H.	Exit angle shall be less than 12 degrees	about 0 degrees	Pass

**A, B, and C are required. D, E, F, and H are desired. G is not applicable for this test.*

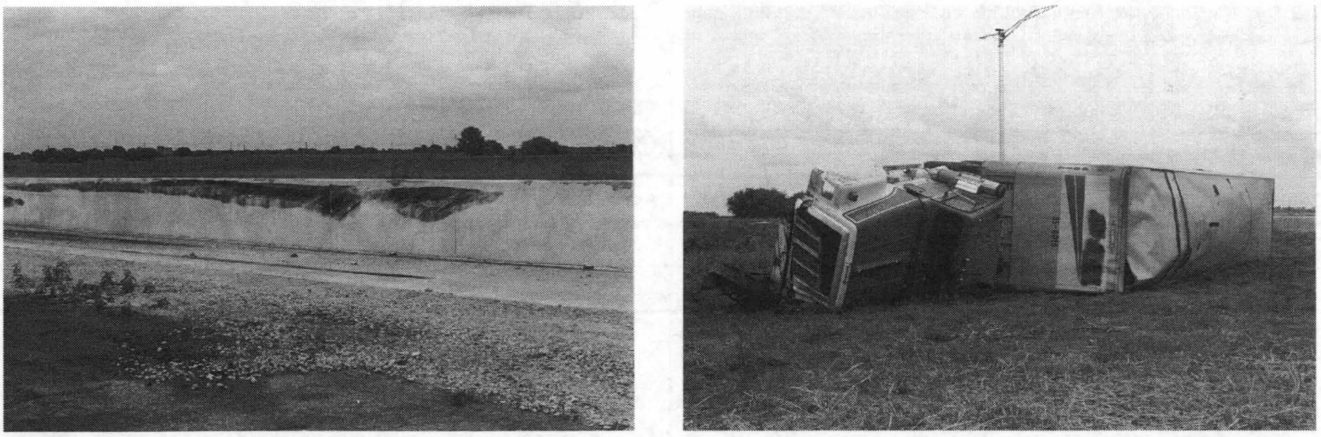

FIGURE 8 Damage to concrete parapet and tractor trailer, Test 7069-13.

cle from penetrating or rolling over the bridge railing. The vehicle remained upright during contact with the bridge railing; however, the vehicle rolled on its side after exiting the installation. As indicated in Table 5, it is desirable, but not required, that the vehicle remain upright after the test. Additional information pertinent to this test is presented in Figure 9. Performance of the concrete parapet bridge railing was judged acceptable.

SUMMARY AND CONCLUSIONS

Two bridge railings meeting the requirements of l/PL3 of the 1989 AASHTO guide specifications have been developed and proven after full-scale crash tests. One is a 1.07-m (42-in.) high F-shape concrete parapet and the other is a 1.07-m (42-in.) high vertical-faced concrete parapet.

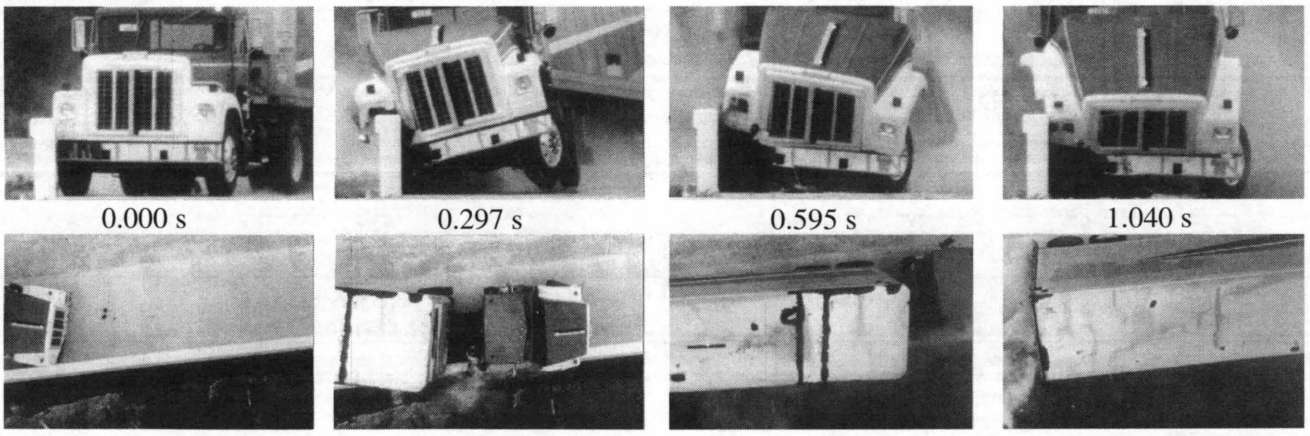

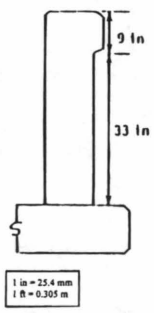

Test No.	7069-13
Date	7/11/88
Test Installation	1.07 m (42-in) Concrete Parapet
Installation Length	30 m (100 ft)
Test Vehicle	1979 International Tractor w/van-trailer
Vehicle Weight	
Empty Weight	12 571 kg (27,690 lb)
Test Inertia	22 723 kg (50,050 lb)
Maximum Vehicle Crush	457 mm (18.0 in)

Impact Speed	82.7 km/h (51.4 mi/h)
Impact Angle	16.2 deg
Exit Speed	N/A
Exit Trajectory	0 deg
Vehicle Accelerations (Max. 0.050-sec avg)	
Longitudinal	-3.3 g
Lateral	3.7 g
Occupant Impact Velocity at true c.g.	
Longitudinal	3.2 m/s (10.5 ft/s)
Lateral	3.8 m/s (12.5 ft/s)
Occupant Ridedown Accelerations	
Longitudinal	-2.2 g
Lateral	4.6 g

FIGURE 9 Summary of results for tractor-trailer test on concrete parapet, Test 7069-13.

REFERENCES

1. *Guide Specifications for Bridge Railings.* AASHTO, Washington, D.C., 1989.
2. *Guide Specifications for Bridge Railings* (proposed). AASHTO, Washington, D.C., 1987.
3. Buth, C. E. *Safer Bridge Railings.* FHWA Report FHWA/RD-82/072. Federal Highway Administration, U.S. Department of Transportation, Washington, D.C., June 1984.
4. Beason, W. L., and T. J. Hirsch. *Measurement of Heavy Vehicle Impact Forces and Inertia Properties.* Final Report for FHWA Contract DTFH61-85-00101. Texas Transportation Institute, Texas A&M University, College Station, Tex., Jan. 1989.
5. Hirsch, T. J. *Analytical Evaluation of Texas Bridge Rails to Contain Buses and Trucks.* Research Report 230-2. Texas Transportation Institute, Texas A&M University, College Station, Tex., August 1978.
6. Buth, C. E., T. J. Hirsch, and C. F. McDevitt. Performance Level 2 Bridge Railings. In *Transportation Research Record 1258,* Transportation Research Board, National Research Council, Washington, D.C., 1990.
7. Michie, J. *Recommended Procedures for the Safety Performance Evaluation of Highway Appurtenances.* NCHRP Report 230. Transportation Research Board, National Research Council, Washington, D.C., March 1981.

Publication of this paper sponsored by Committee on Roadside Safety Features.

Performance Level 2 and Test Level 4 Bridge Railings for Timber Decks

BARRY T. ROSSON, RONALD K. FALLER, AND MICHAEL A. RITTER

The Midwest Roadside Safety Facility, in cooperation with the Federal Highway Administration and U.S. Department of Agriculture Forest Service, Forest Products Laboratory, developed and tested two bridge railings for use on longitudinal timber bridge decks: (*a*) a steel railing system (TBC-8000) and (*b*) a glulam timber railing system (GC-8000). The test for the TBC-8000 was conducted according to Performance Level 2 as specified in the AASHTO *Guide Specifications for Bridge Railings* (1989). The tests for the GC-8000 were conducted according to Test Level 4 as specified in *NCHRP Report 350*. The safety performance of each of the bridge railings was acceptable according to each applicable crash test criterion. Both railings provide aesthetically pleasing and economical alternatives for use on higher-service-level timber bridges.

Most crashworthy bridge railing systems have been developed using materials such as concrete, steel, and aluminum. In addition, most of these railing systems have been constructed on reinforced concrete decks. However, many of the existing bridge railings have not been adapted for use on timber decks. The demand for crashworthy railing systems on timber decks has become increasingly important with the increased use of timber bridges on local roads and secondary highways.

Only recently have researchers begun to develop crashworthy railing systems for timber bridge decks. Further, all of these railing systems were designed for low-to-medium service-level bridges. For timber to be a viable material in the new construction of higher service-level bridges, additional bridge railing systems must be developed and crash-tested for timber bridges.

LITERATURE REVIEW

In 1988, the Texas Transportation Institute (TTI) conducted a safety performance evaluation of the Missouri thrie-beam bridge rail system and transition for the Missouri Highway and Transportation Department (*1*). The bridge rail consisted of W6 × 20 steel posts spaced on 1.90 m (6 ft 3 in.) centers and mounted to the surface of a reinforced concrete bridge deck. A 10-gauge thrie-beam rail was mounted to the traffic-side face of the posts without spacer blocks. To further strengthen the rail, a C8 × 11.5 structural steel channel was mounted to the top of the steel posts at a height of 77.8 cm (2 ft 6⅝ in.). Two full-scale crash tests were conducted on the bridge rail according to *NCHRP Report 230* (*2*). The first test was performed with a 823-kg (1,815-lb) minicompact with impact conditions of 95.9 km/hr (59.6 mph) and 15.0 degrees. The second test was performed with a 2,039-kg (4,495-lb) sedan with impact conditions of 98.0 km/hr (60.9 mph) and 24.0 degrees. According to TTI researchers, the Missouri thrie-beam bridge rail was acceptable according to *NCHRP Report 230* criteria (*2*).

In 1988, Southwest Research Institute (SwRI) performed an evaluation of a longitudinal glulam timber and sawed lumber curb railing system attached to a longitudinal spike-laminated timber deck (*3*). The system evaluated at SwRI was constructed and tested with sawed lumber post 20.3 cm (8 in.) wide × 30.5 cm (12 in.) deep. The system also had been constructed with a nonstandard-size glulam rail 15.2 cm (6 in.) × 27.3 cm (10¾ in.). The curb rail had dimensions of 15.2 cm (6 in.) × 30.5 cm (12 in.) and was attached to the deck with four 1.9-cm (3/4-in.)-diameter ASTM A325 bolts. Two crash tests were conducted according to the AASHTO *Guide Specifications for Bridge Railings (4):* the first was a PL1 test using a 2,383-kg (5,254-lb) pickup traveling at a speed of 76.4 km/hr (47.5 mph) and at an angle of 20 degrees; the second was a PL2 test using an 825-kg (1,818-lb) minicompact traveling at a speed of 95.3 km/hr (59.2 mph) and at an angle of 20 degrees. Although the system met AASHTO PL1 requirements, delamination of several of the deck timbers and minor pull-out of several spikes was observed. Although this system was widely used, and was the only available crash-tested railing for timber bridges, the demand continued for crashworthy bridge railings that would not damage the timber decks and that would be adaptable for use on other timber decks.

In the early 1990s, Forest Product Laboratory and Midwest Roadside Safety Facility (MwRSF) researchers developed and tested three PL1 bridge railings (two glulam timber railing systems and one steel railing system) for use on longitudinal timber decks (*5,6*). This research effort provided several aesthetically pleasing and economical bridge railings for timber bridge decks on low-to-medium service-level highways. The geometry of the PL1 thrie-beam "steel system" railing was essentially unchanged from the previously tested California thrie-beam bridge rail (*7*). Therefore, it was considered unnecessary to perform a test with the minicompact sedan (which was successfully tested during the California development) because there was no potential for wheel snagging or concern for occupant risk. Because the basic geometry of the PL1 glulam timber "curb system" railing was unchanged from the timber system tested by SwRI (*3*), it was deemed unnecessary to perform the test with a minicompact sedan as well. However, the structural components and load transfer mechanisms for both railings were significantly modified, thus requiring crash testing with a 2,449-kg (5,400-lb) pickup truck.

RESEARCH OBJECTIVES

Following the successful development of the three MwRSF PL-1 bridge railings on longitudinal timber decks, a research project was planned to further develop aesthetic and economical bridge railings

B. T. Rosson and R. K. Faller, Midwest Roadside Safety Facility, Civil Engineering Department, 1901 Y Street, Building C, University of Nebraska-Lincoln, Lincoln, Nebr. 68588-0601. M. A. Ritter, U.S. Department of Agriculture Forest Service, Forest Products Laboratory, One Gifford Pinchot Drive, Madison, Wis. 53705.

for timber bridges on higher service-level roadways. The Midwest Roadside Safety Facility in cooperation with the USDA Forest Service, Forest Products Laboratory, and the Federal Highway Administration, developed a PL2 (*2*) thrie-beam railing and a TL-4 (*8*) glulam timber railing that would be compatible with the existing types of longitudinal timber bridge decks. The first bridge railing was a steel system constructed using thrie-beam with a channel attached above spacer blocks (TBC-8000). The second railing was constructed using a glulam timber rail with a curb mounted on scupper blocks (GC-8000).

EVALUATION CRITERIA

Throughout the development of the TBC-8000, crash test criteria of the 1989 AASHTO *Guide Specifications for Bridge Railings* (*4*) were used. To be considered an AASHTO PL2 bridge railing, the railing must satisfy the safety requirements from three full-scale vehicle crash tests. The required PL2 tests are:

1. An 816-kg (1,800-lb) minicompact traveling at 96.6 km/hr (60 mph) and 20 degrees;
2. A 2,449-kg (5,400-lb) pickup traveling at 96.6 km/hr (60 mph) and 20 degrees; and
3. An 8,165-kg (18,000-lb) single-unit truck traveling at 80.5 km/hr (50 mph) and 15 degrees. The guide specifications require that the full-scale crash tests be conducted and reported in accordance with *NCHRP Report 230: Recommended Procedures for the Safety Performance Evaluation of Highway Appurtenances* (*2*).

NCHRP Report 350: Recommended Procedures for the Safety Performance Evaluation of Highway Features (*8*) was published and adopted by the FHWA while the GC-8000 was being developed. Consequently, the GC-8000 railing was evaluated using the TL4 crash test criteria. The required TL4 tests are:

1. An 820-kg (1,808-lb) minicompact traveling at 100 km/hr (62.1 mph) and 20 degrees;
2. A 2,000-kg (44,409-lb) pickup traveling at 100 km/hr (62.1 mph) and 25 degrees; and
3. An 8,000-kg (17,637-lb) single-unit truck traveling at 80 km/hr (49.7 mph) and 15 degrees.

TBC-8000 SYSTEMS

System Development

The previously accepted AASHTO PL1 "steel system" for timber decks (*5,6*) was selected as the basis for the design of the AASHTO PL2 steel bridge railing. Because the Missouri combination steel railing system successfully met the *NCHRP Report 230* safety performance evaluation, and would likely meet the AASHTO PL2 pickup truck crash test criteria as well, concepts from the Missouri railing were used in the design of the new PL2 railing for timber bridge decks.

The minicompact vehicle test conducted on the Missouri thrie-beam bridge railing was performed at 15 degrees, as the *NCHRP Report 230* evaluation criteria require (*2*). Thus, the test results would have been similar if the Missouri railing system had been conducted at 20 degrees, because there was no observable tendency for the vehicle to snag or underride the bridge railing. Also, because the Missouri bridge railing successfully met the *NCHRP Report 230* strength test using a 2,039-kg (4,495-lb) sedan at 98.0 km/hr (60.9 mph) and 24.0 degrees, the AASHTO PL2 strength test (with a 2,449-kg (5,400-lb) pickup traveling at 96.6 km/hr (60 mph) and 20 degrees) would have yielded similar results to the sedan strength test because the impact severity of the sedan crash test was determined to be 132 kJ (97 k-ft), whereas the impact severity for the pickup test was only 103 kJ (76 k-ft). Although the center of mass of the pickup is higher than that of the sedan and would produce slightly higher bending moments in the posts if the impact severities were the same, the actual lower impact force of the pickup test, even when applied at a slightly higher level, would not produce moments of sufficient magnitude to overcome the difference in severity levels. Therefore, with the TBC-8000 consisting of similar structural members as the Missouri railing, only the 8,165-kg (18,000-lb) single-unit truck crash test would have to be conducted for the new railing to meet PL2 crash test criteria.

It was concluded that the PL1 steel system design should be stiffened to meet AASHTO PL2 standards since three of the posts had significant deformation from the PL1 pickup test (*5,6*). In addition, the Missouri thrie-beam railing had 15.9 cm (6.25 in.) of permanent set deflection when hit by the sedan (*1*). Therefore, a C8 × 11.5 steel channel was mounted above the spacer block of the PL1 steel system (Figure 1) to strengthen the bridge rail and meet PL2 strength standards. The top of the steel channel section has a mounting height of 84.5 cm (2 ft 9¼ in.) to provide clearance above the thrie-beam. This provides vertical support for the bottom of the truck box during impact, thus reducing the amount of roll motion of the truck box.

Design Details

The TBC-8000 bridge railing consists of four major components: (*a*) structural steel posts and spacer blocks; (*b*) steel thrie-beam rail; (*c*) structural steel channel rail; and (*d*) structural steel mounting plates. An illustration of the TBC-8000 bridge railing is shown in Figure 1.

Fifteen galvanized ASTM A36 W6 × 15 structural steel posts 93.3 cm (3 ft 3/4 in.) long were used to support the steel railing. The steel posts were attached to the longitudinal glulam timber deck with ASTM A36 structural steel mounting plates. Fifteen steel mounting plates 1.9 cm (3/4 in.) thick, 27.3 cm (10¾ in.) deep, and 61.0 cm (24 in.) long were attached to the deck with two ASTM A722 high-strength bars 2.5 cm (1 in.) in diameter and 1.37 m (4 ft 6 in.) long, spaced at 40.6 cm (16 in.) and located 7.6 cm (3 in.) below the top surface of the deck. Design details for the bearing plates located at the other end of the rods are included in a study by Ritter et al. (*6*). Each steel post was bolted to a steel mounting plate with four 2.2 cm (7/8 in.) diameter ASTM A325 galvanized hex head bolts. Four recessed holes were cut into the edge of the timber deck so the steel mounting plates would bolt flush against the vertical deck surface. The lower rail consisted of a 10-gauge thrie-beam mounted 78.4 cm (2 ft 6⅞ in.) above the timber deck surface. The thrie-beam rail was offset 15.2 cm (6 in.) away from the posts with galvanized ASTM A36 W6 × 15 structural steel spacer blocks 58.7 cm (1 ft 11⅛ in.) long. The upper rail consisted of galvanized ASTM A36 C8 × 11.5 structural steel channel sections attached to the top of the steel spacer blocks. The top of the channel rail was 84.5 cm (2 ft 9¼ in.) above the asphalt surface. The channel rail sections were attached to the spacer blocks with 3½ × 3½ × 5/16 ASTM A36 structural steel angles. Each channel rail section was spliced together with ASTM A36 structural steel splice plates.

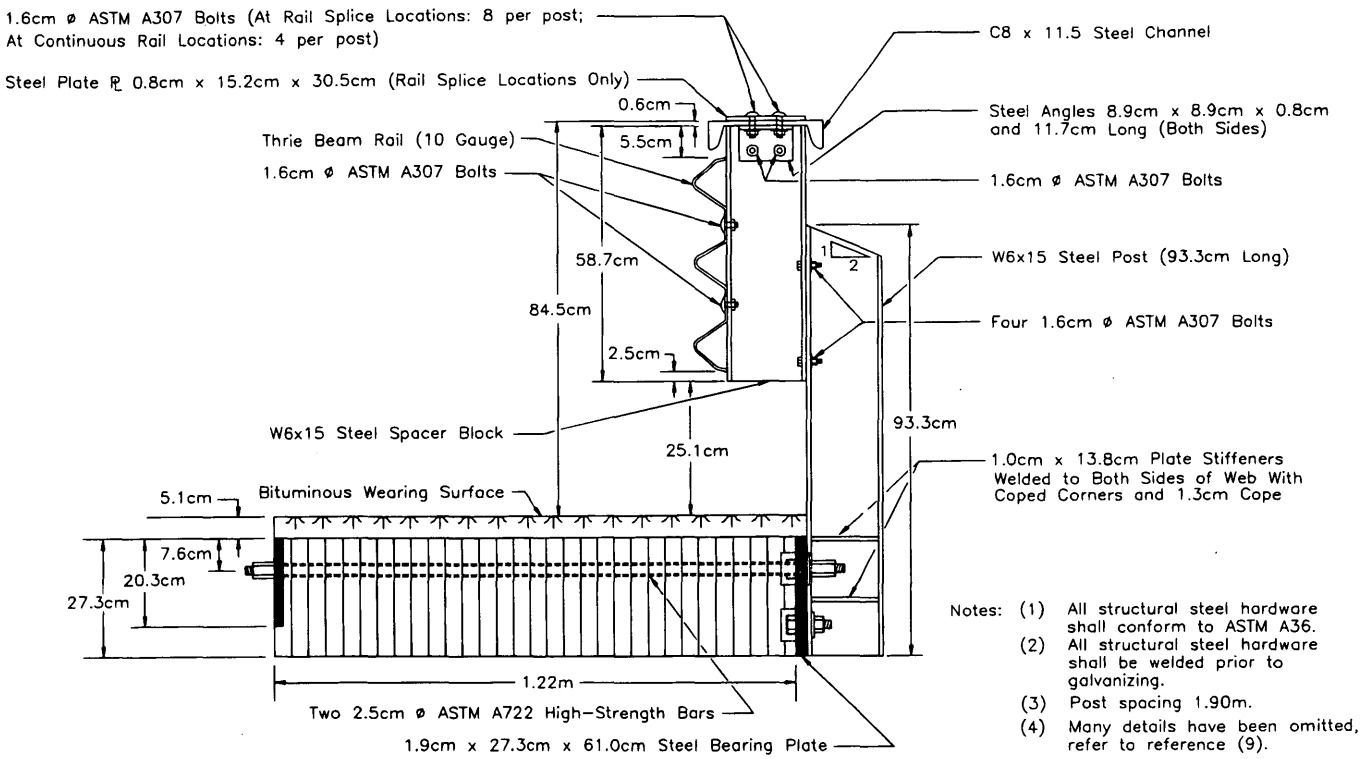

FIGURE 1 Thrie-beam with channel bridge railing (TBC-8000).

An approach guardrail transition was constructed on the upstream end of the TBC-8000 bridge railing. Details of the approach guardrail transition can be found in the Forest Product Laboratory Report on the TBC-8000 (*9*).

The rail was attached to a longitudinal glulam timber deck supported by concrete abutments. A full-size simulated timber bridge system was constructed at the Midwest Roadside Safety Facility to simulate an actual timber bridge installation. The inner three concrete bridge supports had center-to-center spacings of 5.71 m (18 ft 9 in.), and the outer two spacings were 5.56 m (18 ft 3 in.). The longitudinal glulam timber deck consisted of 10 rectangular panels measuring 1.22 m (3 ft 11⅞ in.) wide, 5.70 m (18 ft 8½ in.) long, and 27.3 cm (10¾ in.) thick. It was constructed so that two panels formed the width and five panels formed the length of the installation. The longitudinal glulam timber deck was fabricated with Combination No. 2 West Coast Douglas Fir and treated with pentachlorophenol in heavy oil to a minimum net retention of 9.61 kg/m^3 (0.6 lb/ft^3) as specified in American Wood-Preservers' Association Standard C14 (*10*). At each longitudinal midspan location of the panels, stiffener beams were bolted transversely across the bottom of the deck per AASHTO bridge design requirements. The stiffener beams measured 13.0 cm (5⅛ in.) wide, 15.2 cm (6 in.) thick, and 2.44 m (8 ft) long. The timber deck had a 5.1-cm (2-in.) asphalt surface on top to represent actual field conditions.

Computer Simulation

After the preliminary design of the TBC-8000, computer simulation modeling with *BARRIER VII (11)* was performed to analyze the dynamic performance of the bridge railing before full-scale crash testing. The simulation was conducted modeling a 8,165-kg (18,000-lb) single-unit truck striking the rail at 80.5 km/hr (50 mph) and 15 degrees.

The simulation results indicated that the TBC-8000 bridge railing would successfully redirect the 8,165-kg (18,000-lb) single-unit truck. In addition, the modeling indicated that all structural hardware would remain functional during the impact. The maximum dynamic deflections of the C-rail and thrie-beam were 34.8 cm (13.7 in.) and 29.2 cm (11.5 in.), respectively. The maximum permanent set deflections of the C-rail and thrie-beam were 17.8 cm (7.0 in.) and 15.2 cm (6.0 in.), respectively. The maximum 0.010-sec average lateral and longitudinal decelerations were 2.7 and 2.0 *g*, respectively. The peak 0.050-sec average impact force perpendicular to the bridge railing was approximately 222 kN (50 kips). The truck became parallel to the bridge railing at 0.350 sec. At 0.680 sec, the truck exited the bridge railing at an angle of 11.4 degrees.

Full-Scale Crash Test

Test FSTC-1 [8,165-kg (18,000-lb), 76.3 km/hr (47.4 mph), 16.1 degrees] struck the bridge railing at Post No. 4 (Figure 2). A summary of the test results and the sequential photographs is presented in Figure 3.

After the initial impact with the bridge railing, the right-front corner of the bumper and quarter panel crushed inward. The truck became parallel with the rail at 0.399 sec with a velocity of 66.6 km/hr (41.4 mph). At 0.523 sec, the front-end of the truck began to yaw away from the rail, and at 0.622 sec, the truck box reached a maximum clockwise roll angle of approximately 18 degrees. The truck exited the bridge rail at approximately 1.504 sec and 1.8 degrees. The effective coefficient of friction was determined to be 0.31.

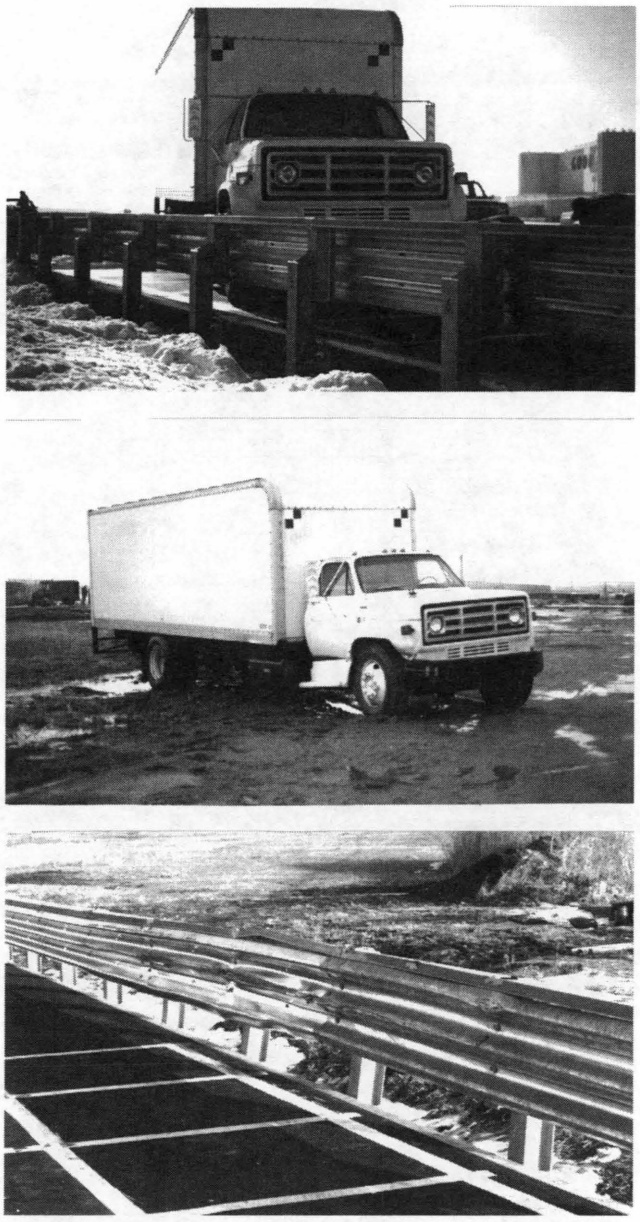

FIGURE 2 Impact location, vehicle damage, and bridge rail damage, Test FSTC-1.

Vehicle damage was relatively minor and was limited to the right-front corner of the truck cab, box, and front bumper (Figure 2). The bridge rail damage was moderate, consisting mostly of deformed thrie-beam sections, C-rail sections, and steel posts (Figure 2). Examination of the top and bottom surfaces of the timber deck laminations revealed no physical damage or separation.

The length of vehicle contact along the top of the C-rail was approximately 11.4 m (37 ft 6 in.). Physical evidence revealed that lateral buckling of the C-rail occurred between Post Nos. 4 and 5 (Figure 2). The physical damage to the thrie-beam rail revealed that approximately 7.6 m (25 ft) of rail was damaged. The maximum permanent set deflections of the C-rail and thrie-beam rail were 19.3 cm (7.6 in.) and 20.8 cm (8.2 in.), respectively.

Test FSTC-1 was evaluated according to the AASHTO PL2 criteria. The TBC-8000 bridge rail contained and smoothly redirected the test vehicle with controlled lateral deflection of the bridge rail. There were no detached elements or fragments that showed potential for penetrating the occupant compartment or that presented undue hazard to other traffic. The test vehicle did not penetrate or ride over the bridge rail, and it remained upright during and after the crash. The occupant compartment was not damaged. The effective coefficient of friction, $\mu = 0.31$, was fair ($0.26 \leq \mu \leq 0.35$). The occupant risk values for occupant impact velocities and ridedown decelerations were satisfactory. The vehicle's trajectory revealed minimum intrusion into adjacent traffic lanes. The vehicle's exit angle from the bridge railing was less than 12 degrees.

GC-8000 SYSTEM

System Development

After the successful development and full-scale vehicle crash testing of the AASHTO PL1 curb system *(5,6)*, it was determined that the PL1 bridge railing had adequate structural capacity and could be modified to meet a higher performance level. Therefore the AASHTO PL1 "curb system" was used as the basis for the design of the *NCHRP Report 350* TL4 glulam railing.

The glulam rail previously tested at SwRI *(3)* was crash-tested using an 825-kg (1,818-lb) minicompact at 95.3 km/hr (59.2 mph) and 20 degrees and a 2,383-kg (5,254-lb) pickup at 76.4 km/hr (47.5 mph) and 20 degrees. Because the basic geometry of the PL1 curb system and the newly developed GC-8000 were essentially the same as the system tested at SwRI, repeating the minicompact sedan test was deemed unnecessary. However, to meet TL4 criteria, the 2,000-kg (4,409-lb) unballasted pickup test at 100 km/hr (62.1 mph) and 25 degrees and the 8,000-kg (17,637-lb) single-unit truck test at 80 km/hr (49.7 mph) and 15 degrees would have to be conducted.

Development of the GC-8000 consisted of re-sizing the structural components previously used with the AASHTO PL-1 curb system to withstand the higher impact forces generated from the TL4 crash test conditions. The components changed included the timber glulam rail, lumber posts, spacer and scupper blocks, and structural steel hardware. The PL1 curb system was constructed with sawed lumber Douglas Fir posts 20.3 cm (8 in.) wide and 20.3 cm (8 in.) deep, and the glulam rail was 17.1 cm (6¾ in.) wide and 26.7 cm (10½ in.) deep. However, computer simulation modeling indicated that the GC-8000 bridge rail posts needed to be 20.3 cm (8 in.) wide and 25.4 cm (10 in.) deep, and the glulam rail needed to be 17.1 cm (6¾ in.) wide and 34.3 cm (13½ in.) deep. The scupper blocks, used to support the sawed lumber curb rail and transfer the impact forces into the timber deck, were increased in length from 0.91 to 1.22 m (3 to 4 ft) and in depth from 14.0 to 19.1 cm (5½ to 7½ in.). The increase in length of the scupper blocks was required to accommodate the six ASTM A307 1.9 cm (3/4 in.) diameter bolts needed to carry the increased impact forces into the deck. The increase in depth of the scupper blocks was used to accommodate a 5.1-cm (2-in.) asphalt-wearing surface placed on the timber deck.

Design Details

The GC-8000 consisted of five major components: (*a*) sawed lumber scupper blocks; (*b*) sawed lumber curb rail; (*c*) sawed lumber posts; (*d*) longitudinal glulam timber rail; and (*e*) timber spacer blocks. An illustration of the GC-8000 bridge railing is shown in Figure 4.

One timber scupper block was bolted to the timber deck at each post location with six ASTM A307 1.9 cm (3/4 in.) diameter, 66.0

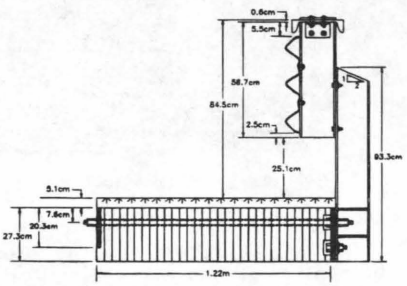

Test Number	FSTC-1
Date	12/9/92
Bridge Rail Installation	Steel Thrie and Channel Bridge Rail
Total Length	28.57 m
Steel Thrie Beam Rail	
Size	10 Gauge (AASHTO M180)
Top Mounting Height	78.4 cm
Steel Channel Rail (C-rail)	
Size	C8 x 11.5 (A36)
Top Mounting Height	84.5 cm
Steel Posts (No. 1 through 15)	W6 x 15 (A36)
Length	93.3 cm
Steel Spacer Blocks (No. 1 through 15)	W6 x 15 (A36)
Length	58.7 cm
Vehicle Model	1986 GMC 7000 Series Straight Truck
Test Inertial Weight	8,165 kg
Gross Static Weight	8,165 kg
Vehicle Speed	
Impact	76.3 km/hr
Exit	Not Available

Vehicle Angle	
Impact	16.1 degrees
Exit	1.8 degrees
Vehicle Snagging	None
Vehicle Stability	Satisfactory
Effective Coefficient of Friction (μ)	0.31
Normalized Occupant Impact Velocity	
Longitudinal (Not Required)	3.3 m/s (9.1 m/s) *(4)*
Lateral (Not Required)	4.8 m/s (7.6 m/s) *(4)*
Occupant Ridedown Deceleration	
Longitudinal (Not Required)	1.8 g's (15 g's) *(4)*
Lateral (Not Required)	6.1 g's (15 g's) *(4)*
Vehicle Damage	Minor
TAD	1-RFQ-2
VDI	01RYEW1
Bridge Rail Damage	Moderate
Maximum Vehicle Rebound Distance	17.8 cm @ 40.54 m
Maximum Permanent Set Deflection	
C-Rail	19.3 cm
Thrie Beam	20.8 cm

FIGURE 3 Summary of test results and sequential photographs, Test FSTC-1.

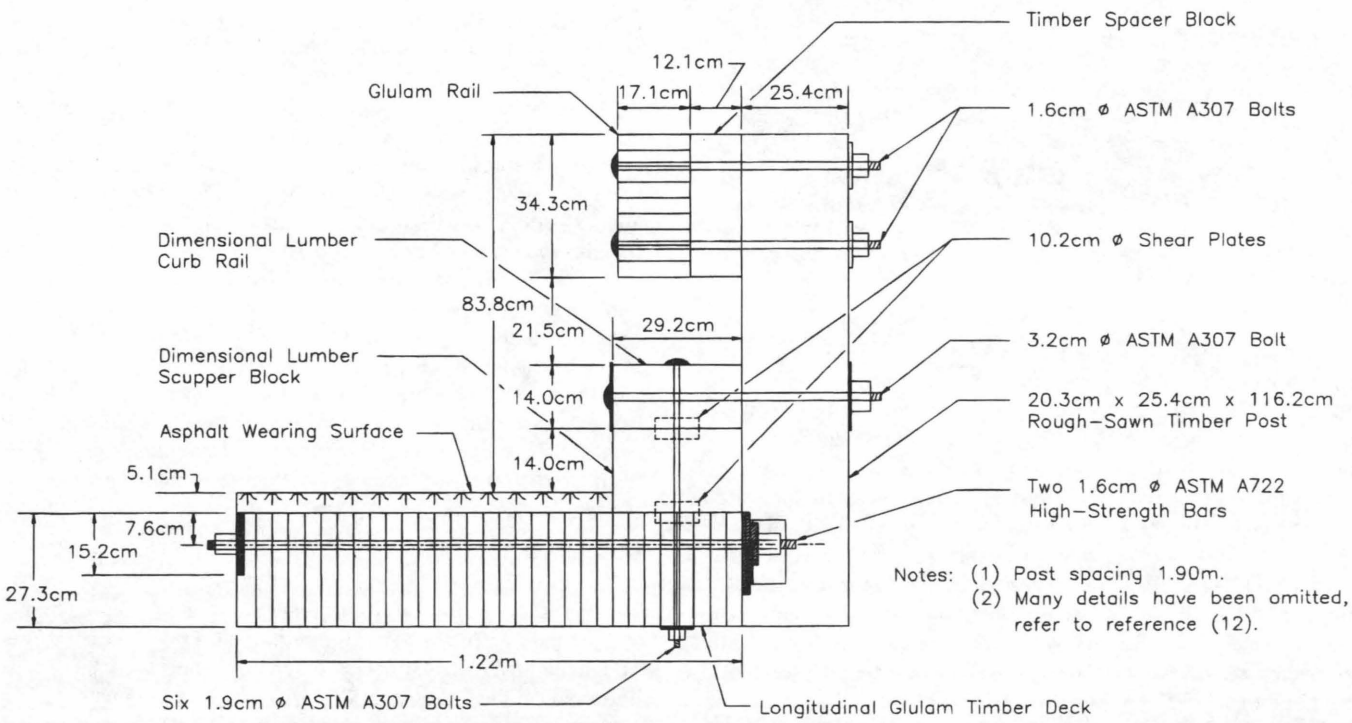

FIGURE 4 Glulam timber with curb bridge railing (GC-8000).

cm (26 in.) long galvanized dome head bolts. The scupper blocks were fabricated with S4S No. 1 Grade Douglas Fir 19.0 cm (7½ in.) thick, 29.2 cm (11½ in.) wide, and 1.22 m (4 ft) long. They were attached to the curb rail and timber deck surface with 10.2 cm (4 in.) diameter shear plate connectors. The curb rail was fabricated with S4S No. 1 Grade Douglas Fir 14.0 cm (5½ in.) deep and 29.2 cm (11½ in.) wide, with the top of the curb rail positioned 28.0 cm (11 in.) above the asphalt-wearing surface. One ASTM A307 3.2 cm (1¼ in.) diameter, 63.5 cm (25 in.) long dome head bolt was used to attach each of the 15 bridge posts to the curb rail. Two 1.37 m (4 ft 6 in.) long high-strength bars were placed 55.9 cm (22 in.) apart transversely through the outer timber deck panel at each post. Fifteen No. 1 Grade rough-sawed lumber Douglas Fir posts approximately 20.3 cm (8 in.) wide, 25.4 cm (10 in.) deep, and 1.16 m (3 ft 9¾ in.) long were used to support the upper glulam railing at a spacing of 1.90 m (6 ft 3 in.) on centers. The posts were treated to meet AWPA Standard C14 with 192.22 kg/m^3 (12 lb/ft^2) creosote *(10)*. The longitudinal glulam rail was fabricated from Combination No. 2 West Coast Douglas Fir and treated in the same manner as the timber deck. The glulam rail was 17.1 cm (6¾ in.) wide and 34.3 cm (13½ in.) deep. The top mounting height of the glulam rail was 83.8 cm (2 ft 9 in.) above the asphalt-wearing surface. The glulam rail was offset from the posts with timber spacer blocks 12.1 cm (4¾ in.) thick, 20.3 cm (8 in.) wide, and 34.3 cm (13½ in.) deep. Two ASTM A307 1.6 cm (5/8 in.) diameter 61.0 cm (24 in.) long galvanized dome head bolts were used to attach the glulam rail to the timber posts. The rail was attached to a longitudinal glulam timber deck similar to the one used in the TBC-8000 crash test.

An approach guardrail transition was constructed on the upstream end of the GC-8000 bridge railing and crash-tested with a 2,041-kg (4,500-lb) sedan at 100.4 km/hr (62.4 mph) and 24.8 degrees. The crash test was evaluated according to the safety performance criteria provided in *NCHRP Report 230 (2)* and was acceptable. The sedan crash test was performed on the guardrail transition according to *NCHRP Report 230* criteria because at the time the transition was tested the GC-8000 was not intended to meet *NCHRP Report 350 (8)* TL4 criteria. Further details concerning the approach guardrail transition can be found in the Forest Product Laboratory Report on the GC-8000 *(12)*.

Computer Simulation

After the preliminary design of the GC-8000, computer simulation modeling with BARRIER VII *(11)*) was performed to analyze the dynamic performance of the bridge railing before full-scale crash testing. Computer simulations were conducted with an 8,165-kg (18,000-lb) single-unit truck hitting the rail at a speed of 80.5 km/hr (50 mph) and impact angle of 15 degrees, and with a 1,996-kg (4,400-lb) pickup truck traveling at a speed of 100 km/hr (62.1 mph) and having impact angle of 25 degrees.

The simulation results indicated that the GC-8000 bridge railing would satisfactorily redirect the 8,000-kg (17,637-lb) single-unit truck. In addition, all structural hardware would remain functional during the impact; the maximum dynamic and permanent set deflections of the glulam rail were 15.2 cm (6.0 in.) and 4.1 cm (1.6 in.), respectively. The maximum 0.010-sec average lateral and longitudinal decelerations were 3.3 and 2.1 *g*, respectively. The peak 0.050-sec average impact force perpendicular to the bridge railing was approximately 285 kN (64 kips). The truck became parallel to the bridge railing at 0.323 sec. At 0.625 sec, the truck exited the bridge railing at an angle of 12.3 degrees.

The simulation results also indicated that the railing would satisfactorily redirect the 2,000-kg (4,409-lb) pickup truck. In addition, all structural hardware would remain functional during the impact; the maximum permanent set and dynamic deflections of the glulam rail were 7.4 cm (2.9 in.) and 17.8 cm (7.0 in.), respectively. The maximum 0.010-sec average lateral and longitudinal decelerations were 13.2 and 10.9 *g*, respectively. The peak 0.050-sec average impact force perpendicular to the bridge railing was approximately 276 kN (62 kips). The truck became parallel to the bridge railing at 0.180 sec. At 0.260 sec, the truck exited the bridge railing at an angle of 9.4 degrees.

Full-Scale Crash Tests

Test FSCR-1 [8,165-kg (18,000-lb), 82.4 km/hr (51.2 mph), 16.8 degrees] hit the bridge rail at approximately 45.7 cm (1 ft 6 in.)

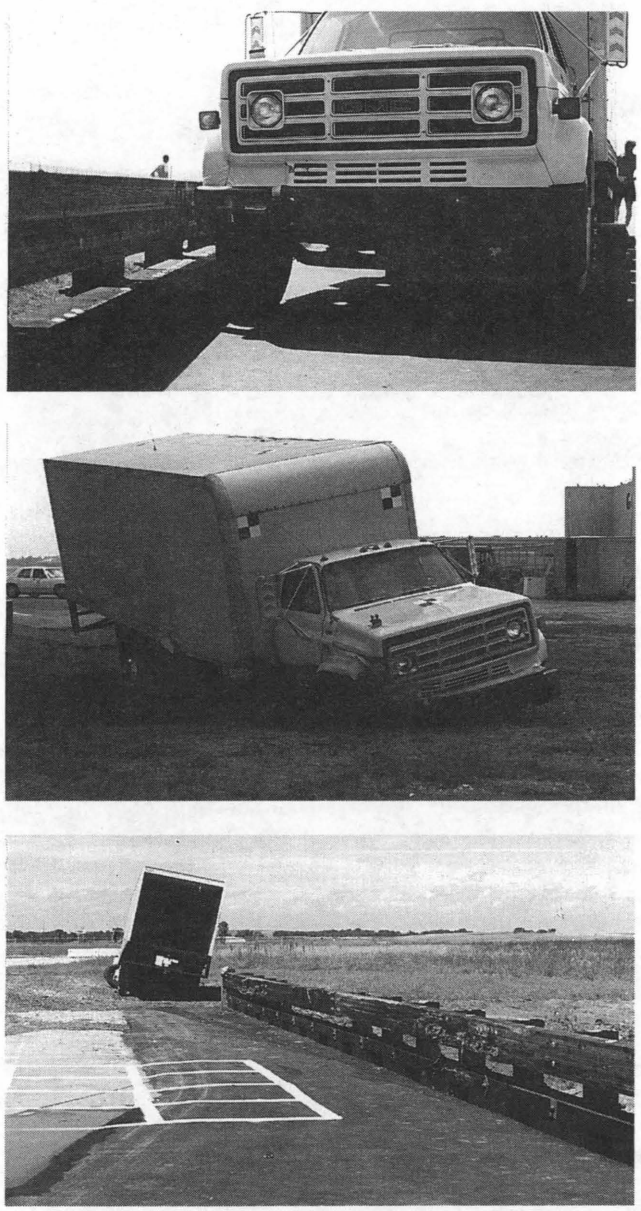

FIGURE 5 Impact location, vehicle damage, and bridge rail damage, Test FSCR-1.

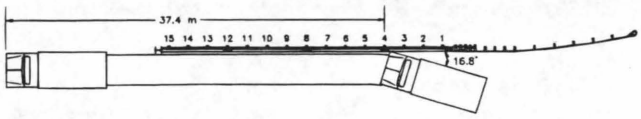

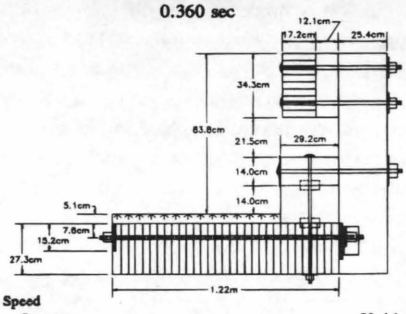

Test Number	FSCR-1
Date	8/12/93
Bridge Rail Installation	Glulam Timber Bridge Rail With Sawn Lumber Curb Rail
Length	28.57 m
Upper Rail	
Width	17.1 cm
Depth	34.3 cm
Top Mounting Height	83.8 cm
Material	Glulam Rail-Comb. No. 2
Lower Rail (Curb)	
Width	29.2 cm
Depth	14.0 cm
Top Mounting Height	27.9 cm
Material	S4S No. 1 Grade Douglas Fir
Posts (No. 1 through 15)	
Size	20.3 cm x 25.4 cm x 116.2 cm
Material	No. 1 Grade Rough Sawn Douglas Fir
Bridge Deck Installation	Longitudinal Glulam Timber Bridge Deck Panels
Panel Size	27.3 cm x 1.22 m x 5.71 m
Material	Glulam Timber Deck Comb. No. 2
Vehicle Model	1986 GMC 7000 Series Single-Unit Truck
Test Inertial Weight	8,165 kg
Gross Static Weight	8,165 kg

Vehicle Speed	
Impact	82.4 km/hr
Exit	66.5 km/hr
Vehicle Angle	
Impact	16.8 degrees
Exit	0 degrees
Vehicle Snagging	Truck Box on Top of Timber Posts and Spacer Blocks
Vehicle Stability	Satisfactory
Effective Coefficient of Friction (μ)	0.38 (Marginal)
Occupant Impact Velocity - Normalized	
Longitudinal (Not Required)	2.7 m/s (9.1 m/s) *(4)*
Lateral (Not Required)	2.1 m/s (7.6 m/s) *(4)*
Occupant Ridedown Deceleration - 10-msec average	
Longitudinal (Not Required)	1.0 G's (15 G's) *(4)*
Lateral (Not Required)	1.8 G's *(15 G's)* *(4)*
Vehicle Damage	Moderate
TAD	1-RFQ-5
VDI	01RYEW3
Vehicle Rebound Distance	0 m
Bridge Rail Damage	Moderate
Maximum Post or Midspan Rail Deflection	
Permanent Set	3.0 cm
Dynamic	16.5 cm

FIGURE 6 Summary of test results and sequential photographs, Test FSCR-1.

upstream from Post No. 4 (Figure 5). A summary of the test results and the sequential photographs are presented in Figure 6.

After the initial impact with the bridge rail, the right-front corner of the bumper and quarter panel crushed inward. At 0.103 sec, the maximum dynamic lateral deflections were measured at Post No. 5 and the front end of the truck cab began to lift and roll clockwise toward the rail. At 0.124 sec, the longitudinal centerline of the truck cab and box remained parallel, and at 0.145 sec, the truck box began rotating toward the rail while the truck cab began rotating away from the rail. At 0.160 sec, the right-front corner of the truck box extended over the rail and the right-front tire was crushed inward under the engine. At 0.340 sec, the truck cab began rotating toward the rail. The left-rear tire lost contact with the ground at 0.400 sec. At 0.413 sec, the truck cab was approximately parallel to the bridge rail with a velocity of 69.8 km/hr (43.4 mph). The truck box achieved a maximum roll angle of approximately 31 degrees toward the rail at 0.649 sec. At the same time, the right-rear tire also lost contact with the ground. The truck cab achieved a maximum roll angle of approximately 23 degrees toward the rail at 0.739 sec. At 1.500 sec, the truck box rolled away from the rail, and at 1.739 sec, the left-front tire contacted the ground and the vehicle exited the bridge railing at a speed of approximately 66.5 km/hr (41.3 mph) and at a 0-degree angle. The effective coefficient of friction was determined to be approximately 0.38.

Exterior vehicle damage was moderate (Figure 5). Vehicle damage occurred to several body locations, including the door and quarter panels, engine hood, front bumper, right-side wheels and rims, front axle, engine hood, truck box and support frame, side-mounted foot steps, and fuel tank. The right-corner of the front bumper and the right-side door and quarter panels were crushed inward. The front axle, with attached tires and steel rims, became detached from the truck and came to rest under the left-side of the truck cab. The right-front and right-rear (outer dual) tires were deflated.

The moderate bridge railing damage near the impact area is shown in Figure 5. The downstream end of the glulam rail adjacent to Post No. 4 was fractured on the lower part of the rail. The curb rail received significant gouging between Post Nos. 4 and 5. Deep gouges and scrapes occurred to the top of the glulam rail from Post Nos. 7–14. Nine timber bridge posts, Post Nos. 7–15, were damaged during the crash test, as shown in Figure 5. The glulam timber bridge deck received some superficial surface cracks near Post No. 4. The crack width ranged between 1.6 to 3.2 mm (1/16 and 1/8 in.).

The maximum lateral permanent set deflections for midspan rail and post locations, as determined from field measurements in the impact region, were approximately 3.0 cm (1.2 in.) and 2.8 cm (1.1 in.), respectively. The maximum dynamic lateral deflections for midspan rail and post locations (determined from high-speed film analysis) were 14.5 cm (5.7 in.) and 16.5 cm (6.5 in.), respectively.

The GC-8000 bridge railing was originally designed and was to be evaluated according to the AASHTO PL2 *(4)*) guidelines. However, following the successful 8,165-kg (18,000-lb) single-unit truck test, it was determined that the bridge railing could potentially

meet the *NCHRP Report 350 (8)* pickup truck strength test. Therefore, the 2,000-kg (4,409-lb) pickup test at 100 km/hr (62.1 mph) and 25 degrees was conducted instead of the 2,449-kg (5,400-lb) pickup test at 96.6 km/hr (60 mph) and 20 degrees.

Test FSCR-4 [2,087-kg (4,600-lb), 98.0 km/hr (60.9 mph), 24.9 degrees] impacted the bridge rail at approximately 1.76 m (5.77 ft) upstream from Post No. 8 (Figure 7). A summary of the test results and the sequential photographs are presented in Figure 8.

After the initial impact with the bridge rail, the right-front corner of the bumper and quarter panel crushed inward. At 0.054 sec, the right-front tire blew out due to contact with the sawed lumber curb rail. At 0.126 sec, maximum dynamic lateral deflections were observed at Post No. 8. The entire vehicle became airborne at approximately 0.217 sec. At 0.223 sec, the pickup truck was approximately parallel to the bridge rail with a velocity of 66.5 km/hr (41.3 mph) with a slight roll angle toward the bridge rail. At 0.418 sec, the vehicle exited the bridge railing at a speed of approximately 62.9 km/hr (39.1 mph) and angle of 10.4 degrees. The vehicle's right-front tire contacted the ground at 0.512 sec, and its the left-front tire contacted the ground at 0.620 sec. The effective coefficient of friction was determined to be approximately 0.54.

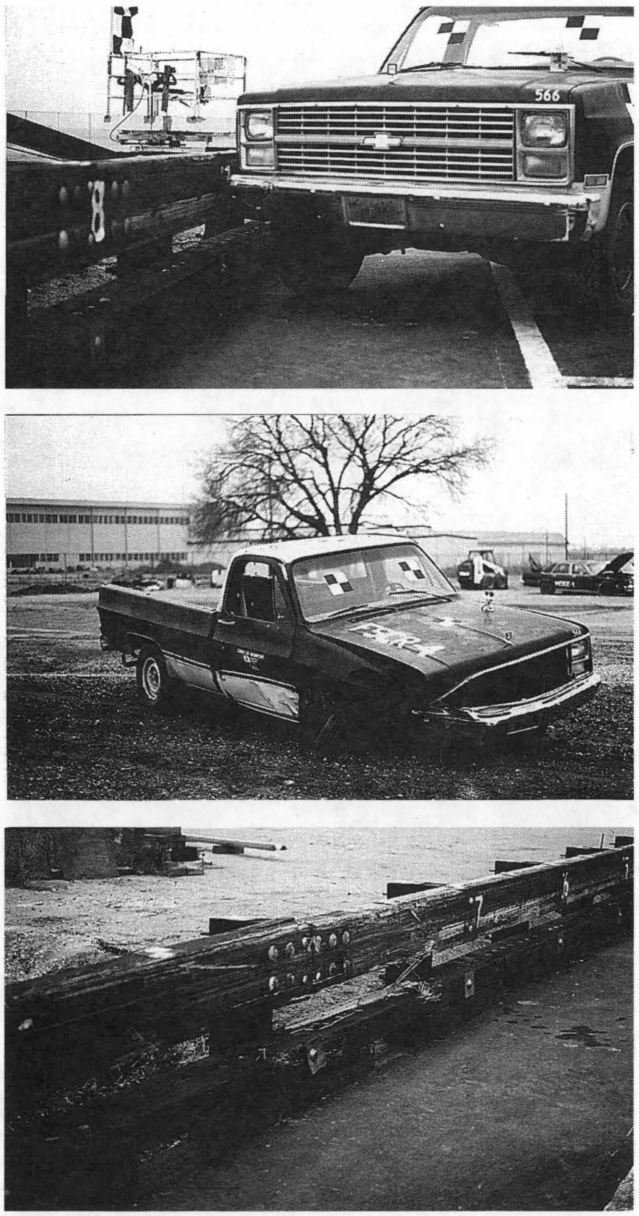

FIGURE 7 Impact location, vehicle damage, and bridge rail damage, Test FSCR-4.

Exterior vehicle damage was moderate (see Figure 7). Vehicle damage occurred to several body locations, including the door and quarter panels, front bumper, right-side tires and rims, rear bumper, engine mount, and interior floorboard. The right-front tire was deflated and partly removed from the rim. In addition, the right-front tire, rim, and attached steering mechanism were pushed backward, and the right-side engine mount was deformed toward the engine. Interior vehicle deformation to the occupant compartment was not sufficient to cause injury to the vehicle occupants.

The minor bridge railing damage downstream from the impact location is shown in Figure 7. Scrapes and gouging occurred to the upper glulam timber and sawed lumber curb rails. Significant tire and rim contact on the curb rail was evident from the downstream side of Post No. 7 to the downstream side of Post No. 8. Longitudinal cracking occurred toward the bottom traffic-side face of the glulam rail at Post No. 8. The downstream-side of the glulam rail splice located at Post No. 8 was fractured. The flexural failure occurred in the tension region of the glulam rail (or the backside of the vertical saw-cut section) and near the downstream end of the steel splice plate. No physical damage occurred to the timber bridge posts or spacer blocks. Additional curb rail damage consisted of cracking along a vertical plane through the longitudinal centerline of the bolts. The glulam timber bridge deck received some superficial surface cracks. The crack width ranged between 1.6 and 6.4 mm (1/16 and 1/4 in.).

The maximum lateral permanent set deflections for midspan rail and post locations (determined from field measurements in the impact region) were approximately 5.3 cm (2.1 in.) and 4.8 cm (1.9 in.), respectively. The maximum dynamic lateral deflections for midspan rail and post locations were 29.2 cm (11.5 in.) and 36.1 cm (14.2 in.), respectively.

Tests FSCR-1 and FSCR-4 were evaluated according to the AASHTO PL2 and NCHRP 350 TL4 criteria. The GC-8000 bridge rail contained and smoothly redirected the test vehicles. The test vehicles did not penetrate, underride, or override the bridge railing, although controlled lateral deflection of the bridge rail is acceptable. There were no detached elements, fragments, or other debris from the bridge railing that showed potential for penetrating the occupant compartment or that presented undue hazard to other traffic. Deformations of, or intrusions into, the occupant compartment that could cause serious injuries did not occur. For Tests FSCR-1 and FSCR-4, the effective coefficients of friction were marginal [$\mu = 0.38$ and $\mu = 0.54$ ($\mu > 0.35$)]. The test vehicles remained upright during and after collision. The occupant risk values for occupant impact velocities and ridedown decelerations were satisfactory. The vehicle trajectories revealed no intrusion into adjacent traffic lanes. For Tests FSCR-1 and FSCR-4, the vehicle exit angles of 0 and 10.4 degrees, respectively, were less than 60 percent of the impact angles of 15 and 25 degrees.

CONCLUSIONS AND RECOMMENDATIONS

The safety performance evaluations of an AASHTO PL2 thriebeam with channel (TBC-8000) rail and an *NCHRP Report No. 350*

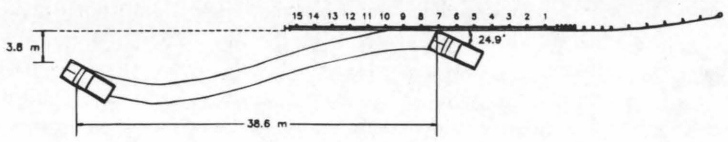

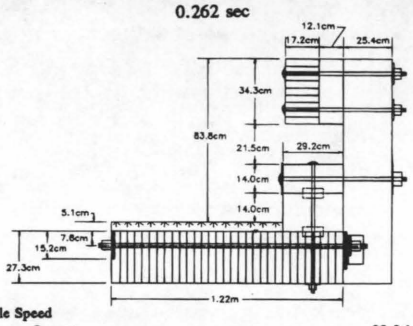

Test Number	FSCR-4
Date	11/23/93
Bridge Rail Installation	Glulam Timber Bridge Rail With Sawn Lumber Curb Rail
Length	28.57 m
Upper Rail	
Width	17.1 cm
Depth	34.3 cm
Top Mounting Height	83.8 cm
Material	Glulam Rail-Comb. No. 2
Lower Rail (Curb)	
Width	29.2 cm
Depth	14.0 cm
Top Mounting Height	27.9 cm
Material	S4S No. 1 Grade Douglas Fir
Posts (No. 1 through 15)	
Size	20.3 cm x 25.4 cm x 116.2 cm
Material	No. 1 Grade Rough Sawn Douglas Fir
Bridge Deck Installation	Longitudinal Glulam Timber Bridge Deck Panels
Panel Size	27.3 cm x 1.22 m x 5.71 m
Material	Glulam Timber Deck Comb. No. 2
Vehicle Model	1984 Custom Deluxe 20 Pickup Truck
Test Inertial Weight	2,087 kg
Gross Static Weight	2,087 kg

Vehicle Speed	
Impact	98.0 km/hr
Exit	62.9 km/hr
Vehicle Angle	
Impact	24.9 degrees
Exit	10.4 degrees
Vehicle Snagging	None
Vehicle Stability	Satisfactory
Effective Coefficient of Friction (μ)	0.54 (Marginal)
Occupant Impact Velocity - Normalized	
Longitudinal (Preferred/Maximum)	8.2 m/s (9 m/s/12 m/s) *(8)*
Lateral	7.4 m/s
Occupant Ridedown Deceleration - 10-msec average	
Longitudinal (Preferred/Maximum)	10.0 G's (15 G's/20 G's) *(8)*
Lateral	12.5 G's
Vehicle Damage	Moderate
TAD	1-RFQ-5
VDI	01RYEW4
Vehicle Lateral Rebound Distance (Right-side)	6.0 m
Bridge Rail Damage	Minor
Maximum Post or Midspan Rail Deflection	
Permanent Set	5.3 cm
Dynamic	36.1 cm

FIGURE 8 Summary of test results and sequential photographs, Test FSCR-4.

TL4 glulam rail with curb (GC-8000) were tested according to the applicable guidelines, and both were acceptable. The result is two new crashworthy bridge railings that are recommended for use on longitudinal timber bridges. Although the two rails were tested on a longitudinal glulam timber bridge deck, both could be adapted for use on other longitudinal timber bridge decks.

The development of the TBC-8000 bridge railing satisfied the concern for economy while also providing a crashworthy bridge railing system for timber bridge decks on higher performance roadways. Although both railings performed similarly according to the evaluation factors of structural adequacy, occupant risk and vehicle trajectory, the vehicle damage to the 8,000-kg (17,637-lb) single-unit truck was more extensive for the GC-8000 impact, and its repair costs also would be higher.

The TBC-8000 was easy to install; therefore it should have low construction costs. The material cost for the TBC-8000 was approximately $174/m ($53/ft). The glulam curb system (GC-8000) is aesthetically pleasing but more expensive than the thrie-beam with channel (TBC-8000) system. The material cost for the GC-8000 was approximately $354/m ($108/ft).

Further testing should be conducted if it is deemed necessary that both transitions and the TBC-8000 railing meet *NCHRP Report 350* TL4 criteria. Further testing will be required because no 8,000-kg (17,637-lb) single-unit truck test or 2,000-kg (4,409-lb) pickup truck test was conducted on either transition. In addition, the TL4 pickup truck test has the potential for significant occupant compartment deformation and could cause the TBC-8000 railing to fail the *NCHRP Report 350* TL-4 crash standards.

ACKNOWLEDGMENTS

The authors thank the following organizations, which have contributed to the success of this research project: the American Institute of Timber Construction, Englewood, Colorado, for donating the glulam materials for the deck and rail construction; Laminated Concepts, Inc., Elmira, New York, for donating structural hardware for the bridge rails; Western Wood Structures, Inc., Tualatin, Oregon, for drafting the preliminary designs and shop drawings; and the Center for Infrastructure Research, University of Nebraska-Lincoln, for matching support.

REFERENCES

1. Mak, K. K., and W. L. Campise. *Testing and Evaluation of Missouri Thrie-Beam Bridge Rail System and Transition.* Final Report to the Missouri Highway and Transportation Department, Final Report No. 87-4. Texas Transportation Institute, Texas A & M University, College Station, Tex., May 1988.
2. *NCHRP Report 230: Recommended Procedures for the Safety Performance Evaluation of Highway Appurtenances* TRB, National Research Council, Washington, D.C., March 1981.

3. Hancock, K. L., A. G. Hansen and J. B. Mayer. *Aesthetic Bridge Rails, Transitions, and Terminals for Park Roads and Parkways.* Report FHWA-RD-90-052. FHWA, U.S. Department of Transportation, May 1990.
4. *Guide Specifications for Bridge Railings,* AASHTO, Washington, D.C., 1989.
5. Faller, R. K., M. A. Ritter, J. C. Holloway, B. G. Pfeifer, and B. T. Rosson, Performance Level 1 Bridge Railings for Timber Decks. *Transportation Research Record 1419,* TRB, National Research Council, Washington, D.C., October 1993, pp. 21–34.
6. Ritter, M. A., R. K. Faller, J. C. Holloway, B. G. Pfeifer, and B. T. Rosson. *Development and Testing of Bridge Railings for Longitudinal Timber Decks by Full-Scale Crash Testing,* U.S. Department of Agriculture, Forest Service, Forest Products Laboratory, Madison, Wis. 1994 (in preparation).
7. Stoughton, R. L., D. Glauz, J. Jewell, J. J. Folsom,and W. F. Crozier. *Vehicle Crash Tests of Steel Bridge Barrier Rail Systems for Use on Secondary Highways.* Division of New Technology, Materials and Research, Office of Structural Materials, California Department of Transportation (in preparation).
8. *NCHRP Report 350: Recommended Procedures for the Safety Performance Evaluation of Highway Features.* TRB, National Research Council, Washington, D.C., 1993.
9. Ritter, M. A., R. K. Faller, and B. T. Rosson. *Development of the TBC-8000 Bridge Railing.* U.S. Department of Agriculture, Forest Service, Forest Products Laboratory, Madison, Wis. 1994 (in preparation).
10. American Wood-Preservers' Association Book of Standards, American Wood-Preservers' Association, Woodstock, Md., 1991.
11. Powell, G. H. *BARRIER VII: A Computer Program for Evaluation of Automobile Barrier Systems.* Report FHWA RD-73-51, FHWA, U.S. Department of Transportation, April 1973.
12. Ritter, M. A., R. K. Faller, B. T. Rosson, and J. C. Holloway. *Development of the GC-8000 Bridge Railing and Transition.* U.S. Department of Agriculture, Forest Service, Forest Products Laboratory, Madison, Wis. 1994 (in preparation).

Publication of this paper sponsored by Committee on Roadside Safety Features.

Risk of Rollover in Ran-Off-Road Crashes

JOHN G. VINER

Linked Illinois state accident and roadway data files were used to explore the nature and importance of vehicle rollovers in "ran-off-road" crashes. Rollovers are known to be a major roadside safety problem—the Illinois data examined in this study indicate that rollovers are involved in one-half of rural roadside crash driver fatalities. The risks of rollover in ran-off-road crashes are compared by land use, road type, and object struck. Side slopes and ditches were found to be the dominant vehicle tripping mechanism involved in rollovers. The findings support the need for closer attention to rollover risks on side slopes and ditches. In particular, the risk of rollover on specific slope and ditch configurations needs to be defined.

Rollover crashes are known to be severe, with most occurring on the roadside. Nationwide data from 1985 indicate that vehicle overturns account for 11 percent of the total harm resulting from police reported crashes, that is, in all traffic crash types (*1*). Further, these data indicate that three-fourths of the first harmful events in all rollover crashes occur outside the shoulder, and that overturns are the cause of one-third of "ran-off-road" crash fatalities. It is estimated from General Estimating System data that 115,000 single-vehicle passenger car off-road rollover crashes occurred in 1989, according for 83 percent of all single-vehicle passenger car rollovers (*2*).

Griffin (*3*) found that the probability of rollover in single-vehicle passenger car crashes (1980 Texas data) was highly dependent on vehicle curb weight and influenced by road type. For example, the 1980 Texas data indicated the risk of rollover in single-vehicle crashes of a 1,450-kg (3,200-lb) car to vary from 20 percent for county roads to 4 percent for city streets. The data indicated rollover risk to vary for Interstate highways from 3 percent for 2,350-kg (5,200-lb) cars to 30 percent for 730-kg (1,600-lb) cars.

Examination of similar data from 1981 Texas files showed risk of driver fatality to be 1.9 times higher in rollovers than nonrollovers (*4*). This study also found the risk of driver fatality or incapacitating injury (K + A injuries) in overturned vehicles to be independent of curb weight. K = killed, A = incapacitating injury, B = nonincapacitating evident injury, C = possible injury, and 0 = no injury; from ANSI D20.1, "Data Element Dictionary for Traffic Record Systems.")

Klein (*5*) examined rollover rates of passenger cars and light trucks using data from five state accident files. The percentage of single-vehicle crashes that resulted in rollover varied by body type from 40 percent for sport utility vehicles to 15 percent for passenger cars.

Hinch et al. (*6*) found that land use produced the largest difference in rollover risk in single-vehicle accidents involving cars, light trucks, and vans: 25 percent in rural accidents compared with 6 percent in urban cases. Malliaris and DeBlois (*7*) found higher police estimated speeds in rollover car crashes compared with all other crashes from both the GES and Fatal Accident Reporting System.

Overturns are the outcome of some tripping mechanism in the crash sequence. It is necessary to identify these mechanisms in any effort aimed at reducing rollovers. This in turn requires information on the sequence of crash events and object struck. A bilevel investigation of police-reported accidents by Harwin and Emery (*8*) is the only study known to the author that contains this needed information.

Harwin and Emery reported the vehicle tripping mechanisms found in a data collection effort involving all Maryland police-reported, single-vehicle rollovers involving cars, light trucks, and vans from August 1987 through December 1988. The data collected were verified by trained accident reconstructionists. Taken together, side slopes and ditches were found to be the predominant cause of rollover in these crashes. Side slopes (including "flat") and ditches were found to be the vehicle tripping mechanism in 50 percent of urban and 70 percent of rural rollovers.

In terms of fixed objects, "curb/wall" was the leading cause of rollover in urban areas, accounting for about 17 percent of urban rollovers compared with 4 percent of rural rollovers in this Maryland study (*8*). "Guardrail/barrier" was the leading fixed object cause of rollover for rural areas, accounting for about 7 percent of rural and 10 percent of urban rollovers. These combined definitions of object types clearly limit the utility of these findings. For example, the Maryland data did not contain a code for median barriers, thus, shaped concrete median barrier cases could be coded as either curb/wall or guardrail/barrier impacts.

Extensions of the Harwin and Emery study (*8*) are needed to more clearly define the ran-off-road rollover problem. In particular, the Maryland data base used did not contain information on nonrollovers, thus the likelihood of a rollover in a crash with any specific object of interest is not known. For example, although curb/walls were found to be the leading urban fixed object tripping mechanism, the risk of overturn in curb/wall impacts could actually be relatively low if there were large numbers of nonrollover curb/wall involvements. Also, the Maryland data base lacked information on roadway type, had a relatively limited description of objects struck, and was limited to cars and light trucks.

Further, in safety problem identification studies, it is useful to examine more than one state due to differences between states in roadway and traffic conditions. Findings of similar results from more than one state, especially states with somewhat different topographies and roadside characteristics, make it more probable that the results will be useful nationwide.

The purpose of this study was to expand on the work of Harwin and Emery in examining the risk of overturn in police-reported roadside crashes in terms of potential tripping mechanisms and other highway variables and to examine the risk of death or serious injury in these crashes.

DATA

Illinois files from the Highway Safety Information System were selected for use in this study. HSIS contains linked accident, road-

Turner Fairbank Highway Research Center, HSR-20, 6300 Georgetown Pike, McLean, Va. 22101.

way, and traffic data from eight states. Linking the Illinois accident and roadway data permitted examination of road type, land use, number of lanes, and speed limit. Illinois files were selected for this study because they contain information on both object struck and relation to the roadway for the first three "involvements" in the crash sequence. Furthermore, the Illinois accident data contains a more detailed list of objects struck than most state accident files.

The data used were on all vehicle crashes in which either the first, second, or third involvement in the crash sequence occurred outside the shoulder. Data were for all vehicle types except motorcycles and covered the years 1985 to 1989. The resulting file contained 115,858 cases: 16,453 rollovers and 99,405 nonrollovers.

It was originally thought that the Illinois file would produce information on the first, second, and third harmful events in these crashes from the data in the first, second, and third involvement variables. It was found, however, that the involvement variables contained a code for "ran off road" and that the first involvement was given this code in essentially all of the cases of this subject file. In practice, this means that the second involvement variable in the data of this study was really the first harmful event (FHE) in the crash sequence, and the third involvement variable was the second harmful event. The analyses that follow interpret the variables in this way.

RESULTS

Risk of Rollover in Roadside Crashes

Rollover and nonrollover outcomes by land use and road type are shown in Table 1. Rural ran-off-road vehicle crashes were 3.5 times as likely to result in rollover as urban crashes (26.3 percent versus 7.3 percent). Rural Interstates and rural two-lane roads had comparable rollover rates (28.9 percent and 28 percent, respectively). Urban Interstates had higher rollover rates than did other urban roads (9.1 percent versus 6.5 percent).

The very large number of case vehicles in this study (115,858) meant that differences reported were statistically significant. For example, a chi-square value of 154 was found for the comparison of percent of overturned vehicles between urban Interstates (9.1 percent) and other urban roads (6.5 percent) as previously noted. This was much higher than the critical chi-square value of 6.6 required to demonstrate a 99% chance ($P < .01$) that this difference is statistically significant.

TABLE 1 Involved Vehicles by Road Type

ROAD TYPE	ROLLOVER	NONROLLOVER	PERCENT ROLLOVER
	RURAL		
INTERSTATE	3,156	7,746	28.9%
2–LANE	6,623	17,041	28.0%
OTHER	1,262	6,159	17.0%
RURAL TOTALS	11,041	30,946	26.3%
	URBAN		
INTERSTATE/FREEWAY	2,108	21,090	9.1%
OTHER	3,302	47,327	6.5%
URBAN TOTALS	5,410	68,417	7.3%

As a second example, a chi-square value of 3.35 was found for the comparison of the seemingly equal rollover rates between rural Interstates (28.9 percent) and rural two-lane roads (28 percent). This result indicates that there is a 90 percent chance ($P < .10$) that the Interstate value is really higher. From a practical point of view, it is difficult to imagine anyone taking an action on the basis of such small differences between rollover percentages. This is simply another illustration of the statistical significance of meaningful differences found from the data.

Table 1 shows that two-thirds of the Illinois ran-off-road rollovers occurred on rural roads. Because the risk of rollover in a rural roadside crash was similar to that for two-lane roads and Interstates (28 percent versus 28.9 percent), the difference in the total counts of rollover vehicles between these road types was essentially caused by differences in the number of reported roadside crashes.

FHEs in rollover crashes by land use are listed in Table 2. In general these FHEs represent the probable cause of rollover. Likely exceptions would be objects such as delineator posts in which contact forces during a collision are relatively minor. In such collisions, some event after object contact such as a ditch or steep slope could well be the true vehicle tripping mechanism.

The dominant cause of overturns was "tire-soil forces" on side slopes and ditches, which caused 80.6 percent of rural and 72 percent of urban rollovers. By comparison, ditches and embankments accounted for 2.2 percent of rural and 1.0 percent of urban rollovers.

Tire-soil forces on side slopes and ditches are not a listed sequence of event variable in the Illinois file. Rather, they are deduced as being the most probable vehicle tripping mechanism for the very large number of cases in which the sequence of events was "ran-off-road" then "overturn." The event location variable in the file indicated that in 98 percent of these cases the rollover occurred on the roadside; thus, the tires were interacting with some roadside surface, generally soil, at the point of vehicle tripping. In the other 2 percent of these cases, the vehicle returned to the roadway and overturned, thus tire-pavement forces generated the tripping forces.

As noted previously, "ditch/embankment" is another sequence of event variable the police officer could have selected as preceding rollover. The surprisingly small number of ditch/embankment rollovers compared with "tire-soil force" rollovers suggests that relatively flat slopes and gently rounded ditches may have been involved in most of these tire-soil cases.

Conceptually at least, hard cornering in loss of control maneuvers could result in tires being rolled off the rim and contribute to rollover propensity on side slopes and ditches. However, Emery was able to locate and examine about 1,500 rollover vehicles, about one-half of the number of vehicles in the Maryland study (8), and not one such case was observed (unpublished data). Thus, this mechanism cannot explain these results.

Rollover caused by either an impact with a fixed object such as a small drainage structure or rock outcropping; or a pavement edge dropoff are probably included in the tire-soil force rollovers in Table 2. Data from a special study by Terhune (9) of 1,000 car and light truck single-vehicle crashes in the National Accident Sampling System were examined to obtain an estimate of the importance of these tripping mechanisms.

Terhune (9) identified rollover type by examining case slides, scene diagrams, and narratives. Of the 159 slope or ditch rollover cases in the file, 21 involved impact with ditch backslopes, which could have included vehicle body contact as well as tire-ditch interaction forces, and 7 were complex cases involving more than one tripping mechanism. Tipping on extremely steep slopes (vehicle

TABLE 2 Rollovers by First Harmful Event

FIRST HARMFUL EVENT	RURAL NUMBER	RURAL PERCENT	URBAN NUMBER	URBAN PERCENT
OTHER THAN FIXED OBJECT				
"TIRE–SOIL FORCES" (1)	8,886	80.6%	3,885	72.0%
SNOW BANK	43	0.4%	26	0.5%
VEHICLE	40	0.4%	34	0.6%
OTHER NONCOLLISION	2	0.0%	1	0.0%
OTHER – SUBTOTAL	8,971	81.3%	3,946	73.1%
FIXED OBJECT				
OTHER OBJECT	456	4.1%	401	7.4%
GUARDRAIL	409	3.7%	306	5.7%
DITCH/EMBANK	248	2.2%	53	1.0%
HIGHWAY SIGN	200	1.8%	110	2.0%
FENCE OTHER	165	1.5%	56	1.0%
DELINEATOR POST	123	1.1%	33	0.6%
TREE	123	1.1%	87	1.6%
UTILITY POLE	104	0.9%	80	1.5%
BRIDGE RAIL/END	85	0.8%	38	0.7%
MAILBOX	52	0.5%	22	0.4%
CULVERT HEADWALL	24	0.2%	4	0.1%
CONC. MEDIAN BARRIER	19	0.2%	80	1.5%
LIGHT STANDARD	15	0.1%	82	1.5%
BARRICADE	10	0.1%	15	0.3%
TRAFFIC SIGNAL	6	0.1%	22	0.4%
UNDERPASS STRUCT	3	0.0%	9	0.2%
BRIDGE ABUTMENT	3	0.0%	2	0.0%
BUILDING	3	0.0%	5	0.1%
IMPACT ATTENUATOR	3	0.0%	0	0.0%
CURB/ISLAND CUR	3	0.0%	28	0.5%
ADVERTISING SIGN	2	0.0%	6	0.1%
MEDIAN FENCE	2	0.0%	3	0.1%
RR SIGNAL	1	0.0%	1	0.0%
WATER HYDRANT	1	0.0%	10	0.2%
FIXED OBJECT – SUBTOTAL	2,060	18.7%	1,453	26.9%
TOTALS	11,031	100.0%	5,399	100.0%

(1) SEE TEXT

center of gravity outboard of wheels) accounted for another 15 cases. In addition to these 159 cases, another 3 cases involved pavement edge dropoff-induced rollovers. Tire-soil forces were the tripping mechanism for the remaining 72 percent of these slope/ditch rollovers. Thus, the Terhune data support the view that tire-soil forces are the tripping mechanism for most of the Illinois "ran-off-road" then "overturn" cases.

Guardrail impacts accounted for the largest number of fixed object impact rollovers: 3.7 percent of all rural and 5.7 percent of all urban rollovers. No other specific fixed object accounted for as much as 3 percent of either the rural or urban rollover totals.

For rural fixed object impacts, the average rollover rate was 8.1 percent. Figure 1 shows the rural and urban rollover rates for each object that had a rural rollover rate greater than 8.1 percent. Rural overturn rates were higher than urban for each object, and culvert headwalls posed the greatest overturn risk.

As discussed previously, overturns subsequent to a delineator, as well as many highway sign and mail box impacts, may not be due to contact forces with these objects because they tend to be relatively minor in nature. Guardrail end impacts may be the cause of the higher than average fixed object rollover rate found for guardrails.

For urban fixed object impacts, the average rollover rate was 3.0 percent. The leading urban fixed object rollover rates not shown in Figure 1 were curb/channelizing island, 8.4 percent; median fence, 7.3 percent; and concrete median barrier, 5.1 percent.

Figure 2 shows the combined effects of vehicle type and land use on rollover rates. Each bar shown in this figure is based on at least 1,000 observations. Vans, straight trucks, and pickup trucks had the highest rollover rates, and large cars had the lowest rollover rate. Rollover was more probable on rural than urban roads for each vehicle type, ranging from 2.4 times for pickup trucks to 3.9 for large cars.

Vehicles in single-vehicle ran-off-road crashes were much more likely to overturn than vehicles that left the road in multivehicle

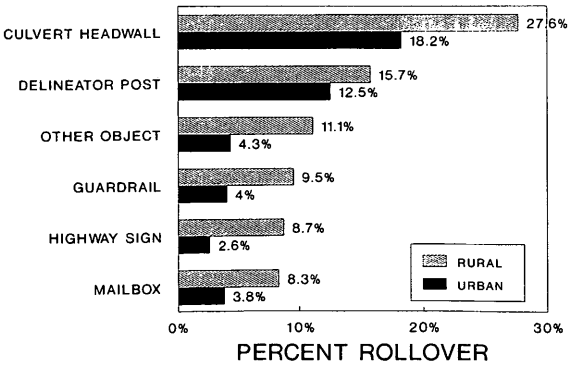

FIGURE 1 Percent rollover by object struck.

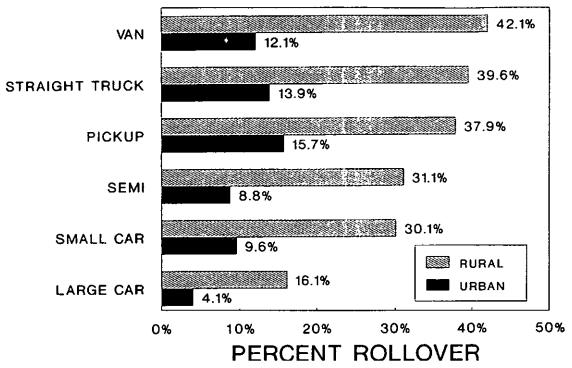

FIGURE 2 Percent rollover by vehicle type.

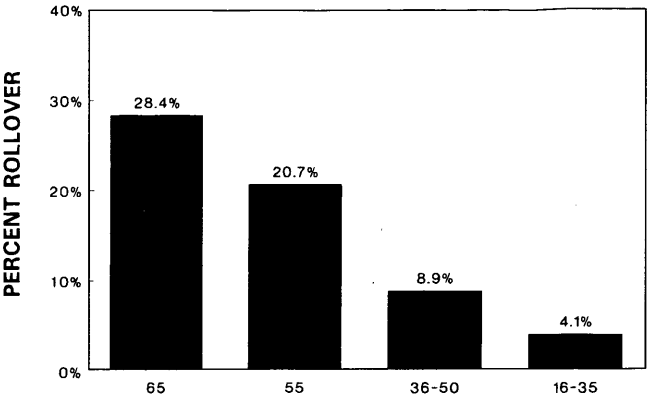

FIGURE 4 Percent rollover by speed limit.

crashes as shown in Figure 3. Further, if three or more vehicles were involved, the rollover risk to a vehicle leaving the road was less than if two vehicles were involved.

The probable explanation for rollover risk decreasing as the number of involved vehicles increases is that rollover is dependent on speed at impact with potential tripping mechanisms. Collision with another vehicle reduces speed and thus overturn risk in subsequent collision events.

Figures 4 and 5 reinforce the notion that roadside rollovers increase with speed. Figure 4 shows a consistent increase in percent of rollovers with increasing speed limit. Figure 5 shows a higher percent of rollovers on dry pavements, which, on average, have higher operating speeds than wet or snow-covered surfaces. Further, higher rural rollover risk than urban rollover risk was found for every comparison made in this study. Higher operating speeds were associated with higher posted speed limits and less speed constraint from traffic volumes on most rural roads.

Figure 6 compares the effect of the location of the FHE on the percentage of vehicles that rolled over for rural Interstates and two-lane roads. Median crashes on Interstates were more likely to result in rollovers than ran-off-road right departures (35.5 percent versus 25.8 percent). Differences in obstacle-free recovery areas and slopes and ditches may account for these median-roadside rollover risk differences.

No difference was seen between ran-off-road left and right departures for rural two-lane roads. Recovery areas, obstacles, and slopes and ditches encountered for left-side departures were similar to right-side departures on two-lane roads. Differences in average speed and angle at departure may have occurred, however. These results indicate that the effects of differences in left or right departure conditions on rollover risk on rural two-lane roads may be minor.

The cases in which the first event was on the road represent 9 percent of the Interstate and 11 percent of the two-lane road cases. A relatively large number of these cases were probably multivehicle, thus explaining the lower rollover risk found.

Risk of Death or Injury in Roadside Crashes

The main reason for concern about rollover risk in roadside crashes is the large known increase in severity of these crashes. The percent of the total number of driver injuries associated with vehicles that overturned at each level of the KABCO injury scale is shown in Figure 7 for rural roads and Figure 8 for urban roads. Illinois KABCO injury definitions are consistent with ANSI D20.1.

Clearly, in Illinois rollover was the predominant cause of death or serious injury on rural roads. On rural roads, rollovers accounted for nearly one-half of the ran-off-road fatalities (47.8 percent) and 41 percent of the A injuries. For nonrollovers, the cause of death or serious injury was impact with some object in essentially all cases. Thus, for nonrollovers, the cause of death or injury was split among impacts with the objects listed in Table 2.

On urban roads, rollover caused a very significant but smaller percent of total serious driver injuries: 22.8 percent of ran-off-road fatalities and 15 percent of A injuries.

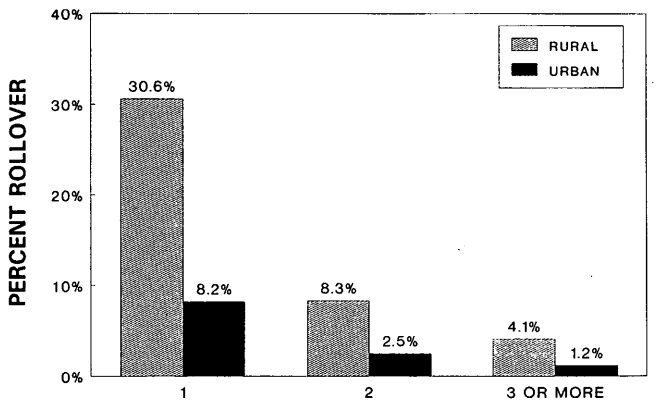

FIGURE 3 Percent rollover by number of involved vehicles.

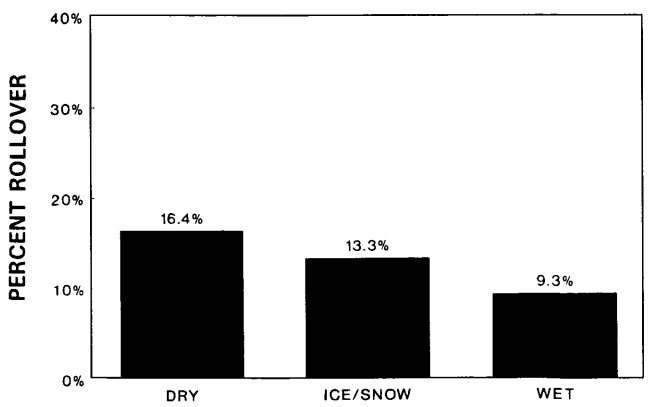

FIGURE 5 Percent rollover by road surface condition.

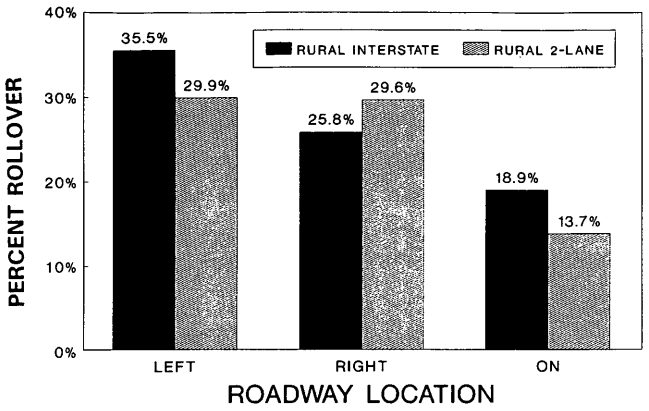

FIGURE 6 Percent rollover by first involvement location, rural interstate versus rural two-lane road.

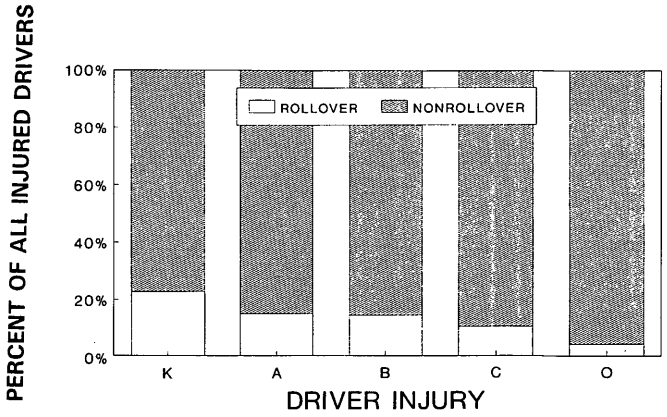

FIGURE 8 Percent of urban ran-off-road driver injuries in rollovers by injury severity.

The percent of the total number of driver fatalities and A injuries due to rollovers on rural Interstates and two-lane roads are shown in Figure 9. Rollovers accounted for a similar fraction of the total fatalities occurring on both rural interstates and two-lane roads. The percent of the total number of A injuries due to rollover was higher on rural interstate (46.3 percent) than on two-lane roads (41.3 percent).

Roadside obstacle-free zones, terrain, and predominant obstacle type varies between states. These differences affect the percentage of total ran-off-road driver fatalities and injuries associated with rollover crashes. For example, a state with large areas of rural woodlands might well show a larger percent of rural driver fatalities and injuries due to tree impacts than in a prairie state like Illinois. In a state with rural woodland, the percentage of total rural fatalities and injuries would be expected to be lower than the losses found in Illinois, as shown in Figures 8 and 9.

Table 3 provides insight on the risk of driver death or serious injury (K + A injuries) by roadside crash type. Rollover is the most severe crash type shown; almost one-fourth of drivers in these crashes suffered fatal or A injuries (24.7 percent). Of the nonrollovers, the most severe crash type found was drivers in vehicle-vehicle collisions in which some second crash impact occurred (22.5 percent K + A).

Driver fatalities or A injuries occurred in 10.6 percent of all nonrollover fixed-object collisions. The risk of driver fatality or A injury in overturn crashes (22.5 percent) was 2.3 times greater than this fixed-object crash risk.

The risk of driver fatality or A injury increased if there was a second reported crash impact for each of the nonrollover crash types shown. Crashes with more than one impact event were likely to have been at a higher speed, on average, than single event crashes; this could be the primary reason for the difference in risk.

CONCLUSIONS

The findings of this study on the general nature of the roadside rollover problem are consistent with the literature; crash severity, rural roads, and vehicle type are factors strongly associated with ran-off-road rollovers. This study also found, as did Harwin and Emery (*8*) from Maryland data, that ditches and slopes were the dominant ran-off-road tripping mechanism. Rollover risks on rural Interstates and two-lane roads were found to be similar.

The findings of this study offer insight on the nature of this problem. Specifically, this analysis of all ran-off-road vehicle crashes in Illinois, motorcycles excluded, resulted in the following principal findings.

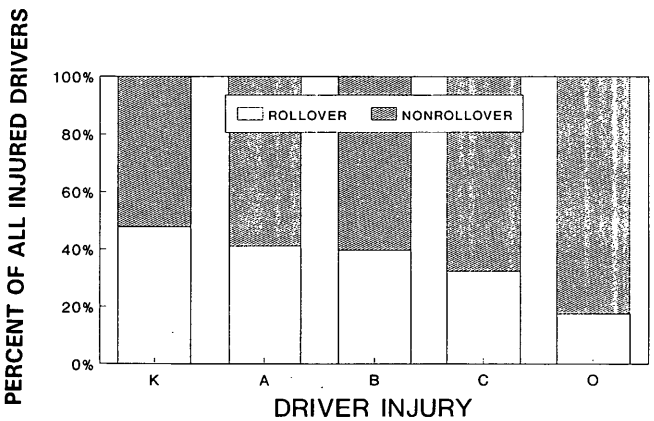

FIGURE 7 Percent of rural ran-off-road driver injuries in rollovers by injury severity.

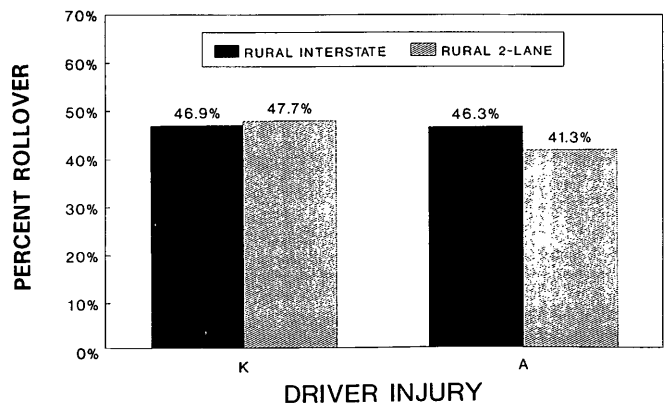

FIGURE 9 Percent of ran-off-road (K + A) severe driver injuries in rollovers, rural interstate versus rural two-lane roads.

TABLE 3 Percent of Driver (K + A) Injuries, Rollover Versus Nonrollover

FIRST HARMFUL EVENT	SECOND HARMFUL EVENT		TOTALS
	YES	NONE	
ALL ROLLOVER VEHICLES			24.7%
ALL NONROLLOVER VEHICLES			
VEHICLE COLLISION	22.5%	12.7%	15.3%
OTHER/UNKNOWN	14.2%	4.5%	10.9%
FIXED OBJECT	15.1%	9.7%	10.6%
ALL NONROLLOVERS	14.9%	9.3%	10.9%

Nature of the Ran-Off-Road Rollover Problem

1. The risk of driver fatality or A injury was greater in rollover crashes than in any nonrollover crash type examined.
2. Roadside rollover risks were much higher in rural areas: 26 percent of involved vehicles on rural roads overturned, compared with 7 percent on urban roads.
3. Rollovers were the dominant rural roadside safety problem. In Illinois, 48 percent of all rural ran-off-road driver fatalities occurred in rollovers. The remaining fatalities were split among a long list of struck objects.
4. Rollover rate was highly dependent on vehicle type. In rural crashes the percent of overturn vehicles varied from 42 percent for vans to 16 percent for large cars.
5. Rollover risk appeared to be strongly dependent on crash speed.

Cause of Vehicle Tripping

6. Slopes and ditches were the principal cause of ran-off-road rollovers, associated with 83 percent of rural and 73 percent of urban rollovers (Table 2). Tire-soil forces were the probable tripping mechanism in most slope/ditch rollovers. Mechanisms contributing to tire-soil forces included: rate of slope, slope changes, soil cover, and tire plowing in soft soil. Police-reported accident files, such as the Illinois data used in this study, do not provide the level of detail required to sort out the relative importance and interaction of these variables as tripping mechanisms.
7. The average overturn rate in rural fixed-object impacts was 8.1 percent. Two objects that exceeded this rate are worthy of note, culvert headwalls (27.6 percent) and guardrails (9.5 percent). The rate for culverts points out the severe nature of impacts with these structures. Guardrail end impacts may be the cause of the higher-than-average guardrail overturn rate.
8. In urban areas, the average overturn rate in fixed-object impacts was 3.0 percent. Culvert headwalls had the highest rate at 18.2 percent, curb/channelizing islands had a rate of 8.4 percent, and concrete median barriers a rate of 5.1 percent.

Road Type: Comparison of Rural Interstates and Two-Lane Roads

9. The risk of overturn, given a ran-off-road crash, was similar for rural Interstates and rural two-lane roads (28.9 percent versus 28.0 percent).
10. Left roadway departures resulted in the same rollover risk as right roadway departures on two-lane roads. For interstates, left-side (median) events had higher rollover rates than right-side events (35.5 percent versus 25.8 percent).
11. Overturns accounted for about the same fraction of total ran-off-road driver fatalities on both rural roadway types (46.9 percent on Interstates versus 47.7 percent on two-lane roads).
12. Overturns accounted for more of the total driver A injuries on Interstate (46.3 percent) than two-lane roads (41.3 percent).

RECOMMENDATIONS

As noted previously the dominance of slopes and ditches found as the probable vehicle tripping mechanism is in general agreement with the findings of the Maryland study (*8*). Further problem identification studies of rollovers on slopes and ditches are recommended, specifically:

1. National accident data bases should be examined to study further the nature and importance of slopes and ditches as a tripping mechanism.
2. The importance of specific slope and ditch configurations as potential tripping mechanisms also should be studied further. Additional field data will be required to conduct accident analyses on this issue because needed data for these analyses are not contained in existing data bases. Computer simulation studies will require refined information on vehicle conditions as they leave the roadway. The literature suggests that lateral skidding occurs at tripping in many rollovers (*8,9*).
3. Issues such as the effects of soft soil and terrain irregularities on overturn risk also need to be examined.

These studies are needed to develop specific cost-effective recommendations to reduce rollover risk on slopes and ditches. Recommendations that might result from these investigations include the following:

- Identification of areas of roadways, such as the outside of horizontal curves, that might justify special attention.
- Revised severity indices for slope and ditch configurations resulting in changes in barrier warrants.
- Recommendations to maintenance personnel about maintaining relatively flat roadsides.
- Defining the importance of countermeasures that would reduce the likelihood of loss of control such as antilock brakes or higher pavement surface friction.

ACKNOWLEDGEMENTS

The author is grateful for the assistance provided by Amy R. Kohls, a former CO-OP student who did the computer runs for the analyses in this study and graphics for the report figures. The assistance of Carol Conley in assembling the analysis file and serving as Ms. Kohls' mentor in SAS programming is also gratefully acknowledged.

REFERENCES

1. Viner, J. G. Harmful Events in Crashes. *Accident Analysis and Prevention,* Vol. 25, No. 2, April 1993, pp. 139–145.

2. National Highway Traffic Safety Administration. Rollover Prevention. Advanced Notice of Proposed Rulemaking. *Federal Register,* Vol. 57, No. 2, Jan. 3, 1992.
3. Griffin, L. I. III. *Probability of Overturn in Single Vehicle Accidents as a Function of Road Type and Passenger Car Curb Weight.* Texas Transportation Institute, Nov. 1981.
4. Viner, J. G. Implications of Small Passenger Cars on Roadside Safety. *Public Roads,* Vol. 48, No. 2, Sept. 1984, pp. 54–62.
5. Klein, T. M. A Statistical Analysis of Vehicle Rollover Propensity and Vehicle Stability. *Vehicle Dynamics and Rollover Propensity Research,* SP-909. Society of Automotive Engineers, Paper 920584, Feb. 1992.
6. Hinch, J., S. Schadle, and T. M. Klein. NHTSA's Rollover Rulemaking Program—Results of Testing and Analysis. *Vehicle Dynamics and Rollover Propensity Research,* SP-909. Society of Automotive Engineers, paper 920584, Feb. 1992, pp. 109–122.
7. Malliaris, A. C. and J. H. DeBlois. Pivotal Characterization of Car Rollovers. Presented at 13th International Technical Conference on Experimental Safety Vehicles. Paris, France, Nov. 1991.
8. Harwin, E. A. and L. Emery. *The Crash Avoidance Rollover Study: A Database for the Investigation of Single Vehicle Rollover Crashes.* National Highway Traffic Safety Administration, May 1989.
9. Terhune, K. H. Contributions of Vehicle Factors and Roadside Features to Rollover in Single-Vehicle Crashes. DOT HS 807 735. National Highway *Traffic Safety Administration,* March 1991.

Publication of this paper sponsored by Committee on Roadside Safety Features.

Clear Zone Requirements for Suburban Highways

KING K. MAK, ROGER P. BLIGH, AND HAYES E. ROSS, JR.

The growth of an urban area typically extends outward along arterial highways. The nature of the land use along the highways gradually changes from rural and agricultural use to suburban use with strip commercial developments. The resulting growth in traffic volume and frequent turning movements cause congestion and increased accident experience, which necessitates widening the existing two-lane highways to four or more lanes. Under current design guidelines, urban roadways must have a minimum clear zone width of 0.46 m (18 in.) beyond the face of the curb. On the other hand, high-speed rural arterial highways typically require a clear zone width of 9.1 m (30 ft) or more beyond the edge of the travelway. Some intermediate design requirements of clear zone width are needed for this transitional type of suburban, high-speed, curb-and-gutter roadway. Furthermore, the widening of the highway reduces the available clear zone width unless additional right-of-way is purchased. In other words, after the highway is widened the typical clear zone width of 9.1 m (30 ft) common to rural highways may be needed to provide more travel lanes. This paper presents the results of a study to determine an appropriate and cost beneficial clear zone requirement for such suburban, high-speed, arterial highways in an upgrading or reconstruction situation.

The growth of an urban area typically extends outward along major arterial highways. The nature of the land use along the highways gradually changes from rural and agricultural to suburban with strip commercial developments, such as service stations, fast food restaurants, and shopping centers. The resulting growth in traffic volume and frequent turning movements can cause congestion and increased accident experience, which may necessitate widening the existing two-lane highways to four or more lanes. Also, in anticipation of future growth, these suburban arterial highway sections are designed with curb-and-gutter cross sections and often with two-way left-turn center lanes, typical of urban type roadways. However, these highway sections will remain suburban in nature for a period of time, i.e., with moderate traffic volume and high speed, and speed limits ranging from 80.5 to 88.6 km/hr (50 to 55 mph). The land use and resulting traffic volume will continue to grow until these highway sections become urban roadways with high traffic volume and lower speed limits [i.e., 72.4 km/hr (45 mph) or less].

These suburban arterial highway sections pose some interesting problems because they serve as a transition from rural- to urban-type highways at the fringes of urban areas. Under current design guidelines (*1*), low-speed [i.e., 72.4 km/h (45 mph) or less] urban roadways with curb-and-gutter cross sections and no shoulders must have a minimum clear zone width of 0.46 m (18 in.) beyond the face of the curb. On the other hand, high-speed rural arterial highways with shoulders and parallel drainage ditches are typically required to have a clear zone width of 9.1-m (30-ft) or more beyond the edge of the travelway (i.e., edgeline or edge of pavement).

Texas Transportation Institute, Texas A&M University System, College Station, Tex. 77843.

Widening a two-lane highway within the existing right-of-way (ROW) reduces the available clear zone width. In other words, unless additional ROW is purchased, the typical clear zone width of 9.1 m (30 ft) common to rural arterial highways may be needed to provide more travel lanes. The problem then is to determine what clear zone width is required for such suburban, high-speed, arterial highways and under what conditions the improvements will be cost-effective.

A study was undertaken by the Texas Transportation Institute (TTI) for the Texas Department of Transportation to determine an appropriate and cost-effective clear zone requirement for suburban, high-speed, arterial highways with curb-and-gutter cross sections in an upgrading or reconstruction situation (*2*). This article presents the details of the study, including the research approach, study results, and recommendations.

STUDY APPROACH

A cost-effectiveness procedure based on the encroachment probability model previously developed at TTI was used to assess the incremental benefits and costs associated with various clear zone widths (*3*). The basic concept behind the benefit-cost (BC) analysis is that public funds should be invested only in projects in which the expected benefits are equal to or exceed the expected direct costs of the project. Benefits are measured in reductions in accident or societal costs resulting from decreases in the frequency or severity of accidents. Direct highway agency costs are comprised of initial installation, maintenance, and accident repair costs. An incremental BC ratio of 1.0 was used for the analysis. This indicates that the additional benefits associated with the improvement option over the existing conditions or another improvement option is equal to the increased costs and that the improvement investment is therefore appropriate.

The major activities undertaken in the analysis included:

1. Define typical site conditions for study.
2. Conduct BC analysis on the various clear zone widths for the typical site conditions.
3. Develop clear zone guidelines.

Typical Site Conditions

An effort was made to define the typical site conditions for suburban, high-speed, curb-and-gutter arterial highways from review of field data obtained for a sample of highway sections meeting the study criteria. A total of 16 highway sections were included in the sample, some of the pertinent information obtained for the sampled

highway sections is summarized in Table 1. Photographs of typical highway sections sampled in the study are shown in Figure 1.

The typical site conditions selected for use with the BC analysis are shown in Table 2. Review of the sampled highway sections showed that the highway types could be categorized into one of the following categories:

1. Four-lane, two-way undivided highways,
2. Four-lane, two-way undivided highway with two-way left-turn center lanes, or
3. Four-lane divided highways.

The more prevalent highway types were four-lane, two-way undivided highways with or without a two-way left-turn center lane, thus, this type was selected for analysis.

Speed limits on these sampled highway sections were between 80.5 to 88.5 km/hr (50 to 55 mph). The highways typically had a 3.7 m (12 ft) lane width with curb-and-gutter cross sections. Most of the sampled highway sections had no shoulders but a few had shoulders 2.4 to 3.05 m (8 to 10 ft) in width. The alignment of the highways was typically straight and level. The traffic volumes on the sampled highway sections varied greatly, ranging from approximately 2,000 to 20,000 average daily traffic (ADT).

For the BC analysis, the speed limit was set at 80.5 to 88.5 km/hr (50 to 55 mph). A lane width of 3.7 m (12 ft) was selected with curb-and-gutter cross sections. The alignment was assumed to be straight and level. To arrive at an incremental BC ratio of 1.0 the traffic volume was varied as needed.

The roadside conditions for these highway sections typically are flat terrain beyond the curb. There was generally a line of utility poles at the ROW line on one side of the highway, with trees, fences, commercial signs, and buildings beyond the ROW line. The density of roadside objects beyond the ROW line varied for each highway section. There were numerous driveways and access points along the highway. The clear zone width typically varied with the ROW width and was clear of obstacles, except for occasional sign supports.

For the BC analysis, the clear zone was assumed to extend to the ROW line and varied in width, starting with a minimum of 3.05 m (10 ft) and increasing in 1.52-m (5-ft) increments. Flat terrain was assumed beyond the curb. A line of utility poles was assumed at the ROW line spaced 76.2 m (250 ft) apart. This spacing is a conservative estimate given that utility pole spacing on rural highways can range from 121.9 to 152.4 m (400 to 500 ft).

As discussed previously, the presence and location of roadside objects beyond the ROW line varied greatly among the sampled highway sections. For the BC analysis, the layout was simplified by using a line of trees as the surrogate for the various roadside objects. Three levels of roadside hazard rating are defined as follows:

1. Low. A line of utility poles at ROW line with 76.2-m (250-ft) spacing and clear roadside beyond ROW line.
2. Medium. A line of utility poles at ROW line with 76.2-m (250-ft) spacing and a line of trees 1.52 m (5 ft) beyond ROW line spaced 30.5 m (100 ft) apart.
3. High. A line of utility poles at ROW line with 76.2-m (250-ft) spacing and a line of trees 1.52 m (5 ft) beyond ROW line spaced 15.2 m (50 ft) apart.

These three roadside hazard ratings represent varying roadside conditions, from a relatively clear roadside (low rating) to a roadside cluttered with hazards (high rating). The rating that best describes the roadside condition for the specific highway section under study can be selected. For a high hazard rating with trees spaced 15.2 m (50 ft) apart, the probability that an approaching

TABLE 1 Site Conditions for Sampled Highway Sections

Site No.	County	Highway	Section Length km (mi)	Description	AADT	Shoulder Width m (ft)	Clear Zone m (ft)	ROW Cost $/m² ($/ft²)
1	Lamb	Loop 430	0.84 (0.52)	4-lane undivided	1,750	2.4 (8)	3.0 (10)	64.58 (6.0)
2	Lamb	US 84	0.31 (0.19)	4-lane TWLTL[a]	4,700	None	6.1 (20)	168.99 (15.7)
3	Tom Green	FM 584	4.98 (3.10)	4-lane TWLTL	5,900	None	≥9.1 (≥30)	N/A[c]
4	Henderson	SH 31	2.19 (1.36)	4-lane TWLTL	13,000	None	N/A	N/A
5	Rusk	US 79	5.03 (3.13)	4-lane TWLTL	5,700	None	7.6 (25)	322.92 (30.0)
6	Smith	SH 64	7.63 (4.74)	4-lane TWLTL	8,900	3.0 (10)	7.6 (25)	122.71 (11.4)
7	Smith	SH 155	7.45 (4.63)	4-lane TWLTL	11,200	None	≥9.1(≥30)	N/A
8	Gregg	Loop 281	4.98 (3.09)	5-lane TWLTL	18,300	None	3.0 (10)	25.83 (2.4)
9	Victoria	SH 185	1.17 (0.73)	4-lane TWLTL	10,200	2.4 (8)	N/A	N/A
10	Calhoun	SH 35	1.62 (1.01)	4-lane divided	12,500	3.0 (10)	N/A	N/A
11	Bastrop	SH 21	1.61 (1.00)	4-lane divided, LT[b] bays	21,000	3.0 (10)	≥9.1 (≥30)	N/A
12	Williamson	US 79	0.99 (0.61)	4-lane undivided	5,500	3.0 (10)	N/A	N/A
13	Comal	SH 46	0.48 (0.30)	4-lane TWLTL	8,200	None	8.2 (27)	69.97 (6.5)
14	Nueces	FM 2444	3.12 (1.94)	4-lane TWLTL	9,200	None	N/A	N/A
15	San Patricio	SH 35	1.88 (1.17)	4-lane divided	10,900	None	N/A	N/A
16	Mills	US 84	0.48 (0.30)	4-lane undivided	3,500	3.0 (10)	5.8 (19)	24.76 (2.3)

Notes,
[a] TWLTL -- Two-Way, Left-Turn Lane
[b] LT -- Left-Turn
[c] N/A -- Not Available

(a)

(b)

(c)

FIGURE 1 Typical sampled highway sections: (*a*) four-lane, two-way undivided, (*b*) four-lane, two-way undivided with two-way left-turn lane, and (*c*) four-lane divided.

vehicle would hit a tree is 0.852. For a medium hazard rating with trees spaced 30.5 m (100 ft) apart, the probability an approaching vehicle would hit a tree is 0.426. Photographs illustrating the three roadside hazard ratings are shown in Figure 2.

The hazards associated with curbs, driveways, and small sign supports within the clear zone were not included in the analysis. The rationale for excluding these hazards in the BC analysis is twofold. First, because the analysis was comparative or incremental in nature, the effects of these hazards would be the same for all clear zone widths, and thus would cancel each other out. Second, the severity associated with these hazards was relatively low and their presence is independent of the clear zone width.

TABLE 2 Typical Site Conditions

- 4-Lane, 2-Way Undivided Highway with or without Center 2-way Left-Turn Lane
- 3.7-m (12-ft) Lane Width, Curb-and-Gutter Section
- No Shoulder/3.05-m (10-ft) Shoulder
- Straight and Level Alignment
- 50-55 mph Speed Limit
- AADT - Varies
- Clear-Zone Width - Varies, Extends to Right-of-Way Line
- Roadside Conditions
  - Flat Terrain beyond Curb
  - Utility Poles
  - Trees
- Roadside Hazard Rating
  - Low - Utility Poles at ROW Line, 76.2-m (250-ft) Spacing
  - Medium - Utility Poles at ROW Line 76.2-m (250-ft) Spacing + Line of Trees 1.5 m (5 ft) beyond ROW Line, Spaced 30.5 m (100 ft) Apart
  - High - Utility Poles at ROW Line 76.2-m (250-ft) Spacing + Line of Trees 1.5 m (5 ft) beyond ROW Line, Spaced 15.2 m (50 ft) Apart
- Estimates of Direct Costs
  - Unit Right-of-Way Acquisition Cost = \$21.53/m^2 to \$64.58/m^2 (\$2/ft^2 to \$6/ft^2)
  - Unit Clearing and Grading Cost = \$0.25/m^2 (\$1,000/acre)
  - Unit Relocation of Utility Pole Cost = \$1,500 per pole
- Traffic Growth Factor = 2.5% Annually
- Percent Trucks = 0% (i.e., All Passenger Car Traffic)
- Life of Project = 10 Years
- Discount Rate = 4%

The severity indexes used in the analysis (Table 3) were obtained from the update to the 1988 AASHTO *Roadside Design Guide* (*4*), now in preparation. As Table 3 shows, the severity associated with an accident increases with impact speed. For the BC analysis, trees were considered rigid point objects and were assigned severity values corresponding to the upper end of the range shown in the table. Although utility poles can also be considered rigid point objects for some impact conditions, accident studies (*5*) and crash tests (*6*) have shown that utility poles will fracture at ground level when the impact energy exceeds a certain level. The impact energy is a function of the mass and speed of the approaching vehicle. Based on a distribution presented by Mak and Mason (*5*) for all vehicle types, 50 percent of utility poles are knocked down when hit at a speed of 64.4 km/hr (40 mph). For this reason, the utility pole hazards were assigned average severity values for the ranges shown in the table.

The accident cost figures in the 1988 AASHTO *Roadside Design Guide* (*4*) were used to convert the accident severity to accident or societal costs, as shown in the following table. Other assumptions were made for the inputs to the BC model, including a traffic growth factor of 2.5 percent annually, 0 percent trucks (i.e., all passenger car traffic), 10 years for the life of the project, and a 4 percent discount rate. The traffic growth factor of 2.5 percent annually represents the upper bound for traffic growth on such highways. The vehicle mix (i.e., percent trucks) is believed to have little or no effect on the clear zone width and to simplify the analysis was thus assumed to be all passenger car traffic. The rationale for selecting a project life of 10 years was that the development and traffic growth on these suburban arterial highways will be such that they will effectively become urban roadways with high traffic volume and lower speed limits in 10 years. Thus, the cost for higher clear zone width requirements would have to be amortized over a period of 10 years, which may or may not be the actual life of the project. The discount rate of 4 percent is a typical value used with BC analyses.

(a)

(b)

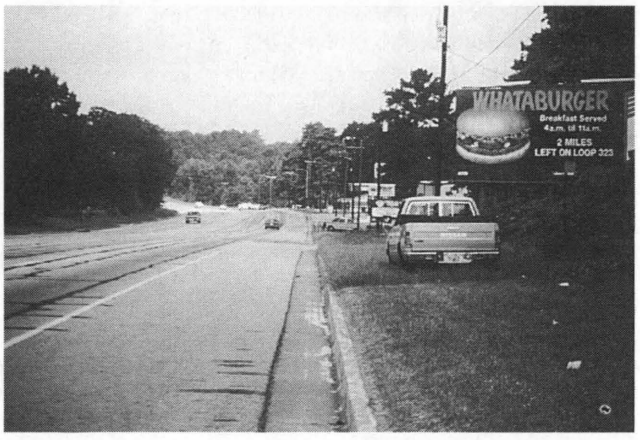

(c)

FIGURE 2 Three roadside hazard ratings: (*a*) low, (*b*) medium, and (*c*) high.

Injury Severity	*Accident Cost*
Fatality	$500,000
Severe injury	110,000
Moderate injury	10,000
Slight injury	3,000
Property damage only (Level 2)	2,000
Property damage only (Level 1)	500

TABLE 3 Severity Indexes Used in Analysis

Type of Hazard	Impact Speed							
	64.4 km/h (40 mph)		80.5 km/h (50 mph)		96.5 km/h (60 mph)		112.6 km/h (70 mph)	
	Range	Avg.	Range	Avg.	Range	Avg.	Range	Avg.
Tree, Diameter > 102 mm (4 in.)	2.6-5.0	3.8	3.2-6.0	4.6	3.8-7.2	5.5	4.4-8.6	6.5
Utility Pole	2.6-5.0	3.8	3.2-6.0	4.6	3.8-7.2	5.5	4.4-8.6	6.5

The direct costs associated with increasing the clear zone width include: ROW purchase cost, clearing cost, and the cost to relocate the utility poles. The cost to purchase additional ROW for the sampled highway sections varied from a low of $\$21.53/m^2$ ($\$2/ft^2$) to a high of $\$322.92/m^2$ ($\$30/ft^2$) with a median of approximately $\$64.58/m^2$ ($\$6/ft^2$). The cost to clear and grade the additional clear zone was assumed to be $\$0.25/m^2$ ($1,000/acre). The cost to relocate the utility poles to the new ROW line was estimated to be $1,500 per pole based on best available estimates.

BC Analysis

The next task was to determine the incremental benefits and costs associated with the various clear zone widths based on the typical site conditions. For this analysis, incremental BC ratios were calculated for various combinations of:

- Clear-zone width,
- Traffic volume (annual ADT),
- Roadside hazard rating, and
- ROW purchase cost.

A baseline clear zone width was assumed for each analysis. The baseline clear zone width was defined as the clear zone width that would be available after a roadway was widened, assuming no additional ROW was acquired. Data from the sampled highway sections indicated that a minimum of at least 3.05 m (10 ft) was typically available for the clear zone width after widening. This should generally be the case given that most two-lane rural highways have at least a 9.1-m (30-ft) clear zone before widening. If the roadway is widened to include four travel lanes and a two-way, left-turn lane, the clear zone would be reduced to a baseline value of approximately 3.7 m (12 ft), assuming 3.7-m (12-ft) lane widths. Thus, the analysis began with a baseline clear zone width of 3.05 m (10 ft).

For this analysis, the alternatives included widening the clear zone width above the baseline value in 1.5-m (5-ft) increments. In other words, if the baseline clear zone width was 3.05 m (10 ft) for Alternative 1, the clear zone width would be 4.6 m (15 ft), 6.1 m (20 ft), 7.6 m (25 ft), and 9.1 (30 ft) for Alternatives 2–5, respectively. The analysis would then be repeated for baseline clear zone widths of 4.6 m (15 ft), 6.1 m (20 ft), and 7.6 m (25 ft).

The objective of the analysis was to determine under what conditions the other alternatives were cost-effective. In other words, when considering a widening or reconstruction project, the analysis is used to determine when it is cost-effective to make capital outlays to provide additional clear zone over the baseline value that would already be available after the roadway is improved.

For each baseline clear zone width, the analysis covered various combinations of roadside hazard rating (i.e., low, medium, and

high) and ROW purchase cost. Analysis of these options and determination of appropriate clear zones were based on an incremental BC analysis. For a given roadside hazard rating and ROW purchase cost, the ADT value at which the incremental BC ratio becomes 1.0 was determined for each pair of alternatives under consideration. The appropriate alternative was then determined by first comparing each alternative with the baseline clear zone option and then to each other. The results are summarized in tabular format and discussed in the next section.

STUDY RESULTS

Benefit-Cost Analysis Results

Results of the BC analysis were used to develop tables that identify the most cost-effective clear zone width option for given combinations of baseline clear zone width, roadside hazard rating, and unit ROW acquisition cost. Tables 4–7 show the range of traffic volumes (ADT) for which additional clear zone width is cost-effective for baseline clear zone widths of 3.05 m (10 ft), 4.6 m (15 ft), 6.1 m (20 ft), and 7.6 m (25 ft), respectively. The data in each of these tables are further subdivided according to high, medium, and low roadside hazard ratings, which are denoted as *a*, *b*, and *c*, respectively.

When developing the tables, the unit ROW acquisition cost was varied in increments of $21.53/m² ($2/ft²), starting at $21.53/m² ($2/ft²), until the ADT at which the baseline clear zone width ceased to be cost-effective exceeded 20,000 vehicles/day. As shown in Table 1, and ADT of 20,000 was the upper limit of the range observed for the sampled sections of highways. For unit ROW acquisition costs above those shown in the tables, it would not be cost-effective to purchase the additional ROW.

Some general observations can be made from the tables. First, as the ROW acquisition cost increases, the ADT required to justify a particular clear zone width also increases. This is expected if one considers that as the direct costs increase, a corresponding increase in benefits is necessary to maintain a BC ratio of 1.0. In the BC analysis, benefits are measured in terms of reductions in accident costs, which are directly related to the traffic volume. In other words, the same safety improvement can result in more benefits (i.e., reduced accident costs) when implemented on a roadway with a higher ADT.

Second, for a given unit ROW acquisition cost, higher ADT values are required to justify the acquisition of additional clear zone width. This observation is similar to the first in that an increase in direct costs must be offset by a corresponding increase in benefits. However, in this case, the increase in direct costs is the result of purchasing additional ROW instead of higher unit acquisition price.

For all the baseline clear zone widths considered, it is not cost-effective to purchase 1.5 m (5 ft) or less of additional ROW. As shown in Tables 4–7, a 1.5-m (5-ft) increase in clear zone width is either not cost-effective or has such a small range of ADT for which it could be considered cost-effective that it would be impractical to implement. This is due to the fact that the incremental benefits achieved over the baseline clear zone width are too small to justify the additional costs. For such small ROW purchases, the direct costs are driven by the utility pole relocation cost, which is a fixed cost based on the number of utility poles. As the clear zone width is further increased, the utility pole relocation cost becomes a smaller percentage of the direct costs, and the incremental benefits become large enough to justify the increased expenditures.

TABLE 4 ADT Range for Which Providing Additional Clear Zone Width is Cost-Effective Based on Baseline Clear Zone Width of 3.0 m (10 ft): (*a*) High, (*b*) Medium, and (*c*) Low Roadside Hazard Rating

(a)

Clear Zone Width, m (ft)	Unit Right-of-Way Acquisition Cost, $/m² ($/ft²)		
	21.53 (2.0)	43.06 (4.0)	64.58 (6.0)
3.1 (10)*	<7,200	<16,000	<22,300
4.6 (15)	N/A	16,000-17,400	22,300-25,700
6.1 (20)	7,200-11,400	17,400-24,400	25,700-34,000
7.6 (25)	11,400-17,100	24,400-32,200	34,000-43,700
9.1 (30)	≥17,100	≥32,200	≥43,700

(b)

Clear Zone Width, m (ft)	Unit Right-of-Way Acquisition Cost, $/m² ($/ft²)		
	21.53 (2.0)	43.06 (4.0)	64.58 (6.0)
3.1 (10)*	<12,000	<22,000	
4.6 (15)	--	22,000-23,500	
6.1 (20)	12,000-16,700	23,500-31,500	
7.6 (25)	16,700-23,200	31,500-40,800	
9.1 (30)	≥23,200	≥48,800	

(c)

Clear Zone Width, m (ft)	Unit Right-of-Way Acquisition Cost, $/m² ($/ft²)		
	21.53 (2.0)	43.06 (4.0)	64.58 (6.0)
3.1 (10)*	<37,800		
4.6 (15)	--		
6.1 (20)	37,800-45,300		
7.6 (25)	45,300-57,000		
9.1 (30)	≥57,000		

* Baseline condition - clear zone width available after widening without any additional right-of-way purchase

For unit ROW acquisition costs of $64.58/m² ($6/ft²) or greater, it is not cost-effective to provide additional clear zone width through the purchase of additional ROW. Because $64.58/m² ($6/ft²) was found to be the median ROW cost for the sampled highway sections, this would indicate that it is not cost-effective to provide additional clear zone width beyond the existing baseline condition for most roadways.

The use of these tables to select a suitable clear zone width requires only basic information such as ADT, baseline clear zone width, unit ROW acquisition cost, and roadside hazard rating. For example, consider a highway section that has an ADT of 9,000, a baseline clear zone width of 3.05 m (10 ft), a unit ROW acquisition cost of $43.06/m² ($4/ft²), and a high roadside hazard rating [these specifications correspond to the conditions in Table 4(*a*)]. The table indicates that a clear zone width of 3.05 m (10 ft) is cost-effective under those conditions. Because this is equivalent to the baseline clear zone width, no additional ROW purchase would be required. If the same highway section had an ADT of 18,000, Table 4(*a*) indicates that a 6.1-m (20-ft) clear zone width would be cost-effective, justifying the purchase of an additional 3.05 m (10 ft) of ROW.

The data presented in Tables 4–7 are further condensed to provide some general clear zone width guidelines for suburban, high-speed arterial highways with curb-and-gutter cross sections. These guidelines are presented in Tables 8–10 for high, medium, and low roadside hazard ratings, respectively. Use of these tables requires the same basic roadway and roadside data but is presented in a dif-

TABLE 5 ADT Range for Which Providing Additional Clear Zone Width is Cost-Effective Based on Baseline Clear Zone Width of 4.6 m (15 ft): (*a*) High, (*b*) Medium, and (*c*) Low Roadside Hazard Rating

(a)

Clear Zone Width, m (ft)	Unit Right-of-Way Acquisition Cost, $/m² ($/ft²)		
	21.53 (2.0)	43.06 (4.0)	64.58 (6.0)
4.6 (15)*	<12,600	<22,600	
6.1 (20)	--	22,600-24,300	
7.6 (25)	12,600-17,200	24,300-32,300	
9.1 (30)	≥17,200	≥32,300	

(b)

Clear Zone Width, m (ft)	Unit Right-of-Way Acquisition Cost, $/m² ($/ft²)		
	21.53 (2.0)	43.06 (4.0)	64.58 (6.0)
4.6 (15)*	<18,000	<29,500	
6.1 (20)	--	29,500-31,500	
7.6 (25)	18,000-23,200	31,500-40,700	
9.1 (30)	≥23,200	≥48,700	

(c)

Clear Zone Width, m (ft)	Unit Right-of-Way Acquisition Cost, $/m² ($/ft²)		
	21.53 (2.0)	43.06 (4.0)	64.58 (6.0)
4.6 (15)*	<47,800		
6.1 (20)	--		
7.6 (25)	47,800-57,000		
9.1 (30)	≥57,000		

* Baseline condition - clear zone width available after widening without any additional right-of-way purchase

TABLE 6 ADT Range for Which Providing Additional Clear Zone Width is Cost-Effective Based on Baseline Clear Zone Width of 6.1 m (20 ft): (*a*) High, (*b*) Medium, and (*c*) Low Roadside Hazard Rating

(a)

Clear Zone Width, m (ft)	Unit Right-of-Way Acquisition Cost, $/m² ($/ft²)		
	21.53 (2.0)	43.06 (4.0)	64.58 (6.0)
6.1 (20)*	<18,700	<30,500	
7.6 (25)	--	30,500-32,200	
9.1 (30)	≥18,700	≥32,200	

(b)

Clear Zone Width, m (ft)	Unit Right-of-Way Acquisition Cost, $/m² ($/ft²)		
	21.53 (2.0)	43.06 (4.0)	64.58 (6.0)
6.1 (20)*	<25,000		
7.6 (25)	--		
9.1 (30)	≥25,000		

(c)

Clear Zone Width, m (ft)	Unit Right-of-Way Acquisition Cost, $/m² ($/ft²)		
	21.53 (2.0)	43.06 (4.0)	64.58 (6.0)
6.1 (20)*	<60,000		
7.6 (25)	--		
9.1 (30)	≥60,000		

* Baseline condition - clear zone width available after widening without any additional right-of-way purchase

TABLE 7 ADT Range for Which Providing Additional Clear Zone Width is Cost-Effective Based on Baseline Clear Zone Width of 7.6 m (25 ft): (*a*) High, (*b*) Medium, and (*c*) Low Roadside Hazard Rating

(a)

Clear Zone Width, m (ft)	Unit Right-of-Way Acquisition Cost, $/m² ($/ft²)		
	21.53 (2.0)	43.06 (4.0)	64.58 (6.0)
7.6 (25)*	<26,800		
9.1 (30)	≥26,800		

(b)

Clear Zone Width, m (ft)	Unit Right-of-Way Acquisition Cost, $/m² ($/ft²)		
	21.53 (2.0)	43.06 (4.0)	64.58 (6.0)
7.6 (25)*	<34,500		
9.1 (30)	≥34,500		

(c)

Clear Zone Width, m (ft)	Unit Right-of-Way Acquisition Cost, $/m² ($/ft²)		
	21.53 (2.0)	43.06 (4.0)	64.58 (6.0)
7.6 (25)*	<76,500		
9.1 (30)	≥76,500		

* Baseline condition - clear zone width available after widening without any additional right-of-way purchase

ferent format. For instance, consider a highway section that has an ADT of 14,000, a baseline clear zone width of 4.6 m (15 ft), a unit ROW acquisition cost of $21.53/m² ($2/ft²), and a high roadside hazard rating [these specifications correspond to the conditions in Table 8(*a*)]. The table indicates that a 7.6-m (25-ft) clear zone is cost-effective. With a baseline clear zone width of 4.6 m (15 ft), the purchase of an additional 3.05 m (10 ft) of ROW will be required to attain a clear zone width of 7.6 m (25 ft).

Clear Zone Width Guidelines

Although the data is rather straightforward, it is complicated by the use of different tables depending on specific site conditions. An alternative may be to use a single table as a statewide guideline for establishing clear zone width requirements for suburban, high-speed arterial highways with curb-and-gutter cross sections. Further discussion of Tables 8–10 follows.

For highway sections with a high roadside hazard rating, Table 8 indicates that additional clear zone width is not cost-effective when the unit ROW acquisition cost exceeds $43.06/m² ($4/ft²). For highway sections with a medium hazard rating, Table 9 indicates that it is not cost-effective to provide additional clear zone width when the unit ROW acquisition cost equals or exceeds $43.06/m² ($4/ft²). For highway sections with a low roadside hazard rating, Table 10 indicates that keeping the existing baseline clear zone width is the most cost-effective option for all unit ROW acquisition costs considered in the analysis.

Based on data collected on the sampled highway sections, the typical or average suburban, high-speed arterial highway with curb-and-gutter cross sections would have a medium roadside hazard rating and a median unit ROW acquisition cost of $64.58/m² ($6/ft²), which corresponds to the conditions specified in Table 9(*b*). It is interesting to note that for these average site conditions, the purchase of additional clear zone width is not cost-effective, regardless of the ADT or baseline clear zone width.

TABLE 8 Clear Zone Requirements for High Roadside Hazard Rating: Unit Right-of-Way Acquisition Cost is (*a*) $21.53/m² ($2.00/ft²), (*b*) $43.06/m² ($4.00/ft²), and (*c*) $43.06/m² (4.00/ft²)

(a)

Baseline Clear Zone Width m (ft)	AADT			
	<8,000	8,000-12,000	12,000-16,000	>16,000
3.1 (10)	Do Nothing	6.1 (20)	7.6 (25)	9.1 (30)
4.6 (15)			7.6 (25)	9.1 (30)
6.1 (20)				9.1 (30)
7.6 (25)				

(b)

Baseline Clear Zone Width m (ft)	AADT			
	<8,000	8,000-12,000	12,000-16,000	>16,000
3.1 (10)	Do Nothing			6.1 (20)
4.6 (15)				
6.1 (20)				
7.6 (25)				

(c)

Baseline Clear Zone Width m (ft)	AADT			
	<8,000	8,000-12,000	12,000-16,000	>16,000
3.1 (10)	Do Nothing			
4.6 (15)				
6.1 (20)				
7.6 (25)				

The most conservative conditions would be a combination of a high roadside hazard rating and the lowest unit ROW acquisition cost [i.e., $21.53/m² ($2/ft²)], which corresponds to the conditions specified in Table 8(*a*). This table indicates that for traffic volumes greater than 16,000 ADT a 9.1-m (30-ft) clear zone width is cost-effective for baseline clear zone widths up to and including 6.1 m (20 ft). For traffic volumes between 12,000 and 16,000 ADT, a 7.6-m (25-ft) clear zone width is cost-effective for baseline clear zone widths of 3.1 m (10 ft) and 4.6 m (15 ft). For traffic volumes between 8,000 and 12,000 ADT, a 6.1-m (20-ft) clear zone width is cost-effective for a baseline clear zone width of 3.1 m (10 ft).

The conditions depicted in Table 8(*b*) [i.e., high roadside hazard rating and unit ROW acquisition cost of $43.06/m² ($4/ft²)] are somewhere between the average and the most conservative conditions. The roadside hazard rating is high, although the unit ROW acquisition cost of $43.06/m² ($4/ft²) is between the lowest cost of $21.53/m² ($2/ft²) and the median cost of $64.58/m² ($6/ft²). The only instance in which additional clear zone width is cost-effective is for traffic volumes greater than 16,000 ADT and a baseline clear zone width of 3.1 m (10 ft).

Similarly, the conditions specified in Table 9(*a*) [i.e., medium roadside hazard rating and unit ROW acquisition cost of $21.53/m² ($2/ft²)] are between the average and the most conservative conditions. The roadside hazard rating is medium, whereas the unit ROW acquisition cost is the lowest at $21.53/m² ($2/ft²). This table indicates that for traffic volumes greater than 16,000 ADT, a 7.6-m (25-ft) clear zone width is cost-effective for baseline clear zone widths of 3.1 m (10 ft) and 4.6 m (15 ft). For traffic volumes between 12,000 and 16,000 ADT, a 6.1-m (20-ft) clear zone width is cost-effective for a baseline clear zone width of 3.1 m (10 ft).

TABLE 9 Clear Zone Requirements for Medium Roadside Hazard Rating: Unit Right-of-Way Acquisition Cost is (*a*) $21.53/m² ($2.00/ft²) and (*b*) $43.06/m² ($4.00/ft²)

(a)

Baseline Clear Zone Width m (ft)	AADT			
	<8,000	8,000-12,000	12,000-16,000	>16,000
3.1 (10)	Do Nothing		6.1 (20)	7.6 (25)
4.6 (15)				7.6 (25)
6.1 (20)				
7.6 (25)				

(b)

Baseline Clear Zone Width m (ft)	AADT			
	<8,000	8,000-12,000	12,000-16,000	>16,000
3.1 (10)	Do Nothing			
4.6 (15)				
6.1 (20)				
7.6 (25)				

Clear zone guidelines should be conservative so that the site conditions on which the guidelines are based are valid for a majority of the roadways for which they will be applied. However, overly conservative guidelines could lead to too many applications that are not cost-effective. The average conditions depicted in Table 9(*b*) are not conservative enough, whereas the conditions specified in Table 8(*a*) are too conservative. Thus, the choice is between conditions depicted in Table 8(*b*) or Table 9(*a*) which are both conservative but not extremely so.

After careful consideration, the conditions in Table 8(*b*), [i.e., high roadside hazard rating and unit ROW acquisition cost of $43.06/m² ($4/ft²)] are considered the more appropriate choice and therefore are recommended. As mentioned previously, the results in this table are still very conservative with the highest roadside hazard rating and a below median ROW acquisition cost of $43.06/m² ($4/ft²).

The recommendations contained in Table 8(*b*) are rather straightforward. For a baseline clear zone width of 3.05 m (10 ft) and an ADT greater than 16,000, a 6.1-m (20-ft) clear zone width is recommended. This would require the purchase of 3.05 m (10 ft) additional ROW. For all other baseline clear zone and ADT combinations, the purchase of additional ROW is not cost-effective.

The site conditions on which the recommended table is based are conservative by design. This is necessary due to the wide range of roadway and roadside conditions for which these guidelines will be

TABLE 10 Clear Zone Requirements for Low Roadside Hazard Rating (All Unit Right-of-Way Acquisition Costs)

Baseline Clear Zone Width m (ft)	AADT			
	<8,000	8,000-12,000	12,000-16,000	>16,000
3.1 (10)	Do Nothing			
4.6 (15)				
6.1 (20)				
7.6 (25)				

applied. However, it is obvious that there will be some sites for which these recommendations will be very conservative and for which a reduced clear zone width may be justified. In these situations, it may be desirable to make a more precise determination of an appropriate clear zone width based on the actual characteristics of the roadway under consideration. The data tabulated in Tables 4–7 can be used for this purpose because the roadside hazard rating, ADT, baseline clear zone width, and unit ROW acquisition cost are known.

Consider a roadway that has a baseline clear zone of 3.05 m (10 ft), a low roadside hazard rating, a unit ROW acquisition cost of $\$21.53/m^2$ ($\$2/ft^2$), and an ADT of 20,000. The clear zone guidelines shown in Table 8(*b*) would indicate a 6.1-m (20-ft) clear zone. However, a more site-specific evaluation using Table 5(*c*) indicates that the baseline clear zone width of 3.05 m (10 ft) is cost-effective and that no additional ROW purchase is required.

SUMMARY AND RECOMMENDATIONS

This study was undertaken to determine the most appropriate and cost-effective clear zone width requirements for suburban, high-speed arterial highways with curb-and-gutter cross sections. Typical site conditions for this class of roadway were defined based on field data obtained from a selected sample of highway sections. An incremental BC analysis was used to determine incremental BC ratios for various combinations of clear zone width, traffic volume (ADT), roadside hazard rating, and unit ROW acquisition cost. The results of this analysis were tabulated to identify ADT ranges for which different clear zone widths become cost-effective. Based on these results, the following general observations were made.

- It is not cost-effective to purchase 1.5 m (5 ft) or less of additional ROW.
- For unit ROW acquisition costs greater than $\$43.06/m^2$ ($\$4/ft^2$), it is not cost-effective to provide additional clear zone width through the purchase of additional ROW.
- For roadways with a low roadside hazard rating, it is not cost-effective to provide additional clear zone width beyond the existing baseline clear zone width.

A general clear zone policy should be established based on the results in Table 8(*b*). For a baseline clear zone of 3.05 m (10 ft) and an ADT greater than 16,000, a 6.1-m (20-ft) clear zone width is recommended. This would require the purchase of 3.05 m (10 ft) additional ROW. For all other baseline clear zone width and ADT combinations, the purchase of additional ROW is not cost-effective and therefore is not recommended.

However, because of the probabilistic nature of the BC analysis and the assumptions inherent therein, a certain degree of judgment should be exercised in applying this data. The typical site conditions (e.g., straight and level alignment, flat terrain beyond curb, 0 percent truck use, etc.) used in the analyses are based on the sampled highway sections included in this study and may not be representative of site conditions throughout the nation. Thus, great care should be taken in applying the study results to other states. A sensitivity analysis to assess the effects of the various parameters included in the typical site conditions would be helpful. Unfortunately, a sensitivity analysis was beyond the scope of this study.

REFERENCES

1. *A Policy on Geometric Design of Highways and Streets,* AASHTO, Washington, D.C., 1990.
2. Texas Transportation Institute. *Design Criteria for Suburban High Speed Curb and Gutter Sections.* Texas A&M University System, College Station, Texas (ongoing).
3. Sicking, D. L., and H. E. Ross, Jr. Benefit-Cost Analysis of Roadside Safety Alternatives. In *Transportation Research Record 1065,* TRB, National Research Council, Washington, D.C., 1986.
4. *Roadside Design Guide.* AASHTO Washington, D.C., Oct. 1988.
5. Mak, K. K., and R. L. Mason. *Accident Analysis—Breakaway and Nonbreakaway Poles Including Sign and Light Standards Along Highways.* Report DOT-HS-5-01266. FHWA, U.S. Department of Transportation, Washington, D. C., Aug. 1980.
6. Ivey, D. L., and J. R. Morgan. *Safer Timber Utility Poles.* Report DTFH-61-83-0-00009. FHWA, U.S. Department of Transportation, Washington, D.C., Sept. 1985.

Publication of this paper sponsored by Committee on Roadside Safety Features.

Development and Implementation of an Automated Facility Inventory System

ANGELA MASTANDREA, BILL SWINDALL, AND GARY KLASSEN

Infrastructure assets are a vital investment in the well-being of a society. If they are not managed properly, the inevitable degradation of these assets could become a source of liability and a significant financial burden to a public agency. Therefore, infrastructure facility management requires reliable and accurate information. Monitoring infrastructure facilities requires extensive data collection efforts. Because present data collection methods are costly and time-consuming, automated methods of data collection are needed to meet evolving management needs. Roadware Corporation has introduced a subsystem for its Automatic Road Analyzer that addresses the need for automated data collection of roadside furniture. Surveyor™ is a new technology used to make measurement from images recorded on videotape. With computer-scaled video and measurement data, an operator at an engineering workstation can measure the size and location of objects quickly and accurately. This information is flexible because the data output is fully compatible with Geographic Information Systems and Computer Automated Design systems. Sign management is one of the primary function of this technology, but there are several applications. Surveyor addresses those issues that make data collection and postprocessing efforts difficult and labor intensive. Implementing an automated data collection system ensures a more comprehensive data base, allowing for more accurate prediction and performance models. Automated data collection provides accurate data in a timely and cost-effective manner.

Infrastructure assets are a vital investment in the present and future well-being of a society. If these assets are not managed properly, their inevitable degradation could become a liability and a significant financial burden to a public agency. To manage infrastructure facilities successfully, reliable and accurate information is required. This need for data has been recognized by many government bodies and is currently used for the Highway Performance Monitoring System (HPMS), which is regulated by the FHWA.

Of the types of data required for infrastructure management, the most critical for developing a comprehensive system are inventory and location of facilities. For facilities to be managed effectively, (*a*) they must be inventoried and classified according to type, (*b*) their condition must be recorded, (*c*) their locations must be registered. An accurate record of location is necessary to (*a*) reduce the possibility of confusing similar facilities that are in close proximity, (*b*) allow for quick and accurate identification while in the field, and (*c*) create unique facility locations for data base management systems, including Geographic Information Systems (GIS).

Transportation agencies that are required to collect the infrastructure inventory and location information generally consist of state departments of transportation, county roads and public works departments, and city engineering departments. With such a wide variety of data users, applications for infrastructure data have expanded and include GIS, facility management data bases, and inventory surveys.

Maintaining and monitoring infrastructure facilities require extensive data collection efforts, which can be costly and labor intensive. To effectively manage the network, managing agencies require the timely delivery of this data. This need will only become more urgent as traffic demands increase, budgets shrink and time constraints on management grow. Current data collection methods for conducting a facility inventory and recording its location are costly and time-consuming. Aerial and remote sensing are expensive data collection methods, and the resulting data do not provide the detailed feature information many transportation agencies require. For example, using aerial methods to identify mile markers, culverts, fire hydrants, and signs is often inaccurate and inefficient. A portion of the costs associated with remote sensing may be attributed to the high capital and operational cost of the required equipment and personnel. Aerial data collection methods are therefore limited by unreliable information.

Currently, manual surveys are conducted to obtain the detailed information required for various management purposes. Data are collected using a variety of methods, from pen-based computers to paper and pencil. Although the data obtained during manual surveys are very specific and detailed, there are several drawbacks to manually collected data:

- Because the entire process is done manually, there is a long turnaround time for the completion of the survey. This includes all survey tasks: from data collection and verification to data input and implementation. If the researcher does not use automated data collection techniques, the effort required does not allow for the timely completion of a survey project.
- Production rates are susceptible to environmental factors, because it is difficult to conduct a field survey during adverse weather conditions.
- Personnel safety is a concern while the field crew is collecting data on-site. The presence of crew members on the road and in traffic poses the danger of serious accidents.
- Much of the data collection effort is associated with the set-up and dismantling of the necessary traffic control devices.
- Incorrect and inaccurate information may be reported as a result of the previously mentioned conditions. Data discrepancies can also be attributed to inconsistencies in the data collection methods and to fatigue.
- There is no permanent or visual record with which to compare the data readings unless the field crew go out into the field again and resurvey the infrastructure facility. Even if photographs are taken in the field, the quality of the resulting photos is not immediately known due to processing delays.

A. Mastandrea, 123 Boulding Avenue, Waterdown, Ontario, L0R 2H3, Canada. B. Swindall and G. Klassen, Roadware Corporation, 147 East River Road, Paris, Ontario, N3L 3E1, Canada.

These deficiencies in performing inventory and location surveys using manual procedures show that a more automated approach is needed.

AUTOMATED RIGHT-OF-WAY DATA COLLECTION

Automated methods of data collection that meet present and future management requirements are clearly needed. These methods use a host vehicle traveling at highway speed while recording the appropriate infrastructure data. The data acquisition vehicle collects all the required data in a single pass of the facility. The vehicle uses video and other sensors (e.g. lasers, ultrasonic sensors, etc.) to capture data automatically, allowing for subsystem processing at an office workstation. The collected data can then be related to a referencing system such as mile marker or Global Position System (GPS).

With automated methods of collecting road data, departments can reap the following benefits:

- An increase in daily production rates during favorable weather conditions;
- Storage of the information for postprocessing;
- Collection of more data items on a per diem basis;
- Reduced expenses;
- Reduced susceptibility to weather because the data collection effort requires significantly less time in the field;
- Information that is processed at an engineering workstation, in an office environment;
- Field data collection that is completed in the vehicle, eliminating the need for crew members to work near the traffic flow;
- Equipment and capital costs that are significantly less than those associated with remote sensing;
- Time requirements that are lower than for a manual survey;
- Accuracy and data detail that are not compromised;
- Quality control procedures that are easier to implement, and discrepancies that can be easily rectified; and
- A visual record of the facility that department members can view at any time.

Automated data collection that provides the user with accurate and consistently reliable data, along with flexibility, will save the department time and money without compromising quality.

INTRODUCTION TO SURVEYOR

Roadware Corporation has developed a new automated facility inventory and location system for right-of-way (ROW) measurements called Surveyor. The Automatic Road Analyzer (ARAN) is a high-speed, mobile data acquisition platform that carries the Surveyor subsystems. The ARAN collects and stores the road data in one pass while traveling at highway speeds.

Surveyor is a patented technology used to make measurements from images recorded on videotape or other video recording media. Associated software uses location information from the distance measuring instrument (DMI), Geometrics System, and GPS to accurately determine the location and attitude (three-dimensional orientation) of the vehicle. This information, along with multiple-frame video images, can be used at an office workstation to establish with accuracy the location of signs, guide rails, bridges, culverts, and other roadway features that can be seen in the ROW video. With ROW video and measurement data, an operator at an engineering workstation can measure the size and location of objects quickly and accurately. To make linear measurements of an object, the video image is digitized at the workstation and the operator uses the computer mouse to select an object on the screen. The computer automatically calculates and reports the object's x and y coordinates and the location (Figure 1). Height, width, and other measurements can also be made. Data output is fully compatible with GIS and Computer Automated Design (CAD) systems.

The vehicle data collection subsystems required for video measurements include the following:

- DMI—An optical shaft encoder, driven by a speedometer cable from the rear wheel, produces a stream of 1,800 pulses per wheel revolution. These pulses are sent to a central data acquisition computer for use by other subsystems. The DMI readings are accurate to within 0.02 percent of the total distance traveled by the vehicle.
- ROW Video—A full color charge coupled device video camera is mounted between the driver and the passenger, and points forward out the vehicle's front window to record a continuous video log of the road ROW. The ROW camera has a horizontal resolution of 720 television lines and a shutter speed of 1/2,000th of a second. The video subsystem is controlled by a 486-based Smart Video Controller (SVC). The SVC controls the video recording functions of the Super VHS (S-VHS) videotape recorder (VTR). Identification and measurement information is overlaid onto the video images for later reference. The ROW the data capture for postprocessing is illustrated in Figure 2.

The ROW perspective video is collected using a high resolution video camera to record Super-Video in S-VHS format. Each video frame is automatically computer-encoded using Society of Motion

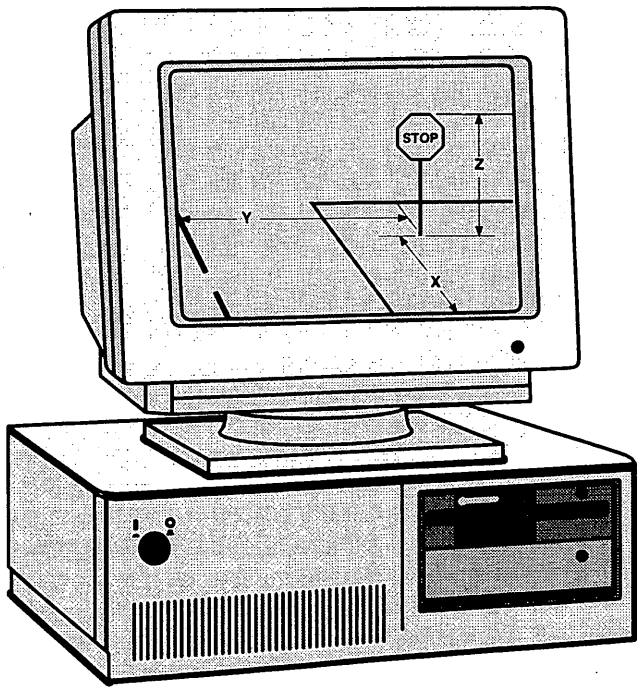

FIGURE 1 ROW video measurements.

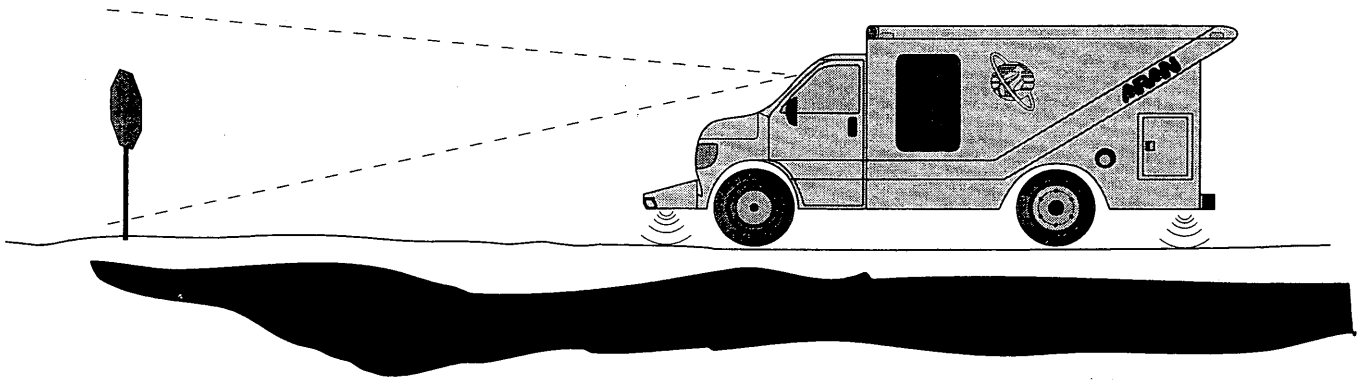

FIGURE 2 ROW data capture.

Picture and Television Engineers (SMPTE) time code and is cross-referenced with distance measurements for rapid access and retrieval during postprocessing. This coding allows the user to review and analyze the video images at a workstation. Associated Search and Find software uses the SMPTE time code, which enables the SVC to position the videotape at any location requested by the user via a keyboard.

- Geometrics System—The geometrics system aboard the data acquisition vehicle uses accelerometers to continuously measure the roll, pitch, and heading of the vehicle. The gyroscope readings provide information on the orientation of the vehicle and the camera with respect to the vehicle's start position.
- Ultrasonic Sensors—These four ultrasonic sensors on the vehicle's chassis measure the vertical displacement of the chassis to the road surface 15 times per second. The distances measured with these sensors are accurate to 1 mm (0.04 in.). The ultrasonic sensor data are used to determine the alignment of the vehicle with respect to the ground to determine the orientation of the camera.

The configuration of the data acquisition system for computer-scaled video is illustrated in Figure 3.

To obtain accurate measurements, the ROW camera must be calibrated to the ultrasonic sensors and the geometrics system. This calibration is completed by performing a factory calibration and a field calibration.

The factory calibration records information specific to the installation of the system on the vehicle. The distances between each ultrasonic sensor and the camera are measured and recorded. An alignment mark is placed on the windshield to align the field calibration with the direction of travel of the vehicle. The factory calibration is performed once, after the system is installed.

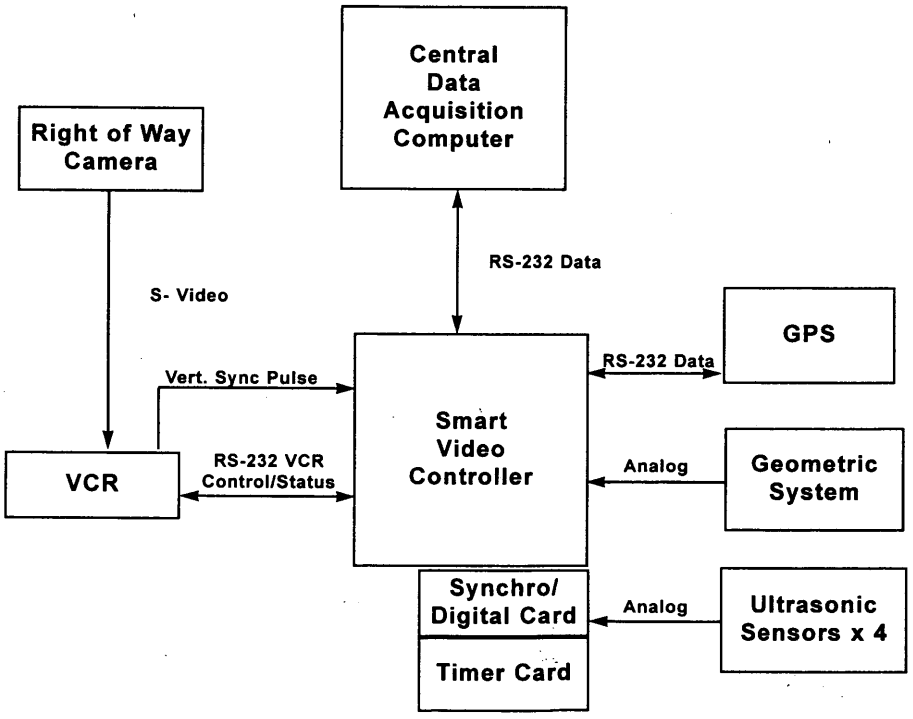

FIGURE 3 Surveyor data acquisition system.

The field calibration is used to calibrate the camera position, focal length, and ultrasonic sensor measurements. A water datum, pendulum, and surveyor's level are used to calibrate all components to a horizontal datum and the direction of travel. The pendulum is placed a known distance from the front of the vehicle. Video of the pendulum is collected while the vehicle is stationary so that a third calibration can be completed at the engineering workstation.

During data collection, geometric and ultrasonic data collected at intervals timed precisely with the shutter of the video camera are collected and stored. This information provides the exact orientation of the vehicle at the time of each video image. As mentioned earlier, all collected data is referenced to the information recorded by the DMI on the data acquisition vehicle.

VIDEO POSTPROCESSING

After the data collection effort is completed, the ROW video is processed at the workstation to record and store all linear measurements. The associated software package is used in the Microsoft Windows environment and allows the operator to select roadway features interactively from the digitized video. The workstation configuration is given in Figure 4.

A software calibration must be performed each time a truck calibration (factory or field) is completed to record the final measurements of the camera position, so the operator may process the video images. The software calibration has two components, a main calibration and a gyroscope calibration. The main calibration uses the videotape of the pendulum taken during the field calibration of the camera, the gyroscope calibration involves updating the calibration files with new gyroscope readings recorded during the field calibration process. When the calibration has been completed, the operator may begin processing the video.

The computer screen consists of four areas: the video area, the menu bar, the VTR control bar, and the object record. The video area is where the digitized VTR image is displayed. All measurements are made from the frame image displayed here.

The menu bar displays functions that are the same as in any other Windows application.

The VTR control bar has two areas, one with five buttons for standard operations, and another with two buttons for shuttle control of the VTR. The counter box displays chainage, frame number, or time. The search button brings up a selection box with detailed search criteria. Figure 5 illustrates the VTR controls.

The object record is where the measured values related to a single object in a single frame are displayed (Figure 6). It also contains an identification hierarchy at the top and an area for user description near the bottom. The position and dimension areas refer to the object being measured on screen. The user description area allows comments to be added and is user-definable.

A computer file is generated corresponding to each videotape. This file is required for postprocessing because it contains ultrasonic sensor and geometric data for each video image.

When the appropriate files are loaded, the user advances the tape. As the tape plays, the video images are digitized and stored in a circular buffer. After the buffer is full, the newest digitized images replace the oldest ones. When the operator has captured the video frames containing an object of interest, the Survey function is selected. The operator then scrolls through the digitized frames that are in the buffer using a scroll bar, and selects the frame that best represents the object. Measurements of the object can now be taken and stored.

The software determines the distance between the object and the camera by recognizing each pixel as a specific distance from the camera, after the video is calibrated. The software is able to accurately determine the linear measurements of the object using an

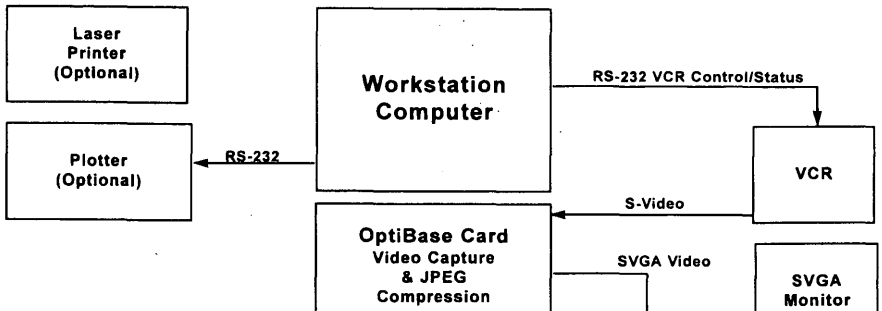

FIGURE 4 Postprocessing workstation configuration.

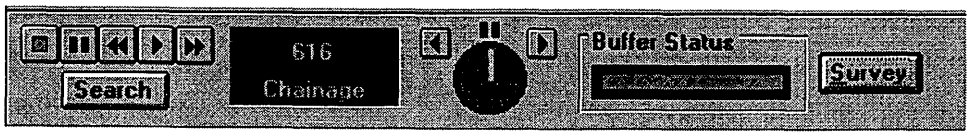

FIGURE 5 VTR control bar.

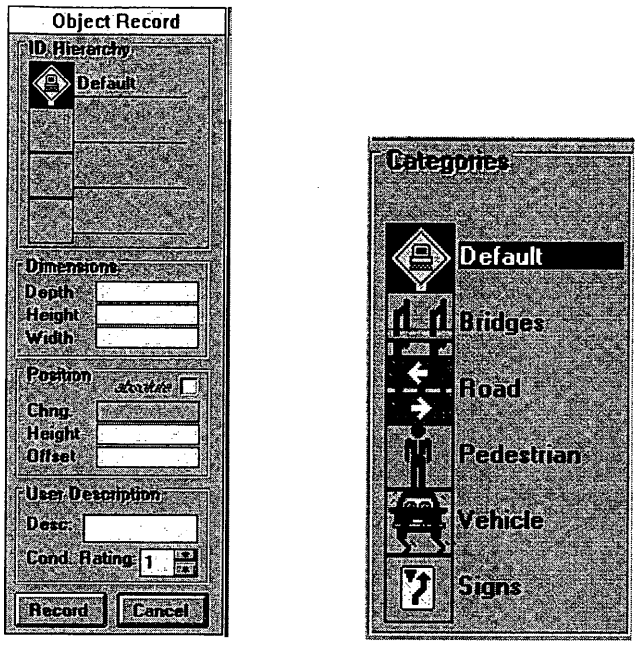

FIGURE 6 Object record and identification hierarchy.

aspect ratio and a radians-per-pixel value. The radians-per-pixel value is calculated from the vertical size of the static pendulum that was recorded during the field calibration procedure. An aspect ratio is used because the vertical size of the pendulum may differ from the horizontal size of the pendulum on the video screen. The aspect ratio is represented as the ratio of the pendulum's horizontal size to its vertical size. The Cartesian coordinates of the road plan and the object are then calculated. The Cartesian coordinates are adjusted for the roll and pitch of the vehicle, as determined from the ultrasonic sensors on the chassis.

All other linear measurements are made assuming the object lies in a vertical plane perpendicular to the direction of travel. Location is measured in relative chainage or geographic (absolute) coordinates. Linear measurements are reported in imperial or metric units. Surveyor is able to make measurements from the video image using one of two methods, single frame and multi-frame.

The single frame mode allows the user to make all measurements using a single video image. All measurements made in the single frame mode must be referenced to the plane of the road. For example, a user who wants to measure a sign begins by identifying the object from where it intersects the plane of the road, at its base. When the object does not intersect the plane of the road or the point of intersection is difficult to discern (because of tall grass, ditches, snow banks, etc.), single frame measurements become impractical.

Multi-frame measurements allow the user to measure objects regardless of where they exist in the image. The user must identify the object in two or more images to make measurements. This method is moderately more time-consuming than the single frame method but provides more flexibility. Multi-frame measurements are made using triangulation calculations.

Both measurement techniques allow the user to measure the three-dimensional position of any object as well as its width, height, and depth.

When all data measurements have been made, the object may be classified in the available identification hierarchy. As the user moves down the classification hierarchy, the object description becomes more specific. The hierarchical structure can be customized for each transportation agency. In the example of a sign inventory, a hierarchical classification such as the one displayed in Figure 7 may exist.

Two additional data inputs are available to the user: condition rating of the object on a scale of 0 to 10 and a comments section to note any irregularities or special characteristics of the facility. When all the information is entered, the operator may save the record in one of three types of file formats: a text file (*.txt), a drawing exchange format (*.dxf) file for use by CAD applications, or a Surveyor file.

APPLICATIONS

The flexibility in file format allows the information to be used in many applications. Collecting additional data items while the vehicle travels the network allows the user to import scaled video data into various software packages, which can be used in any of the following applications.

Sign Management

Sign management practices have not been widespread among transportation agencies in the past, but their implementation is now required by the Intermodal Surface Transportation Efficiency Act. Sign management is one of the primary functions of Surveyor technology, but there are several other applications of this data. Information that would typically be associated with a particular sign includes the following:

- Location (relative or absolute);
- Offset;
- Horizontal width of sign face;
- Vertical height of sign face;
- Height of sign above the road surface;
- Manual on Uniform Traffic Control Device type code;
- Legend (hierarchy);
- Condition assessment;
- Number of signs on the post;
- Number of support posts;
- Type of support post;
- Direction of sign face (north, south, etc.);
- Shared sign post;
- Date installed; and
- Maintenance history.

Traffic Control Signs

Warning Signs

Guide Signs

Regulatory Signs

Right-of-Way Series
Pedestrian Series
Speed Series
Movement Series
Parking Series
Miscellaneous Series

FIGURE 7 Sample identification hierarchy.

GIS

GIS technology is the vehicle used to organize data and understand their spatial associations. GPS and scaled video data may be used together to generate plan view drawings. Because the position data can be represented in (*x-y-z*) format, the information is already in a useful format for input to a GIS as a data overlay. Compatibility with a GIS format is important, because the collection of accurate positioning data for facilities is a difficult and time-consuming data conversion process when using other methods, such as digitizing maps or aerial photographs.

The benefits of linking Surveyor data to a GIS are categorized as follows:

- Data Integration. All GIS data are tied to a common geographic referencing system, (i.e., latitude and longitude coordinates), making all attribute data available (e.g. traffic accident, population, and maintenance records). The combination of data bases provides the user with a more comprehensive picture of the network.
- Data Format and Accessibility. Accessing data base information by pointing and clicking with a mouse is simpler, in most cases, than entering a text query. The results are more easily interpreted because they are visually displayed on the screen, both spatially and by color coding the results.
- Analysis Tool. A comprehensive GIS makes different types of network information available to the last user, allowing the agency to conduct a more thorough analysis of the data.

Facilities Inventory and Condition Assessment

Facilities inventory and condition assessment is possible using the recorded location and the measurements of the features that characterize various highway facilities. The facilities inventory allows the user to locate a facility, determine its condition visually, and attach any special notation that is desired. The condition assessment from video could include noting condition of signs, guardrails, pavement markings, drains, and so forth.

The inventory information can be supplemented using the workstation inventory keyboard. This keyboard can be used to record various types of information relating to pavement condition and facility inventory while the user views the video images at the workstation. Because each video frame is linked to distance and GPS measurements, the information entered at the inventory keyboard is automatically linked to this location data. For example, during inventory of railroad crossings, the operator would press a predefined key when the correct position for the railroad crossing appears on the screen. When the key is pressed, the image number, route number, milepost location, and GPS coordinates would automatically be written to a file for future use. At that point, video measurements of the crossing length and width can be made.

The inventory keyboard uses backlighted liquid crystal display keys that can display a programmable image for each key. In the example of the railroad crossing, a special symbol representing a railroad crossing could be displayed on the key, making the data-entry function straightforward and accurate.

Keys can be defined for virtually any type of inventory or condition assessment. A key can be programmed to toggle on and off, allowing it to be used to indicate the beginning and ending of span-type facilities, such as guardrails, pavement markings, and passing zones.

Preliminary Survey Measurements

Surveyor can also be used in the planning of new infrastructure accessories or modifications. Surveyor can generate a situation diagram, allowing preliminary surveying measurements to be taken from the video before any field work is required. Potential applications include the layout of new structures and modifications of existing lanes (e.g., road widening). This technology can also be used in planning and engineering studies, with respect to selection and location of traffic control devices.

Landmark Survey

A landmark survey can be performed to obtain an accurate location description of the road network. This can be accomplished using GPS data along with Surveyor measurements to record the location of network landmarks. This information can be used to develop a common location referencing system among various departments, similar to milepost identification markers but more accurate.

Traffic Control Planning

When normal traffic flow is interrupted and traffic control is required, a transportation agency may use the recorded video information to plan the set-up of the site in the office, instead of doing the planning in the field, or from maps or sketches.

Visual Historical Record

Video records can be used in the defense of a tort liability case. Having a visual record of the scene in question may help provide information on whether or not an agency was negligent in a specific situation.

Data Reports

Collected data can be formatted to the users' specifications to provide readily available information for determining relevant statistics and planning analysis.

SUMMARY OF BENEFITS

The versatility of scaled video technology is demonstrated by the preceding illustrations. Surveyor addresses the issues that make data collection and postprocessing of inventory and location data difficult and labor intensive. Implementing an automated data-collection system will ensure total data coverage in a timely manner.

The facility inventory and position reference measurements that can be made from the ROW video provide important information for transportation data bases. Knowledge of the location, characterization, and condition of various highway facilities (when quantified by measurements) provides a foundation of accurate information that can be used to manage the infrastructure. This information will provide transportation agencies with the following benefits:

- Operating costs that are lower than traditional data collection methods;

- Automated data collection that can reduce the time required in the field;
- Increased employee safety without the need for traffic control during data collection;
- Easier budgeting and funding allocation;
- Readily available information linked to all other infrastructure information;
- Anomalies that can be checked easily with video;
- Planning of location and layout of new facilities; and
- Information for political considerations.

SURVEYOR IMPLEMENTATION

The following cases illustrate how Surveyor technology has been implemented by some North American transportation agencies:

Commonwealth of Massachusetts

The Massachusetts Department of Transportation has performed field measurement validation of Surveyor measurements, and has found the offset, width, and height measurements to be accurate within 50 to 100 mm (2 to 4 in.). The Department of Transportation is currently evaluating the use of Surveyor in the collection of highway performance monitoring system (HPMS) data, which would include measurements such as lane widths, median distance, and shoulder width.

City of Surrey, British Columbia

The engineering department of the city of Surrey, British Columbia is using Surveyor measurements to establish a GIS layer for public works facilities. Surveyor will be used to determine centerline offset distances and inventory of fire hydrants, bus stops, curb drains, utility poles, and other infrastructure elements of interest to the public works department. A plan view drawing, with *x-y* coordinates for the different features, will be generated by Surveyor in CAD format, and will then be merged with other GIS layers.

State of Rhode Island

Surveyor field data has been collected on approximately 2,900 km (1,800 mi) of highway in the state of Rhode Island. The Rhode Island Department of Transportation is considering using this data for a comprehensive sign inventory, which would include measurements of sign offset, height, size, and related data.

CONCLUSION

The advantages of using a more automated data collection method instead of current manual methods have been clearly illustrated. Collecting data from computer-scaled video allows the user to record more data types simultaneously, creating a more comprehensive data base of the road network. This technology was developed to provide access to the complete picture of the network, meeting today's infrastructure management needs. Initial implementation of this video technology has not been widespread, as the product has only recently been made available to transportation agencies. However, the positive results obtained so far promise a broader acceptance and acquisition of this data collection method.

Publication of this paper sponsored by Committee on Photogrammetry, Remote Sensing, Surveying, and Related Automated Systems.

Development of Evaluation Criteria for Loop Tours

KHALED KSAIBATI, EUGENE M. WILSON, AND DONALD S. WARDER

In the past some historical and cultural heritage areas, wildlife areas, lakes, and areas of scenic beauty were not exposed to tourists in the United States. Realizing this fact, the FHWA, state departments of transportation, and tourism departments introduced scenic byways to expose these features to the public. In Wyoming, a loop tour program was developed in 1989 in conjunction with the already-existing scenic byways to enhance tourism and divert traffic from interstate to state routes. The University of Wyoming and the Wyoming Division of Tourism conducted a research project to determine the effectiveness of the Wyoming loop tours. As a part of this study, a nationwide survey was conducted to determine the national trends in loop programs. In this paper are summarized the findings from the Wyoming study and the nationwide survey.

The United States is a country with a very diverse culture and heritage. It also has a vast variety of wildlife, lakes, and scenic beauty. Tourism is important to the American economy; it creates jobs, promotes retail sales, and even encourages the creation of new businesses. There is an increasing recognition of the need to establish programs that encourage growth of tourism travel. The following facts reflect the importance of tourism (*1*, p. 48):

- Travel and tourism is a $350 billion a year industry and the nation's third largest retail industry (after automobile dealers and food stores).
- Travel and tourism ranks as one of the largest employers in 37 of the 50 states. Travel and tourism comprises 6.7 percent of the gross national product and 13 percent of the service sector.
- In 1989, travel and tourism generated $42.8 billion in tax revenue and a total industry payroll of $73.5 billion. It is America's second largest employer (health care employment is the largest). About 5.8 million people are directly employed in travel and tourism, and another 2.5 million are employed indirectly in providing goods and services to the industry.

In an attempt to promote tourism in the United States, many programs have been undertaken by the federal government, tourism departments, and state departments of transportation. The scenic byways program is one of them. In this program, many existing roads have been designated scenic byways. These scenic and historic roads possess unique cultural features. The objective of designating roads as scenic byways is to preserve and promote the scenic quality of roads and to improve the economy of the local communities. In addition to designating scenic byways, the Wyoming Department of Transportation and the Wyoming Tourism Department introduced loop tours to promote tourism in the state of Wyoming. The Wyoming loop tour program was developed in the late 1980s to introduce wildlife and historic landmarks to tourists visiting Wyoming. Loop tours are short-duration pleasure trips that are usually traveled in a day's time. Tourists begin their loop tour at one point and return to the same point. Loop tours are also called circle trips in certain states.

The University of Wyoming recently conducted a research study on the Wyoming loop tour program. The main objective of this research was to develop criteria for designating loop tours and to use these criteria in evaluating the existing loop tours. The major findings from this research are discussed in this paper.

University of Wyoming, P.O. Box 3108, Laramie, Wyo. 82071.

WYOMING LOOP TOURS

In the late 1980s, the Wyoming Division of Tourism initiated the loop tour program. Initially, this program consisted of three loop tours located in different parts of Wyoming. In 1992 this program was expanded and an additional three loop tours were added. The Wyoming Division of Tourism developed a brochure containing descriptions of each loop tour (*2*). These brochures are normally distributed to tourists at tourist information centers located throughout the state of Wyoming. Information about loop tours is also printed in newspapers and on Wyoming state maps, which are available at information centers.

LOOP TOUR PROGRAMS ACROSS THE UNITED STATES

A literature review failed to find any mention of loop tour programs in the United States. Therefore, the University of Wyoming conducted a nationwide survey to determine which states have loop tour programs similar to the one in Wyoming. Copies of the survey were sent to all 50 state departments of transportation. Of the 50 questionnaires mailed, 37 responses were received. Out of the 37 states responding to the questionnaire, only 11 states indicated that they currently had loop tour programs (Table 1). Oregon reported the highest number of loop tours (20), whereas Wisconsin, with the fewest, reported having only 2 loop tours. New Mexico indicated that a loop tour program was currently under consideration. Only Texas had conducted studies to determine the effectiveness of its loop tour program. Most states considered historic points and scenic quality among the factors for selecting the routes and locations of loop tours. A few states such as Connecticut and South Dakota required paved routes in their loop tours.

LOOP TOUR SELECTION CRITERIA

The purpose of loop tours is to stimulate the economies of local communities by diverting the through traffic from its original route for a short distance. Due to the long distances between attractions

TABLE 1 States Having Loop Tour Programs

STATE	NUMBER OF LOOP TOURS
Connecticut	7
Hawaii	Not available
Oregon	20+
Pennsylvania	4
South Dakota	12
Maryland	Not available
Michigan	4
Minnesota	2
Texas	10
Wisconsin	2
Wyoming	6

in Wyoming, a maximum length of 320 km (200 mi) was used in designing a loop tour. The intent was for through traffic to be diverted if the attractions were of significant interest to the traveler. In this study, all the anchor attractions were classified as to their potential importance, either local or national and international importance. Examples of attractions in the latter category include Yellowstone National Park, Grand Teton National Park, Fort Laramie, and Devils Tower. These national attractions, if present on the loop tours, help to make loop tours popular. Local attractions include state parks, museums, historic sites, lakes, and other attractions that are primarily known locally or in neighboring states. Glendo State Park, Guernsey State Park, and the Wyoming Territorial Prison are a few examples of this category of attraction.

Any loop tour should contain at least one nationally or internationally known attraction or several local attractions. If a route has only great scenic value and no anchor attractions, making it a scenic byway should be considered.

The criteria developed to evaluate loop tours and route links or segments were divided into two levels. In Level I the attractions are selected, and it is determined whether an interstate highway and a round trip of less than 320 km (200 mi, or approximately 4 hr driving time) provide access to the attractions. In Level II the specific route segments to be included in the loop tour are evaluated. Factors considered in Level II include the roadway conditions, scenic beauty, and tourist services of potential route segments.

Level I Evaluation

The following tasks should be performed in a Level I evaluation.

1. Identify nationally, internationally, and locally significant attractions.
2. Identify potential points of diversion (origin) from the interstate routes that are the major through facilities.
3. Identify route segments and routing alternatives from an origin to the proposed sites that are within a total travel time of 4 hr or a maximum distance of about 320 km (200 mi).
4. Routes considered should be safe for driving and should accommodate recreational vehicles (motor homes). Any paved, secondary, or primary route will satisfy this criterion. If the route is not a paved, primary, or secondary highway, then turning radii, superelevation, sight distance, slope, alignment, and grades should be examined to determine whether the safety criteria are met. All these specifications should meet the requirements specified under the Local Rural Roads section in AASHTO's *A Policy on Geometric Design* (*3*).

Level II Evaluation

After identifying the appropriate routes, evaluations are conducted in Level II to select the best route segments. Level II criteria include rating loop tours on the basis of roadway conditions, anchor attractions, communities by population, and scenic beauty. These evaluations are rated on a scale of 1 to 5, on which 5 is "excellent" and 1 is "poor." The Level II criteria are as follows.

1. Roadway conditions. The American Automobile Association's (AAA's) criteria for designating scenic byways are proposed for evaluating roadway conditions. AAA's criteria evaluate the road for surface, shoulder, alignment, and grade factors (*4*). In this loop tour study, AAA's ranking of 1 to 5 was reversed so that 1 reflected poor road conditions and 5 reflected excellent road conditions. An average route segment value of 3 was proposed as the cut-off value in a loop tour.
2. Anchor attractions. All of the route segments that satisfy the roadway condition criteria are rated on the availability of attractions. Ratings are assigned based on the significance of each attraction. International and national attractions are assigned 2 points, whereas local attractions are assigned 1 point. The points assigned are totaled to obtain the final rating for the route segment on a scale of 1 to 5. Any value greater than 5 is assigned a rating of 5.
3. Communities by populations. Population size is directly related to tourist services such as service stations, lodging, restaurants, motels, and information centers. Therefore, any community with a population of 10,000 or above is assigned a rating of 5. This emphasis on smaller population groups reflects the desire to use loop tours to stimulate the economy of smaller local communities. The population sizes and their respective ratings are listed below.

Population	*Numerical Value*
Less than 500	1
500–1,500	2
1,500–5,000	3
5,000–10,000	4
More than 10,000	5

4. Number of communities. The total number of communities present on a particular route is one of the deciding factors rating the route under consideration. This criterion reflects the number of different service opportunities in which expenditures may occur. The rating criteria are as follows:
   a. If there are fewer than five communities on a route segment, then the rating assigned is equal to the number of communities on the route segment itself.
   b. If there are more than five communities, then a rating of 5 will be assigned to the route.
5. Scenic beauty. Each route segment is then evaluated for scenic beauty along the route. The research study conducted by B. Lynne Boyd, Visual Preferences of Natural Landscapes in Southern Wyoming, is proposed for evaluating natural beauty (*5*). In Boyd's study, the main features present in Wyoming are classified as mountains, lakes, streams, and prairies. These features are rated on a scale of 1 to 5 with 5 being excellent.

6. Finally, provisions are made to include roadways necessary to complete loop tours without penalizing the evaluation. Route segments that complete loop tours are evaluated using consistent criteria but tradeoffs are made only on parallel competing facilities.

All of the calculated values of Level II criteria are then tabulated in a matrix and multiplied by appropriate weighting factors. These factors were obtained based on the recommendations of a panel of experts. This delphi procedure produced factor weights deemed appropriate for Wyoming's environment. Roadway conditions and scenic beauty were assigned a weighting factor of 1. Because attractions and tourist services are the main components of loop tours, a weighting factor of 1.5 was used for these components. A weighting factor of 1.3 was used for the number of communities. The best loop tour routing is then selected based on the highest loop tour value.

APPLICATION OF THE DEVELOPED CRITERIA TO THE CHEYENNE AND OREGON TRAIL LOOP TOUR

The loop tour evaluation criteria developed in this research project were validated by evaluating alternate routes on two loop tours in the state of Wyoming (*6*). This article includes the results from evaluating the Cheyenne and Oregon Trail loop tour only.

Level I Evaluation

As shown in Figure 1, this loop tour originates from the state capital, Cheyenne, and passes through Douglas, Glendo State Park, Guernsey, Guernsey State Park, Fort Laramie, and Torrington. Information about travel time and distances is presented in Table 2. The total travel time for the existing loop tour route is 5 hr; it covers a distance of 452 km (283 mi). These figures exceed the maximum limits specified for a loop tour in Level I evaluation.

Fort Laramie, located on US-26, is a national historic site and thus falls under the national/international attraction category. Cheyenne, located near I-80, is the origin for this loop tour. Cheyenne has several local attractions such as the Wyoming state capitol, Wyoming State Museum and Art Gallery, National First Day Cover Museum, Cheyenne Frontier Days Old West Museum, F.E. Warren Air Force Base, and the Wildlife Visitor Center. There are two local attractions in Torrington, the Goshen County Museum and the Torrington Depot. The existing loop tour then passes from Torrington to Guernsey where two other local attractions, Register Cliff and Oregon Trail Ruts National Historic Landmark, are located. The loop then proceeds from Guernsey to Hartville and merges with I-25 at Orin Junction. The route segment from Guernsey to Orin Junction has no anchor attractions. Three alternate route segments that also merge with I-25 were identified. These

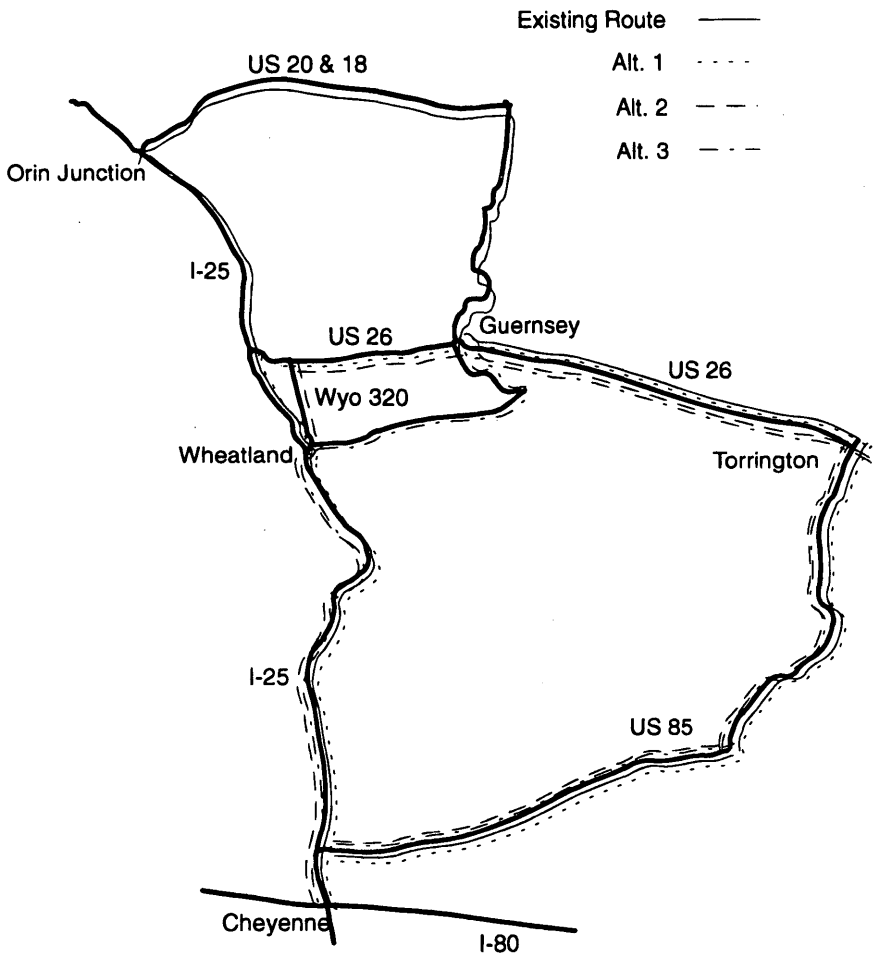

FIGURE 1 Location of existing Cheyenne and Oregon Trail loop tour routes and alternative route segments.

TABLE 2 Travel Times and Lengths for Cheyenne Loop Tour Routes

ROUTE	TIME TRAVEL (Minutes)	DISTANCE (km)
Cheyenne to Torrington (US 85)	84	124
Torrington to Ft. Laramie (US 26)	22	32
Ft. Laramie to Guernsey (US 26)	15	21
Guernsey to Wheatland Exit via Orin Jct. (WYO 270, US 18, & I-25)	125	195
Wheatland Exit to Cheyenne (I-25)	55	80
TOTAL	**301**	**452**

alternate route segments and the original loop tour routing are shown in Figure 1. Of the three alternate route link segments identified, two route segments pass through Wheatland, which has significant tourist services. The existing loop tour routes and the proposed alternate route segments are paved secondary routes and can accommodate recreational vehicles.

Level II Evaluation

As shown in Figure 1, the three alternate and existing routes have two common segments on the loop tours, Cheyenne to Guernsey, and Wheatland exit to Cheyenne. Only the sections that are not held in common were included in Level II evaluation because the common sections had identical ratings. This evaluation included the combined weighting of roadway conditions, scenic beauty, anchor attraction assessment, and community population criteria.

Evaluation of Roadway Conditions

The alternate route segments were selected on the basis of their proximity to the existing loop tour route. They were evaluated and compared with the existing loop tour route using the same criteria (Table 3). All of the alternate routes, except the route from Guernsey to Wheatland via the Goshen County road, received a "good" rating. The route from Guernsey to Wheatland via the Goshen County road was evaluated as "fair" and did not satisfy the roadway condition criterion. Therefore, this route segment was not considered for further evaluation. The travel time and the length of the acceptable alternate route segments are presented in Table 4.

Evaluation of Anchor Attractions

All of the attractions discussed in the Level I evaluation were tabulated according to route segment. Evaluations were carried out based on the criteria developed in this study. The anchor attraction ratings were 0, 0, and 1 for the existing segment, Alternate 1, and Alternate 2, respectively.

Evaluation of Communities by Population

The communities were rated according to their population. These ratings were 0, 0, and 3 for the existing segment, Alternate 1, and Alternate 2, respectively.

TABLE 3 Evaluations of Alternative Route Segments Present Around Cheyenne Loop Tour

ROUTE	ROADWAY				
	Surface	Shoulder	Align	Grade	Avg.
Guernsey to Wheatland Exit via Orin Jct. (WYO 270, US 18 & I-25) Existing Route	3.3	3.6	3.7	3.7	3.6
Guernsey (US 26) to Wheatland Exit via I-25 Alternate #1	4.0	4.0	3.8	4.0	3.9
Guernsey to Wheatland (US 26 & WYO 302) Alternate #2	4.0	3.0	3.3	4.0	3.5
Guernsey to Wheatland via Goshen County Rd Alternate #3	2.1	2.0	2.3	2.8	2.3

Evaluation of Number of Communities

The number of communities located on individual route segments was totaled and the final rating for each route segment was assigned. These ratings were 0, 0, and 1 for the existing segment, Alternate 1, and Alternate 2, respectively.

Evaluation of Scenic Beauty

The results of the scenic beauty evaluations for existing and alternate loop tour route segments are shown in Table 5.

Selection of Best Loop Tour Route

Based on the previous analysis and travel distance data, the existing loop tour route segment from Guernsey to Wheatland junction on I-25 via Orin Junction and the two alternate route segments, Guernsey to I-25 (US-26, Alternate 1) and Guernsey to Wheatland via WYO-320 (Alternate 2), were considered. The ratings for

TABLE 4 Travel Times and Lengths for Alternative Route Segments

ROUTE	TRAVEL TIME (Minutes)	DISTANCE (km)
Guernsey to Wheatland Exit via Orin Jct. (WYO 270, US 18 & I-25) Existing Route	129	212
Guernsey (US 26) to Wheatland Exit via I-25 Alternate #1	31	45
Guernsey to Wheatland (WYO 320 & US 26) Alternate #2	31	45

TABLE 5 Evaluation of Scenic Beauty for Alternative Route Segments

ROUTE	SCENIC BEAUTY				
	Stream	Lake	Mountain	Praries	Avg.
Guernsey to Wheatland Exit via Orin Jct. (WYO 270, US 18 & I-25) Existing Route	0	0	0	3.1	0.8
Guernsey (US 26) to Wheatland Exit via I-25 Alternate #1	0	0	0	3.6	0.9
Guernsey to Wheatland (US 26 & WYO 302) Alternate #2	0	0	0	3.6	0.9

anchor attractions, communities, roadway conditions, and scenic beauty for each route segment, in addition to travel distances, were entered in a matrix (Table 6). It is clear that the alternate route segment from Guernsey to Wheatland via WYO-320 has the highest loop tour value according to the proposed criteria. This alternate route adds a new attraction to the loop tour, and it goes through the city of Wheatland, which has numerous tourist facilities. Thus, this route segment is recommended to replace the existing route segment from Guernsey to Wheatland on I-25 via Orin Junction. [The existing route has a distance of 195 km (122 mi) with a few opportunities for direct access to the population. The proposed changes shorten the length of the loop tour by 150 km (195 km − 45 km = 150 km). In other words, the total length of the loop tour will become 302 km (452 km − 150 km = 302 km), which is less than the maximum length specified in this research study.]

CONCLUSIONS

In this research project, criteria were developed for designating loop tours based on roadway conditions, scenic beauty, local communities, tourist services, and national and local anchor attractions. A rating system was developed to evaluate these features. These features were rated on a scale of 1 to 5, on which 1 was "poor" and 5 was "excellent." Alternate routes on the Cheyenne and Oregon Trail loop tour were then evaluated based on the criteria developed. This research lead to the following conclusions.

1. Currently, there are no national standard criteria for selecting sites and routes for loop tour programs. The judgment of the person or committee in charge plays a major role in designating loop tours.
2. The criteria developed in this study have two levels. Level I determines the attractions and accessibility to these attractions from all Interstate highways. A round trip of less than 320 km (200 mi) or a driving time of approximately 4 hr was considered accessible in designing loop tours. Level II criteria evaluate the specific route segment and overall routing on the basis of roadway conditions, anchor attractions, communities by population, number of communities, and scenic beauty. The results from these weighted Level II evaluations can be used to find the best loop tour route segments.
3. An alternate loop tour routing was recommended for the Cheyenne and Oregon loop tour. The alternate route segment, from Guernsey to Wheatland via WYO-320, was found to be more effective in achieving the loop tour objectives than the original loop tour segment from Guernsey to Orin Junction via Hartville. The alternate loop tour routing focuses directly on Wheatland and shortens the Cheyenne and Oregon loop tour route by 150 km (94 mi).

Finally, all factors developed in this study reflect the conditions encountered in Wyoming (small and scattered populations, long distances between attractions, etc.). If this evaluation technique is to be used by other states, the weighting factors should be reexamined to reflect local conditions.

TABLE 6 Loop Tour Values Calculations

	R.C.	S.B	A. AT.	POP.	# L.C		WT. Fac		L.T.V		Distance (km)
Existing Route	3.6	0.8	0	0	0		1 1		4.4		195
Alternate #1	3.9	0.9	0	0	0	X	1.5 1.5	=	4.8		45
Alternate #2	3.5	0.9	1	3	1		1.3		11.7		45

R.C. Roadway Conditions
S.B. Scenic Beauty
A.AT. Anchor Attractions
POP. Population
#L.C. Number of Local Communities
L.T.V. Loop Tour Value

ACKNOWLEDGMENTS

This cooperative study was funded by the U.S. Department of Transportation's University Transportation Program through the Mountain-Plains Consortium, the Wyoming Division of Tourism, and the University of Wyoming. The authors would like to express their appreciation to Gene Bryan of the Wyoming Division of Tourism for his support throughout the study.

The authors are solely responsible for the contents of this paper, and the views expressed do not necessarily reflect the views of the research sponsors.

REFERENCES

1. *National Scenic Byways Study.* FHWA, U.S. Department of Transportation, Jan. 1991.
2. *Wyoming Loop Tour Brochures.* Wyoming Travel Commission, Cheyenne, 1993.
3. *A Policy on Geometric Design of Highways.* AASHTO, Washington, D.C., 1990.
4. Final Case Study for the National Scenic Byways Study. *The History of AAA's Scenic Byways Program.* FHWA, U.S. Department of Transportation, Sep. 1990.
5. Boyd, B. L. *Visual Preferences of Natural Landscapes in Southern Wyoming.* MS thesis, University of Wyoming, Laramie, 1980.
6. Ksaibati, K., E. Wilson, D. Warder, and G. Bryan. *Evaluation Criteria for Scenic Loop Tours.* MPC Report No. 94-29, March 1994.

Publication of this paper sponsored by Committee on Landscape and Environmental Design.

Geometric Design for Adequate Operational Preview of Road Ahead

J. L. GATTIS AND JOHN DUNCAN

Minimum geometric conditions must exist to provide an ample amount of preview sight distance (PVSD) for comfortable and safe traffic operations. The PVSD concept is based on the assumption that the driver views or previews the roadway surface and other cues that lie ahead to obtain the information needed for vehicular control and guidance. The driver needs a minimum PVSD to perceive and respond to upcoming alignment cues; the roadway geometry affects how much PVSD is available for the driver. A roadway designed with geometric features adequate to the design speed would in many cases provide ample PVSD, but a roadway with constrained design features could have inadequate PVSD. The paper includes a derivation of equations to calculate the available preview sight distance on a crest vertical curve and discusses two applications of the PVSD concept to sharp horizontal curves. When a geometric analysis finds that inadequate PVSD exists, upgraded signing or pavement marking to provide drivers with extra positive guidance may be considered as a means of compensating for inadequate PVSD.

A well-designed roadway should provide the driver with an adequate line-of-sight ahead or along the roadway. The AASHTO "Green Book" (*1*) states that, as a minimum, all roadways should provide the driver with adequate stopping sight distance (SSD). Decision sight distance, passing sight distance, and intersection sight distance are also needed for certain situations. Traffic engineering reference books discuss the sight distance needed to perceive and react to a changing traffic signal. But the driver has other sight distance needs in addition to stopping for hazards ahead, passing slower vehicles, negotiating an intersection, or reacting to a signal. To have a relaxed, comfortable, and safe ride, the driver also needs an adequate view of the roadway alignment ahead. This view of the road surface and other appurtenances ahead provides cues needed for control and guidance, and has been referred to, in a context of pavement marking adequacy, as preview distance (*2*). Herein it is referred to as preview sight distance (PVSD).

The outline and shape of the roadway ahead provide visual cues to help the driver guide the vehicle along and into a proper path. The actual road shape can be defined by pavement edges and curbs, and surface pavement markings may act as surrogates to define roadway outlines and shapes. For instance, the driver's view of upcoming lane lines and curb edges sweeping to the right shows the driver that a horizontal curve to the right is ahead. Other cues, such as traffic control signs or the background environment (i.e., tree lines, guardrails, etc.), may also be present to help guide the driver. Where vehicle densities are high, drivers may rely on the outline of the vehicle stream ahead for guidance.

This study focuses on the minimum crest curvature geometry that must exist to provide an ample amount of PVSD for traffic operations. Two applications of the PVSD concept to sharp horizontal curves are briefly discussed. Where ample PVSD exists, drivers can perceive upcoming alignment cues in advance and respond in order to control and guide the vehicle.

J. L. Gattis, Mack-Blackwell Transportation Center, 4190 Bell Engineering Center, University of Arkansas, Fayetteville, Ark. 72701. J. Duncan, Department of Mathematical Sciences, 301 Science-Engineering Building, University of Arkansas, Fayetteville, Ark. 72701.

DESCRIBING INADEQUATE PVSD CONDITIONS

One could assume that horizontal and vertical curvature that is flat enough to provide adequate SSD would automatically provide an adequate PVSD. Even if a roadway with adequate SSD automatically has ample PVSD, the many sections of roadways that do not conform to current geometric design standards may have inadequate PVSD.

Some of today's roads were first trails or wagon roads, and were paved after the automobile age arrived. If such roads ever were designed, it was for a much lower speed than that at which drivers now operate. It would seem that the potential for PVSD deficiencies would be greater on the many miles of older local or secondary roadways, especially those with curved alignments, than on modern primary highways. Certain locations on these subpar roads may be candidates for upgraded signing or pavement marking to provide the driver with positive guidance as a way of compensating for inadequate PVSD.

Scenario Illustrating Inadequate PVSD

A scenario involving inadequate PVSD can easily be envisioned, as in the case of an undivided urban four-lane minor arterial street in rolling terrain. The horizontal and vertical alignments were designed for 48 km/hr (30 mi/hr), but the actual 85th percentile speed on the street is over 65 km/hr (40 mi/hr). There is a 24.4-m (80-ft) omission in the centerline and lane line markings because of an intersecting street at the crest of a vertical curve. A horizontal curve to the right begins near the intersection and crest. A driver who is unfamiliar with the area, traveling in the inside lane, rapidly approaches the crest of the vertical curve. Upon entering the area bounded by the intersecting street, the driver is briefly in a cueless zone (with no lane lines or curb edge). Although now in a horizontal curve, the driver has erroneously assumed that the roadway continues straight ahead. The vehicle is well into the horizontal curve before the driver again sees roadway curvature cues, that is, the curb edge and pavement markings. If the driver cannot correct the mistake and steer into the curve quickly, the vehicle could cross over into the next lane to the left, which is an oncoming traffic lane.

In this example, the combination of a crest vertical curve and omitted pavement markings created a gap in the series of cues being provided to the driver. Fog or overdriving the headlights may cre-

ate the same effect. If for any reason the flow of cues on which the driver is relying for guidance is inadequate, then there is a greater potential for guidance levels falling below what is needed for safe and comfortable vehicle operation. The inadequate PVSD may result in erratic positioning of the vehicle within a lane, driving outside of the lane boundaries, or an accident. Vehicle control errors have more severe consequences on roads with narrow lanes. For instance, an additional 0.3-m (1-ft) deviation in lane position due to inadequate PVSD in addition to normal lateral variation may not be critical when driving in a wide lane, but the same amount of deviation on a narrow lane could cause the vehicle to encroach on adjacent lanes.

Breaking the Problem Into Components

Analyzing the adequacy of the PVSD along a roadway segment involves a comparison of the available PVSD with the needed PVSD. However, available research does not fully define all of the parameters of such an analysis.

Available PVSD may be constrained by near and far limits. As the driver looks through the front windshield to gather cues for vehicle guidance, the driver's close-up view is obstructed by the front hood. The driver cannot see any closer ahead than this minimum distance. The far limit of the driver's view of roadway surfaces and markings may be governed by the roadway geometry. In the absence of supplementary cues, cues are derived from that length of roadway between the near and far limits of the driver's view of the pavement surface.

The needed PVSD is not so easily defined. Conceptually, it is the length of roadway traveled while the driver perceives and reacts to upcoming roadway guidance cues. It is not easy to measure driver preview time precisely. In order to approximate needed preview time, the author made a number of measurements while driving three winding highways and one city street, all of which appeared to have limited sight distance. In roadway sections that had a preview that seemed uncomfortably small, a stopwatch was used to roughly measure the elapsed time from when the driver (i.e., the author) fixed on a point on the roadway surface ahead for guidance until the vehicle passed that point. The fixed point was located the least distance ahead that allowed the driver to feel marginally comfortable, as he controlled and guided the vehicle. Measurements indicated that a minimum preview time might be on the order of 1.3 to 1.7 sec.

It should be noted that these measurements were made under the following conditions:

1. The driver's only task was to control and guide the vehicle;
2. The driver exercised a very high level of attention;
3. Attention was not diverted to perform other tasks; and
4. Although sight distance was restricted, the roadway had no unexpected gross alignment changes.

It should not be inferred that these values are suitable for design. The amount of preview needed at a given location may depend on the rigor of the required control and guidance efforts at that location. Allowances for driver fatigue, driving task-sharing, and variations among drivers could necessitate greater preview times, if the requirements of a large portion of the driving public are to be comfortably accommodated. Additional information about needed PVSD can be obtained from other studies, including some performed to assess pavement marking adequacy.

Comment

Inadequate PVSD arises when the available viewing distance of the roadway is less than the driver needs to react and make vehicle guidance adjustments. It is assumed that, other elements being equal, a driver would need more guidance on a curved alignment than on a straight alignment. On the basis of the author's driving experience, it was hypothesized that on a horizontal curve, a pavement edge can be a less effective cue on an undivided multilane roadway than it is on a two-lane roadway. This is probably because a driver in the inside lane of an undivided multilane roadway sees a wider pavement and therefore the pavement edges are a less precise "target." In addition, there is no immediately adjacent right pavement edge to help guide the driver and prevent encroachment on the adjacent lane or lanes. Perhaps the driver on an undivided multilane roadway relies more on the lane line markings for guidance through the horizontal curve than does the driver on a two-lane roadway with a well defined edge.

RELATED LITERATURE

Guidance in selecting or evaluating proper PVSD is not contained in the Green Book (*1*) or in many other common geometric design references. But discussions of various topics related to PVSD can be found in human factors literature and geometric design literature.

Tracking and Preview Time

A study on a two-lane road reported by Gordon (*3*) concluded that "On the basis of the driver's fixations, the road edges and the centerline are essential information a driver needs." Gordon noted that the "forward reference distance" of the drivers in the sample and the points they fixed on varied greatly between drivers. Among different drivers, increased forward reference distance did not correlate with increased speed. On curves to the right, drivers' fixation points on average did shift to the left but did not cross over the center line. In a subsequent article (*4*) Gordon wrote, "It is unfortunate that so little is known about the important factor of anticipation in driving. Exploratory studies are needed to determine optimal or minimal anticipation distances applicable to road signs, barriers, [and] curves."

McLean and Hoffman (*2*) reported the preview findings of a number of studies. As Table 1 shows, the findings of the various studies were not consistent. Differences between the various study methods could have contributed to the variation of the findings. Conducting studies of driver steering behavior at 32 km/hr (20 mi/hr) and at 48 km/hr (30 mi/hr), McLean and Hoffman found that for preview times of 2.5 sec or more, steering behavior did not appreciably change. When preview times were less than 2.5 sec, there was an increase in erratic steering behavior. At both 32 km/hr (20 mi/hr) and 48 km/hr (30 mi/hr), about 21 m (70 ft) of far sight distance was needed for drivers to align their cars adequately. At 40 km/hr (25 mi/hr), 21 m (70 ft) is traversed in 1.9 sec. These studies were conducted on a straight road in a traffic-free environment.

When studying the adequacy of pavement markings, Allen et al. (*5*) noted that "the road perspective is determined within the first few hundred feet down the road." They concluded from previous research that sight distances of 30–61 m (100–200 ft) were adequate.

TABLE 1 Preview Times Reported by Various Researchers

Author(s)	Driving situation	Speed m/sec (ft/sec)	Preview time sec.
Gordon	gently meandering	6.1 (20)	7
Hoffman, Joubert	slalom course	7.6 (25)	2
Kondo, Ajimine	straight	3.0-16.8 (10-55)	2-9
Kondo, Ajimine	tight curves	3.0-7.6 (10-25)	2-4
Mourant, Rockwell	open highway	21.3-30.5(70-100)	$\geq$3
Wierwille, Gagne, Knight	simulated highway	30.5 (100)	~3

Time for Other Tasks

Drivers have to perform other tasks that take time. In a synthesis of studies conducted to determine how much glance time is consumed while performing such tasks as checking vehicle instruments, checking mirrors, or reading street name signs, Taoka (*6*) listed average values ranging from 0.62 sec to well over 1 sec.

Amount of Available Visibility

Allen and O'Hanlon (*7*) discussed the need for roadway markings or delineation to provide the driver with positive guidance. The visibility of a given target is defined by its size and contrast. Steering performance is a function of the configuration of delineation and its contrast. The contrast of the target can be affected by light characteristics and environmental factors such as fog, snow, dust, and rain. At night, apparent contrast drops off more rapidly due to headlight scattering.

Currently, headlights on American cars are not uniform in either position or performance. Fambro et al. (*8*) noted that low-beam headlights should provide 15,000–20,000 candela, and high-beam lights up to 75,000 candela. Headlights do not provide an even pattern of light ahead, but rather are aimed and create "hot" spots. A low-beam light 0.6 m (24 in.) above the pavement (the average headlight height) will hit the pavement 70 m (230 ft) ahead and 1.8 m (6 ft) to the right. Presently, pavement reflectances are not well defined, but tend to be in the ranges of 10–20 percent at distances of 61–122 m (200–400 ft). Objects of 14% reflectance are visible at 119 m (390 ft) when illuminated by a source of 25,000 candela, and are visible to 158 m (520 ft) when illuminated by 75,000 candela. The reduction of light transmitted to the driver due to tinted windshields and the impact of oncoming vehicle glare must be considered. Table 2 presents findings from an older study, which approximate visibility with current low-beam headlights, both with and without glare from oncoming vehicles. Fambro et al. (*8*) noted that accident reports do not often list the accident cause as poor headlight visibility (3 percent in one study, 3–23 percent in a pedestrian accident study). The number of cases in which inadequate headlight illumination contributed to an accident but the police report listed a more easily identified factor, such as driver error or excessive speed, is unknown.

Inferences from Literature Concerning PVSD

A number of authors have recognized the need to relate the available sight distance to the sight distance needed for vehicle control and guidance. Although the reported values of needed preview time vary between research studies, the use of values no less than 2.0–3.0

TABLE 2 Visibility Distances Considering Glare

Target	Distances - m (feet)	
	No Glare	Glare
Large objects	39-88 (127-290)	32-114 (105-375)
Small objects	61-89 (201-291)	46-69 (150-228)

sec seem well supported, especially when the need for the driver to perform other tasks in addition to control and guidance is considered. Further study may show the need for a preview greater than 3.0 sec. The values reported in Table 2 imply that a driver traveling at highway speed [27 m/sec (90 ft/sec)] and dimming the headlights while meeting an oncoming vehicle's headlights would briefly have less than 2.0–3.0 sec of preview time. That is, the PVSD available for the driver could be less than is desirable.

EQUATIONS TO SOLVE FOR AVAILABLE PVSD

The amount of needed PVSD may vary according to the complexity of the driving task ahead. A basic need is to be able to see the roadway alignment cues, specifically the lane lines and pavement edges or curbs, far enough ahead to control and guide the vehicle into the roadway. The following equations can be used to estimate the amount of PVSD provided in certain situations.

Solution for Crest Vertical Curve

Figure 1 shows terms used in the derivation of a solution for a parabolic crest vertical curve of the form $x^2 = -4ay$, with the x coordinate of the vertex being 0. The parameter a is uniquely defined by knowing the slope g at any point (other than at the vertex) of known horizontal distance x from the vertex; $a = x/2g$. Suppose that at a point a horizontal distance (q) to the left of the vertex the slope is $g_1 = \tan\theta$. Taking the first derivative of the equation and substituting yields the following.

$$x^2 = -4ay \tag{1}$$

$$2x = -4ay' \tag{2}$$

$$2q = 4ag_1 \tag{3}$$

$$2q/g_1 = 4a \tag{4}$$

If point x is at the point of vertical curvature (PVC), then $2q$ is the length of the horizontal chord.

Now let the slope of a tangent to the parabola at another point x be $-g_2$ when $x = p$, given $p > 0$. Let L_{qp} be the horizontal distance between the points $x = q$ and $x = p$.

$$2p = 4ag_2 \tag{5}$$

$$L_{qp} = q + p = 2a(g_1 + g_2) \tag{6}$$

$$L_{qp}/[(g_1 + g_2)/2] = 4a \tag{7}$$

$$L_{qp}/[(g_1 + g_2)/2] = 2q/g_1 \tag{8}$$

Note that $(g_1 + g_2)/2$ is the average slope between the pair of points $x = -q$ and $x = p$.

The profile tangent sight distance (PTSD when used as a term, or c when used as a dimension) will be defined as the line of sight from the driver's eye to a point that intercepts and is tangent to the curvature of the pavement surface. If the roadway surface is entirely relied on for guidance cues through a crest vertical curve, the PTSD becomes the available PVSD. In deriving a simple formula, this distance c may be measured horizontally (as is done in the field) without significant error. Similarly, the height h of the driver's eye above the pavement surface may be measured vertically. Assuming that both the driver and the point at which the line of sight intercepts the pavement surface are within the limits of the crest vertical curve, PTSD extends from the driver's position at the coordinates $(x - c, f(x - c) + h)$ to the intercept point $[x, f(x)]$.

A parabola has a constant PTSD in both directions, that is, from left to right or from right to left. (It is an interesting mathematical exercise to show that any twice-differentiable curve with a constant PTSD in both directions, measured horizontally, must be a parabola.) The condition for a constant PTSD is given by

$$f(x) - f(x - c) - h = c\,f'(x) \tag{9}$$

If

$$f(x) = -kx^2 \tag{10}$$

then this delay differential equation becomes

$$-kx^2 + kx^2 - 2kcx + kc^2 - h = -2kcx \tag{11}$$

The PTSD for the parabolic vertical curve is thus found by the following substitutions.

$$x^2 = -4ay \tag{12}$$

$$y = x^2/-4a = -kx^2 \tag{13}$$

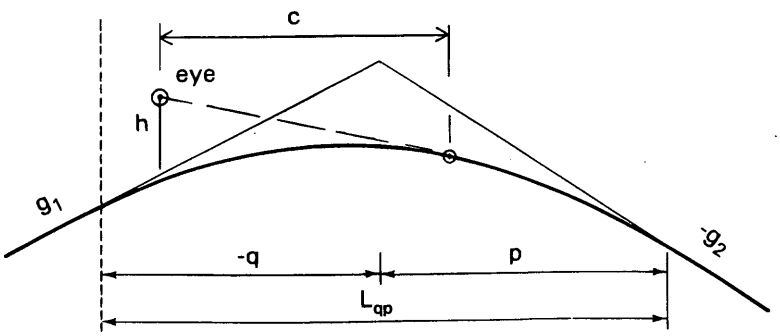

FIGURE 1 Derivation of PTSD for crest vertical curve, driver within curve.

where $k = 1/4a$

$$c^2 = \frac{h}{k} = \frac{h}{1/4a} = 4ah = \frac{2gh}{g_1} \quad (14)$$

Taking the square root,

$$c = \sqrt{\frac{2gh}{g_1}} = \sqrt{4ah} \quad (15)$$

for a parabolic vertical curve in which both gradients have an equal absolute value. For a vertical curve in which the two gradients are unequal, further substitution yields the generalized equation

$$c = \sqrt{\frac{L_{qp}\,h}{(g_1 + g_2)/2}} = \sqrt{\frac{2\,L_{qp}\,h}{g_1 + g_2}} = TSD \quad (16)$$

The common formula for stopping sight distance when SSD $< L$ is, in effect, a summation of two of these equations to find c. One part calculates c_1 with a driver's eye height (h_1) of 1.07 m (3.5 ft) and the line-of-sight tangent to the vertical curve surface; the other calculates c_2 from the point at which the line of sight touches the curve surface to the point at which an object is a height h_2 of 0.15 m (0.5 ft) above the surface.

$$SSD = c_1 + c_2 = \sqrt{4ah_1} + \sqrt{4ah_2} \quad (17)$$

Solution for Crest Vertical Curve with Driver in Advance of Curve

The preceding solution assumed that both the driver and the point at which the driver's line of sight intercepted the pavement surface were within the limits of the crest vertical curve (i.e., needed sight distance was less than vertical curve length). When a driver is approaching the beginning PVC but is still a distance b in advance of the PVC (see Figure 2), then a different equation must be derived.

The physical or actual vertical curve commences at the PVC. However, a theoretical vertical curve parabola exists in advance of the actual PVC. There is a vertical distance j between a driver's actual elevation on the tangent grade in advance of the PVC and a point on the theoretical crest vertical curve parabola beneath the driver. For a driver positioned in advance of the PVC, the PTSD now becomes

$$c = \sqrt{\frac{L_{qp}\,(j + h)}{(g_1 + g_2)/2}} = \sqrt{\frac{2L_{qp}\,(j + h)}{g_1 + g_2}} \quad (18)$$

The value of j may be found as follows.

$$b = \sqrt{\frac{L_{qp}\,j}{(g_1 + g_2)/2}} \quad (19)$$

$$j = \frac{b^2\,(g_1 + g_2)/2}{L_{qp}} \quad (20)$$

If a value for the PTSD when both the driver and the line-of-sight intercept are within the vertical curve has been determined, then the PTSD for a driver located in advance of the PVC may be simply found by

$$c = \sqrt{\frac{L_{qp}\,h}{(g_1 + g_2)/2} + b^2} \quad (21)$$

If the vertical curve length is greater than the needed PVSD, the equation implies that the available PTSD for a vehicle in advance of the PVC will be greater than the available PTSD for a vehicle that has passed the PVC but is still within the limits of the vertical curve.

Examining a Horizontal Curve

In a horizontal curve, the driver's view of the roadway ahead may be less than what is needed to give an adequate preview. Restricted PVSD can occur if other vehicles or roadside objects restrict the PVSD, or if the roadway curves out of sight.

A sharp curve to the right can illustrate two possible assumptions. In one approach, it is assumed that even if adjacent vehicles in the right lane limit the distance ahead that the driver can view his own lane, the absence of oncoming traffic allows the driver to receive cues from the opposing lane's pavement edge or lane lines. In a more conservative approach, it is assumed that the driver must obtain advance cues from the driver's own lane.

Using the more conservative assumption, the distance ahead over which the driver must preview the road surface will not be adequate if the needed line of sight is blocked by a roadside object or another vehicle on the inside of the curve. The available PVSD may be approximated by the common Green Book (*1*) formula for an obstruction blocking the view around a horizontal curve.

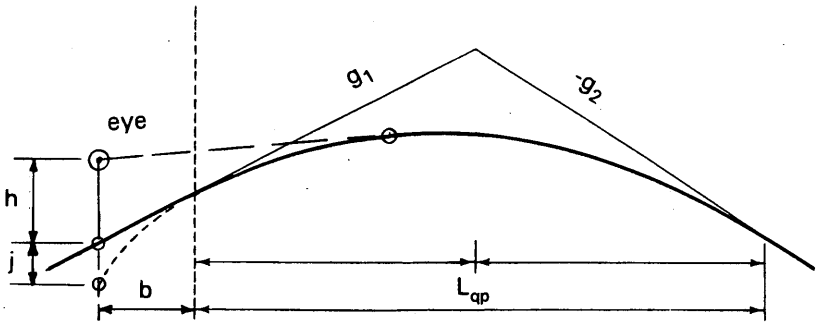

FIGURE 2 Derivation of PTSD for crest vertical curve, driver ahead of curve.

$$\text{available PVSD} = \arccos\left(1 - \frac{M}{R}\right) * \frac{R}{28.648} \quad (22)$$

where R is the radius in feet of the path traveled by the vehicle and M is the lateral offset distance from the path traveled by the vehicle to the object obstructing the driver's view. This view-restricting object may be a vehicle in the next lane or a roadside object.

The other causal situation is related to a horizontal curve being so sharp that the roadway ahead falls outside of the driver's normal high-resolution vision cone. If the conservative assumption is used, the driver must retain in his or her cone of vision the lane markings defining the driver's own lane. Continuing with the curve to the right, assume a lane width W, limits of well-defined vision on either side of a "straight ahead line of sight" defined by a cone of 2θ, and the driver's head turned ϕ degrees into the curve. The outside (i.e., to the left of the driver) lane line will fall outside the cone's right edge at a distance ahead of the driver equal to the needed PVSD for any radius R less than the R approximated in the following equations.

$$\sqrt{R^2 - [PVSD * \cos(\theta + \phi)]^2} = R - \frac{W}{2} - PVSD * \sin(\theta + \phi) \quad (23)$$

$$R = \frac{PVSD^2 + \frac{W^2}{4} + W * PVSD * \sin(\theta + \phi)}{W + 2 * PVSD * \sin(\theta + \phi)} \quad (24)$$

R is a radius of the outside (left) line of the travel lane, shown in Figure 3. For a two-lane roadway, the outside lane line is the centerline.

APPLICATION FOR A DESIGN ANALYSIS

The previously discussed "easily envisioned scenario involving inadequate PVSD" is a location where the construction plans show a +3.68 percent grade followed by a −4.64 percent grade. These grades are connected by a crest vertical curve of 73.2 m (240 ft), on which the design speed is 48 km/hr (30 mi/hr). An intersecting street forms a T intersection at the crest. The calculated stopping sight distance, according to the 1990 Green Book (*1*) is 59.6 m (195.7 ft).

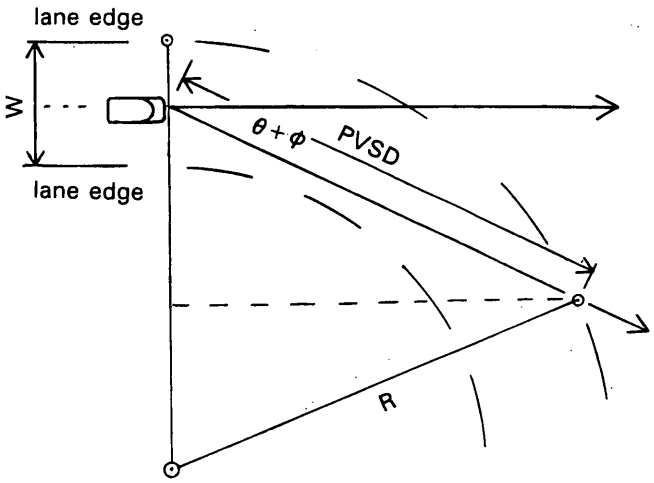

FIGURE 3 Horizontal alignment curving out of sight.

Using Equation 16, the calculated distance at which a driver loses sight of the pavement surface over the crest of the vertical curve is

$$\text{TSD} = \sqrt{\frac{2 * 73.2 * 1.067}{0.0368 + 0.0464}} = 43.3 \quad (25)$$

$$(\text{TSD} = \sqrt{\frac{2 * 240 * 3.5}{0.0368 + 0.0464}} = 142.06 \text{ ft})$$

The PVSD needed for the 85th percentile speed of 71 km/hr (44 mi/hr) and an assumed 2.5 sec to react and maneuver is 49.2 m (161.3 ft). Thus, the available PTSD is slightly less than the needed PVSD. When driving through the actual intersection, the driver momentarily experiences an absence of control and guidance cues while approaching the crest. (The road surface in the crest area lacks pavement markings.) Providing short dashed markings through the intersection would be one way of addressing this situation and helping unfamiliar drivers to negotiate the roadway.

RELATION TO CURRENT RESEARCH

The preview sight distance issue is related to the ongoing study of driver workload and design consistency. A driver who travels a roadway that has continuous geometric design inadequacies and who perceives the inadequacies may have the advantage of being more alert than a driver on a 10-km straight road who suddenly encounters the one 35-km/hr curve, but neither driver has the ability to anticipate or respond to a design inadequacy until it comes into view. It seems that on a roadway that has continuous design inadequacies, the driver would devote a greater proportion of attention to road-following, thus diminishing the attention that can be devoted to other tasks such as monitoring vehicles and pedestrians entering from the side. Indeed, a prolonged, continual state of heightened alertness may accelerate driver fatigue.

The preview sight distance concept also affects the re-evaluation of stopping sight distance criteria. Current criteria for visibility over a crest vertical curve allow a driver with a 1.06-m (3.5-ft) eye height to see a 0.15-m (0.5-ft) high object in time to stop, assuming a 2.5-sec perception-reaction time. For a tangent gradient difference of 7.0% and a 90-km/hr (56-mi/hr) design speed, a 490-m (1608-ft) vertical curve results. If the object height were revised upward to a 0.38-m (1.25-feet) taillight height, then needed vertical curve length would decrease to 365 m (1196 ft). Such a vertical curve would provide 106 m (346 ft) of PTSD, while 100 m (328 ft) would be needed to allow a 4.0-sec preview for perception-reaction and maneuver. At higher design speeds, the 0.38-m (1.25-feet) object height would permit 4.0 sec or more preview time, but crest curves designed for this object height on roadways with design speeds less than 82 km/hr (51 mi/hr) would not have an available PTSD that allows 4.0 sec of roadway surface preview.

Table 3 presents the SSD for given speeds along with the PVSD required for a 4.0-sec preview. The listed object heights (h_2) are those that, when used for vertical curve–SSD design, would also yield an adequate PTSD.

CONCLUSION

Although roadways designed to meet current stopping sight distance standards may also have more than adequate preview sight

TABLE 3 Vertical Curve Design Object Heights To Provide PVSD

	Design speed - km/hr			
	50	65	80	90
Needed SSD - m (ft)	63	97	140	169
PVSD for 4.0 sec. - m (ft)	56	72	89	100
Object height (h_2) - m (ft)	0.016	0.13	0.34	0.50

1 km/hr = 0.62 mph
1 m = 3.28 ft

distances, roadway sections on which the running speeds exceed the design speeds may have inadequate PVSD. Where inadequate PVSD exists, the flow of vehicle control and guidance cues to the driver may be deficient, causing the driver to either sacrifice vehicle control or to concentrate on control to the exclusion of other driving tasks (such as monitoring other traffic).

A summary of needed preview times measured by other researchers showed findings ranging from 2 to 9 sec, with variations in speed and experiment conditions explaining part but not all of the variations between the studies. Preview times measured by the author were slightly lower than those found in the literature. Given that the author's lower values represent only one subject, and that a "best case performance" was measured, the author's lower values are not surprising.

The equations that were presented can be used to evaluate the geometry of existing designs in suspect or problem roadway segments. When establishing design values for PVSD, the engineer must remember that the driver cannot perform all driving tasks simultaneously. Therefore a minimal PVSD, measured when the driver is only concentrating on control and guidance, may be inadequate for all but simple driving situations. Previous research and the author's experience suggest that PVSD values of from 2.5 to 4.0 sec or more sec may be needed. Additional research into human factors could better define the amount of time a driver needs to preview adequately the upcoming roadway alignment and still have time to perform other necessary driving tasks. Even though more effort is needed to define desirable PVSD for various situations, designers can still be cognizant of the concept. One application of the PVSD principle is the design of the roadway in advance of exit ramp gores located in crest vertical curves.

An analysis can identify sections of roadway that have insufficient PVSD. These sites may be candidates for upgrading traffic control devices or other remedial actions to provide the driver with an adequate flow of roadway cues for control and guidance. If inexpensive countermeasures such as upgrading traffic control devices prove to simplify the driving task or reduce accidents, then the roadway agency investment would be easily justified.

ACKNOWLEDGMENT

The support of the Mack-Blackwell National Rural Transportation Study Center at the University of Arkansas made this paper possible.

REFERENCES

1. *A Policy on the Geometric Design of Streets and Highways. AASHTO,* Washington, D.C., 1990.
2. McLean, J. R. and E. R. Hoffman. The Effects of Restricted Preview on Driver Steering Control and Performance. *Human Factors,* Vol. 15, No. 4.
3. Gordon, D. A. Experimental Isolation of Drivers' Visual Input, *Public Roads,* Vol 33, No. 12. Bureau of Public Roads, Washington, D.C., Feb. 1966, pp. 266–273.
4. Gordon, D. A. Perceptual Basis of Vehicular Guidance, *Public Roads,* Vol. 34, No. 3. Bureau of Public Roads, Washington, D.C., Aug. 1966, pp. 53–68.
5. Allen, R. W., J. F. O'Hanlon, D. T. McRuer, et al. *Driver's Visibility Requirements for Roadway Delineation, Vol. I.* FHWA-RD-77-165. Federal Highway Administration, Washington, D.C., Nov. 1977, p. 125.
6. Taoka, G. T. Duration of Drivers' Glances at Mirrors and Displays, *ITE Journal,* Vol. 60, No. 10. Institute of Transportation Engineers, Washington, D.C., Oct. 1990, pp. 35–39.
7. Allen, R. W., and J. F. O'Hanlon. Effects of Roadway Delineation and Visibility Conditions on Driver Steering Performance, *Transportation Research Record 739.* TRB, National Research Council, Washington, D.C., 1979, pp. 5–8.
8. Fambro, D. B., K. Fitzpatrick, L. I. Griffin, K. B. Kahl, R. J. Koppa, and V. J. Pezoldt. *Determination of Stopping Sight Distances,* Interim Report, NCHRP Project 3-42. Texas A&M University, College Station, Tex. Dec. 1992.

Publication of this paper sponsored by Committee on Operational Effects of Geometrics.

Evaluation of Flush Medians and Two-Way, Left-Turn Lanes on Four-Lane Rural Highways

KAY FITZPATRICK AND KEVIN BALKE

Three types of medians are typically used on four-lane rural highways in Texas: raised (or depressed) medians, two-way, left-turn lanes (TWLTLs), and flush medians. On roads with flush medians, the area between the travel lanes is paved and can easily be traversed by a vehicle. This type of median is typically used in areas that shift from rural to suburban. Research was conducted to examine the differences in the operation and safety of four-lane rural highways with TWLTLs and four-lane rural highways with flush medians. A review of accident rates found no statistical differences in the number of accidents on highways with TWLTLs and highways with flush medians when driveway densities were low. Field studies also found no difference in the way these two median treatments operate in rural areas. Therefore, it was concluded that drivers use flush medians and TWLTLs similarly. However, Texas law prohibits the use of flush medians as a storage area or an acceleration/deceleration area for turning left into and out of adjacent properties. The results of the research suggest that drivers ignore the meaning of the solid yellow lines used to mark flush medians. Therefore, to promote uniformity and consistency, it is recommended that flush medians be used only on highways on which the frequency and spacing of driveways permit individual median openings at each driveway. On four-lane rural highways on which this is not possible, it is recommended that TWLTLs be used.

AASHTO defines the median as "the portion of divided highway separating the traveled way for traffic in opposing directions" (*1*). Because medians increase the separation between two opposing vehicles, it may be argued that medians, regardless of type, improve traffic safety by reducing the potential for head-on collisions and by providing an area in which errant or out-of-control vehicles can recover before entering oncoming traffic lanes. Depending on their width, medians also improve safety by reducing headlight glare and by providing an area out of the traffic stream for disabled vehicles to stop in case of emergencies. Medians also improve traffic flow by providing motorists with a place to store (or wait) while making a left turn. Many motorists use the median to accelerate or decelerate when turning on or off a highway. In some cases, medians are used to reserve right-of-way for future roadway expansion.

Median types include median islands and two-way, left turn lanes (TWLTL). Each median type is used in different situations to achieve different levels of control over left-turn access to adjacent properties. The type of median used on a highway depends on several factors, including the following (*1*):

- Functional classification and location of the highway,
- Availability of right-of-way,
- Design speed of the highway,
- Type and intensity of development adjacent to the highway, and
- Desired level of control over left-turn access.

K. Fitzpatrick, Transport Operations Program, Texas Transportation Institute, College Station, Texas 77843-3135. K. Balke, Traffic Management and Information Systems, Texas Transportation Institute, College Station, Texas 77843-3135.

Median islands offer the highest degree of control over left turns into adjacent properties. They use a physical barrier or island to separate opposing directions of traffic. Left-turn access is controlled through the placement of established breaks, or openings, in the median and at intersections. The median can range in width from as little as 1.2 m in highly developed areas, where right-of-way is extremely limited, to 23.8 m in suburban and rural areas, where right-of-way is typically less constrained. In general, raised medians are used on a higher functional class of highways, on which it is desirable to maintain as little interruption to the through movement of traffic as possible.

TWLTLs are at the other end of the spectrum in terms of the amount of control that can be exercised over left turns into adjacent properties. With TWLTLs, left-turning vehicles have unlimited access to adjacent properties. TWLTLs can be used by left-turning vehicles from either direction on the highway and can be used as a storage area for left-turning vehicles waiting for gaps in the opposing traffic stream. Traffic engineering research has shown that because the vehicle is physically removed from the main traffic stream, both traffic safety and flow can be dramatically improved with the installation of a TWLTL on a highway (*2–4*). AASHTO (*1*) provides the following recommendation on the use of TWLTLs: "In general, continuous left-turn lanes should be used only in an urban setting where operating speeds are relatively low and where there are no more than two through lanes in each direction."

The task of highway planners is to determine what type of median is most appropriate on highways whose roadside development shifts from rural to urban or suburban conditions. The problem becomes particularly acute where rural highways enter small urban communities. In those areas, the amount of roadside development increases the demand for left-turn areas. There may be situations in which it is desirable to separate opposing traffic streams and control access to adjacent properties without the expense of installing a median island.

In these situations, some jurisdictions in Texas have used flush medians to separate opposing traffic streams. Flush medians combine many of the attributes and features of raised medians and TWLTLs. With the flush median design, the area between the travel lanes is at-grade. The median area is marked with either a single solid yellow line or double solid yellow line. Left-turn access to adjacent properties is provided at left-turn bays that have been striped at established locations. Since the median area is at-grade, it

can be easily traversed by drivers turning into and out of adjacent properties. Many drivers use flush medians as if they were TWLTLs; however, this appears to be a violation of Texas law. Article VI, Section 62 "Driving on Divided Highway" of the *Texas Motor Vehicle Laws* (*5*) states:

> Whenever any highway has been divided into two (2) or more roadways by having an intervening space or by a physical barrier or clearly indicated dividing section so constructed as to impede vehicular traffic, every vehicle shall be driven only upon the right-hand roadway unless directed or permitted to use another roadway by official traffic-control devices or police officers. No vehicle shall be driven over, across or within any such dividing space, barrier or section, except through an opening in such physical barrier or dividing section or space or at a crossover or intersection as established by authority.

This section of the law has been interpreted as prohibiting the use of a flush median as a refuge area for left turns as well as prohibiting vehicles from turning across a flush median, except at established openings (*6*). Therefore, there appears to be a discrepancy between the law and the way drivers use flush medians.

The purpose of this research was to examine the differences in the operation and safety of four-lane rural highways marked with TWLTLs and four-lane rural highways marked with flush medians. Field studies were performed in a Texas Department of Transportation (TxDOT) district (Lufkin) to measure how four-lane highways in fringe areas operate when they are marked with either a TWLTL or a flush median. A comparison of accidents on four-lane highways marked with TWLTLs and four-lane highways marked with flushed medians also was performed to determine whether there is a difference in the safety of highways with these types of median treatments. On the basis of the results of these analyses, recommendations were made on the application of flush medians on rural four-lane highways.

METHODOLOGY

Field studies were performed to evaluate the traffic operational characteristics of flush medians and TWLTLs on four-lane rural highways. The primary goal of the field studies was to determine whether there is any difference in the operations at these different median treatments. It was reasoned that if the frequencies of particular maneuvers (i.e., left turns from a through lane, left turns from within the median treatment, etc.) were similar at each type of median treatment, then the two median treatments were considered to be performing similar functions (i.e., serving as refuge or storage area for left turning vehicles, etc.). To test this hypothesis, field studies were performed to observe how drivers use the two median treatments in rural areas to make left turns into and out of adjacent businesses.

Study Sites

Operational data were collected at four sites. Three of the sites were located on US-69 west of Lufkin, Texas. One of these was located along a section of US-69 that had been striped with a TWLTL (Site 1). At this site, traffic was observed entering and exiting a gasoline station/convenience store. The other two sites on US-69 were located along a portion of the highway that had been striped with a flush median. One of these two driveways provided access to a self-service laundry (Site 2), and the other provided access to a construction company storage yard (Site 3). No high-volume generators that could be used in the data collection effort were located in the flush median section of US-69.

The fourth site (Site 4) was located on US-59/Loop 224 on the outskirts of Nacogdoches, Texas. US-59/Loop 224 is, for the most part, a divided roadway that passes to the west of Nacogdoches; however, a portion of roadway (approximately 0.8 km) was striped as a flush median. The driveway that provided access to a gasoline station/convenience store was selected for the study. This particular site was similar in characteristics and traffic volumes to the two-way, left-turn site on US-69 in Lufkin (Site 1).

Data Collection

Manual turning movement counts were performed at each of the four sites. Two hours of turning movement data during three data collection periods were gathered: a.m. (7:00 to 9:00), noon (11:30 to 1:30), and p.m. (4:30 to 6:30). These time periods were assumed to have the greatest probability of traffic performing the desired turning movements into the selected study locations. Turning movement volumes were recorded in 15-min intervals for the entire duration of the 2-hour data collection period.

Traffic volume and turning movement counts were performed for traffic traveling on the highway and for traffic exiting the selected driveway at each site. For the highway traffic, vehicle turning movements were grouped into the following categories:

- Total traffic: the sum of all through and turning traffic traveling in both directions on the highway at the driveway location;
- Total left-turning traffic entering driveway: the sum of all left-turning traffic entering the study driveway by turning left from the through lanes, turning left from the median area, or turning right after executing a U-turn at a nearby median opening;
- Left turn from median area: the number of vehicles entering the study driveway by turning left from within the median area;
- Left turn from through lanes: the number of vehicles entering the study driveway by turning left from a through travel lane; and
- Right turn after U-turn at median opening: the number of vehicles entering the study driveway by making a right turn after performing a U-turn at a nearby median opening.

For vehicles exiting the study driveway, vehicle turning movements were grouped into the following categories:

- Total exiting traffic: the sum of all left-turning and right-turning traffic exiting the site through the study driveway;
- Exiting left turn: the number of vehicles exiting the site through the study driveway by performing a left-turn maneuver; and
- Number of two-stage movements: the number of left-turning exiting vehicles that used the median either as an acceleration lane or as a storage (or waiting) area to execute a two-stage, left-turn maneuver.

Videotapes also recorded operations at each of the study sites during the times for which turning movement data were collected. The videotape served as a backup to the manual counts in case additional post hoc analyses were desired or if clarifications of the data were required.

Data Reduction

A summary table showing the number of vehicles performing each type of maneuver is presented in Table 1 for the three data collection periods (a.m., noon, and p.m.). These data were then used to compute the following operational measures:

- The percentage of left-turning traffic that turned from within the marked median (i.e., used the median as a storage area),
- The percentage of left-turning traffic entering the driveway that turned outside of the marked median (i.e., turned left from a through lane), and
- The percentage of exiting traffic that used the median for a two-stage left turn maneuver.

For the most part, traffic volumes and driveway density were higher, and more development existed in the section of US-69 that contained the TWLTL site (Site 1). Generally, the flush median sites were located in a more rural area with lower driveway densities and lower traffic volumes. As a result, a limited amount of traffic entering and exiting the driveways for the two flush median sites on US-69 was observed (Sites 2 and 3).

STUDY RESULTS

The percentage of vehicles entering and exiting the sites for the three data collection periods revealed that most drivers executed their turns from the median area, regardless of how it was striped. At all but one location, almost all the traffic observed entering the four study sites did so using the median area.

No vehicles were observed turning left from the through lane at any of the flush median sites. The data suggest that drivers do not perceive the striped median as an area prohibited to travel and use the flush median as they would a TWLTL.

Except for the a.m. period at Site 2, relatively few vehicles were observed traveling to an established median opening and performing a U-turn to gain access to the sites. At Site 2, 40 percent of the vehicles entering the site did so after making a U-turn at a nearby median opening; however, this observation was based on an extremely limited number of vehicles entering the driveway. In terms of actual counts, the 40 percent of traffic entering the site after making a U-turn represents two of the five vehicles using the driveway.

Less than 10 percent of the left-turn exiting traffic at each of the sites was observed using the median as a storage area or as an acceleration lane. A test of proportions was used to determine whether the differences in the observed percentages of exiting traffic using the median for storage or acceleration at Site 1 and Site 4 were statistically significant. Although a greater percentage of left-turn traffic exiting the driveway at the TWLTL site used the median, the test indicated that there was no statistical difference in the percentages for Site 1 and Site 4 in both the a.m. and noon data collection periods. Because of a malfunction in the video recording equipment, the p.m. period data for Site 4 were not available. Therefore, a comparison of the use of the median at Site 1 and Site 4 could not be performed for the p.m. peak. However, comparison of the a.m. and noon periods suggests no difference in the way motorists use a flush median or TWLTL when existing the driveways.

FINDINGS AND DISCUSSION

The results of the field studies indicated that for all practical purposes, there was no difference in the way the flush medians and TWLTLs function on four-lane rural highways when comparing data for each of the periods observed. For the most part, the proportion of drivers using the flush median as a storage area (both when entering and exiting a driveway) was equal to the proportion of drivers using the TWLTL for the same purpose. In fact, nearly all the vehicles observed entering the driveway at all of the sites turned left from the median area. Very few were observed turning left from the through lanes or going to a nearby median opening to gain access to the study sites. Therefore, the operational data collected indicate no difference in the way flush medians and TWLTLs function on four-lane, rural highways.

The fact that drivers are using flush medians and TWLTLs similarly suggests that either type of median would be appropriate for these roadways. The Manual on Uniform Traffic Control Devices (*7*) recognizes the need for the uniform application of traffic control devices and states that similar situations should be treated in similar ways. Since Texas law prohibits using a flush median as a left-turn lane to gain access to adjacent properties, the findings of this research suggest that, in situations in which denying access to adjacent properties is not needed, the TWLTLs may be more appropriate than a flush median on a four-lane rural highway. Using TWLTLs in these situations would promote the uniform application

TABLE 1 Traffic Counts at Operational Field Study Sites

Time Period	A.M.				Noon				P.M.			
Site Number	1	2	3	4	1	2	3	4	1	2	3	4
Major Road Total Traffic	1784	902	815	1899	1597	871	726	2251	2284	1489	909	2396
Total # of Left-Turns Entering Driveway	24	5	3	43	21	1	3	45	34	0	0	28
Left Turn from Through Lane	0	0	0	0	0	0	0	0	0	0	0	0
Left Turn from Median Area	24	3	3	42	21	1	3	45	34	0	0	28
Right Turn After U-turn at Median Opening	0	2	0	1	0	0	0	0	0	0	0	0
Minor Road Total Traffic	53	5	4	100	36	2	5	109	56	8	5	94
Exiting Left Turn	26	0	1	38	12	2	1	55	31	5	3	44
Number of Two-Stage Maneuvers	2	0	0	1	1	0	0	2	2	0	NA*	NA*

* Data are not available due to equipment malfunction.

of pavement markings in situations where left turns are permitted to adjacent properties.

The use of flush medians should be reserved for situations in which operational and safety concerns warrant that access to adjacent properties be controlled. In such cases, however, a high level of enforcement will be needed to ensure that drivers use the flush median as intended. Without enforcement, flush medians do *not* appear to be effective in controlling access to adjacent properties. Therefore, almost constant enforcement will be required to restrict left-turn access across flush medians. Since constant enforcement is impractical in most situations, the only truly effective way to control left-turn access is by installing a physical barrier, such as a raised or depressed median island or a median barrier. With this type of treatment, left-turn access to adjacent properties is limited to established median openings, the location and design of which can be controlled by the highway agency.

ANALYSIS OF ACCIDENTS

It is well-documented that installing a TWLTL on a roadway that was previously undivided can substantially improve safety and operations. Research shows that accident rates decrease by approximately 20 percent or more after installing TWLTLs on previously undivided highways (*2,3*). Furthermore, TWLTLs can reduce some types of accidents, such as rear-end and sideswipe accidents, by as much as 30 percent (*3*). The reason is that TWLTLs provide an area for left-turning vehicles to queue outside of the through travel lanes while waiting to turn. TWLTLs also provide a refuge and merging area for vehicles turning left out of adjacent properties.

Little, however, is known about the safety benefits of flush medians. A review of the literature did not reveal any studies evaluating the safety benefits of installing a flush median on a roadway that previously was undivided. Furthermore, no studies comparing the operational and safety effects of TWLTLs and flush medians were found.

A comparison of accident rates and accident severity for roadways marked with TWLTLs and flush medians is discussed. The comparison is based on 3 years of accident data. Both total accident and mid-block accident rates are used in the comparison. All the sites used in the comparison were located near Lufkin, Texas, in an attempt to control for regional differences between drivers.

Analysis Procedures

A comparative approach was used to evaluate the safety effects of TWLTLs and flush medians on four-lane rural highways in Texas. Accident rates from sites that experienced similar traffic volumes and roadside development, but had different median treatments (i.e., either a TWLTL or a flush median), were used in the comparison. Analysis of variance procedures was used to determine whether there was a statistical difference in the accident rates between the roadways marked with the different median treatments. Initially, the analysis sought to compare differences in accident rates and accident severity on four-lane rural highways with median islands, TWLTLs, and flush medians; however, the raised/depressed median sites had to be eliminated from the analysis because they did not have the same operating characteristics (i.e., traffic volumes and roadside development levels) as the TWLTL and flush median groups for the sites available in the Lufkin district.

Study Sites

When a comparative approach is used in studying accident statistics, it is important that the study locations have similar operating characteristics and roadside development levels. This is done to ensure that the effects of the different median treatments, not differences in study locations, are evaluated. For this reason, all the sites used in the accident analysis were taken from the Lufkin district in Texas. By using study locations from the same district, it was believed that regional differences in driving population and growth patterns would be controlled in the analysis. Also, the Lufkin district is primarily rural. Since the emphasis of this study was on the operational and safety effects of TWLTLs and flush medians in rural areas, the study focused on the rural driving population. Finally (and perhaps most importantly), flush medians are a common type of median treatment in the Lufkin district, which made locating potential study sites for both the safety and operational studies somewhat easier.

Potential sites were initially identified using TxDOT's Roadway Inventory Data Base. Candidate locations were identified based on pavement width, number of lanes, and roadway classification (i.e., rural versus urban). Transportation officials from the Lufkin district were then asked to identify the type of median treatment used at each of the candidate locations. In addition, officials from the Lufkin district provided drive-through video recordings of all the flush median and TWLTL sites. The video recordings were later used to estimate the driveway densities at each site.

Table 2 provides a summary of the locations used in the analysis. Initially, six sites were located on highways with TWLTLs, and three sites were located on highways with flush medians.

Accident Rates

Accident frequencies were obtained for each of the study sites using the Texas Accident Data Base maintained by the Texas Department of Public Safety. The accident frequencies were then converted to accident rates using the corresponding traffic volumes from each of the study sites. Accident rates were used to account for differences in the length of each of the study sites. Rates were developed using 3 years (1989, 1990, and 1991) of accident statistics at each of the sites. Both total accident rates and mid-block accident rates were computed for each year from these statistics. Table 2 lists the rates for each site.

To compute the total accident rate, all reported accidents occurring at a study location were used (including those accidents classified as intersection and intersection-related in the TxDOT accident data base). It was believed that this rate provided a true representation of the total accident experience on highways with the different median treatments. This rate included accident data from both signalized and unsignalized intersections.

Mid-block accident rates also were used in an attempt to isolate the effects of the median treatment on safety. The rates were developed using the accidents identified in the data base as occurring in the mid-block sections between intersection locations. They do not include accidents classified as occurring at signalized or unsignalized intersections. However, the rate does include accidents specifically related to vehicles entering and exiting adjacent properties through driveways. It was hypothesized that a high mid-block accident rate indicated potential problems with vehicles using the median to turn into and out of adjacent properties.

TABLE 2 Characteristics of Accident Sites

Median Treatment	Highway	Length (km)	Speed Limit (kmph)	ADT (1991)	Driveway Density (Drwy/km)	Total Accident Rate*			Mid-Block Accident Rate*		
						1989	1990	1991	1989	1990	1991
TWLTLs	US 59	1.29	80	11,605	100.6	8.03	4.44	7.79	3.78	1.48	4.38
	FM 1275	2.25	72	17,503	47.1	8.98	11.28	10.91	4.19	6.38	5.55
	US 59	1.61	88	5,780	9.6	0.00	0.00	1.48	0.00	0.00	1.48
	SH 103	2.1	72	7,802	30.9	7.05	5.02	1.65	3.13	2.93	0.41
	US 69	1.61	88	13,010	24.1	1.62	1.18	1.16	1.62	1.18	0.93
	LP 304	1.61	80	7,353	12.9	2.83	5.13	3.92	2.83	5.13	3.36
Flush Median	LP 224/US 59	0.97	88	17,486	13.3	1.33	2.79	1.17	1.33	2.79	1.17
	US 59	2.41	88	7,017	14.0	3.24	1.63	0.80	1.62	0.81	0.40
	US 69	5.63	88	6,799	12.4	1.16	0.94	1.11	0.97	0.75	0.55

* Accidents per Million Vehicle Kilometers

In addition to examining the effects of the different median treatments on accident rates, the analysis also examined how the different median treatments may have affected the severity of accidents at a site. Since major accidents (i.e., those resulting in fatalities) tend to be random events on rural highways, mid-block accident statistics were grouped into three categories based on the severity rating assigned to each accident by the investigating police officer:

- Severe: accidents that resulted in a fatality or incapacitating injury,
- Minor: accidents in which the reporting officer noted a non-incapacitating or possible injury as a result of the accident, and
- Noninjury: accidents that resulted in property damage only.

Using these categories, accident severity rates were developed for each of the 3 years at each study site.

Accident Analysis

Analysis of variance techniques were used to determine whether accident rates and severity of accidents differed on highways with flush medians and highways with TWLTLs. Using these techniques, it was possible to determine what proportion of the total difference in accident rates and accident severity on the highways could be attributed to the different median treatments, and what proportion was due to random effects within sites with similar median treatments. Three years of accident statistics were used in the analysis. The analysis examined the total and mid-block accident rates, as well as severe, minor, and noninjury accident rates. Differences in accident rates were assessed at a 95 percent confidence level.

Table 3 summarizes the results of the comparison. As shown in this table, statistically significant differences were found in all the accident rates, except in the rates of severe and minor accidents.

TABLE 3 Summary of Accident Analysis

	Analysis Using All Sites			Analysis Using Sites with Low Driveway Densities	
	TWLTL (6 sites)	Flush Medians (3 sites)	Significant Difference?	TWLTL (3 Sites)	Significant Difference?
Average Accident Rates (Accidents/Million Vehicle Kilometers)					
Total	4.85	1.58	Yes	2.22	No
Midblock	2.70	1.16	Yes	2.14	No
Average Accident Severity Rates (Accidents/Million Vehicle Kilometers)					
Severe	0.18	0.16	No	0.19	No
Minor	0.80	0.43	No	0.47	No
Non-Injury	1.72	0.58	Yes	1.48	No

Note: The initial analysis used data from all the TWLTL sites and compared the average of the TWLTL sites to the average of the flush median sites. The second analysis only used the data from the three TWLTL sites with low driveway density. Its average was also compared to the average of the flush median sites.

This suggests that highways with TWLTLs typically experience higher accident rates, in terms of both total and mid-block accidents, than do highways marked with flush medians. These results also suggest that, in general, the rates of noninjury accidents tend to be higher on roadways with a TWLTL than on those with a flush median.

However, these results were not supported by the results of the operational field studies. For this reason, a more detailed review of the characteristics of the individual sites was performed. As shown in Table 2, considerable differences existed between the characteristics of some of the TWLTL sites and the flush median sites. Several of the TWLTL sites had considerably higher driveway densities. Since the number of access points is expected to have a significant impact on accident rates on a highway, the TWLTL sites with high driveway densities could not be considered comparable to the flush median sites. Therefore, those TWLTL sites that had more than 14.5 driveways per km were dropped.

After eliminating the TWLTL sites that had significantly higher driveway densities, accident and severity rates were compared again using analysis of variance techniques. As indicated in Table 3, the results of the analysis showed that there was no significant difference in either total accident rate or mid-block accident rate for highways marked with a TWLTL and highways using a flush median treatment. Neither was any statistical difference observed between the rates of severe, minor, and noninjury accidents. Therefore, it can be concluded that on highways with comparable characteristics (i.e., driveway densities and posted speed limits) one type of median treatment is not superior to the other, at least from a safety standpoint.

It should be noted, however, that this conclusion is only valid for highways with a relatively low level of development (i.e., with a driveway density of less than 14.5 driveways per km). Where driveway densities are higher, a significant difference in the safety performance of highways using TWLTL and flush median treatments may be observed. But since highways with flush medians and high driveway densities could not be found for this analysis, this hypothesis remained untested in this study.

SUMMARY

Medians on rural and urban highways serve many functions, including separating opposing streams of traffic, reducing headlight glare, providing a recovery area for errant vehicles, and providing storage and acceleration/deceleration areas for turning vehicles. The type of median (i.e., flush, raised or depressed, or TWLTL) that should be used on a highway depends on a number of factors. This study offers guidelines on what type of median is most appropriate on highways where the roadside development shifts from rural to suburban. In these situations, some TxDOT districts use flush medians to separate opposing traffic streams. Flush medians combine many of the attributes and features of raised or depressed medians and TWLTLs. Unfortunately, there are no clear guidelines indicating when flush medians are appropriate on four-lane rural highways.

The purpose of this research was to examine differences in the operation and safety of four-lane rural highways with TWLTLs and four-lane rural highways with flush medians. Safety was evaluated by reviewing 3 years of accident records from four-lane rural highways with both of these types of median treatments in the TxDOT Lufkin district. Total accident rates, mid-block accident rates, and three levels of accident severity were analyzed. This review found no statistical difference in accident rates and severity between highways with TWLTLs and highways with flush medians when driveway densities were low (i.e., less than 14.5 driveways per km). Because of the limited number of flush median sites, however, it was not possible to determine whether a difference in safety between these two median treatments exists at higher levels of development (i.e., with driveway densities greater than 14.5 driveways per km).

Field studies evaluating the traffic operational characteristics of flush medians and TWLTLs on four-lane rural highways were performed. Observations of how vehicles used the median area on highways with these two median treatments were also performed. Turning movement volumes at select driveway locations on four-lane rural roadways striped with a flush median or a TWLTL were collected. These data were used to assess whether there was a significant difference in the way left-turning vehicles used the median area.

The field studies found that for all practical purposes, there was no difference in the way drivers used highways marked with TWLTLs and highways marked with flush medians. The number of drivers observed using the flush median as a storage area and as an acceleration lane was about equal to the number of drivers observed using the TWLTL for those maneuvers. Based on the operational data, it was concluded that there was no difference in the way flush medians and TWLTLs function on four-lane rural highways.

RECOMMENDATIONS

On the basis of the results of this study, it appears that drivers are ignoring the meaning of the flush median marking. The results have indicated that drivers use flush medians and TWLTLs similarly. Therefore, it is recommended that in order to promote uniform application of traffic control devices, flush medians should be used only in situations in which the location and spacing of driveways permit left-turn bays at every driveway location. This would provide drivers with an area to store and decelerate when executing a left turn from the highway. If median openings at every driveway are not possible then a TWLTL should be used. Using TWLTLs in these situations would promote the uniform application of pavement markings in situations where left turns are permitted to adjacent properties. However, if there is an operational or safety need to prevent left turns from the median, some form of physical barrier (such as a raised or depressed median island, or a median barrier) should be used to physically prohibit drivers from using the median area. Flush medians should not be used to control access to adjacent properties unless strict enforcement can also be provided.

ACKNOWLEDGMENT

This research was sponsored by the Texas Department of Transportation and the Federal Highway Administration. The technical coordinator for the study was Jerry Shelby.

REFERENCES

1. *A Policy on Geometric Design of Highways and Streets.* American Association of State Highway and Transportation Officials, Washington D.C., 1990.

2. Walton, C. M., R. B. Machemehl, T. W. Horne, and W. K. Fung. Accident and Operation Guidelines for Continuous Two-Way Left-Turn Median Lanes. In *Transportation Research Board 737,* TRB, National Research Council, Washington D.C., 1979, pp. 43–54.
3. Thakkar, J. S. Study Effect of Two-Way Left-Turn Lanes on Traffic Accidents. In *Transportation Research Board 960,* TRB, National Research Council, Washington D.C., 1984, pp. 27–33.
4. Nemeth, Z. Two-Way Left-Turn Lanes: State-of-the-Art Overview and Implementation Guide. In *Transportation Research Board 681,* TRB, National Research Council, Washington D.C., 1978, pp. 62–69.
5. *Texas Motor Vehicle Laws.* Issued by the Texas Department of Public Safety, Austin, Tex.
6. Balke, K., and K. Fitzpatrick. *An Evaluation of Flush Medians and Two-Way, Left-Turn Lanes on Four-Lane Rural Highways.* Texas Transportation Institute, College Station, Texas. FHWA/TX-94/1293-1. Nov. 1993.
7. *Manual on Uniform Traffic Control Devices.* U.S. Department of Transportation, FHWA, Washington D.C., 1988.

Publication of this paper sponsored by Committee on Operational Effects of Geometrics.

Travel Efficiency of Unconventional Suburban Arterial Intersection Designs

JOSEPH E. HUMMER AND JONATHAN L. BOONE

A great need exists for lower-cost design strategies to reduce congestion on major suburban arterials on which conventional techniques have been exhausted. This study examines the possible gains in travel efficiency from three unconventional strategies: the median U-turn, in which left turns are made using crossovers on the arterial approximately 180 m from the main intersection; continuous green T-intersection (CGT), in which one or two lanes at the top of the "T" receive a constant green indication; and the North Carolina State University (NCSU) Bowtie, developed during the project, in which left-turning traffic uses roundabouts on the side street approximately 180 m from the main intersection. The study used Traf-Netsim 4.0 to simulate the unconventional configurations and a conventional intersection for comparison in three factorial experiments.The experiments showed that the unconventional alternatives have the potential to provide for more efficient travel. The CGT configurations reduced travel time and stops substantially at three-legged intersections for through volumes of more than 400 vehicles per hour per lane. The median U-turn became more efficient than the CGTs at higher through volumes. An experiment with a four-legged intersection showed that the NCSU Bowtie reduced travel time and stops from the conventional configuration at about 900 or more critical through vehicles per hour. Questions remain about the unconventional strategies, but that they potentially provide for more efficient travel is clear.

Traffic congestion is a growing problem in most cities in North America, especially on major suburban arterials. Traffic engineers often face arterials on which:

- Nothing further can be done to relieve congestion with signal phasing, signal coordination, signal actuation, and other conventional operational techniques;
- Additional through or turn lanes are prohibitively expensive;
- Grade separations at intersections are too costly and are resisted fiercely by local merchants; and
- Intelligent vehicle-highway systems are not yet mature enough to provide a reliable solution.

There is a great need for a set of lower-cost operation and design strategies to reduce congestion at these locations.

North Carolina State University (NCSU) undertook a project to investigate such a set of strategies for the North Carolina Department of Transportation (NCDOT) and the FHWA. The project identified four promising unconventional strategies and investigated the key outstanding issues associated with each strategy. This project performed investigations into the travel efficiency of the strategies. There are obviously many other key variables of concern to engineers contemplating installation of an unconventional alternative, such as accident rates, acceptance by the traveling public, right-of-way costs, and construction costs. However, if an unconventional alternative does not reduce travel times, engineers will not consider it, and its effects on these other variables are unimportant. The project report (*1*) describes the effects of some of these other variables.

J. E. Hummer, Department of Civil Engineering, North Carolina State University, Box 7908, Raleigh, N.C. 27695. J. L. Boone, Hayes, Seay, Mattern, and Mattern, 225 Hillsborough Street, Suite 120, Raleigh, N.C. 27603.

STRATEGIES STUDIED

The four strategies investigated during the project included the continuous green T-intersection (CGT), the median U-turn, the NCSU Bowtie, and the continuous flow intersection. The project team selected these 4 from a list of 12 initial ideas because these had the most potential for widespread application in North Carolina and provoked questions that could be addressed within the scope of the research.

Figure 1 shows the CGT commonly used in Florida. The outside through lane at the top of the "T" receives a constant green signal, whereas the rest of the intersection operates with a typical three-phase signal. Agencies use markings and reflectors to separate the free-flow lane from the through lane subject to the signal. The project also investigated a version of the CGT used at a few locations in North Carolina, in which both through lanes at the top of the T receive a constant green signal, while left turns from the side street are directed into a merging lane in the median. The project team found no existing literature on the efficiency of either version of the CGT.

Figure 2 presents a median U-turn at a four-legged intersection. At the primary intersection, engineers prohibit left turns and specify a two-phase signal. Left-turning vehicles use the crossovers on the arterial. Median U-turns are also feasible at three-legged intersections, using one crossover and one direct left turn. The project team found some speculation in the literature about efficiency gains from median U-turns, but the only systematic study documented was a preliminary one conducted by one of the authors (*2*).

Figure 3 shows an NCSU Bowtie intersection. The authors conceived this strategy during the project; to their knowledge, this strategy has not been proposed or implemented before. The NCSU Bowtie was inspired by median U-turn placements on the side street and by the "raindrop" interchange used in Great Britain and elsewhere (*3*), in which modern roundabouts are placed at the off-ramp terminals of a diamond interchange. In the United States, raindrop interchanges have been proposed in Maryland and California. At the primary intersection of an NCSU Bowtie, engineers prohibit left turns and specify a two-phase signal. Left-turning vehicles use the roundabouts on the side street. An NCSU Bowtie is feasible at a three-legged intersection, but the efficiency gains appear to be minimal and substantial extra right-of-way (ROW) is required, so this project investigated only four-legged applications. The NCSU Bowtie is intriguing because it places the roundabouts on the side

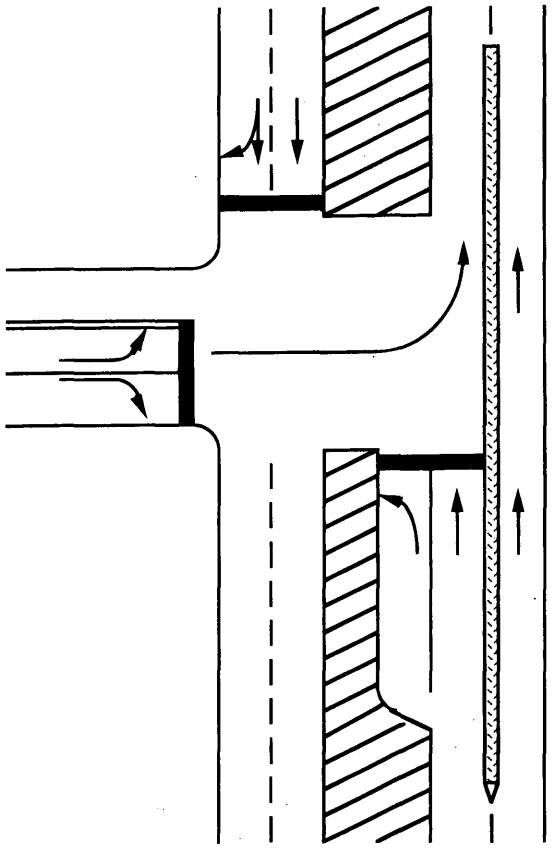

FIGURE 1 Continuous green T-intersection.

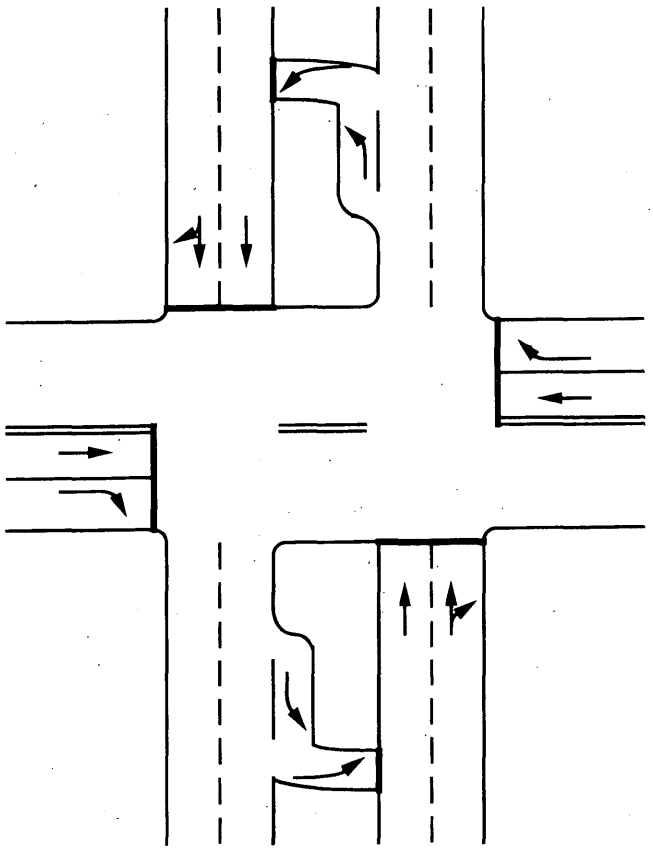

FIGURE 2 Median U-turn intersection.

street rather than the arterial [in keeping with recommended practice in Australia (*4*), for example], and because the extra ROW required for four-legged applications is not large.

The fourth strategy was a continuous flow intersection, shown in Figure 4. The continuous flow intersection crosses a left-turning movement past the oncoming through traffic at a signal upstream of the main intersection, and then guides it to the cross street near the main intersection. At the main intersection, a single signal phase then allows those left turns to move, protected, simultaneously with the through movements. This patented innovation has been implemented only once (as of November 1994), but analyses (*5,6*) and theory suggest that engineers can expect great efficiency gains from it. Since the most outstanding questions regarding this strategy center on safety and human factors, this project concentrated on those issues and did not study the efficiency of the strategy.

EXPERIMENT DESCRIPTION

The project team conducted three experiments on the efficiency of the strategies:

1. A three-legged intersection between a four-lane arterial and a two-lane side street,
2. A three-legged intersection between a six-lane arterial and a two-lane side street, and
3. A four-legged intersection between a four-lane arterial and a two-lane side street.

The primary purpose of the experiments was to determine whether the unconventional alternatives showed promise of more efficient travel within the common ranges of several key variables. The project team could not model every possible combination of volumes and did not attempt to model them all. If the unconventional alternatives showed promise, engineers could create their own models to examine conditions at the specific intersections of interest to them.

Each experiment used Traf-Netsim 4.0 (*7*) to compare the applicable unconventional strategies to a conventional design with direct, protected left turns from a single left-turn lane. Traf-Netsim was the best choice for the experiment because of its ability to simulate an entire network (needed for the unconventional alternatives), its credibility in the profession, and its large range of measures of effectiveness (MOEs).

The project team calibrated and validated Traf-Netsim for the unconventional strategies. The project team traveled to Michigan to collect data at two median U-turn intersections, to Florida to collect data at six CGT intersections, and to Maryland to collect data at the first modern roundabout in the eastern United States. The calibration data included critical gap distributions and saturation flow estimates for the median U-turn, lane distributions for the CGT, and critical gap distributions and circulation speeds for the roundabout. The validation effort encompassed travel time and stopped delay at the two Michigan median U-turn intersections and the Maryland roundabout. The results showed that field data compared reasonably well to Traf-Netsim MOEs. Model calibration and validation details are described elsewhere (*1*).

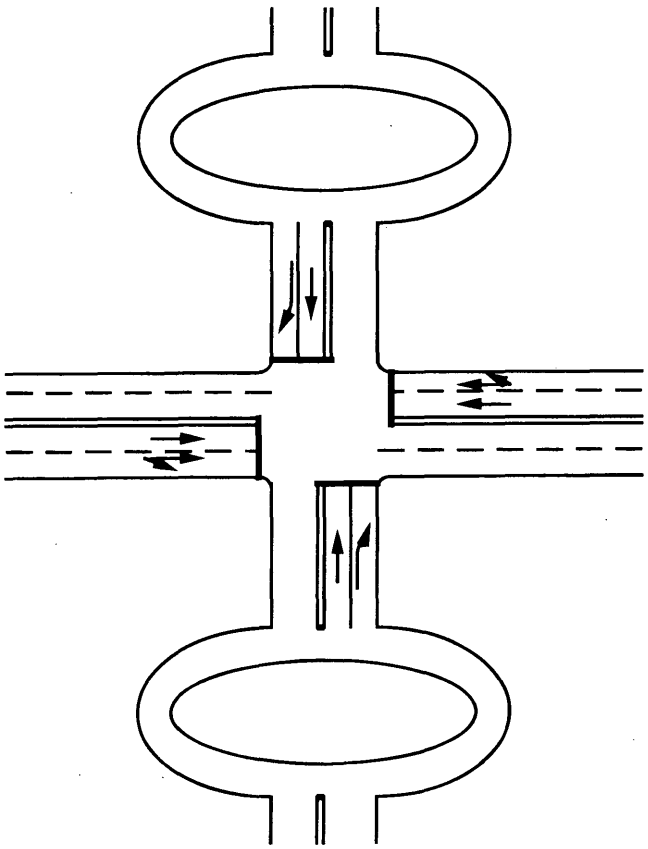

FIGURE 3 NCSU bowtie intersection.

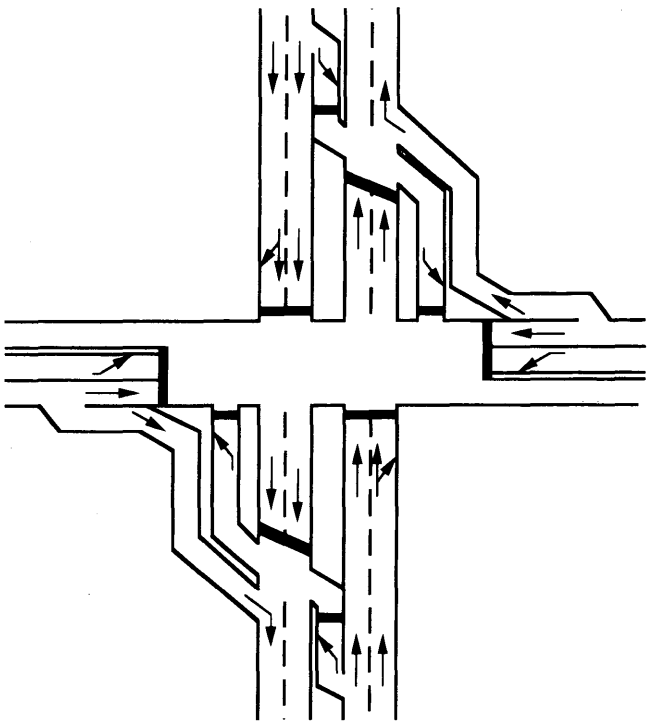

Not to scale.

FIGURE 4 Continuous flow intersection (design patented by Mier).

The project team used 30-min simulation runs after a warm-up period that did not exceed 10 min. The team used the total travel time and the total number of stops within a constant data collection boundary, which extended 488 m in each direction from the primary intersection, as the primary MOEs. Although many analyses use delay as an MOE, total travel time allowed the analysts to compare properly strategies that require vehicles to traverse a circuitous route to execute a desired movement. The team also examined the total travel time and the total stopped delay experienced by left-turning vehicles. This allows judgments about whether methods with indirect left turns penalize those motorists too severely, which could lead to violations and negative public reactions.

The project team used fixed-time signal-phasing schemes timed with Webster's method (*8*). Fixed-time signals are appropriate because many suburban arterials have them to establish progression, because the traffic volumes are high and stable during the congested peak hours of most interest (actuated phases usually reach their maxima anyway), and because the median U-turn alternative needs to coordinate the crossover and main intersection signals. For each traffic volume combination in an experiment, the project team chose a cycle length to satisfy a minimum pedestrian crossing time and to minimize the delay for the conventional intersection treatment. The cycle length was then held constant for that volume combination across each configuration and phase times were developed. This method of signal timing ensured that any differences in the MOEs were due to the configurations, not to different cycle lengths.

To isolate the effects of the strategies, several parameters were held constant in each experiment, including:

- 90-degree intersections;
- Desired free-flow speeds (72 km/hr arterial, 56 km/hr side street);
- 200 right-turn vehicles per hour;
- Right turn on red allowed;
- No left turn on red from crossovers allowed;
- 0 percent grade; and
- Single-lane turn bays, crossovers, and roundabouts.

Each experiment was a full factorial design. The team used an analysis of variance (ANOVA) technique in SAS (*9*) on a UNIX-based workstation to draw conclusions from the data.

EXPERIMENT 1

Set-Up

Experiment 1 compared the median U-turn, the Florida version of the CGT, the North Carolina version of the CGT, and the conventional strategy at the three-legged intersection of a four-lane arterial and a two-lane side street. The three factors in the experiment included the strategy, the through volumes on the arterial, and volumes of the left turn movements. Based on the *Highway Capacity Manual* (*10*) planning analysis, a total critical volume of 1,300 vehicles per hour constitutes congested conditions. The experiment therefore included three levels of through volumes [700, 400, and

100 vehicles per hour per lane (vphpl)] and three levels of left turn volumes [300, 200, and 100 vehicles per hour (vph)] to represent congested, moderate, and uncongested conditions. The team completed two replicates of the experiment with 36 runs ($4 \times 3 \times 3$) in each replicate. The only parameters that were changed between replicates were the random number seeds (the values used to decide which vehicles turn at a given intersection, assign individual driver characteristics, etc.).

Building the simulation models presented several challenges. First, the team had to choose the distance between the crossover and the primary intersection for the median U-turn. On the basis of the literature and measurements collected during model calibration (*1*), the team selected a distance of 183 m. Second, the team selected the median U-turn configuration with the direct left turn from the arterial. If the volumes of the two left-turn movements at a three-legged intersection were similar, the direct left turn from the arterial was considered superior because a direct left turn from the side street requires a difficult merge onto the arterial. Third, the team based the percentage of traffic using the free-flow lane in the Florida CGT on fifty-four 15-min observations made at three sites in Jacksonville (*1*). Finally, although there are locations in Michigan where the median crossover is stop sign–controlled, given North Carolina's typical practice regarding left turns onto multiple lane facilities, the analysts introduced a signal to control operations for the median U-turn, at the crossover. The team chose cycle, phase, and offset times for this signal that allowed for progression of the left turn from the arterial through both signals.

Travel Time Results

The ANOVA on the travel time data showed that the configuration factor and the two-factor interaction between through volume and configuration were both significant at the 99.99 percent confidence level. Additionally, the two-factor interaction between the left-turn volume and the configuration was significant at the 95 percent confidence level.

Student-Newman-Keuls (SNK) and Tukey's (*11*) means tests indicated that the median U-turn configuration accrued significantly less travel time (a mean of 1,600 minutes per run) than the other three configurations. The Florida CGT and the North Carolina CGT provided the next lowest total travel times (1,753 and 1,855 minutes per run, respectively); they did not differ significantly from each other. The North Carolina CGT and the conventional configuration (1,913 minutes per run) did not differ significantly from each other.

Table 1 shows that the efficiency of the median U-turn increased as the through volumes increased. For the low and moderate through volumes, the CGT configurations were the most efficient. At the highest through volume level, the median U-turn reduced total travel time by 12 percent to 39 percent over the standard configuration.

Stop Results

The ANOVA on the total number of stops data indicated that the configuration factor and the two-factor interaction between through volume and configuration were significant at the 99.99 percent confidence level. In addition, the two-factor interaction between the left-turn volume level and the configuration was significant at the 99 percent confidence level, while the three-factor interaction between through volume, left-turn volume, and configuration was significant at the 95 percent confidence level.

SNK and Tukey's (*11*) means tests indicated that at the 95 percent confidence level the median U-turn (mean of 724 stops per run) required significantly fewer stops than any other configuration. The North Carolina CGT and Florida CGT had means of 843 and 856 stops per run, respectively; they did not differ significantly from each other. The standard intersection, at a mean of 965 stops per run, was significantly higher than the others.

Table 1 reveals that for the lowest through volume, the Florida CGT was clearly the most efficient, with about 20 percent fewer stops than the standard configuration and 3 to 15 percent fewer stops than the North Carolina CGT, regardless of left-turn volume. For low through volumes, the median U-turn was the least efficient. At a moderate through volume level, regardless of the left-turn volume, the CGT techniques required about 20 percent fewer stops than the standard configuration, whereas the median U-turn ranged from about 10 percent better to 10 percent worse than the standard configuration. At the highest through volume, the CGTs required slightly fewer stops and the median U-turn required 30 to 60 percent fewer stops than the conventional alternative. The median U-turn performed relatively worse as the left-turn volume increased.

Left Turn MOEs

For left-turn travel time, SNK and Tukey's (*11*) means tests revealed that, at a 95 percent confidence level, the median U-turn had the highest average left-turn travel while the Florida CGT had the lowest. The standard configuration and the North Carolina CGT did not differ significantly. Table 1 shows that these results were consistent across the through volume levels, and that the only important variation across left-turn volume levels was for the median U-turn. The relative inefficiency of the median U-turn decreased as the left turn volume increased.

For left-turn stopped delay, SNK and Tukey's (*11*) means tests revealed that, at a 95 percent confidence level, the median U-turn penalized the left-turn vehicles the most, whereas the standard, North Carolina CGT, and Florida CGT configurations did not differ significantly. The patterns in Table 1 are interesting. For the CGT configurations, the relative efficiency decreased as through volume increased. For the median U-turn, the relative efficiency decreased as through volume increased and as left-turn volume decreased.

EXPERIMENT 2

Experiment 2 compared the median U-turn, the Florida CGT, the North Carolina CGT, and the conventional strategy at the three-legged intersection of a six-lane arterial and a two-lane side street. The six-lane arterial was a concern because the relatively larger proportions of through vehicles may favor unconventional strategies more than for a four-lane arterial. The factors, levels, and analysis methods were the same for this experiment as they were for Experiment 1, and the simulation models differed only slightly.

Table 2 summarizes the results from Experiment 2. Comparing Table 2 with Table 1 for the four-lane arterial experiment reveals only two important differences. First, there was less distinction between the configurations for the travel time MOE. The median U-turn was still the best, but its overall mean was not significantly different from the CGT configurations. The standard configuration was still the worst, but its overall mean also was not significantly

TABLE 1 Summary of Experiment 1 Results

Measure of effectiveness	Through volume, vphpl	Left turn volume, vph / Alt.	Percent difference between the alternative and the conventional configuration: 100	200	300
Travel time	100	NC CGT	- 3	- 2	- 2
		FL CGT	- 9	- 9	-13
		Median U-turn	+ 5	+ 9	+ 8
	400	NC CGT	- 5	- 4	- 4
		FL CGT	-12	-11	-13
		Median U-turn	- 4	0	- 4
	700	NC CGT	- 2	- 4	- 2
		FL CGT	- 3	- 4	-11
		Median U-turn	-39	-12	-31
Stops	100	NC CGT	-18	-11	- 8
		FL CGT	-22	-20	-23
		Median U-turn	+20	+31	+38
	400	NC CGT	-22	-17	-16
		FL CGT	-23	-19	-21
		Median U-turn	- 9	+ 8	+11
	700	NC CGT	-11	-13	- 9
		FL CGT	- 5	0	- 9
		Median U-turn	-61	-29	-46
Left turn travel time	100	NC CGT	- 3	- 2	- 1
		FL CGT	-32	-28	-33
		Median U-turn	+43	+30	+21
	400	NC CGT	- 1	- 1	+ 4
		FL CGT	-30	-25	-32
		Median U-turn	+52	+35	+19
	700	NC CGT	+ 2	- 1	0
		FL CGT	- 8	-22	-32
		Median U-turn	+62	+43	+14
Left turn stopped delay	100	NC CGT	- 8	- 4	- 2
		FL CGT	-11	- 6	-23
		Median U-turn	+56	+20	+ 1
	400	NC CGT	- 3	- 3	+ 9
		FL CGT	- 7	+ 1	-22
		Median U-turn	+82	+33	+ 2
	700	NC CGT	+ 4	- 2	+33
		FL CGT	+51	+ 2	+ 2
		Median U-turn	+105	+50	+31

different from the CGT configurations. The median U-turn and standard were still significantly different from each other. Second, the North Carolina CGT experienced relatively more left-turn stopped delay in Experiment 2 than in Experiment 1. In Experiment 2, the North Carolina CGT had an overall mean that was still significantly better than the median U-turn but now was significantly worse than the Florida CGT and the standard configuration. Other than these two differences, Experiment 2 results were very similar to Experiment 1 results.

EXPERIMENT 3

Set-Up

Experiment 3 compared a standard configuration to the median U-turn and the NCSU Bowtie at the four-legged intersection of a four-lane arterial and a two-lane side street. In developing the simulation models, several design and operation issues required attention. As in the three-legged experiments, the researchers needed to select the appropriate distance between the primary intersection and the U-turn crossovers. Ultimately, a 183-m separation between the primary intersection and the crossover was selected. The researchers verified this selection by conducting a preliminary analysis to determine the maximum queue length associated with the operation of the U-turn crossover for the heaviest volumes. This analysis revealed that a 183-m separation performed satisfactorily. There was uncertainty about the optimal separation between the primary intersection and the roundabouts for the NCSU Bowtie. Adequate storage between the primary intersection and the roundabouts was a concern. Based on preliminary simulation runs, a 183-m distance and two lanes on the approach to the primary intersection proved adequate. Finally, based on the literature and a trip to the first modern roundabout on the East Coast (in Lisbon, Maryland),

TABLE 2 Summary of Experiment 2 Results

Measure of effectiveness	Through volume, vphpl	Left turn volume, vph / Alt.	Percent difference between the alternative and the conventional configuration: 100	200	300
Travel time	100	NC CGT	- 4	- 2	- 2
		FL CGT	-12	-10	-10
		Median U-turn	+ 1	+ 9	+ 8
	400	NC CGT	- 5	- 4	- 4
		FL CGT	-12	-12	-14
		Median U-turn	- 4	- 1	- 9
	700	NC CGT	- 7	-12	- 3
		FL CGT	-13	-11	+ 7
		Median U-turn	-37	-14	-18
Stops	100	NC CGT	-22	-12	-12
		FL CGT	-23	-11	-18
		Median U-turn	+11	+37	+29
	400	NC CGT	-22	-18	-19
		FL CGT	-20	-21	-24
		Median U-turn	-14	+ 5	+ 2
	700	NC CGT	-17	-33	- 6
		FL CGT	-19	-16	- 7
		Median U-turn	-59	-36	-44
Left turn travel time	100	NC CGT	- 2	- 1	+ 4
		FL CGT	-33	-30	-31
		Median U-turn	+42	+64	+29
	400	NC CGT	+ 1	+ 3	+ 6
		FL CGT	-29	-24	-30
		Median U-turn	+61	+42	+20
	700	NC CGT	+ 6	+ 7	+31
		FL CGT	-11	-23	-18
		Median U-turn	+66	+45	+37
Left turn stopped delay	100	NC CGT	- 8	- 2	+11
		FL CGT	-13	- 9	-14
		Median U-turn	+54	+20	+18
	400	NC CGT	+ 3	+ 7	+12
		FL CGT	- 4	+ 4	-19
		Median U-turn	+109	+52	+ 3
	700	NC CGT	+16	+16	+74
		FL CGT	+42	- 2	+ 5
		Median U-turn	+116	+54	+40

the team selected a roundabout diameter of 30 m, a vehicle speed in the roundabout of 24 km/hr, and a more aggressive gap-acceptance distribution than the default distribution (*1*).

For the experiment, the team selected five independent variables: configuration, main street through volume, main street left-turn volume, side street through volume, and side street left-turn volume. Each volume variable had three levels, with the highest levels together corresponding to a total intersection critical volume of 1,400 vph. The analysts completed one full replicate during the experiment, resulting in the analysis of $3 \times 3 \times 3 \times 3 \times 3 = 243$ runs. One full replicate of the experiment was appropriate for two reasons. First, the analysts chose to include the four- and five-way interactions into the error term in the ANOVA. Interpreting the trends associated with the higher-level interactions would be very complicated. Additional replicates are more appropriate when attempting to interpret those interactions. Secondly, by including those interactions in the error term of the model, the F statistic and therefore the analysis would be more conservative. The team examined the same four MOEs as during the first two experiments.

Travel Time Results

The ANOVA on the travel time results showed that the configuration factor; the 4 two-factor interactions involving configuration; and the three-factor interactions between configuration, main street through volume, and side street through volume were significant at the 99 percent confidence level. SNK's and Tukey's means tests indicated that the median U-turn configuration required significantly greater travel times (mean of 2,817 min per run) than the standard configuration (2,578 min per run) and NCSU Bowtie configuration (2,586 min per run) at the 95 percent confidence level. The means for the standard configuration and NCSU Bowtie did not differ significantly.

Although their overall mean travel time values were similar, the interaction results in Table 3 show that the standard configuration performed best at the low and moderate main and side street through volume levels, whereas the NCSU Bowtie configuration responded more favorably to the higher through volumes. Across the highest main and side street through volume levels, the Bowtie accumulated approximately 7 percent less total travel time than the standard configuration. Looking at the three-way interaction results in Table 3, the breakpoint at which the NCSU Bowtie begins to operate more efficiently than the conventional alternative was about 900 critical through vehicles per hour. The travel time savings were about 15 percent at the highest combination of through volume levels. There was little relative variation between the standard and NCSU Bowtie configurations across left-turn volume levels. The median U-turn required the most total travel time over almost all volume combinations considered.

Stop Results

The ANOVA on the number of stops revealed that the following factors were significant at the 99 percent confidence level: the configuration; the two-factor interactions involving configuration and each of the remaining four factors; and the three-factor interaction involving the configuration, the main street through volume, and the side street through volume. In addition, the three-factor interaction between the configuration, the main street left turn, and the side street through volume factors was significant at the 98 percent confidence level. SNK and Tukey's (*11*) means tests indicated that overall, each of the three configurations differed at the 95 percent confidence level. The median U-turn had a mean of 1,833 stops per run, the NCSU Bowtie had a mean of 1,550 stops per run, and the standard configuration had a mean of 1,503 stops per run.

Table 4 shows the two-factor interaction results. The most pronounced trend in these results suggests that the NCSU Bowtie provides the most promise at intersections with high main street through volumes. For the side street through volume, there was no strong trend for the NCSU Bowtie relative to the standard intersection. For main and side street left-turn volumes, Table 4 reveals a slight trend toward fewer stops for the Bowtie with low volumes. The significant three-way interactions yielded no noteworthy trends.

Left Turn MOEs

SNK and Tukey's (*11*) means tests indicated that, at the 95 percent confidence level, the median U-turn required the most left-turn travel time and stopped delay, the NCSU Bowtie the next highest, and the standard configuration the least. Typically, the NCSU Bowtie meant an increase of 20 percent to 60 percent and the median U-turn meant an increase of 60 percent to 130 percent for these MOEs compared to the standard configuration.

CONCLUSIONS

The results of the three experiments described above show that unconventional alternatives have the potential to provide more efficient travel at some suburban arterial intersections. The experiments with three-legged intersections revealed that the Florida and North Carolina versions of the CGT provided substantial reductions in

TABLE 3 Experiment 3 Travel Time Results for Significant Two-Way and Three-Way Interactions Involving Configuration

		Percent difference between the alternative and the conventional configuration	
Variables and units	Levels	Median U-turn	NCSU Bowtie
Main street through volume, vphpl	300	+ 12	+ 6
	400	+ 12	+ 4
	500	+ 5	- 7
Side street through volume, vph	100	+ 16	+ 5
	300	+ 12	+ 5
	500	+ 3	- 6
Main street left turn volume, vph	50	+ 6	0
	125	+ 9	+ 2
	200	+ 13	+ 1
Side street left turn volume, vph	50	+ 4	- 3
	125	+ 9	+ 1
	200	+ 14	+ 4
Main street through volume, vphpl * Side street through volume, vph	300 * 100	+ 17	+ 12
	300 * 300	+ 14	+ 8
	300 * 500	+ 5	+ 5
	400 * 100	+ 19	+ 9
	400 * 300	+ 14	+ 8
	400 * 500	+ 5	- 3
	500 * 100	+ 10	- 5
	500 * 300	+ 9	+ 1
	500 * 500	- 2	- 15

TABLE 4 Experiment 3 Stop Behavior Results for Significant Two-Way Interactions Involving Configuration

		Percent difference between the alternative and the conventional configuration	
Variable and units	Level	Median U-turn	NCSU Bowtie
Main street through volume, vphpl	300	+ 28	+ 11
	400	+ 23	+ 6
	500	+ 17	- 9
Side street through volume, vph	100	+ 31	- 3
	300	+ 24	+ 7
	500	+ 15	0
Main street left turn volume, vph	50	+ 11	- 2
	125	+ 21	+ 2
	200	+ 32	+ 4
Side street left turn volume, vph	50	+ 10	- 4
	125	+ 21	0
	200	+ 33	+ 7

travel time and stops. As through volumes grow somewhere between 400 and 700 vphpl, the median U-turn becomes more efficient than the CGT configurations. The four-legged intersection experiment showed that the NCSU Bowtie was more efficient than the standard intersection at about 900 or more critical through vehicles per hour.

Engineers should be confident of these results because of the statistical significance of the factors in the ANOVAs and because the results match previous expectations. The median U-turn and NCSU Bowtie alternatives essentially reward through travelers at the expense of left-turn travelers, so it makes sense that the relative efficiency of those alternatives rises as through volumes rise. The project team urges engineers contemplating an unconventional alternative for a particular intersection to create Traf-Netsim models of the conventional and alternative intersections with the design volume levels.

While the relative efficiency of the median U-turn and NCSU Bowtie, in terms of overall travel time and stops, varied with through volume, those alternatives consistently led to substantially more travel time and stopped delay for left-turning vehicles than the standard configuration did. It is possible that these penalties on left-turn movements would lead to violations of the left-turn prohibition at the main intersection. However, existing situations in which left-turning vehicles experience extra delay show that motorists will tolerate those penalties without many violations. First and foremost, left-turning drivers in many states tolerate longer delays from protected left turns than from permissive left turns with very low violation rates. Second, left-turning drivers in Michigan use median U-turns without major violations. Finally, left-turning drivers in New Jersey tolerate extra travel time while negotiating jughandle intersections with few violations. Although there may be some level of excessive left-turn travel time that would cause many violations, the evidence suggests that with good traffic control devices, enforcement, and more than a few isolated applications, the unconventional alternatives should not cause those violations.

Many questions remain about the unconventional alternatives. This paper is focused only on the question of travel efficiency, so safety, human factors, ROW, construction costs, and other questions are out of its scope. The project report explores some of those other questions (*1*). Remaining questions regarding the efficiency of the unconventional alternatives include the following;

- How much more efficient are the median U-turn and NCSU Bowtie with two-lane crossovers and roundabouts?
- Do the increased opportunities for progression offered by the unconventional alternatives that reduce signal phases result in still greater efficiency than that demonstrated herein for individual intersections? In particular, how well would a superstreet, made up of a series of three-legged median U-turn intersections allowing each direction of an arterial to progress independently (*12*), perform?
- Is it wise to use an unconventional intersection that is superior at the higher volumes of, for example, 4 peak hours each day, and inferior for the other 20 hours each day? How do the MOEs look over a full day or week?
- The method used to time the signals in the experiments (holding cycle length constant across different strategies) was very conservative. Would using the optimum cycle length for each strategy result in lower cycle lengths and improved MOEs for the unconventional alternatives that require only two phases? Likewise, would using actuated signals provide an advantage for the conventional and CGT configurations that use multiphase signals?

In addition, when resources allow, the project team plans additional analysis of the Experiment 3 data to determine the amounts of travel time, stops, and delay shifted from the arterial to the side street at the NCSU Bowtie. This shift may increase the arterial level of service dramatically even for cases in which there is little or no change in the intersection system-wide MOEs.

ACKNOWLEDGMENTS

FHWA and NCDOT provided support for the research described in this paper. The authors thank Troy Peoples and Jim Dunlop of the NCDOT for their guidance, Stephanie Kolb for setting up some of the Traf-Netsim runs, and Diane Schwarzman of the Howard County (Md.) Department of Public Works for providing sample Traf-Netsim input. The views and opinions expressed in this paper are those of the authors and do not necessarily reflect the views and

opinions of FHWA, NCDOT, or NCSU. The authors assume full responsibility for the accuracy of the data and conclusions presented in this paper.

REFERENCES

1. Boone, J. L., and J. E. Hummer. *Unconventional Design and Operation Strategies for Over-Saturated Suburban Arterials.* Draft Final Report. NCDOT, Raleigh, N.C., June 30, 1994.
2. Hummer, J. E., and T. D. Thompson. A Preliminary Study of the Efficiency of Median U-turn and Jughandle Arterial Left Turn Alternatives. Presented at 72nd Annual Meeting of the Transportation Research Board, Washington, D.C., Jan. 1993.
3. Ourston, L. Wide Nodes and Narrow Roads. Presented at 72nd Annual Meeting of the Transportation Research Board, Washington, D.C., Jan. 1993.
4. Troutbeck, R. J. The Capacity and Design of Roundabouts in Australia. Presented at 72nd Annual Meeting of the Transportation Research Board, Washington, D.C., Jan. 1993.
5. F. Mier and Associates. *Tillary Street Corridor Improvement Project.* New York City Department of Transportation, N.Y., May 1991.
6. Goldblatt, R., F. Mier, and J. Friedman. Continuous Flow Intersections. *ITE Journal,* Vol. 64, No. 7, July 1994, pp. 35–42.
7. *TRAF User Reference Guide.* Version 4.2. Office of Safety and Traffic Operations R&D, FHWA, McLean, Va., Feb. 1994.
8. Khisty, C. J. *Transportation Engineering: An Introduction.* Prentice Hall, Englewood Cliffs, N. J., 1990, p. 275.
9. *SAS Procedures Guide.* Version 6, 3rd ed. SAS Institute, Inc., Cary, N.C., 1990.
10. *Special Report 209: Highway Capacity Manual.* TRB, National Research Council, Washington, D.C., 1985.
11. Anderson, V. L., and R. A. McLean. *Design of Experiments: A Realistic Approach.* Marcel Decker, Inc., New York, 1974, p. 10.
12. R. Kramer. New Combinations of Old Techniques to Rejuvenate Jammed Suburban Arterials. *Proc., Conference on Strategies to Alleviate Traffic Congestion,* Institute of Transportation Engineers, Washington, D.C., 1987.

Publication of this paper sponsored by Committee on Operational Effects of Geometrics.

Tangent Length and Sight Distance Effects on Accident Rates at Horizontal Curves on Rural Two-Lane Highways

KENNETH L. FINK AND RAYMOND A. KRAMMES

Most models for evaluating operating-speed consistency on two-lane rural highways estimate operating-speed profiles based on tangent length and degree of horizontal curvature. Some models also consider the effect of sight distance to horizontal curves. To add insight on the effects of these variables on safety and operations at horizontal curves, a base relationship between accident rates at horizontal curves and degree of curvature was established, and the effects of approach tangent length and approach sight distance on this relationship were examined. The results confirm that degree of curvature is a good predictor of accident rates on horizontal curves. Although the effects of approach tangent length and sight distance were not as clear, the results suggest that the adverse safety effects of long approach tangent length and short approach sight distance become more pronounced on sharp curves.

Accident research has consistently found that accident rates on horizontal curves are 1.5 to 4 times the accident rates on tangent sections of rural two-lane highways (*1*). Most studies have found that the degree of curvature is the primary factor in the prediction of accidents on horizontal curves. (In the metric system of measurements, degree of curvature—the angle subtended by a 100-ft arc of curve—is replaced by radius as the measure of curve sharpness.)

Geometric design consistency principles suggest that, in addition to its degree of curvature, a curve's location relative to adjacent horizontal alignment features (i.e., tangent lengths) and vertical alignment features (i.e., sight distance to the curve) is an important factor in safe operations on curves. The standard procedure for evaluating geometric design consistency on rural two-lane highways is to develop a profile of 85th percentile speeds along the alignment and estimate the speed reductions required between successive horizontal alignment features (principally between approach tangents and curves). Whereas tangent length is a key variable in all procedures for evaluating operating-speed consistency, there are conflicting views on the role of sight distance. Some procedures assume sight distance to curves has no effect on operating-speed profiles, whereas other procedures account for sight distance.

Consistency evaluations require additional effort in the design process. In order to justify this additional effort, it would be necessary to demonstrate that it yields additional insight into the safety and operational effects of alternative alignment geometries. Krammes et al. (*2*) developed a speed-profile model for evaluating operating-speed consistency and conducted accident analysis to assess the benefits of speed reductions as a predictor of accident rates at horizontal curves on rural two-lane highways.

Alternative forms of the speed-profile model employed different assumptions about the effect of sight distance on speed profiles. One form assumed that sight distance has no effect on speed profiles; that is, the distance upstream of the curve at which any necessary deceleration begins is independent of the distance upstream at which the curve becomes visible, which may be a reasonable assumption for drivers familiar with the roadway. The alternative form assumed that the distance upstream of the curve at which any necessary deceleration begins cannot be greater than the distance upstream at which the curve becomes visible, which is a more reasonable assumption for unfamiliar drivers. These different assumptions affect speed reduction estimates only for a subset of curves at which drivers would accelerate to a higher speed on the approach tangent due to the limited available approach sight distance than if greater approach sight distance were available.

The accident analysis compared speed reduction estimates and degree of curvature as predictors of accident rates at horizontal curves. A sample of 1,126 curve sites was grouped into intervals of speed reduction or degree of curvature. The mean speed reduction or degree of curvature and mean accident rate for the curves in each interval were computed, and the mean speed reductions or mean degrees of curvature were regressed against the mean accident rates. For intervals of curve sites requiring no speed reduction (i.e., degree of curvature $\leq 4°$), mean accident rates did not differ significantly; whereas for intervals of curve sites requiring speed reduction (i.e., degree of curvature $> 4°$) mean accident rates increased approximately linearly with both mean degree of curvature and mean speed reduction. It was also concluded that considering the effect of sight distance to curves in the speed-profile model improved the prediction of mean accident rates. These results suggest that speed reduction estimates do provide additional insights into accident experience at horizontal curves and imply that tangent length and/or sight distance may explain some of the variability in accident rates left unexplained by degree of curvature alone.

This study describes follow-up research that was performed to examine more explicitly the effect of approach tangent length and sight distance on accident rates at horizontal curves on rural two-lane highways. First, design guidelines and accident research on tangent length and sight distance to horizontal curves are reviewed. Second, the analysis methodology is described. Next, the analysis results are presented. The final section provides a summary and conclusions.

BACKGROUND

Design Guidelines

The AASHTO (*3*) briefly addresses the issues of tangent length and sight distance relative to horizontal curve design in *A Policy on Geometric Design of Highways and Streets*. AASHTO provides the

K. L. Fink, Kimley-Horn and Associates, Inc., 3001 Weston Parkway, Cary, N.C. 27513. R. A. Krammes, Texas Transportation Institute, Texas A&M University, College Station, Tex. 77843.

guidance that "sharp horizontal curves should not be introduced at the end of long tangents" (*3*). Unfortunately, AASHTO does not define what constitutes a "sharp" curve and a "long" tangent. The guidance on vertical sight distance to horizontal curves is also limited: "sharp horizontal curves should not be introduced at or near the top of a pronounced crest vertical curve" (*3*). Again the designer is left to define "sharp," "near," and "pronounced."

Other countries that employ speed-consistency-based procedures are more precise. Germany, France, and Switzerland have guidelines on maximum lengths for tangents to avoid driver fatigue (*4*). In Germany, tangent lengths are limited by the design speed.

Sight distance criteria in the United States and Europe are similar. Most countries use a stopping sight distance model to determine the minimum allowable sight distance for a given speed along a roadway. U.S. criteria are relatively conservative. French guidelines also set a minimum value for sight distance to horizontal curves (measured from the driver's eye to the pavement surface at the beginning of the curve) as three seconds at the 85th percentile speed on the approach tangent (*5*). The Swiss have a similar guideline that sight distance to a curve should be greater than the required deceleration distance to the curve at 0.8 mpss (2.6 fpss) (*6*).

Literature Review

Four previous studies have considered tangent length among a set of candidate predictors of accident rates at horizontal curves (*7–10*). Their findings with respect to tangent length were mixed. Datta et al. (*7*) found tangent length to be a significant predictor of outside-lane accident rates for one subset of their 25 curve sites in Michigan. Terhune and Parker (*8*) evaluated tangent length (among other variables) using data bases of 78 curves in New York, 40 curves in Ohio, and 41 curves in Alabama, and concluded that tangent length was not significant. Matthews and Barnes (*9*) studied 4,666 curves on the rural two-lane portion of a State highway in New Zealand; they found a significant relationship that involved tangent length in combination with other variables and concluded that accident risk was particularly high on short radius curves at the end of long tangents, on steep down grades, and on relatively straight sections of roads. Zegeer et al. (*10*) evaluated the significance of the minimum and maximum distance to the adjacent curve; although neither variable was significant, they observed, "there appears to be evidence that tangents above a certain length may result in some increase in accidents on the curve ahead." Although these studies are far from conclusive, they suggest a possible effect of tangent length that warrants further examination.

Four studies that examined the safety effects of sight distance on rural two-lane highways were relevant (*11–14*). Although only the study by Glennon et al. (*11*) focused on horizontal curves, the other studies' analyses of accident experience versus sight distance are pertinent to this study. Two of the four studies found a relationship between sight distance and accident rates. Both Olson et al. (*12*) and Paniati and Council (*14*) concluded that the available sight distance has a significant effect on accident rates. Paniati and Council (*14*) used a surrogate measure (the distance from the crest of a vertical curve to the accident) to represent sight distance, so the results cannot be taken literally as an effect of sight distance. Glennon et al. (*11*) concluded that approach sight distance was not a significant variable in a discriminant analysis of curve sites with high and low accident rates. Fambro et al. (*13*) concluded that available stopping sight distance is not a good indicator of accidents, with the exception that "when there are intersections within limited sight distance portions of crest vertical curves, there is a marked increase in accidents." The question about the effect of sight distance on accident rates at horizontal curves remains unanswered.

ANALYSIS METHODOLOGY

The primary objectives of the analysis were to evaluate whether there are statistically significant relationships between the following:

- Accident rates on horizontal curves and the approach tangent length; and
- Accident rates on horizontal curves and the sight distance to the curve.

The analysis was performed on the same database as the Krammes et al. (*2*) study. A base regression model of accident rate as a function of degree of curvature was established. Then, analyses were conducted to determine whether tangent length and sight distance were statistically significant when added to the base model.

Hypotheses

Driver expectancy and design consistency concepts suggest general relationships among degree of curvature, tangent length, sight distance, and accident rates at horizontal curves. These effects were stated as hypotheses that guided the analysis.

It is hypothesized that, at a given degree of curvature, accident rates are higher than average for curves with short approach tangents where drivers do not have enough time to recover from the previous feature, accident rates decrease for moderate approach tangent lengths, and they increase again when the tangent length becomes so long that the horizontal curve is unexpected and the driver is not mentally prepared for it. The effect of tangent length is hypothesized to increase as the degree of curvature at the end of the tangent increases.

It is further hypothesized that, for a given degree of curvature, accident rates decrease as sight distance to the curve increases. As sight distance decreases the driver has less time to react and prepare for the horizontal curve, thus creating a greater opportunity for accidents. This effect is expected to be more pronounced for higher degrees of curvature.

Database

The database contained geometry and accident data for a sample of curve sites selected from roadways in three States: New York, Washington, and Texas. Table 1 summarizes the site selection controls and criteria.

The database included 563 curves. Because approach tangent length and sight distance to the curve vary by direction, each curve lane (direction) was treated as a separate site. Thus, the final database consisted of curve geometry and accident data for 1,126 curve sites. Pertinent geometric and identifying information for each direction of each curve was obtained from both roadway plans and field measurements. Sight distance was measured as the distance upstream from the beginning of the curve at which the curve became visible to the driver.

Police accident reports for the roadway segments were studied in

TABLE 1 Site Selection Controls and Criteria

Control	Criteria
Area Type	Rural
Administrative Classification	State
Functional Classification	Collector or Arterial
Design Classification	Two-Lane
Design Speed	≤ 88.5 km/h (55 mph)
Posted Speed Limit	≤ 88.5 km/h (55 mph)
Terrain	Level to Rolling
Grade	≤ 5 percent
Pavement	High Type
Traffic Volumes	400-3500 vpd
Lane Widths	3.05-3.66 m (10-12 ft)
Shoulder Widths	0-2.44 m (0-8 ft)
Plan-Profile Sheets	Available
Accident Data	Available
RRR Improvements	None within past 5 years
Length of Route	≥ 4.0 km (2.5 miles)
Distance from a Town	≥ 0.8 km (0.5 miles)
Distance from End of Roadway	≥ 0.8 km (0.5 miles)
Intersections	None within Curve Site

order to obtain detailed descriptions of each accident and to verify the type and location of accidents. Five years of accident data (1987 through 1991) were included for the curve sites in Washington and Texas. In New York, however, the police accident reports had been destroyed through October 1988; therefore, only 3 years and 2 months of accident data were included for sites in New York. The accident reports were analyzed to eliminate accidents that were clearly unrelated to the geometry of the roadway (e.g., animal in road, driver asleep) and to include only accidents within the curve proper (i.e., between the point of curvature and point of tangency). Furthermore, due to the limited number of accidents involving large trucks and motorcycles, they were also excluded from the analysis. Thus, the database contained 235 reported accidents involving passenger vehicles at horizontal curves. The accidents included all severity levels: property-damage-only (129 accidents), and injury/fatality (106 accidents). Accident types included run off the road (213 accidents) and both same-direction and opposite-direction multiple vehicle collisions (22 accidents)—types identified by Zegeer et al. (*10*) as being "overrepresented on curves when compared to tangents."

Statistical Analysis

Regression analysis was performed with accident rate as the dependent variable. The independent variables were degree of curvature, approach tangent length, and sight distance to the curve. Previous analysis of this database considered several additional independent variables (state, deflection angle, travel-way width, and total pavement width) and concluded that they were not statistically significant predictors of accident rates (*2*).

Because degree of curvature has proven to be a good predictor of accidents, the first step in the analysis was to establish a regression model between accident rate and degree of curvature that would serve as the basis for the analysis of tangent length and sight distance. Due to the limited size of the database, sites were grouped into nine categories of degree of curvature. The mean degree of curvature in each category was computed. The mean accident rate per million vehicle kilometers of travel at the curve sites in each category was computed by dividing the total number of reported accidents (including all accident types and severity levels) at the curve sites in the category by the sum of the vehicle kilometers traveled at those curve sites during the time period covered by the accident data. Table 2 summarizes the characteristics of the curve sites in each category.

The base regression model had the following form:

$$\text{Mean accident rate} = \beta_0 + \beta_1 \text{ mean degree of curvature}$$

The natural logarithm of the mean accident rate was also considered as the form of the dependent variable.

The effects of tangent length and sight distance were evaluated separately. Within each degree of curvature category, the curve sites were further grouped into tangent length or sight distance categories. Indicator (0–1) variables were added to the base regression model so that different intercepts and slopes could be estimated for each tangent length or sight distance category. Differences between the slopes and intercepts of the relationships between mean accident rate and mean degree of curvature for different tangent length or sight distance categories were tested for statistical significance. Figures 1 and 2 illustrate the hypothesized differences.

The significance level for all statistical tests was at $\alpha = 0.05$. Analyses were performed using the Statistical Analysis System (SAS) (*15*).

RESULTS

Mean Accident Rate Versus Mean Degree of Curvature

The regression model for mean accident rate per million vehicle kilometers versus mean degree of curvature was as follows:

$$\text{Mean accident rate} = 0.05 + 0.23 \text{ mean degree of curvature.}$$

Figure 3 is a plot of the regression model. The model has an r^2 value of 0.94. The root mean square error was 0.33 accidents per million vehicle kilometers. The model was statistically significant at $\alpha = 0.05$. These results suggest a strong and approximately linear relationship. The r^2 value is much higher than typically observed in accident analyses, because the unit of observation is a grouping of curve sites into degree-of-curvature categories which eliminates much of the variability among individual sites.

Relationship Between Accident Rate and Approach Tangent Length

Several stratifications of tangent length were tested. For example, one stratification used the three cases of tangent length based on

TABLE 2 Curve Site Characteristics by Degree-of-Curvature Category

Category	# of Curve Sites	# of Accidents	Range of D (°)	Mean D (°)	Mean Tangent Length (m)	Mean Sight Distance (m)
1	112	10	≤1	0.9	455	211
2	154	14	1-≤2	1.9	380	184
3	136	22	2-≤3	2.9	420	174
4	160	20	3-≤4	3.8	321	180
5	84	19	4-≤5	4.9	354	161
6	128	27	5-≤6	5.8	343	208
7	106	40	6-≤8	7.5	291	177
8	120	44	8-≤11	9.8	248	135
9	126	39	>11	18.3	314	170

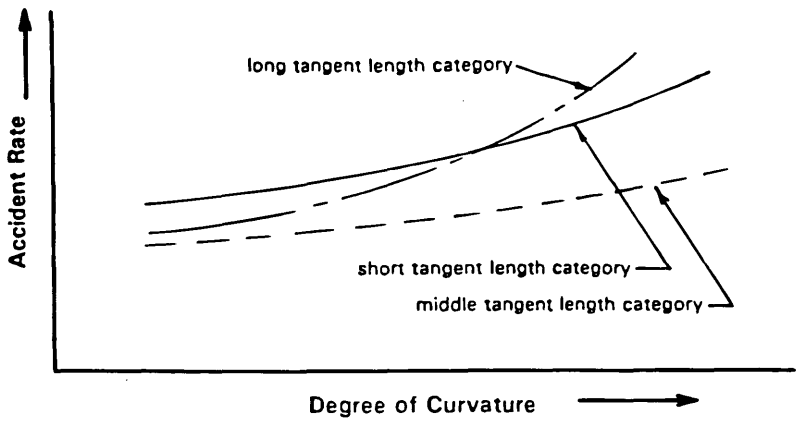

FIGURE 1 Hypothesized relationship between curve accident rate and degree of curvature category for three tangent length categories.

acceleration-deceleration patterns between successive curves in the speed-profile model; unfortunately, the paucity of data in the shortest tangent length category made the regression results unreliable.

In order to ensure a reasonable number of curve sites representing short, moderate, and long tangent lengths, three categories were defined representing the shortest 25 percent [≤107 m (350 ft)], middle 50 percent [107 m (350 ft) to 427 m (1400 ft)], and longest 25 percent [>427 m (1400 ft)] of tangent lengths in the database. The regression models were as follows:

- Shortest 25%: mean accident rate = 0.35 + 0.16 mean degree of curvature;
- Middle 50%: mean accident rate = −0.30 + 0.32 mean degree of curvature;
- Longest 25%: mean accident rate = 0.52 + 0.20 mean degree of curvature.

Figure 4 illustrates the relationships. The results indicate that the slope and intercept for the middle 50 percent of tangent lengths are significantly different from the slope and intercept for the longest 25 percent (at $\alpha = 0.05$). Although there are some statistically significant effects, the lack of consistently strong patterns in Figure 4 tempers the strength of conclusions that can be drawn. Two general findings seem warranted. First, the results support the hypothesis that the effect of longer approach tangents becomes more pronounced at higher degrees of curvature. Second, the results do not support the hypothesis that short tangent lengths increase safety problems.

Relationship Between Accident Rate and Sight Distance to a Curve

The process of selecting sight distance categories was similar to the one for establishing the tangent length categories. Several stratifications of sight distance were considered.

One stratification was based on the French sight distance criterion (i.e., a distance equivalent to 3 s at the 85th percentile approach speed). The database was broken into two categories of sight distance values: less than or equal to the French sight distance criterion, and greater than the criterion. The results with this analysis yielded no significant differences between the categories.

Another stratification was based on the deceleration distance on the approach tangent upstream of the curve calculated by the speed-profile model (*2*). The database was divided into categories of sight distances less than or equal to the required deceleration distances and sight distances greater than the required deceleration distance.

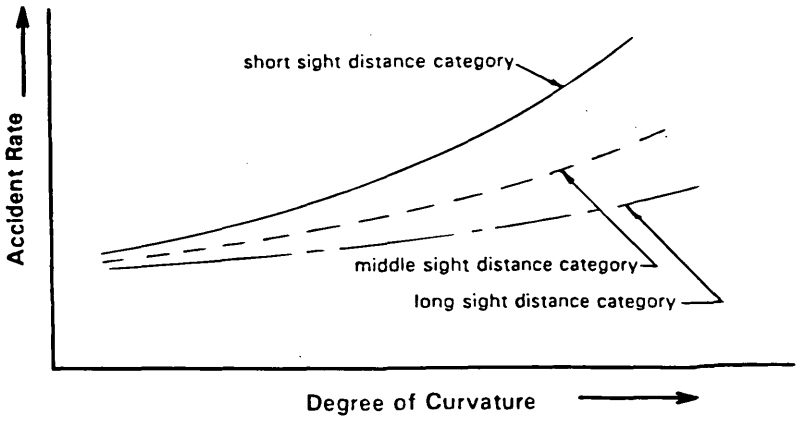

FIGURE 2 Hypothesized relationship between curve accident rate and degree of curvature category for three sight distance categories.

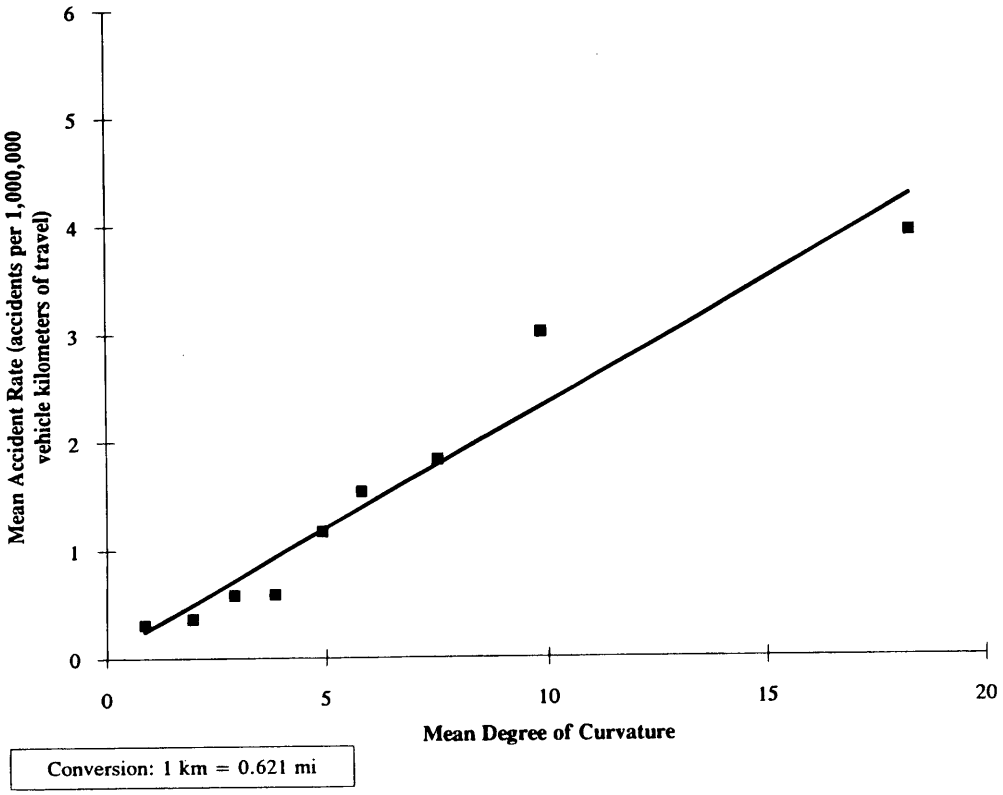

FIGURE 3 Mean accident rate versus mean degree of curvature.

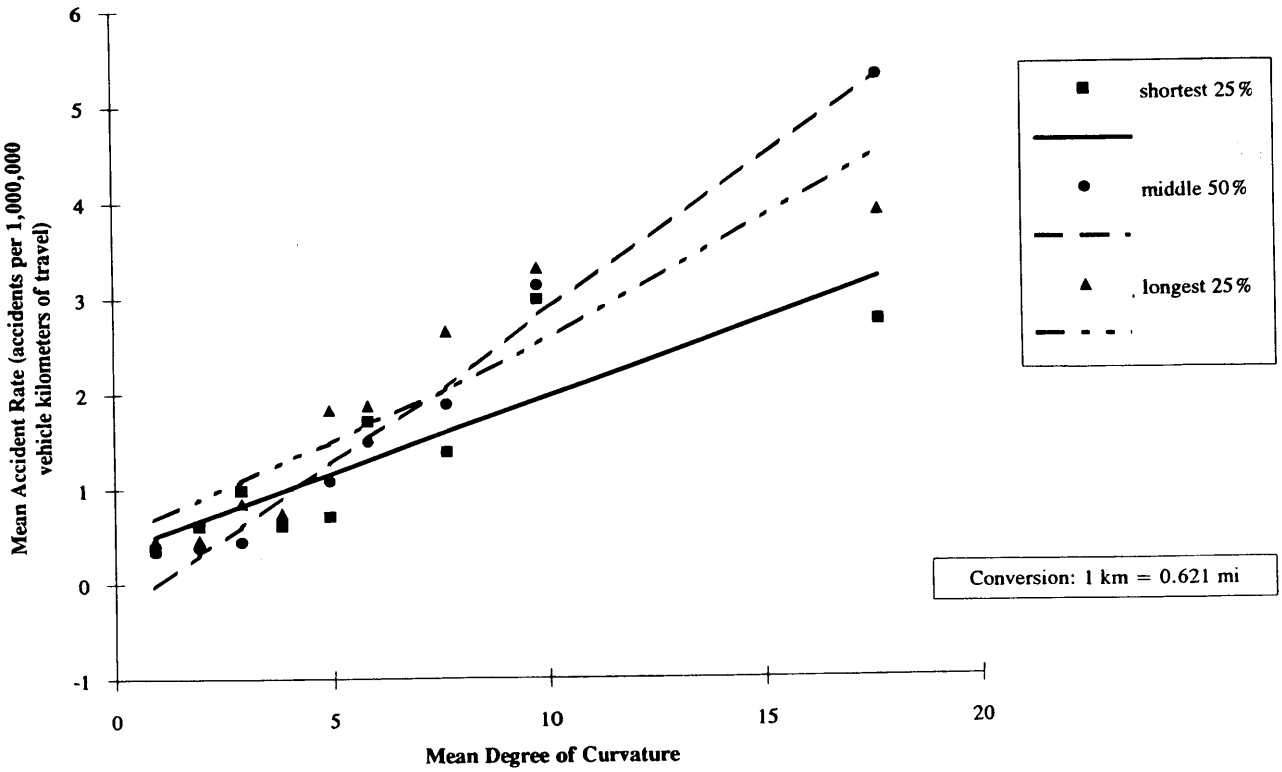

FIGURE 4 Mean accident rate versus tangent length category.

Because only 6 percent of the curve sites had approach sight distance less than the required deceleration distance, the analysis with these categories was not considered reliable.

The results presented in this study are based on categories representing the shortest 25th percent [≤61 m (200 ft)], middle 50th percent [61 m (200 ft) to 213.5 m (700 ft)], and longest 25 percent [>213.5 m (700 ft)] of sight distances in the database. With respect to stopping sight distance guidelines, the shortest sight distance category corresponds to design speeds less than 50 km/h (approximately 30 mi/h), the middle to design speeds between 50–100 km/h (approximately 30–60 mi/h), and the longest to design speeds greater than 100 km/h (approximately 60 mi/h).

The regression models for these three categories are:

- Shortest 25%: mean accident rate = −0.29 + 0.30 mean degree of curvature;
- Middle 50%: mean accident rate = 0.52 + 0.16 mean degree of curvature;
- Longest 25%: mean accident rate = −0.12 + 0.29 mean degree of curvature.

Figure 5 illustrates the relationships. Although the intercepts of the three equations do not differ significantly, the slopes for the shortest and longest sight-distance categories are significantly different from the slope for the middle sight-distance category (at $\alpha = 0.05$). As with the tangent length results, the scatter in Figure 5 tempers the conclusions that can be drawn. The steeper slope for the shortest sight distance category compared to the middle sight distance category is as hypothesized and suggests that the adverse safety effects of short approach sight distance—corresponding to design speeds less than 50 km/h (approximately 30 mi/h)—become more pronounced as the sharpness of curve increases. Contrary to the hypothesized relationships, however, the slope for the longest sight distance category is also steeper than the middle sight distance category. This result may be explained by the likelihood that most sites with long approach sight distance also have long approach tangent lengths. The greater speed reductions associated with long tangents may outweigh the benefits of long sight distance.

CONCLUSIONS

The results in this study are consistent with previous research: the relationship between accident rates and degree of curvature is clear and easy to quantify, whereas the effect of other factors is less clear and more difficult to quantify. A strong relationship between accident rate and degree of curvature category was developed.

The effects of approach tangent length and sight distance are not as clear. The results suggest that the effect of long tangent lengths becomes more pronounced on sharper curves, which is consistent with conventional wisdom and previous research and supports the benefits of evaluating speed consistency. The analysis of sight distance effects also suggests that extreme approach conditions (both long and short approach sight distance) may contribute to higher accident rates on sharper curves. Additional research to more clearly define critical ranges of approach tangent lengths and sight distance seem warranted.

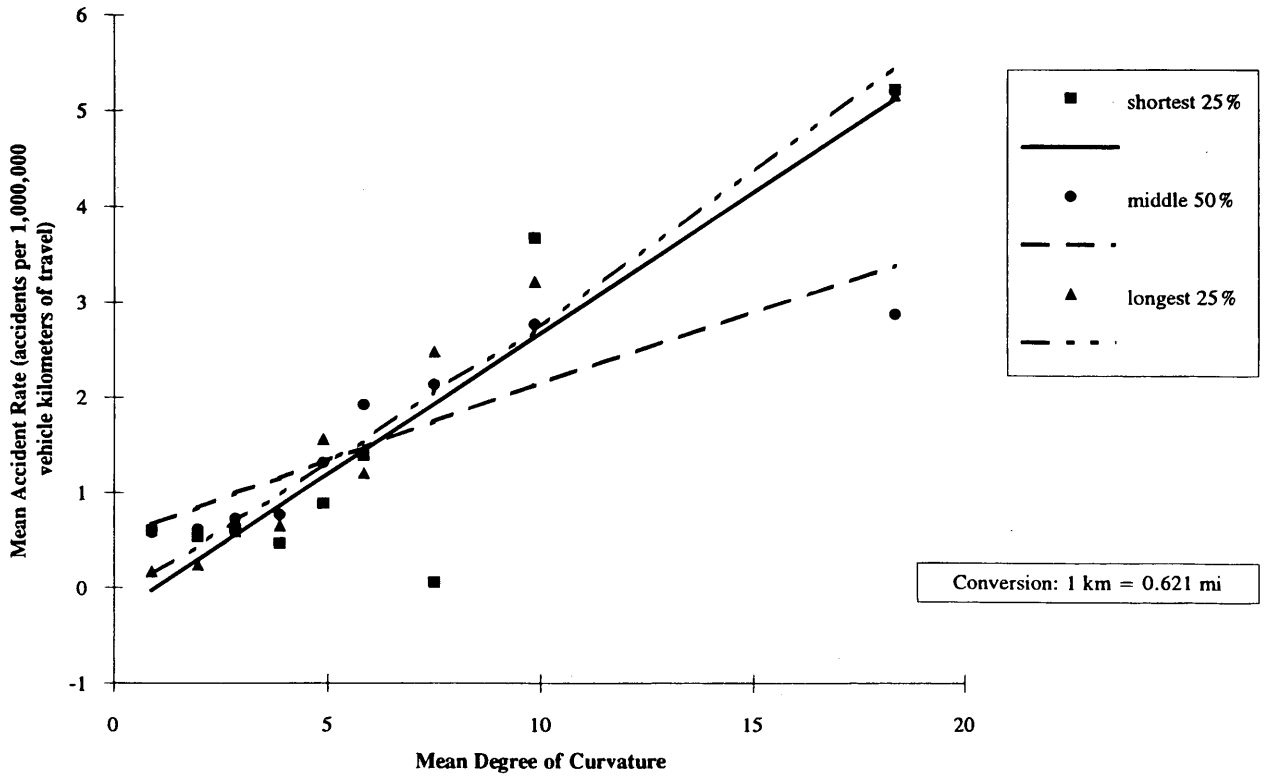

FIGURE 5 Mean accident rate versus sight distance category.

ACKNOWLEDGMENTS

This material is based on work supported by the Federal Highway Administration. Any opinions, findings, and conclusions or recommendations expressed in this publication are those of the authors and do not necessarily reflect the view of the FHWA.

REFERENCES

1. Zegeer, C. V., J. M. Twomey, M. L. Heckman, and J. C. Hayward. *Safety Effectiveness of Highway Design Features, Vol. II, Alignment.* Report FHWA-RD-91-045. FHWA, U.S. Department of Transportation, 1992.
2. Krammes, R. A., R. Q. Brackett, M. A. Shafer, J. L. Ottesen, I. B. Anderson, K. L. Fink, K. M. Collins, O. J. Pendleton, and C. J. Messer. *Horizontal Alignment Consistency for Rural Two-Lane Highways.* Report FHWA-RD-94-034. FHWA, U.S. Department of Transportation, 1994.
3. *A Policy on Geometric Design of Highways and Streets.* AASHTO, Washington, D.C., 1990.
4. Lamm, R., E. M. Choueiri, and J. C. Hayward. The Tangent as an Independent Design Element. In *Transportation Research Record 1195*, TRB, National Research Council, Washington, D.C., 1988, pp. 123–131.
5. *Amenagement des Routes Principales en dehors Agglomerations: Recommendations Techniques pour la Conception Geometrie de la Route* (Draft). Service d'Etudes Techniques des Routes et Autoroutes, Paris, France.
6. *Geschwindigkeit als Projektierungselement.* Swiss Norm 640 080b. Vereingung Schweizerischer Strassenfachleute, Zurich, Switzerland, 1992.
7. Datta, T. K. *Accident Surrogates for Use in Analyzing Highway Safety Hazards.* Report FHWA/RD-82/103. FHWA, U.S. Department of Transportation, 1983.
8. Terhune, K. W., and M. R. Parker. *An Evaluation of Accident Surrogates for Safety Analysis of Rural Highways, Vol. 2. Technical Report.* Report FHWA/RD-86/128. FHWA, U.S. Department of Transportation, 1986.
9. Matthews, L. R., and J. W. Barnes. Relation Between Road Environment and Curve Accidents. *Proc., 14th Australian Road Research Board Conference*, Victoria, Australia, Vol. 14, Part 4, 1988.
10. Zegeer, C., R. Stewart, D. Reinfurt, F. Council, T. Neuman, E. Hamilton, T. Miller, and W. Hunter. *Cost-Effective Geometric Improvements for Safety Upgrading of Horizontal Curves.* Report FHWA-RD-90-021. FHWA, U.S. Department of Transportation, 1991.
11. Glennon, J. C., T. R. Neuman, and J. P. Leisch. *Safety and Operational Considerations for Design of Rural Highway Curves.* Report No, FHWA/RD-86/035. FHWA, U.S. Department of Transportation, 1985.
12. Olson, P. L., D. E. Cleveland, P. S. Fancher, L. P. Kostyniuk, and L. W. Schneider. *NCHRP Report 270: Parameters Affecting Stopping Sight Distance.* TRB, National Research Council, Washington, D.C., June 1984.
13. Fambro, D. B., T. Urbanik II, W. M. Hinshaw, J. W. Hanks, Jr., M. S. Ross, C. H. Tan, and C. J. Pretorius. *Stopping Sight Distance Considerations at Crest Vertical Curves on Rural Two-Lane Highways in Texas (TX-90/1125-1F).* Texas Transportation Institute, College Station, 1989.
14. Paniati, J. F., and F. M. Council. The Highway Safety Information System: Applications and Future Directions. *Public Roads*, Vol. 54, No. 4, 1991, pp. 271–278.
15. *SAS/Stat® User's Guide.* Version 6, Fourth Edition. SAS Institute, Inc., 1990.

Publication of this paper sponsored by Committee on Operational Effects of Geometrics.

Estimating Safety Effects of Cross-Section Design for Various Highway Types Using Negative Binomial Regression

MOHAMMED A. HADI, JACOB ARULDHAS, LEE-FANG CHOW, AND JOSEPH A. WATTLEWORTH

Improvements in cross-section design are expected to reduce crash rates. Previous studies on the subject have concentrated on two-way, two-lane highways and given less attention to other types of highways. In addition, several of those studies used conventional regression analyses that are not suitable to estimate a discrete non-negative variable like crash frequency. This study uses negative binomial regression analyses to estimate the effects of cross-section design elements on total, fatality, and injury crash rates for various types of rural and urban highways at different traffic levels. The results show that, depending on the highway type investigated, increasing lane width, median width, inside shoulder width, and/or outside shoulder width are effective in reducing crashes. The results also indicate that on four-lane urban highways, the raised median is safer than the two-way left-turn lane median and that the use of an open-graded friction course in lieu of a dense-graded friction course does not have any effect on crash rates.

Many studies have been conducted in the last four decades to investigate the effects of various highway designs on safety. The design elements that have been found to affect safety include cross-section design, horizontal alignment, vertical alignment, roadside features, intersection designs, interchange designs, narrow bridges, lighting, access control, pavement conditions, pavement edge drops, speed limit, marking, signing, delineation, railway crossings, pedestrian facility designs, and bicycle facility designs.

Previous studies indicated that improvements to highway design could produce significant reductions in the number of crashes. However, only a few quantitative relationships have been developed to relate various design elements to crash rates. The development of such relationships is necessary because they provide the information required to make the trade-off between the cost and the benefit of better highway designs. In addition, they permit better prioritization of safety improvement projects.

This study quantifies the effects of cross-section design elements on total, fatality, and injury crash rates for various types of rural and urban highways using data from Florida at different traffic levels. Poisson regression and negative binomial regression are investigated for possible use in deriving the estimation equations.

BACKGROUND

A large proportion of the available research on the safety effects of highway design elements has been devoted to two-way, two-lane rural highways; less attention has been given to other highway types. As discussed in a later section, regression analyses were used in some studies to develop quantitative relationships that estimate crashrate as a function of cross-section design elements. The majority of the studies that employed regression analyses used conventional regression to derive the required relationships.

Conventional regression analyses assume that the dependent variable is continuous and normally distributed with a constant variance. These assumptions are not correct when estimating crashes. Crash frequency is a discrete non-negative variable, and its variance depends on its mean. Thus, Poisson regression and negative binomial regression have been used in recent studies for crash data analysis (*1–3*).

Zegeer and Deacon (*4*) reviewed 30 studies performed until the mid-1980s and concluded that no satisfactory quantitative model relating crash rates to lane and shoulder width could be found. Therefore, they calibrated a regression model that estimates the most likely relationships between crashes and lane width, shoulder width, and shoulder type on two-lane rural highways. This model was derived using data obtained from four previous studies.

Later, Zegeer et al. (*5*) developed another regression model to quantify the benefits of shoulder and lane improvements based on data selected from seven states. Only two-lane roadway sites were investigated.

Several studies were conducted to investigate the effects on safety of median width and type. Few of them produced quantitative relationships. Among these was a study by Squires and Parsonson (*6*) in which regression equations were derived to predict crash rates on sections with raised medians and continuous two-way left-turn lanes (TWLTLs) for four- and six-lane highways. Based on these equations, the following points were concluded:

- For four-lane sections, raised medians had a lower crash rate over the range of data studied.
- For six-lane sections, the results were mixed. Raised medians were found to have lower crash rates for most conditions. However, TWLTLs had a lower crash rate where few concentrated areas of turns, such as signalized intersections and unsignalized approaches, existed.

Hoffman (*7*) examined four TWLTL sites with annual average daily traffic (AADT) ranging form 15,000 to 30,000 vehicles per day (vpd). Existing four-lane undivided highways were widened to five lanes to accommodate a center lane for left turn. Crash data for 1 year before and 1 year after the implementation of a TWLTL were examined. The results showed a 33 percent reduction in total crash frequency.

Transportation Research Center, University of Florida, 512 Weil Hall, Gainesville, Fla. 32611.

Bowman and Vecellio (*8*) compared arterial sections with different median types using statistical comparison tests and found that, in the central business district (CBD) areas, TWLTL medians had a lower vehicle crash rate than both raised curb median and undivided cross sections. Undivided arterials had the highest crash rate. In suburban areas, raised curb medians provided the lowest crash rates. In both CBD and suburban locations, raised medians had a lower injury crash rate than both the TWLTL median and undivided cross-sections.

In another paper, Bowman et al. (*2*), using the same data as those used by Bowman and Vecellio (*8*), developed equations to estimate crashes for urban and suburban arterial sections with different median types. Negative binomial regression was used in the analyses. Three different regression models were developed to estimate crashes for raised curb, TWLTL medians, and undivided cross sections. No attempt was made to compare the safety effects of the three median types using the derived models. The study concluded that the derived models provide better estimates of vehicle crash frequency than did the models from prior research. This conclusion, however, should be taken with caution, because the same data used in deriving the models in that study were used in the comparison.

Knuiman et al. (*3*) studied the effect of median width on crash rate using a negative binomial regression model. For a median without a barrier, it was found that crash rates declined rapidly when median width exceeded about 7.6 m (25 ft). The decreasing trend seemed to become level at median widths of approximately 18.9 to 24.4 m (60 to 80 ft).

DATA ACQUISITION

The largest possible number of roadway segments from the state of Florida roadway system were used in this study. For each segment, roadway, traffic, and crash data were needed for the regression analyses.

Roadway and traffic data were obtained from the Florida Department of Transportation's Roadway Characteristics Inventory (RCI) system. Crash data were obtained from the Department of Highway Safety and Motor Vehicles' computerized accident record system. Data from the two systems were linked through their common location data.

Roadway samples were stratified by location, access type, and number of lanes into nine categories. These categories and the AADT range used in analyzing each category were:

- Rural freeways (5,000–60,000 vpd),
- Four-lane rural divided roads (1,145–40,000 vpd),
- Two-way, two-lane rural roads (200–10,000 vpd),
- Four-lane urban freeways (4,260–136,800 vpd),
- Six-lane urban freeways (20,000–200,000 vpd),
- Two-way, two-lane urban collectors (904–38,680 vpd),
- Four-lane urban divided roads (10,000–50,000 vpd),
- Six-lane urban divided roads (10,000–100,000 vpd), and
- Four-lane urban undivided roads (5,000–40,000 vpd).

The selection of geometric design variables for use in this study was based on the completeness of data (proportion of missing data) and the degree to which those variables are expected to affect safety. The variables selected on the basis of these two factors for possible inclusion as independent variables in the derived models were section length, AADT, lane width, outside paved and unpaved shoulder widths, inside paved and unpaved shoulder widths, median width and type, presence of curb, speed limit, number of intersections (or interchanges in case of freeways) and the use of an open-graded versus a dense-graded friction course. The dependent variables were the total number of crashes, number of injury crashes, and number of fatal crashes in 4 years.

Roadway samples were divided into sections such that the geometric design remained constant within a given section. A minimum highway section length of 0.05 mile was set to exclude short sections that might be influenced by adjacent section characteristics. Variable section lengths were used in this study, but the section length was included as an independent variable in the analyses. A section boundary was formed when one or more of the geometric characteristics changed.

Four years (1988–1991) of crash data were used for analyses. This period is long enough for stable rates of crashes to be obtained. A longer analysis period was not used because of the possibility of significant changes in traffic patterns, highway design features, or land uses over the period.

POISSON AND NEGATIVE BINOMIAL REGRESSION MODELS

Poisson regression is based on the assumption that the response (the dependent) variable is Poisson-distributed. The Poisson distribution models the probability of discrete events such as crashes according to the Poisson process as follows:

$$P(Y) = \frac{e^{-\mu}\mu^{Y}}{Y!} \tag{1}$$

where Y is the number of events in a chosen period and μ is the mean number of events in the chosen period.

The Poisson regression model assumes that the mean number of events is a function of regressor variables. Thus, to estimate crash frequency using Poisson regression, the number of crashes is assumed to be Poisson distributed according to the following equation:

$$P(Y=Y_i) = \frac{e^{-\mu_i(X_i,\beta)}[\mu_i(X_i, \beta)]^{Y_i}}{Y_i!} \tag{2}$$

where

Y_i = the number of crashes observed at road section i for a chosen period of time,
β = a vector representing a set of parameters to be estimated,
$\mu_i(X_i, \beta)$ = the mean number of crashes on road section i, which is a function of a set of regressor variables X, and
X_i = a vector representing the value of the regressor variables for highway section i.

The regressor variables in the above equation can be selected as various design and traffic operational variables that could influence safety.

The function $\mu_i(X_i, \beta)$ in Equation 2, which relates the distribution mean to regressor variables, is called the "link function" (*9*). The function used in this study is as follows:

$$\mu_i(X_i, \beta) = e^{X_i\beta} \tag{3}$$

The regression coefficients (β) in Equations and 3 are estimated using the maximum likelihood estimation.

The model of Equation 2 assumes that crash frequency is Poisson-distributed. This implies that the variance is assumed to be equal to the mean of the process. Although in theory the Poisson model is suitable for count data such as crash frequencies, these have been reported to display extra variation or overdispersion relative to a Poisson model. That is, the variance observed was higher than the mean. The overdispersion in crash data could be because not all relevant variables are normally included in the model and because of the uncertainty in regressor variables (*1*). When using the Poisson regression in the presence of overdispersion, maximum likelihood parameter estimates are consistent, but the variances of these parameters are inconsistently estimated. As a result of this, hypothesis test results become invalid.

To deal with overdispersion, negative binomial regression has been suggested for use instead of Poisson regression (*1–3*). This type of regression allows the variance of the process to differ from the mean. In this study, tests for overdispersion were conducted to decide whether Poisson or negative binomial regression should be used for model development.

The maximum-likelihood estimation of model parameters was performed using the LIMDEP statistical package (*10*). This package estimates the Poisson regression parameters using the Newton's method and the negative binomial regression parameters using a modification to the Davidson, Fletcher, and Powell search procedure (*11*). When using the negative binomial regression, LIMDEP starts with parameter values achieved during a Poisson regression analysis. This is expected to produce better values when maximizing the log-likelihood function.

Because ordinary regression was not used, the selection of variables for inclusion in the final models and statistical tests to determine the significance of the derived relationships could not be done using conventional approaches. Rather, methods that do not assume normality of the dependent variable were used. These are reviewed in the following subsections.

Selection of Regressor Variables

In order to decide which subset of independent variables should be included in a crash estimation model, the Akaike's information criterion (AIC), was used. AIC was defined as follows (*12*):

$$\text{AIC} = -2 \cdot ML + 2 \cdot K \tag{4}$$

where K is the number of free parameters in the model and ML is the maximum log-likelihood.

The smaller the value of AIC, the better the mode. Starting with the full set of independent variables listed in the previous section, a stepwise procedure was used to select the best model based on minimizing the AIC value.

Testing Individual Coefficients

Individual parameters in the β vector of Equation 2 were tested to investiage the null hypothesis that a given parameter β_j is zero. The method used was based on the standard errors of coefficients, which is an analog to the *t*-test used in conventional regression analyses. In this method, the following term is computed (*9*):

$$\chi^2 = \frac{b_j^2}{(SE_j)^2} \tag{5}$$

where b_j is the estimate of β_j and SE_j is the standard error of the coefficient β_j.

A chi-square test with one degree of freedom was used to test the hypothesis that the parameter β_j is zero.

Testing for Overdispersion

Two tests for detecting overdispersion in the Poisson process were performed in this study to decide whether Poisson regression or negative binomial regression should be used in analyzing crash data. The first test was suggested by Cameron and Trivedi (*13*). This test involved simple least-squares regressions to test the significance of the overdispersion coefficient.

Another test for overdispersion was performed using outputs from the procedure that estimated the negative binomial regression in LIMDEP. These outputs (an overdispersion parameter and its standard error) were used to test the hypothesis that the overdispersion parameter was zero. Failure to reject this hypothesis would indicate insignificant dispersion and allow the use of Poisson regression.

Goodness of Fit

To measure the goodness of fit, the Pearsons chi-square statistic was used. This statistic was calculated as follows:

$$\chi^2 = \sum \frac{(Y_i - \mu_i)^2}{\mu_i} \tag{6}$$

The degree of freedom of this statistic equals the number of observations minus the total number of estimated parameters.

MODEL ESTIMATION AND TESTING

The Poisson regression and negative binomial regression analyses described in the previous section were considered for use in establishing the required relationships between cross-section design elements and total number of crashes, fatal crashes, and injury crashes. Separate sets of models were developed for each of the nine highway categories investigated in this study. In addition, the analyses were performed separately for nonintersection, or midblock, crashes and all crashes. The latter include, in addition to midblock crashes, intersection crashes, interchange crashes, and railway crossing crashes.

The independent variables in the models were selected based on the AIC value from the total set of geometric design and operational variables extracted from the RCI. The square, square root, and logarithmic terms of several of the variables were investigated for possible inclusion in the final models. In addition, interaction terms that include multiplications of variables that were thought to interact with each other were also tested for inclusion in the models.

Categorical variables (variables, each observation of which belongs to one of several distinct categories) such as median type, curb presence, and friction course type were represented as dummy

variables. To represent K categories of a categorical variable, $K - 1$, binary (0 or 1) dummy variables were created.

The AADT, section length, number of intersections, number of interchanges, lane width, shoulder width, and median width were represented as continuous variables. However, there was some concern that models with continuous representation of cross-section design elements might not be able to identify thresholds above which improvements to these elements do not reduce crash rates. For example, if increasing lane width from 2.8 m to 4.0 m (9 ft to 13 ft) decreased crash rate, but increasing lane width from 4.0 m to 4.3 m (13 ft to 14 ft) did not, a continuous model might attempt to smooth the data according to the assumed transformation and thus might estimate incorrect reduction in crashes due to a widening a lane from 4.0 m to 4.3 m (13 ft to 14 ft).

For the above reason, additional Poisson and negative binomial regression analyses were performed in which lane width, shoulder width, and median width were represented as categorical variables. Based on the results of these analyses, the category of each variable that produced the minimum crash rate was identified and used to determine the threshold above which no reduction in crash rate was expected from improvements to that variable.

The LIMDEP package produced some of the information required to perform statistical inferences on the models developed in this study. Information not produced automatically by the package such as the AIC and the chi-square goodness-of-fit statistics was calculated using LIMDEP commands.

Tests for overdispersion indicated that overdispersion in crash data was significant for all types of highway investigated. Thus, it was decided to use negative binomial regression rather than Poisson regression to estimate model parameters in all cases investigated.

All derived Poisson and negative binomial models failed to pass the chi-square goodness-of-fit test at the 0.05 confidence level. Similar results were reported by other researchers who tried to estimate crashes based on geometric and operational design elements (*1,2*). Bowman et al. (*2*) pointed out that the chi-square test is not suitable for nonlinear problems such as the one under investigation. Miaou et al. (*1*) suggested that the lack of goodness of fit could also be related to the following:

- A large proportion of the roadway sections have very few or no crashes. The chi-square test is not appropriate for these conditions.
- There may have been uncertainties or omitted variables in the data.

Thus, they suggested using the following criteria for model acceptance:

- The signs of all model parameters are as expected.
- AIC is the lowest possible.
- Each individual parameter is accepted when tested using appropriate statistical testing.

TABLE 1 Models Derived To Estimate Total Crash Frequency in 4-Year Period

Highway Type	Crash Location	Model[a]
two-lane rural	mid-block	exp(-10.26 +.8249Llen +.8783Ladt -.0857Lw -.0130Sp +.0589Is -.0150Ts)
	total	exp(-9.053 +.7212Llen +.8869Ladt -.0435Lw -.0262Sp +.1145Is -.0123Ts)
four-lane rural divided	mid-block	exp(-9.545 +.6706Llen +.7205Ladt -.0524Su +.1746Is -.0458Sm)
	total	exp(-7.908 +.4140Llen +.7672Ladt -.0129Su -.3503Is -.0688Sm)
four-and six lane rural freeways	mid-block	exp(-12.89 +.9020Llen +.9156Ladt -.0272Ip +.2164Ic-.0252Sm)
	total	exp(-12.14 +.8533Llen +.9032Ladt -.0252Ip +.4679Ic -.0472Sm)
two-lane urban undivided	mid-block	exp(-10.62 +.8966Llen +.9008Ladt -.0355Lp -.0234Sp +.1707Co +.0603Is - .0323Up)
	total	exp(-8.263 +.7212Llen +.8560Ladt -.0246Lp -.0307Sp +.3652Co +.1111Is - .0387Up)
four-lane urban undivided	mid-block	exp(-8.275 +.8646Llen +.8318Ladt -.1127Lw -.0301Sp -.2831Co +.0427Is)
	total	exp(-4.251 +.6914Llen +.6950Ladt -.1056Lw -.0536Sp -.3101Co +.8251Is - .0309Ps)
four-lane urban divided	mid-block	exp(-13.88 +.7009Llen +1.195Ladt -.0299Ps +.1131Is -.0588Sm +.0982D1 -.2008D2 - .0871D3)
	total	exp(-9.996 +.4890Llen +1.026Ladt -.0367Ps +.2053Is -.1060Sm +.1115Ci)
six-lane urban divided	mid-block	exp(-12.04 +.8223Llen +1.072Ladt -.0270Sp +.0631Is -.0412Sm +.1671Co)
	total	exp(-8.766 +.6335Llen +.8152Ladt -.0026Mw +.1309Is +.2819Co)
four-lane urban freeways	mid-block	exp(-8.837 +.7848Llen +1.213Ladt -.3909Lw -.0263Up -.0225Sp +.2786Ic - .0801Sm)
	total	exp(-8.972 +.0.7292Llen+1.171Ladt -.2585Lw -.0268Sp +.3674Ic - .0926Sm)
six lane urban freeways	mid-block	exp(-13.56 +.8753Llen +1.454Ladt -.3504Lw -.0667Ps +.1787Ic - .0345Sm)
	total	exp(-8.163 +.8049Llen +1.178Ladt -.3740Lw -.0445Ps -.0310Sp +.2935Ic)

[a] *Lw = lane width (ft), Lp = pavement width (ft), Ps = paved shoulder width (ft), Up = unpaved shoulder width (ft), Ts = total shoulder width (ft), Mw = median width (ft), Sm = (median width)$^{.5}$, Su = (unpaved shoulder width)$^{.5}$, Ip = inside paved shoulder, Sp = posted speed limit (mph), Is = number of intersections, Ic = number of interchanges, Co = presence or absence of outside curb (1,0), Ci = presence or absence of inside curb (1,0), Llen = log of (1000 • section length in miles), Ladt = log (AADT), D1 = TWLTL median, D2 = grass median, D3 = raised curb median and median type is crossover resistance when D1=D2=D3= 0*

TABLE 2 Models Derived To Estimate Injury Crash Frequency in 4-Year Period

Highway Type	Crash Location	Model[a]
two-lane rural	mid-block	exp(-10.72 +.8157Llen +.8681Ladt -.0787Lw -.0108Sp +.0601Is -.021Ts)
	total	exp(-9.478 +.7064Llen +.8806Ladt -.0426Lw -.0236Sp +.1155Is -.013Ts)
four-lane rural divided	mid-block	exp(-9.91 +.6288Llen +.6919Ladt +.1973Is)
	total	exp(-8.36 +.3849Llen +.76Ladt +.3617Is -.0455Sm -.0223Sp)
four-and six lane rural freeways	mid-block	exp(-14.032 +.9107Llen +.9599Ladt -.0407Ip +.2127Ic)
	total	exp(-13.19 +.88667Llen +.9527Ladt -.0307Ip +.43Ic -.0463Sm)
two-lane urban undivided	mid-block	exp(-11.415 +.933Llen +.9137Ladt -.0489Lp -.0201Sp +.056Is -.0342Up)
	total	exp(-9.065 +.7451Llen +.864Ladt -.0337Lp -.0253Sp +.108Is -.043Up + 1.48Co)
four-lane urban undivided	mid-block	exp(-9.584 +.8831Llen +.8317Ladt -.1037Lw -.015Sp -.3318Co +.0395Is)
	total	exp(-5.285 +.699Llen +.6993Ladt -.128Lw -.0371Sp -.3407Co +.08Is)
four-lane urban divided	mid-block	exp(-14.023 +.7979Llen +1.216Ladt -.0303Ps +.0839Is -.0325Sm -.0295Sp)
	total	exp(-11.2 +.5254Llen +1.0625Ladt -.0353Ps +.3617Is -.0833Sm +.1191Ci)
six-lane urban divided	mid-block	exp(-14.0 +.8164Llen +1.0934Ladt +.0701Is -.0501Sm +.2202Co)
	total	exp(-8.536 +.7022Llen +.8491Ladt +.113Is +.1311Co -.05Sm -.0278Sp)
four-lane urban freeways	mid-block	exp(-10.61 +.7733Llen +1.1832Ladt -.307Lw -.0232Up -.0154Sp +.24Ic -.06Sm)
	total	exp(-12.6 +.712Llen +1.1373Ladt -.0223Sp +.3512Ic -.0706Sm)
six lane urban freeways	mid-block	exp(-14.04 +.93Llen +1.405Ladt -.339Lw -.0594Ps -.031Sm)
	total	exp(-8.507 +.8418Llen +1.14Ladt -.3845Lw -.0370Ps -.0302Sp +.2433Ic)

[a] *Lw = lane width (ft), Lp = pavement width (ft), Ps = paved shoulder width (ft), Up = unpaved shoulder width (ft), Ts = total shoulder width (ft), Mw = median width (ft), Sm = (median width)$^{.5}$, Su = (unpaved shoulder width)$^{.5}$, Ip= inside paved shoulder, Sp = posted speed limit (mph), Is = number of intersections, Ic = number of interchanges, Co = presence or absence of outside curb (1,0), Ci = presence or absence of inside curb (1,0), Llen = log of (1000 • section length in miles), Ladt = log (AADT).*

These three criteria were used in this study. All of the models derived and discussed in the following section satisfied the above three criteria. Tables 1–3 present the models derived to estimate total, injury, and fatal crash frequencies for a 4-year period. Table 3 indicates that in most cases, the best model found to estimate fatal crashes included only the section length and AADT as explanatory variables. This might be because the number of fatal crashes were too low to allow for correct estimation of the effect of other variables.

MODEL IMPLEMENTATION

This section presents results obtained from the regression analyses for each of the nine highway types investigated. These results were obtained using examples in which the effects of each significant variable on safety was investigated by changing its value while keeping the other significant variables constant at values representing typical roadway sections for the investigated highway type. The models with continuous representation of lane, shoulder, and median width were used in the analyses. However, the thresholds obtained based on categorical representation, as explained in the previous section, were also considered.

The values presented in the following discussion are those for midblock crashes. All-location crashes generally follow similar trends. In the following presentations, crash frequency is expressed in number of crashes per year (C/Y) and crash rate is expressed in number of crashes per million vehicle-kilometers (C/MVKM).

Annual Average Daily Traffic

The derived models presented in Tables 1–3 indicate that crash frequency increases with higher AADT for all highway types investigated. Figure 1 indicates that when comparing different rural highways with the same AADT, two-way, two-lane highways have the highest crash rates, followed by freeways, then by four-lane divided highways. For all three rural highway types, increasing the AADT decreased crash rates. The rate of this decrease, however, is lower for rural freeways than for the other two highway types; this may be due to the higher volumes on freeways.

For urban highways, Figure 2 suggests that crash rates decreased in the following order: four-lane undivided, two-way two-lane, six-lane divided, six-lane freeways, four-lane freeways, and four-lane divided. The crash rates for the last two highway types were very close. Higher AADT levels were associated with lower crash rates for two-way two-lane and four-lane undivided highways. However, higher AADT levels resulted in higher crash rates for urban freeways and other urban divided highways.

Lane Width

Significant relationships could be found between lane width and crashes for undivided highways and urban freeways. For other highway types, no such relationship could be identified. Table 4 shows that, based on categorical representation of lane width, for two-lane

TABLE 3 Models Derived To Estimate Fatal Crash Frequency in 4-Year Period

Highway Type	Crash Location	Model[a]
two-lane rural	mid-block	exp(-15.47 +1.025Llen +.9624Ladt -.1428Lw)
	total	exp(-14.401 +.875Llen +.9362Ladt -.097Lw)
four-lane rural divided	mid-block	exp(-12.644 +.7904Llen +.6036Ladt)
	total	exp(-10.526 +.6404Llen +.541Ladt)
four- and six-lane rural freeways	mid-block	exp(-14.758 +.9714Llen +.7057Ladt)
	total	exp(-14.054 +.947Llen +.6673Ladt)
two-lane urban undivided	mid-block	exp(-12.504 +.8872Llen +.6675Ladt -.11Lp)
	total	exp(-10.93 +.9793Llen +.467Ladt -.0777Lp)
four-lane urban undivided	mid-block	exp(-17.8 +1.281Llen +.854Ladt)
	total	exp(-14.839 +1.0812Llen +.7735Ladt +.4849Co)
four-lane urban divided	mid-block	exp(-14.321 +1.0237Llen +.6193Ladt)
	total	exp(-13.59 +.9514Llen +.6765Ladt)
six-lane urban divided	mid-block	exp(-14.251 +.945Llen +.676Ladt)
	total	exp(-10.88 +.73Llen +.5376Ladt +.0754Is)
four-lane urban freeways	mid-block	exp(-13.861 +.9116Llen +.6326Ladt)
	total	exp(-13.723 +.789Llen +.727Ladt)
six-lane urban freeways	mid-block	exp(-19.835 +1.2169Llen +1.01Ladt)
	total	exp(-12.41 +1.242Llen +1.152Ladt)

[a] *Lw = lane width (ft), Lp = pavement width (ft), Ps = paved shoulder width (ft), Up = unpaved shoulder width (ft), Ts = total shoulder width (ft), Mw = median width (ft), Sm = (median width)$^{.5}$, Su = (unpaved shoulder width)$^{.5}$, Ip = inside paved shoulder, Sp = posted speed limit (mph), Is = number of intersections, Ic = number of interchanges, Co = presence or absence of outside curb (1,0), Ci = presence or absence of inside curb (1,0), Llen = log of (1000 • section length in miles), Ladt = log (AADT).*

rural, two-lane urban, four lane urban undivided, and urban freeways, widening lane width up to 4.0 m, 3.7 m, 4.0 m, and 4.0 m (13 ft, 12 ft, 13 ft, and 13 ft), respectively, could be expected to decrease crash rates.

Figure 3 shows that the highest benefits of lane widening were estimated for urban freeways, followed by four-lane undivided urban highways, then by two-lane rural highways. For two-lane urban highways, there was a significant relationship between pavement width (lane width plus paved shoulder width) and crash frequency, rather than between lane width and crash frequency, when continuous representations of variables were used. The effect of lane width on crash rate for this highway type was lower than for other highway types.

Shoulder Width

Figure 4 indicates that the safety significance of outside total shoulder width, paved shoulder, and unpaved shoulder widths depends on the highway type investigated. Increasing paved shoulder width

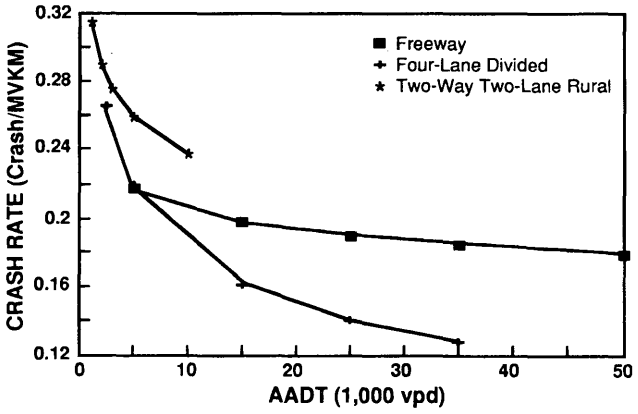

FIGURE 1 Effect of AADT on midblock crash rates of rural highways.

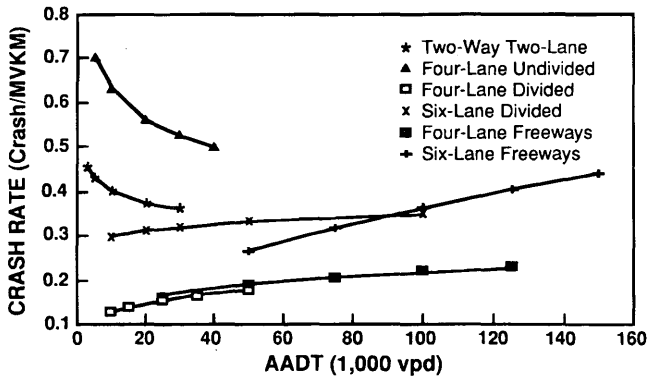

FIGURE 2 Effect of AADT on midblock crash rates of urban highways.

TABLE 4 Values of Lane and Shoulder Widths That Produced Lowest Crash Rates Based on Models Derived Using Categorical Representations of These Variables

Highway Type	Significant Variable	Variable Range[a] (m)[b]	Category with the Minimum Crashes (m)[b]
two-lane rural	lane width	2.8-4.6	4.0
	total shoulder width	0.6-3.7	3.0-3.7
four-lane rural divided	unpaved shoulder width	0.0-3.7	3.0-3.7
rural freeway	inside paved shoulder	0.0-1.8	-[c]
two-lane urban	lane width	3.0-4.6	3.7
	paved shoulder width	0.0-2.4	1.5-2.1
	unpaved shoulder width	0.0-3.0	2.4-3.0
four-lane urban undivided	lane width	2.7-4.0	4.0
four-lane urban divided	paved shoulder width	0.0-3.0	3.0
four-lane urban freeway	lane width	3.7-4.0	4.0
	unpaved shoulder width	0.0-3.0	3.0
six-lane urban freeways	lane width	3.4-3.7	-[c]
	paved shoulder width	0.0-3.7	-[c]

[a] *the range in the RCI data base*
[b] *1 m = 3.28 ft*
[c] *'-' indicates that no model could be developed based on categorical representation of this variable. Only a continuous model could be developed.*

was estimated to produce lower crash rates on six-lane urban freeways, two-lane urban highways, and four-lane urban divided highways. Increasing unpaved shoulder width was estimated to decrease crash rates on four-lane rural highways, two-lane urban highways, and four-lane urban freeways. Greater total shoulder width (paved plus unpaved) was associated with lower crash rates on two-lane rural highways.

It appears from Figure 4 that greater outside shoulder width was particularly effective in reducing crashes on six-lane urban freeways and two-lane urban highways. Table 4 shows that, based on categorical representations of variables, widening outside shoulder width to between 3.0 and 3.7 m (10 and 12 ft) produced the best results, in most cases. In urban two-lane highways, unpaved shoulder width of 2.4–3.0 m (8–10 ft) and a paved shoulder of about 1.5–2.1 m (5–7 ft) produced the best results.

Use of an inside paved shoulder 1.2–1.8 m (4–6 ft) wide was found to be very effective in decreasing crashes on rural freeways. It was found that using a 1.8-m (6-ft) shoulder width could decrease crash rate by 15.7 percent.

Median Width

In spite of several attempts, useful models that use categorical representation of median width could not be derived in this study. Therefore, the results presented for median width are based on continuous models.

Figure 5 shows the effects of median width on mid-block crash rates. It appears that significant reduction in crash rates could be expected from greater median width for all highway types. In all cases, the square root of median width, rather than median width,

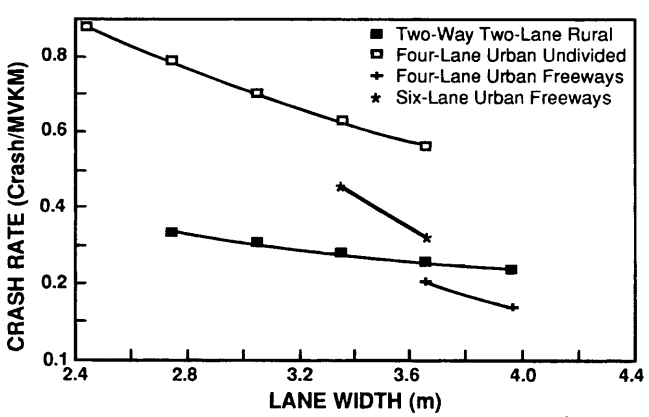

FIGURE 3 Effect of lane width on midblock crash rates.

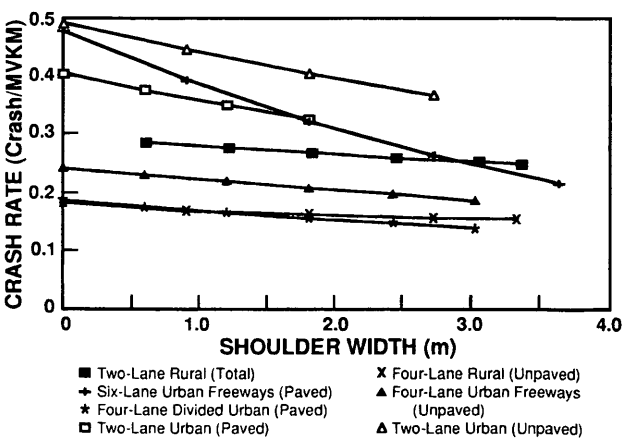

FIGURE 4 Effect of shoulder width on midblock crash rates.

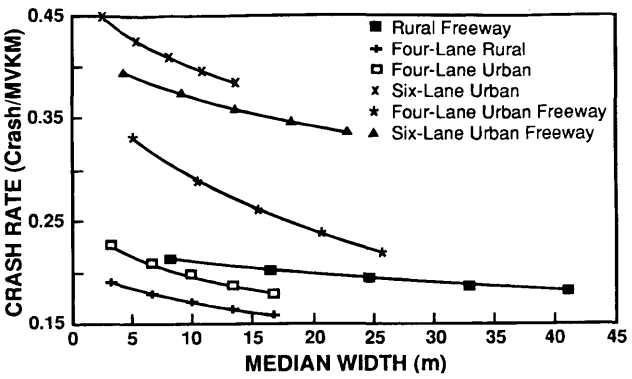

FIGURE 5 Effect of median width on midblock crash rates.

was the significant variable included in the models. This indicated that, as expected, the benefits of greater median width decreased as the median width increased. The safety benefit of increasing median width seems to be the highest in four-lane urban freeways and six-lane urban highways followed by six-lane urban freeways and four-lane urban highways followed by four-lane rural highways and rural freeways.

Median Type

A significant relationship was found between median type and crash experience only in four-lane divided urban highways. Sections with four median types were examined for this highway type. It was found that the safety of median type decreased in the following order: flush unpaved median (grass), raised curb, crossover resistance, and TWLTL. However, the differences in the median width between median types should be noted. For these four median types, the median width ranges based on the RCI database were 4.9–19.5 m, 0.9–11.3 m, 1.8–12.2 m, and 3–4.9 m (16–64ft, 3–37 ft, 6–40 ft, and 10–16 ft), respectively.

Other Elements

Longer section lengths and higher speed limits were associated with lower crash rates. This could be because longer section lengths indicate more uniform cross-section design and sections with higher speed limits generally have higher design speeds. The type of friction course (open-graded versus dense-graded) was not found to be significant in affecting safety.

The presence of more intersections on non-freeway highways and more interchanges on freeways increased crash rates significantly. The effect of intersection/interchange presence in rural highways decreased in the following order: freeways, four-lane divided, and two-lane. For urban highways, the effect decreased in the following order: four-lane freeways, six-lane freeways, four-lane divided, six-lane divided, two-lane undivided, and four-lane undivided.

In all urban highways except four-lane urban undivided highways, the presence of a curb had an adverse affect on vehicular safety.

POSSIBLE MODEL APPLICATIONS

The models derived in this study, along with any relevant models found in the literature, are being used to assess the cost-effectiveness of cross-section design standard requirements. In this analysis, an exhaustive search optimization procedure is being performed to determine the optimal cross-section designs that maximize the cost-effectiveness for each highway type, taking traffic level into consideration. The optimized cost includes four components: crash, construction, travel time, and vehicle operation costs.

The models derived in this study could also be used to examine the cost-effectiveness of improving cross-section design at a specific location. The four cost components mentioned previously could also be used.

CONCLUSIONS

On the basis of the findings of this study it can be concluded that several cross-section design elements affect safety. Increasing lane width to 3.7–4.0 m (12–13 ft), depending on highway type, is estimated to reduce crash rates for urban freeways and undivided highways. In general, increasing outside shoulder width to 3–3.7 m (10–12 ft) also decreases crash rates. An inside paved shoulder 1.2–1.8 m (4–6 ft) wide is effective in decreasing crashes on rural freeways. Median width is significant in affecting safety for all types of divided highway investigated. Median type affects crash rates: four-lane urban divided highways with flush unpaved (grass) medians are the safest, followed by raised curb medians, then crossover resistance, then TWLTL.

Sections with higher AADT levels are associated with higher crash frequencies for all highway types. Higher AADT levels result in higher crash rates on urban divided highways but in lower crash rates on rural highways and urban divided highways.

Other elements that adversely affect safety include nonuniform cross-section design, lower speed limit and thus lower design speed, the presence of a curb (in most cases), and the presence of interchanges or intersections. There is no significant difference between the safety of sections with an open-graded and a dense-graded friction course.

The models developed in this study could be used in conjunction with other relevant models from the literature to assess the cost-effectiveness of geometric design standards and to assign priority to geometric design improvement projects.

ACKNOWLEDGMENTS

This paper presents partial results of a project sponsored by the Florida Department of Transportation. The authors thank Cheng-Tin Gan, a graduate research assistant in the University of Florida Transportation Research Center, for his help in extracting the data from the computerized data bases.

REFERENCES

1. Miaou, S. P., H. S. Patricia, T. Wright, A. K. Rathi, and S. C. Davis. Relationship between Truck Accidents and Highway Geometric Design: A Poisson Regression Approach. In *Transportation Research Record 1376*, TRB, National Research Council, Washington, D.C., 1992, pp. 10–18.

2. Bowman, B. L., R. L. Vecellio, and J. Miao. *Estimating Vehicle and Pedestrian Accidents Resulting from Different Median Types.* Presented at the 73rd Annual Meeting of the TRB, Washington, D.C., January 1994.
3. Knuiman, M. W., F. M. Council, and D. W. Reinfurt. The Effect of Median Width on Highway Accident Rates. In *Transportation Research Record 1401,* TRB, National Research Council, Washington, D.C., 1993, pp. 70–80.
4. Zegeer, C. V. and J. Deacon. Effect of Lane Width, Shoulder Width, and Shoulder Type on Highway Safety. In *Relationship Between Safety and Key Highway Features, A Synthesis of Prior Research,* TRB, National Research Council, Washington, D.C., 1987, pp. 1–21.
5. Zegeer, C. V., D. W. Reinfurt, J. Hummer, L. Herf, and W. Hunter. Safety Effects of Cross-Section Design for Two-Lane Roads. In *Transportation Research Record 1195,* TRB, National Research Council, Washington, D.C., 1988, pp. 30–32.
6. Squires, C. A., and P. S. Parsonson. Accident Comparison of Raised Median and Two-Way Left-Turn Lane Median Treatments. In *Transportation Research Record 1239,* TRB, National Research Council, Washington, D.C., 1989, pp. 30–40.
7. Hoffman, M. R. Two-Way, Left-Turn Lanes Work! In *Traffic Engineering,* Vol. 44, No. 11, Institute of Transportation Engineers, Washington, D.C., 1974, pp. 24–27.
8. Bowman, B. L., and R. L. Vecellio. *The Effect of Urban/Suburban Median Types on Both Vehicular and Pedestrian Safety.* Presented at the 73rd Annual Meeting of the TRB, Washington, D.C., January 1994.
9. Myers, R. H. *Classical and Modern Regression with Applications.* PWS-KENT Publishing Company, Boston, Mass., 1992.
10. Green, W. H. *LIMDEP Version 6.0 User's Manual and Reference Guide.* Econometric Software, Inc., Bellport, N.Y., 1991.
11. Fletcher, R. *Practical Methods of Optimization.* John Wiley and Sons, New York, N.Y., 1980.
12. Gilchrist, W. *Statistical Modelling.* John Wiley and Sons, Inc., New York, N.Y., 1985.
13. Cameron, A., and P. Trivedi. Regression Based Tests for Overdispersion in the Poisson Model. *Journal of Econometrics,* Vol. 46, 1990, pp. 347–364.

The opinions, findings, and conclusions expressed in this publication are those of the authors and not necessarily those of the Florida Department of Transportation or the U.S. Department of Transportation.

Publication of this paper sponsored by Committee on Operational Effects of Geometrics.

Consistency of Horizontal Alignment for Different Vehicle Classes

HASHEM R. AL-MASAEID, MOHAMMAD HAMED, MOHAMMAD ABOUL-ELA, AND ADNAN G. GHANNAM

The objective of this study was to develop guidelines for evaluating the consistency of horizontal alignment of two-way two-lane highways. A number of simple and continuous horizontal curves were selected for this purpose. Roadway geometric design variables were obtained from design plans and field measurements. The speed of passenger cars, light trucks, and trucks was measured on tangent and horizontal curves. In the analysis, the speed reduction between tangent and curve or successive curves was considered the inconsistency indicator. The results of the analysis indicate that the degree of curve, length of vertical curve, gradient, and pavement condition have a significant effect on consistency of simple horizontal curves. For successive curves separated by a short common tangent, the speed reduction was found to be highly affected by the radii of curves. Also, the results reveal that a good consistent design can be achieved if the radii of successive curves are equal. Finally, the speeds on a common tangent between successive curves are investigated. For each type of vehicle, the results indicate that the degree of successive curves and the tangent length significantly influence the speed on the common tangent.

Roadway consistency may be defined as the degree to which highway systems are designed and constructed to avoid critical driving maneuvers, which can lead to unnecessary accident risk. A common case of geometric inconsistency is the existence of a sharp horizontal curve after a long tangent highway section. Studies indicate that half of the total accidents on two-lane rural highways may be indirectly attributed to improper speed adaptation (*1*). Most errors due to excessive speed may be related to inconsistency in horizontal alignment. Therefore, achieving geometric consistency is vital in the design and redesign of two-lane rural highways.

Although many studies have addressed the issue of roadway consistency, most have focused on the operating speed of passenger cars on simple curves. Therefore, more research is needed on highway sections with different types of curves and vehicle classes.

PURPOSE AND SCOPE OF RESEARCH

The purpose of this study is to develop guidelines that will help highway designers and decision makers evaluate and select the best alignment alternatives. The scope of this study is limited to two-way two-lane rural highways. Multi-lane highways are not included because inconsistency in the geometric design of these highways does not lead to hazardous conditions similar to those of two-lane highways. Although traffic accidents are a necessary component in the development of consistent design guidelines, the unavailability of reliable accident information precluded including this variable in the analysis.

Civil Engineering Department, Jordan University of Science and Technology, P. O. Box 3030, Irbid, Jordan.

METHODOLOGY

Four primary rural roads were selected. The availability of geometric design plans in the Jordan Ministry of Public Works and Housing was the sole criterion for selection. The following criteria were adopted to select a roadway section:

1. The selected section should be far from the influence of intersections or any physical features that may create abnormal hazards, such as narrow bridges.
2. The pavement and shoulder widths should be constant for both tangent and curve sections.
3. The tangent and subsequent curves should have the same pavement conditions.

These criteria are recommended in several studies (*2*). Based on these criteria, 57 simple horizontal curve sections and 36 continuous horizontal curves were selected. In this study, a simple horizontal curve is a circular curve preceded by a straight tangent section with a length of at least 800 m. The curve may or may not be accompanied by transition curves. A continuous curve consists of two successive horizontal curves separated by a short tangent with a maximum length of 300 m. Lamm et al. (*3*) indicated that a tangent length of up to 260 m (850 ft) may be considered a nonindependent tangent if the traffic speed is approximately 80 km/hr (52 mph). For nonindependent tangents, the sequence between curves controls the design process.

Different methods have been proposed for evaluating horizontal alignment consistency. These methods include the graphic speed-profile technique proposed for use in the United States, the theoretical speed model used by the Swiss Highway Design Community, and a German procedure using a design parameter known as the curvature change rate (*1*). In this study, the inconsistency indicator is defined in terms of speed reduction, expressed by the 85th percentile, between tangent and curve or successive curves. The effects of geometric design and traffic variables on the speed reduction were investigated using multiple regression analysis.

DATA COLLECTION

Roadway geometric elements were obtained from the design plans of the Ministry of Public Works and Housing, Jordan. Field measurements were conducted to determine some geometric elements.

The geometric elements included degree of curve, deflection angle, length of horizontal curve, length of vertical curve within the horizontal curve, gradient, superelevation, length of spiral, and widths of the lane and shoulder.

The data also included the length of common tangent for continuous curves. as well as prevailing terrain, pavement conditions and posted speed limits. Prevailing terrain was evaluated for each section and described as mountainous, rolling, or level. Pavement conditions for each roadway section were evaluated by a panel of raters. The pavement condition was expressed in terms of Present Serviceability Rating (PSR). Posted speed limits for passenger cars and trucks were obtained from a field survey.

Free-flow speeds were determined by measuring the time required to traverse a 40-m trap length. The measurements were taken for individual vehicles with a minimum gap of 6 sec (*4*). For simple horizontal curves, the measurements were taken along the central part of the curve, and on the preceding tangent about 250 m from the start of the curve section (*2*). Different studies reported that the minimum value of free-flow speed occurred near the curve center (*5–7*).

For continuous curves, measurements were taken at three locations. Two measurements were taken along the central part of each curve and the third on the common tangent. For each location and type of vehicle, the speed distribution was found to be normal. Previous studies by Mclean (*8*) reported similar results. Therefore, the 85th percentile driver in the tangent speed distribution would be the 85th percentile driver in the curve speed distribution. Thus, the speed reduction between tangent and curve or successive curves was estimated as the difference between the 85th percentile speeds.

DEVELOPMENT OF CONSISTENCY MODELS

The information included in the data base was used to develop statistical models that express the speed reduction as a function of geometric, pavement condition, prevailing terrain, and posted speed variables. For each type of vehicle, separate analyses were conducted for simple and continuous curves. The results are presented in the following sections.

Consistency Models for Simple Curves

For each type of vehicle, a correlation matrix was established between speed reduction and the variables included in the data base. The analysis indicated that speed reduction is highly correlated with the degree of horizontal curve, length of vertical curve within horizontal curve, gradient, and pavement condition (*9*). It was also found that the radius of curve and deflection angle are highly correlated with the degree of curve. In addition, the analysis revealed that lane and shoulder widths, superelevation rate, prevailing terrain, and posted speed for passenger cars and trucks had no effect on the speed reduction. Although posted speeds for cars and trucks are important variables, their variances in this study were very low and they did not significantly affect the speed reduction.

Based on stepwise regression analysis, the degree of horizontal curve was the most important variable for predicting the estimated speed reduction. The speed reduction for passenger cars, light trucks, trucks, and for all vehicles are presented, in the following equations:

$$\Delta V_P = 3.64 + 1.78DC \quad (1)$$

$$\Delta V_L = 2.0DC \quad (2)$$

$$\Delta V_T = 4.32 + 1.44DC \quad (3)$$

$$\Delta V_A = 3.30 + 1.58DC \quad (4)$$

where ΔV_P, ΔV_L, ΔV_T, and ΔV_A represent the speed reduction (km/hr) between tangent and curve for passenger cars, light trucks, trucks, and all vehicles, respectively, and DC is the degree of curve (angle in degrees, subtended at the center by an arc of 30 m in length).

The coefficients of multiple determination values were 0.51, 0.69, 0.42, and 0.62 for passenger cars, light trucks, trucks, and all vehicles, respectively. Based on the preceding equations, the estimated speed reductions associated with a curve having a degree of curve of 8 degrees (radius = 215 m) are 17.9, 16.0, and 15.8 km/hr for passenger cars, light trucks, and trucks, respectively. The corresponding speed reduction for all vehicles is 16 km/hr. By inspection, the estimated speed reduction for each type of vehicle is not significantly different from the speed reduction of all vehicles.

Further improvement in prediction precision was achieved when other significant variables were considered. These variables included length of vertical curve within the horizontal curve, gradient, and pavement condition. The length of vertical curve was found to be highly correlated with gradient. Therefore, separate models were developed to show the effects of vertical curve and gradient separately. The resulting equations for all vehicles were as follows:

$$\Delta V_A = 1.84 + 1.39DC + 4.09PC + 0.07G^2 \quad (5)$$

$$\Delta V_A = 1.45 + 1.55DC + 4.00PC + 0.00004V_C^2 \quad (6)$$

where

PC = pavement condition (for PSR $\geq$ 3, PC = 0, otherwise PC = 1),
G = gradient (in percent, average slope between the points of speed measurements on the tangent and the curve center), and
V_C = the length of vertical curve within the horizontal curve (m).

Both models and their parameters were statistically significant at the 95 percent confidence level. The coefficients of multiple determination values were 0.77 and 0.76 for Equations 5 and 6, respectively. Similar equations were developed for each vehicle type. Most of the data included high gradients, which are associated with up-grade and crest curves.

Consistency Models for Continuous Curves

The reduction in the 85th percentile speeds between the first and second curve as the dependent variable was modeled as a function of curve geometric variables. The analysis indicated that the radii of the continuous curves had the most significant effect on speed reduction. The direction of the second curve with respect to the first one was introduced as a dummy variable. However, the analysis revealed that this variable had no effect on speed reduction. Similarly, Mintsis (*10*) reported that the direction of the curve did not affect vehicle

speeds. The speed reductions for passenger cars, light trucks, trucks, and all vehicles are presented in the following equations:

$$\Delta V_P = \frac{5{,}708}{R_2} - \frac{5{,}689}{R_1} \quad (7)$$

$$\Delta V_L = \frac{4{,}957}{R_2} - \frac{4{,}888}{R_1} \quad (8)$$

$$\Delta V_T = \frac{5{,}463}{R_2} - \frac{5{,}463}{R_1} \quad (9)$$

$$\Delta V_A = \frac{5{,}081}{R_2} - \frac{5{,}081}{R_1} \quad (10)$$

where R_1 and R_2 represent the radius of the first (preceding) and the second curve, respectively. The models and their parameters in Equations 7–10 were statistically significant at the 95 percent confidence level. The coefficients of multiple determination values were 0.72, 0.77, 0.66, and 0.81 for Equations 7, 8, 9 and 10, respectively. Based on these models, the speed reduction could be estimated for each vehicle type. The estimated speed reduction might be negative. This occurs if the radius of the first curve is smaller than the radius of the second one. For example, if the radii of the first and second curve are 150 and 200 m, respectively, the estimated speed reductions would be −9.4, −7.8, −9.1, and −8.5 km/hr for passenger cars, light trucks, trucks, and all vehicles, respectively. This example demonstrates that the speed reduction for all vehicles is not significantly different from the speed reduction for each type of vehicle. The relationship between speed reduction and radii of continuous curves for all vehicles is shown in Figure 1.

Consistency Models for Common Tangent

The length of the common tangent between successive curves (non-independent tangent) is considered one of the important geometric design consistency variables. For each type of vehicle, the results indicate that the speed on the common tangent was found to be strongly correlated with the length of common tangent, degree of successive curves, and the deflection angles. However, the degrees of curves were also found to be positively correlated with their deflection angles. Therefore, separate models were established with the aim of developing geometric design guidelines for highway planners.

Based on the length of common tangent and deflection angles, speed on the common tangent can be estimated from Equations 11, 12, 13, and 14 for passenger cars, light trucks, trucks, and all vehicles, respectively.

$$V_P = 115.0 - \frac{3{,}722}{LT} - 0.70\left(\frac{DF_1 * DF_2}{DF_1 + DF_2}\right) \quad (11)$$

$$V_L = 106.0 - \frac{3{,}391}{LT} - 0.73\left(\frac{DF_1 * DF_2}{DF_1 + DF_2}\right) \quad (12)$$

$$V_T = 99.3 - \frac{3{,}099}{LT} - 0.75\left(\frac{DF_1 * DF_2}{DF_1 + DF_2}\right) \quad (13)$$

$$V_A = 108.3 - \frac{3{,}498}{LT} - 0.71\left(\frac{DF_1 * DF_2}{DF_1 + DF_2}\right) \quad (14)$$

where

V_P, V_L, V_T, and V_A = 85th percentile speed of passenger cars, light trucks, trucks, and all vehicles (km/hr), respectively;
L_T = length of common tangent (m); and
DF_1 and DF_2 = deflection angles of first and second curve (in degrees), respectively.

The parameters of the preceding models were statistically significant at the 95 percent confidence level. The coefficients of multiple determination values were 0.68, 0.71, 0.72, and 0.72 for Equations 11, 12, 13, and 14, respectively. Although each type of vehicle had its own distinct speed, the length of common tangent and deflection angles had approximately the same effects. For all vehicles, Figure 2 shows the relationship between the speed on the common tangent

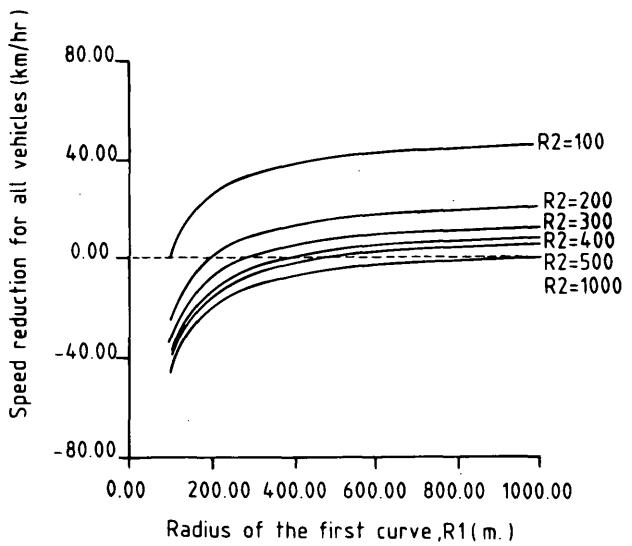

FIGURE 1 Relationship between speed reduction and radii of successive curves for all vehicles.

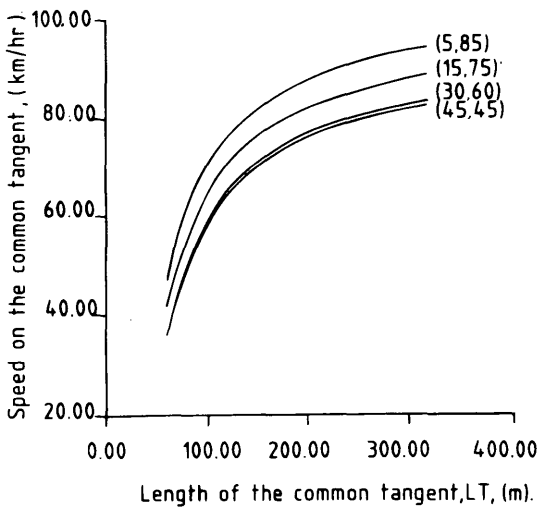

FIGURE 2 Relationship between estimated speed on tangent and both length of tangent (LT) and deflection angles (DF1, DF2) for all vehicles.

and its length for different deflection angles. This figure indicates that for the same total deflection angle ($DF_1 + DF_2$) the lowest speed can be obtained if the two angles are equal. Thus, deflection angles of successive curves should not be the same if higher speeds are desired.

Similarly, models were developed to estimate traffic speed on common tangent as a function of the length of common tangent and the degree of successive curves. For each type of vehicle, the models were similar in form. The developed model for all vehicles may be expressed as

$$V_A = 105.47 - \frac{3{,}792}{LT} - 0.27\,(DC_1 * DC_2) \qquad (15)$$

where DC_1 and DC_2 represent the degree of successive curves for the first and second curve respectively. The preceding model and its parameters were statistically significant. Compared with Equation 14, Equation 15 had lower coefficient of determination ($R^2 = 0.63$). Figure 3 shows the estimated speed for all vehicles as a function of the length of common tangent and degree of successive curves.

DISCUSSION OF RESULTS

In this study, speed reduction is considered as a quantitative measure of an inconsistent design. Several studies suggested a design criterion based on this measure (*11–14*). Previous studies have estimated speed reduction through speed-profile models (*3, 12*) or speed difference distribution (*15*). In this study, speed reduction models were developed to estimate directly the reduction in operating speed. This approach was adopted for the following reasons. First, speed reduction is the most common outcome of an inconsistent design, and it is easier to estimate it directly using appropriate models. Second, it was found through the course of this study that the speed reduction models provided a sound statistical characteristic specifically for continuous and reverse curves. Finally, the

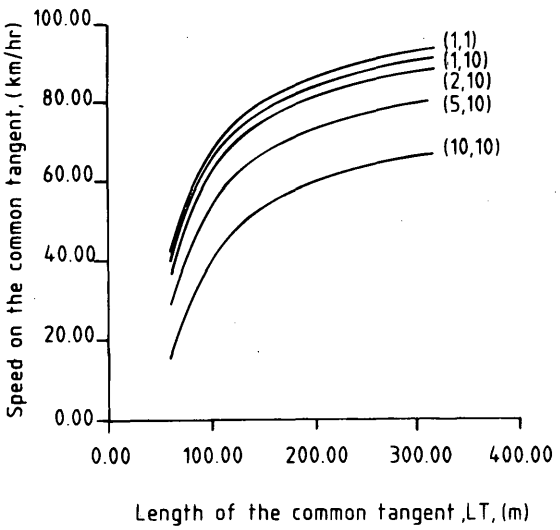

FIGURE 3 Relationship between estimated speed on tangent and both length of tangent (LT) and degree of curves (DC1, DC2) for all vehicles.

results of this study were found to be generally comparable with the results of previous studies. For simple curves, the overall operating speeds on tangents were approximately equal because the tangents were selected to be independent and the selected roads have approximately the same posted speed limits. For continuous curves, the speed on the second curve is dictated by the speed on the preceding one. Thus, modeling the speed reduction directly is not an unreasonable approach.

For simple horizontal curves, the analysis revealed that speed reduction is significantly affected by the degree of curves, gradient, length of vertical curve within horizontal curve, as well as pavement condition. The degree of curve was found to be the most important variable. Although previous studies did not develop speed prediction for each type of vehicle, those studies found that the degree of curve had the greatest impact on the speed of passenger cars on horizontal curves (*4, 16*). Moreover, Lamm et al. (*4*) indicated that gradient did not have a significant influence on the speed of passenger cars. The difference between these results might be attributed to the fact that Lamm et al. (*4*) did not include a gradient steeper than 5 percent, whereas this study included a gradient up to 7 percent. Kanellaidis et al. (*17*) indicated that superelevation rate, lane and shoulder widths, and grade up to 3 percent did not have a statistically significant effect on curve speed. Therefore, results of this study agree with those of previous research.

As stated, speed reduction models were developed for each type of vehicle. Investigation of Equations 1–4 reveals that the speed of passenger cars is affected to a greater extent by the degree of curve, specifically for a medium to high degree of curve. However, for a degree of curve 4 to 10 degrees, the difference between the speed reduction values for all vehicles and for each type of vehicle was not significant in this study. This result is compatible with the results of previous studies. Lamm et al. (*3*) indicated that the difference between operating speeds of passenger cars and trucks increases with increasing degree of curve, but not in a manner that could result in critical maneuvers.

Based on safety considerations, Lamm et al. (*12*) reported that the degree of simple curve should be limited to 5 degrees (radius = 345 m) and the speed reduction to 10 km/hr to achieve a good design. In this study, Equation 5 indicates that for a good pavement condition and grade of up to 4 percent, the degree of curve corresponding to a speed reduction of 10 km/hr is 5.06 degrees (radius = 340 m). Therefore, the results are comparable and the small discrepancy might be attributed to differences in driver attitudes.

For continuous curves, the speed reduction on successive curves, separated by a relatively short tangent, is highly affected by the radii of curves. An inspection of Equations 7–10 reveals that for equal radii, the speed reduction would be negligible. Furthermore, an increase in both radii would minimize the speed reduction and provide better consistency. Compared with other vehicle types, the speed of passenger cars is affected to a greater extent by the curve radii.

For comparison purposes, Equation 7 can be used to determine the radius of the second curve for a given radius of the first curve and specific level of speed reduction. Lamm et al. (*12*) indicated that a good consistent design can be achieved if the speed reduction is less than 10 km/hr. Based on this criterion, if the radius of the first curve is 100 m, then the second curve should have a radius in the range of 85 to 122 m to achieve a good consistent design for passenger cars. This value is comparable with the results of previous research. For good design, Lamm et al. (*12*) showed that a curve

having a radius of 100 m can be combined with a curve having a radius in the range of 81–130 m.

The results indicate that the speed on the common tangent would be increased by increasing the length of common tangent or by reducing the deflection angles. Furthermore, the developed equations indicate that the increase in the length of the common tangent will permit the use of a large degree of curve or deflection angles. Again, one should remember that the results of this study indicate that the degree of curves was found to be strongly correlated with their deflection angles. Thus, the speed on the common tangent would be increased by reducing the degree of successive curves.

PRACTICAL APPLICATION

The ultimate objective of speed reduction models is to develop guidelines for designing or redesigning two-way two-lane highway. The literature reveals that good consistent design can be achieved if the speed reduction is less than 10 km/hr (*12*). For simple horizontal curves, Equation 4 indicates that this condition can be achieved if the degree of the curve is less than 4.24 degrees. Moreover, effect of grade, pavement condition, and the length of vertical curve can be used to determine the maximum degree of curve for a good consistent design. Considering the effects of pavement condition and gradient, Equation 5 can be used to determine the maximum degree of curve that would guarantee a good consistent design for all vehicles. Table 1 presents the maximum degree of curve for different pavement conditions and gradient. For example, if the pavement condition is good or better and the gradient is 6 percent, then a good consistent design would be achieved if the degree of simple curve is less than or equal to 4 degrees (radius = 430 m). Similarly, Table 2 presents the maximum degree of curve for different pavement condition and length of vertical curve. Table 2 was developed using Equation 6. For example, if the pavement condition is good or better and the length of vertical curve is 240 m, then the maximum degree of curve should be limited to 4 degrees (radius = 430 m) to achieve a good design.

For continuous horizontal curves, similar guidelines can be developed using curve radii instead of degree of curves. Table 3 presents the limit of horizontal curve radii that would guarantee a good consistent design. The radius of the first curve was assumed, and the minimum and maximum values of the radius of the second curve were computed using Equations 7 and 10 for passenger cars and all vehicles, respectively. In computing the minimum and maximum radius of the second curve, the speed reductions were taken to be −10 and +10 km/hr, respectively. For example, if the radius of the first curve is 300 m, the second curve should have a radius in the range of 189 to 732 m to achieve a good design for all vehicles. However, if the radius of the first curve is 500 m, then the minimum radius of the second curve is 252 m and no maximum limit (straight section) could be used.

The developed models in this study can be used to estimate the speed on a short common tangent. To achieve a desired speed, the length of the common tangent can be estimated for a given combination of curve degrees or deflection angles.

TABLE 1 Maximum Degree of Horizontal Curve That Would Guarantee Consistent Design for Different Pavement Conditions and Gradients

Pavement Condition	Gradient (%)	Maximum Degree of Curve (degree)
Good or very Good (PSR ≥ 3)	2	5.71
	4	5.06
	6	4.00
	8	2.51
Fair or Poor (PSR < 3)	2	2.74
	4	2.11
	6	1.40
	8	0.00

TABLE 2 Maximum Degree of Horizontal Curve That Would Guarantee Consistent Design for Different Pavement Conditions and Length of Vertical Curve

Pavement Condition	Length of Vertical Curve (m)	Maximum Degree of Curve (degree)
Good or very Good (PSR ≥ 3)	320	2.85
	240	4.00
	160	4.86
	80	5.38
Fair or Poor (PSR < 3)	320	0.23
	240	1.43
	160	2.23
	80	2.69

CONCLUSIONS

In addition to the degree of simple horizontal curve, the length of vertical curve within the horizontal curve, gradient, and pavement condition had a significant effect on consistency of horizontal alignment. Speed reduction, as a measure of alignment consistency, was greatly affected by the degree of curves. Considering all types of vehicles, a good consistent design can be achieved if the degree of curve is less than 4.24 degrees. The radii of successive horizontal curves separated by a short common tangent determined the speed reduction between the curves. For a good consistent design, the curves should have approximately equal radii. Although consistency models for different type of vehicles were developed, the consistency models for passenger cars provided the most conservative geometric design values. For each type of vehicle, the speed on a short common tangent was highly affected by the length of the common tangent and degree of successive horizontal curves. Also, the speed was significantly affected by the value of deflection angles.

TABLE 3 Limits of Horizontal Curve Radii That Would Guarantee Consistent Design on Continuous Curve

Radius of the First Curve (m)	Passenger Cars		All Vehicles	
	Radius of the Second Curve, R2, (m.)		Radius of the Second Curve, R2, (m.)	
	Maximum	Minimum	Maximum	Minimum
100	122	85	124	84
200	309	148	330	144
300	630	197	732	189
400	1352	236	1880	224
500	4018	267	NL*	252
600	NL	293	NL	275
700	NL	315	NL	294
800	NL	334	NL	311
900	NL	350	NL	325
1000	NL	360	NL	337

* : No Maximum Limit (straight).

REFERENCES

1. Lamm, R., J. Hayward, and J. Cargin. Comparison of Different Procedure for Evaluating Speed Consistency. In *Transportation Research Record 1100,* TRB, National Research Council, Washington, D.C., 1986, pp. 10–19.
2. Polus, A., and D. Dagan. Models for Evaluating the Consistency of Highway Alignment. In *Transportation Research Record 1122,* TRB, National Research Council, Washington D.C., 1987, pp. 47–55.
3. Lamm, R., E. Choueiri, and J. Hayward. Tangent as an Independent Design Element. In *Transportation Research Record 1195,* TRB, National Research Council, Washington, D.C., 1988, pp. 123–131.
4. Lamm, R., E. Choueiri, and T., Mailaender. Comparison of Operating Speed on Dry and Wet Pavement of Two-Lane Rural Highways. In *Transportation Research Record 1280,* TRB, National Research Council, Washington, D.C., 1990, pp. 199–207.
5. Kneebone, D.C. Advisory Speed Signs and Their Effect on Traffic. *Proc., 2nd Conference, Australian Road Research Board,* Nunawading, 1964, pp. 524–538.
6. Neuhardt, J., G. Herrin, and T. Rockwell. *Demonstration of a Test-Driver Technique to Assess the Effects of Roadway Geometric and Development on Speed Selection.* Project EES 326B, Department of Industrial Engineers, Ohio State University, 1971.
7. Wong, Y. D., and A. Nicholson. *Speed and Lateral Placement on Horizontal Curves.* Road and Transport Research, Australian Road Research Board, Vol. 2, No. 1, March 1993, pp. 74–87.
8. Mclean, J. R. *Speeds on Curves. Internal Reports AIR 200-1 to 200-5.* Australian Road Research Board, Nunawading, 1970.
9. Adnan, G. *Geometric Design Consistency of Horizontal Alignment for Different Traffic Classes.* Master's thesis. Jordan University of Science and Technology, Irbid-Jordan, 1994.
10. Mintsis, G. *Speed Distribution on Road Curves.* Traffic Engineering and Control, Jan. 1988, pp. 21–27.
11. Leisch, J. E., and J. P. Leisch. New Concept in Speed Design Application. In *Transportation Research Record 631,* Transportation Research Council, Washington, D.C., 1977, pp. 4–15.
12. Lamm, R., E. Choueire, J. Hayward, and A. Paluri. Possible Design Procedure to Promote Design Consistency in Highway Geometric Design on Two-Lane Rural Roads. *Transportation Research Record 1195,* Transportation Research Council, Washington, D.C., 1988, pp. 111–122.
13. Mclean, J. R. *Driver Speed Behavior and Rural Road Alignment Design.* Traffic Engineering and Control, Vol. 22, No. 4, 1981, pp. 208–213.
14. Ben-Akiva, M., M. Hirsh, and J. Prashker. Probabilistic and Economic Factors in Highway Geometric Design. *Transportation Science,* Vol. 19, No. 1, 1985, pp. 11–19.
15. Moshe, H. Probabilistic Approach to Consistency in Geometric Design. *Journal of Transportation Engineering,* ASCE, Vol. 113, No. 3, 1987, pp. 268–276.
16. Talfeha, J. *Road Geometric Design Consistency Based on Speed Changes on Horizontal Curves.* Master's thesis. Jordan University of Science and Technology, Irbid-Jordan, 1991.
17. Kanellaidis, G., J. Golias, and S. Efstathiadis. Drivers' Speed Behavior on Rural Road Curves. *Traffic Engineering and Control,* July/Aug. 1990, pp. 404–415.

Publication of this paper sponsored by Committee on Operational Effects of Geometrics.

Calibrating and Validating Traffic Simulation Models for Unconventional Arterial Intersection Designs

JONATHAN L. BOONE AND JOSEPH E. HUMMER

Computer simulation has become an important tool for evaluating transportation strategies quickly and efficiently. Simulation is especially critical in assessing the potential of innovative traffic control alternatives. The calibration and validation of simulation models characterized by unconventional design and operation strategies is presented. This effort was part of a project to investigate unconventional traffic control alternatives for the North Carolina Department of Transportation. Three alternatives were selected for in-depth investigation: the Florida continuous green T-intersection, an application of the modern roundabout, and the Michigan median U-turn intersection. These strategies were examined using Traf-Netsim 4.0 and the macroscopic analysis package SIDRA 4.07. Models for each of the three alternatives were developed and efforts were made to calibrate and, in two cases, validate them with field data collected in Florida, Maryland, and Michigan. The highlights of the calibration included (*a*) updated critical gap distributions for the six-lane median U-turn and the roundabout, (*b*) a larger saturation flow rate for the median U-turn, (*c*) an average roundabout speed, and (*d*) a distribution of traffic into the free flow lane(s) for the continuous green T-intersection. The validation effort showed that the Traf-Netsim and SIDRA results compared reasonably well to field measurements.

Computer simulation has become one of the most viable evaluation tools that transportation engineers have. With dwindling transportation budgets and high public expectations, the engineer must be able to evaluate transportation strategies quickly and efficiently. As traffic congestion reaches unprecedented levels, innovative techniques will be needed to increase the capacity of existing transportation facilities and maximize the benefits of future proposed facilities. Evaluating the potential of new and innovative traffic control alternatives is one area where simulation techniques can make a significant contribution.

Computer simulation provides a host of benefits to the transportation engineer. First, simulation is a much less expensive means of experimentation than most other alternatives. Evaluation through computer simulation requires no expensive construction, can be completed relatively quickly, and does not impair the safety or convenience of motorists. Simulation allows an analyst to control many variables that would be difficult or impossible in a field test. Finally, adjustments are easier to make with simulation modeling than with field tests.

Although traffic simulation can provide many benefits, analysts must use caution when using this approach. The results provided by such models are only as good as the data that go into them; hence engineers must make an effort to ensure that the models are developed properly and function reliably. The calibration and validation of simulation models characterized by unconventional design and operation strategies is presented. This effort was part of a large project investigating unconventional traffic control alternatives for the North Carolina Department of Transportation (*1*).

Four alternatives were selected for an in-depth investigation. Three of them—the Florida continuous green T-intersection, an application of the modern roundabout, and the Michigan median U-turn intersection—were examined using Traf-Netsim (*2*). Traf-Netsim is a microscopic, stochastic simulation package developed by the FHWA. To supplement Traf-Netsim during the analysis of the modern roundabout application, the team used SIDRA (*3*). SIDRA is a macroscopic intersection analysis package developed by the Australian Road Research Board designed to evaluate roundabouts explicitly. During the research, models were developed for each of the three alternatives and efforts were made to calibrate and in most instances validate each of them.

The research team made data collection trips to Florida, Michigan, and Maryland (home of one of the East Coast's first modern roundabout installations) to collect calibration and validation data on working installations of the three alternatives. The data collection trips targeted both geometric and traffic flow data. Some of the data collected in the field was used to calibrate the models. The rest was used to validate the models by examining the models' ability to forecast the behavior observed in the field for a given set of conditions. Each of the alternatives is discussed separately, and the team's data collection efforts and attempts to calibrate and validate the models are described.

MEDIAN U-TURN

To calibrate and validate the median U-turn model, a data collection trip was made to the Detroit, Michigan area during the summer of 1993. The team visited numerous intersections where left turns were facilitated using median U-turn crossovers (see Figure 1). Two locations were selected for data collection based on three criteria. First, the team wanted to examine four-lane and six-lane arterial applications. Second, the analysts wanted to evaluate signalized and stop-controlled median U-turn crossovers. Third, the team preferred sites where driveways did not significantly influence the behavior observed at the intersection. Based on these criteria, the analysts selected the intersection of Big Beaver and Livernois (two 4-lane arterials with one set of signal-controlled U-turn crossovers) and the intersection of Mound and Hall/M59 (a six-lane and a four-lane arterial with one set of Stop sign-controlled U-turn crossovers).

J. L. Boone, Hayes, Seay, Mattern, and Mattern, Inc., 225 Hillsborough Street, Suite 120, Raleigh, N.C. 27603. J. E. Hummer, Department of Civil Engineering, North Carolina State University, Box 7908, Raleigh, N.C. 27695.

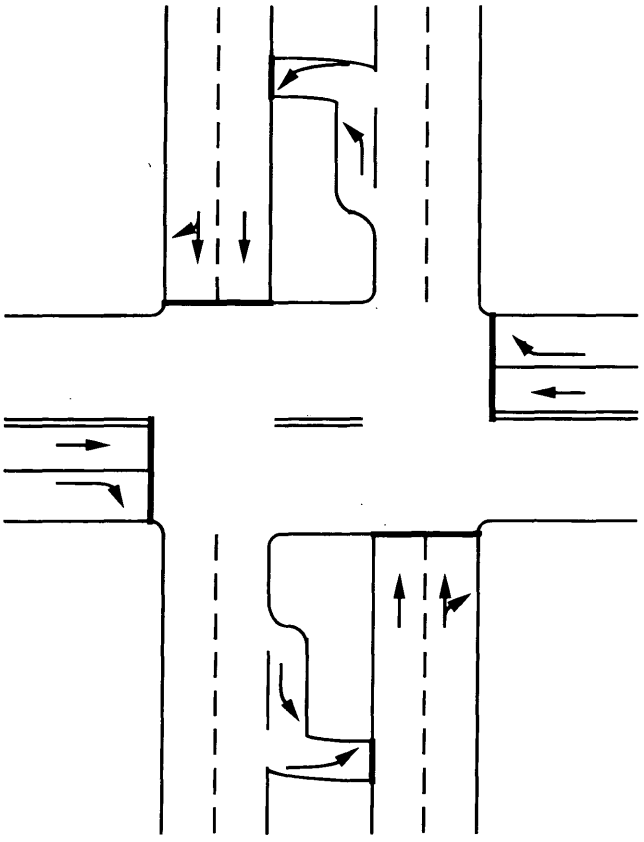

FIGURE 1 Median U-turn intersection.

Model Calibration

To calibrate the models before simulation, the researchers collected saturation flow data at the primary intersection and gap acceptance data at the crossovers. For each intersection, the data collection team recorded mean ideal saturation flows slightly higher than 2,000 passenger cars per hour per lane. Traf-Netsim provided a default value of 1,800 vehicles per hour per lane.

To investigate local motorists' gap acceptance behavior, approximately 1 hr 30 min of videotape was recorded at one of the Stop sign-controlled median crossovers at the intersection of Mound and Hall/M59. After downloading the data using Traffic Data Input Manager (TDIP *4*), Ramsey and Routledge's (*5*) method was applied to obtain a critical gap distribution. The analysis included 224 accepted gaps and 377 rejected gaps.

Although gap acceptance data were not collected at the intersection of Big Beaver and Livernois, the data associated with the two inside through lanes at the intersection of Mound and Hall/M59 were adapted for this purpose. A comparison of the values obtained during the analysis with the default values provided by Traf-Netsim indicates that the Traf-Netsim default values adequately describe the behavior exhibited at the crossovers along Big Beaver (a four-lane arterial), but not at Mound and Hall/M59. Figures 2 and 3 illustrate the comparison between the observed values and the Traf-Netsim default distribution. Based on the derived distribution, motorists turning left onto Mound (a six-lane arterial) from a U-turn crossover exhibit more aggressive behavior. This is not surprising given the high volumes along the six-lane arterial.

Model Validation

After collecting the data to calibrate the models, volume, travel time, and stopped delay data were gathered to validate the models. To collect the volume data, counts were taken over two consecutive 15-min intervals, alternating between the primary intersection and the median U-turn crossovers. For those alternating periods when the team did not count, they interpolated from the available data.

The team applied the average vehicle technique to conduct the travel time study. In all, 36 runs were completed over a 2-hr span for each intersection. At each intersection, data was collected on six movements, including left turns from each approach and through movements along the arterial with the U-turn crossovers.

On the day after collecting the travel time data, for the same 2-hr period, the stop delay behavior was recorded for two of the approaches at each intersection. For each approach, the team collected two 30-min periods of stopped delay data, counting the number of stopped vehicles at consecutive 15-sec intervals.

Based on the Michigan data, the research team developed a model for the intersection of Mound and Hall/M59 and three potential models for the intersection of Big Beaver and Livernois. Three potential models were considered because motorists in Michigan

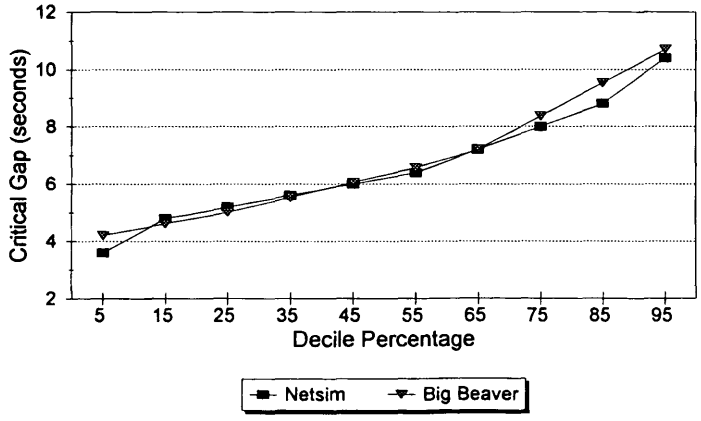

FIGURE 2 Observed Big Beaver and Livernois critical gap distribution versus Traf-Netsim default distribution.

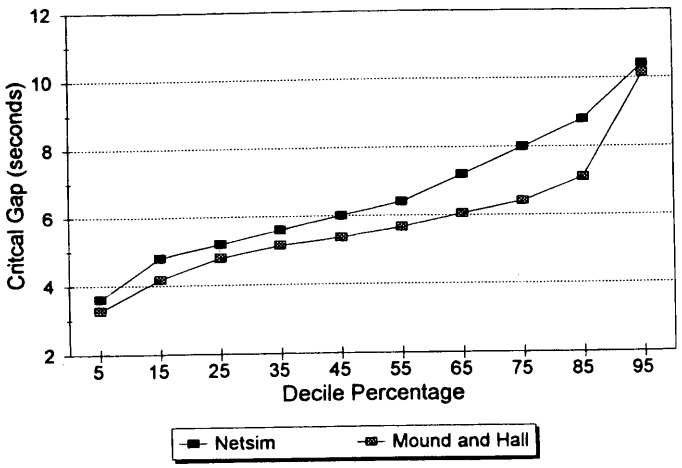

FIGURE 3 Observed Mound and Hall/M59 critical gap distribution versus Traf-Netsim default distribution.

observe the Western left turn rule. This rule allows a motorist to turn left from a crossover during the red signal phase. Traf-Netsim does not allow this type of movement. To emulate this behavior, the researchers first modeled the crossover as a conventional signalized T-intersection with no turns allowed during the red phase. The second model incorporated a signal on the arterial, 15 m upstream of the U-turn crossover, allowing the crossover to act as an unsignalized intersection subject to the gap acceptance parameters recorded during the trip. Figure 4 illustrates this alternative. Finally, a model converting the left turns at the crossover to right turns was developed as shown in Figure 5.

The analysts compared the three models using similar volumes, signal timing plans, and gap acceptance parameters to determine the most appropriate model. The researchers created a model for each 30-min observation period and compiled average results based on 10 runs per observation period. The runs within an observation period differed only in their random number seeds (the numbers used by Traf-Netsim to assign driver characteristics, decide whether a vehicle should turn at a given intersection, etc.).

Big Beaver and Livernois Validation Results

As mentioned previously, the analysts developed three models in an attempt to accurately simulate the behavior at this particular intersection. Table 1 summarizes the field measurements and the estimates provided by each of the models. As expected, the first model, without left turns on red, overestimated the travel times in the range of 3 to 60 percent. As a whole, however, the model overestimated the total travel time for all six movements by less than 20 percent. Given that the model did not allow left turns onto the arterial during the red phase of the signal cycle, its performance is impressive. In terms of stopped delay, the first model also performed reasonably well. For the southbound approach at the primary intersection, the model estimated an average stopped delay of 43.6 sec, a value 27 percent less than that observed in the field. The stopped delay estimate for the U-turn crossover was less than 55 percent of that observed in the field. This is particularly interesting considering that a left turn on red is not allowed by this particular model. The second model, with the signal just upstream of the U-turn model, provided the best travel-time estimates. As with the other two competing models, it overestimated the travel time for the eastbound through movement, but otherwise performed reasonably well. Overall, in terms of estimating the total travel time for the six movements, the model provided an estimate 10 percent higher than that observed in the field. Although the second model adequately esti-

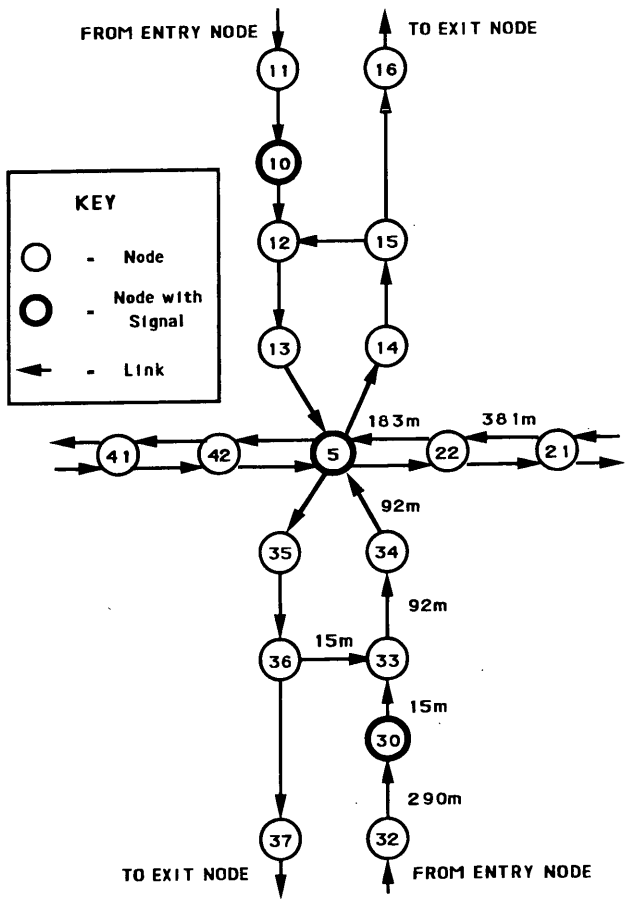

FIGURE 4 Traf-Netsim network for median U-turn option with signals before crossovers.

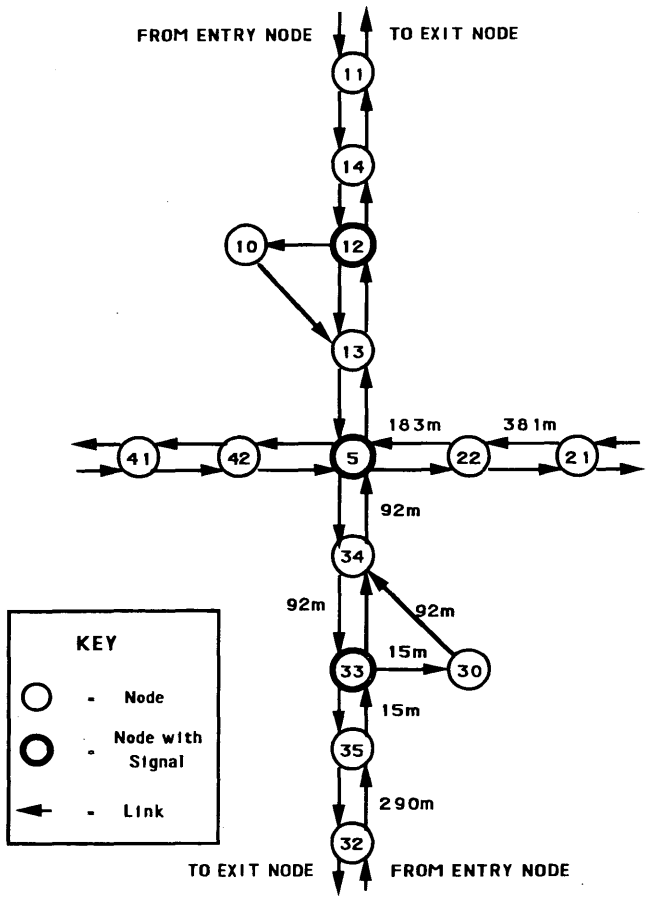

FIGURE 5 Traf-Netsim network for median U-turn option converting left turns from crossover to right turns.

mated the stopped delay for the southbound approach to the main intersection, it significantly underestimated the delay observed at the U-turn crossover. This indicates that relying on an upstream signal to model the left turns on red at the crossover may not properly imitate the behavior observed in the field. The third model provided the most consistent results of the three models evaluated. Besides the eastbound through movement, each of the travel time estimates ranged between 3 and 20 percent of the observed values. The stopped delay estimates provided by this model were also more reasonable, with 8 to 56 percent differences from the observed values. For the most part, each of the three models failed to accurately predict the stopped delay behavior associated with the U-turn crossover, although the third model provided better estimates.

Mound and Hall/M59 Validation Results

The analysts developed one model to simulate the intersection of Mound and Hall/M59. The results, shown in Table 2, indicate that Traf-Netsim was a reasonable predictor of the behavior observed in the field. A two-sample t-test revealed that four of the six pairs of travel time results were not significantly different at the 95 percent confidence level. The remaining two travel estimates provided by the model are within 10 and 20 percent of the times recorded in the field. The stopped delay estimates were also fairly consistent with the delay observed in the field. Although the differences range from 40 to 88 percent of the observed delay, because the delays observed in the field were relatively low, the difference between the observed and estimated values was not particularly alarming.

While developing the model, some difficulties were encountered due to the high volumes and the very high eastbound right turn volume. The version of Traf-Netsim used during the experiment (4.0) lacks the capability to assign vehicles to a given lane based on future actions by the vehicle. In particular, Traf-Netsim lacked the ability to direct vehicles wishing to turn right on the downstream link to the outside lane of the preceding upstream link. For several of the scenarios evaluated (due to the heavy volumes involved), vehicles in the inside through lane wishing to turn right from the next downstream link would stop and wait for an adequate gap to merge into the adjacent through lane to access the right turn lane. This caused midblock queues greater than 300 m long during a 30-min simulation period. To remedy this, an additional through lane was added to links experiencing the queueing problems. The through lane helped minimize the effects associated with this behavior, but it did not completely resolve the problem. Future versions of Traf-Netsim are expected to address this problem with an improved lane-changing algorithm (*6*).

MODERN ROUNDABOUT

Although traffic circles are not uncommon in the United States, few modern roundabouts have been constructed in recent years. As a

TABLE 1 Big Beaver and Livernois Model Validation

Measure of Effectiveness	Movement	Mean value of MOE			
		Field Measurement	Model 1 (no LTOR)	Model 2 (Fig. 4)	Model 3 (Fig. 5)
Travel Time (sec./veh.)	WB Through	95	110	113	110
	EB Through	71	113	117	116
	WB Left	183	188	171	176
	NB Left	157	165	141	152
	EB Left	132	171	151	161
	SB Left	186	227	201	220
Stopped Delay (sec./veh.)	SB Through	60	44	69	65
	Crossover	57	26	11	25

TABLE 2 Mound and Hall model validation

Measure of Effectiveness	Movement	Mean value of MOE	
		Field Measurement	Model
Travel Time (sec./veh.)	WB Through	136	139
	EB Through	99	107
	WB Left	229	228
	NB Left	179	215
	EB Left	178	163
	SB Left	140	180
Stopped Delay (sec./veh.)	SB Through, Time 1	5	10
	SB Through, Time 2	11	17
	WB Through, Time 1	7	11
	WB Through, Time 2	23	13

result, selecting an appropriate site to collect the data necessary to validate the roundabout models was difficult. Based on the project literature review (*1*), the most recent modern roundabout installation on the East Coast at the time of the study was at the junction of Routes 94 and 144 in Lisbon, Maryland, 50 km west of Baltimore. After constructing a temporary version of the roundabout in April 1993, the Maryland State Highway Association (SHA) finalized the design and constructed the current version of the roundabout in the fall of 1993.

Software Selection and Model Calibration

Two software packages were used to analyze the modern roundabout. Although not specifically intended for the analysis of roundabouts, Traf-Netsim 4.0 was chosen as one means to model the roundabout. Of particular importance was its ability to track individual vehicles as they approached and negotiated the roundabout and the surrounding road network. This ability to model an entire network is critical when attempting to evaluate situations such as the "raindrop" (*7*), in which individual roundabouts make up only a portion of the configuration. SIDRA 4.07, a macroscopic intersection analysis package developed by the Australian Road Research Board, was also selected to analyze the roundabout (*3*).

During a visit to Lisbon, the data collection team collected estimates of travel time, stopped delay, time in queue, and percentage stops at entry. Because of the differences between the two analysis packages, the research could only compare the stopped delay estimate for the two models. SIDRA does not estimate travel times and, although Traf-Netsim provides an estimate for the total number of stops, it cannot differentiate between stops associated with queueing and stops at the entry to the roundabout.

To calibrate the Traf-Netsim roundabout model depicted in Figure 6, the team collected gap acceptance data and recorded roundabout circulation speeds. Eight hours of gap acceptance behavior were collected on two approaches to the roundabout. After reducing the data with the aid of TDIP (*6*), the analysts applied Ramsey and Routledge's (*5*) method to obtain an estimate of the critical gap distribution. The comparison between the observed critical gap distribution and the Traf-Netsim default critical gap distribution shown in Figure 7 indicated that motorists entering the roundabout exhibited more aggressive behavior than the behavior described by the Traf-Netsim default distribution. An analysis of the circulation speed within the roundabout revealed an average circulation speed of 24 km/hr. To obtain the speed estimate, average speeds for three of the primary movements at the intersection were obtained and then weighted by the corresponding movement volume.

Because of relatively low volumes at the site and the importance of driver variation for the analysis, travel-time data were collected through a license plate study. The data collection crew examined two approaches to the intersection; one person was stationed along

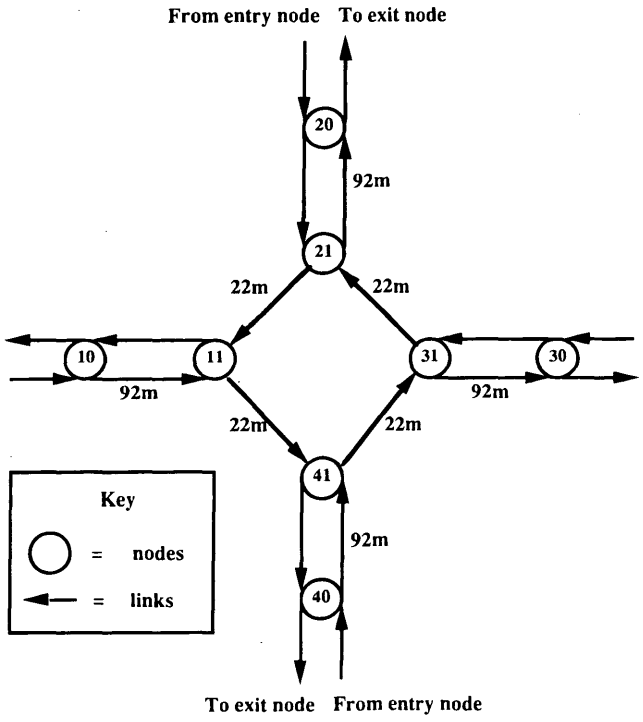

FIGURE 6 Traf-Netsim diagram for roundabout.

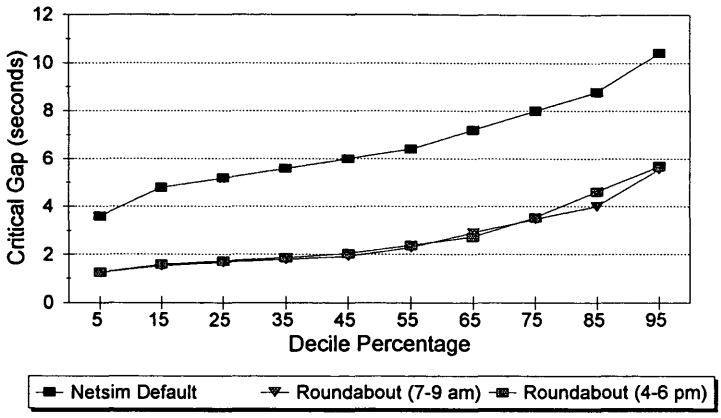

FIGURE 7 Observed roundabout critical gap distribution versus Traf-Netsim default distribution.

the approach leg and the other person moved from one downstream leg to another every 20 min.

Relatively light volumes at the intersection allowed the data collection team to collect the approach volume, stopped delay, and percentage stop data simultaneously. Because tracking vehicles through the roundabout to obtain turning percentages was difficult, the team recorded only the gross approach volumes. To estimate turning movement percentages, a set of November 1990 turning movement counts for the intersection were obtained from the SHA. A comparison of the approach volumes recorded during the trip and those provided by the SHA showed that the overall volumes had changed very little since November 1990.

The average stopped delay was estimated using the same technique as the median U-turn study. Based on the field data, vehicles entering the intersection during the morning or afternoon peak experienced an average stopped delay ranging from 0.5 sec to less than 3 sec. The results also indicate that many of those vehicles approaching the roundabout enter without having to stop.

Validation Results

Table 3 compares the parameters observed in the field with those predicted by Traf-Netsim and SIDRA. The travel time estimates reveal that, on the whole, Traf-Netsim provided a reasonable prediction of the travel times observed in the field with a tendency toward underestimation. Traf-Netsim also provided a low estimate of the number of stops. This is particularly striking considering that the stop percentage estimate provided by Traf-Netsim includes stops resulting from queueing and entry to the roundabout. In terms of stopped delay and time in queue, the values provided by Traf-Netsim also appear somewhat conservative. However, considering the relatively small amount of delay experienced at the intersection, the difference is insignificant. SIDRA also tended to underestimate the average stopped delay. In terms of stops upon entry, SIDRA provided a consistently accurate estimate, particularly as the number of stops increased.

CONTINUOUS GREEN T-INTERSECTION

To gather the data necessary to analyze the continuous green T-intersection (CGT), the team completed a 4-day data collection trip to Jacksonville, Florida. The CGT alternative may be applied to three-legged intersections with little pedestrian activity and high through volumes. Figure 8 illustrates this alternative.

To model this configuration, the team identified two primary areas where additional information was needed. First, the team investigated the typical geometry of the CGT, and then examined the typical distribution of traffic between the free-flow lane(s) and the signalized through lane associated with this configuration. In the first area, the team collected geometric data at 11 sites to develop a model that would represent the typical CGT application. The most significant piece of information to come from this portion of the investigation was the average distance upstream of the intersection where the vehicles were segregated into the outside free-flow lane(s) and the inside through lane subject to stopped conditions at the intersection. On average, the vehicles were segregated approximately 60 m upstream of the intersection and remained segregated for 60 m downstream of the intersection. With this information, the next step was to develop a model with one or two lanes subject to continuous movement, and another subject to signal control. Figure 9 shows the network developed for the CGT based on the geometric data collected.

The second area of calibration for the CGT was to identify the distribution of vehicles between the free-flow lane(s) and the lane subject to stopping for any given through volume. The team collected 86 15-min data points at six sites for lane distribution analysis. Observations for four-lane and six-lane arterials were represented within the data collected. With these data, least squares regression equations were developed relating the amount of traffic in the free-flow lane(s) to the total through volume. The R^2 values associated with these equations were more than 0.99 and suggest that the percentage of vehicles within the free-flow lane(s) is consistent at about 77 percent for four-lane arterials and 81 percent for six-lane arterials. Figure 10 shows the observations at the four-lane CGTs and the resulting least squares regression equation.

CONCLUSIONS

The calibration and validation of models of three unconventional arterial designs was described. Traf-Netsim was used for all three designs, and SIDRA was used for the roundabout alternative. The highlights of the calibration included updated critical gap distribu-

TABLE 3 Results of Roundabout Analysis Using Traf-Netsim and SIDRA

Time Interval	Movement	Travel Times		
		Observed	Traf-Netsim	SIDRA
7:00 - 8:00	EB Left	27 sec.	25.9 sec.	—
	EB Through	25 sec.	23.6 sec.	—
	EB Right	20 sec.	20.2 sec.	—
	SB Left	32 sec.	24.1 sec.	—
	SB Through	24 sec.	20.7 sec.	—
	SB Right	23 sec.	17.9 sec.	—
8:00 - 9:00	EB Left	27 sec.	25.1 sec.	—
	EB Through	25 sec.	22.7 sec.	—
	EB Right	20 sec.	19.2 sec.	—
	SB Left	32 sec.	23.9 sec.	—
	SB Through	24 sec.	20.3 sec.	—
	SB Right	23 sec.	18 sec.	—

Time Interval		Delay, Queue Time, and Stops		
		Observed	Traf-Netsim	SIDRA
7:00 - 8:00	**Eastbound**			
	Stopped Delay	0.088 hrs.	0.152 hrs.	0.06 hrs.
	Queue Time	0.175 hrs.	0.163 hrs.	—
	Number of Stops	45	30	51
	Southbound			
	Stopped Delay	0.05 hrs.	0.109 hrs.	0.01 hrs.
	Queue Time	0.192 hrs.	0.109 hrs.	
	Number of Stops	19	7	11
8:00 - 9:00	**Eastbound**			
	Stopped Delay	0.017 hrs.	0.061 hrs.	0.03 hrs.
	Queue Time	0.083 hrs.	0.064 hrs.	—
	Number of Stops	25	—	29
	Southbound			
	Stopped Delay	0.087 hrs.	0.068 hrs.	0.02 hrs.
	Queue Time	0.204 hrs.	0.068 hrs.	—
	Number of Stops	28	—	19
4:00 - 4:30	**Eastbound**			
	Stopped Delay	0.05 hrs.	0.014 hrs.	0.015 hrs.
	Queue Time	0.074 hrs.	0.015 hrs.	—
	Number of Stops	19	—	13
4:30 - 5:00	**Southbound**			
	Stopped Delay	0.05 hrs.	0.04 hrs.	0.025 hrs.
	Queue Time	0.117 hrs.	0.043 hrs.	—
	Number of Stops	28	—	21
5:00 - 6:00	**Eastbound**			
	Stopped Delay	0.033 hrs.	0.027 hrs.	0.02 hrs.
	Queue Time	0.038 hrs.	0.027 hrs.	—
	Number of Stops	17	—	19
	Southbound			
	Stopped Delay	0.094 hrs.	0.068 hrs.	0.03 hrs.
	Queue Time	0.183 hrs.	0.068 hrs.	—
	Number of Stops	35	—	35

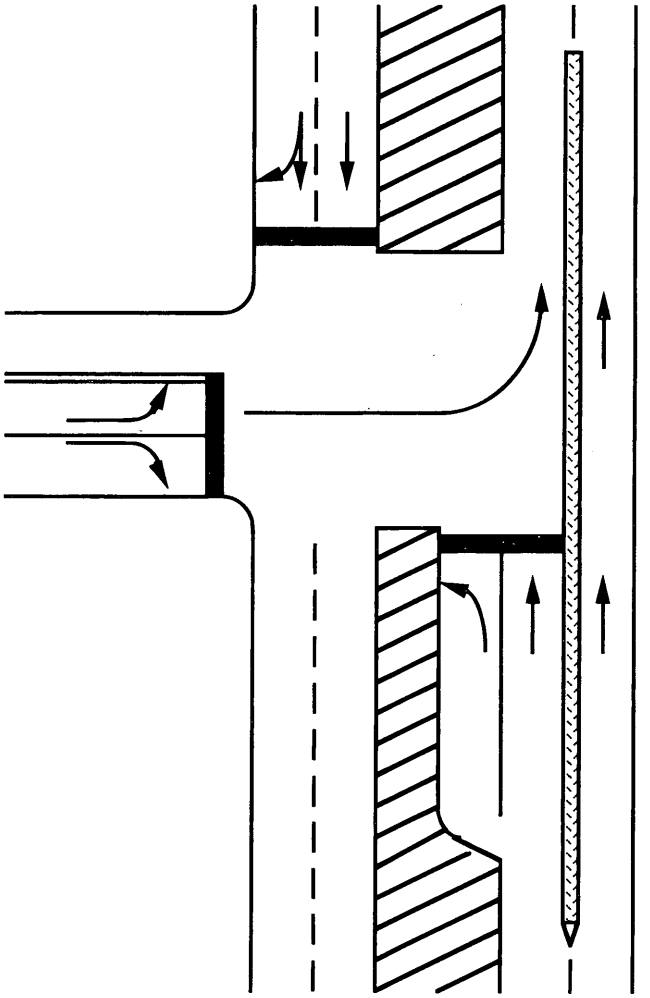

FIGURE 8 Continuous green T-intersection.

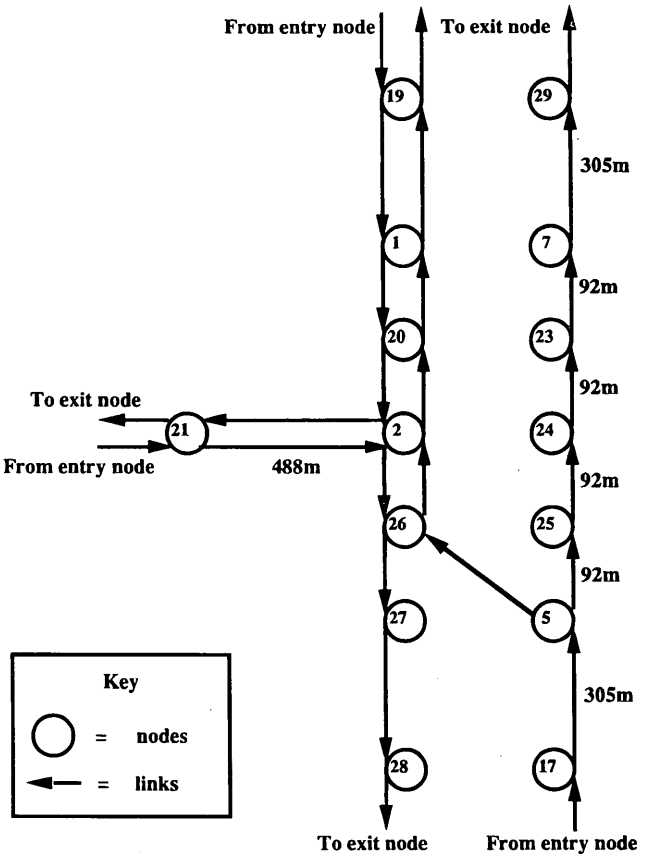

FIGURE 9 Traf-Netsim network for the continuous green T-intersection.

tions for the six-lane median U-turn and the roundabout, a larger saturation flow rate for the median U-turn, an average roundabout speed, and a distribution of traffic into the free-flow lane(s) for the CGT. Although this research investigated only the most important variables in the models that needed calibration, continued interest in these unconventional alternatives may warrant calibrating additional variables.

For validation of the median U-turn model, Traf-Netsim's estimates of travel time and delay for each of the intersections matched the behavior observed in the field reasonably well. Traf-Netsim slightly overestimated the travel time and underestimated the stopped delay. The results also indicate that the third approach to modeling the signal-controlled crossover with left turns on red (treating the crossover as if it operated as a right turn approach) provided the most accurate overall estimates. For validation of the roundabout models, a comparison of the field data with predictions by Traf-Netsim and SIDRA indicates that both provided relatively consistent results. Both Traf-Netsim and SIDRA predicted an insignificant amount of stopped delay and showed that a significant portion of the approaching vehicles entered without having to stop at all. Traf-Netsim also provided an accurate estimate of the travel times observed at the junction. Researchers should consider comparing the two packages and field data at modern roundabouts with higher volumes.

The models developed illustrate how simulation can provide reasonable predictions of field behavior at unconventional intersections. After determining that the models provided reasonable estimates for the measures of interest, the research team was able to gain some insight into what trends could be expected over a wide variety of geometry and traffic volumes.

The research reveals however, that additional work is needed. The CGT model, which appears to provide some potential benefits for application along suburban arterial corridors, still must be validated. As mentioned previously, validation of the roundabout model with higher volumes also would be helpful. Finally, there are several areas in which Traf-Netsim could be improved (e.g., the inability of Traf-Netsim to model left turns on red directly). Modifying Traf-Netsim to model two-lane crossovers and roundabouts would also be a worthwhile enhancement.

ACKNOWLEDGMENTS

FHWA and the North Carolina Department of Transportation (NCDOT) provided support for the research described in this study. The authors thank Troy Peoples and Jim Dunlop of the NCDOT for their guidance; Stephanie Kolb and Paul Sloup for helping collect the data; and engineers with the Michigan Department of Transportation, Maryland State Highway Aministration, and Florida Department of Transportation for their assistance.

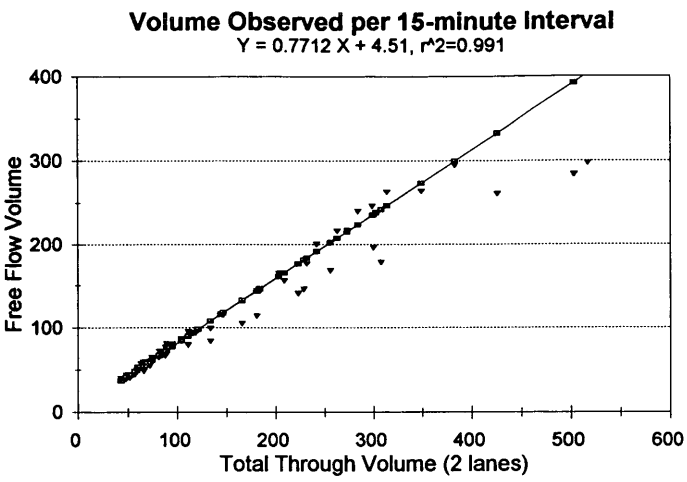

FIGURE 10 Four-lane continuous green T-intersection lane distribution.

REFERENCES

1. Boone, J. L., and J. E. Hummer. *Unconventional Design and Operation Strategies for Over-Saturated Suburban Arterials.* Draft Final Report. North Carolina Department of Transportation, Raleigh, N.C., June 30, 1994.
2. *TRAF User Reference Guide.* Version 4.2. Office of Safety and Traffic Operations R&D, FHWA, McLean, Va., Feb. 1994.
3. Akcelik, R. *Roundabout Capacity and Performance Analysis Using SIDRA.* Working Document TE91/002. Australian Road Research Board Limited, Nunawading, Victoria, Australia, July 1992.
4. Boesen, A., M. Kyte, and B. Rindlisbacher. *TDIP Program Documentation and User's Manual.* University of Idaho, Moscow, Idaho, March 1991.
5. Ramsey, J. B. H., and I. W. Routledge. A New Approach to the Analysis of Gap Acceptance Times. *Traffic Engineering and Control,* Vol. 15, No. 7, Nov. 1973, pp. 353–357.
6. Yedlin, M., E. Lieberman, A. Phlegar, A. Kanaan, and A. Santiago. The New Traf-Netsim: Version 5.0. Presented at the 73rd Annual Meeting of the TRB, Washington, D.C., Jan. 1994.
7. Ourston, L. Wide Nodes and Narrow Roads. Presented at the 72nd Annual Meeting of the TRB, Washington, D.C., Jan. 1993.

The views and opinions expressed in this paper are those of the authors and do not necessarily reflect the views and opinions of the FHWA, the NCDOT, or North Carolina State University. The authors assume full responsibility for the accuracy of the data and conclusion presented in this paper.

Publication of this paper sponsored by Committee on Operational Effects of Geometrics.

Lengths of Left-Turn Lanes at Unsignalized Intersections

PARTHA CHAKROBORTY, SHINYA KIKUCHI, AND MARK LUSZCZ

The required length of left-turn lanes at unsignalized intersections of two-lane roadways is analyzed, and recommended lengths are presented for different conditions. Increasing volumes of turning movements along suburban roadways due to residential and commercial developments warrant an analysis of the adequate length of turn lanes. The existing guidelines and standards for determining lane lengths at unsignalized intersections are incomplete, and the practices of various state agencies are not uniform. A model is developed which calculates the probability that a given length of turning lane will result in overflows. Lane lengths are suggested such that the probability of lane overflow is less than a given threshold value. The parameters considered in the model are the volume of turning vehicles, volume of opposing vehicles, critical gap, threshold probability, and vehicle mix. The validity of the model is checked by computer simulation. The recommended lengths are compared with lengths suggested by AASHTO, and the effects of considering opposing volume and changing the values of the threshold probability are discussed. The results of a field survey on the required space per vehicle in the turn lane are also presented. Recommended lane lengths for various conditions are presented in a set of tables.

As residential and commercial developments proliferate in the suburbs, turning movements, particularly left-turns into and out of minor roadways, are posing significant negative effects on traffic flow and safety of major roadways. A procedure to compute the adequate length of left-turn lanes on major roads at unsignalized intersections is presented. This study was conducted as a part of a series of examinations by the authors of the guidelines on channelization of intersections (*1,2*).

Although the issue of adequate lane length is critical for highway planning, little has been done to develop a consistent volume-based criterion for its selection. Neither AASHTO (*3*) nor the Highway Capacity Manual (*4*) (HCM) provide any definitive guidelines for the selection of lane length. A survey of several states indicates that practices differ widely across the country: some states follow very simple ad hoc criteria, while others use the rigid guide suggested by Harmelink (*5*).

In studying left-turning movements at unsignalized intersections, two questions arise:

1. Is a separate left-turn lane warranted?
2. If it is warranted, what should be the length of the lane?

The work presented addresses the second question. The first question has been dealt with in detail by Kikuchi and Chakroborty (*1*).

The following sections include: a review of existing procedures and practices; identification of the factors relevant to the determination of the length of left-turn lane; analysis of the queueing pattern of the turning vehicles using a generalized queueing model; validation of model results by simulation model; presentation of the suggested left-turn lane lengths; and discussion of the effects of changes in the input parameters with a comparison of the proposed model's results with previously suggested AASHTO values.

P. Chakroborty, Department of Civil Engineering, Indian Institute of Technology, Kanpur, Kanpur 208016, India. S. Kikuchi and M. Luszcz, Department of Civil Engineering, University of Delaware, Newark, Del. 19716.

PROBLEM STATEMENT AND APPROACH

Figure 1 shows an unsignalized intersection in which a major two-lane roadway intersects a minor road. The through traffic on the major road does not stop at the intersection, requiring left-turning vehicles on the major road to wait until a suitable gap is found in the opposing flow. The task is to determine the vehicle storage length L that minimizes the chance of lane overflow; the probability of overflow must be less than a specified threshold value. Lane length L is called the adequate lane length.

EXISTING GUIDELINES

Despite the importance of determining adequate lane length, guidelines for the left-turn lane length at unsignalized intersections have not been systematically compiled.

AASHTO (*3*) suggests the following procedure to calculate lane length: "the storage length, exclusive of taper, may be based on the number of turning vehicles likely to arrive in an average 2-min period within the peak hour." This procedure is obviously ad hoc, and AASHTO acknowledges this when it refers to the 2-min period as "somewhat arbitrary (*3*)." AASHTO recognizes that guidelines on left-turn lane length should be based on the turning as well as the opposing volume, but offers no specifics. NCHRP Report 279, *Intersection Channelization Design Guide* (*6*), also follows the AASHTO guidelines.

When their research revealed a lack of comprehensive guidelines on the subject the authors conducted a survey of various state departments of transportation regarding lane length. Of the fifty questionnaires that were sent out, 25 states responded. It was found that most states follow the rule-of-thumb approach to determine lane lengths. Some states, however, use the lane lengths suggested by Harmelink (*5*).

Harmelink provides a set of figures on recommended lengths for left-turn lanes in his 1967 study (*5*). The suggested lengths are derived based on the criterion that the probability of lane overflow be less than a given value. Harmelink considers most of the relevant factors in his model; however, his derivation suffers from critical errors in the mathematical treatment of probability, which undermine the validity of his recommendations. The shortcomings of Harmelink's derivation were discussed in detail by Kikuchi and Chakroborty (*1*).

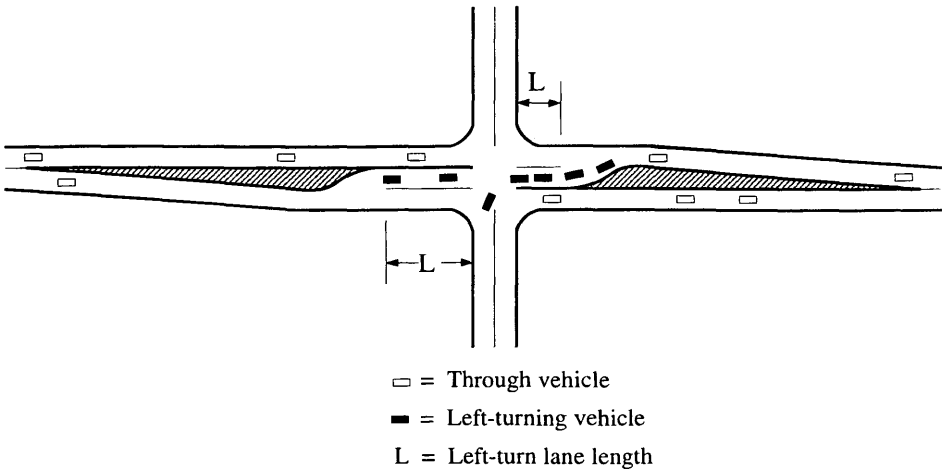

FIGURE 1 Schematic of unsignalized intersection with turning lanes.

Factors Considered in the Analysis

The major factors that must be considered when selecting the left-turn lane length at an unsignalized intersection are:

- Traffic volumes and vehicle mix: left-turn, through, and opposing volume, and composition of vehicle types,
- Critical gap size,
- Space requirement per vehicle, and
- Threshold probability.

Each of these factors is discussed in the following sections.

Traffic Volumes and Vehicle Mix

Left-turn volume is an obvious factor in selecting left-turn lane length. The opposing flow determines the frequency of gaps available to a left-turning vehicle. The type and mix of left-turning vehicles influences the required length in that (*a*) large vehicles require a longer space for storage and (*b*) they often take longer to complete the turn because of a lower acceleration rate and the need for careful maneuvering, which affects their critical gap size.

Critical Gap Size

Critical gap size is the minimum time headway in the opposing flow that is required for a driver to complete a left-turning maneuver. Its value (in seconds) is influenced by several factors, including geometric design, speed of approaching vehicle, dynamic characteristics of the turning vehicle, and driver characteristics. A longer critical gap results in fewer turning opportunities, and hence, the length of the queue increases.

The geometric design of the intersection affects the sight distance of the turning vehicle. The critical gap increases inversely with the available sight distance (*4*). The approach speed of the opposing vehicles also affects the critical gap size. Empirical research has shown that the critical gap size increases with increasing approach speed of the opposing vehicles (*4*). The HCM (*4*) provides guidelines, based on empirical findings, on the value of the critical gap size under different approach speeds and geometric designs. Values ranging from 5 to 7 sec are suggested and shown in Table 1.

Space Requirement Per Vehicle

The space a vehicle requires while standing affects the actual lane length required. The required space per vehicle includes the length of the vehicle and the buffer distance in front of the vehicle. Field surveys were conducted to determine the space requirement of a standing vehicle. The results are provided in the section on the determination of adequate lane length in units of distance.

Threshold Probability of Overflow

The threshold probability defines the acceptable frequency of overflow of vehicles from the left-turn lane into the adjacent through lane. The greater the value of this probability, the greater the chance of lane overflow, and vice versa. A value of 0.015 is used. The selection criteria for the threshold probability and its implications are discussed in a subsequent section.

THE PROPOSED APPROACH

A queueing model of the turning vehicles is constructed and the adequate lane length is then derived by anticipating the probability of lane overflows, which must be less than a given threshold value.

TABLE 1 Critical Gap Size Under Various Conditions

Approach Speed of Opposing Flow	No. of Lanes (in each direction) 1	2
30 mph	5.0 sec	5.5 sec
55 mph	5.5 sec	6.0 sec

Note: In case of restricted sight distance increase the above values by a maximum of 1.0 seconds
Source: HCM [4], Table 10-2.

The proposed procedure for determining the adequate lane length involves:

1. Determining the threshold probability of lane overflow based on the acceptable frequency of lane overflow.
2. Identifying the values of the input parameters based on traffic conditions and intersection characteristics: left-turning volume, opposing volume, critical gap, vehicle mix, and vehicle space requirements.
3. Computing the adequate lane length in units of number of vehicles using the model. The probability of lane overflow (or a queue length greater than the lane length) should be less than the threshold value.
4. Converting the lane length to distance by multiplying the adequate lane length in vehicle units (obtained in step 3) by the factor that converts the vehicle units to the distance requirements considering vehicle mix and the buffer between vehicles.

NOTATION

The following notations are used in explaining the model:

- λ_o = Arrival rate of opposing vehicles in vehicles per second,
- λ_l = Arrival rate of left-turning vehicles in vehicles per second,
- T_c = Critical gap in seconds,
- t_i = Time headway of the ith gap in the opposing flow,
- τ = Threshold probability of lane overflow,
- μ = Service time for a left-turning vehicle (service time of the first vehicle in the queue),
- ν = The number of left-turning vehicles in the queue. The term queue includes the vehicle that is being served (i.e., the vehicle at the top of the queue, as well as the other vehicles waiting behind it),
- N_i = Arbitrary value of the lane length in number of vehicles,
- N^* = The adequate lane length in number of vehicles,
- IN^* = Nearest integer to N^*,
- L = The adequate lane length in units of distance,
- χ = Factor accounting for the vehicle mix while calculating L, and
- S = Space required by a stationary passenger car in meters.

Model Formulation

The queueing process being modeled is as follows:

Left-turning vehicles arrive randomly at the intersection and form a queue. The first vehicle in the queue waits for an acceptable gap in the opposing flow. The service time of this queueing process is actually the waiting time of the first vehicle with no apparent server. The queueing system is assumed to be an M/G/1 system. That is, the arrival process is Poisson distributed, and the service time distribution is unspecified; the queue discipline is first-in-first-out (FIFO). Because of the unique service pattern and service time distribution, the queue distribution is complex. The M/G/1 queue is analyzed using the concept of Markov chains. The outcome of the analysis is the mean and variance of the queue length. From the knowledge of the mean and variance of the queue length, an upper bound probability of lane overflow is obtained using Chebyshev's inequality.

Vehicle Arrival Process

The left-turning and opposing vehicles are assumed to arrive according to the Poisson distribution. The probability of k vehicles arriving within a time period t is given as

$$P(k) = \frac{(\lambda t)^k e^{-\lambda t}}{k!} \tag{1}$$

where λ is either λ_l or λ_o depending on the flow being considered.

Vehicle Departure (Service) Process

A left-turning vehicle at the top of the queue waits until a suitable gap (i.e., gap size $\geq T_c$) becomes available in the opposing flow and then accepts it to make the turn. In this queueing model, the time a vehicle spends at the top of the queue is considered the service time. That is, if the first gap (t_1) is greater than the critical gap size ($t_1 < T_c$), the service time is zero. If the second gap (t_2) is the first acceptable gap ($t_1 < T_c$ and $t_2 > T_c$), the service time is t_1 seconds (i.e., the driver rejects the first gap and immediately accepts the second).

Under the assumption of Poisson arrival for the opposing flow, the time headways in the opposing flow are distributed exponentially with parameter λ_o. Assuming that the critical gap T_c is the same for all drivers and is independent of how long the driver has waited, the following equations are obtained from the moment-generating function of the service time distribution according to Drew (*7*).

$$E[\mu] = \frac{e^{\lambda_o T_c} - 1 - \lambda_o T_c}{\lambda_o} \tag{2}$$

where $E[\mu]$ is the mean service time for the left-turning vehicles (or the mean time a left-turning vehicle waits at the top of the queue).

Subsequently, $E[\mu^2]$ and $E[\mu^3]$ are obtained as follows:

$$E[\mu^2] = \frac{2\{\lambda_o E[\mu]\}^2 + 2\lambda_o E[\mu] - \{\lambda_o T_c\}^2}{\lambda_o} \tag{3}$$

$$E[\mu^3] = \frac{6}{\lambda_o^3}\left[2\lambda_o E[\mu]\left\{\lambda_o E[\mu] - \frac{(\lambda_o T_c)^2}{2}\right\} + \{\lambda_o E[\mu]\}^3 + \left\{\lambda_o E[\mu] - \frac{(\lambda_o T_c)^2}{2} - \frac{(\lambda_o T_c)^3}{6}\right\}\right] \tag{4}$$

Also note that the variance of the service time, var[μ], is obtained from Equations 2 and 3 as

$$\text{var}[\mu] = E[\mu^2] - E[\mu]^2 = \frac{e^{2\lambda_o T_c} - 2\lambda_o T_c e^{\lambda_o T_c} - 1}{\lambda_o^2} \tag{5}$$

Queue Length: Mean and Variance

This section focuses on two consecutive left-turning vehicles (the first and second vehicles) at the top of the queue and studies the queue length (the number of vehicles) during the time in which they are served. The following identity holds:

$$\nu' = \nu - \delta + \alpha \tag{6}$$

where

v = number of vehicles in queue when first vehicle reached top of queue,
v' = number of vehicles in queue just after first vehicle's departure,
α = number of arrivals of left-turning vehicles during particular service time, and
δ = dummy variable that takes a value of 1 if $v > 0$, and a value of 0 if $v = 0$.

In the steady state (i.e., when the initial fluctuations are cleared), the following identities hold: $E[v'] = E[v]$, $E[v'^2] = E[v^2]$, and $E[v'^3] = E[v^3]$. The reason is that, in the long run, the distinction between v and v' is lost and they have the same distribution. From these and the preceding identity expressions for $E[v]$, var$[v]$ can be obtained. The expression for $E[v]$ is called the Pollaczek-Kintchine equation and its derivation can be found in many textbooks of probability theory; among them is Taylor and Karlin (*8*). The expression for $E[v]$ is given as

$$E[v] = \lambda_l E[\mu] + \frac{\lambda_l^2 E[\mu^2]}{2(1 - \lambda_l E[\mu])} \tag{7}$$

Using similar logic, the following relationship for the variance of the queue length, var$[v]$, may be determined.

$$\text{var}[v] = 2(E[v] - \lambda_l E[\mu]^2 + 3E[v] - 2\lambda_l E[\mu] + \frac{\lambda_l^3 E[\mu^3]}{3(1 - \lambda_l E[\mu])} - E[v]^2 \tag{8}$$

DETERMINATION OF ADEQUATE LANE LENGTH IN NUMBER OF VEHICLES

Derivation

The adequate lane length is defined as the minimum lane length in number of vehicles N^* for which the probability of lane overflow is less than an acceptable value:

$$N^* = \min_i \{N_i \mid P(v > N_i) \leq \tau\} \tag{9}$$

where

v = the number of vehicles in the left-turn queue,
N_i = the left-turn lane length in number of vehicles, and
τ = the threshold probability of overflow.

To compute the probability $P(v > N_i)$ precisely, the probability density function (PDF) of the number of left-turn vehicles in the queue must be determined. However, determining the PDF is difficult given the complex distribution of the service time. Chebyshev's inequality formula allows the computation of this probability without any specific assumption about the PDF.

According to Chebyshev's inequality (9),

$$P(v > E[v] + \alpha) \leq \frac{\text{var}[v]}{\text{var}[v] + \alpha^2} \tag{10}$$

where α is any real number. The preceding inequality holds for any probability distribution for v.

Substituting $E[v] + \alpha$ by N_i, Equation 10 can be written as

$$P(v > N_i) \leq \frac{\text{var}[v]}{\text{var}[v] + (N_i - E[v])^2} \tag{11}$$

Thus, in the worst case, the probability that the number of vehicles in the queue, v, is greater than the given lane length, N_i (the overflow condition), is found by treating Equation 11 as an equality.

Hence, for the condition $P\{v > N_i\} \leq \tau$ (Equation 9) to be satisfied, the following should hold:

$$P(v > N_i) = \frac{\text{var}[v]}{\text{var}[v] + (N_i - E[v])^2} \leq \tau \tag{12}$$

When Equation 12 is an equality, the value N_i is equal to N^*. That is, when $N_i = N^*$, Equation 12 may be rewritten as

$$(N^*)^2 - 2E[v]N^* + E[v]^2 + \text{var}[v] - \frac{1}{\tau}\text{var}[v] = 0 \tag{13}$$

By solving Equation 13 with respect to N^*

$$N^* = E[v] + \sigma[v] \sqrt{\frac{1}{\tau} - 1} \tag{14}$$

where $E[v]$ is the mean queue length and $\sigma[v] = \sqrt{\text{var}[v]}$ is the standard deviation of the queue length.

The preceding relation is obtained by considering only one of the two possible roots of Equation 13. The other root is discarded because the lane length required should increase when τ decreases, and not vice versa as is suggested by the discarded root.

The values of $E[v]$ and $\sigma[v]$ in Equation 14 are obtained from Equations 7 and 8, respectively, which are in turn determined by Equations 2 and 3. Hence N^*, the adequate lane length in number of vehicles, can be calculated when a set of values for λ_o, λ_l, and T_c is given.

Recommended Lane Lengths for Selected Input Values

Tables 2 through 6 show the adequate lane length obtained from the model for different sets of input values. In the tables, the numbers shown are the nearest integer to N^*, IN^*. The tables are developed for $\tau = 0.015$, and for different combinations of T_c, λ_l, and λ_o: T_c = 5.0, 5.5, 6.0, 6.5, and 7.0 sec; λ_l = 40 vph to 400 vph; λ_o = 100 vph to 1,000 vph.

The tables show that the adequate lane length increases as the left-turn volume increases for the same opposing volume and critical gap size, as expected. Similarly, for a given left-turning volume and critical gap size, the adequate lane length increases for a higher opposing volume. And as the critical gap size increases so does the adequate lane length (for the same left-turning and opposing volumes).

Model Validation

The validity of the proposed model was tested by comparing the recommended left-turn lane lengths in the tables with the results

TABLE 2 Adequate Lane Length at Unsignalized Intersections (in Number of Vehicles), Critical Gap = 5.0 sec, Threshold Probability = 0.015

Left-Turn Volume (vph)	Opposing Volume (in vph)															
	100	160	220	280	340	400	460	520	580	640	700	760	820	880	940	1000
40	0[a]	0[a]	0[a]	0[a]	1[b]	1[b]	1[b]	1[b]	1[b]	1[b]	1[b]	1[b]	1[b]	2	2	2
80	0[a]	1[b]	1[b]	1[b]	1[b]	1[b]	1[b]	2	2	2	2	2	2	3	3	3
120	0[a]	1[b]	1[b]	1[b]	2	2	2	2	2	3	3	3	3	4	4	4
160	1[b]	1[b]	1[b]	2	2	2	2	3	3	3	4	4	4	5	5	6
200	1[b]	1[b]	2	2	2	3	3	3	4	4	4	5	5	6	6	7
240	1[b]	1[b]	2	2	3	3	3	4	4	5	5	6	6	7	8	9
280	1[b]	2	2	3	3	4	4	4	5	6	6	7	8	8	9	11
320	1[b]	2	2	3	3	4	4	5	6	6	7	8	9	10	11	13
360	1[b]	2	3	3	4	4	5	6	6	7	8	9	10	12	14	16
400	2	2	3	4	4	5	6	6	7	8	9	10	12	14	17	21

[a] A zero lane length indicates that a left-turn lane is not warrented. See ref. [1].

[b] For practical purposes, the lane length should be at least two vehicle lengths.

from a computer simulation of the queueing process. A simulation program of the intersection-queueing process (called TSIM) developed by the University of Delaware was used. TSIM was also used to validate Kikuchi and Chakroborty's (*1*) model on left-turn lane warrants at unsignalized intersections. NETSIM was not used because it does not provide adequate simulation of turning conditions at an isolated unsignalized intersection, nor can it capture the lane overflow condition. For the set of input values used in Table 4 and the corresponding recommended lane lengths, the simulation model was executed and the frequencies of queue lengths were observed. From this, the minimum lane length that would result in a probability of overflow less than the threshold value (0.015) was

TABLE 3 Adequate Lane Length at Unsignalized Intersections (in Number of Vehicles), Critical Gap = 5.5 sec, Threshold Probability = 0.015

Left-Turn Volume (vph)	Opposing Volume (in vph)															
	100	160	220	280	340	400	460	520	580	640	700	760	820	880	940	1000
40	0[a]	0[a]	0[a]	1[b]	1[b]	1[b]	1[b]	1[b]	1[b]	1[b]	1[b]	2	2	2	2	2
80	0[a]	1[b]	1[b]	1[b]	1[b]	1[b]	2	2	2	2	3	3	3	3	3	4
120	1[b]	1[b]	1[b]	2	2	2	2	3	3	3	3	4	4	5	5	5
160	1[b]	1[b]	2	2	2	3	3	3	4	4	4	5	5	6	6	7
200	1[b]	1[b]	2	2	3	3	4	4	4	5	5	6	7	7	8	9
240	1[b]	2	2	3	3	4	4	5	5	6	6	7	8	9	10	12
280	1[b]	2	3	3	4	4	5	5	6	7	8	9	10	11	13	16
320	2	2	3	3	4	5	5	6	7	8	9	10	12	14	17	21
360	2	2	3	4	5	5	6	7	8	9	10	12	15	18	23	-
400	2	3	3	4	5	6	7	8	9	10	12	15	18	23	-	-

[a] A zero lane length indicates that a left-turn lane is not warrented. See ref. [1].

[b] For practical purposes, the lane length should be at least two vehicle lengths.

TABLE 4 Adequate Lane Length at Unsignalized Intersections (in Number of Vehicles), Critical Gap = 6.0 sec, Threshold Probability = 0.015

Left-Turn Volume (vph)	Opposing Volume (in vph)															
	100	160	220	280	340	400	460	520	580	640	700	760	820	880	940	1000
40	0[a]	0[a]	1[b]	1[b]	1[b]	1[b]	1[b]	1[b]	1[b]	2	2	2	2	2	2	3
80	0[a]	1[b]	1[b]	1[b]	1[b]	2	2	2	2	3	3	3	4	4	4	5
120	1[b]	1[b]	1[b]	2	2	2	3	3	3	4	4	5	5	5	6	7
160	1[b]	1[b]	2	2	3	3	3	4	4	5	5	6	7	7	8	9
200	1[b]	2	2	3	3	4	4	5	5	6	7	7	8	9	11	13
240	1[b]	2	3	3	4	4	5	6	6	7	8	9	11	12	15	18
280	2	2	3	4	4	5	6	6	7	8	10	11	13	16	21	-
320	2	3	3	4	5	6	6	7	9	10	12	14	18	23	-	-
360	2	3	4	4	5	6	7	8	10	12	14	18	24	-	-	-
400	2	3	4	5	6	7	8	10	11	14	18	23	-	-	-	-

[a] A zero lane length indicates that a left-turn lane is not warrented. See ref. [1].

[b] For practical purposes, the lane length should be at least two vehicle lengths.

TABLE 5 Adequate Lane Length at Unsignalized Intersections (in Number of Vehicles), Critical Gap = 6.5 sec, Threshold Probability = 0.015

Left-Turn Volume (vph)	Opposing Volume (in vph)															
	100	160	220	280	340	400	460	520	580	640	700	760	820	880	940	1000
40	0[a]	0[a]	1[b]	1[b]	1[b]	1[b]	1[b]	1[b]	2	2	2	2	2	3	3	3
80	1[b]	1[b]	1[b]	1[b]	2	2	2	3	3	3	3	4	4	5	5	5
120	1[b]	1[b]	2	2	2	3	3	3	4	4	5	5	6	7	7	8
160	1[b]	2	2	3	3	3	4	4	5	6	6	7	8	9	11	13
200	1[b]	2	2	3	4	4	5	5	6	7	8	9	11	13	16	20
240	2	2	3	4	4	5	6	7	8	9	10	12	15	18	25	-
280	2	3	3	4	5	6	7	8	9	11	13	16	21	-	-	-
320	2	3	4	5	6	7	8	9	11	13	16	22	-	-	-	-
360	3	3	4	5	6	7	9	11	13	16	22	-	-	-	-	-
400	3	4	5	6	7	8	10	12	16	21	-	-	-	-	-	-

[a] A zero lane length indicates that a left-turn lane is not warrented. See ref. [1].

[b] For practical purposes, the lane length should be at least two vehicle lengths.

found. Table 7 compares the simulation and the proposed model's results for different combinations of λ_l and λ_0. The value of T_c used was 6.0 sec.

Table 7 suggests that the two cases are very similar with a maximum difference of two car spaces (for some of the higher-volume combinations considered). The lane lengths derived from the simulation are equal to or shorter than those calculated by the model. This difference is due to the use of Chebyshev's inequality, which models a worst-case scenario, making the results somewhat conservative.

DETERMINATION OF ADEQUATE LANE LENGTH IN UNITS OF DISTANCE

So far the adequate lane length has been considered (in Equation 14 and Tables 2 through 6) in numbers of vehicles. For application to geometric design, however, the length should be provided in units of distance using the following steps:

1. Establish the average space per passenger car when it is waiting in the left-turn lane. This space includes the buffer between two adjacent cars as well as the vehicle length.
2. Analyze the effect of larger vehicles on space requirement and derive passenger car equivalency factors for non-passenger cars.
3. Determine the lane length in units of distance after considering the vehicle mix.

Step 1: Space Requirement of a Standing Passenger Car

The space requirement for a standing passenger car was determined through field observations at several intersections in Newark, Delaware. The number of passenger cars in the queue and the corresponding space required was measured. One hundred twenty-four such queues (containing 383 passenger cars) were measured. The queues sampled in this analysis contained only passenger cars. Figure 2 provides the observations and the least squares regression line obtained for the data.

The relationship between the space requirement y in meters and the number of passenger cars in the queue x is obtained as

$$y = 7.66x - 2.92 \qquad R^2 = 0.989 \tag{15}$$

Equation 15 indicates that the space required per passenger car is approximately 7.7 m (25 ft) including a buffer zone between cars. However, the required space for the first vehicle in the queue is only (approximately) 4.6 m (15 ft), because no buffer zone is needed between the first car and the stop line. This accounts for the nonzero intercept in the calculated regression line.

TABLE 6 Adequate Lane Length at Unsignalized Intersections (in Number of Vehicles), Critical Gap = 7.0 sec, Threshold Probability = 0.015

Left-Turn Volume (vph)	Opposing Volume (in vph)															
	100	160	220	280	340	400	460	520	580	640	700	760	820	880	940	1000
40	0[a]	1[b]	1[b]	1[b]	1[b]	1[b]	1[b]	2	2	2	2	3	3	3	3	4
80	1[b]	1[b]	1[b]	2	2	2	3	3	3	4	4	4	5	5	6	7
120	1[b]	1[b]	2	2	3	3	4	4	5	5	6	6	7	8	9	11
160	1[b]	2	2	3	3	4	5	5	6	7	8	9	10	12	15	19
200	2	2	3	3	4	5	6	6	7	9	10	12	15	19	26	-
240	2	3	3	4	5	6	7	8	9	11	13	17	23	-	-	-
280	2	3	4	5	6	7	8	9	11	14	18	25	-	-	-	-
320	2	4	4	5	6	8	9	11	14	18	26	-	-	-	-	-
360	3	4	5	6	7	9	11	14	18	25	-	-	-	-	-	-
400	3	5	5	7	8	10	13	16	23	-	-	-	-	-	-	-

[a] A zero lane length indicates that a left-turn lane is not warrented. See ref. [1].

[b] For practical purposes, the lane length should be at least two vehicle lengths.

TABLE 7 Comparison of Length Requirements (in Number of Vehicles): Proposed Model and Simulation

Left-turning Vol.(vph)	Opposing Volume (vph) 100		160		220		280		340		400	
	S	M	S	M	S	M	S	M	S	M	S	M
120	1	1	1	1	1	1	1	2	2	2	2	2
160	1	1	1	1	1	2	1	2	2	3	2	3
200	1	1	1	2	2	2	2	3	2	3	2	4
240	1	1	1	2	2	3	2	3	2	4	2	4

Left-turning Vol.(vph)	Opposing Volume (vph) 460		520		580		640		700		760	
	S	M	S	M	S	M	S	M	S	M	S	M
120	2	3	2	3	3	3	3	4	3	4	4	5
160	2	3	3	4	3	4	4	5	4	5	4	5
200	3	4	3	5	4	5	5	6	6	7	7	7
240	3	5	4	6	5	6	5	7	6	8	7	9

S: Derived from simulation
M: Derived from the proposed model
Threshold probability = 0.015
Critical gap = 6.0 seconds

Step 2: Effects of Large Vehicles on Space Requirement

Large vehicles affect the adequate lane length in two ways: (*a*) they require a longer space, and (*b*) their lower acceleration capability and maneuverability result in a larger critical gap size.

The first point is addressed by assuming passenger car equivalencies, which account for the difference in sizes of large vehicles relative to the passenger car. The equivalency factors are computed from AASHTO's standard on vehicle lengths [Table II-1 of AASHTO Green Book (*3*)] and are provided in Table 8.

The factor of critical gap size in relation to vehicle size requires further research. When large vehicles form a substantial percentage of the total left-turning volume, data should be collected on their gap acceptance characteristics. A critical gap size that reasonably represents the characteristics of the entire traffic stream may be chosen. However, since the analysis presented represents a conservative scenario (by use of Chebyshev's inequality), the lane length computed from the model should be acceptable as long as the percentage of large vehicles is small.

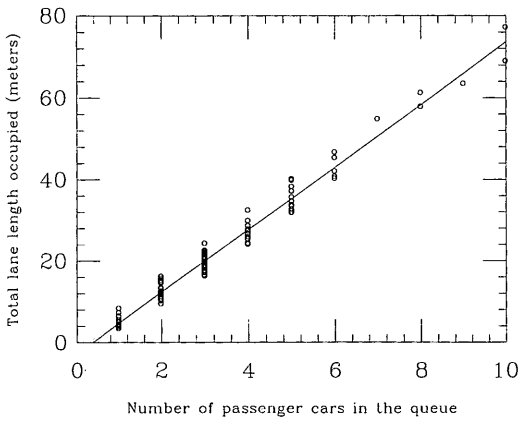

FIGURE 2 Distance occupied versus number of passenger cars.

TABLE 8 Passenger Car Equivalency Factors Based on Vehicle Length

Vehicle Type	Symbol	Equivalency Factor
Passenger Car	E_{PC}	1.0
Bus	E_B	2.1
Truck (WB40-WB60)	E_T	2.6 - 3.4
Recreational Vehicle (MH - MH/B)	E_{RV}	1.6 - 2.8

Note: Computed based on vehicle lengths from AASHTO [3], Table II-1

Step 3: Lane Length in Units of Distance

When the vehicle mix is given, determining the lane length in units of distance follows the method presented by Kikuchi et al (2). In this method it is assumed that the percentage of larger vehicles in the queue equals the percentage of larger vehicles in the left-turning volume.

For a given value of IN^* the required lane length in meters is computed as

$$L = (7.66\, IN^* - 2.92)\, \xi \tag{16}$$

where the expression in parentheses represents the space occupied by IN^* passenger cars (see Equation 15) and ξ is a conversion factor obtained from the following equation:

$$\xi = 1 + (E_B - 1)P_B + (E_T - 1)P_T + (E_{RV} - 1)P_{RV} \tag{17}$$

where P_T, P_B, and P_{RV} are the proportion of buses, trucks, and recreational vehicles in the left-turning volume, and E_T, E_B, and E_{RV} are passenger car equivalency factors given in Table 8, which is based on AASHTO's (*3*) standard on vehicle length.

DISCUSSION OF RESULTS

In the following sections the suggested lane lengths obtained from the model are compared with the guides provided by AASHTO, and the selection of the value of the threshold probability is discussed.

Comparison with AASHTO Guidelines

The results obtained from the proposed model are compared with AASHTO's guidelines. Figure 3 shows the adequate lane length for the two cases as a function of left-turn volume. The bold line represents AASHTO's guideline, and the lighter lines represent the results from the proposed model for a threshold probability of 0.015. AASHTO does not incorporate the opposing volume in its guideline, hence, only one line corresponds to AASHTO's guideline (which is used for any opposing volume).

Figure 3 shows that the AASHTO guideline is a conservative estimate for left-turn volume greater than 150 vph; in particular, when the opposing volume is low, the AASHTO values result in overdesign. However, for left-turn volume less than 150 vph, AASHTO suggests shorter lane lengths than our estimate only when the opposing volume is fairly large (more than 700 vph).

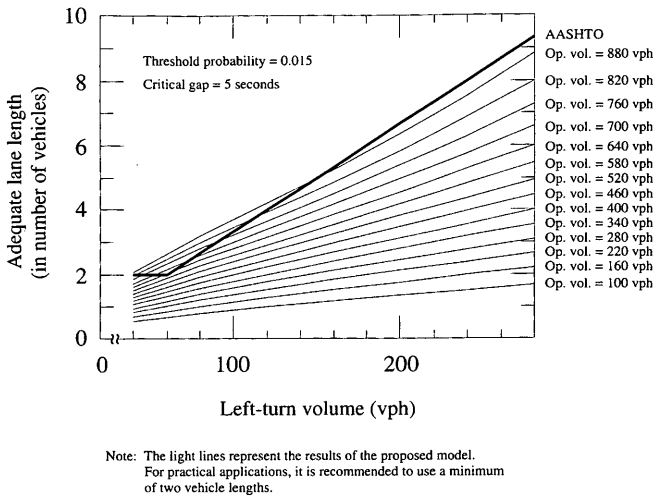

Note: The light lines represent the results of the proposed model. For practical applications, it is recommended to use a minimum of two vehicle lengths.

FIGURE 3 Comparison of AASHTO and proposed model lane lengths.

Choice of Thresholxd Probability

Figure 4 shows how the adequate lane length, N^*, varies with the threshold probability, τ. It is plotted for left-turn volumes of 100 and 200 vph under different combinations of opposing volume (600 and 800 vph) and critical gap (5.0, 5.5, 6.0, and 6.5 sec). The figure confirms that as τ increases, N^* decreases; in other words, shorter lane lengths are justified as more chances of vehicle overflow are allowed. N^*, on the other hand, increases as τ decreases. However, the data suggest some important trade-off considerations when choosing the value of threshold probability.

For a value of τ greater than approximately 0.1, N^* is not only small but also insensitive to changes in τ. AASHTO suggests a minimum lane length of two cars; therefore, the selection of a large τ value will not affect the lane length. However, for large values of τ, the frequency of lane overflow increases, and as a result, the delay to the through movement due to lane blockage also increases.

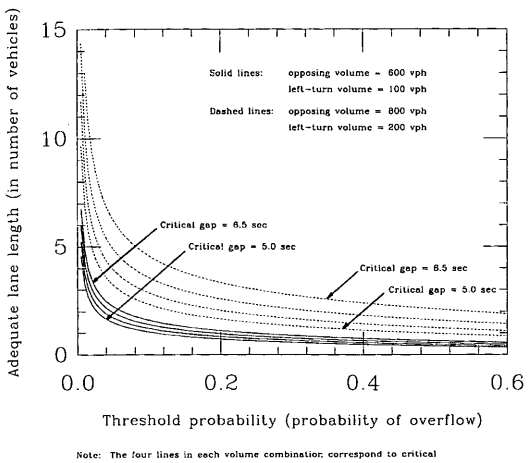

Note: The four lines in each volume combination correspond to critical gap sizes of 5.0, 5.5, 6.0 and 6.5 sec in ascending order.

FIGURE 4 Adequate lane lengths versus threshold probability.

For a value of τ smaller than approximately 0.05, N^* increases rapidly. This suggests that a small change in τ has a large effect on construction cost while having very little effect on the delay of through movement.

In addition, the selection of the threshold probability must consider the volume of through vehicles (traveling in the same direction as the left-turning vehicles, not the opposing traffic). For a higher volume of through vehicles, the threshold probability should be small in order to minimize the delay caused by the overflowing turning vehicles that are blocking the lane. For smaller volumes of through vehicles, the threshold probability can be kept higher. The authors consider that the threshold probability is a parameter that must be chosen based on site-specific conditions.

Unfortunately, none of the traffic engineering manuals, such as the AASHTO Green Book (*3*), HCM (*4*), and MUTCD (*10*) provide any guidelines on the value of the threshold probability. However, the values of the threshold probability used in related problems in the past range from 0.01 to 0.02. For example, this range was used in studying the warrant conditions for left-turn lanes at unsignalized intersections by Kikuchi and Chakroborty (*1*). AASHTO's (*3*) left-turn lane warrant adopts Harmelink's (*5*) derivation, which is based on the value of 0.015.

CONCLUSIONS

A mathematical model for determining the adequate left-turn lane length at an unsignalized intersection is presented. This subject has not been systematically addressed in the literature, and no unified method has been practiced; in particular, the effect of opposing volume on the turning lane length has not been addressed. The model simulates the arrival, waiting, and turning of the left-turning vehicles (the queueing process). The formulation of the model is complicated by the difficulty in deriving the service time distribution. In the model, the wait of the first vehicle in the queue when searching for a necessary gap in the opposing flow is considered the service time; the Pollazek-Kintchine formula and Chebyshev's inequality are used to derive the adequate lane length. Determining adequate left-turn lane length requires keeping the probability of left-turn lane overflow less than a threshold value. After the model derived the length in terms of the number of vehicles, the values were converted to the actual distance, taking into account the space required for different types of vehicles. For this, a series of surveys were conducted to determine the necessary space per vehicle.

The model results were validated by computer simulation. Using the model, a set of tables for recommended left-turn lane lengths were prepared for different combinations of representative values for left-turning volume, opposing volume, critical gap, and for a threshold probability of 0.015. The results were also compared with existing AASHTO guidelines, and the effect of the opposing volume on the recommended model, which the proposed model considers but AASHTO does not, is discussed.

This study provides a model and a formula to compute adequate left-turn lane length based not only on the left-turning volume but also on critical gap, opposing volume, and vehicle mix. While further studies on the determination of the threshold probability of acceptable overflow and critical gap size for large vehicles are important, the proposed formulation provides a more comprehensive and systematic procedure for determining the adequate left-turn lane length at isolated unsignalized intersections than the existing procedures.

REFERENCES

1. Kikuchi, S., and P. Chakroborty. Analysis of Left-Turn Lane Warrants at Unsignalized T-Intersections on Two-Lane Roadways. *Transportation Research Record 1327,* TRB, National Research Council, Washington, D.C., 1991, pp. 80–88.
2. Kikuchi, S., P. Chakroborty, and K. Vukadinovic. Lengths of Left-Turn Lanes at Signalized Intersections. *Transportation Research Record 1385,* TRB, National Research Council, Washington, D.C., 1993, pp. 162–171.
3. *A Policy on Geometric Design of Highways and Streets.* AASHTO, Washington, D.C., 1990.
4. *Special Report 209: Highway Capacity Manual.* TRB, National Research Council, Washington, D.C., 1985.
5. Harmelink, M. D. Volume Warrants for Left-Turn Storage Lanes at Unsignalized Grade Intersections. In *Highway Research Record 211,* HRB, National Research Council, Washington, D.C., 1967, pp. 1–18.
6. *Intersection Channelization Design Guide.* National Cooperative Highway Research Program Report 279, Transportation Research Board, 1985.
7. Drew, D. *Traffic Flow Theory and Control.* McGraw-Hill, New York, N.Y., 1968.
8. Taylor, H. and S. Karlin. *An Introduction to Stochastic Modeling.* Academic Press, Inc., 1984.
9. Sheldon, R. *A First Course on Probability,* 3rd ed., Macmillan Publishing Company, New York, 1988.
10. *Manual on Uniform Traffic Control Devices for Streets and Highways.* U.S. Department of Transportation and Federal Highway Administration, Washington, D.C., 1978.

Publication of this paper sponsored by Committee on Operational Effects of Geometrics.